Polymer Science and Technology

# Advances in Polymers for Biomedical Applications

Deepak Pathania
Bhuvanesh Gupta
Editors

NOVA

Nova Biomedical

# ADVANCES IN POLYMERS FOR BIOMEDICAL APPLICATIONS

# POLYMER SCIENCE AND TECHNOLOGY

Additional books and e-books in this series can be found
on Nova's website under the Series tab.

POLYMER SCIENCE AND TECHNOLOGY

# ADVANCES IN POLYMERS FOR BIOMEDICAL APPLICATIONS

DEEPAK PATHANIA
AND
BHUVANESH GUPTA
EDITORS

**Library of Congress Cataloging-in-Publication Data**

Names: Pathania, Deepak, editor. | Gupta, Bhuvanesh, editor.
Title: Advances in polymers for biomedical applications / editors, Deepak Pathania and Bhuvanesh Gupta (Central University of Jammu, Rahya Suchani, Bagla, Distt. Samba, Jammu and Kashmir, India).
Description: Hauppauge, New York : Nova Science Publisher's, Inc., [2018] | Series: Polymer science and technology | Includes bibliographical references and index.
Identifiers: LCCN 2018021037 (print) | LCCN 2018021542 (ebook) | ISBN 9781536136135 (ebook) | ISBN 9781536136128 (hardcover) | ISBN 978-1-53613-613-5 (ebook)
Subjects: LCSH: Polymers in medicine.
Classification: LCC R857.P6 (ebook) | LCC R857.P6 A39 2018 (print) | DDC 610.28/4--dc23
LC record available at https://lccn.loc.gov/2018021037

*Published by Nova Science Publishers, Inc. † New York*

# CONTENTS

# PREFACE

Polymers have generated considerable interest in a large number of technologically important fields such as human healthcare systems. Polymers represent a very important domain of materials and have become an integral part of day to day human life. Polymers exist in nature; they have been and continue to be an integral part of the universe. This book is intended for scientists and researchers to use in their research or in their professional practice in polymer chemistry and its biomedical applications. Multiple biological, synthetic and hybrid polymers are used for multiple medical applications. A wide range of different polymers are available, and they have the advantage to be tunable in physical, chemical and biological properties and in a wide range to match the requirements of specific applications. This book gives a brief overview about the introduction and developments of polymers for different applications. The biomedical polymers comprise not only bulk materials, but also coatings and pharmaceutical nano-carriers for drugs. The surface modification of the inorganic nanoparticles with a physically or chemically end-tethered polymer chain has been employed to overcome the problems associated with the polymers. Chemically attached polymer chains not only stabilize the inorganic nanoparticles, but also lead to photosensitivity, bioactivity, biocompatibility and pharmacological properties in the composites. Polymer encapsulated silica nanocomposites (mesoporous) have potential applications in different fields, such as optics, bio-catalysis, microelectronics bone tissue engineering, coatings cosmetics, inks, agriculture, drug release systems, diagnoses, enzyme imaging, temperature-responsive materials, and thermosensitive vehicles for cellular imaging. Polymer grafted nanosized particles are known to have excellent properties such as good dispersion ability in solvents and polymer matrices. Polymer-based controlled drug delivery systems have some specific advantages, such as improved efficiency and reduced toxicity. The incorporation of a thermoresponsive polymer layer often enhances protein absorption and specific biomolecular tagging through hydrogen bonding. As a result, the nanocomposite gets cleared from the body at a faster rate (blood residence becomes low). This book is composed of fourteen edited chapters; it is intended for scientists and researchers to use in their research or in their professional practice in polymer chemistry and its biomedical applications.

Chapter 1 - The build-up of new functional materials with controlled structures and properties in micro - and nano-dimensional scale is of essential interest because of their use in biomedicine, pharmaceuticals, tissue engineering, and regenerative medicine. From that point of view, the layer-by-layer deposition of polyelectrolytes on a substrate is imposed and

comparatively easy to realize. It is a technique, which includes a wide range of materials and surfaces, thanks to which it is possible to make nanostructured multilayer coatings.

The polyelectrolyte structures formulated by layer-by-layer deposition represent an outstanding and successful solution to the high demands of pharmaceutical science, where innovative therapeutic systems that provide sustained release in a specific target area with improved efficacy of well-known medical substances are targeted.

The present chapter summarizes the investigations on the formulation and physicochemical properties of polyelectrolyte multilayer (PEM) deposited onto planar polymer substrates, with a potential application as drug delivery carriers on buccal mucosa. The progress and success in the designed PEM was monitored by the newest, modern methods for characterization of the PEMs such as FT-IR, UV-VIS spectroscopy, XPS, SEM, AFM, laser refractometry. Biocompatible polymers, like polypropylene, poly-ε-caprolactone, and polylactic acid were used as substrates of PEM.

Multilayers were formulated from different natural polyelectrolytes – chitosan, xanthan, pectin, poly-L-lysine, carboxymethylcellulose. The layer-by-layer deposition process was accomplished by two methods, spin-coating and dipping.

The novelty in the PEMs presented here is the corona pretreatment of the substrate, which guaranteed an excess of charge on the substrate surface and improved the conditions for polyelectrolyte anchoring.

The experimental results suggested a successful, irreversible deposition of these well formulated PEMs. Changes in the deposition conditions led to corresponding changes in the PEMs structure, which gave one the route to precise modification of their properties in a desired direction, in accordance with the potential application.

The effect of the surrounding environment – pH and ionic strength on the formulation and stability of the PEMs was also investigated.

Chapter 2 - The application of nanoparticles to intracellular drug delivery has attracted increasing attention in the last few decades. Among them, mesoporous silica nanoparticles (MSNs) have emerged as promising nanomaterials which have shown great potential towards incubation of both hydrophobic and hydrophilic drugs and their further internalization at the targeted site in physiological environment for the treatment of large number of diseases. Excellent properties of MSNs such as good stability control over morphology and tunable particle size and the pore structure gives them an edge over other organic or inorganic based nanoparticles. With these properties, there is a great scope in designing novel MSNs with functionalization at the surface as well as within the pores using biocompatible and biodegradable polymers, stimuli responsive groups, proteins etc. MSNs have shown great potential in biotechnological and biomedical applications. Efforts are also made to increase the biocompatibility and circulation time of drug loaded MSNs by coating various polymers onto the surface of MSNs. Extensive work on MSNs has been reported in the literature which is however scattered. In the present chapter, the authors have dealt with the advances made in MSNs as controlled and targeted drug delivery systems using either synthetic or natural polymers specifically towards cancer treatment.

Chapter 3 - Since last three decades polymeric biometrials are being replaced by biodegradable shape-memory polymers and its nanocomposites for biomedical applications because of their good mechanical properties, controlled drug delivery, sterilization capability, biodegradability, biocompatibility and dual shape capability i.e., they can change their shape from shape I to shape II on introduction of an appropriate external stimuli. Among various

shape memory polymers, biodegradable polyurethanes with shape memory effect are in great demand as their physical and chemical properties can be varied in a controlled way by varying the percentage of the composition of soft and hard segments that helps in adjusting the shape recovery temperature of shape memory polyurethane near to the body temperature i.e., 37–40°C.

This study provides a comprehensive review that integrates the breakthroughs in studying biodegradable shape memory polyurethane (SMPU) and their derivatives, such as composites and compound structures, as well as their current applications. Concepts, principles/modeling, structures and related synthesis methods, applications and future trends are also reviewed.

Chapter 4 - Polymeric drug delivery systems (DDSs) are always attractive candidates which can be designed to enhance the therapeutic efficiency, i.e., to decrease the side effects and raise the anticipated effects of drugs. A DDS involves intramuscular, intravenous, enteral or oral administration of a pharmacologically active material for a targeted response after the administered drug or bioactive compound was released in the body. Moreover, controlled DDSs are widely investigated using polymeric based systems especially smart polymers which are sensitive to pH, light, temperature and so on. Indeed, controlled drug delivery is one of the most interesting research areas. A smart DDS must be capable of controlling kinetics (release rate) and operational window in the desired site(s). In other words, appropriate drug DDSs should have high efficacy, bioavailability, safety, controlled and prolonged release time and anticipated therapeutic response. It is noteworthy that computational studies are also carried out on the polymeric DDSs to predict the effectiveness of the designed drug carriers. This is because of the importance of such systems in pharmaceutics industry. Natural and synthetic polymeric drug carriers offer valuable advantages as efficient drug delivery and release. For instance, chitosan has commonly been applied in designing drug delivery systems due to its abundant hydroxyl and amine functionalities, non-toxicity, antibacterial and hemostatic characteristics. Other polymers that are frequently used as DDSs include polylactic acid, polyethyleneglycol, polylactic-co-glycolic acid and molecularly imprinted polymers. Also, these polymers have numerous applications in fabrication of wound dressing materials to protect the wounded areas from environmental harmful factors such as microbial infections. Wound healing is one of the most prevailing and economically difficult healthcare treatments universal. The treatment of severe burns requires preventing the bacterial growth, predominantly when eschar and damaged tissues exist. Accordingly, an antimicrobial treatment of wound is essential to inhibit bacterial proliferation and to accelerate the wound healing process. This chapter presents the most significant recently reported experimental and computational findings using chitosan, polylactic acid, polyethyleneglycol, polylactic-co-glycolic acid and molecularly imprinted polymers in both drug delivery and wound healing applications. Moreover, original research results achieved by means of DFT computations on simulated polymeric drug delivery systems will be presented and discussed.

Chapter 5 - Biopolymers are natural substance that contains multiple units of saccharides, nucleic acids, amino acids and they are produced by a variety of mechanisms. The major biopolymer classification based on biopolymers which is derived from microbial systems, extracted from plants or synthesized by chemical methods. Biopolymers have immense application in the field of medical materials, cosmetics, food additives, clothing fabrics, water treatment, bioremediation, absorbents, biosensors, targeted drug delivery, tissue engineering and even data storage elements. Polyesters, proteins and polysaccharide are the major types of

biopolymers. Among the various polymers, natural polymers are extensively used due to its biocompatibility but not used widely because of its physical properties such as solubility, stability and mechanical strength. These drawbacks can be overcome by functional modifications on biopolymer surface renders them as a suitable and smart biomaterial for medical as well as drug delivery applications. In this chapter, the authors would like to discuss about some polysaccharide based modified biopolymers and its potential applications in various diversified fields, particularly in drug delivery, disease diagnosis and cancer therapy. Chemical modifications are desired for improving the function and targeting its specific applications. The modification technique includes chemical, photochemical, enzymatic, radiation and graft copolymerization. However, these chemical modifications of biopolymers may lead to toxicity issues, increase the cost of production and increased complexity of the synthesis process. In this chapter, the authors discussed about the toxicity issue due to functional modifications and appropriate solutions to overcome these limits by suitable coating or surface stabilization techniques.

Chapter 6 - Multidrug resistance (MDR) is a phenomenon by which the targeted organisms resist antimicrobials that are aimed at eradicating the organism. The present study was aimed at evaluating the antibacterial activity of nano bis-demethoxy curcumin analog (NBDMCA). NBDMCA was prepared by solvent-assisted process and characterized using HRTEM, DLS, FTIR and NMR. The morphology and size of NBDMCA which was determined by HRTEM and DLS was found to be around 90 nm. Antibacterial activity of NBDMCA was determined by using Agar disc diffusion method and compared with various groups of antibiotics. Further, Bacteria-NBDMCA interaction was visualized using optical microscope. Also Resazurin assay was carried out to determine the Minimal Inhibitory concentration of the drug. Investigation of antimicrobial activity of the derivative demonstrated the ability to inhibit Gram-positive and Gram negative microorganisms with zone of inhibition ranging from 10 mm to 20 mm. In addition to this, the mobility of the BDMCA treated bacteria was found to be reduced when compared to the untreated bacteria. Applications of BDMCA based on these findings may lead to valuable discoveries in various fields such as medical devices and antimicrobial systems.

Chapter 7 - Polycaprolactone (PCL) has been extensively used for biomedical applications because of its strength and its slow rate of biodegradation. However, its inert nature has stimulated the surface functionalization of PCL, without the compromise of its bulk properties which can be carried out by plasma functionalization. Thus, this chapter highlights the plasma modification of PCL surface so that immobilization of biomolecules transforms the inert PCL surface to a bioreceptive surface finding vivid applications in tissue engineering. Emphasis has been made on generating specific chemical functionalities on PCL surface by the modulation of the nature of the gas. This consequently changes the surface properties; wettability, nanotopography and nanoroughness which play a vital role in cell adhesion and proliferation. Moreover, the reactive functionalities and the altered surface properties facilitate the covalent attachment of biopolymers and bioreactive substrates rendering durability and ligands for cell receptors to adhere to the PCL surface. The chapter details the application of the plasma modified surface for bioimmobilization and tissue engineering applications. Greater cell adhesion and proliferation was observed with the plasma modified PCL surface enhancing its biocompatibility. Therefore, plasma modification of PCL could elevate its applicability in the biomedical field.

Chapter 8 - Medical research has been greatly benefited with the discovery of biomedical application of natural or synthetic polymers as biomaterial which could help in medical treatment. In this chapter, the authors are going to discuss the use of biomaterials for the directional delivery of molecules that could either modulate the gene expression or directly benefit a tissue or cell. Materials like poly(lactide-co-glycolide), polyacetals, collagen, polysaccharides, chitin, polyanhydrides and other polymers are discussed with respect to their applications for delivering DNA or siRNA.

Chapter 9 - Chitosan, an aminopolysaccharide with strong positive electrical charge, is of great interest as a biomaterial for tissue engineering. Chitosan-based biomaterials show a wide variety of physico-chemical characteristics as: they are non-toxic, biocompatible, bioabsorbable, biodegradable, arise from renewable resources, offering also antimicrobial, haemostatic, analgesic and stimuli responsiveness activities. This chapter reviews the applications of the chitosan containing biomaterials, as hydrogel, powder, porous scaffold, sponge, film, fiber, and nanoparticles in tissue engineering. Tissue engineering, a multidisciplinary research, is devoted to the reconstructing or regenerating damaged biological tissue in clinical/pathological situations, such as lesions, infections, traumas, and sequelae. Chitosan – containing systems exhibit affinity for biomolecules, are promising biomaterials to develop biological substitutes capable to restore, maintain, or to improve the organs and tissues function. Such biomaterials in combination with cells or bioactive molecules (such as cytokines and growth factors) can promote cell proliferation, differentiation, and migration.

Chapter 10 - In this chapter, better wound management using different herbal drugs loaded wound dressing materials has been discussed. The wound healing is a complex phenomenon and it passes through mainly three overlapping phases, where cell to cell and cell to matrix interactions take place. Due to complexity of the wounds, different types of dressing materials are required for faster healing. The traditional herbal medicines have a long history of wound management but often their low bioavailability decreases their efficacy. The encapsulation of herbal drug in polymer matrix increases their efficiency for wound healing. Amongst modern dressing materials, hydrogels, polymeric films and scaffolds have the capability to load very high concentration of drug and also have the ability to release them in a controlled and sustained manner which is essential for optimal therapeutic concentration. Further, they have the capability to absorb the exudate, pass the oxygen and also help the cells to be attached and proliferate. *In-vivo* and clinical studies show better healing efficiency of the herbal drug loaded dressing materials as compared to pure drug or pure dressing materials.

Chapter 11 - Many kinds of stimuli-responsive hydrogels that respond to the change in their surroundings such as solvent composition, temperature, pH, and supply of electric field have been developed in the past decades. Gamma radiation induced graft copolymerization of hydrophilic monomers onto polymeric films has been shown particularly useful for the functionalization of surfaces with stimuli-responsive properties. This method involves the formation of active sites (free radicals) onto the polymeric backbone as a result of the exposition to high-energy radiation, in which a proper microenvironment for the reaction among monomer and/or polymer and the active sites takes place, thus leading to propagation which forms side chain grafts. The modification of polymers using high-energy irradiation may be performed by the following methods: direct or simultaneous, pre-irradiation oxidative and pre-irradiation. The most frequent ones correspond to the pre-irradiation oxidative

method and the direct one. Radiation-grafting has many advantages over conventional methods considering that it does not require catalyst nor additives to initiate the reaction, and in general, no changes on the mechanical properties with respect to the pristine polymeric matrix are observed. This review focuses on the synthesis of stimuli responsive smart hydrogels by the use of gamma radiation induced grafting. In addition, diverse applications of these materials in the biomedical field are also discussed.

Chapter 12 - Hydrogels are three-dimensional networks that are able to absorb large quantities of water or biological fluids, and hence have the potential to be used as primary candidates, for various drug delivery systems, and carriers or matrices, for cells in tissue engineering. Hydrogels prepared from natural materials *viz.*, polysaccharides and polypeptides, along with different types of synthetic hydrogels from the recent reported literature, are presented in this chapter. The most widely employed natural polymers for the preparation of hydrogels are cellulose, chitosan, hyaluronic acid, dextran and alginate, while synthetic polymers are poly(ethylene glycol), poloxamer, Poly(hydroxyethyl methacrylate) (pHEMA), Polyacrylamide (PAAm) and polyvinyl alcohol. All the classifying properties of hydrogels affect their applicability, and types of therapeutic areas, in which they can be utilized.

Chapter 13 - Nowadays, advancements in imaging technology would give a more detailed and accurate image for better diagnosis and treatment planning. The requirements of probes for bioimaging include high target selectivity, high stability, low cytotoxicity, biocompatibility, and high contrast. To this aim, the authors need new materials and approaches.

This chapter reports some fundamental results of biomaterials used to design rational architectures for biomedical imaging application.

Chapter 14 - There is a tremendous progress in the field of drug delivery in last few decades with introduction of novel delivery systems for improving therapeutic objectives, and minimizing side effects. Polymeric Drug Delivery Carrier Systems (PDDCS) have emerged as systems of choice, for targeted and controlled release formulations. PDDCS improve both pharmacokinetic and pharmacodynamic profiles of biopharmaceuticals by altering plasma half-life, decreasing immunogenicity, improving solubility, and stability of drug. For developing an ideal PDDCS, safety, efficacy, hydrophilicity, absence of immunogenicity, biological inertness, suitable pharmacokinetics, and the presence of functional groups for covalent conjugation of drug, targeting moiety, or formation of copolymer are important. Discussion covering various factors impacting the success of PDDCS is very broad and cannot be covered exhaustively in this chapter, so this review focuses on:

1. General introduction to various types of PDDCS and their various therapeutic advances
2. Types of polymers used and essential properties of an ideal carrier for drug delivery
3. Responsive PDDCS based on physical and chemical stimuli
4. Mechanism of drug release from the PDDCS

Chapter 15 - Conventional textile based wound dressing materials are cost-effective and good absorbents. However, cross linked polymer nanocomposites are best choice due to their ability to provide optimal wound healing conditions like homeostasis, non-adherence, maintenance of a moist wound bed etc. electrospun polymer web, by virtue of their micro fibrous structures provide suitable environment for wound healing. In this study, the authors have optimized the preparation of a blend of sodium alginate and polyvinyl alcohol of

different proportions. The authors have mixed the blend with different proportions of citric acid for cross linking. The blend was then made into fibrous web using electrospinning apparatus. Calcium alginate has many advantages over sodium alginate such as web stability and high performance especially with bleeding wounds. Getting commercial calcium alginate is also expensive. Therefore, the authors first made the web using sodium alginate and then replaced the sodium for calcium by using calcium chloride. Thus, the authors formed a web of calcium alginate crosslinked with citric acid.

The web samples were then taken for physiochemical characterization using scanning electron microscopy, Fourier infrared spectroscopy; thermogravimetric analyser and moisture vapour transmission analyser. The SEM micrograph revealed the presence of many interconnections and densely crosslinked web. Moreover, the cross linking was good in the web made from blend as compared to the web made with the individual component. The SEM images clearly suggest that the cross linked web has ideal morphology to give better performance in the process of wound healing. The FTIR spectra clearly revealed the interaction between the groups of the polymer constituents and the groups involved in cross linking. This confirms the role of citric acid in making a high performance web. The spectral findings are in line with the SEM morphological images. Thermogravimetric plot is an evidence for the stability of the material under study. The cross linked web has better stability than the non-cross linked counterpart. Also, the stability increased with an increase in the concentration of the cross linking agent. Thus the authors speculate that, the web which was found to be better as per the SEM micrograph and the FTIR spectra was also stable enough, which is a pre-requisite for a high performance wound healing. MVTR results show that the loss of water is reduced in citric acid crosslinked alginate blend. Since cross linking increases the water absorption capacity of the alginate it would provide moist environment to the wound, which helps in rapid healing thereafter. Compared to the crosslinked web, the non-crosslinked ones showed greater water vapour permeability. The cross linked web was found to inhibit the growth of the *staphylococcus aureus*as evidenced by zone of inhibition in the growth medium.

# ACKNOWLEDGMENTS

The accomplishment of this book has been a very creative contribution of eminent scientists and scholars from various organizations. Shaping these articles into a well-designed academic structure of the book under Nova Publishers is highly appreciated. We would like to acknowledge authors for their strong support during this work. It was a wonderful opportunity for all of us to have a creative interaction with all the authors under the umbrella of Nova Publishers to execute this project in a dynamic manner.

A focused direction and vision is needed for any activity. Here we would like to extend our sincere thanks to Professor P.K. Khosla, Vice Chancellor, Shoolini University and Professor Ashok Aima, Vice Chancellor, Central University of Jammu for their generosity, goodwill and motivation throughout this project. We would extend our sincere thanks to Dr. Arush Sharma, Shoolini University for providing necessary help whenever needed.

A special thanks to our colleagues at IIT Delhi, Central University of Jammu and Shoolini University for all the support and enthusiasm during the work.

It is our sincere effort to appreciate and thank all the people who have been helpful directly or indirectly while executing various aspects of the book preparation at different stages.

*Deepak Pathania*
*Bhuvanesh Gupta*
*Editors*

In: Advances in Polymers for Biomedical Applications ISBN: 978-1-53613-612-8
Editors: Deepak Pathania and Bhuvanesh Gupta 

*Chapter 1*

# INNOVATIVE BIOPOLYMER NANO-MULTILAYERED FILMS FOR BIOMEDICAL APPLICATIONS: FABRICATION AND PHYSICAL PROPERTIES

***M. Marudova[1,*], A. Viraneva[1], S. Sotirov[1], I. Bodurov[1], G. Exner[1], I. Vlaeva[2] and T. Yovcheva[1]***

[1]Faculty of Physics and Technology, University of Plovdiv
"PaisiiHilendarski," Plovdiv, Bulgaria
[2]Department of Mathematics and Physics,
University of Food Technologies, Plovdiv, Bulgaria

## ABSTRACT

The build-up of new functional materials with controlled structures and properties in micro - and nano-dimensional scale is of essential interest because of their use in biomedicine, pharmaceuticals, tissue engineering, and regenerative medicine. From that point of view, the layer-by-layer deposition of polyelectrolytes on a substrate is imposed and comparatively easy to realize. It is a technique, which includes a wide range of materials and surfaces, thanks to which it is possible to make nanostructured multilayer coatings.

The polyelectrolyte structures formulated by layer-by-layer deposition represent an outstanding and successful solution to the high demands of pharmaceutical science, where innovative therapeutic systems that provide sustained release in a specific target area with improved efficacy of well-known medical substances are targeted.

The present chapter summarizes the investigations on the formulation and physicochemical properties of polyelectrolyte multilayer (PEM) deposited onto planar polymer substrates, with a potential application as drug delivery carriers on buccal mucosa. The progress and success in the designed PEM was monitored by the newest, modern methods for characterization of the PEMs such as FT-IR, UV-VIS spectroscopy, XPS, SEM, AFM, laser refractometry. Biocompatible polymers, like polypropylene, poly-ε-caprolactone, and polylactic acid were used as substrates of PEM.

* Corresponding Author Email: margo@uni-plovdiv.bg.

Multilayers were formulated from different natural polyelectrolytes – chitosan, xanthan, pectin, poly-L-lysine, carboxymethylcellulose. The layer-by-layer deposition process was accomplished by two methods, spin-coating and dipping.

The novelty in the PEMs presented here is the corona pretreatment of the substrate, which guaranteed an excess of charge on the substrate surface and improved the conditions for polyelectrolyte anchoring.

The experimental results suggested a successful, irreversible deposition of these well formulated PEMs. Changes in the deposition conditions led to corresponding changes in the PEMs structure, which gave one the route to precise modification of their properties in a desired direction, in accordance with the potential application.

The effect of the surrounding environment – pH and ionic strength on the formulation and stability of the PEMs was also investigated.

**Keywords**: polyelectrolyte multilayers, corona discharge, PEMs stability, pH, ionic strength, biopolymers

## 1. INTRODUCTION

Polyelectrolyte multilayers (PEMs) are one of the promising and intensively investigated (in the past decades) systems in the field of nanomaterial science. Their build up is based on the so-called layer-by-layer (LbL) deposition process, which consists of consecutive adsorption of polyanions and polycations from solutions onto a solid substrate. The interactions between the polyelectrolytes have electrostatic origin [1].

The building mechanism of multilayer structures of polyions or other charged molecules on substrates are schematically presented in Figure 1. The prerequisite for successful deposition is the existence of an excess charge on the surface of the substrate. The charged substrate contacts the first polyelectrolyte solution, charged oppositely to the substrate. After the first layer deposition, a rinsing step is required, during which the loosely connected molecules are removed. Then the contact with the second solution leads to the second layer build up. After that, another rinsing follows. This way, a cycle is closed and the process repeats again, as many times as needed [2]. Because the process involves only the adsorption of polyelectrolytes from solution, there are no limitations on the size and topology of the substrate.

Once again, the successful formation of the next single layer in PEM is the charge overcompensation of the previously adsorbed layer [3] resulting in:

- Repulsion of the like charged molecules and self-regulation of the adsorption to obtain a monomolecular layer;
- Possibility for the oppositely charged molecules to be adsorbed onto the layer.

The high stability of the PEMs is explained by the formation of ion pairs between oppositely charged polymer segments in the consecutive layers [4-6]. Since the polymers are predominantly flexible, the resulting architecture represents an arbitrary structure [7]. The polyelectrolyte deposition from a solution on a solid substrate is a non-equilibrium process, resulting in a loose structure containing numerous defects. The advantage of using

polyelectrolytes in comparison to low-molar-mass molecules, is in the formation of multiple ionic bonds, which ensure the adhesion of the polyelectrolyte layer onto the substrate or previous layer.

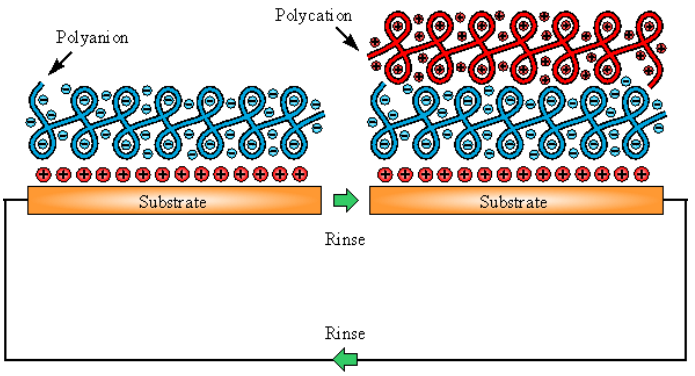


Figure 1. Layer-by-layer deposition of polyelectrolyte multilayers on charged planar substrate.

Following the Decher's technique, a successful PEM is possible when the adsorption process of polyelectrolytes is irreversible during the multilayer structuring [8].

In recent years, studies on the PEMs have focused on identification of an appropriate mechanism of film growth and its relationship to the structure of the individual layers. The results show that the film thickness increases either linearly or exponentially with an increasing number of layers. In PEMs made of highly charged polyelectrolytes, the overall thickness increases linearly. Such PEMs consist of thick layers structures, where each layer partially penetrates into the adjacent layers [9]. For the PEM's obtained from weak polyelectrolytes, the overall thickness increases exponentially with the number of adsorbed layers [10]. Lavalle's model explained the observed differences in the structural formation by suggesting that the polyions in strongly charged polyelectrolytes are tightly bonded together and the surface charge of the film is almost entirely compensated. Such PEMs are not prone to swelling and are more stable with respect to environmental changes. When the interactions between the polyelectrolytes are weaker, part of the charge compensation is achieved by the low-molecular ions from salt. The mobile macromolecular segments may diffuse into or out of the film surface and/or interact with other counterions. Thus, they form neutral complexes with the oppositely charged polyelectrolyte, weakly connected to the film surface. This process implies PEM's swelling, increase in roughness and exponential thickness growth.

The main factors affecting a successful LbL deposition process include the initial substrate charge, the deposition technique, the ionic strength of the solution, the polyelectrolyte concentration, and the pH of the solutions. These factors also determine the area of application of the structures. The PEMs possess a good ability to immobilize biomolecules, being in well preserved activity because LbL deposition:

- does not require drastic conditions in order to build the structures and the process is very often done in water;

- tolerate different environmental conditions (pH and ionic strength), which ensures the construction of PEMs with loose structure and functional groups, capable of binding molecules.

The release rate of the immobilized substances can be controlled in a very broad range through a change of the polyelectrolyte partners in the structures. It can also be controlled through the depth of immobilization in the volume of the PEMs or through a change in environmental conditions of drug release- pH, temperature and ionic strength.

The present chapter summarizes the methods of the LbL deposition process and environmental conditions' influence on the PEMs composition and structure, physical properties and stability, parameters playing an important role in PEMs applications as drug delivery systems.

## 2. RESULTS

### 2.1. Effect of the Substrate Properties on the PEMs Deposition

The formulation of PEMs on polymer substrates is an innovative approach. This possibility extends PEM's spectrum of applications to medicine, pharmaceuticals, and more. A prerequisite of the successful deposition of PEMs on polymer substrates is the existence of an active surface. The activation may be accomplished in a variety of ways - by chemical binding of ionic groups or non-polar emulsifiers, by the application of plasma, etc. [11, 12]. One possibility for substrates activation is to treat them in corona discharge [13].

The chapter deals exactly with corona treated substrates prior to the PEMs built-up. This experimental set-up is a home-made, point-to-plane three-electrode corona discharge system, consisting of a corona electrode (needle), a grounded plate electrode, and a metal grid placed between them. Either positive or negative voltage of magnitude 5 kV was applied to the corona electrode with the same polarity but a magnitude of 1 kV to the grid. The samples were charged under standard room conditions for 1 min.

Employing such treatment, the achieved charge density and its stability depends on the different factors such as: the degree of crystallinity of the material, the charge polarity, the substrate porosity and excess charge stability. The charge stability is expected to influence the properties of the PEMs obtained.

#### *2.1.1. Degree of Crystallinity*

As an example of the effect of substrate crystallinity, we consider pectin/chitosan PEMs, deposited on corona pre-charged polylactic acid - PLLA and PDLA substrates. It is known that PLLA is partially crystalline with a degree of crystallinity of about 37% [14] whereas PDLA is entirely amorphous [15]. For each of the substrates, three series of samples, differing in their number of layers – 4, 10, and 16 –were investigated. In all investigated cases, a successful deposition by the dipping of pectin/chitosan PEMs was gained, as confirmed by FT-IR analysis [16], where in both cases (PLLA and PDLA substrate) a new band in the absorbance spectra was found. Mainly, a broad asymmetric absorption peak with a maximum at 1580 $cm^{-1}$, associated with the $\delta_{N-H}$b and of glucosamine in chitosan at 1582

$cm^{-1}$ and $\nu_{C=O}$b and of carboxylate in pectin at 1610 $cm^{-1}$ [17]. It was also found that the intensity of the typical band rose with the increase of the number of the deposited layers. Hence, it could be concluded that the binding of pectin and chitosan is irreversible and the amount of the polyelectrolites increases gradually during the process of layer deposition.

The exact amount of the polyelectrolytes in the deposited layers was estimated by the surface refractive index (sRI), $n_s$ measurements performed with preliminary swollen in acetate buffer PEMs structures. The sRIs were measured by means of the disappearing diffraction pattern method, using a laser refractometer at wavelengths of 532 nm and 632.8 nm [18]. Applying the one-oscillator Sellmeier's model for two wave lengths, the dispersion curves in the visible range for PEMs on the PLLA and the PDLA substrates were obtained [16]. The results showed that independent of the substrate type, the sRI decreased with the layers' number increase, due to the higher amount of the absorbed buffer solution in the PEMs. The refractive index of the buffer solution is lower than those of the substrate and deposited polyelectrolytes [19-21] and hence the adsorbed buffer in the multilayers decreased the sRI. More significant was that the sRI decreases for the PEMs on a PDLA substrate, which was attributed to the deposition of bigger amount of polyelectrolytes. Hence, it can be speculated that the amorphous substrates promote better polyelectrolyte anchoring.

As an alternative method for estimation of the amount of the deposited chitosan on the PLLA and PDLA substrates, the color reaction of chitosan with ninhydryn [16] could be used. The PEMs structures were treated with ninhydrin solution and the changes in the transmittance at 570 nm were followed. The neat effect of the PEMs was gained after an appropriate normalization of the transmission spectra with respect to the effect of the substrate and that of the samples untreated with ninhydrin. The normalized transmittance of the PEMs with a different number of layers on both types of substrates are shown in Figure 2.

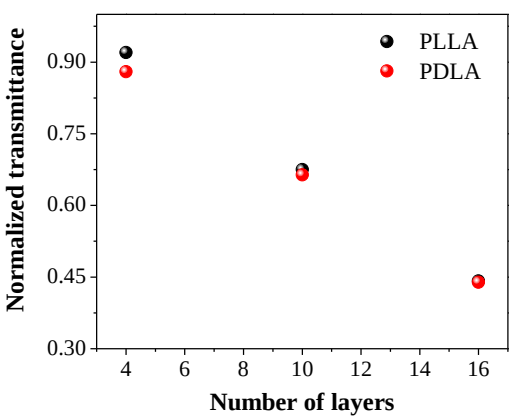


Figure 2. Normalized transmittance at 570 nm for pectin/chitosan PEM onto semicrystalline PLLA and amorphous PDLA for different number of layers.

With an increase in the number of layers, the transmittance decreases. Hence, the assumption was made that the amount of chitosan deposited on the substrates increased with the number of layers and since it is gradual with the number of layers, it is considered to be irreversible. The amount of the polyelectrolytes for the first two bilayers deposited onto the PDLA substrate was slightly higher than that onto the PLLA substrate. The results are in accordance with the before mentioned positive effect of the amorphous structure of the

substrate on the deposition. As some other authors pointed out, the highly regular structure restricts the stable charge trapping [22]. The effect of the substrate decreases, with the number of layers becoming negligible for PEM's with more than 10 layers [23].

### *2.1.2. Corona Polarity*

Examples of pectin/chitosan PEMs will be given where polylactic acid (PLA) substrates were treated in both - positive and negative corona discharges [24]. One has to mention that corona treatments with different corona polarity results in an excess surface charge with the same polarity. Hence, the polyelectrolites layers alternated i.e., for positively charged substrate, the first PEM layer was of polycation and *vice versa* when the substrate was negatively charged, the first PEM layer was of polyanion. This way, two different PEMs structures with alternative ordering were prepared: the first one – chitosan/pectin multilayers on negatively charged PLA substrates, and the second one – pectin/chitosan multilayers on a positively charged PLA substrate. For each type, three different series with different numbers of layers – 4, 10, 16, were studied. The results, gathered by FT-IR spectra analysis showed that the band at 1610 $cm^{-1}$, which is characteristic for the carboxylate ion in pectin [17], was more pronounced and the absorption peaks were deeper in the case of the negatively charged substrate. Therefore, the amount of pectin and chitosan deposited on the negatively charged substrates was considered larger than in the case of the positively charged one.

Applying the same method of sRI measurements to swollen PEMs of chitosan/pectin onto PLA, for $\lambda = 633$ nm and $\lambda = 532$ nm, the results showed that, independent of the substrate polarity, the sRI decreased with the number of layers because of the higher amount of absorbed distilled water. The sRI of distilled water is lower than those of the substrate and deposited polyelectrolytes, hence the absorbed water in the multilayers would decrease the sRI values corresponding to its amount into the PEMs. The results indicated that the amount of absorbed water into the PEMs on negative substrates was higher in comparison with those absorbed in the PEMs on positive substrates.

There are two possible reasons for different swelling behavior of the PEM structures. Because the PLA does not swell in water, the observed swelling is entirely due to the polyelectrolyte multilayers. Therefore, the higher amount of water could be attributed to the bigger amount of pectin and chitosan bound to the negative substrate. Such reasoning is in good agreement with the spectral characterization results. Nevertheless, one should not exclude the possibility that the stability of the PEMs during the swelling in distilled water might be altered i.e., it is possible that some of the polyelectrolytes dissolve in the water. For that reason, the PEMs stability was also independently investigated.

The stability of PEMs was found to be proportional to the changes in the absorption band at 570 nm of those treated in ninhydrin dry and swollen samples [24]. For this purpose, the difference between the absorptions of the dry and swollen samples was calculated:

$$\Delta A(\lambda = const) = A_d - A_s \tag{1}$$

where $A_d$ was the absorption of the dry sample, and $A_s$ was the absorption for the swollen sample. Figure 3 represents the results of the analysis. They clearly showed that the absorption decreased, independent of the corona polarity and it is more pronounced in the

case of a positive corona. These results suggest that a partial dissolution of chitosan during the swelling tests took place for the PEMs on the positively charged substrate.

Using the same absorption spectra, the changes in the absorption band at 660 nm [25] gave the amount of the absorbed water [24]. The increase of the absorption for the swollen samples was attributed to the bound water and the degree of swelling. The findings suggested greater absorption for the PEMs on a negatively pretreated substrate.

Based on the presented results, it could be assumed that the multilayers constructed on the positively charged substrates are less stable than those on the negatively charged substrates.

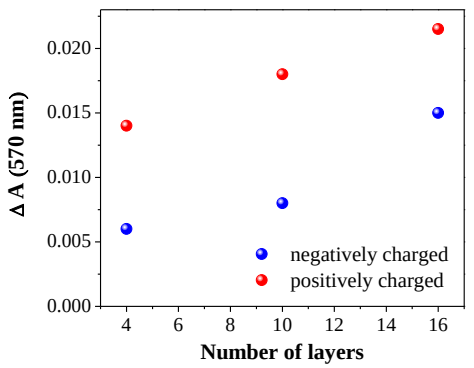


Figure 3. Absorption differences at 570 nm between dry and swollen PEMs of chitosan/pectin onto PLA substrate caused by chitosan dissolution from multilayer structures.

### *2.1.3. Substrate Porosity*

The effect of substrate structure was examined for chitosan/xanthan PEMs deposited on solvent casted or lyophilized PLA substrates. Both substrates were preliminary corona charged, applying the same corona polarity, at the same conditions.

In order to further characterize the stability of the surface charge, the effect of storage time of the PLA and lyophilized PLA substrates on the surface potential decay was investigated [26]. Time dependences of the normalized surface potential for all investigated samples are presented in Figure 4.

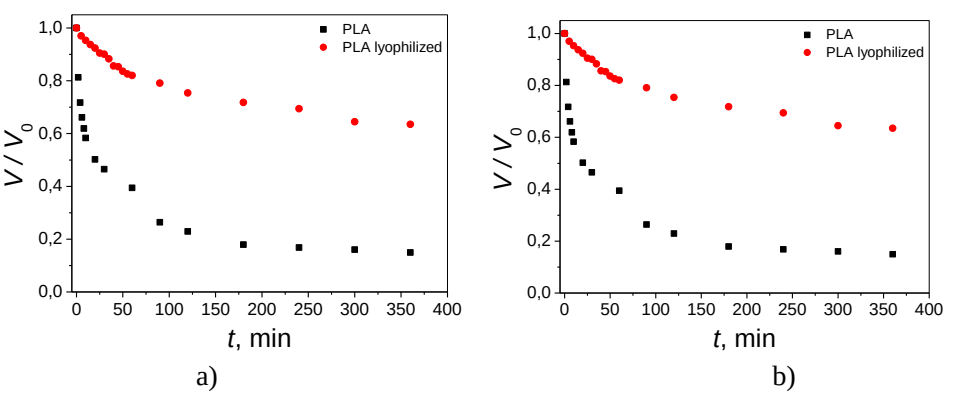


Figure 4. Normalized surface potential time dependences for PLA and lyophilized PLA substrate a) positive corona charge and b) negative corona charge.

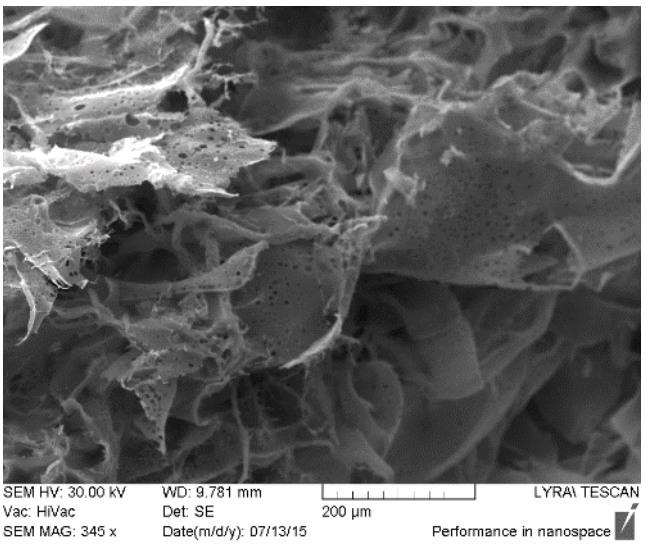


Figure 5. SEM morphology of lyophilized PLA substrate.

The experimental results obtained showed that:

- The normalized surface potentials decay was exponential in the first 60 minutes and then it slowly approaches a constant value within 360 minutes. Such behavior could be explained by the presence of various localized surface states that trapped charges. Similarly, exponential decay was observed by other authors [27];
- The normalized surface potential was higher for the lyophilized PLA substrates irrespective of the corona polarity. It was assumed that the porous structure of the lyophilizing PLA (as shown in Figure 5) significantly improved the ability to store and stabilize the charges [28].

## 2.2. Methods of Deposition

In general, the LbL deposition is a solution-dipping method and its main disadvantage is the long time required to assemble even a monomolecular layer. Usually, the process may take up to 1h per layer depending on the adsorbing systems. The duration of the process is determined as a two-step adsorption process: polymer chains anchor to the surface by some segments (a fast initial step) and then the molecules relax to pack densely (a slower second step) [29]. One reasonable solution to reduce the assembly time is a spin-coating method, where the time for single layer is about 20 s. In addition, a smoother interface between the oppositely charged layers and the PEMs surface is achieved [30].

A comparison between the properties of PEMs prepared by dipping and by spin-coating was made for chitosan/xanthan PEMs on corona pretreated PLA substrates [31].

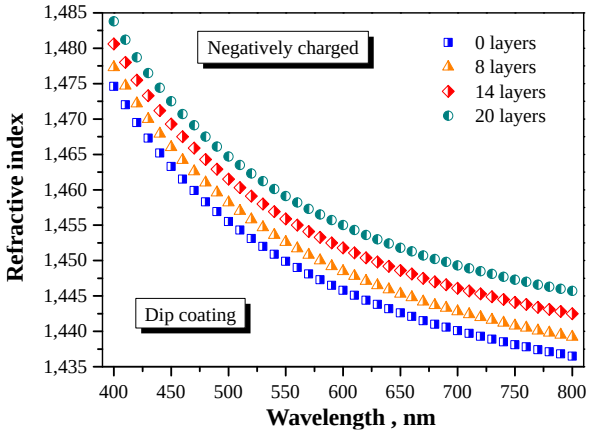


Figure 6. Dispersion curves of negatively charged PLA and PEMs of chitosan/xanthan, made by dipping.

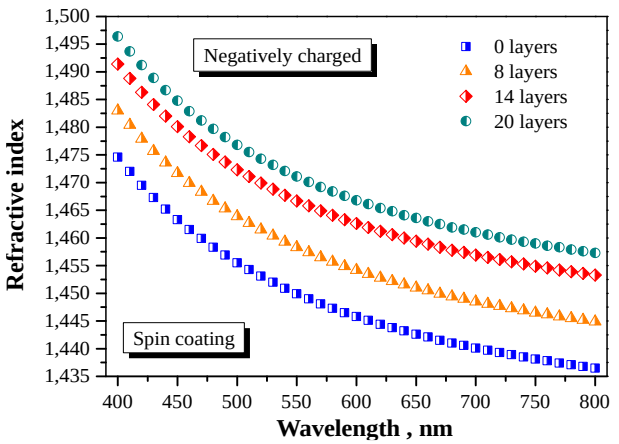


Figure 7. Dispersion curves chitosan/xanthan PEMs on corona pretreated PLA substrates, made by spin-coating.

The optical properties and the thickness of the layers were investigated by sRI measurements. Applying the one-term Sellmeier's model for two wavelengths (532 nm and 635nm), the dispersion curves in the VIS spectral range far from the fundamental absorption band were calculated [32]. Representative plots of such dependences for chitosan/xanthan PEMs on corona pretreated PLA substrate are given in Figure 6 for the dipping method and Figure 7 for the spin-coating method.

The dispersion curves possessed similar behavior for all samples, shifting to higher surface refractive index values with increasing numbers of deposited layers. Hence, the dispersion curves indicated the successful deposition of multilayers. The average sRI, $n_s$, over the penetration depth $d_p$ of PEMs, obeys Lorentz-Lorenz equation:

$$d_p \frac{n_s^2-1}{n_s^2+2} = d\frac{n^2-1}{n^2+2} + Nd_1\frac{n_1^2-1}{n_1^2+2} + Nd_2\frac{n_2^2-1}{n_2^2+2} \quad d_p = d + N(d_1+d_2) \tag{2}$$

where $d_p$ is the average evanescent wave penetration depth at total internal reflection. The values were estimated to be: $d_p = 0.82$ μm for 532 nm, and $d_p = 0.98$ μm for 635 nm [33]. $N$ is the number of one type of the layers. $d_1$, $n_1$ are the thickness and refractive index of first type of layers (chitosan), respectively. $d_2$, $n_2$ are the thickness and the refractive index of the second type of layers (xanthan) respectively. $d$ is the thickness of the PLA substrate at evanescent wave penetration. $n$ is the refractive index of the charged PLA substrate. When the number of layers increased, the PLA substrate refractive index impact decreased. The corresponding values for 532 nm were calculated to be $n_1 = 1.52$ [34], $n_2 = 1.50$ [20], and $n = 1.47$ for the PLA substrate. Solving equation (2) with those particular values showed an increase in the refractive index of the PEMs with the number of layers. Assuming equal layers, the average layer thickness of a single polyelectrolyte layer would be about (5 ± 0.5 nm) for the spin-coated PEMs and about (10 ± 1.0 nm) for the dipping assembled PEMs. The results agreed well with previous investigation on deposition process of weakly charged polyelectrolytes [35], and could be explained by the inter diffusion and interpenetration of the polyelectrolytes. At pH 4.5 of deposition process, the molecules of both chitosan and xanthan are partially charged (the pKa value of the chitosan is about 6.5 [36] and the pKa values of xanthan is 3.1 [37] and part of their chains are free to move in the interior part of the polyelectrolyte complexes. Therefore, an excess amount of polyelectrolyte could be accumulated in the layer volume so its thickness increases. In contrast, the high centrifugal force by spin-coating causes the film thickness to be lower because it expels most of the unbounded polymer molecules.

The surface topology depending on the PEMs formulation was investigated by means of AFM (Figure 8).

The results clearly showed that the roughness of the spin-coating formulated PEMs is much smaller in comparison with that of PEMs made by dippings. The flat and clearly separated interfaces between the layers suggest the lack of interpenetration in the case of spin-coating. On the contrary, the surface topology of dipped PEMs consists of rough patterns, indicating loose interpenetrating structures.

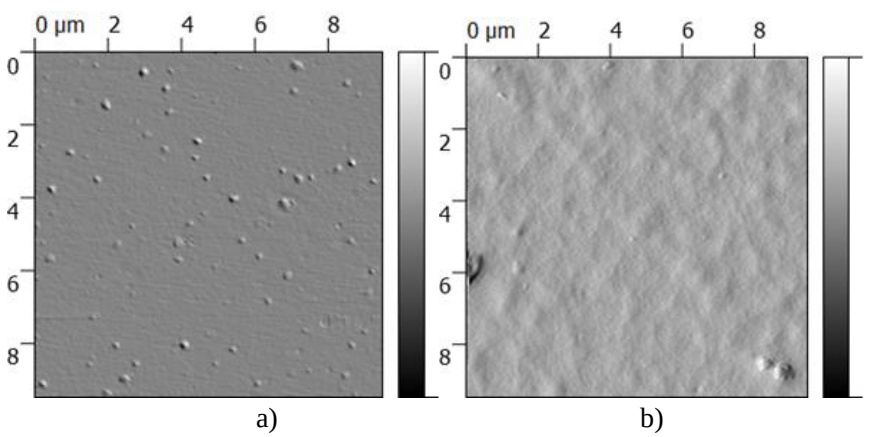


Figure 8. AFM images of spin-coated a) and dipcoated b) multilayered films (chitosan-xanthan) with 20 layers on PLA substrates.

## 2.3. Effect of pH and Ionic Strength on the PEMs Structure

The structure and surface topography of PEMs are among the main factors crucial for their application as drug delivery systems for buccal administration. They determine the depth of drug immobilization in the volume, the drug diffusion kinetics and hence the rate of release. The surface topography on the other hand is responsible for the adhesion properties of the PECs on the buccal mucosa.

Some of the most important parameters affecting the PECs thickness and structure are the ionic strength of the polyelectrolyte solutions, from which the multilayers are built [38, 39].

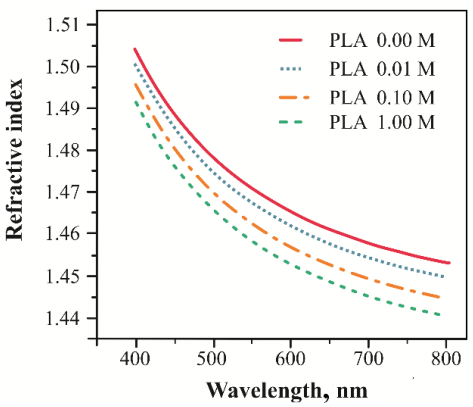


Figure 9. Dispersion curves chitosan/xanthan PEMs on pre-charged PLA substrate, prepared from solution with different ionic strength, given in the plot.

**Table 1. Nitrogen atomic concentration on the surface of chitosan/xanthan PEM on pre-charged PLA substrate at different ionic strength**

| Ionic strength, mol/L | 0.00 | 0.01 | 0.10 | 1.00 |
|---|---|---|---|---|
| N atom. concentration, % | 2.13 | 2.36 | 2.29 | 0.38 |

In this respect, chitosan/xanthan PEMs on pre-charged PLA substrates, prepared from 1% chitosan and 0.1% xanthan solutions with different ionic strength and pH were examined [40]. The thickness of the layers was estimated as already described above from the (sRI) measurements (Figure 9).

The highest values of the sRI were observed for the PEMs prepared from solution with ionic strength 0.01 mol/L, followed by 0.00 mol/L, 0.10 mol/L and 1.00 mol/L. The observed differences in the sRI could be explained once again by a different amount of adsorbed chitosan and xanthan and the gradual decreased impact of substrate refractive index on the apparent sRI. Therefore, the biggest amount of polyelectrolytes was concluded to be deposited when the ionic strength of the solutions was 0.01 mol/L.

Further investigation of the surface chemical composition was done by X-ray photoelectron spectroscopy (XPS). Nitrogen atomic concentration on the surface, related to the amount of adsorbed chitosan at different ionic strengths of the solutions, is presented in Table 1.

The highest amount of chitosan was deposited when solutions with ionic strength 0.01M and 0.10M were used. A decrease of ionic strength to 0.00 M led to a partial desorption of chitosan due to diminution of the electrostatic screening. The lowest amount of chitosan was deposited at the highest ionic strength 1.00 mol/L.

Increasing the ionic strength above critical value led to the destruction of the adsorbed layers [2]. This phenomenon was explained by an ion-exchange model for polyelectrolyte adsorption. According to it, the process of swelling of the multilayer structures begins with the addition of added salts and the excess charge of the polyelectrolyte can spread evenly over the surface. The swelling effect is also affected by the specific interactions between the oppositely charged polyelectrolytes. If the interactions between the segments are strong, the swelling is obstructed and the thickness of the layer increases slowly. The stronger specific interactions lead to higher stability of the layers to the salts concentration.

As the ionic strength increases, the thickness of the layers and the adsorbed amount of polyelectrolyte grows faster than linear [41]. In addition, the surface of the layers at low ionic strength is mostly smooth with small granules, and becomes very rough at large ionic strengths. Thus, the way the film grows is related to the heterogeneous topography of the film. The last statement is confirmed by the results about the surface roughness of the chitosan/xanthan multilayers (Figure 10 and Table 2).

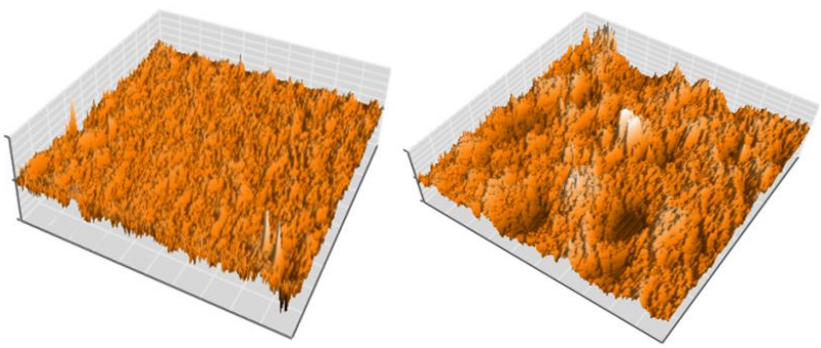

a) b)

Figure 10. Surface morphology of xanthan/chitosan multilayers build-up at ionic strength: a) 0.01mM; b) 1.00M.

**Table2. Roughness of the surfaces of chitosan/xanthan PEM on pre-charged PLA substrate built up from solution with different ionic strength**

| Ionic strength | 0.00M | 0.01M | 0.10M | 1.00M |
|---|---|---|---|---|
| $R_a$, nm | 2.99 | 3.12 | 24.60 | 31.70 |

The multilayers deposited at lower ionic strength solutions were flat and featureless. When multilayers were formed at higher salt concentrations, the surface roughness increased. These results might be explained in terms of a transition from an extended conformation to a more compact form that polyelectrolytes adopt as a function of the solutions' ionic strength [42].

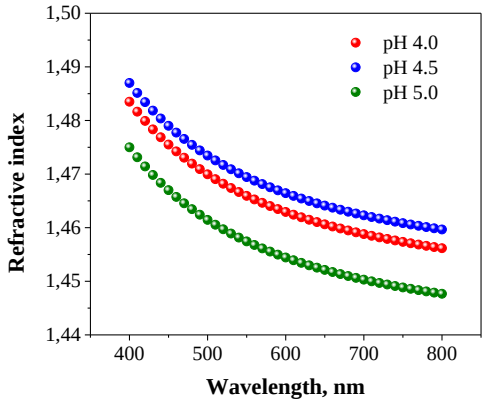


Figure 11. Dispersion curves chitosan/xanthan PEM on pre-charged PLA substrate, prepared from solution with different pH, given in the plot.

**Table 3. Nitrogen atomic concentration on the surface of chitosan/xanthan PEM on pre-charged PLA substrates on the multilayers surfaces at different pH**

| pH | 4.0 | 4.5 | 5.0 |
|---|---|---|---|
| N atom. Concentration % | 1.97 | 2.29 | 1.38 |

In some cases, weak acids and bases (or their salts) are preferred for the design of multilayer films, because it is possible to tune the charge density by changing the solution pH, and hence to control the strength of the electrostatic interactions and the thickness of the adsorbed layers [43]. For these systems, pH has a significant dependence on the polyelectrolyte deposition process.

The sRI of chitosan/xanthan multilayers built at different pH are presented in Figure 11. The highest value of the sRI corresponded to the deposition process at pH 4.5, at which the most compact layer or the adsorption of the biggest amount of polyelectrolytes was observed. The XPS data confirmed this suggestion (Table 3).

The highest amount of chitosan was deposited when the solution had pH 4.5, followed by pH 4.0, and 5.0. Therefore, a conclusion could be made that a pH of 4.5 is optimal pH for xanthan/chitosan deposition process.

Using Katchalsky's theory about the dissociation of weak polyelectrolytes [44], and the information about the $pK_a$ values for chitosan and xanthan [45], the ratios between the protonated amino-groups in the chitosan and the carboxylate ions in the xanthan at different pH were calculated as follows: 1.28 at pH 4, 1.06 at pH 4.5 and 0.90 at pH 5. The nearest 1:1 binding is observed at pH 4.5 where it can be assumed that the most dense network and compact layers were formed.

## 2.4. Physical Properties of PEMs, Swelling, Mechanical Properties

### *2.4.1. Adhesion and Surface Free Energy of PEMs*

As potential medical applications of PEMs are discussed in the present chapter, for drug delivery carriers on buccal mucosa, the adhesive properties become of great importance. In

other words, the surface properties of those systems have to be thoroughly investigated. The mucoadhesion in medicine is usually directly investigated, but the tests require fresh animal mucosa. Instead of that, one may apply preliminary tests involving alternative physical methods such as the method of a small sessile drop. Then after as a later stage, the standard mucoadhesion tests can be limited up to potentially best systems.

In general, the good adhesion in PEMs will be achieved when the contact surface of the drug delivery system possesses high enough surface free energy, $\gamma$. Actually, not only the total values of $\gamma$ matters but the amount of the polar molecules as well, expressed in terms of polarity, *P*.

Small sessile drop, inserted on the solid surface of PEMs, will take a specific shape. The profile of the drop depends on the mutual interactions between all three phases in contact so that the drop rests on the surface displaying particular contact angle, $\theta$. It is defined as the angle between the solid surface and the tangent to the drop at the point of contact [46]. The balance of the surface free energies (tensions) of all three phases in contact, which are the solid surface of the drug delivery system $(s)$, test liquid $(l)$ and the gaseous phase above, which consists of air and the vapor of the test liquid $(g)$ can be described by the Young's equation [47]:

$$\gamma_{lv}\cos\theta = \gamma_{sv} - \gamma_{sl} \tag{3}$$

The surface free energy of any substance, according to Fox, can be represented as a sum of a dispersive $(\gamma^d)$ and polar $(\gamma^p)$ components [47], so that $\gamma = \gamma^p + \gamma^d$ and the polarity is $P = \gamma^p / \gamma$. The dispersive energy summarizes the result of London-van der Waals, Kessom-van der Waals and Lifshitz-van der Waals interactions, whereas the polar part represents the short-range non-dispersive interactions such as hydrogen bonding (acid/base), covalent, metal or ion bonding [48].

There are a number of methods permitting experimental determination of surface free energy, its components, and this way the polarity. For instance that of Owent-Wendt, Zissmann, and Oss-Good-Chaudhury [48-50].

One of the most common experimental methods is that of Owens and Wendt [49], further developed by Kaelble and Uy [51], which ends up with the following dependence:

$$\frac{1+\cos\theta}{2}\frac{\gamma_l}{\sqrt{\gamma_l^d}} = \sqrt{\gamma_s^p}\sqrt{\frac{\gamma_l^p}{\gamma_l^d}} + \sqrt{\gamma_s^d} \tag{4}$$

The analysis of the last equation shows that the dependence $\left[\gamma_l(1+\cos\theta)\right]/\left[2\left(\gamma_l^d\right)^{1/2}\right]$ on $\left(\gamma_l^p/\gamma_l^d\right)^{1/2}$ yields a straight line. By the slope of the linear dependence the values of the polar part of the surface free energy, $\left(\gamma_s^p\right)^{1/2}$ can be extracted whereas from the intercept with the x-axis the dispersive part, $\left(\gamma_s^d\right)^{1/2}$ is obtainable. Gaining the required dependence, at least

two different liquids are demanded, giving different values for $\left(\gamma_l^p / \gamma_l^d\right)^{1/2}$. The most common liquids, polar and non-polar, with their surface free energies values are given in Table 4.

**Table 4. Surface free energy, $\gamma_l$ of different test liquids with its polar, $\gamma_l^p$, and dispersive, $\gamma_l^d$, components [48, 52]**

| Test liquid | $\gamma_l$, mJ/m$^2$ | $\gamma_l^p$, mJ/m$^2$ | $\gamma_l^d$, mJ/m$^2$ |
|---|---|---|---|
| Distilled water | 72.8 | 51.0 | 21.8 |
| Form amide | 58.4 | 26.7 | 31.7 |
| Methylene iodide | 50.8 | 1.3 | 50.8 |
| Ethylene glycol | 48.2 | 16.7 | 31.5 |

The contact angle is experimentally obtainable by inserting a small drop onto the flat solid surface of PEM. The volume drop may vary from 2 up to 10 µl, given the guarantee of no significant gravitational effect is involved. The drops are inserted by means of micro-syringe (*Innovative labor system GMbH, Germany*). For each sample, for the purpose of adequate statistical analysis, at least 5 drops are requested.

The shape and the contact angle can be observed by a commercially available or home-made equipment. A simple set-up can be built employing an USB microscope (*Cs01-200 Digital microscope, Coolingtech, China*) and movable along X-Y plane sample table. The contact angle reading can be done by a special software (ImageJ, *http://imagej.net*), drawing the tangent to the drop in the point of contact with the solid surface. The accuracy of such experiments is of the order of ± 0.01°.

In Figure 12, results for water contact angle onto PEM of chitosan/xanthan onto corona pretreated poly(ε-caprolactone) substrates are shown. They clearly show the $\theta$ dependence on the corona discharge polarity (i.e., the end-layer) and the number of layers (the amount and the polarity of the excess charge). Similar results have been reported by other authors [23, 53].

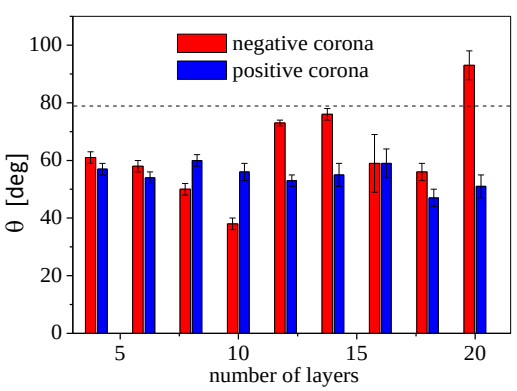


Figure 12. Water contact angle of PEM's of chitosan/xanthan on pretreated in corona discharge poly(ε-caprolactone). The dotted line represents the value for the untreated bare substrate.

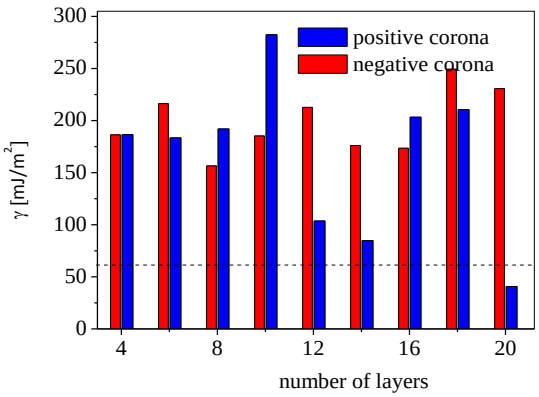


Figure 13. Surface free energy of PEM's of chitosan/xanthan on pretreated in corona discharge poly(ε-caprolactone). Dashed line represents the values of untreated bare substrate.

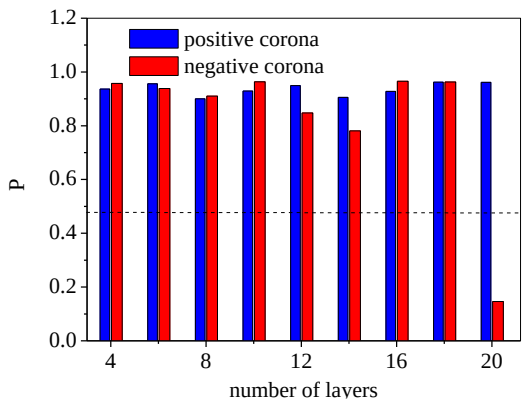


Figure 14. Polarity of PEM's of chitosan/xanthan on pretreated in corona discharge poly(ε-caprolactone). Dashed line represents the value of untreated bare substrate.

For the same PEM's, the surface free energy was determined based on 4 different liquids tests (water, methylene iodide, form amide, ethylene glycol). The results are shown in Figure 13 for the total energy and in Figure 14 the polarity. The results clearly prove the strong dependence of the surface free energy on the end-layer and the positive effect on initial corona discharge pretreatment of the bare substrate. The polarity rises of the expenses of the polar component $\gamma$, which facilitates the adhesion of PEM onto buccal mucosa.

### *2.4.2. Swelling*

Physico-chemical properties of PEMs are extremely important for the overall performance of the structure. Between them swelling is the most closely related to applications as drug delivery systems because it is directly correlated to the permeability of the layers [54]. The swelling behavior of the PEMs depends on both the properties of the films and swelling medium, with substantial swelling observed under certain conditions [55].

The dependence of the total number of layers on the degree of swelling is studied. Such approach has been adopted in the investigation of PEM of poly-L-lysine/

carboxymethylcellulose on PP substrate, pretreated in negative corona discharge, where the swelling was in distilled water [56].

The tests were carried out by dipping the PEMs into the desired solution and leaving the samples until a constant weight is achieved. Ensuing that the deposited layers are stable over the time of swelling, the equilibrium swelling degree is determined as:

$$w = \frac{m - m_0}{m_0} \tag{5}$$

where $m$ is the sample weight at equilibrium swelling and $m_0$ is the weight of the dry sample. The results (Figure 15) show an increase of the degree of swelling with the number of the layers in the specific case of PEMs. It proves the presence of a different number of layers, and correlates with the increasing number of hydrophilic biopolymer molecules. The results also demonstrate the stability of the PEMs in aqueous solutions.

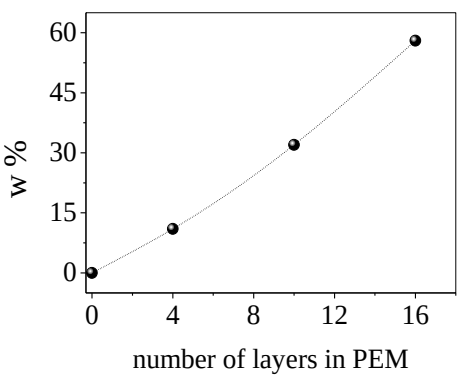


Figure 15. Degree of swelling for PEMof Poly-L-lysine/carboxymethylcellulose on PP substrate, pretreated in negative corona discharge.

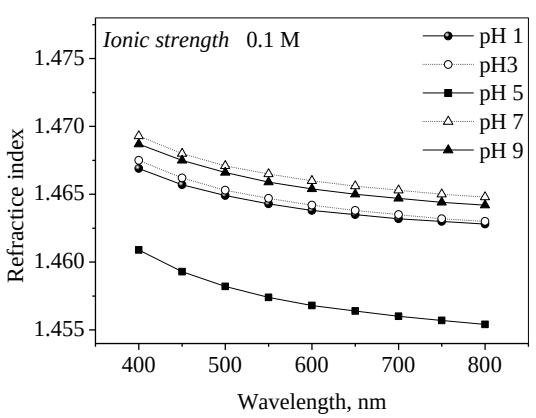


Figure 16. Dispersion of the surface refractive index, $n_s$, of PEM of poly(galacturonic acid)/chitosan onto Poly(DL-lactide) substrate, pretreated in negative corona discharge, at constant ionic strength and different pH for swollen to equilibrium degree samples.

In a number of cases, weak polyelectrolytes are used in the PEMs build-up, and as such their properties in solution are highly sensitive to pH and ionic strength. The internal structure, in combination with the dissociation behavior of the free functional groups within the film, determines the overall swelling behavior of the films. The pH and ionic strength of the swelling medium influence the swelling behavior of the films by affecting the electrostatic forces operating in the hydrated film as well as the dynamics of the ionic cross-links holding the layers together. The control and tuning of the swelling behavior of the multilayer assemblies is important to use these materials in many applications such as controlled release, membrane filtration, and biomaterial coatings.

The influence of pH and ionic strength on the response of poly (galacturonic) acid/chitosan multilayers on corona pretreated polylactic acid substrate was studied by Marudova et al. [57]. The research was done by following the changes in sRI.

In these swelling experiments, a buffer solution of desired pH (1, 3, 5, 7 and 9) and ionic strength (0.001 M, 0.01 M, 0.1 M and 1 M) were used. HCl/KCl, acetate, and phosphate buffers could cover the desired range. The amount of the absorbed water was established by the changes in sRI dependence on the wavelength. As a first step, experiments at fixed pH and varying ionic strength could be performed, followed by a second set, in which the ionic strength was kept constant and pH could be varied. In Figure 16, the results of the surface refractive index for constant values of the ionic strength 0.1 and different pH are given.

The most pronounced swelling is observed at pH 5 and it is attributed to the largest hydrated mass. The higher water adsorption at pH 1 (in comparison to that at pH 3) and at pH 9 (in comparison to that at pH 7), is associated with the formation of more crosslinked structure at these pH that has a reduced tendency to swell [58]. Similar investigations at fixed pH and different ionic strength were also performed [57].

The lower hydration at low ionic strength (0.001 M and 0.010 M) could be attributed to the anti-polyelectrolyte type swelling of a polyampholyte networks. This effect has also been observed for other multilayered structures [59. 60].

### *2.4.3. Mechanical Properties*

The final practical performance of PEMs depends to a great extent on their physico-mechanical properties. The appropriate patient comfort has to be secured. Therefore, the appropriate tests are a necessity in the field of PEMs for drug delivery systems. Results of such tests are given in Figure 17 for dry and hydrated states of PEM of Poly-L-lysine/carboxymethylcellulose on a PP substrate, pretreated in negative corona discharge [56]. The experiments represent a simple extension at a constant deformation rate of 0.1 mm/s (*Stable Microsystems® Texture Analyzer TAXT2i*). The samples (dry film dimensions 10 mm × 4 mm × 0.02 mm) were glued to the metal holders by a cyanoacrylate adhesive. The Young's modulus was determined from a stress-strain curve for deformations less than 3%. According to the results, the PEM improves the mechanical strength in dry as well as in hydrated states [56].

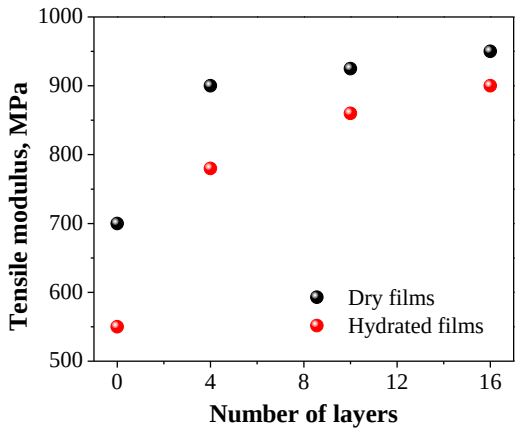


Figure 17. Tensile modulus dependence on the number of layers for PEMof Poly-L-lysine/ carboxymethylcellulose on PP substrate, pretreated in negative corona discharge.

## 2.5. Stability of PEMs at Different Environment Conditions

The multilayer films are non-equilibrium systems, and their structure depends on the method of preparation. The formation of the multilayer is influenced by pH, ionic strength, polymer functionality and polymer concentration. Important structural variables include the extent to which the two polyelectrolytes interpenetrate [61], the extent of crosslinking of individual layers, and the extent of charge compensation of one polymer by another. These structural variables lead to differences in functional behavior, including multilayers stability end environmental response.

On the other hand, the PEMs' stability is of great importance for all of their applications. In the case of pharmaceutical use as drug delivery systems, the most important factors of the environment are pH, ionic strength, and temperature.

As an example to study the PEMs stability, chitosan/pectin multilayers on corona pretreated PLA substrate were chosen.

### *2.5.1. Stability of PEMs at Different Ionic Strength*

A possible approach for characterizing the PEMs stability is investigation of the color reaction between chitosan and ninhydrine [57]. The amount of chitosan is estimated when, after reaching the equilibrium swelling, the multilayers are treated with ninhydrin solutions and the changes in the transmittance at $\lambda = 570$ nm are followed (Figure 18). A normalization towards the substrate value was done. Transmittance was expected to increase in correspondence with dissolving chitosan, depending on the ionic strength of the solution used. The ionic strength governed the rate of the ionic interactions i.e., the polyelectrolyte could be partially dissolved with time, an electrostatic screening effect might appear, and a decrease in hydration ability might be observed [55, 57, 61].

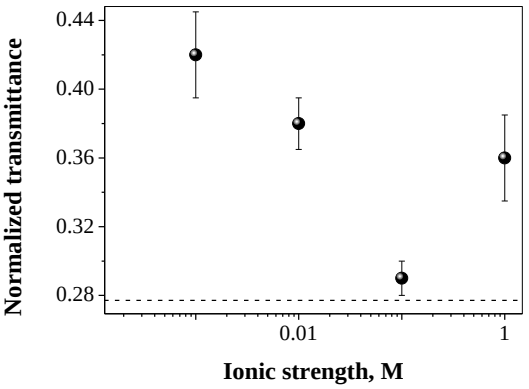


Figure 18. Normalized transmittance with respect to the bare substrate and non-chemically treated at $\lambda = 570$ nm dependence on ionic strength of PEM of Poly(galacturonic) acid/chitosan multilayers deposited onto negative corona pretreated PLA substrate. The samples were treated in 2% ninhydrin solution. The dashed line represent the reference sample value.

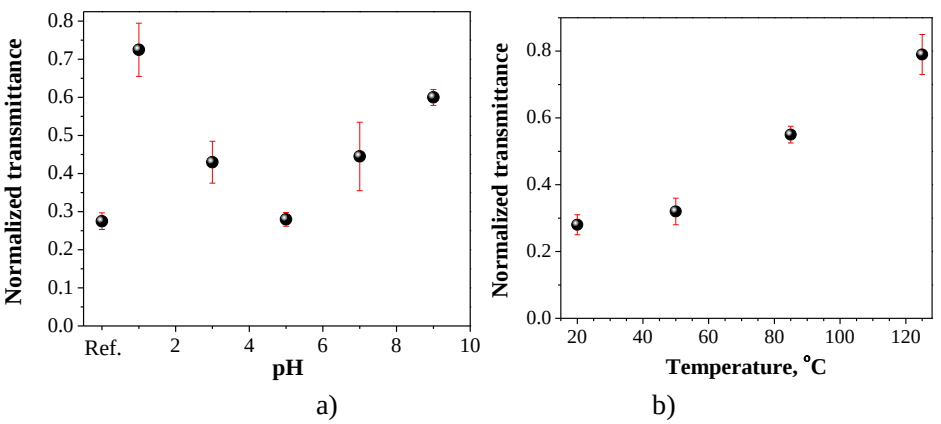


Figure 19. Normalized transmittance at 570 nm of PGA/chitosan multilayers treated with 2% ninhydrin solution dependence on a) pH and b) on temperature.

### *2.5.2. Stability of PEMs at Different pH*

The stability of the multilayers at pH from 1 to 9 was examined again by measuring the transmittance of ninhydrintreated multilayer films – Figure 19a. Normalization of the transmittance towards substrate with outlayers was done. A nonswollen ninhydrintreated sample was used as reference [56].

In the examined ranges, the effect of change in pH on the stability was larger than the effects observed through changing ionic strength. The transmittance at 570 nm increased with the decreasing or the increasing pH (in comparison with pH 5) that was explained with dissolving of chitosan of the multilayers. This behavior was attributed to changes in the charge density of the polyelectrolytes.

Having in mind that the ionization degree of week polyelectrolytes is given by the equations [62]:

$$\alpha\% = \frac{100}{1+10^{(pK_a - pH)}} \text{ (weak acid)} \quad (6)$$

$$\alpha\% = \frac{100}{1+10^{(pH - pK_a)}} \text{ (weak base)} \quad (7)$$

and the values of the dissociation constants pKa for carbohyl groups in PGA (pKa = 3.2) [63] and amino groups in chitosan (pKa = 6.5) [64], the ionization degree of both PGA and chitosan was calculated at different pH. At pH 7 the charge of the chitosan is essentially suppressed (the protonation of the amino group was less than 25%) and the electrostatic interaction between PGA and chitosan was not enough to ensure stable multilayer structure. At pH 3 the ionization of carboxyl groups in PGA was less than 40% and the multilayers were again unstable. The stability of the PGA/chitosan interaction appeared entirely dependent on the electrostatic interactions between PGA and chitosan. The multilayers were most stable at pH 5, where both carboxyl and amino groups were totally charged.

### *2.5.3. Stability of PEMs at Different Temperature*

Thermal behavior of the multilayer films was examined by the transmittance of ninhydrin treated samples (Figure 19b) [56]. The increase of temperature led to the increase in the normalized transmittance at 570 nm, indicating weaker interaction between ninhydrin and amino groups in the chitosan. A possible explanation of this behavior could be the structural rearrangements - at a certain temperature, the polyelectrolyte material softens, thus facilitating any rearrangement [65]. Another possible reason could be converting the–$NH3^{+}$–OOC– salt bonds into amide bonds at 120°C [66]. The samples became more brittle at higher temperatures due to the increased crystallinity of PLLA substrate. At 150°C, the destruction of samples was observed.

## CONCLUSION

The present chapter summarizes an innovative approach of PEMs' deposition onto a preliminary charged (in corona discharge system) polymer substrates.

It was found that the type, structure, and polarity of the substrate influenced the structure and stability of the PEMs. Negatively charged substrates with amorphous and/or porous structures facilitate the deposition process. In these cases, due to structural heterogeneity, the surface charge is more stable and insures irreversible binding of the deposited polyelectrolyte.

In order to optimize the technology of PEMs' formulation, dipping and spin-coating methods for polyelectrolyte deposition were used. In the case of the spin-coating method, flat and clearly separated PEMs were obtained. Films with higher thickness and surface roughness indicating a presence of interpolymer diffusion and interpenetration are constructed with the dip-coating method. The last structures were more appropriate for drug delivery applications of PEMs, as far as the looser structures facilitates higher amount of the drug, at different depths to be immobilized.

Natural weak polyelectrolytes were used in PEMs formulation, for which the degree of ionization depended on the acidity and salt content of the environment. Therefore, the

structure and the properties of PEMs could be regulated very precisely in the context of their application. The PEMs were more stable at pH, which corresponds to the stoichiometric ratio between the negatively and positively charged ionic groups in the deposited polyelectrolytes. The ionic strength was responsible for the screening effect of the low molecular salt. As the ionic strength increased, the PEMs roughness increased. This result is associated with various conformational states of the polyelectrolyte molecules. The PEMs were more stable at ionic strengths between 0.1 mol/l and 1.0 mol/l, when repulsive interactions between charges were screened. The PEMs were stable up to temperatures of about 50°C, which determined their potential use as drug delivery systems.

## ACKNOWLEDGMENT

This study was funded by Bulgarian National Scientific Fund, Project No DFNI B-02/7.

## REFERENCES

[1] Decher, Gero. “Fuzzy nanoassemblies: toward layered polymeric multi-composites.” *Science* 277, no. 5330 (1997): 1232-1237.

[2] Borges, Joao, and Joao F. Mano. “Molecular interactions driving the layer-by-layer assembly of multilayers.” *Chemical Reviews* 114, no. 18 (2014): 8883-8942.

[3] Ariga, Katsuhiko, Yusuke Yamauchi, Gaulthier Rydzek, Qingmin Ji, Yusuke Yonamine, Kevin C. W. Wu, and Jonathan P. Hill. “Layer-by-layer nano architectonics: invention, innovation, and evolution.” *Chemistry Letters* 43, no. 1 (2013): 36-68.

[4] Ariga, Katsuhiko, Jonathan P. Hill, and Qingmin Ji. “Layer-by-layer assembly as a versatile bottom-up nanofabrication technique for exploratory research and realistic application.” *Physical Chemistry Chemical Physics* 9, no. 19 (2007): 2319-2340.

[5] Volodkin, Dmitry, and Regine von Klitzing. “Competing mechanisms in polyelectrolyte multilayer formation and swelling: Polycation–polyanion pairing vs. polyelectrolyte–ion pairing.” *Current Opinion in Colloid & Interface Science* 19, no. 1 (2014): 25-31.

[6] Castelnovo, M., & Joanny, J. F., (2000), Formation of Polyelectrolyte Multilayers, *Langmuir*, 16: 7524-7532.

[7] Abu-Sharkh B. “Structure and mechanism of the deposition of multilayers of polyelectrolytes and nanoparticles.” *Langmuir.* 2006 Mar 28;22(7):3028-34.

[8] Jomaa, Houssam W., and Joseph B. Schlenoff. “Salt-induced polyelectrolyte inter diffusion in multilayered films: A neutron reflectivity study.” *Macromolecules* 38, no. 20 (2005): 8473-8480.

[9] Decher, Gero. “Layer- by- layer assembly (putting molecules to work).” Multilayer Thin Films: *Sequential Assembly of Nanocomposite Materials*, Second Edition (2012): 1-21.

[10] Lavalle, Ph., Gergely, C., Cuisinier, F. J. G., Decher, G., Schaaf, P., Voegel, J. C., and Picart, C. (2002), Comparison of the Structure of Polyelectrolyte Multilayer Films Exhibiting a Linear and an Exponential Growth Regime: An in Situ Atomic Force Microscopy Study, *Macromolecules*, 35 (11): 4458-4465.

[11] Wong, Ieong, and Chih-Ming Ho. "Surface molecular property modifications for poly (dimethylsiloxane) (PDMS) based microfluidic devices." *Microfluidics and Nanofluidics* 7, no. 3 (2009): 291.

[12] Trimukhe, Ajinkya M., Krishnasamy N. Pandiyaraj, AnujTripathi, Jose SavioMelo, and Rajendra R. Deshmukh. "Plasma Surface Modification of Biomaterials for Biomedical Applications." In *Advances in Biomaterials for Biomedical Applications*, pp. 95-166. Springer Singapore, 2017.

[13] McCarty, Logan S., Adam Winkleman, and George M. Whitesides. "Electrostatic Self- Assembly of Polystyrene Microspheres by Using Chemically Directed Contact Electrification." *Angewandte Chemie International Edition* 46, no. 1- 2 (2007): 206-209.

[14] Pan, Pengju, Lili Han, Jianna Bao, Qing Xie, Guorong Shan, and Yongzhong Bao. "Competitive stereocomplexation, homocrystallization, and polymorphic crystalline transition in poly (L-lactic acid)/poly (D-lactic acid) racemic blends: molecular weight effects." *The Journal of Physical Chemistry* B 119, no. 21 (2015): 6462-6470.

[15] Pitt, Colin G., A. Robert Jeffcoat, Ruth A. Zweidinger, and Anton Schindler. "Sustained drug delivery systems. I. The permeability of poly(ε- caprolactone), poly (DL- lactic acid), and their copolymers." *Journal of Biomedical Materials Research Part A* 13, no. 3 (1979): 497-507.

[16] Yovcheva T., M. Marudova, A. Viraneva, E. Gencheva, I. Vlaeva, S. Sainov, G. Mekishev, "Pectin/chitosan multilayers on different poly-lactide substrates," *Journal of Nanostructured Polymers and Nanocomposites*, 5 (3), 2009, 55-59.

[17] Bigucci, F., B. Luppi, T. Cerchiara, M. Sorrenti, G. Bettinetti, L. Rodriguez, and V. Zecchi. "Chitosan/pectin polyelectrolyte complexes: selection of suitable preparative conditions for colon-specific delivery of vancomycin." *European Journal of Pharmaceutical Sciences* 35, no. 5 (2008): 435-441.

[18] Sainov, S., Sarov, Y. and Kurtev, S., "Wide-spectral range laser refractometer", *Appl. Opt.*, 42/13, (2003), 2327.

[19] Garlotta, Donald. "A literature review of poly (lactic acid)." *Journal of Polymers and the Environmen*t 9, no. 2 (2001): 63-84.

[20] Panchev I., Nikolova K., Sainov S. "Laser Refractometry of Edible films." *Proc. SPIE* 5449: (2007)35-40.

[21] K. Nikolova, I. Panchev, S. Sainov, "Optical characteristics of biopolymer films from pectin and gelatin," *Journal of Optoelectronics and Advanced Materials*, vol. 7, No. 3, 2005, pp. 1439-1444.

[22] Gencheva, E. A., T. A. Yovcheva, M. G. Marudova, A. P. Viraneva, I. P. Bodurov, G. A. Mekishev, and S. H. Sainov. "Formation and Investigation of Corona Charged Films

from Polylactic Acid." In *AIP Conference Proceedings*, vol. 1203, no. 1, pp. 495-500. AIP, 2010.

[23] Kolasińska, Marta, and Piotr Warszyński. "The effect of nature of polyions and treatment after deposition on wetting characteristics of polyelectrolyte multilayers." *Applied surface science* 252, no. 3 (2005): 759-765.

[24] Yovcheva, T. A., M. G. Marudova, A. P. Viraneva, E. A. Gencheva, G. A. Mekishev, and S. H. Sainov. "Investigation of Pectin/Chitosan Multilayers Build- up on Corona Charged Polylactide Substrates." In *AIP Conference Proceedings*, vol. 1203, no. 1, pp. 979-984. AIP, 2010.

[25] Pegau, W. S., and J. Ronald Zaneveld. "*Temperature-dependent absorption of water in the red and near-infrared portions of the spectrum*." (1993).

[26] Yovcheva, T. A., M. G. Marudova, A. P. Viraneva, S. I. Sotirov, S. H. Rusev, I. P. Bodurov, B. A. Pilicheva et al. "Various corona treated biopolymer substrates for the deposition of polyelectrolyte multilayers." In *AIP Conference Proceedings*, vol. 1722, no. 1, p. 220026. AIP Publishing, 2016.

[27] Sessler, Gerhard M. "Electrets: recent developments." *Journal of Electrostatics* 51 (2001): 137-145.

[28] Mok, Michelle M., KannanSeshadri, Moses M. David, Seth M. Kirk, and Daniel Carvajal. "*Asymmetric articles with a porous substrate and a polymeric coating extending into the substrate and methods of making the same*." U.S. Patent Application 15/319,111, filed June 30, 2015.

[29] Lvov, Y., Decher, G. *Cryst. Rep*. 1994, 39, 628.

[30] Lee, Seung-Sub, Jong-Dal Hong, Chang Hwan Kim, Kwan Kim, JaPil Koo, and Ki-Bong Lee. "Layer-by-layer deposited multilayer assemblies of ionene-type polyelectrolytes based on the spin-coating method." *Macromolecules* 34, no. 16 (2001): 5358-5360.

[31] Bodurov, I., I. Vlaeva, G. Exner, Y. Uzunova, S. Russev, B. Pilicheva, A. Viraneva et al. "Investigation of multilayered polyelectrolyte thin films by means of refractive index measurements, FT-IR spectroscopy and SEM." In *Journal of Physics: Conference Series*, *vol. 682*, no. 1, p. 012026. IOP Publishing, 2016.

[32] Singh J 2006, *Optical Properties of Condensed Matter and Applications* (Berlin: Wiley–VCH).

[33] Yovcheva T, Sainov S, Meksihev G. (2007) Corona-charged polypropylene films investigated by a laser refractometer. *J Optoelectron Adv Mater* 9: 2087-2090.

[34] Azofeifa, Daniel E., Humberto J. Arguedas, and William E. Vargas. "Optical properties of chitin and chitosan biopolymers with application to structural color analysis." *Optical Materials* 35, no. 2 (2012): 175-183.

[35] Lee Y. M., Park DK, Choe W. S., Cho S. M., Han G. Y., Park J. Y., Pil J. "Spin-Assembled Layer-by-Layer Films of Weakly Charged Polyelectrolyte Multilayer." *Journal of Nanoscience and Nanotechnology* 9: (2009)7467-7472.

[36] Wu, Shao-Jung, Trong-Ming Don, Cheng-Wei Lin, and Fwu-Long Mi. "Delivery of berberine using chitosan/fucoidan-taurine conjugate nanoparticles for treatment of

defective intestinal epithelial tight junction barrier." *Marine Drugs* 12, no. 11 (2014): 5677-5697.

[37] Oprea, Ana-Maria, Manuela-Tatiana Nistor, LenutaProfire, Marcel IonelPopa, Catalina Elena Lupusoru, and Cornelia Vasile. "Evaluation of the controlled release ability of theophylline from xanthan/chondroitin sulfate hydrogels." *Journal of Biomaterials and Nanobiotechnology* 4, no. 2 (2013): 123-131.

[38] Tang, Kan, and Nicolaas A. M. Besseling. "Formation of polyelectrolyte multilayers: ionic strengths and growth regimes." *Soft Matter* 12, no. 4 (2016): 1032-1040.

[39] Selin, Victor, John Ankner, and Svetlana Sukhishvili. "Effects of drying and ionic strength on non-linear growth of polyelectrolyte multilayers." *Bulletin of the American Physical Society* 62 (2017).

[40] Viraneva, A., M. Marudova, S. Sotirov, I. Bodurov, B. Pilicheva, Y. Uzunova, G. Exner, Ts. Grancharova, I. Vlaeva, and T. Yovcheva. "Deposition of polyelectrolyte multilayer films made from chitosan and xanthan on biodegradable substrate: Effect of pH and ionic strength." In *AIP Conference Proceedings*, vol. 1722, no. 1, p. 220025. AIP Publishing, 2016.

[41] Ge, Aimin, Michiya Matsusaki, Lin Qiao, Mitsuru Akashi, and Shen Ye. "Salt effects on surface structures of polyelectrolyte multilayers (PEMs) investigated by vibrational sum frequency generation (SFG) spectroscopy." *Langmuir* 32, no. 16 (2016): 3803-3810.

[42] McAloney, Richard A., Mark Sinyor, Vyacheslav Dudnik, and M. Cynthia Goh. "Atomic force microscopy studies of salt effects on polyelectrolyte multilayer film morphology." *Langmuir* 17, no. 21 (2001): 6655-6663.

[43] Shiratori, Seimei S., and Michael F. Rubner. "pH-dependent thickness behavior of sequentially adsorbed layers of weak polyelectrolytes." *Macromolecules* 33, no. 11 (2000): 4213-4219.

[44] Lifson, S., and Katchalsky. A. (1954), "The electrostatic free energy of polyelectrolyte solutions. II. Fully stretched macromolecules." *J. Polym. Sci*. 13: 43-55.

[45] Argin-Soysal, Sanem, Peter Kofinas, and Y. Martin Lo. "Effect of complexation conditions on xanthan–chitosan polyelectrolyte complex gels." *Food Hydrocolloids* 23, no. 1 (2009): 202-209.

[46] Vlaeva I., Yovcheva T., Viraneva A., Kitova S., Exner G., Guzhova A., Galikhanov M., Contact angle analysis of corona treated polypropylene films, *Journal of Physics: Conference Series*, 2012, 398, art. No. 012054 (6pp).

[47] MatijevicE. Ed. (1969) *Surface and colloid science*, vol. 2. Wiley –Interscience, New York- London- Sydney- Toronto.

[48] Baldan A. *International Journal of Adhesion & Adhesives* 38 (2012) 95–116 Adhesion phenomena in bonded joints.

[49] Owens D., Wendt R. (1969) Estimation of the surface free energy of polymers. *J. Appl. Polym. Sci.* 13 1741-1747.

[50] Kabza K., Gestwizki J., McGrath J. L., *J. Chem. Edu*. 77(1) 63-65 (2000) Contact angle goniometry as a tool for surface tension measurements of solids, using Zisman plot method.

[51] Kaelble D. H., Uy C., *J. Adhesion 2* (1970) 50, A Reinterpretation of Organic Liquid-Polytetrafluoroethylene Surface Interactions.

[52] Skurtys O., Velásquez P., Henriques O., Matiacevich S., Enrione J., Osorio F.(2011) Wetting behavior of chitosan solutions on blueberry epicarp with or without epicuticular waxes. *LWT-Food Sci. Technol*. 44 1449-1457.

[53] Wong J. E., Rehfeldt F., Hänni P., Tanaka M., Klitying R. "Swelling behavior of polyelectrolyte multilayers in saturated water vapor." *Macromolecules* (2004), 37, 7285-7289.

[54] Miller, Matthew D., and Merlin L. Bruening. "Correlation of the swelling and permeability of polyelectrolyte multilayer films." *Chemistry of Materials* 17, no. 21 (2005): 5375-5381.

[55] Burke, Susan E., and Christopher J. Barrett. "Swelling behavior of hyaluronic acid/ polyallylamine hydrochloride multilayer films." *Biomacromolecules* 6, no. 3 (2005): 1419-1428.

[56] Marudova M., T. Yovcheva, R. Todorova, G. Zsivanovits, E. Vozary, A. Viraneva, I. Vlaeva, E. Gencheva, G. Mekishev. "Poly-L-lysine/carboxymethylcellulose multilayers on corona treated polypropylene substrates", *Journal of Optoelectronics and Advanced Materials* 11(10), 2009, 1424 – 1427.

[57] Marudova M., T. Yovcheva, A. Viraneva, E. Gencheva, I. Vlaeva, S. Sainov, G. Mekishev, "Influence of the environmental conditions on the response and stability of poly(galacturonic) acid/chitosan multilayers on biodegradable films," *Journal Of Nanostructured Polymers And Nanocomposites*, 2009, 5/3 60-65.

[58] Moffat, J., Noel, T., Parker, R., Wellner, N. and Ring, S., "The environmental response and stability of PGA and poly-L-lysine multilayers," *Carbohydrate Polymers,* 70 (2007), 422-429.

[59] Dubas, S. and Schlenoff, J., "Swelling and smoothing of polyelectrolyte multilayers by salt," *Langmuir*, 17 (2001), 7725–7727.

[60] Ming G, Gawel K., Stokke B. T. (2014) Polyelectrolyte and antipolyelectrolyte effects in swelling of polyampholyte and polyzwitterionic charge balanced and charge offset hydrogels, *European Polymer Journal* 53, 65-74.

[61] Schlenoff, J. B. and Dubas, S. T., "Mechanism of polyelectrolyte multilayer growth: charge overcompensation and distribution," *Macromolecules*, 34 (2001), 592–598.

[62] Nalwa, H. S., *Handbook of Polyelectrolytes and Their Applications*, American Scientific Publishers, 2003.

[63] Dumitriu, S., *Polysaccharides: Structural Diversity and Functional Versatility*, CRC; 2 edition, 2004.

[64] Jolles, P., Muzzarelli, R. A. A., *Chitin and Chitinases* (ExperientiaSupplementum), Birkhäuser Basel; 1 edition, 2004.

[65] Bernabé P., Peniche C., Argüelles-Monal W., Swelling behavior of chitosan/PGA polyelectrolyte complex membranes. Effect of thermal cross-linking, *Polymer Bulletin*, 55/5 (2005), 367-375.

[66] Kohler K., Shchukin Dg., Mohwald H., Sukhorukov, Gb., Thermal behavior of polyelectrolyte multilayer microcapsules. The effect of odd and even layer number, *J. Phys. Chem. B*, 109/39 (2005), 18250-18259.

In: Advances in Polymers for Biomedical Applications ISBN: 978-1-53613-612-8
Editors: Deepak Pathania and Bhuvanesh Gupta 

*Chapter 2*

# POLYMER GRAFTED SMART MESOPOROUS SILICA NANOPARTICLES: CHALLENGES AND ADVANCES IN CONTROLLED DRUG DELIVERY APPLICATIONS

***Manohar V. Badiger** and Neha Tiwari***
Polymer Science and Engineering Division,
CSIR - National Chemical Laboratory, Pune, India

## ABSTRACT

The application of nanoparticles to intracellular drug delivery has attracted increasing attention in the last few decades. Among them, mesoporous silica nanoparticles (MSNs) have emerged as promising nanomaterials which have shown great potential towards incubation of both hydrophobic and hydrophilic drugs and their further internalization at the targeted site in physiological environment for the treatment of large number of diseases. Excellent properties of MSNs such as good stability control over morphology and tunable particle size and the pore structure gives them an edge over other organic or inorganic based nanoparticles. With these properties, there is a great scope in designing novel MSNs with functionalization at the surface as well as within the pores using biocompatible and biodegradable polymers, stimuli responsive groups, proteins etc. MSNs have shown great potential in biotechnological and biomedical applications. Efforts are also made to increase the biocompatibility and circulation time of drug loaded MSNs by coating various polymers onto the surface of MSNs. Extensive work on MSNs has been reported in the literature which is however scattered. In the present chapter, we have dealt with the advances made in MSNs as controlled and targeted drug delivery systems using either synthetic or natural polymers specifically towards cancer treatment.

**Keywords:** mesoporous silica nanoparticles (MSNs), targeted drug delivery, cancer cells, polymers

*Corresponding Author Email: mv.badiger@ncl.res.in.

## 1. INTRODUCTION

Cancer has become one of the major causes of death worldwide and more than 13 million cancer deaths are predicted in 2030 by World health organization (WHO) [1]. Chemotherapy is a widely accepted treatment for cancer wherein high dosages of chemotherapeutic agents are used. This is unfortunately associated with major side effects like insufficient drug concentrations at the tumor site and toxicity to the healthy cells along with cancer cells [2]. Alternately, controlled drug delivery systems at the targeted site are gaining importance in cancer treatment. The major challenge however is to limit the dosage of drugs at the targeted site with minimal side effects [3]. In this context, as quoted by physicist Richard Feynman, "There is plenty of room at the bottom"; Nanotechnology has emerged as one of the key solutions to overcome the above mentioned drawbacks. Nanoparticles with extremely high surface to volume ratio and possibility of making in different sizes and shapes can be utilized for the encapsulation of both hydrophilic and hydrophobic drugs with enhanced drug bioavailability as well as least damage to the normal cells [4, 5]. Over the past few decades, several nanomaterials have been explored as drug delivery systems (DDS) in *in-vivo* conditions. For an efficient nanomaterial based DDS, nanomaterials must fulfill the following requirements [6, 7]:

1) Biocompatibility
2) High loading of drug molecules
3) Zero premature release before reaching targeted site
4) Efficient cellular uptake
5) Site specificity
6) Control release of drug molecules over a desired period of time

Keeping in mind the above mentioned requirements, a few nanocarriers explored for drug delivery applications are liposomes [8, 9], dendrimers [10, 11], polymeric micelles[12-14], carbon nanotubes [15, 16] and inorganic nanoparticles [17-19] as shown in Figure1. Amongst them, Mesoporous silica nanoparticles (MSNs) have attracted much attention due to their inherent properties like high surface area (>900 $m^2/g$), tunable particle (50-300 nm) and pore size (2-6 nm), pore volume (>0.9 $cm^3/g$), control over the morphology (spheres, ellipsoid, rods and tubes), high stability (resistant to heat, pH, mechanical stress and enzymatic induces hydrolysis) and biocompatibility [6] (Figure 2). MSNs (MCM-41) with ordered pore structure were first synthesized by a group of scientists in Mobil Corporation in 1992. MSNs initially found their wide range of applications in catalysis, adsorption, optics, photochemistry etc. [21]. Although MSNs have been synthesized in early 90s, Vallet-Regi et al. published their first report in 2001 on the MSNs as drug delivery systems. They successfully showed 30 wt% loading of Ibuprofen, an analgesic and anti-inflammatory drug in MSN followed by their release [22]. Later, large number of reports appeared in the literature and showed the immense potential of MSNs in drugs delivery [7, 23, 24], biosensors [25, 26] and gene transfection applications [12, 6]. The highly porous structure of MSNs helps in the loading of large amount of drug molecules and thus minimum amount of carrier is needed for the

delivery of sufficient quantity of drug. The functionalization of the outer surface of MSNs with various organic molecules, polymers, nanoparticles helps in preventing the drug molecules inside the pores from enzymatic degradation or premature release due to diffusion before reaching the cancer site. The surface functionalization of MSNs with various synthetic and natural polymers will be discussed in the later sections. Along with the control over the drug release, another factor that needs to be taken into consideration is the targeted delivery of these nanoparticles at the specific cancer site without affecting the healthy cells. According to the previous studies, it is revealed that MSNs tend to accumulate inside the cancer cells more effectively than normal cells due to Enhanced Permeability and Retention (EPR) effect [27, 28]. Further, various stimuli responsive systems with zero premature release were designed using MSNs wherein the release is triggered by external stimuli like temperature [29-31], pH [32-34], redox [35-37], magnetic field [38, 39] and electric field [40, 41], light [42, 43] and enzymatic action [44-46]. These stimuli will be discussed in detail in later sections taking examples from the literature. Various stimuli responsive polymers (both natural and synthetic) have been explored in the last few decades that not only helps to encapsulate drug molecules inside the porous structure but also incorporate stimuli responsiveness to the nanocarriers which ensures least damage to the healthy cells.

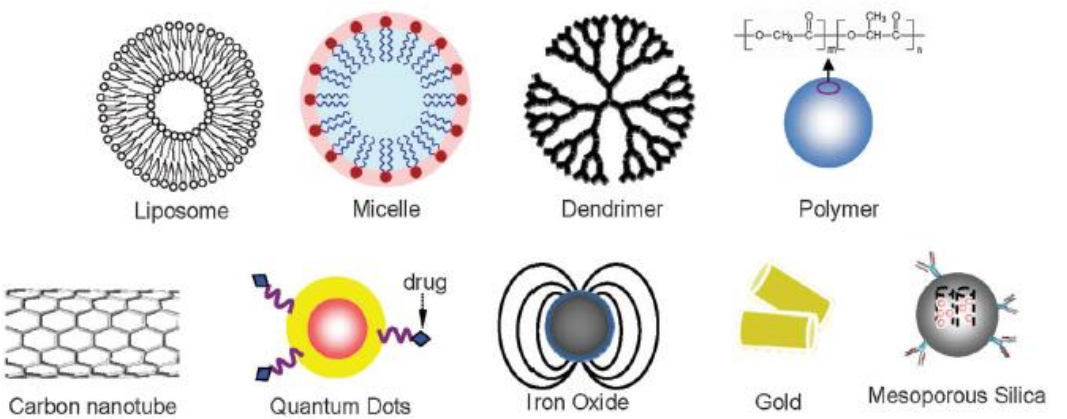


Figure 1. Different carrier systems used as release vehicles for smart drug delivery (Figure is adapted from Ref.[20] with permission of Royal Society of Chemistry).

In the present chapter, we have focused on the synthesis, modification, biocompatibility and applications of MSNs for intracellular drug delivery applications. We have taken information from the extensive literature search we made on the above subject and also included some of our own work in this area. We have summarized the recent strategies designed by various research groups to target cancer cells using MSN-polymer hybrid nanocarriers. Finally, we have discussed the work on the enhanced internalization and drug delivery in cancer cells by modification of the MSN surface with natural polysaccharide, carboxymethyl cellulose carried out in our laboratory.

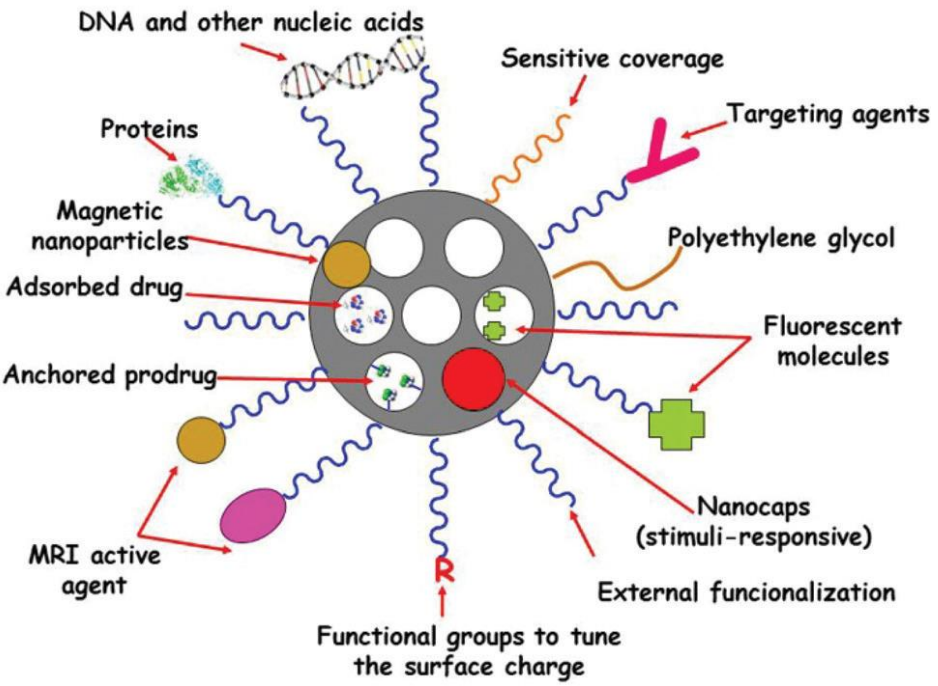


Figure 2. Mesoporous silica nanoparticles as nanomedical multifunctional nanoplatforms (Figure is adapted from Ref.[47] with permission of Royal Society of Chemistry).

## 2. Synthesis of Mesoporous Silica Nanoparticles

Mesoporous Silica Nanoparticles (MSNs) with different particle sizes, pore sizes and morphology was first reported in 1992 by scientists at Mobil Corporation, USA. The design of MSNs such as MCM-41, MCM-48 and SBA-15 was achieved using surfactants as structure directing agents [48]. Several reviews have appeared in the literature on the detailed synthesis of different kinds of MSNs [49, 50]. Amongst many MSNs, MCM-41 is most extensively explored forbiomedical applications owing to its size and shape which is most suitable for intracellular uptake [51]. It is synthesized using Cetyltrialkyl ammonium bromide (CTAB) surfactant as a structure directing agent, tetraethyl orthosilicate (TEOS) as silica precursor and alkali as a catalyst using sol-gel method [52, 49]. A base catalyzed sol-gel process is most extensively employed to produce nanoparticles by means of hydrolysis and condensation reaction as shown below [53]:

Hydrolysis: $OH^- + Si(OR)_4 \rightarrow Si(OR)_3OH + RO^-$
Condensation: $SiO^- + Si(OH)_4 \rightarrow Si\text{-}O\text{-}Si + OH^-$

The pathway for MSN synthesis is given in Scheme 1. In the synthesis, CTAB with hydrophilic head groups and long hydrophobic organic tails self assemble in water to form complex structures above a critical association concentration (CAC). The surfactant molecules adopt different self assembled structures depending on the solution composition and concentration. Around the polar head region of the micelles, silica condenses in the

presence of alkali as a catalyst and form assemblies of desired morphology and size. The surfactant can then be removed to obtain ordered hexagonal arrangement of pores in MSNs.

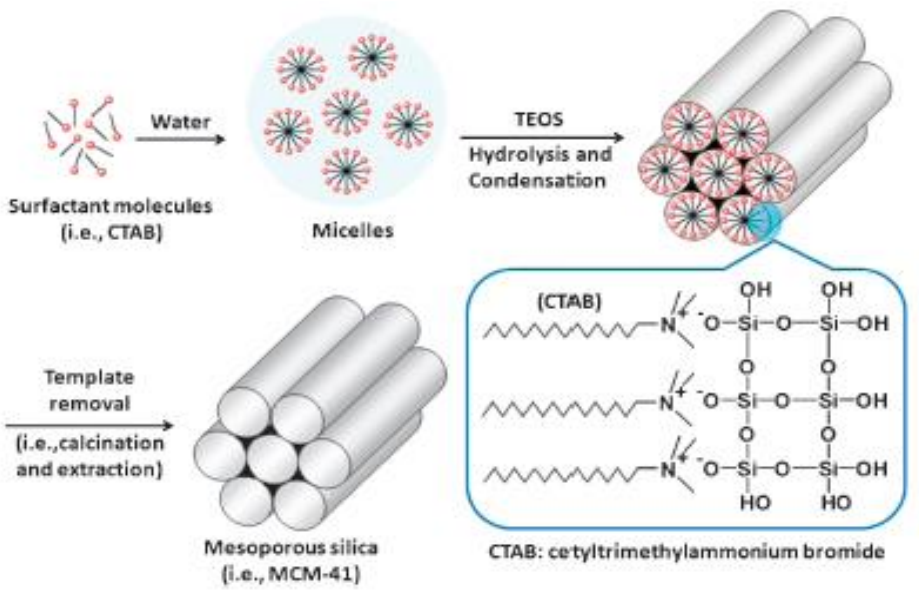


Scheme 1. Synthesis of Mesoporous Silica nanoparticles (MSNs) for drug delivery (Scheme is adapted from Ref.[54] with permission of Royal Society of Chemistry).

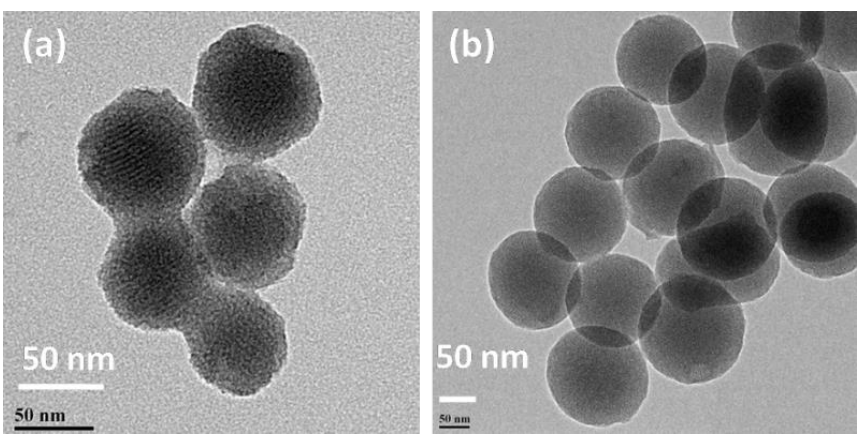


Figure 3. Transmission electron microscopy images of MSNs with different particle size a) 50 nm [58] and b) 100 nm [59].

A precise control over the size, shape, pore size and pore geometry is very important in biomedical applications. The pore size and the geometry of MSNs can be tuned by varying the surfactant templates, pH [55] and addition of organic co solvents [56]. Further, the particle size and morphology can be affected by varying the molar ratios of silica precursors, and surfactants, base catalysts and addition of co-solvents [57]. Figure 3 shows three different MSNs with varying particle sizes and pore diameter.

## 3. Surface Functionalization of Mesoporous Silica Nanoparticles

The isoelectric point of MSN is ~2.0 and thus pure MSNs remain negatively charged under physiological pH of ~7.4 or under malignant tumors <7.0. Thus, tuning the external surface of MSNs is necessary with appropriate functional groups for their application in DDS. The surface modification of MSNs with organic functional groups like alkyl, thiol, amino, cyano, allyl, alkoxy etc. provides increased versatility to MSNs. The surface modification can be successfully carried out using two widely used methods: i) co-condensation [60, 61] and ii) grafting (post synthesis) [62-64, 50]. Figure 4 represents the pictorial representation of co-condensation and post-synthetic grafting methods. In co-condensation method, silica precursor is hydrolytically condensed together with organosilanes in one pot synthesis. Co-condensation is associated with short preparation time and uniform distribution of organic moieties. The co-condensing reagents are organo-substituted trialkoxysilanes and their influence on particle morphology depends upon whether their organic groups stabilize or destabilize the micelles during the formation of MSNs [49]. Homogeneous coverage of functional groups on MSN is one of the major advantages associated with co-condensation method of functionalization. Here, the template can be removed by extraction in organic solvents under reflux conditions after synthesis.

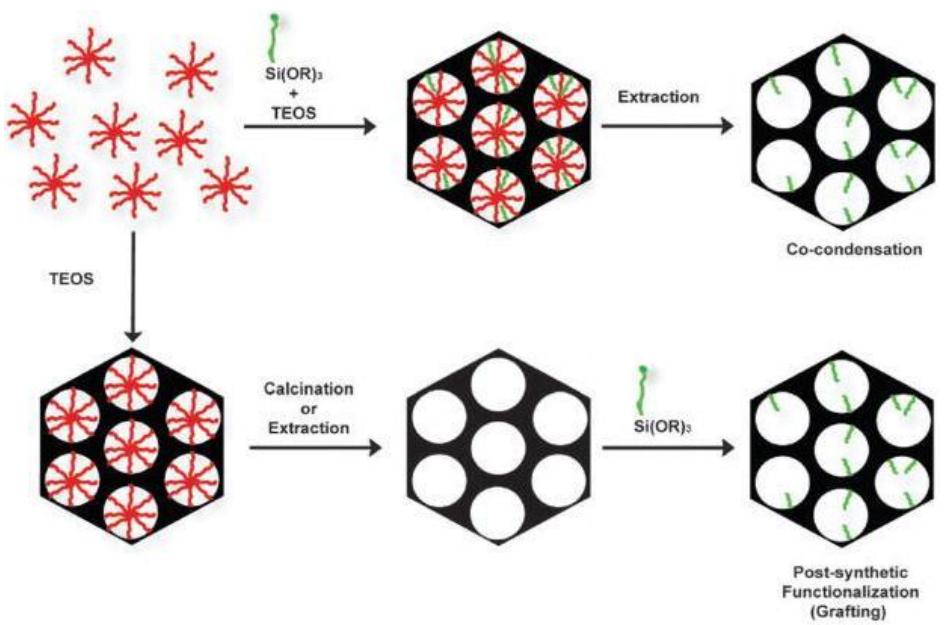


Figure 4. Functionalization of MSNs by co-condensation and post-synthetic method. Green color indicates a trialkoxysilane molecule bearing a functional group and red color shows the structure-directing agent by micelles (Figure adopted from Ref.[65] with permission of Royal Society of Chemistry).

Post synthetic grafting is the most popular method of functionalization wherein functionalization of MSN is performed after its synthesis either before or after the template removal. Grafting is carried out by silylation on free (≡Si-OH) and germinal silanol

(=$Si(OH)_2$) groups. Organic functional groups can be introduced either through covalent or ionic bonding. This method is associated with high surface coverage with functional groups. Various organic molecules and polymers can be used for functionalization of MSN surface [66, 6]. In the post functionalization method, the template can be removed either using calcination (before grafting) or by appropriate extraction in solvent using reflux conditions (after grafting).

## 4. MECHANISM OF CELLULAR UPTAKE OF MSNS

The understanding of pathway of cellular internalization of MSNs is very important for the design of nanoparticles for controlled drug delivery applications. The cellular internalization of MSNs in different cell lines has been reported by various groups [67-70]. The uptake of MSNs is controlled by various factors like size and morphology of the particles, surface functionalization and the interaction between MSNs and cell surface [69-71]. The wide varieties of pathways are mainly divided into two major categories: phagocytosis and pinocytosis (macropinocitosis and endocytosis) [72, 73]. The cells use either of these pathways for internalization depending on the size of the particles. For instance, micro scale particles (>1μm) are internalized via phagocytosis whereas, smaller particles (<200-300 nm) like MSNs are mostly internalized through endocytosis [74-77]. Some of the endocytotic pathways studied are: clathrin dependent, calveolin dependent, receptor-mediated and clathrin and calveolin independent endocytosis [78, 79]. Depending on the functionality present on the surface of MSNs, the nanoparticles follow one of the endocytotic pathways as shown in Figure 5. The uptake of MSN via endocytosis was first published by Lin et al. and they demonstrated the application of poly (amidoamine) (PAMAM) dendrimer capping on MSN for intracellular drug/gene delivery in Chinese hamster ovarian (CHO) using TEM. They showed the clear localization of PAMAM-MSNs near subcellular organelles such as mitochondria and Golgi bodies [80]. The energy dependent cellular uptake of MSNs was studied by Zink et al. They showed that uptake of MSNs was higher at 37 °C than at 4 °C which indicates that uptake of MSNs is driven by energy dependent pathway confirming the endocytotic pathway [81]. MSNs after internalization in the cells have to reach cytoplasm to release drug molecules. The understanding of this intracellular trafficking is important to design more efficient drug delivery systems. After the endocytosis of MSNs, it undergoes series of events: MSNs are first transported to primary endosomes and then to sorting endosomes. From sorting endosomes, a fraction of MSNs are thrown back to the cell exterior while the remaining fuse with lysosomes and enter the cytosolic compartment to release the drug molecules [7, 82]. Intracellular trafficking pathway of FITC labeled MSNs was first studied by Lin et al. wherein the confocal microscopy was performed on MSN using endosome marker [68, 83].

## 5. TARGETING CANCER CELLS

When normal cells show abnormal and excessive behavior of growth they become cancer cells. The regulatory circuits like cell proliferation and maintenance in cancer cells are much

different as compared to normal cells. The MSNs have been successfully used to transfer the therapeutic agents selectively at the tumor site without harming the normal cells. The use of MSNs can reduce the high doses of therapeutic agents that are used in the conventional chemotherapy thus preventing other side effects. Two different strategies have been explored for targeting nanoparticles at the tumor site depending on the size and functionality of the MSNs [84] and are described below:

## 5.1. Passive Targeting

The rapid growth of cells in tumor results in high demand of nutrients and oxygen supply compared to that of normal cells. Thus, the cancer cells undergo the process called angiogenesis in which they acquire the ability to form new blood vessels from the surrounding capillaries. This fast growth of new blood vessels is irregular and results in fenestration of the size 200-2000 nm range. Hence, MSNs in the range of 100-200 nm have a tendency to accumulate much more in the cancer cells than normal cells. Also, due to lack of effective lymphatic drainage in tumor, the accumulated nanoparticles remain longer in the tumor tissue without being cleared by the immune system. This phenomenon is called as Enhanced Permeability and Retention (EPR) effect [85] and was first reported by Matsumura and Maeda in 1986. They showed that macromolecules greater than 50 kDa has a tendency to preferentially enter the tumor interstitium and remain there for an extended period of time [86]. The pictorial representation of EPR effect is shown in Figure 5.

For successful passive targeting, enhanced circulation time of the nanoparticles in the physiological environment and the ability to overcome biological barriers, the particle size of MSNs must be more than 50 nm (in order to keep inherent mesoporosity and to avoid renal clearance) and less than 300 nm (in order to diffuse at the tumor site in sufficient amounts) [87]. Also, surface modification of MSNs to increase the circulation time in order to ensure tumor accumulation is another important factor as it helps to avoid rapid clearance of MSNs from Reticuloendothelial system (RES). Various studies have shown that surface modification of MSNs with hydrophilic polymers like polyethyeleglycol (PEG) helps in increasing the circulation time of MSNs in biological system along with reduction in RES uptake [88-90].

## 5.2. Active Targeting

Cancer cells also over express different surface receptors that are poorly present in normal cells. Thus, the active targeting of nanoparticles could be achieved by modification of the surface of MSNs with antibodies, polysaccharides, polypeptides and appropriate ligands which are specifically selected for a particular receptor that are over expressed on the surface of cancer cells [91, 92]. Different molecular target receptors present on cancer cells which can be used for active targeting by MSNs are transferring, folic acid, VCAM-1, metalloproteinases, lectins, VEGFR, αβ-integrins [87]. By this mechanism, the MSNs are internalized by receptor-mediated endocytosis (Figure 5). Roselholm et al. have reported on the targeting of cancer cells by functionalization of MSNs surface with polyethyleneimine

followed by attachment of folic acid. They showed the higher order of magnitude of MSNs internalization in cancer cells than normal cells [93]. Qi et al. successfully delivered various chemotherapeutic drugs like paclitaxel, cisplatin and 5-florouracil at laryngeal carcinoma using folic acid modified MSNs [94]. Zhang et al. used the cancer over expressed metalloproteinases for the successful internalization of RGD functionalized MSNs drug delivery nanocarriers protected by polyanionic envelope [95]. Similarly, mannose functionalized MSNs have been utilized for targeting cancer cells over expressed with lectins [96]. These studies show that receptor mediated endocytosis by functionalized MSNs using active targeting is beneficial to reducing the side effects of chemotherapeutic agents to the healthy cells.

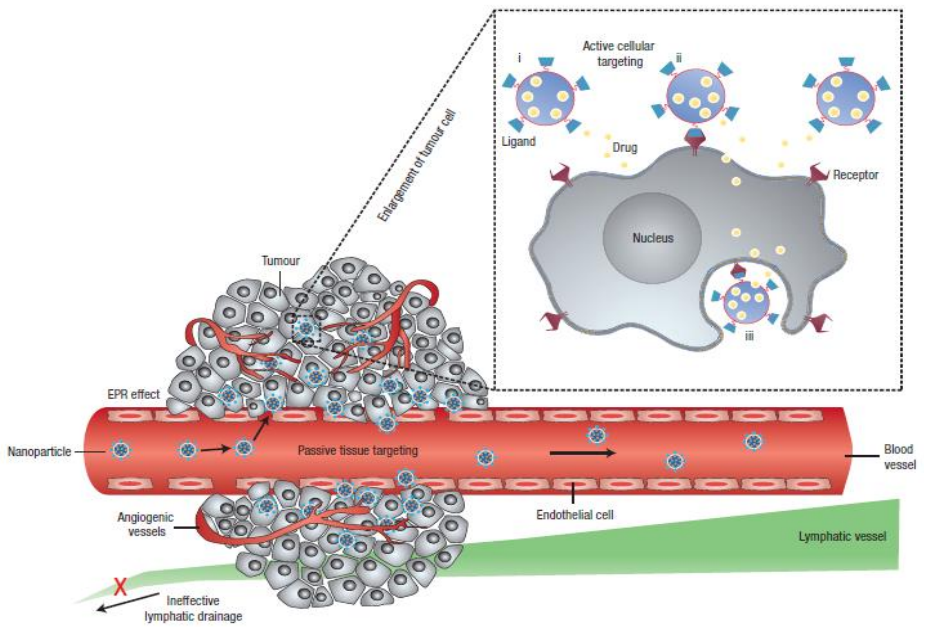


Figure 5. Molecular targets for active and passive targeting of cancer by mesoporous silica nanoparticles (Figure adapted from Ref.[4] with permission of Nature publishing group).

## 6. Biocompatibility and Biodegradation of Mesoporous Silica Nanoparticles

Biocompatibility, biodistribution, retention and clearance are vital factors to be considered for using high potential MSNs for intracellular drug delivery applications. Further, other factors such as concentration, size, surface area and chemical composition of MSNs also play an important role towards toxic triggers in physiological environment [97, 51, 98]. Various groups have studied the biocompatibility of MSNs in different cell lines. For instance, it's been shown that MSNs are biocompatible towards HeLa and CHO at concentrations below 100 µg/ml, by Lin et al. [68, 35]. Above this concentration, MSNs are shown to be toxic and resulted in cell damage. The same group has also shown hemolytic properties of MSNs towards mammalian red blood cells (RBCs) [99].The unmodified silica is

proven to be toxic and results in hemolysis due to the interaction between the silanol groups present on the surface of silica and tetra alkyl groups localized on the membranes of RBCs whereas, MSNs shows much less hemolysis sincemost of the silanol groups are present inside the porous network [100, 101]. Also, both amorphous silica and MSNs grafted with positively and negatively charged groups showed no hemolysis in RBC which further confirms that silanol groups are indeed responsible for toxicity. Another group, Haynes and coworkers coated MSNs with iron oxide nanoparticles showed concentration and size dependent hemolytic behavior on RBCs with exception of the smallest MSNs [102, 103]. In vitro and in vivo studies performed by R. Langer and coworkers using MSNs shows that biocompatibility of MSNs is both concentration and cell-type dependent [104]. Thus, in order to increase the biocompatibility and reduce the hemolysis due to free silanol groups, the surface functionalization of MSNs with polymers, proteins, liposomes and other functional groups has been suggested by different authors. Also, modification of MSNs surface with polymer coatings, charged groups or lipid bilayer was found to decrease the particle aggregation and thus improving the stability of nanoparticles in physiological environment [105-108].

Another important concern associated with MSNs is their biodegradation under physiological conditions after the therapeutic function. It is desired that nanoparticle should be degraded into harmless byproducts and finally get cleared form the body without any potential side effects. Recently, few studies have been performed on silica nanomaterials by M. Sailor and group and they reported that the accumulation of the silica mainly takes place in kidney, liver and spleen. Also, they demonstrated that most of the silica particles got cleared from the body of mice within a period of one week and completely cleared in four weeks. The mechanism of clearance of silica nanoparticles is due to the degradation by lysosomes to soluble orthosilicic acid which is finally excreted through the renal system [109]. Studies performed by K. Wang et al. showed the accumulation of silica was mainly in liver, kidney and urinary bladder after few hours of intravenous injection. They also reported that the blood circulation time of silica can be enhanced effectively by modification of surface with various functional groups and these nanoparticles were shown to be safely excreted via renal system [107].

The above studies on the biocompatibility and biodegradation of MSNs indicate that appropriate functionalization of these nanoparticles can prove to be effective towards better blood circulation, adsorption specificity, biocompatibility and better clearance after their desired action in the physiological environment.

## 7. Surface Functionalization of MSNs with Polymers for Drug Delivery Applications

As mentioned earlier, the importance of surface functionalization of MSNs to be effectively used in the physiological environment and specific cell targeting is well documented [110, 111]. Another advantage associated with the surface coating of MSNs is the control over the release of drug molecules over a desired period of time. The loaded drugs in the pores of MSNs without any coating results in rapid and uncontrolled drug release through diffusion. In case of hydrophilic drugs, due to their high solubility in aqueous media, they would be released as soon as they come in contact with water. In the case of hydrophobic

drugs, although MSNs do provide a control over the release of hydrophobic drugs up to certain limit, a rapid release can occur when MSNs come in contact with the phospholipids present on the cell surface before reaching the targeted interior of cells. In order to overcome these problems, controlled release systems based on MSNs have been developed by applying mechanical controls over the pore openings. The mechanical pore blocks includes groups such as AuNPs [34], CdS nanocrystals [35], $Fe_3O_4$ [112], cyclodextrins [113], ZnO quantum dots [114] and various synthetic and natural polymers [115, 116, 42, 117, 118]. In this chapter, we have dealt with surface modification of MSNs using stimuli-responsive polymers which creates a barrier and affects the controlled release of the drug. These polymer chains completely wrap around the drug loaded MSNs thus blocking the multiple pore openings. The drug molecules can be released from MSNs when pores are exposed at the targeted site by using various stimuli like pH, temperature, enzymatic degradation, magnetic and electric field etc. [53, 119].

## 7.1. Surface Functionalization of MSNs with Synthetic Polymers for Targeted Drug Delivery

Various synthetic polymers have been studied for the surface functionalization of MSNs which help in the controlled release of drug molecules. Polyethylene glycol (PEG) is one such synthetic polymer that has been studied extensively due to its inherent biocompatibility, prolonged circulation time and EPR effect [120-122]. Various stimuli have been used for the release of drug molecules once MSNs enter inside the cancer cells. For example, Li et al. have synthesized PEG chains as the gatekeepers to control the release of guest molecules followed by their release using redox chemistry (Figure 6). They first functionalized the surface of MSNs with thiol moieties using mercaptopropyl-trimethoxysilane (MPTMS) followed by the reaction with polyethylene glycol orthopyridyl disulfide (mPEG-SS-Pyridine). The modified MSNs were loaded with fluorescein as model drug. The MSNs functionalized with PEG using dithiol linkage (MSNs-SS-mPEG) exhibits redox responsive release characteristics in the presence of glutathione (an enzyme present in the cells) as indicated in fluorescence imaging. MSNs-SS-mPEG shows no cytotoxicity to the breast cancer cell line, MCF-7 indicating the biocompatibility of the PEG coated nanoparticles whereas methotrexate (MTX, an anticancer drug) loaded MSNs-SS-mPEG shows noticeable cytotoxicity in MCF-7 due to the release of the drug molecules inside the cell line (PEG-gatekeepers) [123].

Recently, Li et al. have prepared multifunctional pH sensitive MSNs by covalent modification of surface with poly (2- (pentamethyleneimino) ethyl methacrylate) (PPEMA) and poly (ethylene glycol) (PEG) (MSN@PPEMA/PEG). PEG being hydrophilic in nature helps in increasing the circulation time whereas PPEMA helps in the blockage of pores containing drug molecules (Figure 7). PPEMA becomes hydrophobic at neutral pH of the blood thus, preventing DOX.HCl in the pores from premature release. Once, MSN@PPEMA/PEG enter the interior of the cancer cells by EPR effect, the acidic condition helps in the protonation of the PPEMA and it becomes hydrophilic in nature. This leads to the opening of the pores previously blocked by PPEMA followed by release of DOX molecules inside the cancer cells [124].

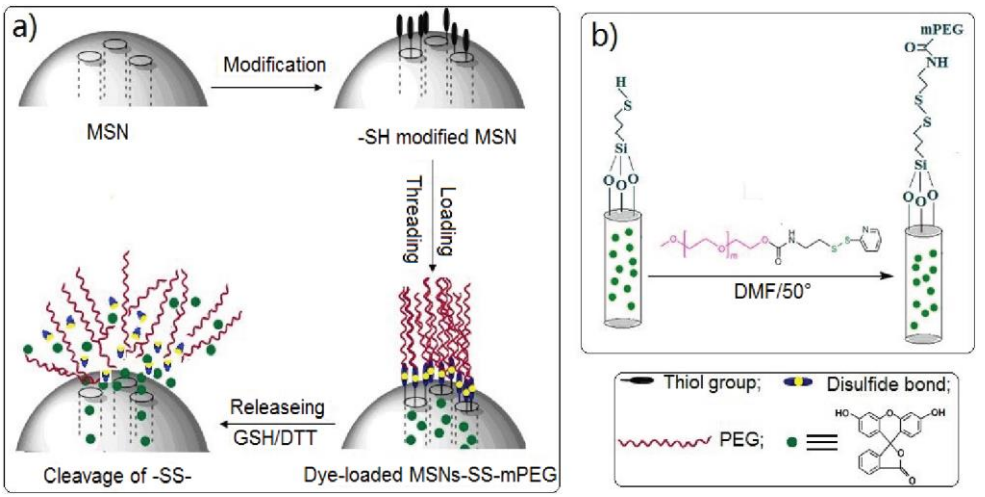


Figure 6. (a) Illustration of (a) Synthesis of the Dye-Loaded MSNs-SS-mPEG Nanoparticles and the Mechanism of Dye Release by Disulfide Cleavage; (b) Exchange Reaction between MSNs-SH and PEG-SS-Pyridine (Figure adapted from Ref.[123] with permission of American Chemical Society).

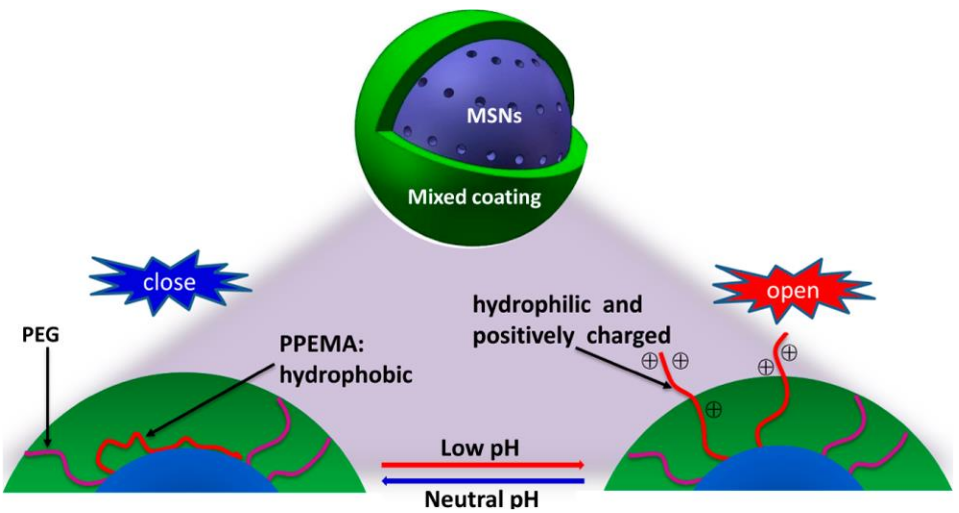


Figure 7. Schematic Illustration of Multifunctional MSN@PPEMA/PEG with Close−Open Transformation for pH Sensitive Drug Delivery (Figure adapted from Ref. [124] with permission of American Chemical Society).

PNIPAM is another synthetic polymer that shows LCST behavior and thus has been explored for the temperature dependent release of drug molecules on grafting PNIPAM on to MSN surface. David et al. has explored this LCST behavior of PNIPAM for the controlled opening and closing of the pores in in-vitro conditions. They functionalized the surface of MSNs using thiol groups by PTMS using co-condensation method. The thiol functionalized MSNs were further reacted with pyridyl disulfide-terminated PNIPAM (PNIPAM-S-S-Py) to prepare MSN-PNIPAM (Figure 8). Loading and release study of fluorescein from MSN-PNIPAM loaded with fluorescein was performed in phosphate buffer saline (PBS) at 25 °C and at 38 °C. It has been observed that fluorescein enters MSNs at 25 °C (below LCST of PNIPAM) and no loading occurs at 38 °C (above LCST of PNIPAM). The similar behavior

was observed for the release of fluorescein at two different temperatures. This indicates that below LCST (25 °C), PNIPAM is in the extended from and thus rendered the pores open for both loading and release of fluorescein molecules whereas above LCST (38 °C), PNIPAM chains are in the collapsed form and thus blocks the pores on MSNs which prevents the release of fluorescein [125].

Another strategy to prevent the premature release of drugs from MSNs is the layer by layer (LBL) assembly that utilizes the electrostatic attraction to assemble polyelectrolyte multilayer on the MSNs surface. One such study was published by Zhang et al. wherein, LBL technique was utilized for the synthesis of pH responsive MSNs nanocarriers using poly(allylamine hydrochloride) (PAH) and sodium poly(styrene sulfonate) (PSS) polyelectrolyte pairs as shells and MSNs (PEM-MSN) as cores (Figure 9). DOX was used as a model drug to conduct the pH dependent release study from PEM-MSN both in in-vitro and in-vivo conditions. The cellular uptake studies of DOX loaded PEM-MSN shows high internalization of the particles in HeLa cell line (lung cancer) resulting in growth inhibition effect as compared to that of L929 cell line (fibroblast cells). Also, DOX loaded PEM-MSN shows prolonged release of the drug inside the cancer cell line due to slow degradation of polymer multilayer. The studies conducted in normal rats showed that DOX loaded PEM-MSN induced a sustained drug concentration in blood plasma and lower concentration in major organs like heart compared to free DOX. The histological results also revealed that DOX loaded PEM-MSNs has lower systemic toxicity than free DOX [126].

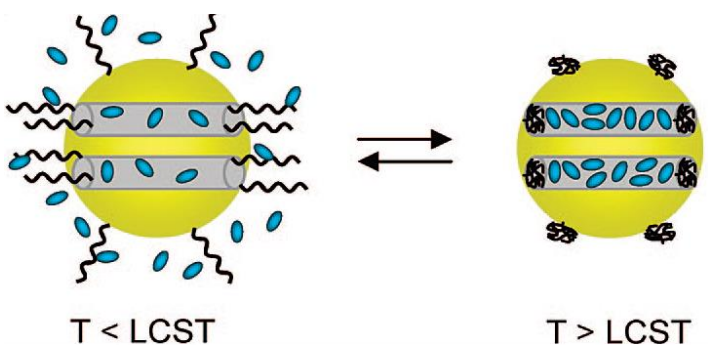


Figure 8. Schematic representation of the principle of action of PNIPAM (blue circles are fluorescein molecules and black chains indicates PNIPAM in extended and collapsed state (Figure adapted from Ref.[125] with permission of American Chemical Society).

Vallet Regi et al. reported the synthesis of thermo responsive hybrid polymer/magnetic MSNs able to release drug molecules in a controlled manner in the presence of magnetic field as external stimuli. Paramagnetic iron oxide nanocrystals were entrapped inside the pores of MSNs (MMSN) to incorporate heating capability under alternating magnetic field and thermo responsive property was incorporated by the surface functionalization of MSNs using poly(N-isopropylacrylamide) (PNIPAM) (Figure 10). PNIPAM is known to exhibit LCST behavior at approximately 32 °C in water. Below this temperature, PNIPAM is in the hydrated state (expanded state) and blocks the release of drugs and upon increasing the temperature the polymer shrinks and opens up the pores which results in the release of encapsulated drug molecules. MMSN was first reacted with 3-(trimethoxysilyl) propyl methacrylate (MPS) to form MMSN-MPS and further with copolymer of poly-NIPAM-b-PEI using in-situ radical

polymerization using MBA as cross linking agent and APS as an initiator. The studies show that MMSN-PNIPAM-PEI shows increase in the release of fluorescein above LCST temperature of PNIPAM due to the shrinkage of the polymer. The sample in the presence of magnetic field shows similar release profile due to the heating of the iron nanoparticles which increases the temperature of the system, thus leading to the collapse of PNIPAM on the surface of MSN causing an increase in release rate of fluorescein molecules [39].

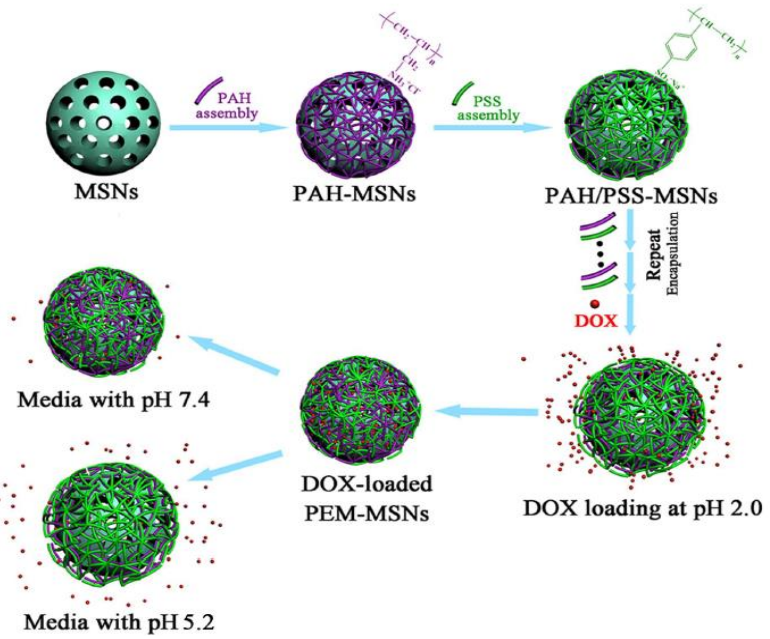


Figure 9. Schematic illustration of pH-responsive carrier systems based on PEM-MSNs (Figure adapted from Ref.[126] with permission of Royal Society of Chemistry).

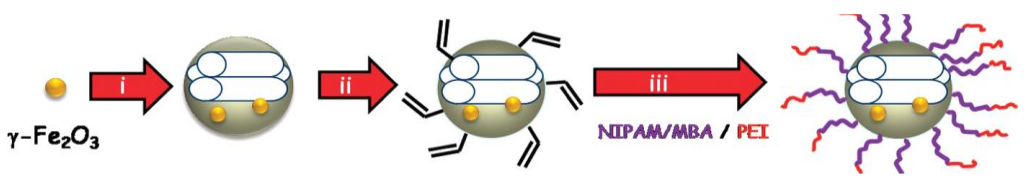


Figure 10. Synthesis of MMSN-NIPAM (Figure adapted from Ref.[39] with permission of American Chemical Society).

## 7.2. Surface Functionalization of MSNs with Natural Polymers for Targeted Drug Delivery

Although synthetic polymers used for DDS are biocompatible, they do not undergo degradation in biological media. As an alternative, researchers have started exploring natural polymers for the surface modification of MSNs for DDS due to their inherent biodegradability and biocompatibility. Various natural polymers that have been explored so far include polysaccharides like chitosan [127], alginate [128], hyaluronic acid [129] etc., and polypeptides including DNA [130, 58, 30]. These natural polymers have been successfully

used as gatekeepers to prevent premature release of drugs and other biomolecules from the pores of MSNs. The uptake of these nanoparticles could take place either through EPR effect or through receptor mediated endocytosis. Once, they reach the inside of cancer cells, the release of drug molecules can be triggered by stimuli as discussed in the previous sections like changes in pH, enzymatic degradation, temperature, light etc. The enzymatic degradation of various natural polymers as gatekeepers is found to be an interesting way to control the drug release in targeted cancer cells.

Various enzymes that are involved in enzymatic degradation include esterases [132, 133], peptidases [134, 135], reductases [136, 137], DNAses [138, 139] and glycosidases [140, 141]. Poly-L-glutamic acid (PGA) is one such polymer that has been used as gatekeeper for the encapsulation of drugs in MSNs as it is highly stable in plasma and can be easily degraded by lysosomal enzyme cathepsin B. PGA is a non toxic and non immunogenic polymer and has already been employed in phase III trial polymer- anticancer drug conjugate, Opaxio. Recently, Ramen et al. have reported an enzyme responsive drug delivery system based on PGA capped MSN conjugates (Figure 11). The pores of MSNs were loaded with the dye rhodamine B or DOX and the external surface was functionalized with PGA. Here, PGA has shown to effectively inhibit the premature release of drug molecules. In the presence of an enzyme pronase, the peptide bonds in PGA are cleaved by hydrolysis resulting in the release of drug. The studies revealed that PGA coated MSNs showed around 20% of drug release in 24 h in the absence of pronase whereas the release was found to be 90% in 5 h in the presence of pronase. The uptake studies of MSN-PGA in SK-BR-3 breast cancer cells showed very high biocompatibility of the nanoparticles whereas DOX loaded MSN-PGA effectively killed more than 90% of the cells confirming the ability of the nanoparticles to deliver drug molecules inside the cells [131].

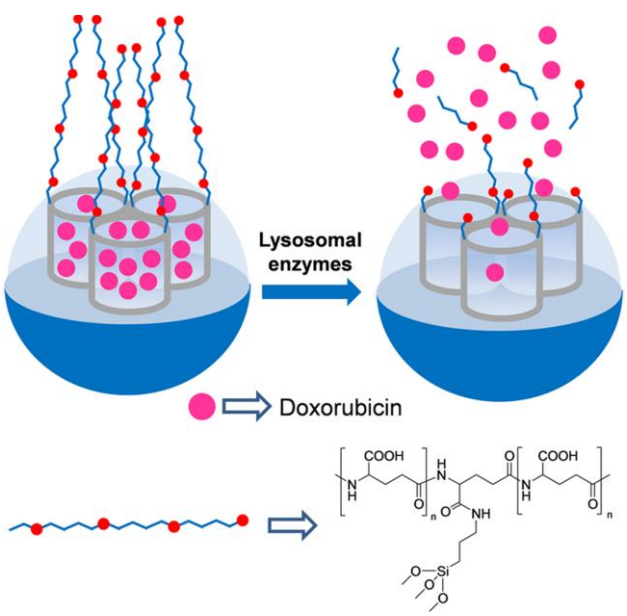


Figure 11. MSNs Capped with PGA: Drug Delivery is Selectively Observed in the Presence of Lysosomal Enzymes (Figure adapted from Ref.[131] with permission of American Chemical Society).

Lin et al. used DNA as a capping agent for drugs inside the $Cu_{1.8}S$ coated MSNs (NC) and the release of two different drug molecules, curcumin (cur) and DOX was triggered by the photosensitized reaction inside the cancer cells. DNA double strands containing GC base pairs are known for loading of DOX (from literature) and by changing the number of GC base pairs the loading DOX molecules can be adjusted. One of the DNA strands is thiolated and helps in binding DNA with $Cu_{1.8}S$ coated MSNs while the other strand is preconjugated with the aptamer for the targeted delivery to the cancer cells (Figure12). Here, the GC rich DNA is used to bind with the DOX molecules and an aptamer AS1411 is used to binding with cancer cells and internalization of nanocarriers occurs via receptor mediated endocytosis. The nanocarriers are represented as DNA (DOX)-NC-cur. The nanocarriers were found to be biocompatible in the absence of drug and show apoptotic molecular mechanism (when loaded with drugs) in MCF-7 breast cancer cell line. The nanocarriers upon irradiation with laser light 980 nm lead to the release of DOX and Cur and thus can be used for multiple drug cancer therapy. The study reveals that nanocarriers have promising future for combination chemotherapy and targeting drug delivery without affecting the surrounding healthy cells [142].

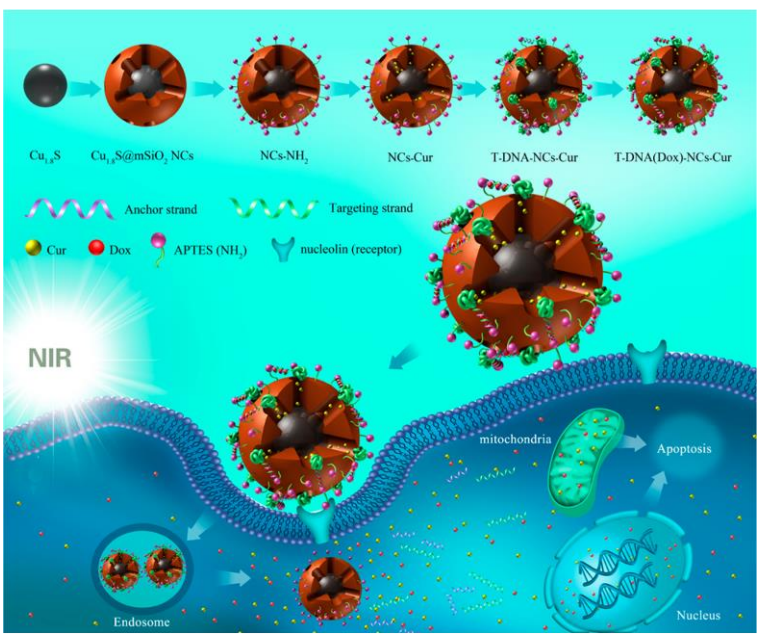


Figure 12. Synthetic Process, Anticancer Drug Loading, and Possible Receptor-Mediated Endocytosis Pathway of the Targeting Cu1.8S@mSiO$_2$ Core−Shell NCs (Figure adapted from Ref.[142] with permission of American Chemical Society).

Hyaluronic acid (HA) is a polysaccharide which is natural ligand for the CD44 receptors over expressed in most of the cancer cells. Recently, Yu et al. synthesized MSNs with a mean particle size of 70-100 nm and functionalized the surface with HA targeting ligands. DOX, an anticancer drug was loaded into the pores of MSN-HA and the internalization of the nanoparticles was studied inside HCT-116 cell line overexpressed with CD44 receptors (Figure 13). HA coated on the surface of MSNs by EDC coupling reaction helped in the internalization of the particles by conjugating with the CD44 receptors over expressed on the

surface of HeLa cancer cell line by receptor mediated endocytosis. The studies reveal that HA modification on MSNs helps in the better internalization of MSN-HA in HCT-116 cancer cell line as compared to unmodified MSNs. Also, DOX loaded MSN-HA showed better anti proliferative effect on HCT-116 as compared to free DOX or DOX loaded unmodified MSN which confirms that HA helps in the internalization and release of DOX inside HCT-116 by CD44 receptor mediated endocytosis pathway [143].

Another study conducted by Gao et al. adopted the LBL methodology using biocompatible polysaccharides, enzyme and polyglycerol for the encapsulation of amoxicillin molecules (AMO), antibacterial drug inside the pores of MSNs thus preventing their premature release. They synthesized carboxyl modified MSNs as a core and coated the surface using Lysozyme (Lys), Hyaluronic acid (HA) and polyglycerol methacrylate (PGMA) via electrostatic interaction (MSN-Lys-HA-PGMA) (Figure 14). The nanoparticles were found to be biocompatible with very low hemolytic effect. Also, they showed effective antibacterial activity both in vitro and in vivo conditions. The Lys and PGMA on MSNs particles showed multivalent binding with the cell wall of bacteria while HA acts as a valve and helps in the release of AMO from the pores of MSNs after degradation from the hyaluronidase enzyme present inside the bacterial cell. HA, Lys, PGMA and AMO showed efficient antibacterial activity towards the drug resistant bacteria as compared to the conventional antibacterial drugs. The studies indicated that LBL coated MSNs showed good pathogenic inhibition towards bacterial-infected wounds. The nanoparticles proved to be a good alternative for the conventional antibiotics [144].

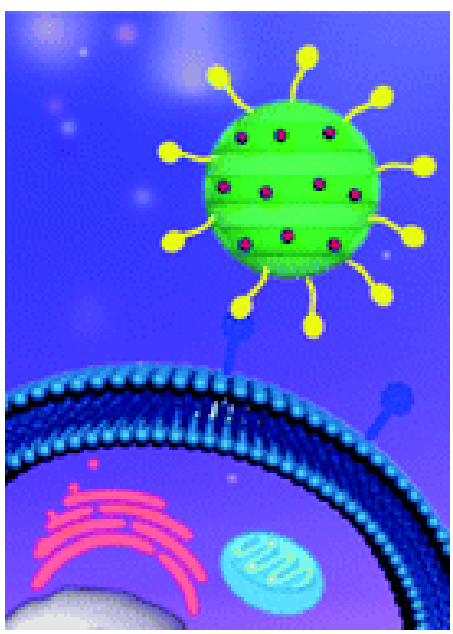

Figure 13. Cellular uptake of DOX@HA-MSNs through a CD44 receptor-mediated endocytosis (Figure adapted from Ref.[143] with permission of Royal Society of Chemistry).

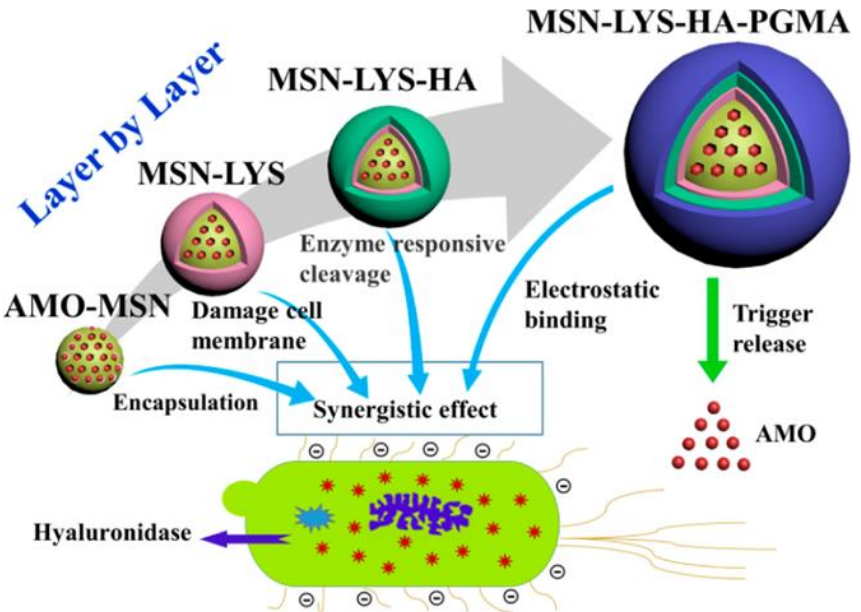


Figure 14. Biocompatible and fluorescent core/shell composite nanoparticles (Figure adapted from Ref.[144] with permission of American Chemical Society).

## 8. Carboxymethyl Cellulose Grafted Mesoporous Silica Nanoparticles (MSN-CMC)

Owing to the immense potential of MSNs and natural polymers hybrids as drug delivery nanocarriers, we explored the cellular uptake ability of carboxymethyl cellulose (CMC) grafted MSNs (MSN-CMC) in cancer cells. We used MSN-CMC hybrid nanoparticles for delivery of anticancer and antibacterial drug, curcumin inside breast cancer cell line (MDA-MB-231). Carboxymethyl cellulose, being a natural polysaccharide imparts biocompatibility and increased circulation time of the hybrid MSNs in the physiological environment along with preventing premature release of curcumin from inside the pores before reaching the cancer cells. In the following sections, we will discuss in detail the synthesis, characterization and in-vitro drug release using MSN-CMC hybrid nanoparticles inside MDA-MB-231 cancer cell line [59].

### 8.1. Synthesis of Mesoporous Silica Nanoparticles

In a typical procedure of synthesis of MSNs, 1 gm of Cetyltrimethylammonium bromide (CTAB) was dissolved in 480 ml of deionized water using an overhead stirrer at room temperature followed by the addition of 2 M NaOH solution (3.5 ml). The solution was allowed to stir for 30 min at 80 °C. 5 ml of tetraethyl orthosilicate was added to the above mixture drop wise. The mixture was stirred for another 2 h at 80 °C at 6000 rpm. The resultant white precipitate was collected by vacuum filtration and washed with copious amount of water. The precipitate was dried in vacuum oven overnight to obtain mesoporous

silica in powder form. The removal of the surfactant was carried out by dispersing 1 gm of MSN in 100 ml methanol and 1 ml of hydrochloric acid. The solution was refluxed for 6 h. The template removed MSN was obtained by vacuum filtration and drying in oven overnight.

## 8.2. Synthesis of Carboxymethyl (CMC) Grafted Mesoporous Silica Nanoparticles (MSNs)

The synthetic route of MSNs and its functionalization with amine moieties and carboxymethyl cellulose is given in Scheme 2. The synthesis of MSNs was performed using sol-gel method using CTAB as a structure directing agent and tetraethyl orthosilicate as a silica precursor as mentioned above. The functionalization of the outer surface of MSNs with amine moieties was performed using aminopropyl triethoxysilane. The amino groups were introduced to further functionalize the MSN surface with Carboxymethyl cellulose (CMC). The amine groups on MSN covalently react with the –COOH groups on Carboxymethyl Cellulose to form amide linkages in the presence of N-hydroxy succinimide (NHS). TEM images of MSNs before and after functionalization showed uniform particle size of ~ 120 nm (Figure 15).

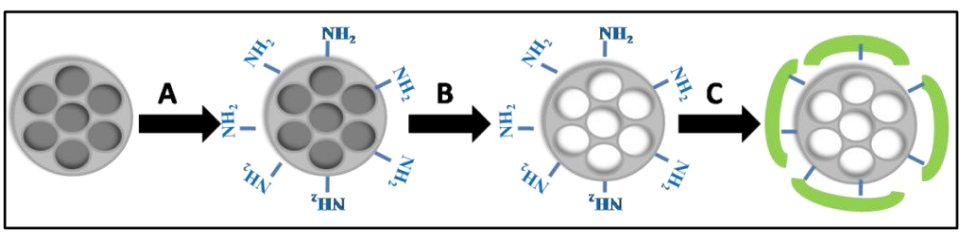


Scheme 2. Synthesis of carboxymethyl cellulose (CMC)-grafted mesoporous silica nanoparticles (MSNs).

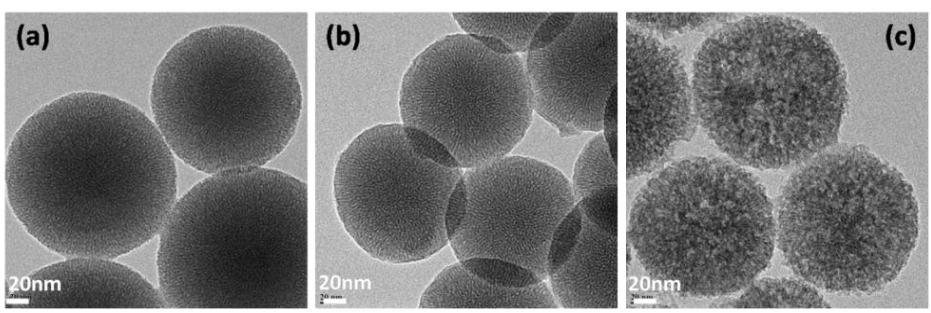


Figure 15. TEM images of (a) MSN, (b) MSN-$NH_2$ and (c) MSN-CMC.

### 8.3. Synthesis of Curcumin Loaded MSN-CMC

Curcumin, an anticancer drug was effectively loaded into the pores of MSNs in order to increase its bioavailability since it is hydrophobic in nature and also to prevent its enzymatic

degradation before reaching the cancer cells by EPR effect. For curcumin incubation, MSN surface was first grafted with amine moieties using aminopropyl triethoxysilane. Curcumin was then physically incubated in to the pores of MSN-$NH_2$ by stirring it with MSN in methanol overnight. The curcumin loaded MSN-$NH_2$ was washed copiously with distilled water to remove any drug molecules adsorbed on the surface. The physical entrapment of curcumin inside the pores of MSN was confirmed from the reduction in the pore diameter of MSN from $N_2$ adsorption-desorption isotherm. In the next step, carboxymethyl cellulose was grafted onto the surface of curcumin loaded MSN-$NH_2$. The –COOH groups on CMC reacts with amine groups on the surface of MSN to form amide linkages by EDC coupling reaction. The curcumin loaded CMC grafted MSN was washed with distilled water in order to remove unreacted molecules and side products. The synthetic scheme of the curcumin loaded MSN-CMC is shown in Scheme 3. The amount of drug loaded in MSN-$NH_2$ and MSN-CMC is given in Table 1.

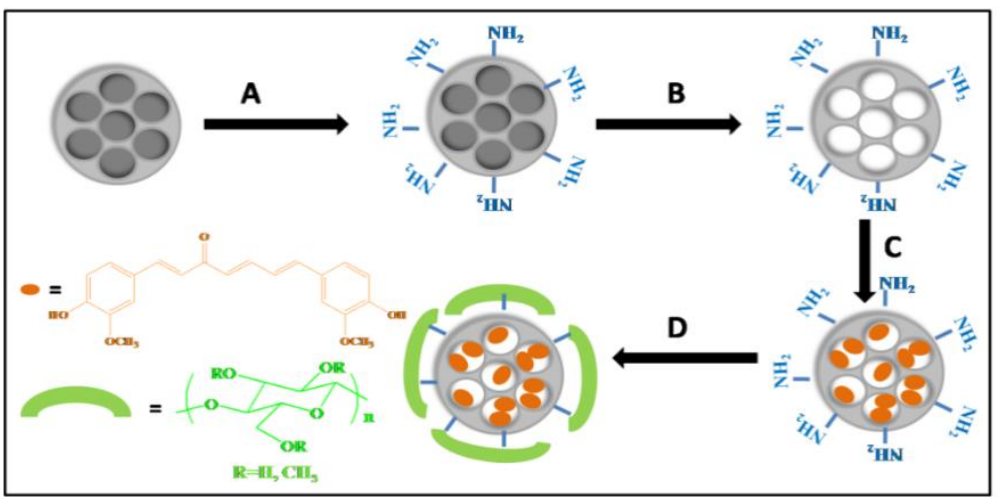


Scheme 3. Synthesis of curcumin loaded carboxymethyl cellulose grafted MSN (A) aminopropyl triethoxy silane in toluene, (B) Methanol in HCl for surfactant removal (C) Curcumin loading in MSN-$NH_2$ nanoparticles and (D) Carboxymethyl cellulose grafting in water in presence of EDC.HCl and NHS.

**Table 1. Curcumin loading in functionalized MSNs**

| Sample Name | Loading of Curcumin (µg/mg) |
|---|---|
| MSN-$NH_2$ | 107 |
| MSN-CMC | 80 |

## 8.4. In Vitro Cytotoxicity Assay

The in vitro cell cytotoxicity of MSN-$NH_2$, MSN-CMC, MSN-cur-$NH_2$, MSN-cur-CMC and free curcumin to MDA-MB-231 cells was investigated using MTT assay. Figure 16 (a) shows that MSN-$NH_2$ and MSN-CMC have no toxic effect to the cancer cells up to a concentration of 200 µg/ml after incubation for around 24 h indicating good biocompatibility

of these nanoparticles. Figure 16 (b) shows the In-vitro cellular toxicity of MSN-cur-$NH_2$, MSN-cur-CMC and free curcumin in MDA-MB-231 cells at different concentrations. It has been observed that free curcumin showed negligible cytotoxicity to the cancer cells. This could be explained due to the fact that curcumin being hydrophobic in nature has very less solubility in the dispersed medium. A comparison of the MTT results of MSN-cur-$NH_2$ and MSN-cur-CMC with the same concentration of curcumin inside the pores showed that MSN-cur-CMC has higher cell inhibitory effect as compared to that of the MSN- cur-$NH_2$. The $GI_{50}$ of MSN-cur-$NH_2$ and MSN-cur-CMC are found to be 8 µg/ml and 1.5 µg/ml respectively. This indicates that CMC functionalization helps in the better internalization of curcumin loaded MSNs resulting into better inhibition of the cancer cells as compared to that of curcumin loaded MSN-$NH_2$.

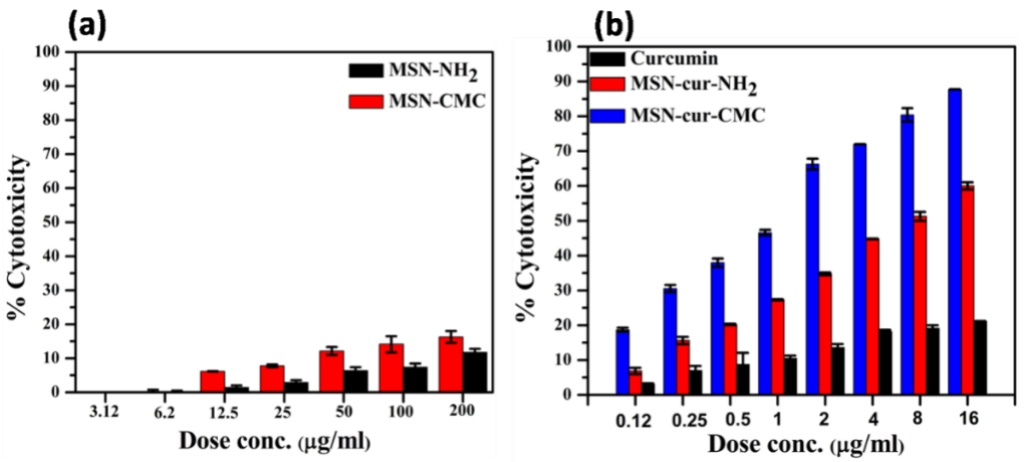


Figure 16. (a) % Cytotoxicity of MDA-MB-231 cells incubated with MSN-$NH_2$ and MSN-CMC and (b) % Cytotoxicity of MDA-MB-231 cells incubated with free curcumin, MSN-cur-$NH_2$ and MSN-cur-CMC keeping the amount of curcumin same in all the samples.

## 8.5. Intracellular Uptake of MSN Particles

For the cellular uptake studies, we incubated the breast cancer cell line MDA-MB-231 with free curcumin (16 µg/ml), MSN-cur-$NH_2$ and MSN-cur-CMC ($GI_{50}$ conc. of around 7 µg/ml and 1.5 µg/ml respectively). Similarly, MSNs without curcumin (MSN-$NH_2$ and MSN-CMC) were used as control in conc. of 200 µg/ml. The auto fluorescence of curcumin inside the cells was captured after 1 h of incubation of the MSNs (with and without curcumin) and free curcumin. It is observed that free curcumin does not show auto fluorescence due to curcumin after 1 h whereas curcumin loaded MSN-cur-$NH_2$ and MSN-cur-CMC showed auto fluorescence of curcumin molecules. It was also evident from Figure 17 that curcumin loaded MSN-cur-CMC showed much better fluorescence due to curcumin as compared to that of curcumin loaded MSN-cur-$NH_2$. This confirms that CMC grafted MSN helps in the better internalization of curcumin inside the cells as compare to MSN-$NH_2$ as $GI_{50}$ of MSN-cur-CMC is much lower compared to that of MSN-cur-$NH_2$.

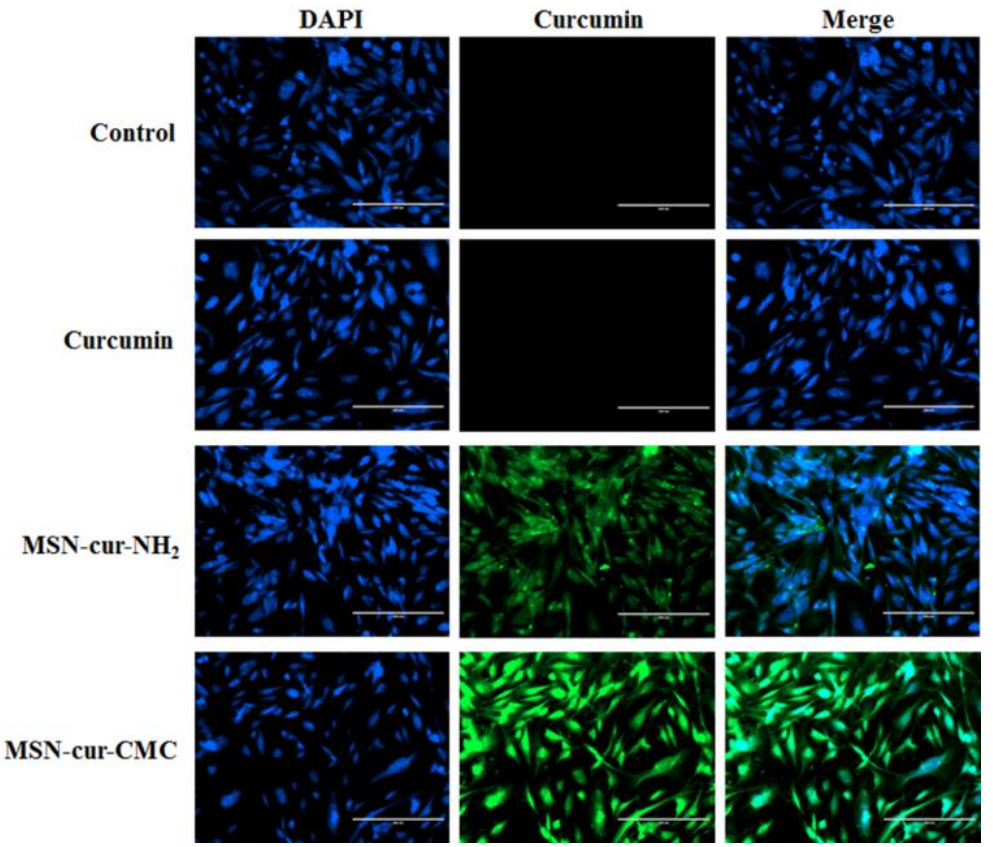


Figure 17.Intracellular uptake of $–NH_2$ and –CMC functionalized MSNs using fluorescence microscopy. Images are at a magnification of 200 µm of MDA-MB-231 incubated with 16 µg/ml of free curcumin, MSN-$NH_2$ ($GI_{50}$=7 µg/ml) and MSN-cur-CMC ($GI_{50}$=1.5 µg/ml). Blue fluorescence is due to nuclei staining of cell with DAPI and green due to auto fluorescence of curcumin release inside the cells.

## 8.6. Apoptosis by Annexin V-FITC PI Staining

We investigated the apoptosis in MDA-MB-231 cells using annexin V-FITC/PI and DAPI as the staining agents. We observed that treatment of cells with free curcumin (16 µg/ml) and $GI_{50}$ concentrations of MSN-cur-$NH_2$ (7 µg/ml) and MSN-cur-CMC (1.5 µg/ml) resulted in increase in the apoptotic cells in 48 h (Figure 18). The calculated apoptotic ratios upon 48 h for control, curcumin, MSN-cur-$NH_2$ and MSN-cur-CMC were found to be 2.5, 9.7, 49 and 69 respectively. The high apoptotic values for MSN-cur-CMC compared to free curcumin and MSN-cur-$NH_2$ further confirms that CMC coating on the MSN surface helps in better uptake of the MSN particles inside the cells and hence more curcumin molecules are released effectively at the targeted site. We also observed that PI positive cells were not observed in the experiment suggesting the absence of necrosis. This experiment proves that MSN-cur-CMC induces cell death in MDA-MB-231 cell line via apoptotic pathway.

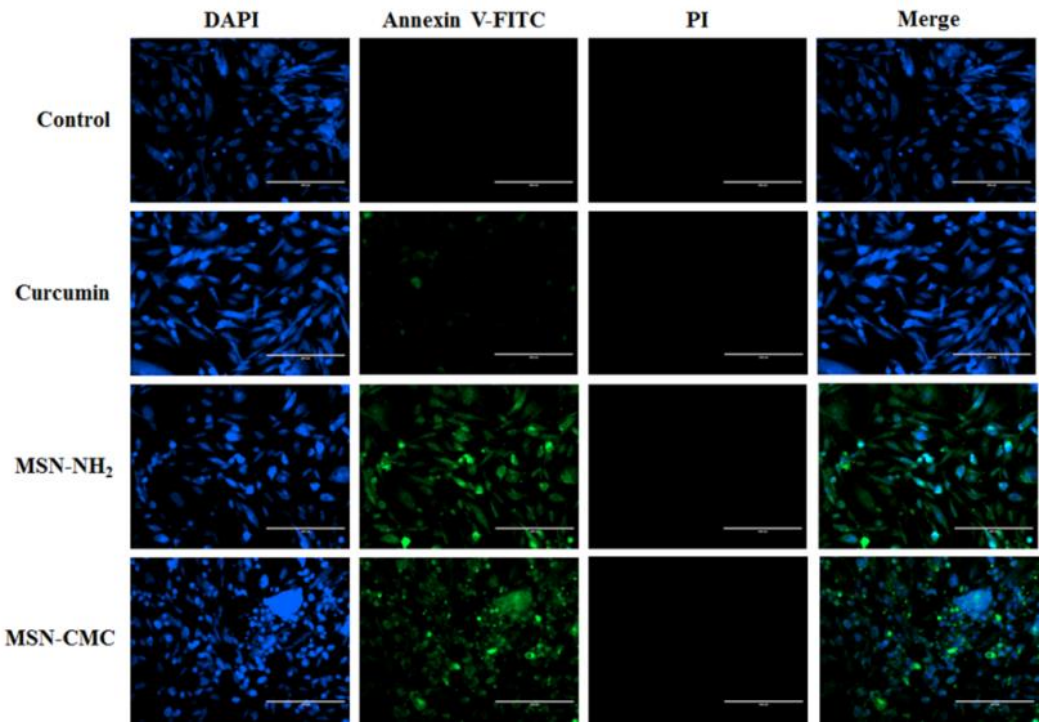


Figure 18. Apoptosis of MDA-MB-231 cells using fluorescence microscopy. Images are at a magnification of 200 µm of MDA-MB-231 incubated with 16 µg/ml of free curcumin, MSN-$NH_2$ ($GI_{50}$ = 7 µg/ml) and MSN-cur-CMC ($GI_{50}$=1.5 µg/ml). Blue fluorescence is due to nuclei staining of cell with DAPI and green fluorescence due to staining of cells by annexin V-FITC.

## CONCLUSION

Since the discovery of MSNs for drug delivery applications in early 2000, they have undergone rapid and drastic development in order to further improve their properties in controlled and targeted drug release. The versatile nature of MSNs in terms of their stability, functionalization and control over the morphology make them one of the most interesting alternatives over other drug delivery nanocarriers. In conclusion, we have highlighted various recent research findings for the potential use of MSNs in drug delivery along with some of our own work on the carboxymethyl cellulose grafted Mesoporous Silica hybrid Nanogels for drug delivery applications. MSNs can be transformed into intelligent systems by grafting the surface with appropriate functional moieties. The smart systems that respond to the various stimuli can help in the targeted delivery of drug molecules specifically inside the cancer cells preventing their premature release. Although they have shown to possess reasonably good biocompatibility after surface functionalization with different organic molecules (to prevent hemolysis due to free silanol groups), yet a deep understanding of their in-vivo biocompatibility and biodistribution needs to be addressed before they can be used in clinical trials.

## ACKNOWLEDGMENTS

Authors are grateful to Council of Scientific & Industrial Research (CSIR), New Delhi and CSIR-NCL for the facilities.

## REFERENCES

[1] McGuire, Shelley. 2016. "World cancer report 2014. Geneva, Switzerland: World Health Organization, international agency for research on cancer, WHO Press, 2015."*Advances in Nutrition: An International Review Journal* no. 7 (2):418-419.

[2] Chabner, Bruce A, and Thomas G Roberts Jr. 2005. "Chemotherapy and the war on cancer." *Nature reviews. Cancer* no. 5 (1):65.

[3] Song, Yuanhui, Yihong Li, Qien Xu, and Zhe Liu. 2017. "Mesoporous silica nanoparticles for stimuli-responsive controlled drug delivery: advances, challenges, and outlook." *International journal of nanomedicine* no. 12:87.

[4] Peer, Dan, Jeffrey M Karp, Seungpyo Hong, Omid C Farokhzad, Rimona Margalit, and Robert Langer. 2007. "Nanocarriers as an emerging platform for cancer therapy." *Nature nanotechnology* no. 2 (12):751-760.

[5] Faraji, Amir H, and Peter Wipf. 2009. "Nanoparticles in cellular drug delivery." *Bioorganic & medicinal chemistry* no. 17 (8):2950-2962.

[6] Slowing, Igor I, Juan L Vivero-Escoto, Chia-Wen Wu, and Victor S Y Lin. 2008. "Mesoporous silica nanoparticles as controlled release drug delivery and gene transfection carriers." *Advanced drug delivery reviews* no. 60 (11):1278-1288.

[7] Vivero-Escoto, Juan L, Igor I Slowing, Brian G Trewyn, and Victor SY Lin. 2010. "Mesoporous silica nanoparticles for intracellular controlled drug delivery." *Small* no. 6 (18):1952-1967.

[8] Ninomiya, Kazuaki, Shinya Kawabata, Hiroyuki Tashita, and Nobuaki Shimizu. 2014. "Ultrasound-mediated drug delivery using liposomes modified with a thermosensitive polymer." *Ultrasonics sonochemistry* no. 21 (1):310-316.

[9] Mo, Ran, Tianyue Jiang, and Zhen Gu. 2014. "Enhanced anticancer efficacy by ATP-mediated liposomal drug delivery." *Angewandte Chemie* no. 126 (23):5925-5930.

[10] Zhang, Chengyuan, Dayi Pan, Kui Luo, Wenchuan She, Chunhua Guo, Yang Yang, and Zhongwei Gu. 2014. "Peptide Dendrimer–Doxorubicin Conjugate-Based Nanoparticles as an Enzyme-Responsive Drug Delivery System for Cancer Therapy." *Advanced healthcare materials* no. 3 (8):1299-1308.

[11] Yavuz, Burçin, Sibel Bozdağ Pehlivan, İmran Vural, and Nurşen Ünlü. 2015. "In vitro/in vivo evaluation of dexamethasone—PAMAM dendrimer complexes for retinal drug delivery."*Journal of pharmaceutical sciences* no. 104 (11):3814-3823.

[12] Ding, Jianxun, Linghui Chen, Chunsheng Xiao, Li Chen, Xiuli Zhuang, and Xuesi Chen. 2014. "Noncovalent interaction-assisted polymeric micelles for controlled drug delivery." *Chemical Communications* no. 50 (77):11274-11290.

[13] Zhu, Lin, Federico Perche, Tao Wang, and Vladimir P Torchilin. 2014. "Matrix metalloproteinase 2-sensitive multifunctional polymeric micelles for tumor-specific co-delivery of siRNA and hydrophobic drugs." *Biomaterials* no. 35 (13):4213-4222.

[14] Ke, Xi-Yu, Victor Wee Lin Ng, Shu-Jun Gao, Yen Wah Tong, James L Hedrick, and Yi Yan Yang. 2014. "Co-delivery of thioridazine and doxorubicin using polymeric micelles for targeting both cancer cells and cancer stem cells." *Biomaterials* no. 35 (3):1096-1108.

[15] Wu, Huixia, Haili Shi, Hao Zhang, Xue Wang, Yan Yang, Chao Yu, Caiqin Hao, Jing Du, He Hu, and Shiping Yang. 2014. "Prostate stem cell antigen antibody-conjugated multiwalled carbon nanotubes for targeted ultrasound imaging and drug delivery." *Biomaterials* no. 35 (20):5369-5380.

[16] Karchemski, Faina, Daniel Zucker, Yechezkel Barenholz, and Oren Regev. 2012. "Carbon nanotubes-liposomes conjugate as a platform for drug delivery into cells." *Journal of controlled release* no. 160 (2):339-345.

[17] You, Peihong, Yang Yang, Mingwei Wang, Xiaoyu Huang, and Xiao Huang. 2015. "Graphene oxide-based nanocarriers for cancer imaging and drug delivery." *Current pharmaceutical design* no. 21 (22):3215-3222.

[18] Maleki Dizaj, Solmaz, Mohammad Barzegar-Jalali, Mohammad Hossein Zarrintan, Khosro Adibkia, and Farzaneh Lotfipour. 2015. "Calcium carbonate nanoparticles as cancer drug delivery system." *Expert opinion on drug delivery* no. 12 (10):1649-1660.

[19] Elbialy, Nihal Saad, Mohamed Mahmoud Fathy, and Wafaa Mohamed Khalil. 2015. "Doxorubicin loaded magnetic gold nanoparticles for in vivo targeted drug delivery." *International journal of pharmaceutics* no. 490 (1):190-199.

[20] Mai, Wilson X, and Huan Meng. 2013. "Mesoporous silica nanoparticles: a multifunctional nano therapeutic system." *Integrative Biology* no. 5 (1):19-28.

[21] Yamamoto, Eisuke, and Kazuyuki Kuroda. 2016. "Colloidal mesoporous silica nanoparticles." *Bulletin of the Chemical Society of Japan* no. 89 (5):501-539.

[22] Vallet-Regi, M, A Ramila, RP Del Real, and J Pérez-Pariente. 2001. "A new property of MCM-41: drug delivery system." *Chemistry of Materials* no. 13 (2):308-311.

[23] Tang, Fangqiong, Linlin Li, and Dong Chen. 2012. "Mesoporous silica nanoparticles: synthesis, biocompatibility and drug delivery." *Advanced Materials* no. 24 (12):1504-1534.

[24] Karimi, Mahdi, Hamed Mirshekari, Masoumeh Aliakbari, Parham Sahandi-Zangabad, and Michael R Hamblin. 2016. "Smart mesoporous silica nanoparticles for controlled-release drug delivery." *Nanotechnology Reviews* no. 5 (2):195-207.

[25] Trewyn, Brian G, Supratim Giri, Igor I Slowing, and Victor S Y Lin. 2007. "Mesoporous silica nanoparticle based controlled release, drug delivery, and biosensor systems." *Chemical communications* (31):3236-3245.

[26] Wang, Yonghong, Lun Jiang, Lei Chu, Wen Liu, Shun Wu, Yaohui Wu, Xiaoxiao He, and Kemin Wang. 2017. "Electrochemical detection of glutathione by using thymine-rich DNA-gated switch functionalized mesoporous silica nanoparticles." *Biosensors and Bioelectronics* no. 87:459-465.

[27] He, Qianjun, Zhiwen Zhang, Yu Gao, Jianlin Shi, and Yaping Li. 2009. "Intracellular localization and cytotoxicity of spherical mesoporous silica nano-and microparticles." *Small* no. 5 (23):2722-2729.

[28] Lu, Jie, Monty Liong, Zongxi Li, Jeffrey I Zink, and Fuyuhiko Tamanoi. 2010. "Biocompatibility, biodistribution, and drug-delivery efficiency of mesoporous silica nanoparticles for cancer therapy in animals." *Small* no. 6 (16):1794-1805.

[29] Aznar, Elena, Laura Mondragón, José V Ros-Lis, Félix Sancenón, M Dolores Marcos, Ramón Martínez-Máñez, Juan Soto, Enrique Pérez-Payá, and Pedro Amorós. 2011. "Finely tuned temperature-controlled cargo release using paraffin-capped mesoporous silica nanoparticles." *Angewandte Chemie International Edition* no. 50 (47):11172-11175.

[30] Schlossbauer, Axel, Simon Warncke, Philipp ME Gramlich, Johann Kecht, Antonio Manetto, Thomas Carell, and Thomas Bein. 2010. "A Programmable DNA-Based Molecular Valve for Colloidal Mesoporous Silica." *Angewandte Chemie International Edition* no. 49 (28):4734-4737.

[31] Jadhav, Sushilkumar A, Ivana Miletto, Valentina Brunella, Gloria Berlier, and Dominique Scalarone. 2015. "Controlled post-synthesis grafting of thermoresponsive poly (N-isopropylacrylamide) on mesoporous silica nanoparticles." *Polymers for Advanced Technologies* no. 26 (9):1070-1075.

[32] Lee, Chia-Hung, Shih-Hsun Cheng, I Huang, Jeffrey S Souris, Chung-Shi Yang, Chung-Yuan Mou, and Leu-Wei Lo. 2010. "Intracellular pH-responsive mesoporous silica nanoparticles for the controlled release of anticancer chemotherapeutics." *Angewandte Chemie* no. 122 (44):8390-8395.

[33] Hu, Chunlin, Lingxue Yu, Zhen Zheng, Jing Wang, Yuan Liu, Yifeng Jiang, Guangzhi Tong, Yanjun Zhou, and Xinling Wang. 2015. "Tannin as a gatekeeper of pH-responsive mesoporous silica nanoparticles for drug delivery." *RSC Advances* no. 5 (104):85436-85441.

[34] Liu, Rui, Ying Zhang, Xiang Zhao, Arun Agarwal, Leonard J Mueller, and Pingyun Feng. 2010. "pH-responsive nanogated ensemble based on gold-capped mesoporous silica through an acid-labile acetal linker." *Journal of the American Chemical Society* no. 132 (5):1500-1501.

[35] Lai, Cheng-Yu, Brian G Trewyn, Dusan M Jeftinija, Ksenija Jeftinija, Shu Xu, Srdija Jeftinija, and Victor S Y Lin. 2003. "A mesoporous silica nanosphere-based carrier system with chemically removable CdS nanoparticle caps for stimuli-responsive controlled release of neurotransmitters and drug molecules." *Journal of the American Chemical Society* no. 125 (15):4451-4459.

[36] Giri, Supratim, Brian G Trewyn, Michael P Stellmaker, and Victor SY Lin. 2005. "Stimuli-responsive controlled-release delivery system based on mesoporous silica nanorods capped with magnetic nanoparticles." *Angewandte Chemie International Edition* no. 44 (32):5038-5044.

[37] Nadrah, Peter, Fabiola Porta, Odon Planinšek, Alexander Kros, and Miran Gaberšček. 2013. "Poly (propylene imine) dendrimer caps on mesoporous silica nanoparticles for

redox-responsive release: smaller is better." *Physical Chemistry Chemical Physics* no. 15 (26):10740-10748.

[38] Thomas, Courtney R, Daniel P Ferris, Jae-Hyun Lee, Eunjoo Choi, Mi Hyeon Cho, Eun Sook Kim, J Fraser Stoddart, Jeon-Soo Shin, Jinwoo Cheon, and Jeffrey I Zink. 2010. "Noninvasive remote-controlled release of drug molecules in vitro using magnetic actuation of mechanized nanoparticles." *Journal of the American Chemical Society* no. 132 (31):10623-10625.

[39] Baeza, Alejandro, Eduardo Guisasola, Eduardo Ruiz-Hernández, and María Vallet-Regí. 2012. "Magnetically triggered multidrug release by hybrid mesoporous silica nanoparticles." *Chemistry of Materials* no. 24 (3):517-524.

[40] Zhu, Yingchun, Huijuan Liu, Fang Li, Qichao Ruan, Hua Wang, Masahiro Fujiwara, Lianzhou Wang, and GQ Lu. 2010. "Dipolar molecules as impellers achieving electric-field-stimulated release." *Journal of the American Chemical Society* no. 132 (5):1450-1451.

[41] Gilman, Marina, and Sander L Gilman. 2008. "Electrotherapy and the human voice: a literature review of the historical origins and contemporary applications." *Journal of Voice* no. 22 (2):219-231.

[42] Yang, Xinjian, Xia Liu, Zhen Liu, Fang Pu, Jinsong Ren, and Xiaogang Qu. 2012. "Near-Infrared Light-Triggered, Targeted Drug Delivery to Cancer Cells by Aptamer Gated Nanovehicles." *Advanced materials* no. 24 (21):2890-2895.

[43] Zhu, Yingchun, and Masahiro Fujiwara. 2007. "Installing dynamic molecular photomechanics in mesopores: a multifunctional controlled-release nanosystem."*Angewandte Chemie International Edition* no. 46 (13):2241-2244.

[44] Schlossbauer, Axel, Johann Kecht, and Thomas Bein. 2009. "Biotin–Avidin as a Protease-Responsive Cap System for Controlled Guest Release from Colloidal Mesoporous Silica." *Angewandte Chemie* no. 121 (17):3138-3141.

[45] Bernardos, Andrea, Elena Aznar, María Dolores Marcos, Ramón Martínez-Máñez, Félix Sancenón, Juan Soto, José Manuel Barat, and Pedro Amorós. 2009. "Enzyme-responsive controlled release using mesoporous silica supports capped with lactose." *Angewandte Chemie* no. 121 (32):5998-6001.

[46] Singh, Neetu, Amrita Karambelkar, Luo Gu, Kevin Lin, Jordan S Miller, Christopher S Chen, Michael J Sailor, and Sangeeta N Bhatia. 2011. "Bioresponsive mesoporous silica nanoparticles for triggered drug release." *Journal of the American Chemical Society* no. 133 (49):19582-19585.

[47] Colilla, Montserrat, Blanca González, and María Vallet-Regí. 2013. "Mesoporous silica nanoparticles for the design of smart delivery nanodevices." *Biomaterials Science* no. 1 (2):114-134.

[48] Kresge, CT, ME Leonowicz, WJ Roth, JC Vartuli, and JS Beck. 1992. "Ordered mesoporous molecular sieves synthesized by a liquid-crystal template mechanism." *Nature*no. 359 (6397):710-712.

[49] Trewyn, Brian G, Igor I Slowing, Supratim Giri, Hung-Ting Chen, and Victor S Y Lin. 2007. "Synthesis and functionalization of a mesoporous silica nanoparticle based on

the sol–gel process and applications in controlled release." *Accounts of chemical research* no. 40 (9):846-853.

[50] Hoffmann, Frank, Maximilian Cornelius, Jürgen Morell, and Michael Fröba. 2006. "Silica-based mesoporous organic–inorganic hybrid materials." *Angewandte Chemie International Edition* no. 45 (20):3216-3251.

[51] Fangqiong, Tang, Li Linlin, and Chen Dong. 2012. "Mesoporous Silica Nanoparticles: Synthesis, Biocompatibility and Drug Delivery." *Advanced Materials* no. 24:1505-1534. doi: 10.1002/adma.201104763.

[52] Kwon, Sooyeon, Rajendra K Singh, Roman A Perez, Ensanya A Abou Neel, Hae-Won Kim, and Wojciech Chrzanowski. 2013. "Silica-based mesoporous nanoparticles for controlled drug delivery." *Journal of tissue engineering* no. 4:2041731413503357.

[53] Li, Zongxi, Jonathan C Barnes, Aleksandr Bosoy, J Fraser Stoddart, and Jeffrey I Zink. 2012. "Mesoporous silica nanoparticles in biomedical applications." *Chemical Society Reviews* no. 41 (7):2590-2605.

[54] Yang, Piaoping, Shili Gai, and Jun Lin. 2012. "Functionalized mesoporous silica materials for controlled drug delivery." *Chemical Society Reviews* no. 41 (9):3679-3698.

[55] Sadasivan, Sajanikumari, Deepa Khushalani, and Stephen Mann. 2003. "Synthesis and shape modification of organo-functionalised silica nanoparticles with ordered mesostructured interiors." *Journal of Materials Chemistry* no. 13 (5):1023-1029.

[56] Stöber, Werner, Arthur Fink, and Ernst Bohn. 1968. "Controlled growth of monodisperse silica spheres in the micron size range." *Journal of colloid and interface science* no. 26 (1):62-69.

[57] Slowing, Igor I, Brian G Trewyn, Supratim Giri, and VS-Y Lin. 2007. "Mesoporous silica nanoparticles for drug delivery and biosensing applications." *Advanced Functional Materials* no. 17 (8):1225-1236.

[58] Kar, Mrityunjoy, Neha Tiwari, Mitali Tiwari, Mayurika Lahiri, and Sayam Sen Gupta. 2013. "Poly-L-Arginine Grafted Silica Mesoporous Nanoparticles for Enhanced Cellular Uptake and their Application in DNA Delivery and Controlled Drug Release." *Particle & Particle Systems Characterization* no. 30 (2):166-179.

[59] Tiwari, Neha, Laxman Nawale, Dhiman Sarkar, and Manohar V Badiger. 2017. "Carboxymethyl Cellulose-Grafted Mesoporous Silica Hybrid Nanogels for Enhanced Cellular Uptake and Release of Curcumin." *Gels* no. 3 (1):8.

[60] Radu, Daniela R, Cheng-Yu Lai, Jianguo Huang, Xu Shu, and Victor S Y Lin. 2005. "Fine-tuning the degree of organic functionalization of mesoporous silica nanosphere materials via an interfacially designed co-condensation method." *Chemical Communications* (10):1264-1266.

[61] Huh, Seong, Hung-Ting Chen, Jerzy W Wiench, Marek Pruski, and Victor SY Lin. 2005. "Cooperative catalysis by general acid and base bifunctionalized mesoporous silica nanospheres." *Angewandte Chemie International Edition* no. 44 (12):1826-1830.

[62] Walcarius, Alain, Mathieu Etienne, and Bénédicte Lebeau. 2003. "Rate of access to the binding sites in organically modified silicates. 2. Ordered mesoporous silicas grafted with amine or thiol groups." *Chemistry of materials* no. 15 (11):2161-2173.

[63] Walcarius, Alain, Mathieu Etienne, Stéphanie Sayen, and Bénédicte Lebeau. 2003. "Grafted silicas in electroanalysis: amorphous versus ordered mesoporous materials." *Electroanalysis* no. 15 (5-6):414-421.

[64] Walcarius, Alain, Mathieu Etienne, and Jacques Bessière. 2002. "Rate of access to the binding sites in organically modified silicates. 1. Amorphous silica gels grafted with amine or thiol groups." *Chemistry of materials* no. 14 (6):2757-2766.

[65] Vivero-Escoto, Juan L, Rachel C Huxford-Phillips, and Wenbin Lin. 2012. "Silica-based nanoprobes for biomedical imaging and theranostic applications." *Chemical Society Reviews* no. 41 (7):2673-2685.

[66] Vinu, Ajayan, Kazi Zakir Hossain, and Katsuhiko Ariga. 2005. "Recent advances in functionalization of mesoporous silica." *Journal of Nanoscience and Nanotechnology* no. 5 (3):347-371.

[67] Lu, Jie, Monty Liong, Jeffrey I Zink, and Fuyuhiko Tamanoi. 2007. "Mesoporous silica nanoparticles as a delivery system for hydrophobic anticancer drugs." *Small* no. 3 (8):1341-1346.

[68] Slowing, Igor, Brian G Trewyn, and Victor S Y Lin. 2006. "Effect of surface functionalization of MCM-41-type mesoporous silica nanoparticles on the endocytosis by human cancer cells." *Journal of the American Chemical Society* no. 128 (46):14792-14793.

[69] Chung, Tsai-Hua, Si-Han Wu, Ming Yao, Chen-Wen Lu, Yu-Shen Lin, Yann Hung, Chung-Yuan Mou, Yao-Chang Chen, and Dong-Ming Huang. 2007. "The effect of surface charge on the uptake and biological function of mesoporous silica nanoparticles in 3T3-L1 cells and human mesenchymal stem cells." *Biomaterials* no. 28 (19):2959-2966.

[70] Huang, Dong-Ming, Yann Hung, Bor-Sheng Ko, Szu-Chun Hsu, Wei-Hsuan Chen, Chung-Liang Chien, Chih-Pin Tsai, Chieh-Ti Kuo, Ju-Chiun Kang, and Chung-Shi Yang. 2005. "Highly efficient cellular labeling of mesoporous nanoparticles in human mesenchymal stem cells: implication for stem cell tracking." *The FASEB journal* no. 19 (14):2014-2016.

[71] Trewyn, Brian G, Jennifer A Nieweg, Yannan Zhao, and Victor S Y Lin. 2008. "Biocompatible mesoporous silica nanoparticles with different morphologies for animal cell membrane penetration." *Chemical Engineering Journal* no. 137 (1):23-29.

[72] Mayor, Satyajit, and Richard E Pagano. 2007. "Pathways of clathrin-independent endocytosis." *Nature reviews Molecular cell biology* no. 8 (8):603-612.

[73] Conner, Sean D, and Sandra L Schmid. 2003. "Regulated portals of entry into the cell." *Nature* no. 422 (6927):37.

[74] Prokop, Ales, and Jeffrey M Davidson. 2008. "Nanovehicular intracellular delivery systems." *Journal of pharmaceutical sciences* no. 97 (9):3518-3590.

[75] Mornet, Stéphane, Olivier Lambert, Etienne Duguet, and Alain Brisson. 2005. "The formation of supported lipid bilayers on silica nanoparticles revealed by cryoelectron microscopy." *Nano letters* no. 5 (2):281-285.

[76] Gemeinhart, Richard A, Dan Luo, and W Mark Saltzman. 2005. "Cellular fate of a modular DNA delivery system mediated by silica nanoparticles." *Biotechnology progress* no. 21 (2):532-537.

[77] Xing, Xinli, Xiaoxiao He, Jiaofeng Peng, Kemin Wang, and Weihong Tan. 2005. "Uptake of silica-coated nanoparticles by HeLa cells." *Journal of nanoscience and nanotechnology* no. 5 (10):1688-1693.

[78] Gao, Huajian, Wendong Shi, and Lambert B Freund. 2005. "Mechanics of receptor-mediated endocytosis." *Proceedings of the National Academy of Sciences of the United States of America* no. 102 (27):9469-9474.

[79] Jiang, Wen, Betty YS Kim, James T Rutka, and Warren CW Chan. 2008. "Nanoparticle-mediated cellular response is size-dependent." *Nature nanotechnology* no. 3 (3):145-150.

[80] Radu, Daniela R, Cheng-Yu Lai, Ksenija Jeftinija, Eric W Rowe, Srdija Jeftinija, and Victor S Y Lin. 2004. "A polyamidoamine dendrimer-capped mesoporous silica nanosphere-based gene transfection reagent." *Journal of the American Chemical Society* no. 126 (41):13216-13217.

[81] Lu, Jie, Monty Liong, Sean Sherman, Tian Xia, Michael Kovochich, Andre E Nel, Jeffrey I Zink, and Fuyuhiko Tamanoi. 2007. "Mesoporous silica nanoparticles for cancer therapy: energy-dependent cellular uptake and delivery of paclitaxel to cancer cells." *Nanobiotechnology* no. 3 (2):89-95.

[82] Maxfield, Frederick R, and Timothy E McGraw. 2004. "Endocytic recycling."*Nature reviews. Molecular cell biology* no. 5 (2):121.

[83] Xu, Shi, Bogdan Z Olenyuk, Curtis T Okamoto, and Sarah F Hamm-Alvarez. 2013. "Targeting receptor-mediated endocytotic pathways with nanoparticles: rationale and advances." *Advanced drug delivery reviews* no. 65 (1):121-138.

[84] Knežević, Nikola Ž, and Jean-Olivier Durand. 2015. "Targeted treatment of cancer with nanotherapeutics based on mesoporous silica nanoparticles." *ChemPlusChem* no. 80 (1):26-36.

[85] van Vlerken, Lilian E, Zhenfeng Duan, Michael V Seiden, and Mansoor M Amiji. 2007. "Modulation of intracellular ceramide using polymeric nanoparticles to overcome multidrug resistance in cancer." *Cancer research* no. 67 (10):4843-4850.

[86] Matsumura, Yasuhiro, and Hiroshi Maeda. 1986. "A new concept for macromolecular therapeutics in cancer chemotherapy: mechanism of tumoritropic accumulation of proteins and the antitumor agent smancs." *Cancer research* no. 46 (12 Part 1):6387-6392.

[87] Martínez-Carmona, Marina, Montserrat Colilla, and Maria Vallet-Regí. 2015. "Smart mesoporous nanomaterials for antitumor therapy."*Nanomaterials* no. 5 (4):1906-1937.

[88] Meng, Huan, Min Xue, Tian Xia, Zhaoxia Ji, Derrick Y Tarn, Jeffrey I Zink, and Andre E Nel. 2011. "Use of size and a copolymer design feature to improve the

biodistribution and the enhanced permeability and retention effect of doxorubicin-loaded mesoporous silica nanoparticles in a murine xenograft tumor model." *ACS nano* no. 5 (5):4131-4144.

[89] Cauda, Valentina, Christian Argyo, and Thomas Bein. 2010. "Impact of different PEGylation patterns on the long-term bio-stability of colloidal mesoporous silica nanoparticles." *Journal of Materials Chemistry* no. 20 (39):8693-8699.

[90] Cauda, Valentina, Axel Schlossbauer, and Thomas Bein. 2010. "Bio-degradation study of colloidal mesoporous silica nanoparticles: effect of surface functionalization with organo-silanes and poly (ethylene glycol)." *Microporous and Mesoporous Materials* no. 132 (1):60-71.

[91] Brannon-Peppas, Lisa, and James O Blanchette. 2004. "Nanoparticle and targeted systems for cancer therapy." *Advanced drug delivery reviews* no. 56 (11):1649-1659.

[92] Sudimack, Jennifer, and Robert J Lee. 2000. "Targeted drug delivery via the folate receptor." *Advanced drug delivery reviews* no. 41 (2):147-162.

[93] Rosenholm, Jessica M, Annika Meinander, Emilia Peuhu, Rasmus Niemi, John E Eriksson, Cecilia Sahlgren, and Mika Lindén. 2008. "Targeting of porous hybrid silica nanoparticles to cancer cells." *ACS nano* no. 3 (1):197-206.

[94] Qi, Xinmeng, Dan Yu, Bo Jia, Chunshun Jin, Xueshibojie Liu, Xue Zhao, and Guangxin Zhang. 2016. "Targeting CD133+ laryngeal carcinoma cells with chemotherapeutic drugs and siRNA against ABCG2 mediated by thermo/pH-sensitive mesoporous silica nanoparticles." *Tumor Biology* no. 37 (2):2209-2217.

[95] Zhang, Jing, Zhe-Fan Yuan, Ya Wang, Wei-Hai Chen, Guo-Feng Luo, Si-Xue Cheng, Ren-Xi Zhuo, and Xian-Zheng Zhang. 2013. "Multifunctional envelope-type mesoporous silica nanoparticles for tumor-triggered targeting drug delivery." *Journal of the American Chemical Society* no. 135 (13):5068-5073.

[96] Brevet, David, Magali Gary-Bobo, Laurence Raehm, Sébastien Richeter, Ouahiba Hocine, Kassem Amro, Bernard Loock, Pierre Couleaud, Céline Frochot, and Alain Morère. 2009. "Mannose-targeted mesoporous silica nanoparticles for photodynamic therapy." *Chemical Communications* (12):1475-1477.

[97] Tarn, Derrick, Carlee E Ashley, Min Xue, Eric C Carnes, Jeffrey I Zink, and C Jeffrey Brinker. 2013. "Mesoporous silica nanoparticle nanocarriers: biofunctionality and biocompatibility." *Accounts of chemical research* no. 46 (3):792-801.

[98] Asefa, Tewodros, and Zhimin Tao. 2012. "Biocompatibility of mesoporous silica nanoparticles." *Chemical research in toxicology* no. 25 (11):2265-2284.

[99] Slowing, Igor I, Chia-Wen Wu, Juan L Vivero-Escoto, and Victor SY Lin. 2009. "Mesoporous silica nanoparticles for reducing hemolytic activity towards mammalian red blood cells." *Small* no. 5 (1):57-62.

[100] Yu, Tian, Alexander Malugin, and Hamidreza Ghandehari. 2011. "Impact of silica nanoparticle design on cellular toxicity and hemolytic activity." *ACS nano* no. 5 (7):5717-5728.

[101] Fubini, Bice, Ivana Fenoglio, Zoe Elias, and Odile Poirot. 2001. "Variability of biological responses to silicas: effect of origin, crystallinity, and state of surface on

generation of reactive oxygen species and morphological transformation of mammalian cells." *Journal of environmental pathology, toxicology and oncology* no. 20 (Suppl. 1).

[102] Lin, Yu-Shen, and Christy L Haynes. 2009. "Synthesis and characterization of biocompatible and size-tunable multifunctional porous silica nanoparticles." *Chemistry of Materials* no. 21 (17):3979-3986.

[103] Lin, Yu-Shen, and Christy L Haynes. 2010. "Impacts of mesoporous silica nanoparticle size, pore ordering, and pore integrity on hemolytic activity." *Journal of the American Chemical Society* no. 132 (13):4834-4842.

[104] Hudson, Sarah P, Robert F Padera, Robert Langer, and Daniel S Kohane. 2008. "The biocompatibility of mesoporous silicates." *Biomaterials* no. 29 (30):4045-4055.

[105] Nash, T, AC Allison, and JS Harington. 1966. "Physico-chemical properties of silica in relation to its toxicity." *Nature* 210, 259–261.

[106] Van Schooneveld, Matti M, Esad Vucic, Rolf Koole, Yu Zhou, Joanne Stocks, David P Cormode, Cheuk Y Tang, Ronald E Gordon, Klaas Nicolay, and Andries Meijerink. 2008. "Improved biocompatibility and pharmacokinetics of silica nanoparticles by means of a lipid coating: a multimodality investigation." *Nano letters* no. 8 (8):2517-2525.

[107] He, Xiaoxiao, Hailong Nie, Kemin Wang, Weihong Tan, Xu Wu, and Pengfei Zhang. 2008. "In vivo study of biodistribution and urinary excretion of surface-modified silica nanoparticles."*Analytical chemistry* no. 80 (24):9597-9603.

[108] He, Qianjun, Jiamin Zhang, Jianlin Shi, Ziyan Zhu, Linxia Zhang, Wenbo Bu, Limin Guo, and Yu Chen. 2010. "The effect of PEGylation of mesoporous silica nanoparticles on nonspecific binding of serum proteins and cellular responses." *Biomaterials* no. 31 (6):1085-1092.

[109] Park, Ji-Ho, Luo Gu, Geoffrey Von Maltzahn, Erkki Ruoslahti, Sangeeta N Bhatia, and Michael J Sailor. 2009. "Biodegradable luminescent porous silicon nanoparticles for in vivo applications." *Nature materials* no. 8 (4):331.

[110] Argyo, Christian, Veronika Weiss, Christoph Bräuchle, and Thomas Bein. 2013. "Multifunctional mesoporous silica nanoparticles as a universal platform for drug delivery." *Chemistry of materials* no. 26 (1):435-451.

[111] Natarajan, Siva Kumar, and Stalin Selvaraj. 2014. "Mesoporous silica nanoparticles: importance of surface modifications and its role in drug delivery." *RSC advances* no. 4 (28):14328-14334.

[112] Gan, Qi, Xunyu Lu, Yuan Yuan, Jiangchao Qian, Huanjun Zhou, Xun Lu, Jianlin Shi, and Changsheng Liu. 2011. "A magnetic, reversible pH-responsive nanogated ensemble based on Fe 3 O 4 nanoparticles-capped mesoporous silica." *Biomaterials* no. 32 (7):1932-1942.

[113] Ferris, Daniel P, Yan-Li Zhao, Niveen M Khashab, Hussam A Khatib, J Fraser Stoddart, and Jeffrey I Zink. 2009. "Light-operated mechanized nanoparticles." *Journal of the American Chemical Society* no. 131 (5):1686-1688.

[114] Muhammad, Faheem, Mingyi Guo, Wenxiu Qi, Fuxing Sun, Aifei Wang, Yingjie Guo, and Guangshan Zhu. 2011. "pH-triggered controlled drug release from mesoporous

silica nanoparticles via intracelluar dissolution of ZnO nanolids." *Journal of the American chemical society* no. 133 (23):8778-8781.

[115] Cauda, Valentina, Hanna Engelke, Anna Sauer, Delphine Arcizet, Joachim Rädler, and Thomas Bein. 2010. "Colchicine-loaded lipid bilayer-coated 50 nm mesoporous nanoparticles efficiently induce microtubule depolymerization upon cell uptake." *Nano letters* no. 10 (7):2484-2492.

[116] Liu, Rui, Puhong Liao, Jikai Liu, and Pingyun Feng. 2011. "Responsive polymer-coated mesoporous silica as a pH-sensitive nanocarrier for controlled release." *Langmuir* no. 27 (6):3095-3099.

[117] Liu, Juewen, Alison Stace-Naughton, Xingmao Jiang, and C Jeffrey Brinker. 2009. "Porous nanoparticle supported lipid bilayers (protocells) as delivery vehicles." *Journal of the American Chemical Society* no. 131 (4):1354-1355.

[118] Akinc, Akin, Mini Thomas, Alexander M Klibanov, and Robert Langer. 2005. "Exploring polyethylenimine-mediated DNA transfection and the proton sponge hypothesis." *The journal of gene medicine* no. 7 (5):657-663.

[119] Sun, Ruijuan, Wenqian Wang, Yongqiang Wen, and Xueji Zhang. 2015. "Recent advance on mesoporous silica nanoparticles-based controlled release system: Intelligent switches open up new horizon." *Nanomaterials* no. 5 (4):2019-2053.

[120] Zhao, Qinfu, Chen Wang, Ying Liu, Jiahong Wang, Yikun Gao, Xiaojing Zhang, Tongying Jiang, and Siling Wang. 2014. "PEGylated mesoporous silica as a redox-responsive drug delivery system for loading thiol-containing drugs." *International journal of pharmaceutics* no. 477 (1):613-622.

[121] Giménez, Cristina, Cristina de la Torre, Mónica Gorbe, Elena Aznar, Félix Sancenón, Jose R Murguía, Ramón Martínez-Máñez, M Dolores Marcos, and Pedro Amorós. 2015. "Gated mesoporous silica nanoparticles for the controlled delivery of drugs in cancer cells." *Langmuir* no. 31 (12):3753-3762.

[122] Palanikumar, L, Eun Seong Choi, Jae Yeong Cheon, Sang Hoon Joo, and Ja-Hyoung Ryu. 2015. "Noncovalent polymer-gatekeeper in mesoporous silica nanoparticles as a targeted drug delivery platform."*Advanced Functional Materials* no. 25 (6):957-965.

[123] Cui, Yanna, Haiqing Dong, Xiaojun Cai, Deping Wang, and Yongyong Li. 2012. "Mesoporous silica nanoparticles capped with disulfide-linked PEG gatekeepers for glutathione-mediated controlled release." *ACS applied materials & interfaces* no. 4 (6):3177-3183.

[124] Chen, Tianchan, Wei Wu, Hong Xiao, Yanxiao Chen, Min Chen, and Jianshu Li. 2015. "Intelligent drug delivery system based on mesoporous silica nanoparticles coated with an ultra-pH-sensitive gatekeeper and Poly (ethylene glycol)." *Acs Macro Letters* no. 5 (1):55-58.

[125] You, Ye-Zi, Kennedy K Kalebaila, Stephanie L Brock, and David Oupicky. 2008. "Temperature-controlled uptake and release in PNIPAM-modified porous silica nanoparticles." *Chemistry of Materials* no. 20 (10):3354-3359.

[126] Feng, Wei, Xiaojun Zhou, Chuanglong He, Kexin Qiu, Wei Nie, Liang Chen, Hongsheng Wang, Xiumei Mo, and Yanzhong Zhang. 2013. "Polyelectrolyte

multilayer functionalized mesoporous silica nanoparticles for pH-responsive drug delivery: layer thickness-dependent release profiles and biocompatibility." *Journal of Materials Chemistry B* no. 1 (43):5886-5898.

[127] Hu, Xiaoxi, Yun Wang, and Bo Peng. 2014. "Chitosan-Capped Mesoporous Silica Nanoparticles as pH-Responsive Nanocarriers for Controlled Drug Release." *Chemistry–An Asian Journal* no. 9 (1):319-327.

[128] Hu, Liang, Changshan Sun, Aihua Song, Di Chang, Xin Zheng, Yikun Gao, Tongying Jiang, and Siling Wang. 2014. "Alginate encapsulated mesoporous silica nanospheres as a sustained drug delivery system for the poorly water-soluble drug indomethacin." *Asian journal of pharmaceutical sciences* no. 9 (4):183-190.

[129] Zhao, Qinfu, Shengyu Wang, Yang Yang, Xian Li, Donghua Di, Chungang Zhang, Tongying Jiang, and Siling Wang. 2017. "Hyaluronic acid and carbon dots-gated hollow mesoporous silica for redox and enzyme-triggered targeted drug delivery and bioimaging." *Materials Science and Engineering: C* no. 78:475-484.

[130] Zhu, Yufang, Wenjun Meng, Hong Gao, and Nobutaka Hanagata. 2011. "Hollow mesoporous silica/poly (L-lysine) particles for codelivery of drug and gene with enzyme-triggered release property." *The Journal of Physical Chemistry C* no. 115 (28):13630-13636.

[131] Tukappa, Asha, Amelia Ultimo, Cristina de la Torre, Teresa Pardo, Félix Sancenón, and Ramón Martínez-Máñez. 2016. "Polyglutamic acid-gated mesoporous silica nanoparticles for enzyme-controlled drug delivery." *Langmuir* no. 32 (33):8507-8515.

[132] Agostini, Alessandro, Laura Mondragón, Lluis Pascual, Elena Aznar, Carmen Coll, Ramón Martínez-Máñez, Félix Sancenón, Juan Soto, M Dolores Marcos, and Pedro Amorós. 2012. "Design of enzyme-mediated controlled release systems based on silica mesoporous supports capped with ester-glycol groups." *Langmuir* no. 28 (41):14766-14776.

[133] DenizáYilmaz, M, and J FraseráStoddart. 2015. "Esterase-and pH-responsive poly (β-amino ester)-capped mesoporous silica nanoparticles for drug delivery." *Nanoscale* no. 7 (16):7178-7183.

[134] Van Rijt, Sabine H, Deniz A Bőlükbas, Christian Argyo, Stefan Datz, Michael Lindner, Oliver Eickelberg, Melanie Königshoff, Thomas Bein, and Silke Meiners. 2015. "Protease-mediated release of chemotherapeutics from mesoporous silica nanoparticles to ex vivo human and mouse lung tumors." *ACS nano* no. 9 (3):2377-2389.

[135] de la Torre, Cristina, Laura Mondragón, Carmen Coll, Félix Sancenón, María D Marcos, Ramón Martínez-Máñez, Pedro Amorós, Enrique Pérez-Payá, and Mar Orzáez. 2014. "Cathepsin-B Induced Controlled Release from Peptide-Capped Mesoporous Silica Nanoparticles." *Chemistry-A European Journal* no. 20 (47):15309-15314.

[136] Xiao, Yu, Tao Wang, Yu Cao, Xue Wang, Ye Zhang, Yunling Liu, and Qisheng Huo. 2015. "Enzyme and voltage stimuli-responsive controlled release system based on β-cyclodextrin-capped mesoporous silica nanoparticles." *Dalton Transactions* no. 44 (9):4355-4361.

[137] Mas, Núria, Alessandro Agostini, Laura Mondragón, Andrea Bernardos, Félix Sancenón, M Dolores Marcos, Ramón Martínez-Máñez, Ana M Costero, Salvador Gil, and Matilde Merino-Sanjuán. 2013. "Enzyme-Responsive Silica Mesoporous Supports Capped with Azopyridinium Salts for Controlled Delivery Applications." *Chemistry-A European Journal* no. 19 (4):1346-1356.

[138] Zhang, Guilong, Minglei Yang, Dongqing Cai, Kang Zheng, Xin Zhang, Lifang Wu, and Zhengyan Wu. 2014. "Composite of functional mesoporous silica and DNA: an enzyme-responsive controlled release drug carrier system." *ACS applied materials & interfaces* no. 6 (11):8042-8047.

[139] Qian, Ruocan, Lin Ding, and Huangxian Ju. 2013. "Switchable fluorescent imaging of intracellular telomerase activity using telomerase-responsive mesoporous silica nanoparticle." *Journal of the American Chemical Society* no. 135 (36):13282-13285.

[140] Agostini, Alessandro, Laura Mondragón, Andrea Bernardos, Ramón Martínez-Máñez, M Dolores Marcos, Félix Sancenón, Juan Soto, Ana Costero, Cristina Manguan-García, and Rosario Perona. 2012. "Targeted cargo delivery in senescent cells using capped mesoporous silica nanoparticles." *Angewandte Chemie International Edition* no. 51 (42):10556-10560.

[141] Park, Chiyoung, Hyehyeon Kim, Saehee Kim, and Chulhee Kim. 2009. "Enzyme responsive nanocontainers with cyclodextrin gatekeepers and synergistic effects in release of guests." *Journal of the American Chemical Society* no. 131 (46):16614-16615.

[142] Zhang, Yuanxin, Zhiyao Hou, Yakun Ge, Kerong Deng, Bei Liu, Xuejiao Li, Quanshun Li, Ziyong Cheng, Ping'an Ma, and Chunxia Li. 2015. "DNA-hybrid-gated photothermal mesoporous silica nanoparticles for NIR-responsive and aptamer-targeted drug delivery."

[143] Yu, Meihua, Siddharth Jambhrunkar, Peter Thorn, Jiezhong Chen, Wenyi Gu, and Chengzhong Yu. 2013. "Hyaluronic acid modified mesoporous silica nanoparticles for targeted drug delivery to CD44-overexpressing cancer cells." *Nanoscale* no. 5 (1):178-183.

[144] Wu, Yuanhao, Yubo Long, Qing-Lan Li, Shuying Han, Jianbiao Ma, Ying-Wei Yang, and Hui Gao. 2015. "Layer-by-layer (LBL) self-assembled biohybrid nanomaterials for efficient antibacterial applications." *ACS applied materials & interfaces* no. 7 (31):17255-17263.

In: Advances in Polymers for Biomedical Applications ISBN: 978-1-53613-612-8
Editors: Deepak Pathania and Bhuvanesh Gupta 

*Chapter 3*

# BIODEGRADABLE SHAPE MEMORY POLYURETHANE AND ITS NANOCOMPOSITES FOR BIOMEDICAL APPLICATIONS

***Dheeraj Ahuja and Anupama Kaushik*[1,*]**
[1]Dr. S.S. Bhatnagar University Institute of Chemical Engineering,
Panjab University, Chandigarh, India

## ABSTRACT

Since last three decades polymeric biometrials are being replaced by biodegradable shape-memory polymers and its nanocomposites for biomedical applications becasuse of their good mechanical properties, controlled drug delievery, steralization capability, biodegradability, biocompatability and dual shape capability i.e., they can change their shape from shape I to shape II on intorduction of an appropriate external stimuli. Among various shape memory polymers, biodegradable polyurethanes with shape memory effect are in great demand as their physical and chemical properties can be varied in a controlled way by varying the percentage of the composition of soft and hard segments that helps in adjusting the shape recovery temperature of shape memory polyurethane near to the body temperature i.e., 37–40°C.

This study provides a comprehensive review that integrates the breakthroughs in studying biodegradable shape memory polyurethane (SMPU) and their derivatives, such as composites and compound structures, as well as their current applications. Concepts, principles/modeling, structures and related synthesis methods, applications and future trends are also reviewed.

**Keywords:** shape memory polymers, nanocomposites, SMPU, biodegradable polyurethanes, stents, medical implants

[*] Corresponding Author: Dr. Dheeraj Ahuja Email: anupamachem@gmail.com.

## 1. INTRODUCTION

Shape-memory materials, including shape-memory alloys [1–3, 4, 5], ceramics [6, 7, 8–12], hydrogels [13–15, 16], and shape memory polymers [17–20, 4, 21, 22], have found wide applications in various fields, such as sensors, transducers, actuators and medical implants [23–27, 28, 29]. In order to qualify as a shape memory material it should possess shape memory effects. Shape memory effects are those in which a material can be deformed and fixed into temporary shape and can return to original permanent shape under cyclic conditions of loading/unloading and thermal swings. Shape memory effect caused by thermal stimuli are more common as in this the recovery takes place with respect to a certrain critical temperature. The first shape memory effect induced smart material was first discovered by Chang and Read in 1932 [23, 26, 27, 30]. Though shape memory materials based on alloys possess excellent mechanical properties and have found a ample of technical applications [15, 31] but then also they have been replaced by ceramics [30, 32] and polymers [31, 33] based shape memory polymers because of the high manufacturing cost, narrow recoverable deformation and appreciable toxicity [23, 8, 17, 34, 35].

A great deal of attention is being focused towards shape memory polymers for the development of smart materials because of their varying mechanical properties and higher degree of deformation offered along with low cost, light weight and easy processibility [36–38, 8, 39, 40]. Further, an added advantage offered by polymers is that they are resistant to chemicals, non toxic, biocompatible and can be made biodegradable [41, 42]. Different kinds of shape memory polymers have been reported and developed after the development of “Polynorbornene” the first shape memory polymer developed by CDF Chimie company (France) in 1984.

Shape memory polymers are those that can adopt a new temporary shape and revert back to original shape under the influence of an external stimulus. In these cases, the shape memory performance not only depends on the molecular structure, but also on the mode of deformation and the programming of the stimulus application process [43, 44, 45]. Obtaining a new shape is dependent on both the nature of stimulus and the mode of deformation. On the other hand, regaining the original shape is always dictated by how the stimulus is applied. The stimulus here refers to heat, light, chemical reaction, electricity, and magnetism. This may be applied independently, e.g., only heat or light, or in complex combinations [17, 46]. The process is shown in Figure 1.

The material having shape memory property should have atleast two independent or synergitically working phased among which one phase should be reversible while the other shall be in the active range of the stimulus [47–49, 50]. Therefore shape memory effects are accomplished during a transition stage i.e., where the reversible phase undergoes changes from temporary to permanent shape and a permananet shape can be acheieved by polymer chains on deformation during this transition state. However it should be noted that on attainment of temporary shape stimulus should be taken away rapidly for achieving the desired form because if the stimulus takes longer time to return to the reference state, polymer chains can relax leading to the poorer shape memory performance [51, 52, 45, 53]. For example, low thermal conductivity of polymers in case of thermal gradients leads to slower cooling and heating where the elastically stored energy [54, 55] plays an important role in

shape memory performances as the polymer chains store an important part of energy during deformation which is used to recover the original shape upon the application of the stimulus. The heat dissipation is another important factor. One more important factor that accounts for shape loss is heat dissipation during deformation and recovery in a single shape memory cycle. However, this type of loss depends on the rheological properties of the materials [56–58, 59]. Stretching/deformation temperature and extent of deformation/strain level along with rheological properties of polymer are the most critical conditions used to determine the recovery force and extent of shape useful in deciding suitable applications of the shape memory polymers. For example magnitude of recovery stress developed by polymers needs to be evaluated carefully while replacing shape memory alloys with shape memory polyurethanes.

Shape memory effects are possessed by a variety of polymers such as theroplastics based on polyethylene and polystyrene copolymers and thermosets based on polyurethanes and polyepoxides [60, 61, 62]. Polyurethanes with shape memory effects have become the most popular among these polymers because of their unique properties such as high shape recoverability with a maximum recoverable strain of >400%, wide range of shape recovery temperature from -30 to 70°C, good processing ability and excellent biocompatiblity [63, 27]. Some other characteristics of the shape memory polyurethanes (SMPU's) that make them prominent material as compared to other shape memory polymers are biodegradability, vast possibilities for synthesis and production from readily available commercial raw materials, and affordable cost.

Shape memory polyurethanes (SMPU's) are one of the most popular groups of materials applied for biomedical applications [63, 64, 65] which may be attributed to their segmented block copolymeric character that endows them for a wide range of versatility in terms of tailoring their physical properties, blood and tissue compatibility [66, 67, 68, 69]. They are usually thermo-responsive, i.e., their temporary deformation can be eliminated and their permanent shape can be restored at a critical temperature (referred as transition temperature or switching temperature), which can be either the glass transition ($T_g$) or the melting temperature ($T_m$) of the materials [70, 71]. Singhal et al. synthesiszed polyurethanes foams with shape memory effecs for embolic biomedical applications [71, 71].

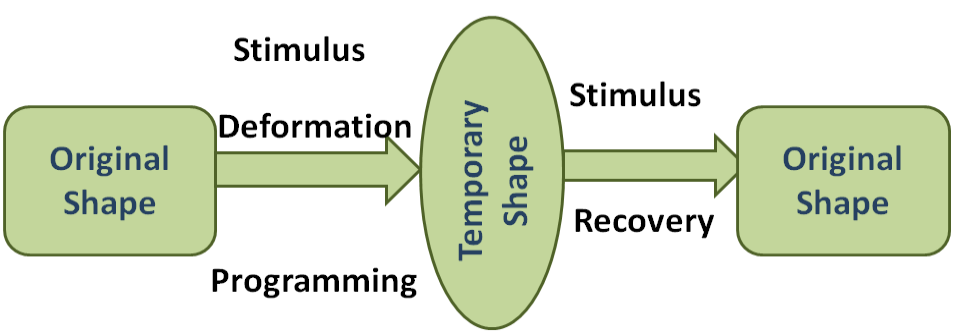


Figure 1. Process of Shape memory polymer.

The usage of polyurethanes as SMPs suffers from several challenges such as thermal degradation, hydrolytic degradation, low stiffness and a dimensional instability after processing leading to the insufficient recovery stress, long recovery time and in some cases low value of shape fixity [71]. The low stiffness of SMPUs results in a relatively small recovery force under constraint (actuation force) compared to alternative active actuation materials or schemes [72]. Thus, in some applications, SMPUs may not generate sufficient recovery force to be viable. This drawback can be overcome by use of high modulud organic or inorganic fillers such as glass fibers [73], ceramic filler, poly (D,L-lactide) [74], silsequioxanes [75, 76], celite [30, 44], carbon nanotubes [44], carbon nanofibers [15], cellulose nanofibers [15, 77] and nanoclay [30] particles to the polymer matrix.

This chapter highlights the critical review of the shape memory polyurethanes and its nanocomposites, their behaviour, properties and application with a special focus on the applications of shape memory polyurethanes in biomedical domain.

## 2. SHAPE MEMORY POLYURETHANES (SMPUS)

Shape memory polyurethane also known as segmented polyurethanes are stimuli-responsive materials i.e., they have the capability of changing their shape upon application of an external stimulus. This stimulus can be heat, stress, magnetic fields, electric fields, pH values, UV light, and even water. Shape memory polyurethanes are generally synthesiszed by polycondensation reaction of macropolyols with polydiiscocyanates consisiting of a two phase structure: semicrystalline and the rigid hard segment dispersed in matrix of soft segments as shown in figure 2 [78].

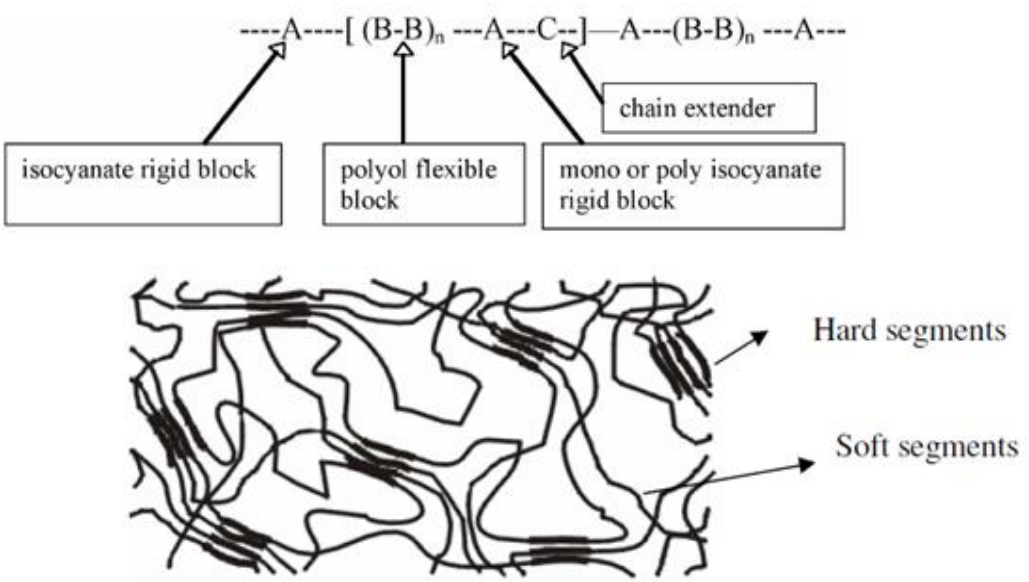


Figure 2. Polyurethane structure showing hard segment dispersed in soft crystallizable phase [55].

Hard segment bundles are formed by the phase separation process. These bundles act as multifunctional physical netpoints because of their higher glass transition temperature ($T_g$) or melting temperature ($T_m$) than the soft segment. Soft segment is the amoprphous matrix with low glass transition temperature. The hard segments mainly consist of the diisocyanate; either aromatic or aliphatic and the chain extender while the soft segments are sequence of macroglycol moieties which are used to maintain the temporary shape [15, 79, 80]. The soft segments, which arise from high-molecular-weight polyols like polyester, polycarbonate, or polyether macroglycols, provide rubbery properties to the resultant polymer. Hard segments have high density of urethane groups with high polarity are rigid at room temperature while soft segments having low polarity and less dense in urethane groups are flexible. The thermodynamically incompatible hard and soft segments are combined end-to-end through covalent urethane bonds making polyurethanes as multiblock copolymers. The differences in polarity between the hard and soft segments render these regions incompatible separation at molecular level, producing a microphase separated structure which results in unique elastomeric properties. Chain extenders are generally low molecular weight diols or diamines used to further couple these pre-polymers [81, 82].

## 3. MECHANISM OF GENERATION OF THERMORESPONSIVE SHAPE MEMORY EFFECTS IN SEGMENTED POLYURETHANES

Thermoresponsive shape memory effects are induced when the change in shape is due to change in temperature. The segmented polyurethanes are conventionally processed for its *permanent shape* followed by deformation to the intended *temporary shape* and recovers to the permanent shape. The polymer maintains this temporary shape until the shape change into the permanent form is activated by a predetermined external stimulus. The mechanism of the shape memory effetcs depends on the molecular network structure of polymers. Original and temporary shape is fixed by interactions between the switching segmetnts. The polymer network consists of molecular switches and netpoints. The netpoints determine the permanent shape of the polymer network and can be of a chemical (covalent bonds) or physical (intermolecular interactions) nature. Physical cross-linking is obtained in a polymer whose morphology consists of at least two segregated domains. Here, domains related to the highest thermal transition temperature ($T_{perm}$) act as netpoints (a hard segment), while chain segments in domains with the second highest thermal transition ($T_{trans}$) act as molecular switches (a switching segment). If the working temperature is higher than $T_{trans}$, then the switching domains are flexible, resulting in an entropic elastic behavior of the polymer network above $T_{trans}$. If the sample has been previously deformed by application of an external stress, it snaps back into its initial shape once the external stress is released. The molecular mechanism of the shape-memory effect is illustrated for the thermally induced shape-memory effect in Figure 3 [83]. The shape-memory polymer network consists of covalent netpoints and switching segments based on a physical interaction [44].

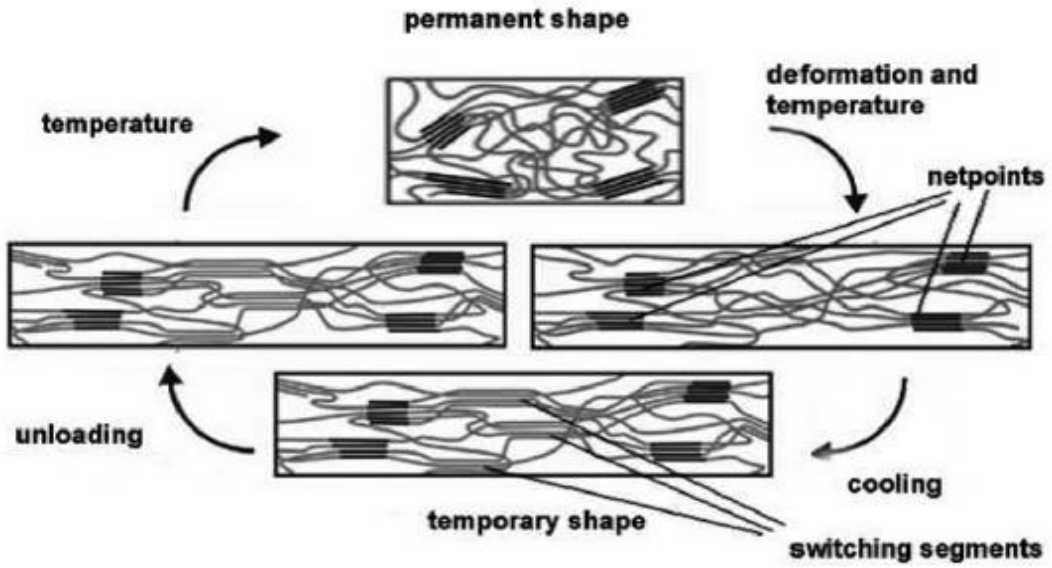


Figure 3. Mechanism of thermally induced shape memory effect [84–88].

## 4. BEHAVIOR AND PERFORMANCE OF SHAPE MEMORY POLYURETHANES (SMPUS)

Microphase seperation and stimulus response is governed by a variety of chemical and structural factors such as chemical structure, number average molecular weight and molecular weight distribution of soft segments, chemical structure and symmetry of the diisocyanate compound, chemical structure of the chain extender, average chain length and length distribution of hard segments, hard/soft segment ratio in the copolymer [34], crystallizability of hard and soft segments [89], extent of competitive hydrogen bonding between hard–hard and hard–soft segments, inherent solubility between hard and soft segments [34], method/polymerization procedure used during the synthesis and the nature of the interfacial region between the soft segment matrix and hard segment domains [89]. By adjusting the molecular weight of the macrodiol moiety and the molar ratio of the soft-to-hard segment, the shape recovery temperature of polyurethane can be successfully adjusted to 37-40$^{o}$C.

Brownian motion and the restricted molecular motion of the soft segment due to the crystalline hard-segment phase leads to the rubber elasticity in these shape memory polyurethanes between the glass transition temperature of soft segment ($T_g$) and the melting temperature of the hard segment ($T_m$) [89]. Once they are deformed in the temperature range between $T_g$ and $T_m$ and subsequently cooled below $T_g$ under a constant strain, the deformed shape is fixed because their micro-Brownian movements are frozen. When they are reheated to a temperature above $T_g$, a shape-memory effect is observed. That is, the original shape is recovered by the elastic force stored during the deformation [90].

Generally, the shape recovery temperature of a medical device is in the vicinity of $T_g$ if its shape memory is based on glass transition [55, 91, 92]. When its $T_g$ is above body temperature, it is necessary to heat the device to a temperature above the $T_g$ value of the

polymer to achieve shape recovery [81, 82]. In this case, the shape-recovered device can retain a high enough rigidity and strength at body temperature, because it is in the glass state. However, heating a medical device that has been implanted in the human body is difficult for many medical applications. If the $T_g$ is equal to or below body temperature, then body temperature can promote the shape recovery process. However, the mechanical strength will be lost at body temperature because the material is in the rubber state. Furthermore, if $T_g$ of a polymer device is much below body temperature, the deformed device should be stored at a temperature below room temperature. This is not convenient. Therefore, it is desirable to have a polymer device with $T_g$ in the vicinity of human body temperature [83].

Thermo-responsive segmented polyurethanes get deformed at a temperature above transition temperature (which can be glass transition, $T_g$ or melting temperature, $T_m$) and suddenly cooled to a temperature below *transition temperature*, the deformed shape becomes frozen. When it is heated above *transition temperature*, the polymer recovers its original shape [93, 94]. Because of the ability of thermo-responsive segmental polyurethanes to recover shape at critical temperature large bulky devices could thus potentially be introduced into the body in a compressed temporary shape by means of minimally invasive surgery and then expand to their permanent shape to fit as required [95]. This property is very useful in cardiovascular stents and sutures. Therefore, shape memory polymers have come to the focal point over the last decade as proposed materials for biomedical implants [82]. Potential biodegradability is an additional functionality of shape memory polymers that can prevent a second surgery for device explantation. With good biodegradability, they would neither stay in the human body for a very long time nor require a second surgery to be removed from the human body. With shape-memory property and a recovery near body temperature, the handling of the corresponding medical devices would be easy.

For medical implantations, the shape-memory polymers are expected to be both biodegradable and to have a recovery temperature near the human body temperature. With good bio-degradability, they neither stay in the human body for a long time nor require a second surgery to be removed from the human body. With a room (recovery) temperature value near body temperature, the handling of the corresponding medical devices would be easy. The temporary deformation may be realized near room temperature, and the original shape may be recovered automatically when the device is implanted into the human body.

Performance of shape memory effects in shape memory polyurethanes can be determined by computing the strain recovery ratio, strain or shape fixity Recovery stress, and Shape recovery time rate from stress vs strain curve obtained from the cyclic conditions of loading/unloading and thermal changes.

Strain recovery ratio is defined as level of deformation recovered on applying the thermal stimuli while rcovering the permanent shape or it may also be defined as the ability of a material to memorize its permanent shape [81].

Shape or strain fixity is the ratio of deformation (e.g., elongation) before and after the temporary shape is formed upon the completion of deformation [55]. In the case of thermal activation, e.g., heat as stimulus, the temporary shape is obtained by heating up the polymer above the activation temperature, stretching it, and then rapidly cooling it below the activation temperature with the load in place. After the specimen is cooled, the stretching force is removed. Because of the inevitable relaxation in some cases, the length of the stretched specimen at the end of deformation and after cooling is not the same. Consequently, the value of shape fixity is less than unity.

Recovery stress is defined as the stress needed to hold a restrained specimen at fixed dimensions while the specimen attempts to undergo shape recovery upon application of the stimulus [96–99]. This is an important qualifying parameter to project particular applications of SMPs. For example, recovery stress in the range of 150-300 MPa are produced by SMAs, while 1-3 MPa by many SMPs [100].

Shape recovery time is another significant property of SMPs which refers to the time that an SMP takes to recover from a strained state (temporary shape) to the original state (permanent shape) [101]. This is possible, so that the SMP article undergoes the fastest recovery of its temporary shape upon application of the stimulus. A typical recovery time for SMPs may be around a few minutes, while it is less than one second for SMAs. Attempts to shorten the recovery time have not met with much success.

Hence it is concluded that the shape memory polyurethanes (SMPU) exhibit remarkable shape memory effects (SME), due to microphase segregation [102]. This is very much interrelated to the chemical nature and the production method of polyurethanes. Typical polyurethanes are produced via insertion polymerization by which the polymerization results in thermodynamically incompatible blocks of hard and soft segments. Thus, this incompatibility creates a system in which different blocks constitute separate phases and form microdomains. This inherent structure of polyurethanes facilitates thermal activation of shape memory, as very different thermal transitions are associated with the soft and hard segments.

## 5. SHAPE MEMORY POLYURETHANES NANOCOMPOSITES

Although shape memory polyurethanes have found extensive applications, but limitations like relatively low recovery stress, which is usually 1–3 MPa compared to 0.5–1 GPa for shape memory metal alloys [103], prevent their widespread usage. The relatively low recovery stress becomes a limiting factor in many applications especially in cases where a large resisting stress during shape recovery is required. One of the best avenue to improve mechanical properties and to add multiple functionalities to the shape memory polyurethanes is to mix with high modulus fillers like carbon nanotubes [104], clays [73] and cellulose nanofibrils [74] etc.. As reoprted in literature these fillers not only enhance the mechanical properties and stiffness but also improve the the theraml conductivity [105] and the value of thermal expansion coefficient [106]. However, it has been observed that there is a trade-off between modulus enhancement and recoverable strain ratio due to the effects of filler particle size, much higher stiffness of fillers, or potential infringement with the polymer networks especially at high filler loadings. For example Liang et al. [75, 76] and Ohki et al. [107] studied the effects of chopped and wove fiberglass and unidirectional kevlar fibers on the properties of shape memory polyurethanes, respectively and find that there was a trade-off between modulus enhancement and recoverable strain. As 400% increase in elastic modulus with no shape memory effects was observed by Liang et at [108] 50% incorporation of continuous glass fibers in the SMPU whereas Ohki et al. [108] observed 50% improvement in modulus with incorporation of 10% chopped glass fibers with a decrease in recovery ratio form 60% to 25%. Also, composites of SMPU with carbon black with crystallizable PCL diol soft segments were synthesized by Li et al. [108] and their effects were studied. A significant increase in the electrical conductivity and storage modulus with a large decrease in the

recovery ratio was observed at 20% filler concentration. Further no significant effect on the modulus and recoverable strain was observed below a ctitical filler loading.

These issues can be alleviated by reducing the size of filler and the loading content which reduces the soft segment crystallinity. The reduction of soft segment crystallinity causes an imbalance of Helmholtz free energy, which in turn, caused a reduction of SM properties [108]. Chopped and continuous, especially continuous nanofillers such as nanoclay [108], carbon nanotubes [108], cellulose nanofibers [108] etc. to improve the mechanical strength of shape memory polymers.

Multiwall carbon nanotubes (MWCNT's) filled SMPU nanocomposites were synthesized by Vaia and coworkers [108]. These authours found that SMPU with 5% MWCNT's showed higher strain recovery than pristine SMPU and SMPU fiulled with 20% carbon black. Functionalized MWCNT/SMPU nanocomposites were developed by Mondal and Hu [108] by solution mixing and improvement in recovery ratio was observed at fileer concentartion of 2.5% only. Elecetroactive shape memory PVA/MWCNT nanocomposites were prpepared by Du et al. [109] and studied the effects of MWCNT concentarion. They found that glass transition temperature, thermal conductivity and recovery ratio improved with increawse in concentration of CNT's. High speed recoverability was reported by Raja M. et al. [110] in the polyurethane/poly(lactic acid)/CNT nanocompoites.

Shape memory properties of SMPU/organoclay nanocomposite based on PCL diol soft segment was reported by Cao and Jana [110]. A good level of dispersion was achieved by the by using melt mixing and bulk polymerization technique developed by Pattanayak and Jana [111] that lead to a great increase in recovery strain. Ahmad Zubir et al. [112] synthesized shape memory polyurethane/clay nanocomposites using using palm oil as polyol. They reported that the shape memory and mechanical properties were highly influenced by reinforcement of clay. The optimum mechanical and shape memory properties were achieved for 3 wt% reinforcement of clay beyond which a decrease in the shape memory behaviour was observed whereas mechanical strength kept on increasing. Shape memory polyurethane clay nanocomposites with better shape memory properties and increased glass trantion temperature were reported by Haghayegh and Mir Mohamad Sadeghi [1–3].

J. T. Kim et al. [4, 5] studied the shape memory pereformance of the synthesiszed polyurethane/graphene nanocomposites and found improvement in the rubbery state modulus, yield strength, galss transtion temperature, shape fixity and shape recovery ratio. Graphene oxide was used as a filler by Qi et al. [6, 7] to synthesize nanocomposites with water induced shape memory effect. It was found that shape memory properties were improved that may be because of crosslinking with graphene oxide. Greater mechanical, thermal and dynamic mechanical properties along with higher shape memory properties of polyurethane nanocomposites develpoed using functionalized graphene were reported by Han and Chun [8–12].

## 6. SHAPE MEMORY POLYURETHANES NANOCOMPOSITES FOR BIOMEDICAL APPLICATIONS

Shape memory polyurethanes (SMPU) are extensively used polymers in biomedical applications because of their durability, elasticity, fatigue resistance, compliance, bio-

stability, biodegradability and tailorable backbone structure from a wide range of available precursors. A thermo-responsive segmented polyurethane get deformed at a temperature above transition temperature (which can be glass transition or melting temperature) and suddenly cooled to a temperature below *transition temperature*, the deformed shape becomes frozen. When it is heated above *transition temperature*, the polymer recovers its original shape [13–15]. Large bulky devices made up of thermoresponsive segmented polyurethanes can be introduced into the body in a compressed temporary shape by means of minimal invasive surgery and then expand to their permanent shape to fit as required because of their ability to recover shape at critical temperature [16]. This property is very useful in cardiovascular stents and sutures. Conventionally shape memory alloys, like Nitinol, are used for cardiovascular stents as they exhibit outstanding features, such as small size and high strength, but show disadvantages like high manufacturing cost, limited recoverable deformation and complicated surgery process [17–20]. Moreover, metal stents being rigid compared to the surrounding vessel, cause abrupt change of compliance in the junction of the host artery and the stent, lead to an abnormal stress concentration which will initiate an adaptive response in the vascular tissue [4, 21, 22]. Therefore, shape memory polymers have come to the focal point over the last decade as proposed materials for stents [23–27]. Potential biodegradability is an additional functionality of shape memory polymers that can prevent a second surgery for device explantation. With good biodegradability, they would neither stay in the human body for a very long time nor require a second surgery to be removed from the human body. With shape-memory property and a recovery near body temperature, the handling of the corresponding medical devices would be easy.

Poly(ε-caprolactone) based polyurethanes, polycaprolactone polylactic acid blends, polyester based polyurethanes (poly(lactic acid) (PLA), poly(butylenes succinate) (PBS), and poly(hydroxyalkanoic acids) (PHA)) have been studied extensively for a number of biomedical applications because of their biodegradability, independence from petroleum and non-toxic degradation products. The properties of independence from petroleum and complete biodegradation are their two major fetching advantages. Biodegradation in this connection means hydrolysable at temperatures up to 50$^{o}$C (e.g., in composting) over a period of several months to one year with the help of naturally occurring microorganisms such as bacteria, fungi, and algae [28, 29]. Non-toxic degradation products are, of course, other important pre-requirements for any potential applications. The polyester and copolyesters of several α-, β- and ω-hydroxy acids have been used widely during the past 20 years. Minna Hakkarainen and Ann-Christine Albertsson [23, 26, 27] studied the degradation of PCL films in different biotic and abiotic environments. The degradation in biotic medium occurred heterogeneously and scanning electron micrographs revealed the formation of parallel grooves, spherical and non-spherical holes in the films. It is reported that the degradation started preferentially at the amorphous regions and for longer time duration, even the crystalline regions were degraded producing large spherical and non-spherical holes which were visible in scanning electron micrographs. Biodegradable polymeric composite based on PCL and starch was developed by Soheila Ali Akbari Ghavimi et al. [30]. Degradation studies were performed in phosphate buffer saline (PBS) containing α-amylase or lipase at 37°C for 4 weeks.

Degradation studies revealed that non-porous composites exhibit potential to develop pores in situ. Such composites have potential to be used as scaffolds for bone tissue engineering applications. Eoin Murray et al. [15] examined enzymatic degradation of

graphene/polycaprolactone composites in phosphate buffered saline. Covalently linked graphene/polycaprolactone showed a consistent degradation profile maintaining the graphene:PCL ratio throughout the degradation process. The degradation products were non-toxic to the proliferating cells and hence, graphene/polycaprolactone composites have proven to be promising substrates for biodegradable tissue engineering scaffolds for electro-responsive tissue types.

Five buffer solutions having pH values 1.6, 3.0, 5.0, 7.4 and 9.6 were used to observe the effect of pH medium on the degradation rate of PLA microcapsules by K. Makino et al. [31]. The decrease in weight average molecular weight ($M_w$) of PLA in degradation medium indicated that a number of ester bonds in the polymer are cleaved and degradation process was observed faster in highly alkaline buffer solution (pH 9.6) than in the highly acidic and slightly alkaline ones. Young You et al. [30] examined the *in vitro* degradation of electrospun polyglycolide (PGA), PLA, and poly(lactide-*co*-glycolide) (PLGA) nanofiber matrices in phosphate buffer solutions (pH 7.4) at 37°C. The degradation rates of the nanofiber matrices were fast, in the order of PGA > PLGA ≫ PLA. Wide-angle X-ray diffraction studies revealed that for the PGA matrix, a significant increase in the crystallinity during the early stage was detected, as well as a gradual decrease during the later period, and this indicated that preferential hydrolytic degradation in the amorphous regions occurred with cleavage-induced crystallization, followed by further degradation in the crystalline region. Wei Z. [32] investigated the *in vitro* degradation behavior of PLA and PLGA films in Hank's solution. The hydrolytic degradation of the PLA and PLGA was monitored by measuring the changes of inherent viscosity and weight loss of the resulting samples. The degradation rate of PLGA was dependent on the composition of the copolymer and increased with increasing the glycolide content increasing. PLGA copolymer has potential application as drug elusion coating on coronary stents. Self-reinforced PLLA plates were also incubated *in vitro* for 5 years by Riitta Suuronen et al. [31]. The material degraded considerably faster in vivo than in vitro. They retained their macroscopic form until the end of the 5-year follow-up. Loss of mass of the plates was 52% ± 8% after 5 years of incubation in vitro.

Haiyan Li et al. [33] investigated the hydrolytic degradation behavior of the PBSU films in the phosphate-buffered saline and the results suggested that the PBSU degraded in the PBS solution with the same behavior as that of the degradable poly(*α*-hydroxyesters). Eun Hwan Jeong et al. [23] studied hydrolytic degradation of PBSU ultrafine fibers. As the degradation proceeded, the surface of the fibers became coarse and the fibers ultimately broke down and finally turned into chunks. The amorphous regions in the ultrafine PBS fibers were degraded first, while the crystalline ones remained as the crystalline layers were stacked between amorphous ones. These can be used in wound dressing materials and tissue scaffolds.

For the development of a resorbable gastrointestinal patch, the *in vitro* degradation of solution-cast films of poly(3-hydroxybutyrate) (PHB) and poly(L-lactide) was examined by Freier T [8, 17, 34, 35]. The molecular weight of pure PHB decreased to one-half after one year in buffer solution with pH 7.4 at 37°C. In vitro degradation of PHAs in the aqueous media proceeds via a random bulk hydrolysis of ester bonds in the polymer chain. To understand mechanisms of PHB biodegradation it is necessary to examine hydrolysis of PHB in vitro. Degradation of films from PHB has been demonstrated under three different conditions: at 37°C in phosphate buffer (pH = 7.4) and at 70°C in phosphate buffer (pH = 7.4), and at 37°C in human blood serum by A.P. Bonartsev [36–38]. At 37°C hydrolysis of PHB was very slow as only 5% weight loss of PHB films was observed for 6 months.

Degradation of PHB films in human blood serum was similar to degradation in phosphate buffer at 37°C with high correlation rate. At 70°C degradation of PHB was much more rapid as 5% weight loss of PHB films was observed for 2.5 months and the complete degradation of PHB films was occurred for 3.5 months.

The perspective area of these degradable polyesters application is development of implanted medical devices for dental, craniomaxillofacial, orthopaedic, hernioplastic and skin surgery. A number of potential medical devices like bioresorbable surgical sutures, biodegradable screws and plates for cartilage and bone fixation, biodegradable membranes for periodontal treatment, surgical meshes, and wound coverings have been developed [8, 39, 40].

An increase of 300% in strength and 2600% in stiffness was by observed Cherian et al. in polyurethane nanocomposite synthesized using celluose nanofibers as fillers [41]. These nanocompistes were used for the synthesis of numerous versaitile medical implants such as heart valves and vascular grafts. Shape memory properties of hyperbranched polyurethanes/MWCNT along with biodegradabilty and bicompatability were studied by Deka et al. [42]. Biodegradability and shape memory properties of nanocomposites was found to be higher than pristine polyurethane leading them to be used as promising shape memory biomaterial.

## CONCLUSION

From the above text, it is evident that the research interest of scientist has grown significantly towards the development of biodegradable polyurethane with shape memory effcets. The properties of shape memory polyurethanes can be customized to fit the exact requirement of the design engineers because of their block copolymeric structure. Therefore they are most widely used in biomedical applications as stents, suture, tissue engineering, drug delivery and various other implants. Moreover, they can be made biodegradable and bicompatible by the addition of a biobased diol or diiscocynate. However, its use is limited because of the inherent restriction such as poor mechanical strength and low recovery stress. In this regard, development of polyurethane matrix by addition of nanofiller in the polymer matrix offers an opportunity for attaining the higher values of recovery stress and higher mechanical strength. But there is a limitation with the use of nanofiller as they are not well dispersed in the polymer matrix leading to non uniform properties. The field is is still being explored.

Henceforth, it can be foreseen, research in this area will grow further as scientists from academia and industries are making significant contributions to the development of technology and fundamental understanding.

## ACKNOWLEDGMENTS

We gratefully acknowledge RGNF, UGC, India for SRF- fellowship to one of its author Mr. Dheeraj Ahuja; CSIR, India; University Grants Commission (UGC), India and Technical

Education Quality Improvement Program (TEQIP-II) by Ministry of HRD, India for rendering their financial assistance to accomplish this research work.

## RÉFÉRENCES

[1] Waitz T (2005) The self-accommodated morphology of martensite in nanocrystalline NiTi shape memory alloys. *Acta Mater* 53:2273–2283.

[2] Elahinia MH, Ahmadian M, Ashrafiuon H (2004) Design of a Kalman filter for rotary shape memory alloy actuators. *Smart Mater Struct* 13:691.

[3] Firstov GS, Van Humbeeck J, Koval YN (2004) High-temperature shape memory alloys: some recent developments. *Mater Sci Eng* A 378:2–10.

[4] Schurch KE, Ashbee KHG (1977) A near perfect shape-memory ceramic material. *Nature* 266:706–707.

[5] Pandit P, Gupta SM, Wadhawan VK (2004) Shape-memory effect in PMN-PT (65/35) ceramic. *Solid State Commun* 131:665–670.

[6] Liu G, Ding X, Cao Y, et al. (2004) Shape memory of hydrogen-bonded polymer network/poly (ethylene glycol) complexes. *Macromolecules* 37:2228–2232.

[7] Osada Y, Matsuda A (1995) Shape memory in hydrogels. *Nature* 376:219.

[8] Lee BS, Chun BC, Chung Y-C, et al. (2001) Structure and thermomechanical properties of polyurethane block copolymers with shape memory effect. *Macromolecules* 34:6431–6437.

[9] Yang JH, Chun BC, Chung Y-C, Cho JH (2003) Comparison of thermal/mechanical properties and shape memory effect of polyurethane block-copolymers with planar or bent shape of hard segment. *Polymer (Guildf)* 44:3251–3258.

[10] Gall K, Dunn ML, Liu Y, et al. (2004) Internal stress storage in shape memory polymer nanocomposites. *Appl Phys Lett* 85:290–292.

[11] Tobushi H, Matsui R, Hayashi S, Shimada D (2004) The influence of shape-holding conditions on shape recovery of polyurethane-shape memory polymer foams. *Smart Mater Struct* 13:881.

[12] Poilane C, Delobelle P, Lexcellent C, et al. (2000) Analysis of the mechanical behavior of shape memory polymer membranes by nanoindentation, bulging and point membrane deflection tests. *Thin Solid Films* 379:156–165.

[13] Schryvers D, Potapov P, Santamarta R, Tirry W (2004) Applications of advanced transmission electron microscopic techniques to Ni–Ti based shape memory materials. *Mater Sci Eng* A 378:11–15.

[14] Kohl M, Brugger D, Ohtsuka M, Takagi T (2004) A novel actuation mechanism on the basis of ferromagnetic SMA thin films. *Sensors Actuators A Phys* 114:445–450.

[15] Lendlein A, Kelch S (2002) Shape-memory polymers. *Angew Chemie Int Ed* 41:2034–2057.

[16] Chang LC, Read TA (1951) Plastic deformation and diffusionless phase changes in metals—the gold–cadmium beta phase. *Trans Aime* 189:47–52.

[17] Wei ZG, Sandstroröm R, Miyazaki S (1998) Shape-memory materials and hybrid composites for smart systems: Part I Shape-memory materials. *J Mater Sci* 33:3743–3762.

[18] Hornbogen E (2004) Review Thermo-mechanical fatigue of shape memory alloys. *J Mater Sci* 39:385–399.
[19] El Feninat F, Laroche G, Fiset M, Mantovani D (2002) Shape memory materials for biomedical applications. *Adv Eng Mater* 4:91–104.
[20] Wataha JC, Hanks CT, Craig RG (1991) The in vitro effects of metal cations on eukaryotic cell metabolism. *J Biomed Mater Res* Part A 25:1133–1149.
[21] Heuer AH, Ruhle M, Marshall DB (1990) On the thermoelastic martensitic transformation in tetragonal zirconia. *J Am Ceram Soc 7*3:1084–1093.
[22] Veitch S, Marmach M, Swain M V (1986) *Strength and toughness of Mg-PSZ and Y-TZP materials at cyrogenic temperatures.* MRS Online Proc Libr Arch 78.
[23] Liu C, Qin H, Mather PT (2007) Review of progress in shape-memory polymers. *J Mater Chem* 17:1543–1558.
[24] Yu Y, Ikeda T (2005) Photodeformable polymers: A new kind of promising smart material for micro-and nano-applications. *Macromol Chem Phys* 206:1705–1708.
[25] Gould P (2007) Nanocantilevers for small-scale sensors: Nanotechnology. *Mater Today* 10:10.
[26] Kim BK, Lee SH, Furukawa M (2005) Shape memory effects of multiblock thermoplastic elastomers. *Handb Condens Thermoplast Elastomers* 521–566.
[27] Behl M, Lendlein A (2007) Shape-memory polymers. *Mater today* 10:20–28.
[28] Uo M, Watari F, Yokoyama A, et al. (2001) Tissue reaction around metal implants observed by X-ray scanning analytical microscopy. *Biomaterials* 22:677–685.
[29] Hornbogen E (2006) Comparison of shape memory metals and polymers. *Adv Eng Mater* 8:101–106.
[30] Ratna D, Karger-Kocsis J (2008) Recent advances in shape memory polymers and composites: a review. *J Mater Sci* 43:254–269.
[31] Beloshenko VA, Varyukhin VN, Voznyak YV (2005) The shape memory effect in polymers. *Russ Chem Rev* 74:265–283.
[32] Nguyen TD, Qi HJ, Castro F, Long KN (2008) A thermoviscoelastic model for amorphous shape memory polymers: incorporating structural and stress relaxation. *J Mech Phys Solids* 56:2792–2814.
[33] Yakacki CM, Satarkar NS, Gall K, et al. (2009) Shape-memory polymer networks with Fe3O4 nanoparticles for remote activation. *J Appl Polym Sci* 112:3166–3176.
[34] Liang C, Rogers CA, Malafeew E (1997) Investigation of shape memory polymers and their hybrid composites. *J Intell Mater Syst Struct* 8:380–386.
[35] Hayashi S (1995) Room-temperature-functional shape-memory polymers. *Plast Eng* 51:29–31.
[36] Krishnan M (2003) *Polyurethane elastomer article with "shape memory" and medical devices therefrom.*
[37] Baer G, Wilson TS, Matthews DL, Maitland DJ (2007) Shape-memory behavior of thermally stimulated polyurethane for medical applications. *J Appl Polym Sci* 103:3882–3892.
[38] Esteban VL, Lantada AD, Morgado PL, et al. (2009) *Physical ageing of a PU based shape memory polymer: influence on their applicability to the development of medical devices.*
[39] Lelah MD, Cooper SL (1986) *Polyurethanes in medicine.* CRC press.

[40] Szycher M (2012) Structure–property relations in polyurethanes. *Szycher's Handb Polyurethanes* 37.

[41] Huang WM, Yang B, Zhao Y, Ding Z (2010) Thermo-moisture responsive polyurethane shape-memory polymer and composites: a review. *J Mater Chem* 20:3367–3381.

[42] Singhal P, Small W, Cosgriff-Hernandez E, et al. (2014) Low density biodegradable shape memory polyurethane foams for embolic biomedical applications. *Acta Biomater* 10:67–76. doi: https://doi.org/10.1016/j.actbio.2013.09.027.

[43] Mathur AB, Collier TO, Kao WJ, et al. (1997) In vivo biocompatibility and biostability of modified polyurethanes. *J Biomed Mater Res* 36:246–257.

[44] Gunes IS, Jana SC (2008) Shape memory polymers and their nanocomposites: a review of science and technology of new multifunctional materials. *J Nanosci Nanotechnol* 8:1616–1637.

[45] Gunes IS, Cao F, Jana SC (2008) Evaluation of nanoparticulate fillers for development of shape memory polyurethane nanocomposites. *Polymer (Guildf)* 49:2223–2234.

[46] Zheng X, Zhou S, Li X, Weng J (2006) Shape memory properties of poly (D, L-lactide)/hydroxyapatite composites. *Biomaterials* 27:4288–4295.

[47] Mather PT, Jeon HG, Romo-Uribe A, et al. (1999) Mechanical relaxation and microstructure of poly (norbornyl-POSS) copolymers. *Macromolecules* 32:1194–1203.

[48] Mather PT, Jeon HG, Haddad TS (2000) Strain recovery in POSS hybrid thermoplastics. *Polym Prepr* 41:528–529.

[49] Jeon HG, Mather PT, Haddad TS (2000) Shape memory and nanostructure in poly (norbornyl-POSS) copolymers. *Polym Int* 49:453–457.

[50] Park JS, Chung Y-C, Do Lee S, et al. (2008) Shape memory effects of polyurethane block copolymers cross-linked by celite. *Fibers Polym* 9:661–666.

[51] Miaudet P, Derré A, Maugey M, et al. (2007) Shape and temperature memory of nanocomposites with broadened glass transition. *Science* (80- ) 318:1294–1296.

[52] Meng Q, Hu J, Mondal S (2008) Thermal sensitive shape recovery and mass transfer properties of polyurethane/modified MWNT composite membranes synthesized via in situ solution pre-polymerization. *J Memb Sci* 319:102–110.

[53] Jimenez G, Jana S (2007) Polyurethane-carbon nanofiber composites for shape memory effects. In: *Antec-Conference Proceedings-*. p 18.

[54] Auad ML, Contos VS, Nutt S, et al. (2008) Characterization of nanocellulose-reinforced shape memory polyurethanes. *Polym Int* 57:651–659.

[55] Cao F, Jana SC (2007) Nanoclay-tethered shape memory polyurethane nanocomposites. *Polymer (Guildf)* 48:3790–3800.

[56] Nakamae K, Nishino T, Asaoka S (1996) Microphase separation and surface properties of segmented polyurethane—Effect of hard segment content. *Int J Adhes Adhes* 16:233–239.

[57] Hood MA, Wang B, Sands JM, et al. (2010) Morphology control of segmented polyurethanes by crystallization of hard and soft segments. *Polymer (Guildf)* 51:2191–2198.

[58] Xu M, MacKnight WJ, Chen CHY, Thomas EL (1983) Structure and morphology of segmented polyurethanes: 1. Influence of incompatability on hard-segment sequence length. *Polymer (Guildf) 2*4:1327–1332.

[59] Mondal S, Martin D (2012) Hydrolytic degradation of segmented polyurethane copolymers for biomedical applications. *Polym Degrad Stab* 97:1553–1561.
[60] Caracciolo PC, De Queiroz AAA, Higa OZ, et al. (2008) Segmented poly (esterurethane urea) s from novel urea–diol chain extenders: Synthesis, characterization and in vitro biological properties. *Acta Biomater* 4:976–988.
[61] Wang Y, Ruan C, Sun J, et al. (2011) Degradation studies on segmented polyurethanes prepared with poly (D, L-lactic acid) diol, hexamethylene diisocyanate and different chain extenders. *Polym Degrad Stab* 96:1687–1694.
[62] Li C, Liu J, Li J, et al. (2012) Studies of 4, 4′-diphenylmethane diisocyanate (MDI)/1, 4-butanediol (BDO) based TPUs by in situ and moving-window two-dimensional correlation infrared spectroscopy: understanding of multiple DSC endotherms from intermolecular interactions and motions leve. *Polymer (Guildf)* 53:5423–5435.
[63] Jaros A, Smola A, Kasperczyk J, Dobrzyński P (2010) Biodegradable shape memory polymers for medical purposes. *Chemik* 64:87–96.
[64] Ning L, De-Ning W, Sheng-Kang Y (1996) Crystallinity and hydrogen bonding of hard segments in segmented poly (urethane urea) copolymers. *Polymer (Guildf)* 37:3577–3583.
[65] Garrett JT, Runt J, Lin JS (2000) Microphase separation of segmented poly (urethane urea) block copolymers. *Macromolecules* 33:6353–6359.
[66] Saiani A, Novak A, Rodier L, et al. (2007) Origin of multiple melting endotherms in a high hard block content polyurethane: effect of annealing temperature. *Macromolecules* 40:7252–7262.
[67] Saiani A, Daunch WA, Verbeke H, et al. (2001) Origin of multiple melting endotherms in a high hard block content polyurethane. 1. Thermodynamic investigation. *Macromolecules* 34:9059–9068.
[68] Privalko VP, Azarenkov VP, Baibak A V, Usenko AA (1996) Thermodynamic characterization of segmented polyurethanes. *Thermochim Acta* 285:155–165.
[69] Noshay A, McGrath JE (2013) *Block copolymers: overview and critical survey*. Elsevier.
[70] Yılgor E, Yılgor I, Yurtsever E (2002) Hydrogen bonding and polyurethane morphology. I. Quantum mechanical calculations of hydrogen bond energies and vibrational spectroscopy of model compounds. *Polymer (Guildf)* 43:6551–6559.
[71] Jeong HM, Lee SY, Kim BK (2000) Shape memory polyurethane containing amorphous reversible phase. *J Mater Sci* 35:1579–1583.
[72] Wang W, Ping P, Chen X, Jing X (2007) Shape memory effect of poly (L-lactide)-based polyurethanes with different hard segments. *Polym Int* 56:840–846.
[73] Khan F, Koo J-H, Monk D, Eisbrenner E (2008) Characterization of shear deformation and strain recovery behavior in shape memory polymers. *Polym Test* 27:498–503.
[74] Lendlein A, Langer R (2002) Biodegradable, elastic shape-memory polymers for potential biomedical applications. *Science* (80- ) 296:1673–1676.
[75] Peng T, Gibula P, Goosen MFA (1996) Role of polymers in improving the results of stenting in coronary arteries. *Biomaterials* 17:685–694.
[76] Bertrand OF, Sipehia R, Mongrain R, et al. (1998) Biocompatibility aspects of new stent technology. *J Am Coll Cardiol* 32:562–571.

[77] Paik IH, Goo NS, Yoon KJ, et al. (2005) Electric resistance property of a conducting shape memory polyurethane actuator. In: *Key Engineering Materials. Trans Tech Publ*, pp 1539–1544.

[78] Kim Y, Verkade JG (2002) A tetrameric titanium alkoxide as a lactide polymerization catalyst. *Macromol Rapid Commun* 23:917–921.

[79] Yan B, Gu S, Zhang Y (2013) Polylactide-based thermoplastic shape memory polymer nanocomposites. *Eur Polym J* 49:366–378.

[80] Liu Y, Du H, Liu L, Leng J (2014) Shape memory polymers and their composites in aerospace applications: a review. *Smart Mater Struct* 23:23001.

[81] Raja M, Ryu SH, Shanmugharaj AM (2013) Thermal, mechanical and electroactive shape memory properties of polyurethane (PU)/poly (lactic acid)(PLA)/CNT nanocomposites. *Eur Polym J* 49:3492–3500.

[82] Du F-P, Ye E-Z, Yang W, et al. (2015) Electroactive shape memory polymer based on optimized multi-walled carbon nanotubes/polyvinyl alcohol nanocomposites. *Compos Part B Eng* 68:170–175.

[83] Liu Y, Li Y, Yang G, et al. (2015) Multi-stimulus-responsive shape-memory polymer nanocomposite network cross-linked by cellulose nanocrystals. *ACS Appl Mater Interfaces* 7:4118–4126.

[84] Tobushi H, Okumura K, Hayashi S, Ito N (2001) Thermomechanical constitutive model of shape memory polymer. *Mech Mater* 33:545–554.

[85] Bhattacharyya A, Tobushi H (2000) Analysis of the isothermal mechanical response of a shape memory polymer rheological model. *Polym Eng Sci* 40:2498–2510.

[86] Liu Y, Gall K, Dunn ML, et al. (2006) Thermomechanics of shape memory polymers: uniaxial experiments and constitutive modeling. *Int J Plast* 22:279–313.

[87] Diani J, Liu Y, Gall K (2006) Finite strain 3D thermoviscoelastic constitutive model for shape memory polymers. *Polym Eng Sci* 46:486–492.

[88] Ameduri S, Pecora R, Karagiannis D (2016) A single slotted morphing flap based on SMA technology. *Smart Struct Syst* 17:819–835.

[89] Ohki T, Ni Q-Q, Ohsako N, Iwamoto M (2004) Mechanical and shape memory behavior of composites with shape memory polymer. *Compos Part A Appl Sci Manuf* 35:1065–1073. doi: https://doi.org/10.1016/j.compositesa.2004.03.001.

[90] Gunes IS, Pérez-Bolivar C, Cao F, et al. (2010) Analysis of non-covalent interactions between the nanoparticulate fillers and the matrix polymer as applied to shape memory performance. *J Mater Chem* 20:3467–3474.

[91] Kaushik A, Ahuja D, Salwani V (2011) Synthesis and characterization of organically modified clay/castor oil based chain extended polyurethane nanocomposites. *Compos Part A Appl Sci Manuf* 42:1534–1541.

[92] Ahuja D, Kaushik A (2017) Castor oil-based polyurethane nanocomposites reinforced with organically modified clay: Synthesis and characterization. *J Elastomers Plast* 49:315–331.

[93] Vaia RA, Koerner H, Powers D, et al. (2005) Polymer nanocomposites as adaptive materials: carbon nanotube–polyurethane stress recovery systems. In: A*bstracts of papers of the american chemical society*. Amer Chemical Soc 1155 16TH ST, NW, Washington, DC 20036 USA, pp U983–U984.

[94] Koerner H, Price G, Pearce NA, et al. (2004) Remotely actuated polymer nanocomposites—stress-recovery of carbon-nanotube-filled thermoplastic elastomers. *Nat Mater* 3:115–120.
[95] Mondal S, Hu JL (2006) Shape memory studies of functionalized MWNT-reinforced polyurethane copolymers. *Iran Polym J* 15:135–142.
[96] Pattanayak A, Jana SC (2005) Thermoplastic polyurethane nanocomposites of reactive silicate clays: effects of soft segments on properties. *Polymer (Guildf)* 46:5183–5193.
[97] Pattanayak A, Jana SC (2005) Properties of bulk-polymerized thermoplastic polyurethane nanocomposites. *Polymer (Guildf)* 46:3394–3406.
[98] Pattanayak A, Jana SC (2005) Synthesis of thermoplastic polyurethane nanocomposites of reactive nanoclay by bulk polymerization methods. *Polymer (Guildf)* 46:3275–3288.
[99] Pattanayak A, Jana SC (2005) High-strength and low-stiffness composites of nanoclay-filled thermoplastic polyurethanes. *Polym Eng Sci* 45:1532–1539.
[100] Ahmad Zubir S, Ahmad S, Ali ES (2013) Palm oil polyol/polyurethane shape memory nanocomposites. In: Applied Mechanics and Materials. *Trans Tech Publ*, pp 2666–2669.
[101] Haghayegh M, Mir Mohamad Sadeghi G (2012) Synthesis of shape memory polyurethane/clay nanocomposites and analysis of shape memory, thermal, and mechanical properties. *Polym Compos* 33:843–849.
[102] Kim JT, Kim BK, Kim EY, et al. (2014) Synthesis and shape memory performance of polyurethane/graphene nanocomposites. *React Funct Polym* 74:16–21.
[103] Qi X, Yao X, Deng S, et al. (2014) Water-induced shape memory effect of graphene oxide reinforced polyvinyl alcohol nanocomposites. *J Mater Chem* A 2:2240–2249.
[104] Han S, Chun BC (2014) Preparation of polyurethane nanocomposites via covalent incorporation of functionalized graphene and its shape memory effect. *Compos Part A Appl Sci Manuf* 58:65–72. doi: https://doi.org/10.1016/j.compositesa.2013.11.016.
[105] Ping P, Wang W, Chen X, Jing X (2005) Poly (ε-caprolactone) polyurethane and its shape-memory property. *Biomacromolecules* 6:587–592.
[106] Surovtsova I (2005) Effects of compliance mismatch on blood flow in an artery with endovascular prosthesis. *J Biomech* 38:2078–2086.
[107] Gupta AP, Kumar V (2007) New emerging trends in synthetic biodegradable polymers–Polylactide: A critique. *Eur Polym J* 43:4053–4074.
[108] Hakkarainen M, Albertsson A (2002) Heterogeneous biodegradation of polycaprolactone–low molecular weight products and surface changes. *Macromol Chem Phys* 203:1357–1363.
[109] Freier T, Kunze C, Nischan C, et al. (2002) In vitro and in vivo degradation studies for development of a biodegradable patch based on poly (3-hydroxybutyrate). *Biomaterials* 23:2649–2657.
[110] Bonartsev AP, Myshkina VL, Nikolaeva DA, et al. (2007) Biosynthesis, biodegradation, and application of poly (3-hydroxybutyrate) and its copolymers-natural polyesters produced by diazotrophic bacteria. *Commun Curr Res Educ Top Trends Appl Microbiol* 1:295–307.

[111] Cherian BM, Leão AL, de Souza SF, et al. (2011) Cellulose nanocomposites with nanofibres isolated from pineapple leaf fibers for medical applications. *Carbohydr Polym* 86:1790–1798. doi: https://doi.org/10.1016/j.carbpol.2011.07.009.

[112] Deka H, Karak N, Kalita RD, Buragohain AK (2010) Biocompatible hyperbranched polyurethane/multi-walled carbon nanotube composites as shape memory materials. *Carbon NY* 48:2013–2022.

In: Advances in Polymers for Biomedical Applications ISBN: 978-1-53613-612-8
Editors: Deepak Pathania and Bhuvanesh Gupta 

*Chapter 4*

# ADVANCES IN POLYMERS FOR DRUG DELIVERY AND WOUND HEALING APPLICATIONS

***Zahra Shariatinia**** *and Ahmad Mohammadi-Denyani*
Department of Chemistry, Amirkabir University of Technology
(Tehran Polytechnic), Tehran, Iran

## ABSTRACT

Polymeric drug delivery systems (DDSs) are always attractive candidates which can be designed to enhance the therapeutic efficiency, i.e., to decrease the side effects and raise the anticipated effects of drugs. A DDS involves intramuscular, intravenous, enteral or oral administration of a pharmacologically active material for a targeted response after the administered drug or bioactive compound was released in the body. Moreover, controlled DDSs are widely investigated using polymeric based systems especially smart polymers which are sensitive to pH, light, temperature and so on. Indeed, controlled drug delivery is one of the most interesting research areas. A smart DDS must be capable of controlling kinetics (release rate) and operational window in the desired site(s). In other words, appropriate drug DDSs should have high efficacy, bioavailability, safety, controlled and prolonged release time and anticipated therapeutic response. It is noteworthy that computational studies are also carried out on the polymeric DDSs to predict the effectiveness of the designed drug carriers. This is because of the importance of such systems in pharmaceutics industry. Natural and synthetic polymeric drug carriers offer valuable advantages as efficient drug delivery and release. For instance, chitosan has commonly been applied in designing drug delivery systems due to its abundant hydroxyl and amine functionalities, non-toxicity, antibacterial and hemostatic characteristics. Other polymers that are frequently used as DDSs include polylactic acid, polyethyleneglycol, polylactic-co-glycolic acid and molecularly imprinted polymers. Also, these polymers have numerous applications in fabrication of wound dressing materials to protect the wounded areas from environmental harmful factors such as microbial infections. Wound healing is one of the most prevailing and economically difficult healthcare treatments universal. The treatment of severe burns requires preventing the bacterial growth, predominantly when eschar and damaged tissues exist.

* Corresponding Author Email: shariati@aut.ac.ir; shariatiz@yahoo.com.

Accordingly, an antimicrobial treatment of wound is essential to inhibit bacterial proliferation and to accelerate the wound healing process. This chapter presents the most significant recently reported experimental and computational findings using chitosan, polylactic acid, polyethyleneglycol, polylactic-co-glycolic acid and molecularly imprinted polymers in both drug delivery and wound healing applications. Moreover, original research results achieved by means of DFT computations on simulated polymeric drug delivery systems will be presented and discussed.

**Keywords:** drug delivery, wound healing, chitosan, polylactic acid, polyethyleneglycol, molecularly imprinted polymer, DFT computations

## 1. INTRODUCTION

Recently, controlled release systems have received great attention because of their potential application as efficient drug delivery systems (DDSs) which are intended to enhance the therapeutic efficacy by reducing side effects and increasing desired drugs effects. In fact, controlled DDSs are widely investigated using inorganic, organic, polymeric and smart hybrid materials such as clays, cyclodextrins, micelles, hydrogels, microspheres, electro-active polymers and nanofibers [1-6]. It is very beneficial for a DDS that drug molecules do not release from carrier before they reach the target site/tissue and instead they are mainly released in the desired organ/tissue. Furthermore, the drug release should be controlled by the designed carrier.

In past decades, advances have been occurred in state-of-the-art therapies which utilize biopharmaceuticals including nucleic acids, proteins, bioactive molecules and peptides as therapeutic agents to diagnose diseases. Such novel drugs necessitate using advanced DDSs in order to increase their pharmacodynamics and pharmacokinetics properties as well as to enhance biocompatibility and tissue/cell specificity. Thus, it is mandatory to develop new DDSs and mechanisms to be able to control them which can lead to the evolution in finding next generation DDSs [7]. The progress in the biomedical science has noticeably affected the development of smart and novel designed DDSs for highly controlled and targeted drug treatment. Indeed, controlled drug delivery is one of the most necessary and fast developing issues which can have numerous benefits compared to traditional dosage forms including enhanced absorption rate, specific targeting of drugs to cell/tissue, biocompatibility, drug safety against degradation by means of proteolytic enzymes, releasing controlled drug amount in the body during long time in therapeutic range [8].

The most promising controlled DDSs are prepared using polymers due to their appropriate characteristics which can simply be manufactured at industrial scale and have the modification potential [9]. Polymers have shown a crucial role in the progress of drug delivery technology because they can offer repeated dosage, release both type of hydrophobic and hydrophilic drug formulations in a synchronized and constant manner during prolonged periods. Polymeric therapeutics comprise linear or branched polymer chain which can work either as the bioactive agents (like polymeric drugs) or as inert carriers to which a drug can covalently be bound (such as polymer-drug, polymer-DNA and polymer-antibody conjugates as well as polymeric micelles, dendrimers, nanosphere, nanocapsule and multicomponent polyplexes) [10]. The polymers used in drug delivery may rationally be classified according

to their characteristics including (a) origin (natural, synthetic or a combination of both), (b) chemical nature (polyanhydride, polyester, cellulose and protein-based compound), (c) backbone stability (biodegradable or nonbiodegradable) and (d) solubility (hydrophobic or hydrophilic) [11, 12]. Nevertheless, all of these features have some limitations, for instance although natural polymers are plentiful and biodegradable, it is hard to purify and reproduce them. Also, synthetic polymers reveal high immunogenicity and this prevent from their long-term treatment. Non-biodegradable polymers must be taken out by surgery subsequent to their drug release at the desired tissue/site. The common features which make the polymers as potential candidates for drug delivery are safety, hydrophilicity, efficacy, non-immunogenicity, satisfactory pharmacokinetics, biological inactivity as well as the existence of functional groups allowing covalent conjugation of drugs/targeting groups and copolymer formation [13]. In other words, some advantages of polymers as inert carriers to which drugs are conjugated include improved pharmacodynamics and pharmacokinetic properties of biopharmaceuticals by several routes like increasing plasma half-life, decreasing immunogenicity, boosting stability of biopharmaceuticals, improving solubility of low molecular weight drugs, and acting as controlled and targeted drug delivery systems [14-16]. For example, the polymer conjugates have been applied to target different diseases such as rheumatoid arthritis, hepatitis B and C, diabetes, ischemia and cancer [17].

Polymeric DDSs have experienced a substantial growth along with the pre-clinical and clinical developments in polymer-based nanomedicine materials and biomedical applications. The significant characteristic of a drug-polymer conjugate is that the drug is physically conjugated to the polymeric vehicle [18]. Thus, problem of burst drug release can be mostly overcome and the drug is bound to the polymer backbone through linkages that are specially designed to release drug in desired sites with a suitable rate [19]. Indeed, the polymer-drug conjugate concept was first presented by Helmut Ringsdorf in 1975 [20], which introduces a perfect polymer-drug conjugate by a hydrophilic polymeric vehicle and a bioactive compound that is commonly lined to the polymeric chains through a biological linker. In order to increase pharmacokinetic performance and therapeutic effectiveness, a solubility enhancer or a targeting fragment may be added to the conjugate [20, 21]. Generally, polymer-drug conjugate DDSs afford some advantages including (a) ability to attain high drug payloads, (b) enhanced drug solubility, (c) modulating the drug pharmacokinetics (such as long plasma exposure and improved bio-distribution which leads to superior therapeutic efficiency), (d) less local and systemic side-effects by very cytotoxic or irritant drugs, (e) greater *in vivo* stability of drugs and (f) controlled rate and site of drug release. Considering these benefits, it is interesting to entirely exploit the polymer-drug conjugates as potential drug delivery vehicles.

Today, polymers are an essential part of DDSs because they have shown enhanced pharmacokinetic features including superior circulation time compared with conventional small drug molecules which result in more specially targeting to the tissues. Therefore, polymers are remarkably used as nano-medicines and therapeutics [22]. Furthermore, polymers have indicated enormous development in case of reservoir formed DDSs like liposomes and hydrogels. Solvent activated and diffusion based DDSs are also exploited for employing various polymers [22]. Solvent activated DDSs which are hydrophilic in nature (such as hydrogels) swell and then release the drug when they are placed in an aqueous medium [23]. In diffusion based DDSs, drug molecule is dissolved in a completely swollen system or a non-swellable matrix which is not decomposed throughout the activation time.

Biocompatible polymers provide a safe path for drug delivery because they have well-engineered architectures which are consistent with changes in the mechanisms of biological processes. In biodegradable polymers, covalent bonds are broken down but in case of bio-erodible polymers, erosion occurs by dissolution of connecting chains without any variations in the chemical structure of polymer [23]. Water soluble, non-immunogenic and nontoxic polymers are preferred to be used as drug carriers because they can act passively to improve circulation time and to minimize drug degradation. The safe elimination of drug is another essential subject [22]. When a non-degradable polymer is used, it must not be accumulated in the body and when the polymer is degradable, its destroyed components must be non-toxic, lower than renal threshold level and should not create any immune response [22]. Polymers that can mimic biological organisms respond to external stimuli like alterations in pH and temperature and their characteristics including hydrophobic/hydrophilic property, solubility, conformation and biomolecule (drug) release can be changed [22].

Natural and synthetic polymeric nanocarriers have presented numerous advantages in drug delivery, targeting and release [24]. For instance, chitosan (CS) is a favorable candidate for drug delivery applications because it is non-toxic, biodegradable, biocompatible as well as it has low manufacturing and disposal costs [25, 26]. CS has often been applied to design DDSs due to it has amine and hydroxyl functional groups as well as it displays good hemostatic and antibacterial features [27–29]. CS is a biopolymer which is well capable of accelerating wound healing in human [30, 31] which is due to its considerable antibacterial efficiency against a broad range of bacteria [32-34]. It is an inexpensive and abundant polymer that has easily been prepared [35].

Molecularly imprinted polymers (MIPs) have been developed as DDSs [36–39] to create suitable dosage devices and forms for clinical applications like diagnostic sensors. The efficacy of MIPs for drug administration by diverse routes (such as oral, transdermal or ocular) has received great attention due to it is possible to control and prolong the drug release [40–42]. MIPs are prepared from synthetic polymers having good thermal stability and selective molecular recognition sites. The recognition sites in the polymeric matrix match to the shape and locations of functional groups of template molecule [43]. The imprinting method is carried out by both non-covalent and reversible covalent bonds formed between template and appropriate functional groups existing on monomers throughout the pre-polymerization process [44]. When the template molecule is removed, the remaining compound is a cross-linked copolymer with specific recognition sites for the template. Molecular imprinting technique is very applicable in the analytical arena which is primarily used to determine diverse substances such as bio-active molecules and drugs in various samples; for example, MIPs were used for nicotine determination [45]. Even though the MIPs were employed to isolate and quantify nicotine in some biological fluids [46] and environmental samples [44], they were not examined as DDSs. The utilization of MIPs as DDSs may afford an effective and safe approach for controlling the drug release. The MIPs can be used as matrixes having higher affinities for drugs and therefore drug diffusion will be modulated.

Skin is one of the most important tissues that protects and preserves homeostasis of body and its injury in any form causes homeostasis deregulation which allows for the entrance of pathogenic microbes inside the body [47]. An instant requirement to defence damaged skin against infection is wound dressing [48]. Materials selected for wound dressing must be non-allergic and non-toxic but having antibacterial potency [49]. A perfect wound healing was

done using biosynthetic dressing possessing salient properties including minimal inflammatory reactions, long life, antimicrobial activity and low antigenicity [50]. An ideal dressing should have antimicrobial property, moist environment, exudates removal and gaseous exchange [49–52]. Recently, chitosan (a deacetylated derivative of chitin) has revealed extraordinary advantages for application in biomedical fields [53]. CS has exclusively been used in wound healing [54, 55], drug delivery [56] and non-viral gene delivery [57]. The occurrence of polycationic amino groups in the CS backbone causes its protonation in aqueous environments at pH<6.5 but this is a restriction for CS that limits its antibacterial activity at physiological pH [50]. Nevertheless, CS films have the drawbacks of low mechanical stability, fragility and high degradation rate by lysozyme and in acidic media [58]. Polyethylene glycol (PEG) is a synthetic polymer which is approved by the food and drug administration (FDA, USA) for internal ingestion and DDSs [59]. PEG cross-linked CS hydrogel displayed improved mechanical characteristics than individual CS and the cross-linked compound was exploited in tissue engineering and wound healing purposses [60, 61].

Polylactic acid (PLA) and its copolymers have a long safety history in human being and a wide sort of applications. PLA is the second frequently used global bioplastic. Also, PLA is an FDA approved polymer for an extensive variety of biomedical applications like medical sutures as well as orthopedic screws and implants due to it is biodegradable by enzymatic activity and hydrolysis, biocompatible and has suitable mechanical features and low immunogenicity. Moreover, PLA is known as a promising polymer for wound dressing purposes because it is biocompatible and shows elasticity and mechanical durability [62]. PLA has been used in numerous preclinical and clinical tests. It is notable that three-dimensional (3-D) printing has provided vast opportunities for biomedical engineering to fabricate various platforms to be employed for a broad range of applications. Also, PLA can be applied as drug carrier similar to liposomes, dendrimers, polymeric nanoparticles and micelles to encapsulate antitumor drugs and avoid systemic toxicity. The clinical application of these methods from preclinical experiments is a developing field with incremental progress.

Annually, some medical costs belong to repairing skin injuries and their associated diseases. The therapeutic methods can be classified to applying synthetic and natural bandages, gauzes, cottons, diverse kinds of debridement (such as biosurgical, surgical and enzymatic), laser therapy, extracorporeal shake wave therapy, hyperbaric oxygen therapy, ultrasound therapy, electrical stimulation, by means of topical products (lotions, gels, ointments, creams and powders) and wound dressing materials [63, 64]. Among these methods, numerous studies have used various wound dressings having exceptional features because this is a safe treatment which can be applied combined with one or more therapeutic procedures stated above [65]. Currently, the best wound dressing (in form of foam, film, hydrogel, hydrocolloid and hydrofiber) should be non-adhesive, nontoxic and biocompatible. Additionally, it must absorb wound exudates and toxic agents, defend the wound against bacteria, support angiogenesis, permit vital gas exchange, maintain moisture in the wound/wound dressing interface, provide thermal insulation in the wound space, be convenient and sterilizable, have a satisfactory quality, be manufactured in diverse sizes in order to cover whole wound area and lastly be economically accessible [66–68].

In this chapter book, the most substantial experimental and computational results achieved for both drug delivery and wound healing applications using chitosan, polylactic acid, polyethyleneglycol, polylactic-co-glycolic acid and molecularly imprinted polymers are

reviewed. Furthermore, our original research data accomplished through DFT computations on simulated polymeric DDSs will be provided and discussed in detail.

## 2. CHITOSAN (CS) DRUG DELIVERY SYSTEMS

Nanocomposites of CS and clays can be produced by electrostatic interactions that offer their potential as advanced DDSs. The microparticles of chitosan-magnesium aluminum silicate (MAS) nanocomposites loaded with propranolol HCl were prepared by spray-drying method [69]. The influences of the MAS amount and adding sodium tripolyphosphate (TPP) as the crosslinking agent were examined. It was found that incorporating MAS created less spherical microparticles. The spray-dried nanocomposite particles had an intercalated structure and the drug was distributed and/or dissolved. A sustained release of propranolol was observed from all kinds of microparticles during several hours in both 0.1 M HCl and phosphate buffer (at pH 7.4) and burst release was not detected. This was a surprising result because the particles had sizes of low micrometer and CS was soluble at acidic pH. This result revealed the significance of drug-MAS and drug-CS interactions in the nanocomposite microparticles. Also, increasing the MAS quantity clearly slowed down the drug release at both low and neutral pH but adding 1-3% TPP only slightly/moderately decreased the release rate, regardless of the release medium used [69].

Since folic acid-polymer conjugates are frequently applied as drug delivery vehicles, the folic acid (FA) was loaded by CS-15 and CS-100 kDa in aqueous medium at physiological pH [70]. Thermodynamic parameters $\Delta H$= -18 to -12 (kJ. $mol^{-1}$), $\Delta S$= -22 to -8 ($J.mol^{-1}.K^{-1}$) and $\Delta G$= -11 to -9 ($kJ.mol^{-1}$) exhibited the FA-CS bindings occurred through both H-bonds and van der Waals interactions. Also, the FA-CS conjugates became more stable when polymer size was enlarged and the FA loading efficiency was 35 to 55%. The TEM images displayed main changes in polymer morphology upon FA addition. Thus, it was concluded that CS nanoparticles were able to deliver FA in vitro [70].

It was shown that physically crosslinked pectin–CS hydrogels could serve as drug carriers in order to explore the mechanism which controlled the release rate [71]. The sustained release behaviors of three drugs (progesterone, mesalamine and curcumin) were examined during 24 h under physiological conditions. The FT-IR, DSC along with the swelling test supported that the extent of interactions highly affected the release rate. Thus, it was stated that the pectin–CS thermoreversible hydrogels could be used to improve the life style of numerous patients through decreasing the uptake of chronic drugs [71].

Biocompatible nanocomposite films of blended CS and PEG-block-poly(propylene glycol)-block-PEG (BP) polymers loaded by metformin (MET) drug and MCM-41 or MCM-41-APS (APS=aminopropylsilane) NPs were designed and developed to achieve DDSs which were valuable for controlled drug release applications [72]. The total pore volume and mesoporous volume of MCM-41 were equal to 1.08 and 1.05 $cm^3/g$ while those of MCM-41-APS were measured to be 0.54 and 0.26 $cm^3/g$ which designated smaller values for the APS functionalized compound. The maximum film thickness was obtained for CS-BP-G-10%MET (70 μm) however it was the minimum for the CS-BP-G-4%MCM-41 (49 μm). The water uptake percent for all of the films was the highest in acidic environment whereas it was

diminished in PBS and the smallest swelling was happened in the alkaline medium. The least and the utmost water uptake was detected for the films contained 4%MCM-41NPs and 4%MCM-41-APS-10%MET, respectively. The SEM images of all of the films after three days water uptake at pH=4 displayed that they were stable against damage (tearing and/or cracking). Also, increasing the MCM-41 or MCM-41-APS content in the films improved the tensile stress however reduced the elongation at break. The MET release was suddenly enhanced during ~22–24 h (burst release) while subsequently the drug release was gradually boosted for the period of 15 days (sustained release). It was concluded that the most promising DDS was the film 4% MCM-41-APS-10%MET NPs for the reason that it had improved hydrolytic stability, hydrophilicity, mechanical properties, biocompatibility and drug release behavior [72].

Some chitosan–polyethylene oxide (CS-PEO) antimicrobial electrospun nanofibrous mats incorporated with ZnO NPs and hydrocortisone-imipenem/cilastatin-loaded ZnO NPs were created using electrospinning method [30]. The SEM micrographs demonstrated that the spherical ZnO NPs had a size of ~70–200 nm and the very uniform CS-PEO nanofibers were free of beads having mean diameters of ~20–130 nm. The water uptakes by all of the nanofibrous mats were the uppermost in acidic environment while they were declined in the buffer solution and the least swelling values were acquired in the alkaline medium. The drug containing mat had its bactericidal potency even after it was used for the release test in the PBS buffer for 8 days. The hydrocortisone release was 82% during the first 12h but the release rate of imipenem/cilastatin was very much slower with only 20% of the drug was released throughout this time which proved this nanofibrous mat was very appropriate to prevent infection (using imipenem/cilastatin antibiotic and ZnO NPs) and inflammation (by hydrocortisone) predominantly for the wound dressing applications [30].

Antimicrobial electrospun CS-PEO nanofibrous mats comprising fumed silica (F. silica), cefazolin and cefazolin-loaded fumed silica NPs were developed to be used in biomedical applications [31]. The SEM images exhibited that the average diameters of F. silica and F. silica-cefazolin NPs were equal to 40±10 and 60±15 nm, respectively. Furthermore, the diameters of fibers were about 160±30, 90±20 and 70±15 nm for the CS-PEO, CS-PEO-1% F. silica and CS-PEO-1% F. silica-0.5% cefazolin nanofibrous mats, respectively which indicated adding F. silica and cefazolin loaded F. silica NPs to the CS-PEO mat decreased the nanofiber diameter. The two CS-PEO mats having 2.5% cefazolin and 1% F. silica-0.50% cefazolin presented 100% antibacterial activities against both *E. coli* and *S. aureus* bacteria. The cefazolin release from mats was abruptly enhanced during first 24 and 6 hours for the CS-PEO mats containing 2.5% cefazolin and 1% F. silica-0.50% cefazolin while after that the drug release was much sluggish. The CS-PEO-1% F. silica-0.50% cefazolin was suggested as the best nanocomposite tissue/device for biomedical applications among the mats CS-PEO-2.5% cefazolin and CS-PEO-1% F. silica because of its superior hydrophilicity, higher tensile strength and sustained drug release. Furthermore, the wound healing capability of the mat CS-PEO-F. silica-cefazolin was assessed on the wounded skins of the female Wistar rats. It was found that the wounded skins of the rats were nearly completely healed after ten days by means of this mat as a wound dressing scaffold [31].

## 3. POLYLACTIC ACID (PLA) DRUG DELIVERY SYSTEMS

Recently, solvent cast polymeric inserts (SCIs) and electrospun nanofiber inserts (ENIs) were developed to be employed in ocular drug delivery [73]. SCIs and ENIs containing 1, 5 and 10%w/w dexamethasone drug were fabricated by means of a blend matrix of PLA and polyvinylalcohol (PVA). All of inserts were characterized for their thickness, morphology, pH, drug crystallinity, drug content, sterility, *in vitro* drug release, chloroform and dimethylformamide (DMF) content as well as cytotoxicity. The thicknesses of 1, 5 and 10% drug loaded ENIs were measured equal to 50, 62.5 and 93.3 μm, respectively, with suitable folding durability. The SCIs were brittle and their thickness values were more than 200 μm. The drug release rates estimated for the 1, 5 and 10% ENIs were determined as 0.62, 1.46 and 2.30 μg/h, respectively whereas those examined for the SCIs were unreliable. The DMF amounts in SCIs and ENIs were 0.123 and 0.007% w/w, respectively but chloroform was not distinguished. Cytotoxicity was not perceived for the ENIs in cultured bovine corneal endothelial cells during 24h. Finally, it was concluded that ENIs were superior to SCIs and they could be exploited as promising DDSs to treat anterior segment ocular diseases [73].

The influences of Manuka and tea tree essential oils (EOs) on the antibacterial activity and mechanical properties of electrospun PLA fibers were studied [74]. It was established that the essential oils acted as plasticizers of PLA by dropping the glass transition temperature of the fabricated composite fibers up to 60% but enhancement of tensile strength and elongation-at-break up to 12 times. Particularly, Manuka EO effectively blocked formation of *Staphylococcus epidermidis* biofilms that were usually resulted in nosocomial infections in implanted devices. Thus, results demonstrated that natural extracts could successfully be used to modulate the mechanical features of PLA fibers and to deliberate antibacterial performance [74].

The single wall carbon nanotubes doped with iron oxide nanoparticles ($Fe_3O_4$-iSWNTs) and coated with PLA-co-methoxy polyethylene glycol copolymeric (PLA-co-mPEG) micelles were prepared as hybrid nanomaterials (HNDDSs) and smart DDSs for the effective chemotherapy drug docetaxel (DTX) [75]. Treatment of the SWNTs in the acidic solution created carboxylate groups on the SWNTs surface and allowed their functionalization with $Fe_3O_4$ NPs. The PLA-co-mPEG was synthesized through ring-opening polymerization reaction and achieved as micelles which coated the $Fe_3O_4$-iSWNTs NPs. The produced nanomaterials were characterized by H-NMR, FT-IR, XRD, SEM-EDX, VSM, TGA and DSC analysis techniques. The SEM images of nanocomposites exhibited that their particle sizes were changed from 15 to 50 nm. The cytotoxicity and *in vitro* drug release tests were accomplished for the DTX loaded $Fe_3O_4$-iSWNTs/PLA-co-mPEG nanocomposites. Docetaxel was released in simulated tumor environment conditions was a sustained release (43.7% release in 348.5 h). The nanocomposite did not show obvious toxicity to MCF7 cancer cells but DTX loaded nanocomposites presented superior antitumor activity compared with free DTX so that 59 and 36% of the cells were viable after incubation, respectively. Hence, it was proposed that these nanocomposites could be used for sustained and targeted delivery of anticancer DTX drug to the cancerous cells/tissues under external magnetic fields [75].

Layered double hydroxide (LDH) materials which were intercalated with chloramphenicol, diclofenac and ketoprofen were dispersed in the semicrystalline PLA matrix [76]. The solids were characterized by FT-IR, XRD and TGA analyses. The drug release from

the DDSs was monitored by means of UV–Vis spectroscopy. It was shown that the ketoprofen drug release was nearly complete after 24 h from the drug-LDH system however lower values were achieved for other drugs (80 and 60% for chloramphenicol and diclofenac, respectively). Also, when the drugs were supported on PLA, their release rates were much slower which could be associated with the polymer degradation [76].

## 4. POLYETHYLENEGLYCOL (PEG) DRUG DELIVERY SYSTEMS

Blending of PEG and β-cyclodextrin (β-CD) in the presence of $K_2CO_3$ produced some gels which were characterized by modulated temperature differential scanning calorimetry (MTDSC), rheology, turbidity measurements and hot stage microscopy [77]. Also, the ability of these gels was investigated for topical drug delivery. The two thermoreversible GelL and GelH supramolecular gels were achieved at low (<50°C) and high (>70°C) temperatures, respectively. It was shown that GelL was changed to GelH through heating. However, by cooling, the GelH (that was more stable than GelL) was precipitated and the GelL was not reformed. GelL may be obtained by simple complexation of β-CD and PEG in the presence of $K_2CO_3$. Nevertheless, GelH probably formed a particular complex or a pseudopolyrotaxane gel. GelL was use for pharmaceutical application instead of GelH due to its forming temperature was near to the human body temperature. Further, the interactions occurred among diclofenac sodium (DS) drug and the gel components were studied by means of the FT-IR spectroscopy. The interactions might be hydrogen bonds and ionic attractions between the carboxylic groups of DS drug and the hydroxyl groups of β-CD or PEG and perhaps the inclusion of the DS aromatic ring inside the β-CD cavity. Additionally, the permeation and release of DS from GelL were considerably greater than those measured for a commercial gel. Consequently, the GelL could be suggested as a useful compound for the topical drug delivery [77].

In another work, β-CD–PEG–polyethyleneimine (PEI) coated iron oxide nanoparticles ($Fe_3O_4$-β-CD-PEG-PEI NPs) were prepared as drug carriers to be utilized in drug delivery purposes using 5-fluorouracil (5-FU) as the model drug [78]. The $Fe_3O_4$-β-CD-PEG-PEI nanoparticles were characterized by FT-IR spectroscopy, XRD, SEM, TEM and VSM techniques. The average particles sizes estimated for the 5-FU loaded $Fe_3O_4$-β-CD, $Fe_3O_4$-β-CD-PEG and $Fe_3O_4$-β-CD-PEG-PEI NPs were changed from 151 to 300 nm and their zeta potential values were obtained from −43 mV to −20 mV. The loading capacity, encapsulation efficiency and in vitro drug release ability of 5- FU drug loaded $Fe_3O_4$-β-CD, $Fe_3O_4$-β-CD-PEG and $Fe_3O_4$-β-CD-PEG-PEI NPs was assessed using UV–vis spectroscopy. In vitro cytotoxicity tests by MTT assay indicated that 5-FU loaded $Fe_3O_4$-β-CD-PEG-PEI NPs were toxic to cancer cells but non-toxic to normal cells. The in vitro release of 5-FU from drug loaded $Fe_3O_4$-β-CD-PEG-PEI composite was accomplished at diverse pH values and temperatures. It was established that 5-FU was faster and more released at pH 6.8 compared with in the acidic medium (pH=1.2). Thus, the $Fe_3O_4$-β-CD-PEG-PEI carrier could find promising application in anticancer drug delivery for the tumor therapy [78].

Ranibizumab is a first line treatment for age-related macular degeneration (AMD). To improve ranibizumab-based therapy, ranibizumab biosimilar (Mab)/PEG-conjugated small gold NPs (core size: ~5 nm) were developed for the Mab delivery [79]. The particles were characterized by TEM images and DLS analysis. The average diameters of Mab/PEG-

conjugated gold NPs and PEG-conjugated gold NPs were different using diverse PEG chain lengths (5 and 10 kDa). The Mab conjugation efficacy was optimized through altering the PEG amount and a great conjugation efficiency was measured (>70%). According to the Matrigel *in vitro*, it was indicated that Mab/PEG-conjugated gold NPs could efficiently inhibit the tube formation by the human umbilical vein endothelial cells. Also, the PEG-conjugated gold NPs without Mab surprisingly prevented the tube formation. The Mab/PEG-conjugated gold NPs did not display cell proliferation in human endothelial cells. Hence, it was proposed that Mab/PEG-conjugated gold NPs could be applied as suitable colloidal material against angiogenesis-associated diseases in local sites like AMD [79].

## 5. POLYLACTIC-CO-GLYCOLIC ACID (PLGA) DRUG DELIVERY SYSTEMS

Pickering emulsion (that forms by stabilization of the emulsion oil/water interface by means of colloids) is a favorable methodology to prepare DDSs for application in biomedical arena [80]. Using Pickering emulsion, solvent evaporation and ultrasonic irradiation, biodegradable PLGA-CS core-shell nanocomposites with a narrow size distribution were fabricated. For this purpose, aqueous-phase CS colloids were utilized in order to develop stabilized hydrophobic PLGA core in absence of surfactants or cross-linkers. The application of high intensity ultrasonic radiation facilitated effective dispersion of emulsion droplets with the particle size of PLGA-CS was controlled (255.1-824.8 nm) using diverse amplitudes. Low amplitude ultrasonic radiation (20% of total power) led to the creation of drug-loaded PLGA-CS with a small diameter (255.1 nm) and great monodispersity (polydispersity index=0.078). The hydrophobic drugs could be loaded to the PLGA core and encapsulated in the CS shell and this system has two functions including (a) PLGA dispersion in aqueous media and (b) modulating the *in vitro* drug release. Thus, these results disclosed that the modified was promising to design and formulate monodisperse polymeric drug carriers [80].

The influence of subcutaneous administration of insulin loaded PEG capped PLGA nanoparticles (ISPPLG NPs) to diabetic rats was examined [81]. Several low molecular weight biodegradable PLGA copolymers were synthesized through melt polycondensation reaction and their ISPPLG NPs were achieved using the water/oil/water (W/O/W) emulsion solvent evaporation process. Then, the PLGA copolymers and their NPs were characterized. The maximum encapsulation efficiency for the ISPPLG4 NPs was 66% and the nanoparticles diameter was ~140 nm. The *in vivo* tests using the ISPPLG NPs were accomplished on diabetic rats by subcutaneous administration and substantial decrease in serum glucose level accompanied by partial repairing in tissue defense systems were observed. Also, histopathological investigation disclosed that ISPPLG NPs restored the damages produced by oxidants throughout hyperglycaemia. Hence, the subcutaneous administrating ISPPLG4 NPs was known as a useful method to reduce hyperglycaemia related complications [81].

Incorporation of paclitaxel (PTX) in PLGA matrixes created films having high tensile rigidity and slow release rate which could not deliver the desired release rate in most biomedical applications including drug eluting stents and cancer treatment. Thus, in order to improve and modify their performance, some poly (diol sebacate)s were synthesized and characterized to be used as additives [82]. Also, the tensile characteristics of PLGA blends

were assessed because they could be applied as coatings in drug eluting stents. Using 20% additive amount, a considerable improvement was observed in mechanical flexibility because it decreased the Young´s Modulus and enhanced the maximum deformation at break. Release of PTX was examined and related to the additive release from the PLGA films. In comparison to the PLGA control film, an increase in the initial burst release was detected for all blends. The PTX release was modulated by varying the hydrophilic degree of the additive or its quantity in the blend. Thus, it was supposed that the PTX was entered in the additive phase. Cytotoxicity tests of additives were accomplished using mouse embryonic fibroblasts NIH/3T3. The NIH/3T3 cells were trypsinized and seeded in 96-well plates in absence and presence of polymer discs to be employed as positive control (TC plastic). It was verified that mouse embryonic fibroblasts NIH/3T3 had a similar performance to that of the TC plastic (+) control [82].

## 6. MOLECULARLY IMPRINTED POLYMER (MIP) DRUG DELIVERY SYSTEMS

The MIPs using nicotine template drug were prepared and the possibility of employing these materials in controlled transdermal nicotine delivery was evaluated [83]. Thus, MIPs were synthesized through free radical polymerization reaction using methacrylicacid monomer and ethylene glycol dimethacrylate cross-linker. The obtained polymeric particles were incorporated in transdermal systems with vehicles of diverse polarities. Some characterization techniques including IR spectroscopy, SEM image and thermal analysis were utilized to examine the drug–polymer interactions/compatibility and particles size/morphology. It was found that non-covalent drug–polymer interactions were occurred in the MIP particles through nicotine adsorption (mostly in non-polar vehicles). The kinetics of the drug release was fitted to Higuchi model which designated drug diffusion from the polymeric matrix. Furthermore, the drug diffusion from the polymer matrix could be improved by selective sites in the imprinted polymeric carrier. Consequently, MIPs could be used as appropriate candidates in controlled transdermal nicotine administration [83].

A nanocomposite of magnetic MIP (MMIP)/graphene oxide (GO) named MMIP@GO was developed using acrylamido-2-methyl-1-propanesulfonic acid monomer and ethylene glycol diacrylate (EGDMA) cross-linker with acrylate functionalized $Fe_3O_4$ NPs, GO and Rivastigmine (RIV) drug template [84]. The MMIP@GO was characterized by TGA, FT-IR, VSM, XRD, SEM and SEM-EDS analyses. The water uptake of MMIP@GO, selectivity and recognition for RIV and a structural derivative were assessed and compared with those of the magnetic non imprinted polymer (MNIP). The RIV adsorption mechanism onto the MMIP@GO obeyed the Langmuir model (the maximum capacity = 71.41 mg $g^{-1}$). The kinetic data were fitted to pseudo first-order model with the selectivity factor was 1.98 compared to the MNIP@GO. The *in vitro* RIV release test was dependent to the pH values (2.2-9.0) and the network structure of hydrogels. It was found that the maximum release of 74% was took place after 7 days at pH 9 [84].

In another work, hybrid pH-sensitive nanospheres were prepared by the application of a simplistic MIP method together with a UV-initiated precipitation polymerization reaction by means of vancomycin (VA) template, 2-hydroxyethyl methacrylate and 2-(diethylamino)

ethyl methacrylate functional monomers and EGDMA cross-linker [85]. The MIP nanospheres showed well-controlled particle sizes and a drug loading quantity of approximately 17% which was greater than that of the non-imprinted polymer (NIP) nanospheres (5%). Also, the VA loading capacity was well related to the crosslinker dosage. The MIP nanospheres demonstrated more controlled and slower VA release rates compared with that of the NIP nanosphere. Besides, the MIP nanospheres were sensitive to pH and thus exhibited an increased VA release rate at the lower pH levels. The VA-loaded MIP nanospheres had greater antibacterial activity (>92%) against *Staphylococcus aureus* (*S. aureus*) but the NIP nanospheres were inactive to *S. aureus*. Hence, the MIP nanospheres could be suggested as promising materials for targeted drug delivery in order to attain specific therapies like killing cancer cells with no damaging in healthy cells/tissues and stopping bacterial infections [85].

## 7. SMART POLYMERIC DRUG DELIVERY SYSTEMS

A smart pH-sensitive drug nano-carrier was developed by a simple method for controlled release of anticancer agents [86]. The nano-carrier had two central parts including the nano-container MCM-41 part and pH-sensitive poly4-vinylpyridine gatekeeper. The MCM-41 was synthesized through template supported sol-gel procedure. Then, polymerized functional groups were bound on pore entrances instead of internal walls. After that, polymeric gatekeepers were attached onto the pore entrances by means of precipitation polymerization reaction of monomers with functionalized MCM-41. The EDX, XRD, FT-IR, TGA, Zeta potentials, DLS, TEM and FE-SEM analyses were used to support the binding of gatekeepers. Additionally, the release of methotroxate (MTX) anti-cancer drug was accomplished in diverse media (pH=4, 5.8 and 7.4) at 37±1°C. It was found that the release rates were entirely pH dependent so that the release was preceded by drop in pH level. It was concluded that at the higher pH, the gatekeepers were in their closed state whereas they switched to the open state due to repulsive forces occurred between positively charged polymeric chains in acidic environments. Therefore, the results proposed that this smart nanocarrier could be accounted for as a proper material for the delivery of therapeutics to cancer tissues [86].

It is known that the targeted delivery of antitumor agents to the tumor cell nucleus is of excessive attention in cancer therapy because the nucleus is one of the most common targets for the drug action [87]. In this context, a smart polymeric conjugate platform was prepared which used stimulus-responsive approaches in order to attain multistage nuclear drug delivery after the systemic administration. The conjugates contained a backbone of N-(2-hydroxypropyl) methacrylamide copolymer and detachable nucleus transport sub-units that were sensitive to lysosomal enzyme. The sub-units had a biforked structure with one end was conjugated to the drug (H1 peptide) and the other end was conjugated to a pH-responsive targeting peptide (R8NLS) which jointed the asset of nuclear localization sequence and cell penetrating peptide. The conjugates displayed long circulation time and outstanding tumor homing capacity. Activation of R8NLS in acidic tumor microenvironment enabled tissue penetration and cellular internalization. When internalized into the cell, the sub-units were released for nuclear transport by nuclear pore complex. These exceptional characteristics led to 50-fold enhancement in nuclear drug accumulation compared with the original polymer-

drug conjugates in vitro, and superb in vivo nuclear drug delivery effectiveness. Hence, the results provided a nuclear drug delivery vehicle through merging the detachable sub-units and microenvironment-responsive structure [87].

A thermosensitive poly(di(ethylene glycol) methyl ether methacrylate) (PDEGMA) polymer was synthesized and then it was electrospun into fibers through blending with ethyl cellulose (EC) [88]. Also, fibers loaded with ketoprofen (KET) drug were produced. The cylindrical fibers were observed in the SEM images even though some beads and fused fibers were detected in the KET-loaded materials. The XRD patterns exhibited that KET was amorphously dispersed in the fibers. The water contact angle analysis revealed that the wettability of the EC/PDEGMA fibers was altered when the temperature was enhanced and the fibers became evidently more hydrophobic. *In vitro* drug release test displayed that KET release was happened during a long time and the fibers had diverse release profiles at 25 and 37ºC, which reflected their thermosensitive features. Besides, the materials had decent biocompatibility towards L929 fibroblasts. Therefore, the prepared fibers could find potential as smart stimuli responsive DDSs [88].

In another study, a biocompatible, multi-stimuli responsive and non-immunogenic smart carrier was designed for targeted delivery and triggered release of hydrophobic drugs [89]. The smart CS-based microcapsules (MSRS-CS-MCs) were fabricated using folic acid (FA) functionalized thiolated CS through a simple sonochemical technique. Immobilization of both of FA targeting moiety and Rhodamine B isothiocyanate (RITC), a red fluorescent dye, was done on the microcapsules shells. Also, oleic acid (OA) modified magnetic $Fe_3O_4$ NPs (OA-$Fe_3O_4$ MNPs) and a hydrophobic drug, green fluorescent dye (Coumarin 6, C6), were encapsulated in the microcapsules. The spherical MSRS-CS-MCs drug carriers with an average size of 500 nm presented outstanding magnetic responsive capacity, interesting reduction-responsive release of hydrophobic drugs and promising selectively folate-receptor-mediated targeting functionality to the HeLa cells. The combination of magnetic and reduction dual-responsiveness, folate-receptor-mediated targeting functionality and fluorescence visualization in the multipurpose microcapsules made MSRS-CS-MCs auspicious nanocarriers for upcoming biomedical applications [89].

An effective DDS was developed for which the carrier was synthesized by combining CMK3 ordered mesoporous carbon and a thermosensitive poly(N-isopropylacrylamide) polymer named PNIPAAm. The polymers were synthesized with two chain lengths (PNIPAAMm-100n and PNIPAAm 400n) and then they were entered in CMK3 to create composite materials [90]. The $N_2$ adsorption isotherms and SEM images of the samples exhibited that PNIPAAMm-100n was uniformly embedded but PNIPAAMm-400n was not evenly embedded. The latter phenomenon was ascribed to great intra-molecular interactions of PNIPAAMm-400n chains and their aggregation over the external surface of the porous structure. Loading of doxorubicin (DOX) drug was performed into the samples and it was shown that the maximum loading abilities for the polymer-embedded samples were decreased. Nevertheless, the release capacities and the loading rates were considerably enhanced. The principal drug release mechanism was found to be the polymer thermosensitivity (irrespective of the polymer chain length, the drug release at 37°C was meaningfully greater than that measured at 4°C). The cytotoxicity tests established that the materials were biocompatible and suitable for forthcoming biological applications. Thus, it was suggested that the composite synthesized using ordered mesoporous carbon and thermosensitive polymer would be an effective carrier in drug loading and release trials.

Furthermore, the drug loading and release could be controlled through modifying the polymeric chain length [90].

## 8. DFT COMPUTATIONS ON DRUG DELIVERY SYSTEMS

Polymeric materials as drug carriers such as PEG, which physically entrap drugs, play a significant role in modern pharmaceutical technology [91-93]. Indeed, they perform the targeted delivery of drugs to specific sites of action in the body. The decreased interactions with blood components (opsonization) lead to activation of the complement system and result in a reduced blood clearance of drug carrier, which is recognized as the stealth effect. PEG is the most frequently used non-ionic hydrophilic polymer with stealth action. In addition, PEG decreases the aggregation of particles by steric stabilization and provides high stability during storage and application [94]. Since it is known that PEG can affect the pharmacokinetic properties of drugs, it is often utilized in numerous established and emerging applications in pharmaceutics. The change in the pharmacokinetics of administered drugs shielded by PEG causes prolonged blood circulation times and as a result increases the possibility of reaching drug to its site of action before being recognized as a foreign particle and cleared from the body. For this reason, many drugs are PEG-containing products [94]. So far, all polymeric stealth drug-delivery systems that have been presented to the market include PEG functionalized products and no other synthetic polymer has yet reached this status [94–96]. Moreover, PEG illustrates a high solubility in organic solvents, thus, end-group modifications are quite simple. At the same time, PEG is soluble in water and has a low intrinsic toxicity which makes the polymer ideally used in biological applications.

The success of PEG in drug-delivery purposes also caused its applications in other medical fields so that it is used in blood and organ storage in order to reduce the aggregation of red blood cells and improve the blood compatibility of poly(vinyl chloride) bags [97–100]. PEG copolymers that are implanted as cardiovascular devices decrease thrombosis [101]. The inhibited interactions of PEG with biomolecules resulted in its antifouling and anti-adhesion applications, for example in Merrifield syntheses [102], ultrafiltration [103], and the protection of contact lenses from pathogenic bacteria and fungi [104, 105]. PEG chains linked to hydrophobic molecules such as oleic acid, can act as a surfactant, and are found as surface-active, viscosity-increasing, and skin-conditioning agents in all kinds of cosmetics—from toothpaste to cleansing agents, such as shampoos, body and bath soaps, to fragrance, aftershave lotion, face powder, and eye shadow [106, 107]. These paradigms confirm that PEG is not only very popular in pharmaceutical applications, but also it is a favored consumer product in our daily life.

Hydrochlorothiazide (HCT) is a diuretic drug belonging to the thiazide class used for the treatment of mild to moderate hypertension. The chemical formula of HCT is $C_7H_8ClN_3O_4S_2$ that is named 6-chloro-1,1-dioxo-3,4-dihydro-2H-1,2,4-benzothiadiazine-7-sulfonamide, as recorded in the IUPAC system. Thiazides work, at least in part, by inhibiting sodium reabsorption in the distal convoluted tubule [108, 109]. Oral administration of HCT causes dieresis within 2 hours [110], indirectly resulting in an initial decrease in plasma volume that attenuates with long-term treatment [111]. Diuretic substances enhance urine flow and decrease the capacity of tubular reabsorption of sodium and water. They reduce blood

volume, decrease blood return to the heart and consequently reduce cardiac output and lower blood pressure. HCT has extensive signs in the treatment of diseases such as renal edema, hypertension, hypercalcemia and nephrogenic diabetes insipidus [112]. HCT is a calcium-sparing diuretic which can help rid the body of excess water, but retain calcium [113, 114]. It is frequently used for the treatment of hypertension, congestive heart failure, symptomatic edema, diabetes insipidus, renal tubular acidosis, and the prevention of kidney stones [115]. It is also occasionally applied for hypercalciuria, Dent's disease, and Ménière's disease. After oral administration, HCT peak concentration in plasma is achieved at 2 h and the half-life of elimination averages 10 h [116, 117]. It is absorbed by the gastrointestinal tract and eliminated mostly by renal excretion; approximately 65–72% of the drug dose is excreted in urine [118, 119].

## 8.1. Delivery of Anti-Hypertensive Hydrochlorothiazide Drug Using Ethyleneglycol

Herein, following our previous works on computational DDSs and polymeric composites [120-125], the structural and electronic properties of six complexes formed through hydrogen bonds between anti-hypertensive hydrochlorothiazide drug and ethylene glycol (EG) as a drug carrier were predicted. For this purpose, DFT computations were conducted at B3LYP and B3PW91 levels in both the gas phase and solution state (in water and ethanol). It was found that complex **4** formed through H-bonds between oxygen and NH hydrogen atoms of sulfonamide in drug and OH from EG is the most stable compound in the gas phase but the complex **6** created by N-H…O hydrogen bond between the NH(ring) moiety of drug and O atom of OH group from EG is the most energetically stable compound in the solution state (water and ethanol); consequently, complex **6** can be selected as the most suitable drug delivery system in the solution state.

### *8.1.1. Computational Methods*

The structures of compounds **1**–**6** (Scheme 1) were first optimized in Hyperchem 7.0 program and then, the quantum chemical calculations were carried out by Gaussian 98 program [126] to fully optimize the geometries of the structures using density functional theory (DFT) at B3LYP and B3PW91 levels and standard 6-31G(d) and 6-31+G(d,p) basis sets in the gas phase and in the solution state (water and ethanol). The SCRF keyword using Tomasi's polarized continuum (PCM) model was utilized to compute the structure in various solvents [127]. The natural bond orbital (NBO) calculations were performed to obtain the HOMO (highest occupied molecular orbital), LUMO (lowest unoccupied molecular orbital), band gap energies, electron density charge transfer energies, contours and surfaces. Nuclear quadrupole coupling constants ($\chi$) were calculated from the equation $\chi = e^2q_{zz}Q/h$ [128], supposing the electric quadrupole moments (Q) of $^2H$ (I=1), $^{17}O$ (I=5/2) and $^{14}N$ (I=1), nuclei are 2.86, 25.58 and 20.44 mb (1 mb $=10^{-31}$ $m^2$), respectively [129]. The topological analysis of the optimized structures **1**–**6** at both B3LYP and B3PW91 levels were accomplished by the Quantum Theory of Atoms in Molecules (QTAIM) of Bader [130] using AIM2000 program [131] in order to evaluate the nature of bonds (covalent, electrostatic and intermediate).

### *8.1.2. Results and Discussion*

#### 8.1.2.1. Optimization and Energies of the Structures

In order to investigate the electronic and structural properties of isolated ethylene glycol (EG, **1**), anti-hypertensive hydrochlorothiazide drug (**2**) and their hydrogen bonded complexes (**3**–**6**) (Scheme 1), DFT computations were performed at B3LYP and B3PW91 levels of theory using 6-31G(d) and 6-31+G(d,p) basis sets in the gas phase as well as in water and ethanol solvents. It is obvious that complexes **3**–**6** differ in the hydrogen bonds formed between EG and drug so that in **3** and **4** the two sulfonamide groups ($SO_2NH_2$) on the phenyl ring and within the ring, respectively, both form the two strong N-H…O and O-H…O hydrogen bonds. In system **5**, the O-H…O hydrogen bond is created between the sulfonyl oxygen (in the ring) and hydrogen atom of OH from EG but in **6**, the N-H…O bond is constructed between the hydrogen atom of ring NH group and OH oxygen atom of EG. Herein, the EG is considered as the drug carrier and complexes **3**–**6** are our drug delivery systems that are evaluated and compared for their structural characteristics.

The binding energies for the isolated and complex compounds were calculated from the equations $\Delta E_{binding}$ = E(molecule) – $\Sigma_i$ E(i), i = atom or ion and $\Delta E_{binding}$ = E(complex) – Σ E[(drug) + E(EG)] + BSSE + ΔZPVE, respectively. The $\Delta E_{binding}$ values were corrected by addition of basis set superposition error (BSSE) energies as well as the zero-point vibrational energies to the binding energies. The zero-point vibrational energy (ΔZPVE) correction was estimated as the difference in zero-point vibrational energies between the complex and the isolated molecules, i.e., ΔZPVE = ZPVE(complex) – [ZPVE(drug) + ZPVE(EG)] [132]. The basis sets superposition errors [133] using counterpoise correction was developed by Boys and Bernardi [134].

The $\Delta E_{binding}$ values (kcal/mol) for compounds **1**–**6** are given in Table 1. It can be seen that among complexes **3**–**6** in the gas phase, compound **4** is the most stable one at both B3LYP and B3PW91 levels with the most negative $\Delta E_{binding}$ and then complex **6** reveals the greatest $\Delta E_{binding}$. The $\Delta E_{binding}$ is the most negative for compound **6** in the solution state (water and ethanol). However, the binding energy of complex **4** is slightly smaller than that of 6 and shows the greatest negative value after **6**. It is notable that complex **3** that has two hydrogen bonds with a very similar structure to that of **4** displays binding energies very smaller than those of its analogue **4**. The least $E_{binding}$ value is computed for complex **5** that is a hydrogen bonded structure between oxygen atom of ring sulfonyl group and H atom from OH group of EG reflecting non-preferred formation of this H-bond relative to other forms. Therefore, considering the $\Delta E_{binding}$, it can be stated that complexes **6** and then **4** will be the most favorable ones in the solution state among systems **3**–**6** examined here. Also, the $\Delta E_{binding}$ values of complexes **4** and **6** are the greatest at the B3LYP/6-31+G(d) level of theory. The optimized structures of the most stable complexes **4** (in the gas phase) and **6** (in water and ethanol) at B3LYP/6-31+G(d) level are presented in Figure 1 displaying the presence of intermolecular hydrogen bonds between the drug and EG.

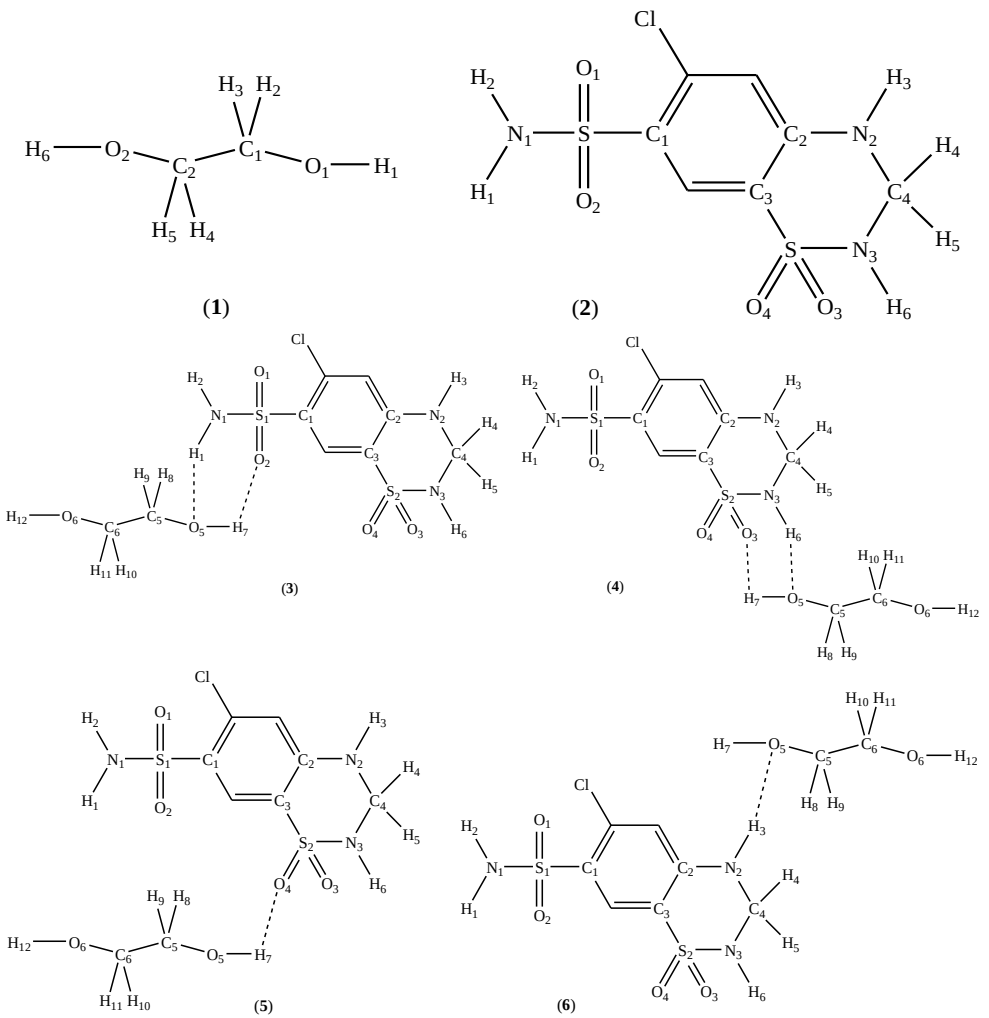


Scheme 1. The molecular structures of compound 1–6 indicating the atom-labeling schemes.

Calculated dipole moments (μ, Debye) for compounds **1**–**6** in the gas phase and in the solution state (water and ethanol) are given in Table 2. The data indicate relatively the same values at both B3LYP and B3PW91 methods. Also, the dipole moments in water and methanol are about 4 Debye greater than those measured in the gas phase. This can be attributed to the polarization effect of polar solvents used here. The greatest dipole moment is obtained for complex 6 in gas phase (~11.0 Debye) and in solvents (~15.0 Debye). The dipole moment of EG (**1**) is zero but the drug (**2**) exhibits a high polarity. All of the complexes **3**–**6** reveal remarkable dipole moments both in the gas phase and in the solution state confirming the existence of strong hydrogen bonding interactions between the two species (**1** and **2**).

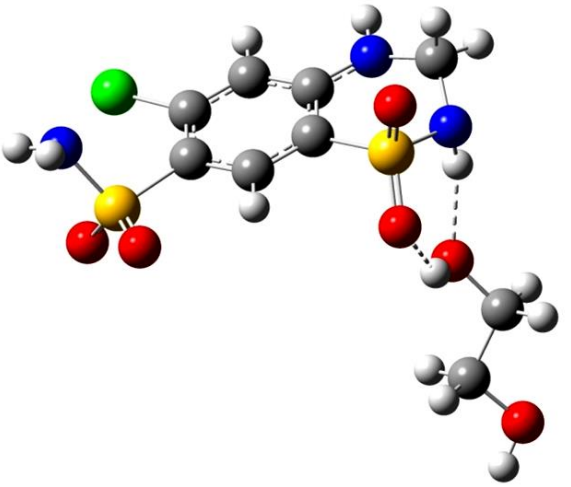

(**4** in gas phase)

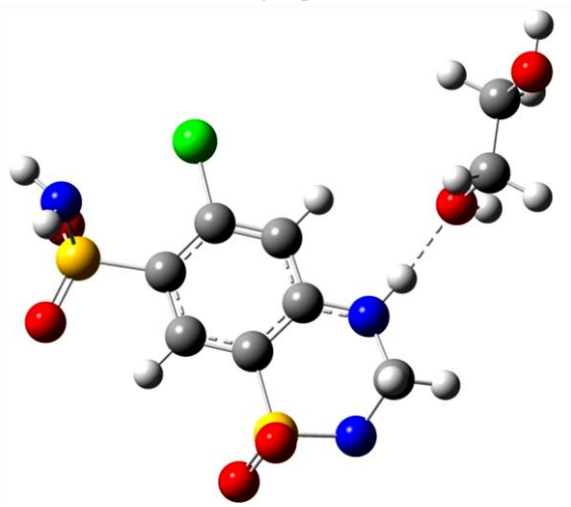

(**6** in water)

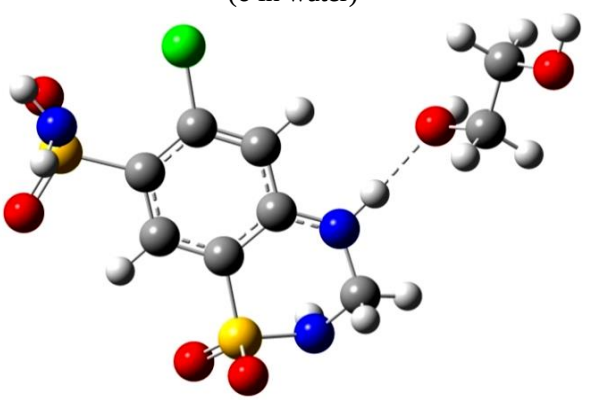

(**6** in ethanol)

Figure 1. The optimized structures of compounds **4** (in gas phase) and **6** (in water and ethanol) at B3LYP/6-31G(d) level of theory.

**Table 1. The computed binding energies ([a]$\Delta E_{binding}$, kcal/mole) for compounds 1–6**

| Compound | $\Delta E_{binding}$ (gas phase) | | | |
|---|---|---|---|---|
| | B3LYP/6-31+G(d) | B3PW91/6-31+G(d) | B3LYP/6-31+G(d,p) | B3PW91/6-31+G(d,p) |
| **1** | -888.543 | -891.115 | -899.007 | -901.432 |
| **2** | -2393.264 | -2432.734 | -2405.199 | -2444.424 |
| **3** | -7.3381 | -6.5166 | -7.4195 | -6.6556 |
| **4** | -10.2166 | -9.6885 | -10.1462 | -9.7009 |
| **5** | -2.8419 | -2.1197 | -2.9491 | -2.2269 |
| **6** | -8.5812 | -8.2674 | -8.4650 | -8.1883 |
| Compound | $\Delta E_{binding}$ (in water) | | | |
| | B3LYP/6-31+G(d) | B3PW91/6-31+G(d) | B3LYP/6-31+G(d,p) | B3PW91/6-31+G(d,p) |
| **1** | -892.987 | -895.553 | -903.210 | -905.619 |
| **2** | -2405.194 | -2444.584 | -2417.007 | -2456.136 |
| **3** | -2.9197 | -2.0696 | -1.7010 | -2.3861 |
| **4** | -5.2730 | -4.5798 | -5.2667 | -4.6897 |
| **5** | -0.9366 | -0.7161 | -0.9242 | -0.7976 |
| **6** | -5.6346 | -5.2632 | -5.6228 | -5.3204 |
| Compound | $\Delta E_{binding}$ (in ethanol) | | | |
| | B3LYP/6-31+G(d) | B3PW91/6-31+G(d) | B3LYP/6-31+G(d,p) | B3PW91/6-31+G(d,p) |
| **1** | -892.783 | -895.349 | -903.017 | -905.426 |
| **2** | -2404.574 | -2443.971 | -2416.392 | -2455.530 |
| **3** | -3.1016 | -2.5292 | -3.3371 | -2.542 |
| **4** | -5.2635 | -4.9705 | -5.3795 | -4.8876 |
| **5** | -1.3914 | -1.0065 | -1.4513 | -0.9027 |
| **6** | -5.7638 | -5.6302 | -5.7325 | -5.3686 |

[a]For compounds **1** and **2**, $\Delta E_{binding} = E_{molecule} - \Sigma E_{atom}$ and for compounds **3**–**6**, $\Delta E_{binding} = E_{complex} - \Sigma(E_{drug} + E_{EG}) + BSSE + \Delta ZPVE$.

The Gibbs free energies ($\Delta G_{interaction}$) and enthalpies of interaction ($\Delta H_{interaction}$) for compounds **3**–**6** are given in Tables 3 and 4, respectively. The $\Delta G_{interaction}$ and $\Delta H_{interaction}$ were calculated using the following equations.

$$\Delta G_{interaction} = G(drug–EG) - \Sigma\,[G(drug) + G(EG)]$$
$$\Delta H_{interaction} = H(drug–EG) - \Sigma\,[H(drug) + H(EG)]$$

It can be observed from the table that comparable $\Delta G_{interaction}$ values are obtained at both B3LYP and B3PW91 levels (Table 3) and the hydrogen bond formation between the drug and EG is only exergonic ($\Delta G_{interaction} < 0$, spontaneous interaction) for compounds **4** and **6** in the gas phase with a much more negative value for compound **4**. This result is in agreement with the binding energies in which the most negative $\Delta E_{binding}$ is measured for complex **4** in the gas phase. All of the $\Delta G_{interaction}$ values are positive (endergonic or non-spontaneous interaction) and comparable in water and ethanol solvents with the smallest value is obtained for **6** and then for complex **4** confirming the binding energy results. Thus, formation of complex **4** in the gas phase and complex **6** in the solution state is more favored compared with other compounds. In addition, the greatest positive values are computed for compound **5** reflecting its formation is not favored in comparison with other structures.

**Table 2. The computed dipole moments (Debye) for compounds 1–6**

| Compound | dipole moment (gas phase) | | | |
|---|---|---|---|---|
| | B3LYP/6-31+G(d) | B3PW91/6-31+G(d) | B3LYP/6-31+G(d,p) | B3PW91/6-31+G(d,p) |
| **1** | 0.0000 | 0.0000 | 0.0000 | 0.0000 |
| **2** | 7.9706 | 7.8977 | 7.9756 | 7.9010 |
| **3** | 6.1570 | 6.1304 | 6.1870 | 6.1636 |
| **4** | 5.9837 | 5.8706 | 6.0103 | 5.9045 |
| **5** | 8.2371 | 8.2139 | 8.2355 | 8.1865 |
| **6** | 11.1805 | 11.1276 | 11.0942 | 11.1151 |
| Compound | dipole moment (in water) | | | |
| | B3LYP/6-31+G(d) | B3PW91/6-31+G(d) | B3LYP/6-31+G(d,p) | B3PW91/6-31+G(d,p) |
| **1** | 0.0000 | 0.0001 | 0.0000 | 0.0001 |
| **2** | 11.8029 | 11.6655 | 11.8371 | 11.6938 |
| **3** | 9.7319 | 9.6068 | 9.9516 | 9.8305 |
| **4** | 11.0536 | 8.5821 | 10.8759 | 8.6561 |
| **5** | 11.5501 | 12.3693 | 11.7160 | 12.4302 |
| **6** | 14.9414 | 14.7489 | 14.9347 | 14.7629 |
| Compound | dipole moment (in ethanol) | | | |
| | B3LYP/6-31+G(d) | B3PW91/6-31+G(d) | B3LYP/6-31+G(d,p) | B3PW91/6-31+G(d,p) |
| **1** | 0.0000 | 0.0000 | 0.0000 | 0.0000 |
| **2** | 11.5587 | 11.4331 | 11.5895 | 11.4586 |
| **3** | 9.5319 | 9.4114 | 9.7053 | 9.5841 |
| **4** | 8.4835 | 8.3802 | 8.5943 | 8.4908 |
| **5** | 12.1161 | 12.1110 | 12.3525 | 12.1927 |
| **6** | 14.6549 | 14.5599 | 14.7201 | 14.5529 |

**Table 3. The computed Gibbs free energies ($\Delta G_{interaction}$, kcal/mol) of interaction for compounds 3–6**

| Compound | $\Delta G_{interaction}$ (gas phase) | | | |
|---|---|---|---|---|
| | B3LYP/6-31+G(d) | B3PW91/6-31+G(d) | B3LYP/6-31+G(d,p) | B3PW91/6-31+G(d,p) |
| **3** | +1.9459 | +2.6292 | +2.1122 | +2.7290 |
| **4** | -1.5179 | -1.2694 | -1.2650 | -0.9559 |
| **5** | +4.7533 | +5.1750 | +4.5902 | +5.2748 |
| **6** | -0.5742 | -0.2064 | -0.2146 | -0.0144 |
| Compound | $\Delta G_{interaction}$ (in water) | | | |
| | B3LYP/6-31+G(d) | B3PW91/6-31+G(d) | B3LYP/6-31+G(d,p) | B3PW91/6-31+G(d,p) |
| **3** | +5.1551 | +5.6848 | +5.4513 | +5.8458 |
| **4** | +2.9750 | +3.4098 | +2.8081 | +3.5171 |
| **5** | +6.8495 | +6.4783 | +6.5755 | +6.6446 |
| **6** | +2.9279 | +2.9003 | +3.1551 | +2.4999 |
| Compound | $\Delta G_{interaction}$ (in ethanol) | | | |
| | B3LYP/6-31+G(d) | B3PW91/6-31+G(d) | B3LYP/6-31+G(d,p) | B3PW91/6-31+G(d,p) |
| **3** | +5.0140 | +5.6981 | +5.2599 | +5.6437 |
| **4** | +3.2956 | +3.7495 | +2.8238 | +3.1551 |
| **5** | +5.6883 | +6.5500 | +6.0121 | +6.9816 |
| **6** | +2.5018 | +2.8954 | +3.0666 | +3.0296 |

The $\Delta H_{interaction}$ values are negative all for compounds **3–6** at both B3LYP and B3PW91 levels reflecting their exothermic reaction behavior (Table 4). The $\Delta H_{interaction}$ vary in the range of -11.1475 (in **4**) to -3.3358 (in **5**) in the gas phase at B3LYP/6-31+G(d) method. Interestingly, the $\Delta H_{interaction}$ values confirm the $\Delta E_{binding}$ and $\Delta G_{interaction}$ results so that the most negative values are measured for complex **4** in the gas phase and complex **6** in the solution state indicating the most convenient formation of these compounds. Furthermore, the least negative values are found for compound **5** revealing its formation is not favored in comparison with other structures.

**Table 4. The computed enthalpies ($\Delta H_{interaction}$, kcal/mol) of interaction for compounds 3–6**

| Compound | $\Delta H_{interaction}$ (gas phase) | | | |
|---|---|---|---|---|
| | B3LYP/6-31+G(d) | B3PW91/6-31+G(d) | B3LYP/6-31+G(d,p) | B3PW91/6-31+G(d,p) |
| **3** | -8.8038 | -8.0703 | -8.5622 | -7.8858 |
| **4** | -11.1475 | -10.7171 | -10.8056 | -10.4303 |
| **5** | -3.3358 | -2.5702 | -3.1532 | -2.4171 |
| **6** | -9.0090 | -8.7367 | -8.7461 | -8.4907 |
| Compound | $\Delta H_{interaction}$ (in water) | | | |
| | B3LYP/6-31+G(d) | B3PW91/6-31+G(d) | B3LYP/6-31+G(d,p) | B3PW91/6-31+G(d,p) |
| **3** | -4.2733 | -3.5021 | -2.5119 | -3.4657 |
| **4** | -5.9732 | -5.4899 | -5.6983 | -5.3087 |
| **5** | -1.9033 | -1.2054 | -1.5996 | -1.0598 |
| **6** | -6.0918 | -5.7379 | -5.9230 | -5.6061 |
| Compound | $\Delta H_{interaction}$ (in ethanol) | | | |
| | B3LYP/6-31+G(d) | B3PW91/6-31+G(d) | B3LYP/6-31+G(d,p) | B3PW91/6-31+G(d,p) |
| **3** | -4.4835 | -3.4297 | -4.3680 | -3.6646 |
| **4** | -6.1357 | -5.4744 | -5.9292 | -5.5314 |
| **5** | -1.8944 | -1.0903 | -1.7244 | -1.1954 |
| **6** | -6.2097 | -5.8927 | -6.0378 | -5.7159 |

The hydrogen bonding data of compounds **3–6** at B3LYP/6-31+G(d) level of theory are presented in Table 5. It is observed that in all cases the d(H...A) distances are below or about 2 Å indicating the formation of strong hydrogen bonds between drug and EG. The smallest d(H...A) distances are measured for complex **6** reflecting its preferred formation relative to other structures. Also, the distances are smaller in the solution state than in the gas phase implying stronger interactions in the solvents.

Selected bond lengths and angles of compounds **4** in the gas phase and **6** in water and ethanol at B3LYP/6-31+G(d) level are listed in Table 6. Comparable results are obtained for the bond lengths in the gas phase and in the solution state. The S2–O3 and S2–O4 bond lengths are about 1.47 and 1.46 Å, respectively, in complex **4** showing the S2–O3 bond length is longer than S2–O4 which is due to the contribution of O3 atom in the formation of O(5)–H(7)...O(3) hydrogen bond but the O4 atom does not take part in the H-bond formation. The S2–O3 and S2–O4 bond lengths are both near 1.47 Å in **6** because none of them form H-bond. In both compounds **4** and **6**, the S-N and S-C bond lengths are almost 1.68-1.69 and 1.79 Å, respectively, and the C2-C3 and C-O bond lengths are approximately 1.40 and 1.40-1.50 Å, respectively.

**Table 5. Hydrogen bonding data (Å, °) for compounds 3–6 at B3LYP/6-31+G(d) level of theory**

| Compound | Computation phase | d(H…A) | d(D–H) | d(H...A) | d(D...A) | ∠DHA[a] |
|---|---|---|---|---|---|---|
| **3** | Gas | N(1)–H(1)...O(5) | 1.0300 | 1.9953 | 2.9570 | 154.24 |
| | Water | | 1.0315 | 1.9676 | 2.9423 | 156.46 |
| | Ethanol | | 1.0314 | 1.9695 | 2.9433 | 156.30 |
| | Gas | O(5)–H(7)...O(2) | 0.9761 | 1.9964 | 2.8301 | 142.00 |
| | Water | | 0.9743 | 2.1137 | 2.5304 | 136.50 |
| | Ethanol | | 0.9744 | 2.1055 | 2.8939 | 136.83 |
| **4** | Gas | N(3)–H(6)...O(5) | 1.0310 | 1.9616 | 2.9103 | 151.63 |
| | Water | | 1.0338 | 1.9168 | 2.8978 | 157.24 |
| | Ethanol | | 1.0324 | 1.9596 | 2.9284 | 155.08 |
| | Gas | O(5)–H(7)...O(3) | 0.9764 | 2.0375 | 2.8537 | 139.80 |
| | Water | | 0.9725 | 2.2582 | 2.9872 | 130.94 |
| | Ethanol | | 0.9751 | 2.1673 | 2.9410 | 135.25 |
| **5** | Gas | O(5)–H(7)...O(4) | 0.9736 | 2.0231 | 2.9542 | 159.34 |
| | Water | | 0.9766 | 1.9085 | 2.8828 | 175.19 |
| | Ethanol | | 0.9760 | 1.9123 | 2.8868 | 176.16 |
| **6** | Gas | N(2)–H(3)...O(5) | 1.0191 | 1.9489 | 2.9676 | 177.95 |
| | Water | | 1.0248 | 1.8823 | 2.9044 | 174.91 |
| | Ethanol | | 1.0244 | 1.8841 | 2.9070 | 176.12 |

[a] D is donor atom, H is hydrogen and A is the acceptor atom.

**Table 6. Selected bond lengths (Å) and angles (°) for compounds 4 (in gas phase) and 6 (in water and ethanol) calculated at B3LYP/6-31+G(d) level of theory**

| **4** in gas phase | | **6** in water | | **6** in ethanol | |
|---|---|---|---|---|---|
| S2–O3 | 1.4717 | S2–O3 | 1.4715 | S2–O3 | 1.4711 |
| S2–O4 | 1.4626 | S2–O4 | 1.4702 | S2–O4 | 1.4697 |
| S2–C3 | 1.7898 | S2–C3 | 1.7818 | S2–C3 | 1.7824 |
| S2–N3 | 1.6846 | S2–N3 | 1.6854 | S2–N3 | 1.6962 |
| C2–C3 | 1.4171 | C2–C3 | 1.4228 | C2–C3 | 1.4227 |
| S1–C1 | 1.7988 | S1–C1 | 1.7892 | S1–C1 | 1.7897 |
| S1–N1 | 1.6914 | S1–N1 | 1.6806 | S1–N1 | 1.6810 |
| C5–O5 | 1.4293 | C5–O5 | 1.4365 | C5–O5 | 1.4366 |
| C5–C6 | 1.5258 | C5–C6 | 1.5250 | C5–C6 | 1.5250 |
| N1–S1–C1 | 103.46 | N1–S1–C1 | 103.18 | N1–S1–C1 | 103.27 |
| N1–S1–O1 | 108.18 | N1–S1–O1 | 110.93 | N1–S1–O1 | 110.68 |
| N1–S1–O2 | 106.94 | N1–S1–O2 | 106.14 | N1–S1–O2 | 106.24 |
| S2–N3–C4 | 112.60 | S2–N3–C4 | 112.49 | S2–N3–C4 | 112.44 |
| C2–C3–S2 | 119.55 | C2–C3–S2 | 119.28 | C2–C3–S2 | 119.26 |
| N2–C4–N3 | 111.83 | N2–C4–N3 | 112.28 | N2–C4–N3 | 112.33 |
| C6–C5–O5 | 111.23 | C6–C5–O5 | 111.12 | C6–C5–O5 | 111.17 |
| C5–C6–O6 | 106.88 | C5–C6–O6 | 106.97 | C5–C6–O6 | 106.93 |

The S1 and S2 atoms of $SO_2$ groups on the phenyl ring and within the aliphatic ring of compounds **4** and **6** are tetrahedral because the angles at these sulfur atoms are about 110°. For example, average of the surrounding angles around S1 and S2 atoms of compound **4** in the gas phase are 109.2280 and 109.1876 Å, respectively. The N1 and N3 atoms are also

tetrahedral but the N2 and ring carbon atoms in compounds **4** and **6** are planar for which sum of surrounding angles are all near 360°.

### 8.1.2.2. NBO Analysis

The band gaps ($E_g$) of compounds **1**–**6** which are the differences of energies between the HOMO and LUMO and are measures of electron conductivities are given in Table 7. Similar results were obtained at the four computational levels and also in the gas phase and in the solution state. It is observed that the band gap of EG is the highest (~8 eV) but those of drug and hydrogen bonded complexes are comparable that are almost ~5 eV.

The HOMO and LUMO molecular orbitals of EG (**1**), drug (**2**) and their corresponding complexes **4**, **6** in the gas phase are depicted in Figure 2. It is clear that the HOMO and LUMO electron densities in **1** are both located on the whole molecule. In compound **2**, the electron density of HOMO orbital is dispersed especially on the two aromatic and aliphatic rings while the LUMO orbital is only observed on aromatic phenyl ring. The HOMO and LUMO orbitals of complexes **4** and **6** are similar to those of drug **2** in which they are placed on the drug and there is not any portion of HOMO and LUMO orbitals on the EG. Very similar results were observed for complexes **4** and **6** in water (Figure 3) and ethanol (Figure 4) but in compound **4**, the negative and positive regions of the wave functions (red and green spaces) are replaced with each other in ethanol.

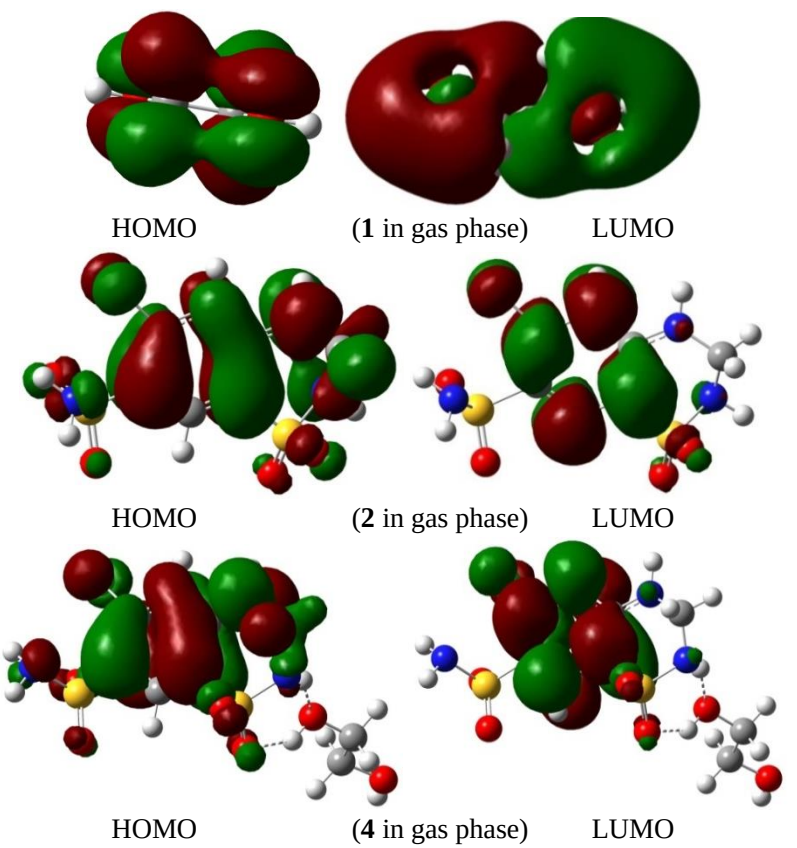


Figure 2. (Continued).

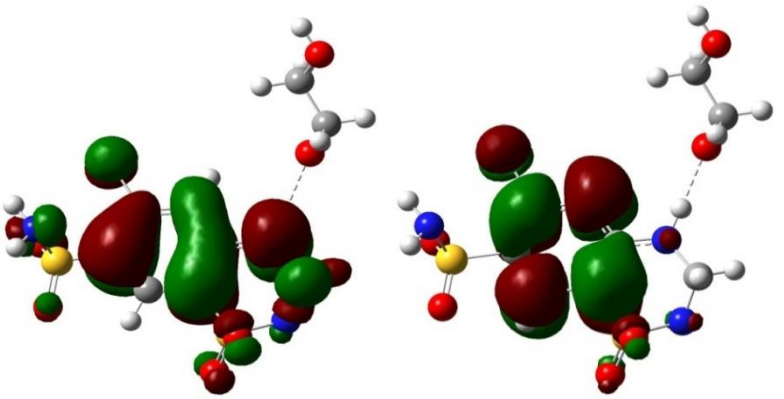


Figure 2. The HOMO and LUMO molecular orbitals of compounds **1**, **2**, **4** and **6** in gas phase at B3LYP/6-31G(d) level. Red and green represent negative and positive regions of the wave functions, respectively.

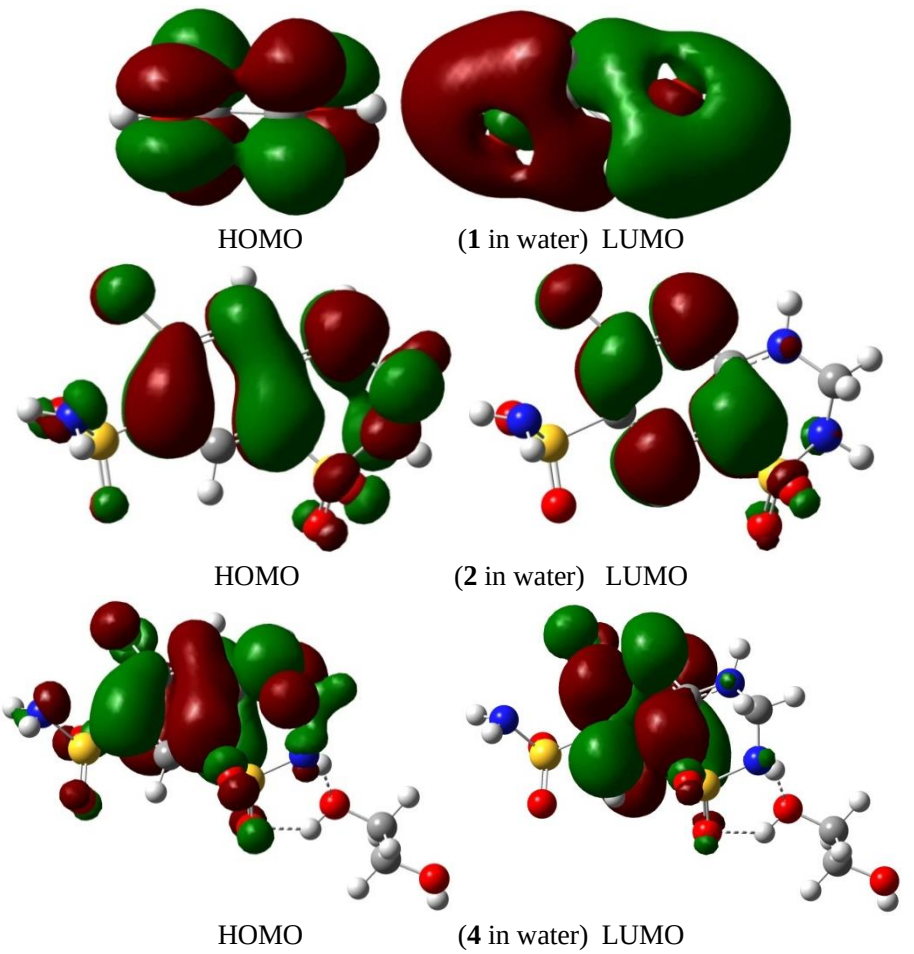


Figure 3. (Continued).

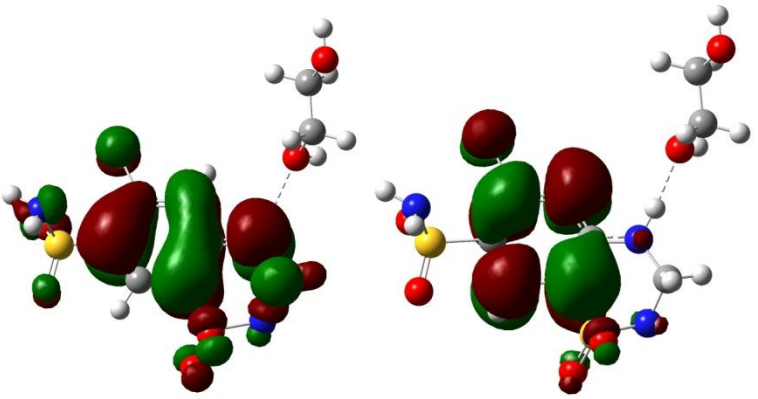


Figure 3. The HOMO and LUMO molecular orbitals of compounds **1**, **2**, **4** and **6** in water at B3LYP/6-31G(d) level. Red and green represent negative and positive regions of the wave functions, respectively.

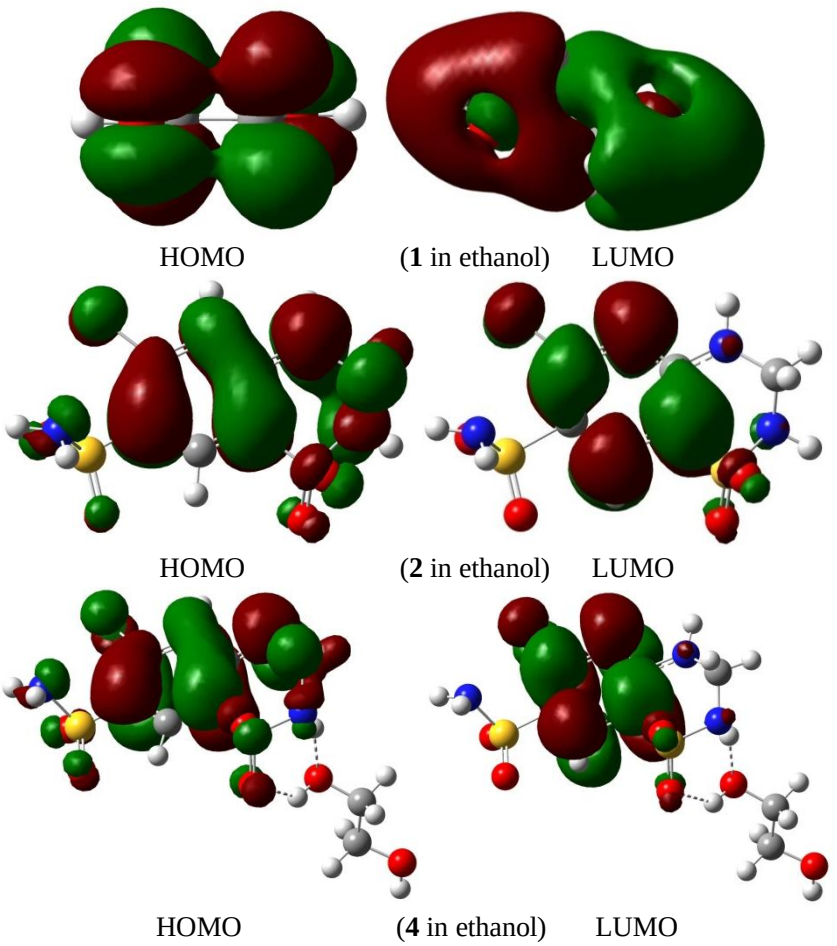


Figure 4. (Continued).

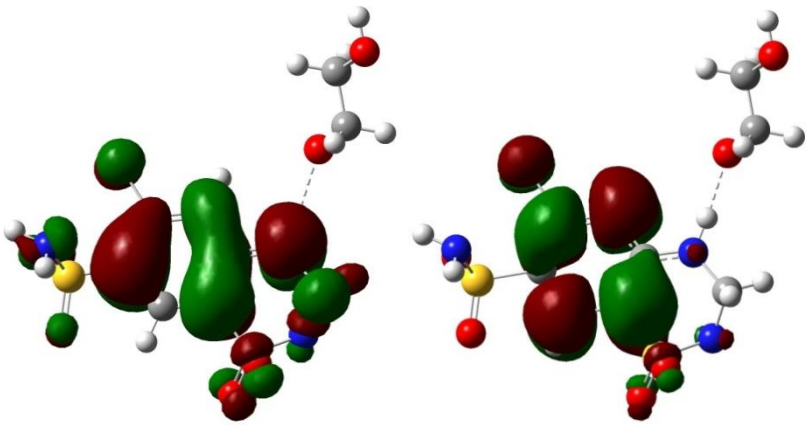


Figure 4. The HOMO and LUMO molecular orbitals of compounds **1**, **2**, **4** and **6** in ethanol at B3LYP/6-31G(d) level. Red and green represent negative and positive regions of the wave functions, respectively.

**Table 7. The computed band gaps ($E_g = E_{HOMO}–E_{LUMO}$, eV) for compounds 1–6**

| Compound | band gap (gas phase) | | | |
|---|---|---|---|---|
| | B3LYP/6-31+G(d) | B3PW91/6-31+G(d) | B3LYP/6-31+G(d,p) | B3PW91/6-31+G(d,p) |
| **1** | 7.5577 | 7.8481 | 7.5820 | 7.8606 |
| **2** | 5.0396 | 5.0551 | 5.0390 | 5.0554 |
| **3** | 5.0377 | 5.0516 | 5.0363 | 5.0511 |
| **4** | 5.0374 | 5.0505 | 5.0336 | 5.0480 |
| **5** | 5.0287 | 5.0444 | 5.0276 | 5.0442 |
| **6** | 4.9786 | 4.9974 | 4.9871 | 4.9952 |
| Compound | band gap (in water) | | | |
| | B3LYP/6-31+G(d) | B3PW91/6-31+G(d) | B3LYP/6-31+G(d,p) | B3PW91/6-31+G(d,p) |
| **1** | 7.9221 | 8.1921 | 7.7934 | 8.1823 |
| **2** | 4.9354 | 4.9473 | 4.9351 | 4.9471 |
| **3** | 4.9155 | 4.9258 | 4.9441 | 4.9256 |
| **4** | 4.9348 | 4.9503 | 4.9332 | 4.9476 |
| **5** | 4.9321 | 4.9427 | 4.9324 | 4.9427 |
| **6** | 4.8809 | 4.8956 | 4.8801 | 4.8943 |
| Compound | band gap (in ethanol) | | | |
| | B3LYP/6-31+G(d) | B3PW91/6-31+G(d) | B3LYP/6-31+G(d,p) | B3PW91/6-31+G(d,p) |
| **1** | 7.9088 | 8.1858 | 7.9164 | 8.1722 |
| **2** | 4.9403 | 4.9522 | 4.9397 | 4.9522 |
| **3** | 4.9226 | 4.9329 | 4.9218 | 4.9326 |
| **4** | 4.9408 | 4.9547 | 4.9394 | 4.9525 |
| **5** | 4.9332 | 4.9476 | 4.9335 | 4.9430 |
| **6** | 4.8867 | 4.9016 | 4.8856 | 4.9005 |

The surfaces and contours or electrostatic potential maps (ESP) for complexes **4** in the gas phase and **6** in water and ethanol are presented in Figure 5. It is obvious that for both compounds, the electrostatic potentials are mainly present on the drug and also within the spaces between the two interacting species (EG and drug). It is evident from contours or ESP

images that the orientation of complex **6** is such that more negative potential (red lines) is present in the bottom of the complex that can lead to a greater dipole moment for the structure compared with complex **4**. Also, similar results are obtained in water and ethanol for **6**.

To further interpret the nature of the binding in these systems, the electronic structures of the thermodynamically most stable states between EG (**1**) and drug (**2**) in compounds **4** and **6** were studied. For this purpose, their density of states (DOS) spectra were calculated and indicated in Figure 6. It is clearly observed that there are some hybridization between the drug and the EG. Consequently, the existence of interactions is deduced quantitatively in terms of the DOS spectra. Moreover, the DOS spectra are very similar and show small discrepancies in water and ethanol but they are different from those obtained in the gas phase. However, the DOS spectra of EG are all almost identical in the gas phase and in the solution state.

The interaction energies from the NBO perturbation theory energy analysis for the transitions from oxygen lone pairs to the vicinal antibonding orbitals or from a bonding σ orbital to a vicinal antibonding σ* orbital in compounds **4** (in the gas phase) and **6** (in water and ethanol) are presented in Table 8. It can be seen that the energies of electron density transitions occurring as σ→σ* and from oxygen lone pair to the vicinal antibonding orbitals have almost comparable high values indicating they are all important transitions. For example, in complex **4**, the energies of σ→σ* and Lp (O)→σ* transitions are within the range 514.55–746.73 and 439.25–784.38 kcal/mol, respectively. Also, very similar results are measured in water and ethanol for **6**. In water, the energies of σ→σ* and Lp (O)→σ* transitions are within the range 533.38–765.55 and 545.92–671.42 kcal/mol, respectively.

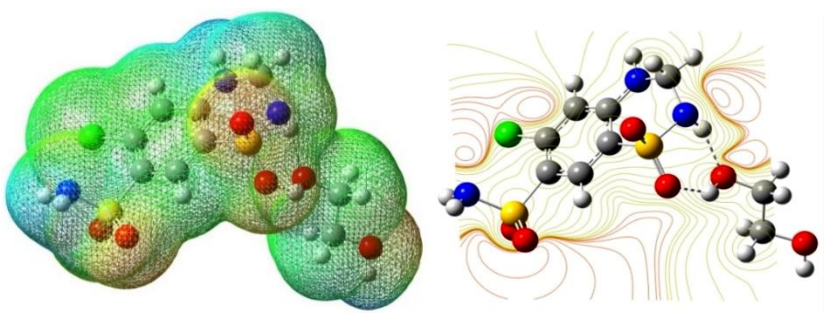

(**4** in gas phase)

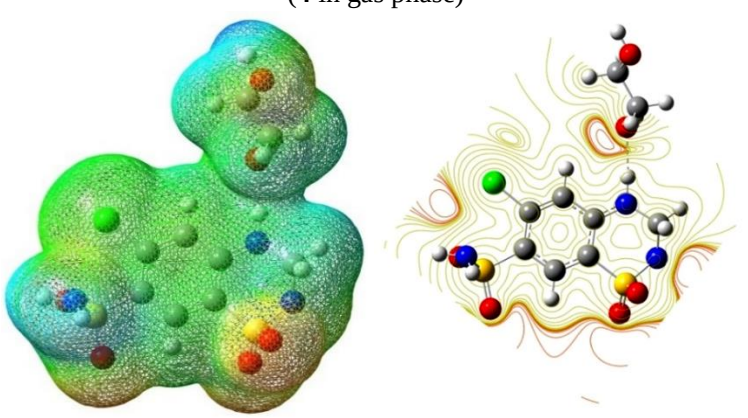

(**6** in water)

Figure 5. (Continued).

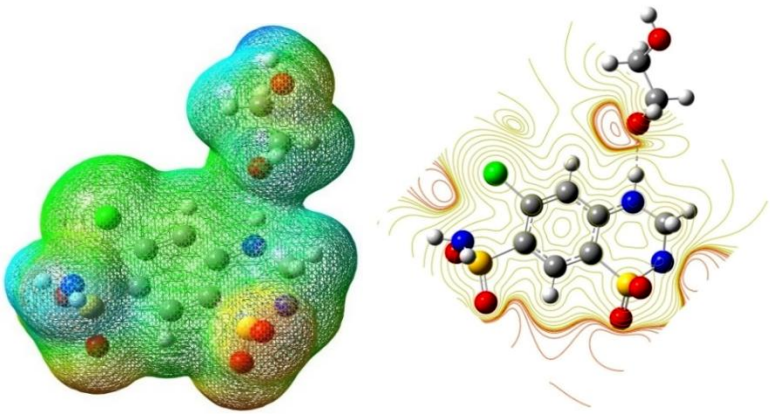

(**6** in ethanol)

Figure 5. The surfaces and contours or electrostatic potential maps (ESP) for complexes **4** and **6** in gas phase, water and ethanol (red lines denote the negative potentials and yellow lines are the positive potentials).

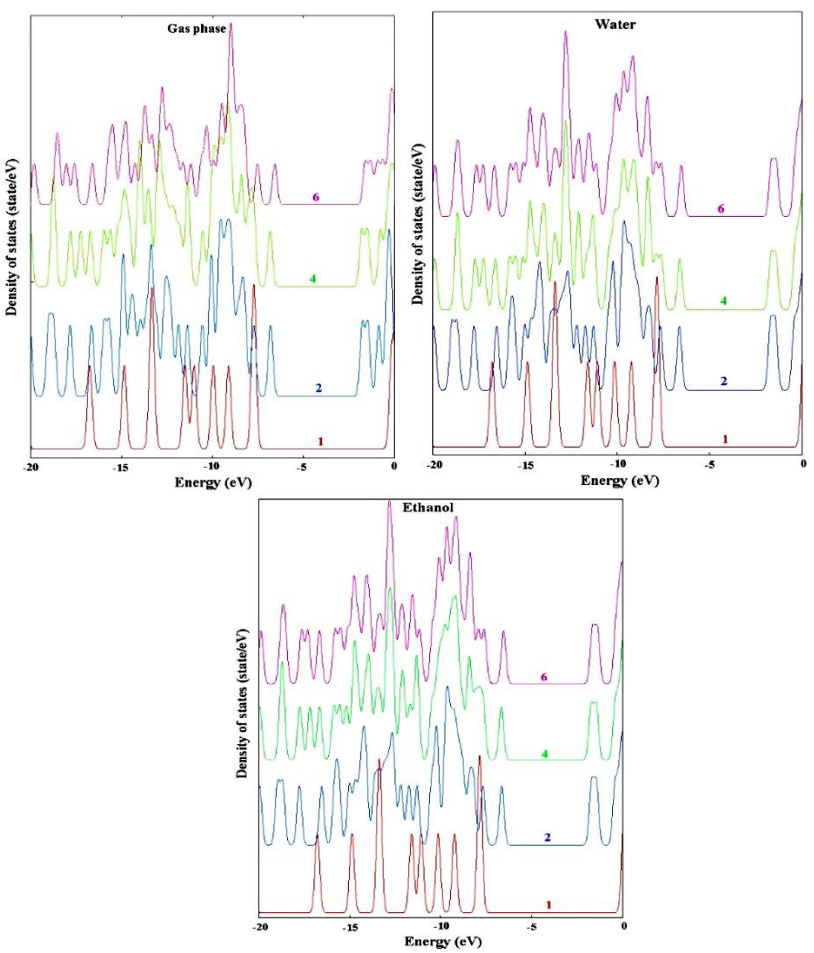


Figure 6. The density of state (DOS) spectra of compounds **1**, **2**, **4** and **6** in gas phase, water and ethanol at B3LYP/6-31G(d) level.

**Table 8. The energies of electron density transfer transitions (kcal/mole) for 4 (in gas phase) and 6 (in water and ethanol) calculated at B3LYP/6-31+G(d) level of theory**

| Compound | Transition type | Energy | Transition type | Energy |
|---|---|---|---|---|
| **4** in gas phase | σ (S1-C1) → σ* (S1-C1) | 527.10 | Lp (O3) → σ* (O5-H7) | 784.38 |
| | σ (S1-C1) → σ* (S1-O1) | 608.68 | Lp (O5) → σ* (N3-H6) | 589.85 |
| | σ (S1-C1) → σ* (S1-O2) | 602.40 | Lp (O5) → σ* (C4-N3) | 439.25 |
| | σ (S1-C1) → σ* (S1-N1) | 514.55 | Lp (O5) → σ* (C3-H6) | 502.00 |
| | σ (S1-C1) → σ* (N1-H1) | 709.08 | Lp (O5) → σ* (C5-H8) | 589.85 |
| | σ (S1-C1) → σ* (N1-H2) | 709.08 | Lp (O5) → σ* (C5-H9) | 583.58 |
| | σ (C2-C3) → σ* (C2-N2) | 746.73 | Lp (O6) → σ* (O5-C5) | 564.75 |
| | σ (C2-C3) → σ* (S2-O3) | 627.50 | Lp (O6) → σ* (C5-C6) | 621.22 |
| | σ (C2-C3) → σ* (N2-H3) | 709.08 | Lp (O6) → π* (C6-H10) | 633.78 |
| **6** in water | σ (S1-C1) → σ* (S1-C1) | 533.38 | Lp (O1) → σ* (S1-O2) | 665.15 |
| | σ (S1-C1) → σ* (S1-O1) | 602.40 | Lp (O2) → σ* (S1-N1) | 589.85 |
| | σ (S1-C1) → σ* (S1-O2) | 602.40 | Lp (O3) → σ* (S2-O4) | 671.42 |
| | σ (S1-C1) → σ* (S1-N1) | 520.82 | Lp (O4) → σ* (S2-O3) | 671.42 |
| | σ (S1-C1) → σ* (N1-H1) | 715.35 | Lp (O5) → σ* (N2-H3) | 589.85 |
| | σ (S1-C1) → σ* (N1-H2) | 715.35 | Lp (O5) → σ* (C5-C6) | 545.92 |
| | σ (C2-C3) → σ* (C2-N2) | 765.55 | Lp (O5) → σ* (C5-H8) | 571.02 |
| | σ (C2-C3) → σ* (S2-O3) | 621.22 | Lp (O6) → σ* (C5-O5) | 558.48 |
| | σ (C2-C3) → σ* (N2-H3) | 740.45 | Lp (O6) → σ* (C5-C6) | 621.22 |
| | σ (N2-H3) → σ* (O5-C5) | 589.85 | Lp (O6) → σ* (C6-H10) | 640.05 |
| | σ (N2-H3) → σ* (O5-H7) | 683.98 | Lp (O6) → σ* (C6-H11) | 640.05 |
| **6** in ethanol | σ (S1-C1) → σ* (S1-C1) | 533.38 | Lp (O1) → σ* (S1-O2) | 665.15 |
| | σ (S1-C1) → σ* (S1-O1) | 602.40 | Lp (O2) → σ* (C1-N1) | 602.40 |
| | σ (S1-C1) → σ* (S1-O2) | 602.40 | Lp (O3) → σ* (S2-O4) | 671.42 |
| | σ (S1-C1) → σ* (S1-N1) | 520.82 | Lp (O3) → σ* (S2-C3) | 608.68 |
| | σ (S1-C1) → σ* (N1-H1) | 715.35 | Lp (O5) → σ* (N2-H3) | 589.85 |
| | σ (S1-C1) → σ* (N1-H2) | 715.35 | Lp (O5) → σ* (C5-C6) | 545.92 |
| | σ (C2-C3) → σ* (C2-N2) | 765.55 | Lp (O5) → σ* (C5-H8) | 564.75 |
| | σ (C2-C3) → σ* (S2-O3) | 621.22 | Lp (O6) → σ* (C5-O5) | 558.48 |
| | σ (C2-C3) → σ* (N2-H3) | 740.45 | Lp (O6) → σ* (C5-C6) | 621.22 |
| | σ (N2-H3) → σ* (O5-C5) | 589.85 | Lp (O6) → σ* (C6-H10) | 640.05 |
| | σ (N2-H3) → σ* (O5-H7) | 683.98 | Lp (O6) → σ* (C6-H11) | 640.05 |

### 8.1.2.3. QTAIM Analysis

The topological studies of electron densities for EG, drug and its corresponding complexes was performed using QTAIM calculations and the computed structures are illustrated in Figure 7 for the most stable compounds **4** (in the gas phase) and **6** (in water and ethanol) with the related data are listed in Table 9. According to the QTAIM theory, values of $\rho(\mathbf{r})$ < 0.1 au are related to a closed-shell (mainly electrostatic) interaction [135, 136] providing an approximately small and positive value of $\nabla^2\rho(\mathbf{r})$ [137]. Nevertheless, for a shared (predominantly covalent) interaction, $\rho(\mathbf{r})$ is usually > 0.1 au [137] and $\nabla^2\rho(\mathbf{r})$ is usually negative [138].

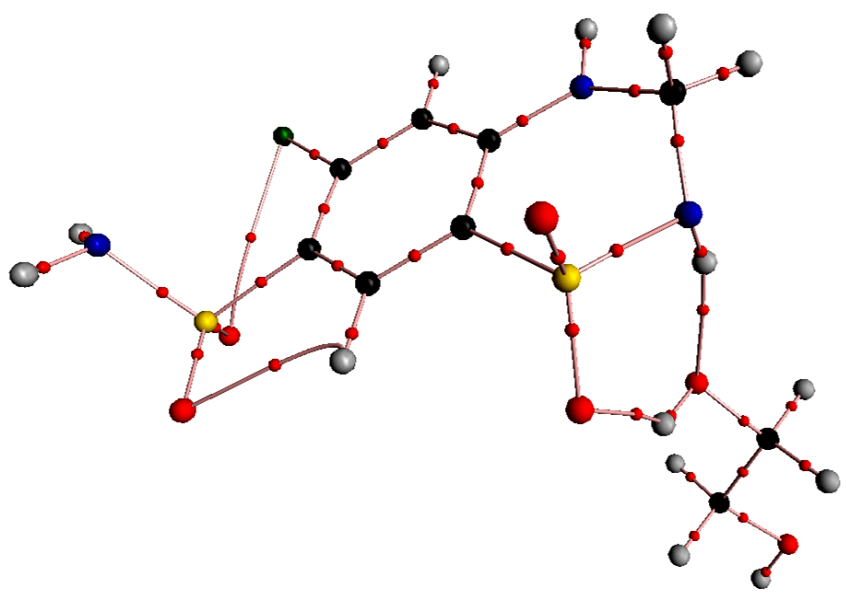

(**4** in gas phase)

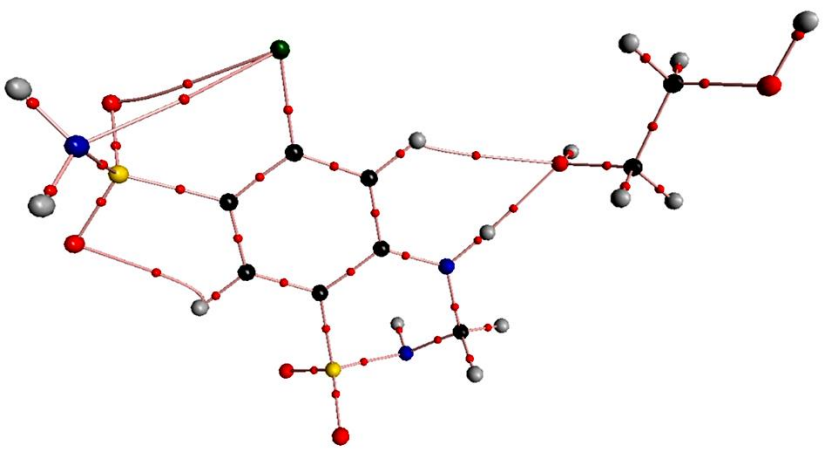

(**6** in water and ethanol)

Figure 7. The molecular graphs (MGs) of compounds **4** (in gas phase) and **6** (in water and ethanol) obtained by QTAIM analysis at B3LYP/6-31G(d) level of theory. Bond critical points: red circles; Bond paths: pink lines.

It is apparent from Table 7 that the large electron densities for $\rho(\mathbf{r})$ values (0.2059–0.3422 $e a_0^{-3}$) at the bcps confirm the shared interaction for the N–H, S=O, S–C, C–C, C–N, C–S, S–N, O–H and C–O bonds in compounds **4** and **6**. Although these bonds are covalent, positive $\nabla^2\rho(\mathbf{r})$ values (0.9398–1.0181 $e a_0^{-5}$) for bcps of the S=O bonds but negative $\nabla^2\rho(\mathbf{r})$ values (from –0.4017 to –1.8225 $e a_0^{-5}$) are obtained for bcps of the N–H, S=O, S–C, C–C, C–N, C–S, S–N, O–H and C–O bonds. Moreover, the electronic energy density values help more precise description of the nature of bonds. Thus, the negative $H(\mathbf{r})$ values in the range from –0.1478 to –0.5139 $e^2 a_0^{-4}$ are indicative of the predominant covalent character for the N–H, S=O, S–C, C–C, C–N, C–S, S–N, O–H and C–O bonds in all species.

**Table 9. The QTAIM data calculated at B3LYP/6-31+G(d) level for bond paths of compounds 4 (in gas phase) and 6 (in water and ethanol)**

| Compound | Bond | $\rho(\mathbf{r})$ | $\nabla^2\rho(\mathbf{r})$ | $G(\mathbf{r})$ | $V(\mathbf{r})$ | $H(\mathbf{r})$ | $\lvert V(\mathbf{r})\rvert/G(\mathbf{r})$ |
|---|---|---|---|---|---|---|---|
| **4** in gas phase | N1–H1 | 0.3231 | -1.6095 | 0.0442 | -0.4908 | -0.4466 | 11.101 |
| | S1–O1 | 0.2851 | 1.0181 | 0.5882 | -0.9220 | -0.3337 | 1.5673 |
| | S1–C1 | 0.2033 | -0.4057 | 0.0463 | -0.1941 | -0.1478 | 4.1888 |
| | C2–C3 | 0.2990 | -0.7759 | 0.0932 | -0.3803 | -0.2871 | 4.0824 |
| | C2–N2 | 0.3153 | -0.9877 | 0.2304 | -0.7076 | -0.4773 | 3.0719 |
| | C3–S2 | 0.2072 | -0.4176 | 0.0492 | -0.2029 | -0.1536 | 4.1199 |
| | S2–N3 | 0.2299 | -0.5132 | 0.1551 | -0.4384 | -0.2834 | 2.8274 |
| | O5–H7 | 0.3370 | -1.7870 | 0.0592 | -0.5651 | -0.5059 | 9.5474 |
| | C5–O5 | 0.2481 | -0.4321 | 0.2383 | -0.5846 | -0.3463 | 2.4533 |
| | N3–H6...O5 | 0.0261 | 0.0824 | 0.0231 | -0.0220 | -0.0007 | 1.0336 |
| | O5–H7...O3 | 0.0214 | 0.0721 | 0.0183 | -0.0185 | -0.0002 | 1.0139 |
| | S1–O1...Cl(ring) | 0.0092 | 0.0339 | 0.0072 | -0.0060 | 0.0013 | 0.8254 |
| | S1–O2...H–C(ring) | 0.0147 | 0.0634 | 0.0135 | -0.0111 | 0.0024 | 0.8251 |
| **6** in water | N1–H1 | 0.3207 | -1.6047 | 0.0423 | -0.4858 | -0.4435 | 11.482 |
| | S1–O1 | 0.2815 | 0.9398 | 0.5651 | -0.8952 | -0.3301 | 1.5842 |
| | S1–C1 | 0.2060 | -0.4116 | 0.0481 | -0.1991 | -0.1510 | 4.1391 |
| | C2–C3 | 0.2962 | -0.7637 | 0.0901 | -0.3712 | -0.2811 | 4.1182 |
| | C2–N2 | 0.3269 | -1.0295 | 0.2511 | -0.7596 | -0.5085 | 3.0250 |
| | C3–S2 | 0.2092 | -0.4210 | 0.0508 | -0.2068 | -0.1560 | 4.0725 |
| | S2–N3 | 0.2303 | -0.5274 | 0.1513 | -0.4345 | -0.2832 | 2.8712 |
| | O5–H7 | 0.3421 | -1.8225 | 0.0582 | -0.5721 | -0.5139 | 9.8245 |
| | C5–O5 | 0.2426 | -0.4031 | 0.2340 | -0.5688 | -0.3348 | 2.4306 |
| | N2–H3...O5 | 0.0303 | 0.0967 | 0.0250 | -0.0257 | -0.0008 | 1.0310 |
| | C–H(ring)...O5 | 0.0052 | 0.0205 | 0.0041 | -0.0030 | 0.0010 | 0.7455 |
| | S1–O1...Cl(ring) | 0.0091 | 0.0329 | 0.0071 | -0.0059 | 0.0011 | 0.8380 |
| | S1–O2...H–C(ring) | 0.0151 | 0.0636 | 0.0137 | -0.0114 | 0.0022 | 0.8379 |
| | N1...Cl(ring) | 0.0078 | 0.0263 | 0.0056 | -0.0046 | 0.0010 | 0.8284 |
| **6** in ethanol | N1–H1 | 0.3208 | -1.6053 | 0.0424 | -0.4859 | -0.4436 | 11.486 |
| | S1–O1 | 0.2817 | 0.9440 | 0.5663 | -0.8966 | -0.3303 | 1.5832 |
| | S1–C1 | 0.2059 | -0.4114 | 0.0480 | -0.1988 | -0.1508 | 4.1425 |
| | C2–C3 | 0.2963 | -0.7639 | 0.0902 | -0.3715 | -0.2812 | 4.1163 |
| | C2–N2 | 0.3264 | -1.0277 | 0.2503 | -0.7576 | -0.5072 | 3.0263 |
| | C3–S2 | 0.2091 | -0.4205 | 0.0507 | -0.2065 | -0.1558 | 4.0737 |
| | S2–N3 | 0.2299 | -0.5275 | 0.1503 | -0.4324 | -0.2821 | 2.8775 |
| | O5–H7 | 0.3422 | -1.8216 | 0.0584 | -0.5721 | -0.5138 | 9.8010 |
| | C5–O5 | 0.2425 | -0.4017 | 0.2341 | -0.5686 | -0.3345 | 2.4290 |
| | N2–H3...O5 | 0.0301 | 0.0964 | 0.0248 | -0.0256 | -0.0007 | 1.0302 |
| | C–H(ring)...O5 | 0.0049 | 0.0192 | 0.0038 | -0.0028 | 0.0010 | 0.7285 |
| | S1–O1...Cl(ring) | 0.0092 | 0.0330 | 0.0071 | -0.0059 | 0.0012 | 0.8376 |
| | S1–O2...H–C(ring) | 0.0151 | 0.0635 | 0.0137 | -0.0114 | 0.0022 | 0.8367 |
| | N1...Cl(ring) | 0.0078 | 0.02635 | 0.0056 | -0.0047 | 0.0010 | 0.8282 |

Figure 7 exhibits that the interactions between EG and drug are of electrostatic nature so that the small positive values for $\rho(\mathbf{r})$, $\nabla^2\rho(\mathbf{r})$ and $H(\mathbf{r})$ at the bcps of N3–H6...O5, O5–H7...O3, S1–O1...Cl(ring) and S1–O2...H–C(ring) in **4** confirm this issue. Similar electrostatic interactions happen in complex **6** in both water and ethanol including

intermolecular strong N2–H3...O5 and weak C–H(ring)...O5 hydrogen bonds as well as intramolecular weak S1–O2...H–C(ring) hydrogen bond plus two S1–O1...Cl(ring) and N1...Cl(ring) interactions.

The $|V(\mathbf{r})|/G(\mathbf{r})$ ratio can be used to categorize the interatomic interactions into three classes including covalent, intermediate and electrostatic bonds [139] so that the electrostatic interactions are associated with $|V(\mathbf{r})|/G(\mathbf{r}) \leq 1$, intermediate interactions $1 < |V(\mathbf{r})|/G(\mathbf{r}) < 2$, and shared interactions $|V(\mathbf{r})|/G(\mathbf{r}) > 2$. The values of $|V(\mathbf{r})|/G(\mathbf{r})$ in Table 9 support the covalent/shared character of the N–H, S–C, C–C, C–N, C–S, S–N, O–H and C–O bonds, the intermediate character of S=O, N3–H6...O5, O5–H7...O3 and N2–H3...O5 bonds while the electrostatic nature of S1–O1...Cl(ring), S1–O2...H–C(ring), C–H(ring)...O5 and N1...Cl(ring) interactions with their corresponding $|V(\mathbf{r})|/G(\mathbf{r})$ values are in the range of 2.4290–11.486, 1.0139–1.5842 and 0.7285–0.8380, respectively. It is notable that the intermolecular strong N–H…O and O–H…O hydrogen bonds have covalent characters reflecting strong interactions occur in complexes **4** and **6** between the EG and drug.

### 8.1.2.4. NQR Analysis

Selected calculated nuclear quadrupole coupling constants (NQCCs, χs) for the quadrupole nuclei $^{2}H$, $^{14}N$ and $^{17}O$ of compounds **4** and **6** are presented in Table 10. Similar results are obtained for both compounds **4** (in the gas phase) and **6** (in water and ethanol). The NQCCs of sulfonyl oxygen atoms in both compounds **4** and **6** are about 8.5–9.0 MHz but those of EG are greater (~10–11 MHz). The hydrogen atoms connected to the carbon atoms reveal much smaller χ values than those connected to nitrogen or oxygen atoms. For example in **4**, the χ values of H1, H2, H4, H5, H8-H11 are in the range of 200.98–297.04 kHz while those of H3, H6, H7 and H12 change within the range 179.40–188.20 kHz. Moreover, the χ values of H nuclei incorporating in the formation of strong intermolecular H-bonds are much less than their related values. For instance, the H3 atom is free in **4** but it is involved in the H-bond creation in **6**. The NQCCs for the H3 atom in **4** is 257.45 kHz but it decreases in **6** to 203.97 (in water) and 204.83 (in ethanol) kHz. Similarly, the H6 atom is engaged the H-bond creation in **4** but it is free in **6**. The NQCCs for the H6 nucleus in **4** is 200.98 kHz but it increases in **6** to 235.76 (in water) and 236.00 (in ethanol) kHz. The nitrogen atoms indicate χ values within the range of 4.2348 (for **6** in water) to 5.0270 MHz (for **4** in the gas phase). Similar results were obtained for the $^{2}H$, $^{14}N$ and $^{17}O$ NQCCs in our previous work [140].

**Table 10. Calculated nuclear quadrupole coupling constants (NQCC, χ) for $^{2}H$ (kHz) and $^{17}O$, $^{14}N$ (MHz) nuclei of compounds 4 (in gas phase) and 6 (in water and ethanol) at B3LYP/6-31+G(d) level**

| Compound **4** in gas phase | NQCC | Compound **6** in water | NQCC | Compound **6** in ethanol | NQCC |
|---|---|---|---|---|---|
| O1 | 8.5085 | O1 | 8.9468 | O1 | 8.9215 |
| O2 | 8.5338 | O2 | 8.5464 | O2 | 8.5403 |
| O3 | 8.8457 | O3 | 8.8311 | O3 | 8.8185 |
| O4 | 8.4489 | O4 | 8.5873 | O4 | 8.5832 |
| O5 | 9.8241 | O5 | 10.075 | O5 | 10.097 |
| O6 | 10.915 | O6 | 10.609 | O6 | 10.628 |

| Compound **4** in gas phase | NQCC | Compound **6** in water | NQCC | Compound **6** in ethanol | NQCC |
|---|---|---|---|---|---|
| H1 | 248.67 | H1 | 243.18 | H1 | 243.55 |
| H2 | 247.69 | H2 | 241.86 | H2 | 242.37 |
| H3 | 257.45 | H3 | 203.97 | H3 | 204.83 |
| H4 | 178.73 | H4 | 180.56 | H4 | 180.57 |
| H5 | 186.97 | H5 | 185.66 | H5 | 185.73 |
| H6 | 200.98 | H6 | 235.76 | H6 | 236.00 |
| H7 | 261.55 | H7 | 285.41 | H7 | 285.66 |
| H8 | 188.20 | H8 | 187.28 | H8 | 187.35 |
| H9 | 182.55 | H9 | 182.80 | H9 | 182.82 |
| H10 | 179.40 | H10 | 179.56 | H10 | 179.54 |
| H11 | 181.80 | H11 | 181.85 | H11 | 181.82 |
| H12 | 297.04 | H12 | 289.91 | H12 | 290.14 |
| N1 | 4.6995 | N1 | 4.6162 | N1 | 4.6268 |
| N2 | 5.0270 | N2 | 4.2348 | N2 | 4.2556 |
| N3 | 4.8610 | N3 | 4.8183 | N3 | 4.8210 |

### *8.1.3. Summary*

The hydrogen bonding interactions were investigated between anti-hypertensive hydrochlorothiazide drug and ethyleneglycol (EG, as drug carrier) using DFT computations at B3LYP and B3PW91 levels of theory in both the gas phase and solution state (water and ethanol). Among systems **3**–**6**, complex **4** containing N(3)–H(6)...O(5) and O(5)–H(7)...O(3) H-bonds showed the most negative binding energies in the gas phase but complex **6** including N(2)–H(3)...O(5) hydrogen bonds is the most satble in both water and ethanol solutions. The NBO analysis exhibited nearly identical band gaps ($E_g \approx 5$ eV) for drug and complexes **3**–**6**. The $\sigma \rightarrow \sigma^*$ and Lp (O)$\rightarrow\sigma^*$ transitions had very comparable energies. The $|V(\mathbf{r})|/G(\mathbf{r})$ ratios obtained from the QTAIM analysis established that there are also weak intramolecular C–H…O hydrogen bonds in compounds **4** and **6** that are electrostatic in nature. Finally, it could be proposed that the complex **6** was expected to work the best as a drug delivery system in the solution state because of its greatest negative binding energy, enthalpy and Gibbs free energy among the six complexes examined here.

## 8.2. MIP Drug Delivery Systems

In recent times, numerous experimental and computational investigations have been conducted on MIP compounds [141–146]. For instance, the hydrogen bonding interactions between both 1S-2S and 1R-2R isomers of methacrylicacid (MAA) and pseudoephedrinium cation (as model drug) were computed by Gaussian 98 software [147]. Eight H-bonded forms were calculated at HF and B3LYP levels of theory using the standard 6-31G(d) and 6-31+G(d,p) basis sets and it was found that for all of the molecules the B3LYP/6-31G* provided the highest stabilization energies. Among four computational methods, B3LYP/6-31G(d) gave the highest H-bonding energy for all of the complexes. The nuclear quadrupole coupling constants (NQCCs) for $^{17}O$ and $^{14}N$ nuclei were measured near 10.0, 0.5−1.0 MHz but for $^{2}H$ atoms, the NQCC was in the range of ~150.0−350.0 kHz [147].

In another work, intermolecular interactions between α-, β-glucose and MAA was investigated [122]. Twenty-two conformations were optimized using the HF and B3LYP levels of theory with the 6-31G(d) basis set. The binding energies $\Delta E_{bind}$ of the optimized systems were calculated taking into account the basis set superposition error (BSSE) and the zero-point vibrational energies corrections. It was indicated that in all complexes, the NQCC values were obtained about 10.0 MHz for $^{17}O$ atoms whereas they varied from ~200.0 to 350.0 kHz for the $^{2}H$ nuclei [122].

The H-bonding interactions between letrozole (Let) anticancer drug and three copolymers of methacrylic acid-trimethylolpropane trimethacrylate (M1-M3 as molecular imprinted polymers) were examined using both B3LYP and B3PW91 methods [123]. The binding energies ($\Delta E_{binding}$) were corrected for the basis set superposition error (BSSE) and zero-point vibrational energies (ZPVE) and the most negative $\Delta E_{binding}$ were acquired for compounds formed between M1 copolymer and endocyclic N1 and N2 atoms of drug, respectively. Also, among complexes in which two copolymers were incorporated in the creation of O-H…N bonds with the drug, compound containing two M1 copolymers displayed the highest $\Delta E_{binding}$ value. The interactions of all copolymers with drug were exothermic and exergonic (spontaneous interaction). Furthermore, the QTAIM analysis proved the covalent nature of the C-N, C-H, N–N, C–O, O–H and O-H…N bonds, the intermediate character of C≡N and C=O bonds while the electrostatic character of C-H…O, HC…HC and CH…N interactions. Considering the $\Delta E_{binding}$, $\Delta G_{interaction}$ and $\Delta H_{interaction}$ values, it was recommended that complexes **7** and **8** (among two particles systems) as well as complex **13** (among three particles systems) could be chosen as the most favorable drug delivery systems [123].

Recently, an MIP was obtained for vanillin by photoinitiated polymerization reaction by means of a mixed semi-covalent and non-covalent imprinting approach. The polymerizable syringaldehyde was used as a dummy template and acrylamide was chosen as a monomer in B3LYP/6-31+G(d,p) computational method [148]. The binding of vanillin onto the MIPs were estimated by three different isotherm models including Langmuir, bi-Langmuir and Langmuir–Freundlich. Results indicated heterogeneity of binding sites. DFT calculations verified that the specific binding of vanillin in the cavities was occurred due to non-covalent interactions of the template with the hydroxyphenyl and the amide groups. Besides, the binding geometry of vanillin was modelled in the MIP cavity. It was concluded that the MIP was very specific for vanillin (with an imprinting factor=7.4) and it was effectively applied to extract vanillin (with a recovery of 80%) from red wine spike with vanillin, vanilla pods as well as natural and artificial vanilla sugar [148].

Effects of the electrostatic force, cavity's backbone atoms and Mulliken charge on the selectivity of MIPs were investigated [149]. Additionally, charge distribution was proposed as a computational parameter to predict the selectivity coefficients of MIP-based sensors. MAA was used as the functional monomer and ethylene glycol dimethacrylate (EGDMA) as the cross linker for hydroxyzine and cetirizine imprinted polymers. The B3LYP method was chosen for the optimization of molecular geometries. Win order to perform the molecular optimization and examine the hydrogen bonding properties, some configurations with 1:n ($n \leq 5$) of template/monomer complexes were drawn and optimized. Considering the most stable configuration, hydroxyzine and cetirizine imprinted polymers were designed. A correlation was achieved between the selectivity coefficients and theoretical charge distributions. Results amazingly revealed that charge distribution based model was capable to guess the selectivity coefficients for the MIP based potentiometric sensors [149].

An enantioselective MIP was computationally designed for S-warfarin using the density functional theory (DFT) method at B3LYP/631G+ (d, p) level [150]. Also, the influence of polymerization solvent was assessed by the polarizable continuum model (PCM) which was measured the interaction energies (ΔE) between S-warfarin and monomers in different polymerization solvents. It was presented that the MAA and acetonitrile provided the highest stabilization energy for the pre-polymerization adducts. Further, the molar ratio of 1:3 gave the highest ΔE, thus, the polymer was synthesized through the thermal bulk polymerization technique with the molar ratio of S-warfarin-$(MAA)_3$. The enantioselective extraction of R and S-warfarin was investigated by polarimetry chiral separation and chromatography procedures. Results exhibited that the proposed S-warfarin MIP had a modest recognition to extract R-warfarin from a racemic mixture but it had no recognition for other foreign drugs. Also, in a racemic mixture of R and S-warfarin, the polymer could remove nearly 20% of R-warfarin. The linearity between response (peak areas) and concentration of S-warfarin in plasma was in the range of 15.4–3080 ng $mL^{-1}$ ($R^2$= 0.999). For a racemic mixture of R, S-warfarin in plasma, the linear range was 12.0–2500 ng $mL^{-1}$ ($R^2$= 0.998). Accurate results were attained for the polymer employed to analyze a real sample [150].

Molecularly imprinted systems that were selective for deltamethrin and aimed to offer a appropriate sorbent for solid phase (SPE) extraction were developed that were further used to implement an analytical method for the trace analysis of a target pesticide in spiked olive oil samples [151]. Thus, an initial assessment of the molecular recognition and selectivity of the MIPs was performed. To examine the complexity of the template selective recognition in these matrices, the quantum chemical approach was accomplished to provide visions about the mechanisms behind template recognition, and particularly the vital roles of crosslinker and solvent. Therefore, DFT calculations confirmed the results achieved from the experimental molecular recognition tests which allow choosing the most proper imprinting material for the extraction which contains acrylamide as a functional monomer and ethylene glycol dimethacrylateas crosslinker. Also, an analytical method including a sample preparation step based on solid phase extraction was realized by means of this tailor made system as the sorbent, for the selective isolation/pre-concentration of deltamethrin from olive oil samples. It was shown that the molecularly imprinted solid phase extraction (MISPE) process effectively cleaned up the spiked olive oil samples (recovery rates were up to 94%) [151].

An electrochemical MIP sensor that was sensitive and selective for minoxidil (MX) was prepared [152]. For this purpose, the MIP film was coated on glassy carbon electrode through electrochemical polymerization in a solution comprising ternary monomer and MX template by means of cyclic voltammetry scans. Then, the coated polymer was modified using Ag nanoparticles. Appropriate functional monomer was selected according to the interactions between diverse monomers and template by means of the DFT computations. The modified electrode was characterized by scanning electron microscopy (SEM), cyclic voltammetry and electrochemical impedance spectroscopy (EIS). Under the optimal conditions, the oxidation peak current was proportionate to MX concentration in the range of 0.03–500 lM and the detection limit was 0.01 lM. The sensor was successfully employed to determine MX concentration in real samples [152].

An electrochemical sensor was fabricated based on mesalamine MIP film coated on a glassy carbon electrode [153]. DFT calculations in both gas and solution phases were carried out to examine the intermolecular interactions in the pre-polymerization mixture and to

determine proper functional monomers for the preparation of MIP. Based on the computational data, gallic acid (GA), o-phenylenediamine (OP) and p-aminobenzoic acid were designated as suitable monomers. The prepared MIP film was put on glassy carbon electrode by electropolymerization of solution incorporated with ternary monomers and followed by deposition of nanobranched Ag dendrites (AgDs). Surface features of the modified electrode (AgDs/MIP/GCE) were investigated by SEM and EIS analyses. The peak current was proportional to the mesalamine concentration ranging from 0.05 to 100 μM, under the optimum conditions, with a detection limit equal to 0.015 μM. The sensor was successfully used to decide mesalamine concentration in real samples [153].

## 9. CS WOUND HEALING MATERIALS

It is known that treatment of bacterial infection is essential in wound healing process. Thus, producing economical antibacterial agents having wound healing properties is of great demand. Recently, chitosan/poly(vinyl alcohol)/zinc oxide (CS/PVA/ZnO) beads were designed as antibacterial agents with wound healing features [154]. The CS/PVA/ZnO beads were characterized using FT-IR, XRD, TEM and SEM analysis techniques. CS showed two peaks at 2θ=10, 20° and the CS/PVA polymer exhibited a peak at 2θ=19.7° and another peak with low intensity at 2θ=11.5°. The ZnO displayed characteristic peaks related to the planes (100), (002), (101), (102), (110), (103), (200) and (112) which were consistent with Wurtzite ore with the hexagonal lattice structure. Also, the bactericidal effects of CS/PVA/ZnO beads against were evaluated *E. coli*, and *S. aureus* microorganisms. It was found that antibacterial activity of CS/PVA/ZnO was greater than those of PVA and CS. biocompatibility and hemocompatibility of CS/PVA/ZnO beads were experienced *in vitro* and wound healing potencies of CS/PVA/ZnO samples were assessed in mice skin wound. The CS/PVA/ZnO presented extraordinary antimicrobial and wound healing effects as well as biocompatibility and hemocompatibility. Therefore, the results powerfully supported the opportunity of using CS/PVA/ZnO materials for the antibacterial and wound healing purposes [154].

In another research, CS–hyaluronic acid composite sponge scaffold containing andrographolide (AND) lipid nanocarriers was produced [155]. Nanocarriers were achieved by solvent diffusion technique and applying $2^3$ factorial design. It was found that the NLC4 had the utmost desirability value (0.882) and hence it was selected as the optimum nanocarrier which demonstrated spherical shape with was 253 nm in size, 83.04% entrapment efficiency and long AND release up to 48h. Also, NLC4 was added into the CS-hyaluronic acid gel and lyophilized for 24h to acquire CS-hyaluronic acid/NLC4 nanocomposite sponge in order to improve AND delivery to the wounded positions. The sponge morphology was characterized by SEM image. Nanocomposites had a porosity of 56.22% with superior swelling. The *in vivo* test in rats revealed that the CS-hyaluronic acid/NLC4 sponge accelerated the wound healing with no scar and enhanced tissue quality. Thus, these findings strongly supported the probability of employing CS-HA/NLC4 sponge in wound care applications [155].

It has been established that halloysite is a natural nanotubular clay mineral (Halloysite Nano Tubes, HNTs) which is chemically equal to kaolinite and because of its good biocompatibility it is an interesting nanomaterial for a wide variety of biological applications.

Moreover, CS oligosaccharides can accelerate wound healing through increasing the functions of inflammatory and repairing cells. Thus, a nanocomposite of HNTs and CS oligosaccharides was developed to be employed as pour powder in order to improve healing in the chronic wounds treatment [156]. A 1:0.05 weight ratio HTNs/CS oligosaccharide nanocomposite was achieved by merely adding the HTNs powder to 1% aqueous CS oligosaccharide solution and it was formed by means of ionic interactions producing a compound with 98.6%w/w HTNs and 1.4%w/w CS oligosaccharide. The HTNs and HTNs/CS oligosaccharide nanocomposite were properly biocompatible *in vitro* with normal human dermal fibroblast cells up to 300 μg/ml concentration, improved *in vitro* fibroblast motility and supported both migration and proliferation. The HTNs/CS oligosaccharide nanocomposite and its two components were separately assessed for healing ability in a murine (rat) model. The HTNs/CS oligosaccharide showed superior skin reorganization and reepithelization compared with HNTs or CS oligosaccharide distinctly. Hence, the results could suggest development of the nanocomposite to be used as a medical device in wound healing [156].

Several CS-bentonite nanocomposite (CBN) films were obtained by means of solvent casting process to be used in wound healing application [157]. The physicochemical properties of the films including folding endurance, thickness, water vapor transmission rate (WVTR) and water absorption capability were examined. The FT-IR spectrum was achieved in order to determine the interactions occurred between negatively charged bentonite and positively charged CS. The surface morphologies of the composite films were investigated by SEM images. As a result of high hydrophilic nature of bentonite, it seriously improved the water absorption potencies of the nanocomposite films. The existence of bentonite in the films enhanced the mechanical strength. Furthermore, the antibacterial activities of the films were tested against both Gram positive and Gram negative bacteria and it was shown that all CBN films had good inhibitory effects against all the bacteria compared with the control. Thus, it was suggested that the CBN films were potential candidates for application as wound healing materials [157].

Chitosan is not soluble in water because of its rigid crystalline structure and this has considerably limited its use in wound healing. Thus, a water-soluble CS derivative, N-succinyl-CS (NSC), was synthesized and its capacity to promote the wound healing process was evaluated [158]. NSC was synthesized using succinic anhydride, alkaline CS and hydrochloric acid under the optimized conditions and characterized by $^{1}$H NMR, FT-IR, TGA, XRD and solubility tests. The NSC cytotoxicity was assessed in L929 cells and its bactericidal property was estimated by the inhibition zone technique and bacterial growth curves analysis. Results exhibited that the NSC solubility was noticeably enhanced compared to CS, the NSC was not toxic and it had good antibacterial activity. Animal wound healing assessment designated that NSC considerably reduced the healing time compared to CS. Histopathological test proposed that the fundamental mechanisms of these effects could be associated with the ability of NSC to accelerate the granulation tissue formation and enhance epithelialization. Thus, the results confirmed good potential of the NSC for application as a wound dressing agent [158].

A wound healing material was achieved by means of two marine biomaterials including squid ink polysaccharide and CS carriers and $CaCl_2$ initiator for coagulation [159]. Using central composite design, response surface methodology, full assessment of appearance quality of composite sponges and water absorption were considered as evaluation indices in

order to recognize the optimized preparation conditions and also estimate the wound healing potency of the squid ink polysaccharide-CS (SIP-CS) sponge. The optimized SIP-CS formulation was contained 2.29% CS, 0.55% squid ink polysaccharide and 2.82% $CaCl_2$ using a volume ratio of 15:5:2. SIP-CS was conducive to sticking on the wound and showed a spongy feature, high absorptivity and tackiness. Rabbit ear arterial, hepatic and femoral artery hemorrhage tests specified that, in comparison to the CS dressings and absorbable gelatin, shorter hemostatic times were and smaller bleeding volume were measured. Besides, SIP-CS absorbed a great quantity of hemocytes which led to rapid hemostasis. The healing zones and wound pathological sections in scalded New Zealand rabbits exhibited that SIP-CS stimulated wound healing more quickly than CS and superior than commercially accessible burn cream. Consequently, SIP-CS was considered as a suitable wound healing material for rapid hemostasis, to promote burn/scalded skin healing and protect against wound infection [159].

## 10. PLA WOUND HEALING MATERIALS

The PLA/Ag nanofibers were fabricated by electrospinning procedure and their *in vitro* biocompatibility, antibacterial and mechanical properties were also evaluated [160]. The colloidal nanosilver added in the system was synthesized by biological reduction reaction using $AgNO_3$ and bitter gourd extract as the reducing agent in a solution containing PLA as the capping agent polymer. The nanofibers were characterized by TEM, SEM, EDS, XRD, AT-IR, DLS, contact angle, fluorescence and UV-Vis analyses. The interaction of the PLA capping agent with colloidal nanosilver particles was established by the XPS technique. Substantial bactericidal activity was detected for PLA/Ag nanofibers against both *E. coli* and *S. aureus* bacteria using agar disc diffusion method. The spherical particles with a mean size of ~5-20 nm were observed in the TEM images. The *in vitro* assay displayed that the biofabricated PLA/Ag nanofibers (Hemolytic percentage<5%) were cytocompatible with fibroblast cells and did not damage cell growth. The WVTR value proved that a local optimum moist medium existed which could promote wound healing. Thus, it was justified that the PLA/Ag nanofibers could be used as wound healing materials to increase the proliferation and functions of fibroblasts and epidermal cells [160].

Single dose interactive nanofibrous wound dressing agents were fabricated using PLA and cellulose acetate (CA) which mimicked extracellular matrix (ECM) and studied for wound treatment [161]. The thymoquinone (TQ) antimicrobial material was added to the scaffolds to prevent usual clinical infections and to promote the wound closure rate and re-epithelialization. The TQ-loaded PLA/CA wound dressings presented several benefits like mimicking the ECM through the 3D nanofibrous structure and accelerated the cell proliferation because of the bioactive and hydrophilic nature of CA. also, these wound dressings inhibited the bacterial infection at the initial stages as a result of TQ existence and preserved the least probable bacterial entrance in the wounded zone by the drug sustained release during 9 days. *In vivo* test established that TQ-loaded PLA:CA (7:3) scaffolds meaningfully stimulated the wound healing course through enhancement of re-epithelialization and adjusting the granulation tissue formation. Thus, the results suggested that the TQ-loaded PLA/CA nanofibrous mats were ideal candidates for wound dressing purposes [161].

Core-shell nanofibers were fabricated by means of electrospinning method using an inclusion complex (IC) of curcumin (CUR) hydrophobic drug formed with cyclodextrin (CD) in the core and PLA polymer in the shell (cCUR/HPbCD-IC-sPLA-NF) [162]. CD-IC of CUR and HPbCD was obtained with a 1:2 molar ratio. Formation of the core-shell nanofibers was confirmed by CLSM and TEM images. cCUR/HPbCD-IC-sPLA-NF slowly released CUR however total value was much more compared with those of PLA-CUR-NF at pH values of 1 and 7.4 because of the CUR restriction in the nanofibers core and solubility enhancement revealed in phase solubility diagram, respectively. Superior antioxidant activity of cCUR/HPbCD-IC-sPLA-NF in methanol:water (1:1) was associated with the solubility increase attained in the aqueous environment. The slow reaction of cCUR/HPbCD-IC-sPLA-NF in methanol was related to the shell which inhibited the rapid CUR release. Conversely, cCUR/HPbCD-IC-sPLA-NF displayed somewhat higher antioxidant activity rate than PLA-CUR-NF in methanol:water (1:1) in consequence of the improved solubility. Thus, slow CUR release was occurred from the core-shell nanofiber and CUR inclusion complexation with HPbCD caused great solubility. It was concluded that electrospinning of core-shell nanofibers with CD-IC core led to slow drug release along with the solubility improvement of hydrophobic drugs [162].

Wound treatment is a challenge to lots of clinicians due to the complexity exists in the wound healing course. Also, the selection of a wound dressing is dependent to several factors like injury extension, wound type, location and the health status of the patient. These factors cause the difficulty and complexity of using a single kind of dressing. Recently, a woven cotton fabric PLA composite was developed as a low drug delivery device to be utilized in biomedical applications through a hand weaving technique to achieve the fabrics and to control their porosity [163]. Fabrics having three different pore sizes of 0.5, 1.0 and 1.5 mm were produced using a natural cotton yarn of 36 Tex and then they were used to prepare the composite. In order to examine the effect of the PLA/fabric ratio on the mechanical characteristics, three diverse PLA concentrations (0.01, 0.03 and 0.06 g/mL) were utilized. The amoxicillin antibiotic drug was employed and the drug release was checked by UV-Vis spectrophotometry. Results indicated that the drug loading capacity was increased by declining the fabric porosity. The release profiles tracked a two stage pattern and the release mechanism was appeared as a mixed transport system including diffusion and perhaps super case II kinetics along with a release caused by damaging the composite surface by dissolution. The concentration amount of released drug surpassed the minimum inhibition concentration of amoxicillin against *S. aureus* bacterium. It was proposed that degradation of the fabric composite influenced the drug release rate. The water absorption capability of composites was reduced by increasing the PLA concentration. The mechanical features of composites were in agreement with the fabric's weight and density. Thus, it was recommended that the developed devices were suitable to be applied in wound dressing purposes on sites needing a water-resistant dressing to aid in preventing bacterial infection of the primary dressing [163].

## 11. PEG WOUND HEALING MATERIALS

Microporous CS-PEG films containing copper ion ($Cu^{2+}$) were produced as multipotent wound dressing materials [164]. The mechanical property, moisture permeability and

swelling behavior and the $Cu^{2+}$ release from hydrogel films with different $Cu^{2+}$ contents were examined. Results proved the improved mechanical stability of the films by increasing $Cu^{2+}$ amount but no cooperation of moisture permeability and absorption capacity of wound exudates. The morphological analysis established the existence of microporous surface and swollen micropores in hydrated forms. Film degradation in lysozyme and $H_2O_2$ validated increasing film stability by enhancement of the $Cu^{2+}$ content up to 30 days. The bactericidal assays discovered dominance in inhibition of biofilm formation compared to CS films. Thus, the in vitro drug release, cell adhesion test and MTT assay verified the efficacy of $Cu^{2+}$ loaded hydrogels for the sustained drug release and antibacterial property with outstanding keratinocyte cell response [164].

Mechanical bowel preparation is a typical practice in elective colon surgery. To confirm the influence of mechanical bowel preparation on the colonic flora, 185 patients undergoing elective open colon surgery were studied, 90 of whom were arbitrarily allocated to take mechanical bowel preparation with PEG [165]. Swabs of the subcutis and the anastomosis were obtained throughout surgery. Additional swabs were prepared from any successive wound infections. It was found that mechanical bowel preparation could not decrease infection of the peritoneal cavity or the subcutis in the course of surgery and it was seemed that more sterile subcutaneous swabs existed in the control group [165].

Wood nanocellulose was proposed for wound dressing application due to its ability to create transparent films having decent liquid absorption capacities which are satisfactory for non-healing and chronic wounds where suitable exudates management is required. Additionally, the transparency allows following the wound repair without the need to eliminate the dressing from the wound. Estimation of the mechanical properties of nanocellulose films and dressings is very significant to tailor optimized wound dressing materials with sufficient strength, porosity, conformability and exudate management. Generally, the mechanical characteristics are evaluated in standard conditions (50% relative humidity, RH) which are not pertinent to a wound management condition. In a recent study, the mechanical features of three nanocellulose grades with variable degree of nanofibrillation were assessed [166]. The influences of PEG addition and nanofibrillation on the elongation, tensile strength and elastic modulus were measured after 24 h in water and in phosphate buffer saline (PBS) solution. Results exhibited the behaviors of the nanocellulose dressing materials after wetting in order to improve mechanical properties in aqueous environments which are relevant to the wound management [166].

Polyethylene glycol fumarate (PEGF) was synthesized through polycondensation polymerization reaction and characterized by diverse analyses to decide its functional groups and physical properties including crystallization and melting temperature, fusion enthalpy and average molecular weight [167]. Wound dressing films fabricated using PEGF, CS and thymol (Th) were obtained by solvent casting process with altered formula containing 80%w/w CS and 20%w/w PEGF polymers and various amounts of Th (0, 0.6, 1.2 and 1.8%v/v) as the pharmaceutical additive. The films were investigated by tensile testing, FT-IR, WVTR, swelling, equilibrium water uptake, water vapor uptake, water solubility, SEM and antibacterial activity analyses. The blend film having 1.8%v/v of Th illustrated optimum properties such as adequate mechanical properties, improved absorption of liquid water and water vapor, greater WVTR and air permeability, satisfactory water solubility, higher swelling level, superior porous structure and rough surfaces and outstanding antibacterial

efficacy against both Gram-positive and Gram-negative bacteria which made it an appropriate candidate to be used in wound dressing purposes [167].

## 12. PLGA HEALING MATERIALS

Recently, nanofibrous drug-loaded collagen/poly-D-L-lactide–glycolide (PLGA) scaffold membranes were developed to provide sustained release of glucophage in wounds related to diabetes [168]. The glucophage, PLGA and collagen were dissolved in 1,1,1,3,3,3-hexafluoro-2-propanol and electrospun into nanofibers through electrospinning method. The *in vitro* and *in vivo* release rates of the drugs from the membranes were assessed by high-performance liquid chromatography and it was found that high glucophage concentrations were released from the nanofibrous membranes for more than three weeks. The hydrophilic character of the glucophage-loaded collagen/PLGA membranes was greater than those of the collagen/PLGA membranes thus they displayed a greater water uptake capability. The glucophage-loaded collagen/PLGA membranes noticeably supported healing of the diabetic wounds. Furthermore, the collagen amounts in diabetic rats treated by drug-eluting membranes were greater than those of the control rats due to the down-regulation of matrix metalloproteinase 9. Hence, it was suggested that the nanofibrous glucophage-loaded collagen/PLGA membranes could increase collagen quantity to treat diabetic wounds thus they could be considered as very fruitful healing promoters for such wounds created at the early stages [168].

It is recognized that wound healing is a complex process which involves numerous overlapping and interdependent series of physiological actions. Also, using exogenous lactate released from the PLGA polymer could accelerate the angiogenesis and wound healing. Curcumin is a familiar topical wound healing compound that can be used for both normal and diabetic-impaired wounds. Therefore, it was imagined that the curcumin encapsulated PLGA NPs will potentially promote the wound healing process [169]. It was found that in a full thickness excisional wound healing mouse, the PLGA–curcumin NPs had a twofold greater wound healing potency than that of curcumin or PLGA. RT-PCR and histology experiments established that PLGA–curcumin NPs displayed advanced granulation tissue formation, re-epithelialization and anti-inflammatory effects. The PLGA NPs provided several advantages for the encapsulated curcumin such as protection against light degradation, improved water solubility and presented a sustained release of curcumin during 8 days. Consequently, the curcumin loaded PLGA NPs could effectively be used for the active wound healing [169].

It is well identified that PLGA provides lactate which can accelerate neovascularization and accelerates wound healing. LL37 is an endogenous human host defense peptide that fights infection and can modulate angiogenesis and wound healing. Therefore, it was assumed that administrating LL37 encapsulated PLGA nanoparticle (PLGA-LL37 NP) could promote wound closure because of the sustained release of both lactate and LL37 [170]. Treatment of full thickness excisional wounds with PLGA-LL37 NP expressively augmented wound healing relative to only administration of LL37 or PLGA. PLGA-LL37 NP treated wounds demonstrated progressive granulation tissue creation through substantial greater collagen deposition, neovascularized and re-epithelialized composition. In fact, the PLGA-LL37 NP enhanced angiogenesis, largely up-regulated IL-6 and VEGFa expression and controlled the

inflammatory wound response. The PLGA-LL37 NP prompted improved in vitro cell migration however it did not influence the proliferation and metabolism of keratinocytes. Also, it exhibited antimicrobial efficiency against *Escherichia coli* microorganism. Thus, a biodegradable material was developed that could accelerate wound healing processes because of the joint effects of LL37 and lactate released from the PLGA-LL37 nanoparticles [170].

Diabetic foot ulcers (DFUs) signify a main clinical issue in the elderly people. In order to find a material for the treatment of this problematic disease, rhEGF-loaded PLGA-alginate microspheres (MS) were achieved through a modified w/o/w-double-emulsion/solvent evaporation process [171]. Diverse designs were estimated to attain optimize properties of microspheres by addition of NaCl into surfactant solution and/or solvent elimination phase and incorporating alginate as the second polymer. It was found that alginate addition improved the encapsulation efficiency (EE) and NaCl incorporation not only increased the EE but also made the particle surface regular and smooth. After the microspheres were optimized, the rhEGF loading was augmented to 1%. Then, the gamma radiation was used to sterilize the particles in order to obtain the precise dosage for *in vivo* tests. The in vitro cell culture assesses established that neither the sterilization process nor the microencapsulation could affect the rhEGF bioactivity or rhEGF wound contraction. Furthermore, the MS were utilized *in vivo* to treat the full-thickness wound in diabetic Wistar rats. rhEGF MS treated animals exhibited a statistically significant reduction in the wounded area after 7 and 11 days, a whole re-epithelization by day 11 and a faster resolution of the inflammatory course. Generally, the results established the favorable potential of rhEGF-loaded PLGA-alginate MS to stimulate effective and earlier wound healing which could be applied for the treatment of DFUs [171].

## CONCLUSION

Microparticles of chitosan-magnesium aluminum silicate (MAS) nanocomposites containing propranolol HCl were obtained by spray-drying process and the effects of the MAS quantity and adding sodium tripolyphosphate (TPP) crosslinker were investigated. A sustained release of propranolol was detected from all microparticles in several hours in both 0.1 M HCl and phosphate buffer (at pH 7.4) but burst release was not observed which was surprising due to the particles were of low micrometer sizes and CS was soluble at acidic pH. Besides, increasing the MAS amount slowed down the drug release at both low and neutral pH media however adding 1-3% TPP merely slightly/moderately decreased the release rate, irrespective of the release environment used.

Solvent cast polymeric inserts (SCIs) and electrospun nanofiber inserts (ENIs) were achieved to be used in ocular drug delivery. SCIs and ENIs comprising 1, 5 and 10%w/w dexamethasone drug were fabricated using a PLA and PVA blend. The drug release rates for the 1, 5 and 10% ENIs were estimated to be 0.62, 1.46 and 2.30 μg/h, respectively while those examined for the SCIs were unreliable. The cytotoxicity was not apparent for the ENIs in cultured bovine corneal endothelial cells during 24h.

Blending of PEG and β-cyclodextrin (β-CD) in the company with $K_2CO_3$ yielded some gels. The thermoreversible GelL and GelH supramolecular gels were produced at low (<50°C) and high (>70°C) temperatures, respectively. The interactions happened among

diclofenac sodium (DS) drug and the gel components were hydrogen bonds and ionic attractions between the carboxylic groups of DS drug and the hydroxyl groups of β-CD or PEG and perhaps the inclusion of the DS aromatic ring inside the β-CD cavity. The DS release from GelL was noticeably greater than those measured for a commercial gel.

The insulin loaded PEG capped PLGA nanoparticles (ISPPLG NPs) were subcutaneous administered to diabetic rats and for this purpose, some low molecular weight biodegradable PLGA copolymers were synthesized and their ISPPLG NPs were produced by means of the water/oil/water (W/O/W) emulsion solvent evaporation procedure. The *in vivo* tests using the ISPPLG NPs on diabetic rats by subcutaneous administration showed a substantial decrease in serum glucose level accompanied by partial repairing in tissue defense systems. As well, histopathological assay revealed that ISPPLG NPs restored the damages produced by oxidants during hyperglycaemia.

Magnetic MIP (MMIP)/graphene oxide (GO) nanocomposite named MMIP@GO was developed by means of acrylamido-2-methyl-1-propanesulfonic acid monomer and ethylene glycol diacrylate (EGDMA) cross-linker with acrylate functionalized $Fe_3O_4$ NPs, GO and Rivastigmine (RIV) drug template. The RIV adsorption mechanism by the MMIP@GO obeyed the Langmuir model and the kinetic data were fitted to pseudo first-order model with the selectivity factor was 1.98 compared to the MNIP@GO. The *in vitro* RIV release test was dependent to the pH values and the network structure of hydrogels. It was found that the maximum release of 74% was happened after 7 days at pH 9.

A biocompatible, multi-stimuli responsive and non-immunogenic smart drug vehicle was developed for targeted delivery of hydrophobic drugs. Smart CS-based microcapsules (MSRS-CS-MCs) were formed using folic acid (FA) functionalized thiolated CS by sonochemical method. Immobilization of both of FA and Rhodamine B isothiocyanate (RITC) as a red fluorescent dye was done on the microcapsules shells. Furthermore, oleic acid (OA) modified magnetic $Fe_3O_4$ NPs (OA-$Fe_3O_4$ MNPs) and a hydrophobic drug, green fluorescent dye (Coumarin 6, C6), were encapsulated in the microcapsules. The spherical MSRS-CS-MCs drug carriers with size of ~500 nm illustrated exceptional magnetic responsive ability, remarkable reduction-responsive release of hydrophobic drugs and favorable selectively folate-receptor-mediated targeting functionality to the HeLa cells. Thus, combination of magnetic and reduction dual-responsiveness, folate-receptor-mediated targeting functionality and fluorescence visualization in the multipurpose microcapsules produced promising MSRS-CS-MCs nanocarriers.

The structural and electronic properties of six complexes formed by hydrogen bonds between anti-hypertensive hydrochlorothiazide drug and ethylene glycol (EG) as a drug carrier were predicted by DFT computations at B3LYP and B3PW91 levels in both the gas phase and solution state (in water and ethanol). It was found that complex **4** formed by means of H-bonds between oxygen and NH hydrogen atoms of sulfonamide group in drug and OH from EG was the most stable compound in the gas phase but the complex **6** created by N-H…O hydrogen bond between the NH(ring) moiety of drug and O atom of OH group from EG was the most energetically stable compound in the solution state (water and ethanol). Accordingly, complex **6** was selected as the most suitable drug delivery system in the solution phase.

An MIP was created for vanillin by photoinitiated polymerization reaction with a mixed semi-covalent and non-covalent imprinting methodology using polymerizable syringaldehyde as template and acrylamide monomer through the B3LYP/6-31+G(d,p) computations. The

DFT calculations confirmed that the specific binding of vanillin in the cavities was related to non-covalent interactions of the template with the hydroxyphenyl and the amide groups. In addition, the binding geometry of vanillin was modelled in the MIP cavity. It was shown that the MIP was much specific for vanillin (imprinting factor=7.4) thus it was efficiently used to extract vanillin (recovery=80%) from red wine spike with vanillin, vanilla pods as well as artificial and natural vanilla sugar.

CS-bentonite nanocomposite (CBN) films were achieved to be employed in wound healing application. Due to great hydrophilic nature of bentonite, it extremely enhanced the water absorption properties of the films. The bentonite presence in the films improved the mechanical strength. Also, the bactericidal activities of the films were assessed against Gram positive and Gram negative bacteria and it was revealed that all CBN films possessed good inhibitory effects against all the bacteria relative to the control. Consequently, the CBN films could be considered as potential materials in wound healing application.

The PLA/Ag nanofibers were produced by electrospinning technique and their *in vitro* antibacterial, mechanical properties and biocompatibility were estimated. Considerable bactericidal property was perceived for PLA/Ag nanofibers against both *E. coli* and *S. aureus* bacteria. The *in vitro* test exhibited that the biofabricated PLA/Ag nanofibers (Hemolytic percentage<5%) were cytocompatible with fibroblast cells and did not inhibit cell growth. The WVTR experiment verified that an optimum moist medium was provided which could promote wound healing. Thus, the PLA/Ag nanofibers could be applied as wound healing materials to enhance the proliferation and functions of fibroblasts and epidermal cells.

Polyethylene glycol fumarate (PEGF) was synthesized by polycondensation polymerization reaction. The wound dressing films obtained using PEGF, CS and thymol (Th) were composed of 80%w/w CS and 20%w/w PEGF polymers and different amounts of Th pharmaceutical additive (0, 0.6, 1.2 and 1.8%v/v). The blend film with 1.8%v/v Th demonstrated optimum properties like improved mechanical properties, adequate absorption of liquid water and water vapor, satisfactory WVTR and air permeability, greater water solubility, superior swelling level, better porous structure and rough surfaces and exceptional antibacterial efficiency against both Gram-positive and Gram-negative bacteria which made it a suitable material for wound dressing application.

Because the diabetic foot ulcers (DFUs) are a main clinical problem in the elderly people and to find an effective material to treat this disease, rhEGF-loaded PLGA-alginate microspheres (MS) were attained by a modified w/o/w-double-emulsion/solvent evaporation method. It was found that alginate addition improved the encapsulation efficiency (EE) and NaCl incorporation not only increased the EE but also made the particle surface regular and smooth. The *in vitro* cell culture test proved that neither the sterilization process nor the microencapsulation affected the rhEGF bioactivity or rhEGF wound contraction. The MS were used *in vivo* to treat the full-thickness wound in diabetic Wistar rats. rhEGF MS treated animals displayed a statistically significant reduction in the wounded zone after 7 and 11 days, a complete re-epithelization by day 11 and a faster resolution of the inflammatory course. Hence, the rhEGF-loaded PLGA-alginate MS could potentially promote wound healing in the treatment of DFUs.

## ACKNOWLEDGMENTS

The financial support of this work by Research Council of Amirkabir University of Technology (Tehran Polytechnic) is gratefully acknowledged. The authors also would like to thank High Performance Computing Cluster of Amirkabir University of Technology for their great help in providing computer services (hardwares and softwares).

## REFERENCES

[1] A. Abbaszad Rafi, M. Mahkam, Preparation of magnetic pH-sensitive film with alginate base for colon specific drug delivery, *Int. J. Polym. Mater. Polym. Biomater*. 64 (2015) 214-219.

[2] X. Chen, H. Yan, W. Sun, Y. Feng, J. Li, Q. Lin, Z. Shi, X. Wang, Synthesis of amphiphilic alginate derivatives and electrospinning blend nanofibers: a novel hydrophobic drug carrier, *Polym. Bull.* 72 (2015) 3097-3117.

[3] Z. Chen, X. Li, H. He, Z. Ren, Y. Liu, J. Wang, Z. Li, G. Shen, G. Han, Mesoporous silica nanoparticles with manipulated microstructures for drug delivery, *Colloid. Surf. B: Biointerfaces* 95 (2012) 274-278.

[4] O. Dogru, S. Abdurrahmanoglu, N. Kayaman-Apohan, Preparation and characterization of modified nanosilica/PNIPAm hybrid cryogels, *Polym. Bull.* 72 (2015) 993-1005.

[5] M. Khimani, S. Yusa, A. Nagae, R. Enomoto, V. K. Aswal, E. Kesselman, D. Danino, P. Bahadur, Self-assembly of multi-responsive poly(N-isopropylacrylamide)-b-poly(N,Ndimethylaminopropylacrylamide) in aqueous media, *Eur. Polym. J.* 69 (2015) 96-109.

[6] T. Potrč, S. Baumgartner, R. Roškar, O. Planinšek, Z. Lavrič, J. Kristl, P. Kocbek, Electrospun polycaprolactone nanofibers as a potential oromucosal delivery system for poorly water-soluble drugs, *Eur. J. Pharmaceut. Sci.* 75 (2015) 101-113.

[7] E. Ruiz-Hernández, A. Baeza, M. Vallet-Regí, Smart drug delivery through DNA/magnetic nanoparticle gates, *ACS Nano 5* (2011) 1259–1266.

[8] S. Grund, M. Bauer, D. Fischer, Polymers in drug delivery-state of the art and future trends, *Adv. Eng. Mater*. 13 (2011) B61-B87.

[9] G. Tiwari, R. Tiwari, B. Sriwastawa, L. Bhati, S. Pandey, P. Pandey, S. K. Bannerjee, Drug delivery systems: An updated review, *Int. J. Pharm. Investig*. 2 (2012) 2–11.

[10] A. Ribeiro, F. Veiga, D. Santos, J. J. Torres-Labandeira, A. Concheiro, C. Alvarez-Lorenzo, Bioinspired imprinted PHEMA-hydrogels for ocular delivery of carbonic anhydrase inhibitor drugs, *Biomacromolecules 12* (2011) 701–709.

[11] H. Masoud, A. Alexeev, Controlled release of nanoparticles and macromolecules from responsive microgel capsules, *ACS Nano 6* (2012) 212–219.

[12] Y. Zhang, J. Yu, H. N. Bomba, Y. Zhu, Z. Gu, Mechanical force-triggered drug delivery, *Chem. Rev. 116* (2016) 12536–12563.

[13] S. Son, E. Shin, B. S. Kim, Light-responsive micelles of spiropyran initiated hyperbranched polyglycerol for smart drug delivery, *Biomacromolecules 15* (2014) 628–634.

[14] E. A. Mourelatou, D. Libster, I. Nir, S. Hatziantoniou, A. Aserin, Nissim Garti, C. Demetzos, Type and location of interaction between hyperbranched polymers and liposomes. Relevance to design of a potentially advanced drug delivery nanosystem (aDDnS), *J. Phys. Chem. B 115* (2011) 3400–3408.

[15] S. Hobel, A. Aigner, Polyethylenimine (PEI)/siRNA-mediated Gene Knockdown in vitro and in vivo, *Methods Mol. Biol*. 623 (2010) 283.

[16] H. M. Pan, H. Yu, G. Guigas, A. Fery, M. Weiss, V. Patzel, D. Trau, Engineering and design of polymeric shells: inwards interweaving polymers as multilayer nanofilm, immobilization matrix, or chromatography resins, *ACS Appl. Mater. Interfaces 9 (***2017)** 5447–5456.

[17] P. D. Cooper, *Activators and inhibitors of complement*, R. B. Sim (Ed.), Kluwer Academic Publishers, Springer Netherlands (1993).

[18] N. Larson, H. Ghandehari, Polymeric conjugates for drug delivery, *Chem. Mater.* 24 (2012) 840-853.

[19] N. Marasini, S. Haque, L. M. Kaminskas, Polymer-drug conjugates as inhalable drug delivery systems: A review, *Curr. Opin. Colloid Interf. Sci.* 31 (2017) 18-29.

[20] H. Ringsdorf, Structure and properties of pharmacologically active polymers, *J. Polym. Sci. Pol. Sym.* 51 (1975) 135-153.

[21] X. Pang, X. Yang, G. Zhai Polymer-drug conjugates: recent progress on administration routes, *Expert Opin. Drug Deliv*. 11 (2014) 1075-1086.

[22] D. Schmaljohann, Thermo and pH responsive polymers in drug delivery, *Adv. Drug Deliv. Rev.* 58 (2006) 1655-1670.

[23] W. B. Liechty, D. R. Kryscio, B. V. Slaughter, N. A. Peppas, Polymers for drug delivery systems, *Ann. Rev. Chem. Biomol. Eng.* 1 (2010) 149-173.

[24] A. D. Martino, V. Sedlarik, Amphiphilic chitosan-grafted-functionalized polylactic acid based nanoparticles as a delivery system for doxorubicin and temozolomide co-therapy, *Int. J. Pharm.* 474 (2014) 134–145.

[25] D. Pathania, D. Gupta, S. Agarwal, M. Asif, V. K. Gupta, Fabrication of chitosan-gpoly(acrylamide)/CuS nanocomposite for controlled drug delivery and antibacterial activity, *Mater. Sci. Eng.* C 64 (2016) 428–435.

[26] I. Kohsari, Z. Shariatinia, S. M. Pourmortazavi, Antibacterial electrospun chitosan–polyethylene oxidenano composite mats containing bioactive silver nanoparticles, *Carbohydr. Polym*. 140 (2016) 287–298.

[27] I. Kohsari, Z. Shariatinia, S. M. Pourmortazavi, Antibacterial electrospun chitosan-polyethylene oxide nanocomposite mats containing ZIF-8 nanoparticles, *Int. J. Biol. Macromol.* 91 (2016) 778–788.

[28] Z. Shariatinia, Z. Nikfar, Synthesis and antibacterial activities of novel nanocomposite films of chitosan/phosphoramide/$Fe_3O_4$ NPs, *Int. J. Biol. Macromol.* 60 (2013) 226–234.

[29] Z. Shariatinia, Z. Nikfar, K. Gholivand, S. Abolghasemi Tarei, Antibacterial activities of novel nanocomposite biofilms of chitosan/phosphoramide/Ag NPs, *Polym. Composit.* 36 (2015) 454–466.

[30] Y. Fazli, Z. Shariatinia, I. Kohsari, A. Azadmehr, S. M. Pourmortazavi, A novel chitosan-polyethylene oxide nanofibrous mat designed for controlled co-release of hydrocortisone and imipenem/cilastatin drugs, *Int. J. Pharmaceut.* 513 (2016) 636–647.

[31] Y. Fazli, Z. Shariatinia, Controlled release of cefazolin sodium antibiotic drug from electrospun chitosan-polyethylene oxide nanofibrous mats, *Mater. Sci. and Eng. C* 71 (2017) 641–652.

[32] L. Jiang, Y. Lu, X. Liu, H. Tu, J. Zhang, X. Shi, H. Deng, Y. Du, Layer–by–layer immobilization of quaternized carboxymethyl chitosan/organic rectorite and alginate onto nanofibrous mats and their antibacterial application, *Carbohydr. Polym.* 121 (2015) 428–435.

[33] Z. Shariatinia, M. Fazli, Mechanical properties and antibacterial activities of novel nanobiocomposite films of chitosan and starch, *Food Hydrocolloid*. 46 (2015) 112–124.

[34] J. Li, Y. Wu, L. Zhao, Antibacterial activity and mechanism of chitosan with ultra high molecular weight, *Carbohydr. Polym*. 148 (2016) 200–205.

[35] B. K. Gu, S. J. Park, M. S. Kim, Y. J. Lee, J. I. Kim, C. H. Kim, Gelatin blending and sonication of chitosan nanofiber mats produce synergistic effects on hemostatic functions. *Int. J. Biol. Macromol.* 82(2016) 89–96.

[36] A. L. M. Ruela, E. C. Figueiredo, G. R. Pereira, Molecularly imprinted polymers as nicotine transdermal delivery systems, *Chem. Eng. J*. 248 (2014) 1–8.

[37] M. S. Silva, F. L. Nobrega, A. Aguiar-Ricardo, E. J. Cabrita, T. Casimiro, Development of molecular imprinted co-polymeric devices for controlled delivery of flufenamic acid using supercritical fluid technology, *J. Supercrit. Fluid*. 58 (2011) 150–157.

[38] K. Rostamizadeh, M. Vahedpour, S. Bozorgi, Synthesis, characterization and evaluation of computationally designed nanoparticles of molecular imprinted polymers as drug delivery systems, *Int. J. Pharm.* 424 (2012) 67–75.

[39] S. Subrahmanyam, A. Guerreiro, A. Poma, E. Moczko, E. Piletska, S. Piletsky, Optimisation of experimental conditions for synthesis of high affinity MIP nanoparticles, *Eur. Polym. J*. 49 (2013) 100–105.

[40] C. Alvarez-Lorenzo, C. González-Chomón, A. Concheiro, Molecularly imprinted hydrogels for affinity-controlled and stimuli-responsive drug delivery, in: C. Alvarez-Lorenzo, A. Concheiro, H. J. Schneider, M. Shahinpoor (Eds.), *Smart Materials for Drug Delivery*, RSC, Cambridge (2013) 228–260.

[41] C. Alvarez-Lorenzo, F. Yañez-Gomez, A. Concheiro, Modular biomimetic drug delivery systems, in: S. Dumitriu, V. Popa (Eds.), *Polymeric Materials, Medicinal and Pharmaceutical Applications*, CRC Press, Boca Raton, Florida, (2013) 85–122.

[42] C. Alvarez-Lorenzo, A. Concheiro, From Drug Dosage Forms to Intelligent Drug Delivery Systems: A Change of Paradigm, in: C. Alvarez-Lorenzo, A. Concheiro (Eds.), *Smart Materials for Drug Delivery*, RSC, Cambridge, (2013) 1–32.

[43] C. Bodhibukkana, T. Srichana, S. Kaewnopparat, N. Tangthong, P. Bouking, G. P. Martin, R. Suedee, Composite membrane of bacterially-derived cellulose and molecularly imprinted polymer for use as a transdermal enantioselective controlled-release system of racemic propranolol, *J. Control. Release* 113 (2006) 43–56.

[44] J. Yang, Y. Hu, J. B. Cai, X. L. Zhu, Q. D. Su, Y. Q. Hu, F. X. Liang, Selective hair analysis of nicotine by molecular imprinted solid-phase extraction: an application for evaluating tobacco smoke exposure, *Food Chem. Toxicol.* 45 (2007) 896–903.

[45] E. C. Figueiredo, D. M. Oliveira, M. E. P. B. Siqueira, M. A. Z. Arruda, On-line molecularly imprinted solid-phase extraction for the selective spectrophotometric determination of nicotine in the urine of smokers, *Anal. Chim. Acta* 635 (2009) 102–107.

[46] J. Alenus, A. Ethirajan, F. Horemans, A. Weustenraed, P. Csipai, J. Gruber, M. Peeters, T. J. Cleij, P. Wagner, Molecularly imprinted polymers as synthetic receptors for the QCM-D-based detection of L-nicotine in diluted salive and urine samples, *Anal. Bioanal. Chem.* 405 (2013) 6479–6487.

[47] C. Y. Gong, Q. J. Wu, Y. J. Wang, D. D. Zhang, F. Luo, X. Zhao, Y. Q. Wei, Z. Y. Qian, *Biomaterials* 34 (2013) 6377–6387.

[48] H. N. Kim, Y. Hong, M. S. Kim, S. M. Kim, K. Y. Suh, *Biomaterials* 33 (2012) 8782–8792.

[49] N. Q. Tran, Y. K. Joung, E. Lih, K. D. Park, *Biomacromolecules* 12 (2011) 2872–2880.

[50] X. Fan, K. Chen, X. He, N. Li, J. Huang, K. Tang, Y. Li, F. Wang, *Int. J. Biol. Macromol.* 91 (2016) 15–22.

[51] E. Dellera, M. C. Bonferoni, G. Sandri, S. Rossi, F. Ferrari, C. D. Fante, C. Perotti, P. Grisoli, C. Caramella, *Eur. J. Pharm. Biopharm.* 88 (2014) 643–650.

[52] S. K. Mishra, D. S. Mary, S. Kannan, Copper incorporated microporous chitosan-polyethylene glycolhydrogels loaded with naproxen for effective drug release and anti-infection wound dressing, *Int. J. Biol. Macromol.* 95 (2017) 928–937.

[53] M. Kongsong, K. Songsurang, P. Sangvanich, K. Siralertmukul, N. Muangsin, *Eur. J. Pharm. Biopharm.* 88 (2014) 986–997.

[54] R. Shukla, S. K. Kashaw, A. P. Jain, S. Lodhi, *Int. J. Biol. Macromol.* 91 (2016)1110–1119.

[55] V. Patrulea, V. Ostafe, G. Borchard, O. Jordan, *Eur. J. Pharm. Biopharm.* 97 (2015) 417–426.

[56] M. H. Nguyen, Y. Hong, T. Y. Kiew, K. Hadinoto, *Eur. J. Pharm. Biopharm.* 96 (2015) 1–10.

[57] M. Koping-Hoggard, K. M. Varum, M. Issa, S. Danielsen, B. E. Christensen, B. T. Stokke, P. Artursson, *Gene Ther.* 11 (2004) 1441–1452.

[58] M. J. Moura, H. Faneca, M. P. Lima, M. H. Gil, M. M. Figueiredo, *Biomacromolecules* 12 (2011) 3275–3284.

[59] D. Cavalla, *Drug News Perspect.* 14 (2001) 495–499.

[60] S. K. Mishra, S. Raveendran, J. M. F. Ferreira, S. Kannan, *In Situ* Impregnation of Silver Nanoclusters in Microporous Chitosan-PEG Membranes as an Antibacterial and Drug Delivery Percutaneous Device, *Langmuir* (2016), 32 (40), 10305–10316.

[61] B. Ozcelik, K. D. Brown, A. Blencowe, M. Daniell, G. W. Stevens, G. G. Qiao, *Acta Biomater*. 9 (2013) 6594–6605.

[62] S. Alippilakkotte, S. Kumar, L. Sreejith, Fabrication of PLA/Ag nanofibers by green synthesis method using Momordica charantia fruit extract for wound dressing applications, *Colloid. Surf. A Physicochem. Eng. Asp.* 529 (2017) 771-782.

[63] J. R. Davidson, Current concepts in wound management and wound healing products, *Vet. Clin. NA Small Anim. Pract.* 46 (2015).

[64] J. S. Boateng, K. H. Matthews, H. N. E. Stevens, G. M. Eccleston, Wound healing dressings and drug delivery systems: a review, *J. Pharm. Sci.* 97 (2008) 2892–2923.

[65] S. Koosehgol, M. Ebrahimian-Hosseinabadi, M. Alizadeh, A. Zamanian, Preparation and characterization of in situ chitosan/polyethylene glycol fumarate/thymol hydrogel as an effective wound dressing, *Mater. Sci. Eng. C* 79 (2017) 66-75.

[66] H. F. Selig, D. B. Lumenta, M. Giretzlehner, M. G. Jeschke, D. Upton, L. P. Kamolz, The properties of an "ideal" burn wound dressing - What do we need in daily clinical practice? Results of a worldwide online survey among burn care specialists, *Burns* 38 (2012) 960–966.

[67] L. I. F. Moura, A. M. a Dias, E. Carvalho, H. C. De Sousa, Recent advances on the development of wound dressings for diabetic foot ulcer treatment - A review, *Acta Biomater*. 9 (2013) 7093–7114.

[68] S. MacNeil, Progress and opportunities for tissue-engineered skin, *Nature* 445 (2007) 874–880.

[69] R. Khlibsuwan, F. Siepmann, J. Siepmann, T. Pongjanyakul, Chitosan-clay nanocomposite microparticles for controlled drug delivery: Effects of the MAS content and TPP crosslinking, *J. Drug Deliv. Sci. Technol.* 40 (2017) 1-10.

[70] P. Chanphai1, V. Konka, H. A. Tajmir-Riahi, Folic acid–chitosan conjugation: A new drug delivery tool, *J. Mol. Liquid*. 238 (2017) 155-159.

[71] L. Neufeld, H. Bianco-Peled, Pectin–chitosan physical hydrogels as potential drug delivery vehicles, *Int. J. Biol. Macromol.* 101 (2017) 852–861.

[72] Z. Shariatinia, Z. Zahraee, Controlled release of metformin from chitosan–based nanocomposite films containing mesoporous MCM-41 nanoparticles as novel drug delivery systems, *J. Colloid Interface Sci.* 501 (2017) 60–76.

[73] R. S. Bhattarai, A. Das, R. M. Alzhrani, D. Kang, S. B. Bhaduri, S. H. S. Boddu, Comparison of electrospun and solvent cast polylactic acid (PLA)/poly(vinyl alcohol) (PVA) inserts as potential ocular drug delivery vehicles, *Mater. Sci. Eng.* C 77 (2017) 895-903.

[74] W. Zhang, C. Huang, O. Kusmartseva, N. L. Thomas, E. Mele, Electrospinning of polylactic acid fibres containing tea tree and manuka oil, *React. Funct. Polym*. 117 (2017) 106-111.

[75] F. Hossein Panahi, S. J. Peighambardoust, S. Davaran, R. Salehi, Development and characterization of PLA-mPEG copolymer containing iron nanoparticle-coated carbon nanotubes for controlled delivery of docetaxel, *Polymer* 117 (2017) 117-131.

[76] M. S. S. Román, M. J. Holgado, B. Salinas, Vicente Rives, Drug release from layered double hydroxides and from their polylactic acid (PLA) nanocomposites, *Appl. Clay Sci.* 71 (2013) 1–7.

[77] A. Klaewklod, V. Tantishaiyakul, N. Hirun, T. Sangfai, Lin Li, Characterization of supramolecular gels based on β-cyclodextrin and polyethyleneglycol and their potential use for topical drug delivery, *Mater. Sci. Eng.* C 50 (2015) 242–250.

[78] G. Prabha, V. Raj, Formation and characterization of β-cyclodextrin (β-CD)–polyethyleneglycol (PEG)–polyethyleneimine (PEI) coated $Fe_3O_4$ nanoparticles for loading and releasing 5-Fluorouracil drug, *Biomed. Pharmacotherap.* 80 (2016) 173–182.

[79] A. Hoshikawa, T. Tagami, C. Morimura, K. Fukushige, T. Ozeki, Ranibizumab biosimilar/polyethyleneglycol-conjugated gold nanoparticles as a novel drug delivery platform for age-related macular degeneration, *J. Drug Deliv. Sci. Technol*. 38 (2017) 45-50.

[80] J. Wang, W. C. Law, L. Chen, D. Chen, C. Y. Tang, Fabrication of monodisperse drug-loaded poly(lactic-co-glycolic acid)-chitosan core-shell nanocomposites via pickering emulsion, *Composit. B Eng*. 121 (2017) 99-107.

[81] S. Saravanan, S. Malathi, P. S. L. Sesh, S. Selvasubramanian, S. Balasubramanian, V. Pandiyan, Hydrophilic poly (ethylene glycol) capped poly(lactic-co-glycolic) acid nanoparticles for subcutaneous delivery of insulin in diabetic rats, *Int. J. Biol. Macromol.* 95 (2017) 1190-1198.

[82] L. Navarro, D. E. Mogosanu, N. Ceaglio, J. Luna, P. Dubruel, I. Rintoul, Novel poly (diol sebacate)s as additives to modify Paclitaxel release from poly (lactic-co-glycolic acid) thin films, *J. Pharm. Sci.* 106 (2017) 2106-2114.

[83] A. L. M. Ruela, E. C. Figueiredo, G. R. Pereira, Molecularly imprinted polymers as nicotine transdermal delivery systems, *Chem. Eng. J*. 248 (2014) 1–8.

[84] K. Hemmati, R. Sahraei, M. Ghaemy, Synthesis and characterization of a novel magnetic molecularly imprinted polymer with incorporated graphene oxide for drug delivery, *Polymer* 101 (2016) 257-268.

[85] C. Mao, X. Xie, X. Liu, Z. Cui, X. Yang, K. W. K. Yeung, H. Pan, P. K. Chu, S. Wu, The controlled drug release by pH-sensitive molecularly imprinted nanospheres for enhanced antibacterial activity, *Mater. Sci. Eng.* C 77 (2017) 84–91.

[86] A. Abbaszad Rafi, M. Mahkam, S. Davaran, H. Hamishehkar, A smart pH-responsive Nano-carrier as a drug delivery system: A hybrid system comprised of mesoporous nanosilica MCM-41 (as a nano-container) & a pH-sensitive polymer (as smart reversible gatekeepers); preparation, characterization and in vitro release studies of an anti-cancer drug, *Eur. J. Pharm. Sci.* 93 (2016) 64-73.

[87] J. Zhong, L. Li, X. Zhu, S. Guan, Q. Yang, Z. Zhou, Z. Zhang, Y. Huang, A smart polymeric platform for multistage nucleus-targeted anticancer drug delivery, *Biomaterials* 65 (2015) 43-55.

[88] H. Li, K. Liu, Q. Sang, G. R. Williams, J. Wu, H. Wang, J. Wu, L. M. Zhu, A thermosensitive drug delivery system prepared by blend electrospinning, *Colloid. Surf B Biointerf.* 159 (2017) 277-283.

[89] X. Cui, X. Guan, S. Zhong, J. Chen, H. Zhu, Z. Li, F. Xu, P. Chen, H. Wang, Multi-stimuli responsive smart chitosan-based microcapsules for targeted drug delivery and triggered drug release, Ultrasonic. *Sonochem.* 38 (2017) 145-153.

[90] M. V. Kiamahalleh, A. Mellati, S. A. Madani, P. Pendleton, H. Zhang, S. H. Madani, Smart carriers for controlled drug delivery: thermosensitive polymers embedded in ordered mesoporous carbon, *J. Pharm. Sci.* 106 (2017) 1545-1552.

[91] O. Yom-Tov, D. Seliktar, H. Bianco-Peled, A modified emulsion gelation technique to improve buoyancy ofhydrogel tablets for floating drug delivery systems, *Mater. Sci. Eng.* C 55 (2015) 335–342.

[92] W. Ke, K. Shao, R. Huang, L. Han, Y. Liu, J. Li, Y. Kuang, L. Ye, J. Lou, C. Jiang, Gene delivery targeted to the brain using an Angiopep-conjugated polyethyleneglycol-modified polyamidoamine dendrimer, *Biomaterials* 30 (2009) 6976–6985.

[93] A. Klaewklod, V. Tantishaiyakul, N. Hirun, T. Sangfai, L. Li, Characterization of supramolecular gels based on β-cyclodextrin and polyethyleneglycol and their potential use for topical drug delivery, *Mater. Sci. Eng.* C 50 (2015) 242–250.

[94] G. Pasut, F. M. Veronese, Polymer-drug conjugation, recent achievements and general strategies, *Progr. Polym. Sci.* 32 (2007) 933–961.

[95] T. M. Allen, P. R. Cullis, Drug delivery systems: entering the mainstream, *Science* 303 (2004) 1818–1822.

[96] R. Duncan, M. J. Vicent, F. Greco, R. I. Nicholson, Polymer–drug conjugates: towards a novel approach for the treatment of endrocine-related cancer, *Endocr. Relat. Cancer* 12 (2005) S189–S199.

[97] I. B. Mosbah, R. Franco-Go, H. B. Abdennebi, R. Hernandez, G. Escolar, D. Saidane, J. Rosello-Catafau, C. Peralta, Effects of polyethylene glycol and hydroxyethyl starch in University of Wisconsin preservation solution on human red blood cell aggregation and viscosity, *Transplant. Proc.* 38 (2006) 1229–1235.

[98] B. Balakrishnan, D. Kumar, Y. Yoshida, A. Jayakrishnan, Chemical modification of poly (vinyl chloride) resin using poly (ethylene glycol) to improve blood compatibility, *Biomaterials* 26 (2005) 3495–3502.

[99] M. Rahman, C. S. Brazel, Review: An Assessment of Traditional Plasticizers and Research Trends for Development of Novel Plasticizers, *Prog. Polym. Sci.* 29 (2004) 1223–1248.

[100] S. Lakshmi, A. Jayakrishnan, Migration resistant, blood-compatible plasticized polyvinyl chloride for medical and related applications, *Artif. Organs* 22 (1998) 222–229.

[101] L. J. Suggs, J. L. West, A. G. Mikos, Platelet adhesion on a biodegradable poly(propylene fumarate-co-ethylene glycol) copolymer, *Biomaterials* 20 (1999) 683–690.

[102] *Encyclopedia of Polymer Science and Technology* (Ed.: H. F. Mark), Wiley, New York, 2007.

[103] A. Asatekin, S. Kang, M. Elimelech, A. M. Mayes, Anti-fouling ultrafiltration membranes containing polyacrylonitrile-graft-poly (ethylene oxide) comb copolymer additives, *J. Membr. Sci.* 298 (2007) 136–146.

[104] K. H. Cheng, S. L. Leung, H. W. Hoekman, W. H. Beekhuis, P. G. H. Mulder, A. J. M. Geerards, A. Kijlstra, Incidence of contact-lens-associated microbial keratitis and its related morbidity, *Lancet* 354 (1999) 179–183.

[105] O. H. Kwon, Y. C. Nho, Y. M. Lee, Radiation-Induced Copolymerization of 2-Hydroxyethyl methacrylate and Polyethylene glycol methacrylate, and Its Protein Adsorption and Bacterial Attachment, *J. Ind. Eng. Chem*. 9 (2003) 138–145.

[106] W. Johnson, Final report on the safety assessment of PEG-25 propylene glycol stearate, PEG-75 propylene glycol stearate, PEG-120 propylene glycol stearate, PEG-10 propylene glycol, PEG-8 propylene glycol cocoate, and PEG-55 propylene glycol oleate, *Int. J. Toxicol*. 20 (2001) 13–26.

[107] C. J. Le Coz, E. Heid, Allergic contact dermatitis from methoxy PEG-17/dodecyl glycol copolymer (Elfacos® OW 100), *Contact Dermatitis* 44 (2001) 308–319.

[108] S. S. Ali, P. K. Sharma, V. K. Garg, A. K. Singh, S. C. Mondal, The target-specific transporter and current status of diuretics as anti-hypertensive, *Fund. Clinic. Pharmacol.* 26 (2012) 175–179.

[109] C. A. Ecelbarger, S. Tiwari, Sodium transporters in the distal nephron and disease implications, *Curr. Hypertens. Rep.* 8 (2006) 158–165.

[110] R. H. Barbhaiya, W. A. Craig, H. P. Corrick-West, P. G. Welling, Pharmacokinetics of hydrochlorothiazide in fasted and nonfasted subjects: a comparison of plasma level and urinary excretion methods, *J. Pharm. Sci.* 71 (1982) 245–248.

[111] S. Shah, I. Khatri, E. D. Freis, Mechanism of antihypertensive effect of thiazide diuretics, *Am. Heart J.* 95 (1978) 611–618.

[112] J. G. Hardman, L. E. Limbird, A. G. Gilman, *Goodman & Gilman's The pharmacological basis of therapeutics*, 12 Ed., McGraw-Hill, New York, 2010.

[113] B. Beermann, M. Groschinsky-Grind, A. Rosén, Absorption, metabolism, and excretion of hydrochlorothiazide, *Clin. Pharmacol. Ther.* 19 (1976) 531–537.

[114] J. D. Duarte, R. M. Cooper-DeHoff, Mechanisms for blood pressure lowering and metabolic effects of thiazide and thiazide-like diuretics, *Expert. Rev. Cardiovasc. Ther.* 8 (2010) 793–802.

[115] *"Hydrochlorothiazide,"* The American Society of Health-System Pharmacists, 2011.

[116] J. Y. Hsieh, C. Lin, B. K. Matuszewski, M. R. Dobrinska, Fully automated methods for the determination of hydrochlorothiazide in human plasma and urine, *J. Pharm. Biomed. Anal.* 12 (1994) 1555–1562.

[117] K. A. Khaled, Y. A. Asiri, Y. M. El-Sayed, *In vivo* evaluation of hydrochlorothiazide liquisolid tablets in beagle dogs, *Int. J. Pharm.* 222 (2001) 1–6.

[118] C. Niemeyer, G. Hasenfuss, U. Wais, H. Knauf, M. Schaferkorting, E. Mutschler, Pharmacokinetics of hydrochlorothiazide in relation to renal-function, *Eur. J. Clin. Pharmacol.* 24 (1983) 661–665.

[119] B. Beermann, M. Groschinsky-Grind, Pharmacokinetics of hydrochlorothiazide in man, *Eur. J. Clin. Pharmacol.* 12 (1977) 297–303.

[120] Z. Nikfar, Z. Shariatinia, Phosphate functionalized (4,4)-armchair CNTs as novel drug delivery systems for alendronate and etidronate anti-osteoporosis drugs, *J. Mol. Graphics Model.* 76 (2017) 86-105.

[121] Z. Nikfar, Z. Shariatinia, DFT computational study on the phosphate functionalized SWCNTs as efficient drug delivery systems for anti-osteoporosis zolendronate and risedronate drugs, *Phys. E* 91 (2017) 41-59.

[122] Z. Shariatinia, M. F. Erben, C. O. Della Védova, M. Abdous, S. Azodi, Hydrogen bonding interactions between α-, β-glucose, and methacrylic acid, *Struct. Chem.* 22 (2011) 1347–1352.

[123] S. Kazemi, A. S. Daryani, M. Abdouss, Z. Shariatinia, DFT computations on the hydrogen bonding interactions between methacrylic acid-trimethylolpropane trimethacrylate copolymers and letrozole as drug delivery systems, *J. Theor. Comput. Chem.* 15 (2016) 1650015.

[124] Z. Shariatinia, A. Mazloom Jalali, F. Afshar Taromi, Molecular dynamics simulations on desulfurization of n-octane/thiophene mixture using silica filled polydimethylsiloxane nanocomposite membranes, *Modelling Simul. Mater. Sci. Eng.* 24 (2016) 035002.

[125] A. Mazloom Jalali, Z. Shariatinia, F. Afshar Taromi, Desulfurization efficiency of polydimethylsiloxane/silica nanoparticle nanocomposite membranes: MD simulations, *Comput. Mater. Sci.* 139 (2017) 115–124.

[126] M. J. Frisch, G. W. Trucks, H. B. Schlegel, G. E. Scuseria, M. A. Robb, J. R. Cheeseman, V. G. Zakrzewski, J. A. Montgomery, R. E. J. Jr Stratmann, C. Burant, S. Dapprich, J. M. Millam, A. D. Daniels, K. N. Kudin, M. C. Strain, O. Farkas, J. Tomasi, V. Barone, M. Cossi, R. Cammi, B. Mennucci, C. Pomelli, C. Adamo, S. Clifford, J. Ochterski, G. A. Petersson, P. Y. Ayala, Q. Cui, K. Morokuma, D. K. Malick, A. D. Rabuck, K. Raghavachari, J. B. Foresman, J. Cioslowski, J. V. Ortiz, A. G. Baboul, B. B. Stefanov, G. Liu, A. Liashenko, P. Piskorz, I. Komaromi, R. Gomperts, R. L. Martin, D. J. Fox, T. Keith, M. A. Al-Laham, C. Y. Peng, A. Nanayakkara, M. P. Challacombe, M. W. Gill, B. Johnson, W. Chen, M. W. Wong, J. L. Andres, C. Gonzalez, M. Head-Gordon, E. S. Replogle, J. A. Pople, *Gaussian 98, Revision A9, Gaussian, Inc*; Pittsburgh, PA, 1998.

[127] S. Mietrus, E. Scrocco, Electrostatic interaction of a solute with a continuum. A direct utilizaion of AB initio molecular potentials for the prevision of solvent effects, *Chem. Phys.* 55 (1981) 117–129.

[128] R. Bersohn, Nuclear electric quadrupole spectra in solids, *J. Chem. Phys.* 20 (1952) 1505–1509.

[129] P. Pyykö, Spectroscopic nuclear quadrupole moments, *Mol. Phys.* 99 (2001) 1617–1629.

[130] R. F. W. Bader, *Atoms in Molecules: A quantum theory*. Oxford University Press, Oxford, UK, 1990.

[131] R. F. W. Bader, *AIM2000 Program ver 2.0*, McMaster University, Hamilton, 2000.

[132] Y. Dimitrova, Theoretical study of structures and stabilities of hydrogen-bonded phenol–water complexes, *J. Mol. Struct. Theochem.* 455 (1998) 9–21.

[133] F. B. van Duijneveldt, J. G. C. M. van Duijneveldt-van de Rijdt, J. H. van Lenthe, State of the art in counterpoise theory, *Chem. Rev.* 94 (1994) 1873–1885.

[134] S. B. Boys, F. Bernardi, The calculation of small molecular interactions by the differences of separate total energies, Some procedures with reduced errors, *Mol. Phys.* 19 (1970) 553–566.

[135] R. F. W. Bader, A quantum theory of molecular structure and its applications, *Chem. Rev.* 91 (1991) 893–928.

[136] R. F. W. Bader, H. Essén, The characterization of atomic interactions, *J. Chem. Phys.* 80 (1983) 1943–1960.

[137] R. G. A. Bone, R. F. W. Bader, Identifying and analyzing intermolecular bonding interactions in van der Waals molecules, *J. Phys. Chem.* 100 (1996) 10892–10911.

[138] M. F. Bobrov, G. V. Popova, V. G. Tsirelson, A topological analysis of electron density and chemical bonding in cyclophosphazenes $P_nN_nX_{2n}$ (X = H, F, Cl; N = 2, 3, 4), *Russ. J. Phys. Chem.* 80 (2006) 584–590.

[139] E. Espinosa, I. Alkorta, J. Elguero, E. Molins, From weak to strong interactions: a comprehensive analysis of the topological and energetic properties of the electron density distribution involving X–H…F–Y systems, *J. Chem. Phys.* 117 (2002) 5529–5542.

[140] Z. Shariatinia, S. Shahidi, A DFT study on the physical adsorption of cyclophosphamidederivatives on the surface of fullerene $C_{60}$ nanocage, *J. Mol. Graph. Model.* 52 (2014) 71–81.

[141] S. Azodi-Deilami, M. Abdouss, D. Kordestani, Z. Shariatinia, Preparation of *N,N-p*-phenylene bismethacryl amide as a novel cross-link agent for synthesis and characterization of the core–shell magnetic molecularly imprinted polymer nanoparticles, *J. Mater. Sci. Mater. Med.* 25 (2014) 645–656.

[142] M. Azenha, P. Kathirvel, P. Nogueira, A. Fernando-Silva, The requisite level of theory for the computational design of molecularly imprinted silica xerogels, *Biosens. Bioelectron.* 23 (2008) 1843-1849.

[143] Z. Shariatinia, M. F. Erben, C. O. D. Védova, DFT calculations on the hydrogen bonding interactions between adrenaline and trimethoxysilylpropylamine, *Main Group Chem.* 11 (2012) 275–284.

[144] Y. Liu, F. Wang, T. Tan, M. Lei, Study of the properties of molecularly imprinted polymers by computational and conformational analysis, *Anal. Chim. Acta* 581 (2007) 137-146.

[145] M. Abdouss, S. Azodi-Deilami, E. Asadi, Z. Shariatinia, Synthesis of molecularly imprinted polymer as a sorbent for solid phase extraction of citalopram from human serum and urine, *J. Mater. Sci. Mater. Med.* 23 (2012) 1543–1552.

[146] J. Yao, X. Li, W. Qin, Computational design and synthesis of molecular imprinted polymers with high selectivity for removal of aniline from contaminated water, *Anal. Chim. Acta* 610 (2008) 282-288.

[147] Z. Shariatinia, N. Arabzadeh, M. Abdous, Ab initio calculations on the hydrogen bonding interactions among pseudoephedrinium cation isomers and methacrylic acid, *Main Group Chem*. 10 (2011) 1–16.

[148] K. Puzio, R. Delepee, R. Vidal, L. A. Agrofoglio, Combination of computational methods, adsorption isotherms and selectivity tests for the conception of a mixed non-covalent–semi-covalent molecularly imprinted polymer of vanillin, *Anal. Chim. Acta* 790 (2013) 47– 55.

[149] A. Azimi, M. Javanbakht, Computational prediction and experimental selectivity coefficients for hydroxyzine and cetirizine molecularly imprinted polymer based potentiometric sensors, *Anal. Chim. Acta* 812 (2014) 184–190.

[150] F. Ahmadi, E. Yawari, M. Nikbakht, Computational design of an enantioselective molecular imprintedpolymer for the solid phase extraction of S-warfarin from plasma, *J. Chromatogr. A* 1338 (2014) 9–16.

[151] N. Martins, E. P. Carreiro, A. Locati, J. P. P. Ramalho, M. J. Cabrita, A. J. Burke, R. Garcia, Design and development of molecularly imprinted polymers for theselective extraction of deltamethrin in olive oil: An integratedcomputational-assisted approach, *J. Chromatogr. A* 1409 (2015) 1–10.

[152] N. Karimian, M. B. Gholivand, F. Taherkhani, Computational design and development of a novel voltammetric sensor for minoxidil detection based on electropolymerized molecularly imprinted polymer, *J. Electroanal. Chem.* 740 (2015) 45–52.

[153] M. Torkashvand, M. B. Gholivand, F. Taherkhani, Fabrication of an electrochemical sensor based on computationally designed molecularly imprinted polymer for the determination of mesalamine in real samples, *Mater. Sci. Eng.* C 55 (2015) 209–217.

[154] G. Yuvaraja, J. L. Pathak, Z. Weijiang, Z. Yaping, X. Jiao, Antibacterial and wound healing properties of chitosan/poly(vinyl alcohol)/zinc oxide beads (CS/PVA/ZnO), *Int. J. Biol. Macromol*. 103 (2017) 234-241.

[155] R. Abdel-Basset Sanad, H. M. Abdel-Bar, Chitosan–Hyaluronic acid composite sponge scaffold enriched with Andrographolide-loaded lipid nanoparticles for enhanced wound healing, *Carbohydr. Polym*. 173 (2017) 441-450.

[156] G. Sandri, C. Aguzzi, S. Rossi, M. C. Bonferoni, G. Bruni, C. Boselli, A. I. Cornaglia, F. Riva, C. Viseras, C. Caramella, F. Ferrari, Halloysite and chitosan oligosaccharide nanocomposite for wound healing, *Acta Biomater*. 57 (2017) 216-224.

[157] N. Devi, J. Dutta, Preparation and characterization of chitosan-bentonite nanocomposite films for wound healing application, *Int. J. Biol. Macromol*. 104B (2017) 1897-1904.

[158] F. Tang, L. Lv, F. Lu, B. Rong, Z. Li, B. Lu, K. Yu, J. Liu, F. Dai, D. Wu, G. Lan, Preparation and characterization of N-chitosan as a wound healing accelerator, *Int. J. Biol. Macromol.* 93 (2016) 1295–1303.

[159] N. Huang, J. Lin, S. Li, Y. Deng, S. Kong, P. Hong, P. Yang, M. Liao, Z. Hu, Preparation and evaluation of squid ink polysaccharide-chitosan as a wound-healing sponge, *Mater. Sci. Eng. C Mater. Biol. Appl.* 82 (2018) 354-362.

[160] Z. Aytac, T. Uyar, Core-shell nanofibers of curcumin/cyclodextrin inclusion complex and polylactic acid: Enhanced water solubility and slow release of curcumin, *Int. J. Pharm.* 518 (2017) 177–184.

[161] S. Alippilakkotte, S. Kumar, L. Sreejith, Fabrication of PLA/Ag nanofibers by green synthesis method using Momordica charantia fruit extract for wound dressing applications, Colloid. Surf. *A Physicochem. Eng. Asp*. 529 (2017) 771-782.

[162] S. F. Gomaa, T. M. Madkour, S. Moghannem, I. M. El-Sherbiny, New polylactic acid/cellulose acetate-based antimicrobial interactive single dose nanofibrous wound dressing mats, *Int. J. Biol. Macromol*. 105 (2017) 1148-1160.

[163] I. J. Macha, M. M. Muna, J. L. Magere, In vitro study and characterization of cotton fabric PLA composite as a slow antibiotic delivery device for biomedical applications, *J. Drug Deliv. Sci. Technol*. 43 (2018) 172–177.

[164] S. K. Mishra, D. Sujitha Mary, S. Kannan, Copper incorporated microporous chitosan-polyethylene glycolhydrogels loaded with naproxen for effective drug release and anti-infection wound dressing, *Int. J. Biol. Macromol*. 95 (2017) 928–937.

[165] P. R. Fa-Si-Oen, C. Verwaest, J. Buitenweg, H. Putter, J. W. de Waard, C. J. H. van de Velde, R. M. H. Roumen, Effect of mechanical bowel preparation with polyethyleneglycol on bacterial contamination and wound infection in patients undergoing elective open colon surgery, *Clinic. Microbiol. Infect.* 11 (2005) 145–163.

[166] F. Sun, H. R. Nordli, B. Pukstad, E. K. Gamstedt, G. Chinga-Carrasco, Mechanical characteristics of nanocellulose-PEG bionanocomposite wound dressings in wet conditions, *J. Mechanic. Behav. Biomed. Mater*. 69 (2017) 377–384.

[167] S. Koosehgol, M. Ebrahimian-Hosseinabadi, M. Alizadeh, A. Zamanian, Preparation and characterization of in situ chitosan/polyethylene glycol fumarate/thymol hydrogel as an effective wound dressing, *Mater. Sci. Eng*. C 79 (2017) 66-75.

[168] C. H. Lee, S. H. Chang, W. J. Chen, K. C. Hung, Y. H. Lin, S. J. Liu, M. J. Hsie, J. H. S. Pang, J. H. Juang, Augmentation of diabetic wound healing and enhancement of collagen content using nanofibrous glucophage-loaded collagen/PLGA scaffold membranes, *J. Colloid Interf. Sci*. 439 (2015) 88–97.

[169] K. K. Chereddy, R. Coco, P. B. Memvanga, B. Ucakar, A. des Rieux, G. Vandermeulen, V. Préat, Combined effect of PLGA and curcumin on wound healing activity, *J. Control. Release* 171 (2013) 208–215.

[170] K. K. Chereddy, C. H. Her, M. Comune, C. Moia, A. Lopes, P. E. Porporato, J. Vanacker, M. C. Lam, L. Steinstraesser, P. Sonveaux, H. Zhu, L. S. Ferreira, G. Vandermeulen, V. Préat, PLGA nanoparticles loaded with host defense peptide LL37 promote wound healing, *J. Control. Release* 194 (2014) 138–147.

[171] G. Gainza, J. J. Aguirre, J. L. Pedraz, R. M. Hernández, M. Igartua, rhEGF-loaded PLGA-Alginate microspheres enhance the healing of full-thickness excisional wounds in diabetised Wistar rats, *Eur. J. Pharm. Sci.* 50 (2013) 243–252.

In: Advances in Polymers for Biomedical Applications ISBN: 978-1-53613-612-8
Editors: Deepak Pathania and Bhuvanesh Gupta 

*Chapter 5*

# MODIFIED BIOPOLYMERS AND ITS POTENTIAL SIGNIFICANCE IN TARGETED DRUG DELIVERY AND DISEASE DIAGNOSIS

***S. Vaidevi[1,2], M. Azeera[2], K. Ruckmani[1,2,*] and S. Lakshmana Prabu[2]***

[1]National Facility for Drug Development for Academia,
Pharmaceutical and Allied Industries (NFDD),
Anna University, BIT campus, Tamil Nadu, India
[2]Department of Pharmaceutical Technology,
Centre for Excellence in Nanobio Translational REsearch (CENTRE),
Anna University, BIT campus, Tamil Nadu, India

## ABSTRACT

Biopolymers are natural substance that contains multiple units of saccharides, nucleic acids, amino acids and they are produced by a variety of mechanisms. The major biopolymer classification based on biopolymers which is derived from microbial systems, extracted from plants or synthesized by chemical methods. Biopolymers have immense application in the field of medical materials, cosmetics, food additives, clothing fabrics, water treatment, bioremediation, absorbents, biosensors, targeted drug delivery, tissue engineering and even data storage elements. Polyesters, proteins and polysaccharide are the major types of biopolymers. Among the various polymers, natural polymers are extensively used due to its biocompatibility but not used widely because of its physical properties such as solubility, stability and mechanical strength. These drawbacks can be overcome by functional modifications on biopolymer surface renders them as a suitable and smart biomaterial for medical as well as drug delivery applications. In this chapter, we would like to discuss about some polysaccharide based modified biopolymers and its potential applications in various diversified fields, particularly in drug delivery, disease diagnosis and cancer therapy. Chemical modifications are desired for improving the

* Corresponding Author Email: hodpharma.aut@gmail.com.

function and targeting its specific applications. The modification technique includes chemical, photochemical, enzymatic, radiation and graft copolymerization. However, these chemical modifications of biopolymers may lead to toxicity issues, increase the cost of production and increased complexity of the synthesis process. In this chapter, we discussed about the toxicity issue due to functional modifications and appropriate solutions to overcome these limits by suitable coating or surface stabilization techniques.

**Keywords:** polysaccharide, biopolymers, biocompatibility, drug delivery, diagnosis

## INTRODUCTION

Biopolymers are polymers that are produced from living organisms, which are classified into three groups: polysaccharides, proteins and nucleic acids. It is important to control particle size, charge, surface morphology and release rate of loaded molecules in biopolymer-based nanoparticles as drug/gene delivery carriers. Biopolymers are suitable materials as nanoparticles for clinical application due to their versatile traits, including biocompatibility, biodegradability and low immunogenicity. Polymeric nanoparticles have been used as a potent therapeutic carrier for delivery of therapeutic molecules such as genes, drugs and for tissue engineering application. Chitosan is the most commonly used cationic polysaccharide for polyion-complex, whereas carboxymethyl cellulose (CMC), dextran sulfate, carrageenan, heparin, hyaluronic acid, alginate was used as anionic polysaccharides. In this chapter, we discussed about polysaccharide based biopolymers and its potential significance in targeted drug delivery and disease diagnosis.

### 1.1. Polysaccharide Based Biopolymers

#### *1.1.1. Functional Modification: Cross Linking*

Preparation of polysaccharide nanoparticles by crosslinking can be achieved by either ionic crosslinking (physical crosslinking) or covalent crosslinking (chemical crosslinking). Covalently crosslinked polysaccharide nanoparticles enable the network structure to be permanent since irreversible chemical links are formed unless biodegradable or stimuli-responsive cross linkers are employed.

Physical crosslinking of polysaccharides are based on ionic interactions between charged polysaccharides and ionic cross linkers. In this method, the prepared nanoparticles are having good reversibility and biocompatiblity. Ionically-cross linked nanoparticles are generally pH sensitive, it is a suitable feature for stimuli-sensitive controlled release.

#### *1.1.2. Polyion-Complex*

Polysaccharide nanoparticles are also prepared by direct electrostatic interactions between oppositely charged polysaccharides in solution. The stability of polyion-complex are determined by the degree of interaction between the polyelectrolytes, which is affected by the charge density, its distribution, chemical environment such as pH of the solution, ionic strength, temperature, the molecular weight of the polyelectrolytes and their flexibility.

## 2. CHITOSAN

Chitosan is a heteropolymer composed of glucosamine and N-acetyl glucosamine residues (Figure 1), and it is obtained by deacetylation of chitin. The physicochemical properties of chitosan are: it is a weak base, soluble in acidic solution (pH 6.5), insoluble in water and organic solvents. Due to its hydrophilic nature and greater solubility in acidic medium, chitosan hydrogels exhibits relatively low mechanical strength and limited ability to control the release of encapsulated compounds. Chitosan (CS) is non-toxic, hydrophilic, biocompatible and biodegradable are the major considerations for consumption in biomedical and pharmaceutical applications including drug delivery, cosmetics and tissue engineering.

The presence of primary hydroxyl and amine groups in its backbone allows it for chemical modifications to control its physical properties and can be used in drug targeting, drug delivery and tumor extracellular targeting. It forms a hydrogel in the presence of multi-valent anions, such as tripolyphosphate (TPP) due to its ionic interaction between the positively charged amino groups of chitosan and the negatively charged counter-ion of TPP.

### 2.1. Modified Chitosan

The primary hydroxyl and amine groups located on the backbone of chitosan are responsible for the reactivity of the polymer and also act as sites for chemical modification. Some important functional modifications of chitosan are carboxymethylation, carboxyethylation, reductive amination with phosphorylcholine glyceraldehydes, thiolated chitosan, N- or O-acylation and alkylation, quaternarization, phosphorylated chitosan and grafted chitosan. These functional modifications in chitosan render them as a suitable carrier for drug delivery applications. However, chitosan has certain limitations in controlled drug delivery and tissue engineering applications. These limitations can be overcome by chemical modification. Thus, modified chitosan hydrogels has gained importance in current research areas such as drug delivery, tissue engineering & disease diagnosis.

Chitosan derivatives such as chitosan succinate and chitosan phthalate microspheres were used for oral delivery of insulin. The chitosan succinate is more hydrophilic than chitosan phthalate and the pharmacological efficacy for chitosan phthalate and chitosan succinate microspheres was almost three fold higher than the efficacy of the oral administration of insulin [1]. In another study, surface modified of chitosan-TBA (4-thiobutyl-amidine) conjugate PLGA nanoparticles used as transmucosal drug delivery system and self-aggregated nanoparticles of cholesterol-modified chitosan conjugate act as a novel carrier loaded with epirubicin for the effective drug delivery to target cells [2].

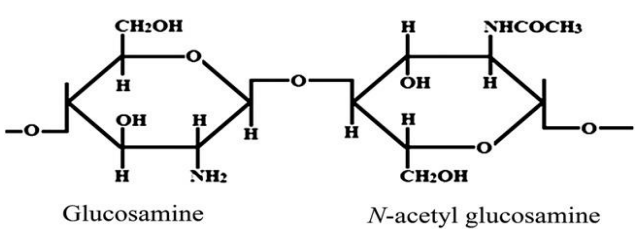


Figure 1. Chemical structure of chitosan.

The polyelectrolyte complexes of chitosan and pectin showed a pH-sensitive and swelling ability on the release behavior of vancomycin for colon-specific delivery [3]. Hydrogels of oxidized dextran (Odex) and N-carboxyethyl chitosan (CEC) without any extraneous crosslinking agent can be used for wound dressing [4]. Novel polyampholyte hydrogels based on carboxymethyl chitosans (CMC) can be used in oral delivery system for protein drugs [5]. Chitosan–TBA (chitosan-4- thiobutylamidine) conjugates can be considered as a vehicle for nasal peptide drug delivery [5]. Some mucoadhesive vaginal gels were prepared using hydroxyethylcellulose (HEC) mixed with chitosan (CS) or its derivative namely 5-methyl pyrrolidinone chitosan (MPCS) loaded with metronidazole (MET) for drug delivery [6].

In another case methoxy poly (ethylene glycol)-grafted-chitosan (mPEG-g-CS) conjugates formed by the formaldehyde linking method. Mono- disperse nanoparticles in aqueous media showed a potential carrier for the sustained release of methotrexate (MTX) [7]. Recently atrial natriuretic peptide-conjugated chitosan-hydrazone-mPEG copolymer nanoparticles identified as pH-responsive carriers for intracellular delivery of prednisone. Chitosan and methoxy-polyethylene glycol (mPEG) polymers were used for synthesis of this novel hydrazone-linked, pH-cleavable chitosan-hydrazone-mPEG copolymer (CH-Hz-mPEG) [8].

Thermoresponsive drug delivery system developed using PNIPAm (poly (N-isopropylacrylamide)) and chitosan. Polymeric nanoparticles prepared by conjugation of amine-terminated PNIPAm with O-carboxymethylchitosan through graft-onto method. FTIR and proton NMR analysis confirmed the synthesis of a copolymer and XRD analysis reveals conjugation reaction of polymeric materials. Doxorubicin loaded polymeric nanoparticles (D-PNPs) were fabricated using copolymer by gelation method. Morphology illustration through TEM showed the spherical shape of DPNPs and particle size measurement indicates thermoresponsive properties of D-PNPs at various temperatures. The release study results reveal that the release of doxorubicin was slower at 25°C, moderately released at 37°C, and faster released at 42°C; may be due to its framework of the prepared D-PNPs. Based on the results such as transmittance measurement, particle size and release studies, it was confirmed that the D-PNPs exhibit temperature-responsive behavior, which could make them appropriate for a thermoresponsive drug delivery [9].

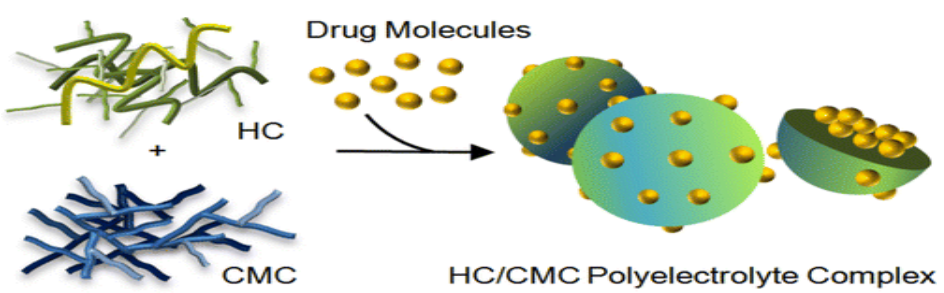


Figure 2. Schematic diagram showing complexation of HC with CMC via electrostatic interactions for encapsulation of drug molecules (Reprinted with permission [11] Copyright © 2015, American Chemical Society).

A targeted drug delivery system was developed using folate-conjugated pluronic F127/chitosan core-shell nanoparticles to deliver doxorubicin (DOX) for the treatment of cancer. In this process DOX was encapsulated in pluronic F127 micelle cores in the presence of sodium dodecyl sulfate (SDS) by a self-assembly method. In the former shell, a layer of either chitosan or folate-conjugated chitosan was deposited onto the pluronic micelles. The encapsulation efficiency was approximately 58.1%. The average size of the core-shell nanoparticles was 37 nm with zeta potential value with 12.9 mV which indicates the presence of a shell layer and stability of particles. *In-vitro* DOX release study reveals, an initial burst release, followed by a sustained release was observed in 24 hours. In addition, the core-shell nanoparticles showed greater cytotoxicity towards MCF-7 cells than free DOX, suggesting a better therapeutic efficacy in treating cancer cells. The uptake rate of the folate-conjugated chitosan nanoparticles were relatively faster than that of the chitosan nanoparticles, possibly due to more effective folate-mediated endocytosis. Both types of nanoparticles exhibited similar toxicity profiles against MCF-7 cells. The study results indicated that the lower cell viability corresponds to a higher DOX concentration and longer incubation time. They concluded that these core-shell nanoparticles performed as promising delivery vectors for the treatment of tumor tissues, particularly breast cancer, in which folate receptors are overexpressed [10].

A novel chitosan-based drug delivery system developed using polyelectrolye *complexes* for effective drug encapsulation and more sustained drug release than the conventional chitosan. In another method polyelectrolyte complexes formed between chitosan (CS) and anionic polymers. Chitosan is copolymerized with hypromellose via a coupling reagent-mediated approach to form a water-soluble, nontoxic CS derivative, namely hypromellose-graft-CS (HC). Hypromellose is cellulose ether commonly used in the fabrication of hydrophilic matrices and the polyelectrolyte complexes was formed via electrostatic interactions by mixing the positively charged CS or HC molecules with the negatively charged CMC chains. Incorporation of Hypromellose to the hydrophobic CS molecules, expected to enhance the aqueous solubility of the resulting product. Then this HC is complexed with carboxymethylcellulose (CMC) to generate a polyampholytic hydrogel. HC is highly water-soluble across a wide pH range, and has a substantially higher pH buffering capacity to provide a pH-stable environment for delivery of drugs. In addition, the polyelectrolyte complex of HC exhibits a drug encapsulation efficiency of over 90% in all drugs tested, which is 1–2 fold higher than the efficiency attainable by the polyelectrolyte complex of conventional CS, with a 2–3 fold longer duration of sustained drug release. These results indicate that HC can act as an excellent promising system for drug development and drug administration both industrially and clinically [11].

## 2.2. Chitosan-Based Nano Medicines for Cancer Treatment

Carboxymethyl chitosan (CMCS) is an amphoteric polymer, and its charge can be changed via the varying the molar ratio of –COOH to $–NH_2$. CMCS is a derivative of chitosan and it is widely used as a surface coating agent and the complex was negatively charged with the shielding of CMCS at physiological conditions; under acidic tumor conditions, the coating material can be removed, and it became positively charged which

enhance cellular uptake via electrostatic absorptive endocytosis. These dendrimers exhibited 1.99 and 1.76 times higher cellular uptake efficiencies at pH 7.4 and pH 6.5 in MCF-7 and A549 cells, respectively. After intravenous administration in mice bearing H22 tumors, doxorubicin-loaded dendrimers exhibited a 1.50-fold greater antitumor activity and presented no obvious systematic toxicity based on histological analysis compared with free drugs. Thus, the nanocarriers could promote the preferential accumulation of DOX in tumor cells to improve the antitumor effect and minimize the nonspecific distribution in normal cells due to the charge reversal target ability and EPR effect. The surface modification of the cationic dendrimer PAMAM with CMCS has been exploited for conventional antitumor drug progressive targeting delivery [12].

In another study grafting performed by using chitosan (CHT) with diisocyanate terminated polyurethane for controlled and sustained drug release system. Solubility studies, swelling behavior and contact angle measurements support the hydrophobic chemical modifications on chitosan molecules. Molecular relaxation phenomena due to the constraint associated with the grafting have been revealed using spin–lattice relaxation time (T1) and shifting of peak position in tan δ curve toward lower temperature in dynamic mechanical measurement at constant frequency indicating the flexible nature of graft copolymers as compared to pure chitosan. In depth biocompatibility studies through platelet aggregation, platelet adhesion, reactive oxygen species of the developed graft copolymers, in-vitro hemolysis assay and cell viability have been performed to understand its potential use in biomedical applications and compared. The chitosan graft copolymer has improved properties when compare with pure chitosan and its bio and hemocompatible nature of chitosan graft copolymers makes them as a potent carrier for controlled and sustained drug release [13].

Transmucosal drug delivery system was developed by ionic gelation technique. In this method chitosan (CS) hydrochloride complexed with pentasodium tripolyphosphate (TPP) and sodium alginate (ALG). Incorporation of a small proportion of ALG increases molecular weight from 4 to 74 kDa and colloidal size from ∼260 to ∼525 nm. Insulin has been taken as a model peptide, was associated to CS-TPP-ALG nanoparticles with efficiencies in the range of ∼41 to ∼52%, irrespective of the molecular weight of the ALG incorporated in the formulation. These CS-TPP-ALG nanoparticles exhibited a capacity to enhance the systemic absorption of insulin after nasal administration to conscious rabbits. Interestingly, it was observed that the duration of the hypoglycemic response was affected by the ALG's Molecular weight. This new nanoparticulate composition can be used as a potential carrier for increasing insulin absorption by nasal [14].

## 3. ALGINATE

Alginate is a natural linear anionic polysaccharide present in the cell wall of brown algae (Phaeophyceae) and widely utilized in food and pharmaceutical industries. The seaweed is extracted with a dilute alkaline solution which solubilizes the alginic acid. Chemically, alginate is constituted by 1, 4-linked-β-D12 mannuronic acid (M) and α-L-guluronic acid (G) residues, generally composed of consecutive G residues, M residues or alternating MG residues (Figure 3). Alginate can be used as an ingredient in the various pharmaceutical

preparations. The alginic acid can be converted into sodium alginate as salt by chemical reaction, which is mainly used for micro encapsulation.

## 3.1. Modified Alginates

Alginates from different sources vary in their proportions of blocks. Hydration of alginic acid leads to the formation of a high-viscosity "acid gel" due to intermolecular binding. After gelation the water molecules are physically entrapped inside the alginate matrix, which is free to migrate. Due to this migration property, it can be used in various applications (e.g., alginate gels for cell immobilization/encapsulation). The water-holding capacity of the gel is due to capillary forces. Heat-stable gels can be developed at room temperature. Alginate has numerous unique properties; it has been utilized for the entrapment and delivery of biomolecules like DNA, proteins and cells.

The mucoadhesive feature of alginate is an important property for delivery of biomolecules to mucosal tissues (other than the GI tract), thereby improving overall drug effectiveness and bioavailability. Modified form of alginate was prepared by using lectins which are conjugated to the surface of spermine-modified alginate beads; these developed beads adhere to epithelial rather than mucosa [15].

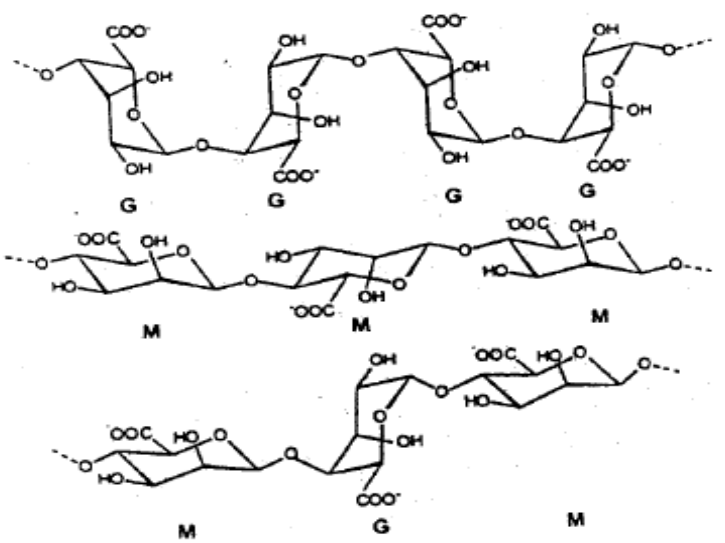


Figure 3. Alginate block types: G- guluronic acid, M-Mannuronic acid.

## 3.2. Hybrid Microparticles

Alginate-based hybrid aerogel microparticles were prepared by emulsion gelation method and drying was performed using supercritical $CO_2$. Spherical hybrid microparticles with mesoporous structure were developed with high specific surface area with better mucoadhesive properties. Pectin interacts with alginate, high degree of crosslinking resulting in lower shrinkage, high specific area and nontoxic nature which renders them as a suitable

novel formulation for delivery of drug through mucosal routes. Drugs such as ketoprofen and quercetin are used to prepare alginate-based aerogel microparticles by supercritical solution and anti-solvent process that never alter the cell growth. The antioxidant activity of quercetin was not affected by loading and supercritical drying. Drug release from alginate/κ-carrageenan aerogel was found to be slightly faster for both drugs compared to alginate/pectin counterpart [16].

### 3.3. Hybrid Aerogels

An alginate based hybrid aerogels was prepared in the form of microparticles (<50 μm) as carriers for mucosal administration of drugs. Low methoxyl pectin and κ-carrageenan were co-gelled with alginate and dried with supercritical $CO_2$. Spherical mesoporous aerogel microparticles were obtained for alginate, hybrid alginate/pectin and alginate/κ-carrageenan aerogels, presenting high specific surface area and mucoadhesive properties [16]. The microparticles were loaded with ketoprofen via adsorption from its solution in sc-$CO_2$, whereas quercetin via supercritical anti-solvent precipitation. Loading of ketoprofen was found to be between 17 and 22% w/w whereas quercetin was found to be between 3.1 and 5.4% w/w. The loading procedure allowed the preservation of antioxidant activity of quercetin. Release of both drugs from alginate/κ-carrageenan aerogel were slightly faster when compare to alginate/pectin. The results indicate that alginate-based aerogel microparticles can be viewed as promising matrices for mucosal drug delivery applications. Biopolymer-based aerogels with mucoadhesive properties are of special interest in pharmaceutical applications which can be designed for administration through various mucosal delivery routes (nasal, buccal, intestinal and vaginal).

### 3.4. Microcapsules

Biocompatible Ca-ALG hydrogel microcapsules were synthesized with good dispersity by using $CaCO_3$ microspheres as a template. After modification with folate-linked lipids uploading photo-sensitizer, the capsules encapsulating chemotherapeutic drugs can be used as multidrug carriers for selectively combined cancer treatment. *In-vitro* cytotoxicity tests showed that the combination of chemotherapy and PDT were much more effective than chemotherapy or PDT alone. The microsystem designed might have a promising way to develop co-delivery carriers for combined therapy with high efficiency. A reactive template method was used to fabricate alginate-based hydrogel microcapsules. The uniform and well-dispersed hydrogel capsules have a higher drug loading capacity. Once they are coated with a folate linked lipid mixture on the surface, the capsules possess higher cellular uptake efficiency by the molecule recognition between folate and the folate-receptor overexpressed by the cancer cells. Moreover, in this bioconjugate the lipid could remarkably reduce the release rate of hydrophilic doxorubicin from the hydrogel microcapsules and encapsulate the hydrophobic photosensitizer hypocrellin B. The biointerfaced capsules could be used as a drug carrier for combined treatment against cancer cell proliferation and it has much more effective than chemotherapy or photodynamic therapy alone [17].

In another study novel controlled release system was developed which is triggered by mechanical stimuli. In this technology, novel dosing strategy enabling on demand administration of medicines through mechanical stimuli; which is intentionally created by patient them self. Ondansetron (ODN), an anti-emetic drug released from hydrogel composed of β-cyclodextrin (β -CyD) derivative and alginate (AL) can be controlled by mild mechanical compressions that mimic operation by a patient's hand. ODN is released in response to mechanical compressions by changing the inclusion ability of CyD moieties, which may be conformed, distorted, and/or suppressed stabilization of the inclusion complex when an external stress is applied. It is revealed that the release can be induced even by the slight conformational restriction for β-CyD due to the mechanical stimulus. This controlled release technology provides a novel dosing strategy enabling on demand administration of medicines through a mechanical stimulus generated intentionally by the patient. The polymeric material described here could provide an implantable delivery system in the gel form that enables the release of drugs simply by massage the gel at an appropriate accessible point on the patient's body [18].

## 3.5. Alginate Hydrogel: Drug Delivery Applications

A novel microparticulate drug delivery system which contains alginate hydrogel core, encapsulated by a biodegradable hydrophobic polymeric shell. These micro-particles were fabricated through concurrent emulsion solvent evaporation and ionotropic gelation processes. The incorporation of alginate within PLGA or PLLA was shown to increase the encapsulation efficiency when metoclopramide HCl (MCA), a model hydrophilic drug, was loaded with the particles and compared to PLGA and PLLA microparticles fabricated without alginate. The shell formed was able to serve as a physical barrier between the MCA-loaded hydrogel core and the PBS medium during the release studies. Thus, these gel-core hydrophobic shell microparticles would allow the improved loading and release of water soluble drugs and potentially for protein loading. Incorporation of alginate within PLGA or PLLA was shown to increase the encapsulation efficiency of a model hydrophilic drug metoclopramide HCl (MCA). Metoclopramide hydrochloride (MCA), a model hydrophilic drug, was used and the release of this drug was compared between this core shell particulate system against a pure system of calcium alginate (CaAlg) beads. The research findings showed the improved drug loading and that the shell served as a membrane in controlling the release of water soluble drugs [19].

A Multifunctional implantable system was developed and it can capable of biosensing, drug delivery and magnetic resonance imaging (MRI) for continuous monitoring, controlled anti-inflammatory drug delivery and imaging, respectively [20]. In this method a glucose biosensor used as biosensor component, diclofenac sodium (Diclo) used as an anti-inflammatory agent and magnetic nanoparticles (MNP) were used as an MRI contrast agent. MNP were synthesized by the co-precipitation technique and particle size found to be 5-15 nm which is loaded with the sensor and drug components into alginate microspheres and the final system after MNP loaded inside alginate microspheres were found to be 10–60 μm. Biosensing studies indicated an excellent glucose response curve, with a regression coefficient of 0.974. *In-vitro* Diclo release shows that MNP loading in alginate microspheres increases the burst release percentage by 11–12% in both 60 and 10 μm particles. MRI

showed significant contrast for both sizes. The particles showed an excellent biocompatibility (>80%) for all combinations of formulations. The system shows a great potential for biosensing with concurrent drug delivery and visualization for biomedical applications.

Hydrophobically modified biomineralized polysaccharide alginate membrane was developed with smart drug release property using sodium palmitate as the hydrophobic component [21]. Indomethacin release profiles of the modified alginate membrane were found to be pH and thermo-responsive. The drug release of modified alginate membrane was around 60% within 12 h, while that of the alginate membrane was higher than 90%. These results indicate that the hydrophobic and biomineralized polysaccharide components can hinder the permeation of the encapsulated drug and reduce the drug release effectively. The resulting membrane can be used as "smart" materials for sustained dual-responsive drug delivery. PNIPAAm and sodium palmitate were employed as a thermal-responsive and hydrophobic components, respectively. Sodium palmitate is a non-toxic fatty acid, sodium salt with an appropriate alkyl chain length, which can effectively inhibit water penetrating into the beads and decrease the water uptake. Biomineralized component ($CaHPO_4$) formed between $Ca^{2+}$ and $HPO_4^{2-}$, the polyelectrolyte formed between positively charged chitosan and negatively charged alginate exist in the resulting membranes. The diffusion-controlled deposition of inorganic minerals and hydrophobic component within porous organic polymeric matrices could prevent the permeation of the encapsulated drug and reduce the drug release effectively. The equilibrium swelling behavior of the modified membranes as well as their controlled delivery performance was investigated as a function of pH and temperature.

Modified alginate for sustained drug delivery was developed by using Chemical a crosslinking technique between AG-G5 hybrid nanogel of alginate (AG) and G5.0 poly (amidoamine) (PAMAM) dendrimer was prepared via carbodiimide chemistry [22]. Anticancer drug epirubicin (EPI) loaded into AG-G5 nanogels via simple physical entrapment process to attain effective and sustained delivery of chemotherapeutic agents. In this method 1-ethyl-3-(3- dimethylamino propyl) carbodiiamide hydrochloride (EDC), was used to activate the carboxylate groups of alginate to covalently interact with PAMAM dendrimer amine groups. EDC, a zero length crosslinker used to create permanent irreversible amide bond between alginate and PAMAM moieties. Finally, the remaining carboxylate groups were crosslinked using calcium chloride ($CaCl_2$). Covalent and ionic interactions in alginate-dendrimer network provide structural stability with high drug entrapment efficiencies. In this method epirubicin (EPI), a model drug used for this study and the anticancer efficacy of EPI ⊂AG-G5 nanogels in human breast cancer (MCF-7) cells was studied. By taking advantage of inherent red fluorescence of EPI, we could track the intracellular distribution of EPI therein. This can be useful in the fluorescence based evaluation of cancer progression and therapy. Although, AG-G5 nanogels can perform as suitable platforms for enhanced drug delivery to cancer cells.

In another study pectinate/alginate microspheres (PAMs) for encapsulating cisplatin were successfully prepared by electrospraying and then coated with Eudragit S100 using a polyelectrolyte multilayer coating technique [23]. *In-vitro* release studies indicated that Eudragit S100-coated PAMs showed markedly reduced drug release in simulated gastric conditions compared to the non-coated PAMs. Hence, Eudragit S100-coated PAMs have the potential to serve as a colonic drug delivery system. The release of cisplatin from the Eudragit S100-coated PAMs was more sustained in simulated gastric fluid than in simulated intestinal

fluid due to the increased solubility of the coating polymer in media with pH 7.0. Drug release from the Eudragit S100-coated PAMs was best described by the Higuchi's square root model and that Eudragit S100-coated PAMs can be a potential carrier for delivery of cisplatin in the colon region.

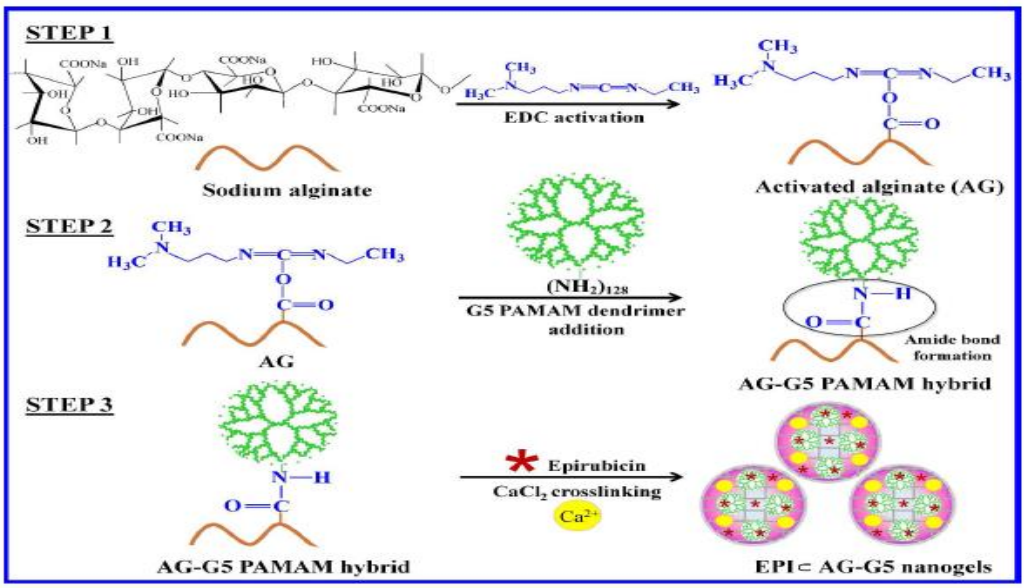


Figure 4. Stepwise representation of the synthesis scheme for EPI⊂AG-G5 nanogels (Reprinted with permission from [22] Copyright © 2016, American Chemical Society).

Biomineralized hydrophobically modified alginate membranes were developed and characterization using SEM and FT-IR revealed that the prepared membranes are covered by a biomineralized polysaccharide layer [24]. The swelling ratio decreased with the introduction of sodium palmitate (SP) into the biomineralized polysaccharide composition. Indomethacin release from the biomineralized hydrophobically modified membranes were found to be around 70% within 720 min, while 100% release is obtained from the nonmodified membranes. A series of biomineralized hydrophobically modified alginate membranes with sustained drug release properties was prepared in one-step method. The results demonstrated that the interaction of the biomineralized polysaccharide composition and the hydrophobic chain could prevent the permeation of the encapsulated drug and endow the hydrophobically modified alginate membranes with sustained release properties.

Hydrogel based delivery systems were developed for control release of drug in mucosal surface. Terbutaline sulfate and bovine serum albumin (BSA)-loaded alginate–poloxamer micro particles were prepared by a w/o-emulsion- and external gelation method. *In vitro* drug release were performed and the result reveals that the drug-release patterns could effectively be adjusted by varying the ‘‘alginate: poloxamer" blend ratio. In addition, the particle size, morphology, calcium and chloride content as well as alginate-release rates could be altered. Erosion was the predominant release mechanism for BSA. The novel hydrogel-based microparticles offering mild conditions for incorporated drugs (e.g., proteins) provide an interesting potential as controlled delivery systems for mucosal surfaces. In addition, the

poloxamer 407 might fill the pores of the alginate gel and act as diffusion barriers for the entrapped drug as well as for the dissolution medium, thereby slowing down the exchange of calcium ions, and consequently the calcium alginate gel degradation [25].

## 4. DEXTRAN

Dextran is a complex branched glucan (polysaccharide made of many glucose molecules) composed of chains of varying lengths (from 3 to 2000 kilodaltons). Chemical structure of dextan was depicted in Figure 5. Dextran mainly used as an antithrombotic antiplatelet agent to reduce blood viscosity and also act as a volume expander in hypovolemia [26].

### 4.1. Dextran Conjugates for Drug Delivery

Dextran conjugates have excellent bioadhesive properties. Prodrugs of dextran are especially useful in colon targeted drug delivery. Liver targeted delivery is also reported for dextran conjugates. Dextran based micelles are useful carriers for anticancer drugs. Dextran coated nanocarriers have long circulating times due to prevention of particles being opsonized. Better solubilization of poorly soluble drugs may be achieved by their conjugation to dextran. Dextran conjugation with cationic polymers enhances the serum stability and reduces their toxicity of those cationic polymers [27]. Macromolecular drug carrier systems have been developed to enhance the selectivity of cytotoxic drugs by coupling them with carriers to enhance the affinity towards the target tissue.

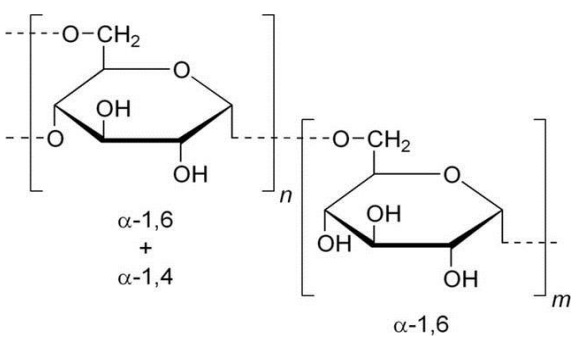


Figure 5. Chemical structure of dextran.

### 4.2. Dextran as Drug Carrier

Advantages of dextran as drug carriers, the main properties are [27]

I. Polymeric chemical structure with repetitive monomers.
II. Highly water solubility.
III. High stability to acidic or alkaline conditions due to stable glucosidic bonds that are not hydrolyzed easily except under extreme pH ranges.

IV. The possibility of derivatization on numerous reactive hydroxyl groups present in its structure.
V. Availability of different molecular weights.
VI. Inert nature due to low toxicity and pharmacological activity.
VII. Protection of conjugated drugs from biodegradation.
VIII. An apparent passive targeting of the soluble macromolecules to solid tumors due to EPR effect.

## 4.3. Modified Dextran

Mucoadhesive NP drug carriers have attracted substantial interest as a potential treatment for anterior eye diseases. In this method NPs composed of PLA-Dex surface functionalized with a mucoadhesive ligand and PBA were developed as drug carriers with particle sizes ranging from 25-28 nm. Using Cyclosporine A as a model drug, NPs encapsulated up to 13.7%w/w, *in -vitro* release study at a clinically relevant dose exhibited sustained release up to 5 days. Fine tuning of the PBA density on the NP surface; maximize the mucin-NP interaction without compromising the particle stability. This block copolymer conjugate may be useful to improve the bioavailability of topical formulations. The surface of the NP formed from a linear block copolymer PLA-Dex was modified with PBA to form a mucoadhesive NP for topical ocular drug delivery application. Moreover, *in-vitro* mucin-NP interaction was facilitated when the NPs were functionalized with PBA molecules, which is difficult to achieve using PEG-based systems. Since PBA functionalization also causes dextran to be more hydrophobic, it is ideal to adjust the amount of PBA to achieve optimal mucin - NP interaction without compromising the colloidal stability of the NPs. The current report involving various *in-vitro* studies provides promising results for the potential use of PLA-Dex PBA NPs to improve the bioavailability of ocular drugs intended to target the anterior segment of the eye [28].

## 4.4. Dextran as Stimuli-Responsive Drug Carriers

Stimuli-responsive drug carriers have great potential to deliver bioactive materials or drug on demand to a specific location within the human body. External or physiological stimuli, such as light, temperature, ultrasound, magnetic force, enzyme, pH, reductive or oxidative stress can be used for triggering the drug release. Among the various stimuli, pH has been considered as one of the most commonly used responsive drug delivery systems. Compared to the neutral pH in most human tissues, acidic environments are found within the cell in endosomes or lysosomes or in tumor microenvironments. Acid-responsive drug carriers can precisely release their cargo in the acidic microenvironments of tumors or in the endosomal or lysosomal compartments within a cell.

In another study acetylated dextran used as an acid-responsive biodegradable polymer for immunotherapy [29]. Water-insoluble acetylated dextran was prepared by modifying a water-soluble dextran with acid-labile acetyl moieties. A novel stimuli responsive (acid responsive) drug delivery system which contains dextran (functionalized with vicinal diols) with

hydrophobic boronate esters. Doxorubicin, hydrophobic anticancer drug encapsulated into the particles. Hydrolysis of the boronate esters under mild acidic conditions recovers the hydrophilic hydroxyl groups of the dextran and disrupts the particles into water soluble fragments thereby leads to a pH-responsive release of the drug. The polymer spontaneously forms acid-responsive nanoparticles in water that undergo a fast hydrolysis and release of an incorporated anticancer drug, doxorubicin, at mild acidic conditions usually present in tumor microenvironments and lysosomes. A confocal fluorescence microscopy study reveals that 100% of the HeLa cells uptake doxorubicin-loaded B-Dex nanoparticles with a preferential accumulation of the nanoparticles in the cytoplasm [30].

## 4.5. Bioresponsive Drug Delivery System

Design and synthesis of bioresponsive nanocarriers are more challenging due to changes in local bioenvironment of the cell. Examples of bioresponsive drug delivery systems are based on metaloenzyme responsive gate opening, oligonucleotide responsive gate opening, glucose responsive drug delivery and other enzyme responsive drug delivery. In particular, glucose responsive drug delivery has great potential in diabetes and cancer treatment. Moreover, it is a very challenging issue due to changes in local bioenvironment. Magnetic Mesoporous Silica (MMS) based drug delivery nanocarrier system that can target specific cell and release drug via glucose-responsive gate [31]. In this method synthesized MMS is functionalized with phenylboronic acid and folate. After drug loading inside the pores of MMS, outside of the pores are closed by dextran via binding with phenylboronic acid. Dextran-gated pores are opened for drug release in the presence of glucose that competes binding with phenylboronic acid. Drugs such as tolbutamide and camptothecin are loaded into MMS to target beta cells and cancer cells, respectively. The drug release depends upon the bulk glucose concentration and produces the glucose concentration dependent cytotoxicity.

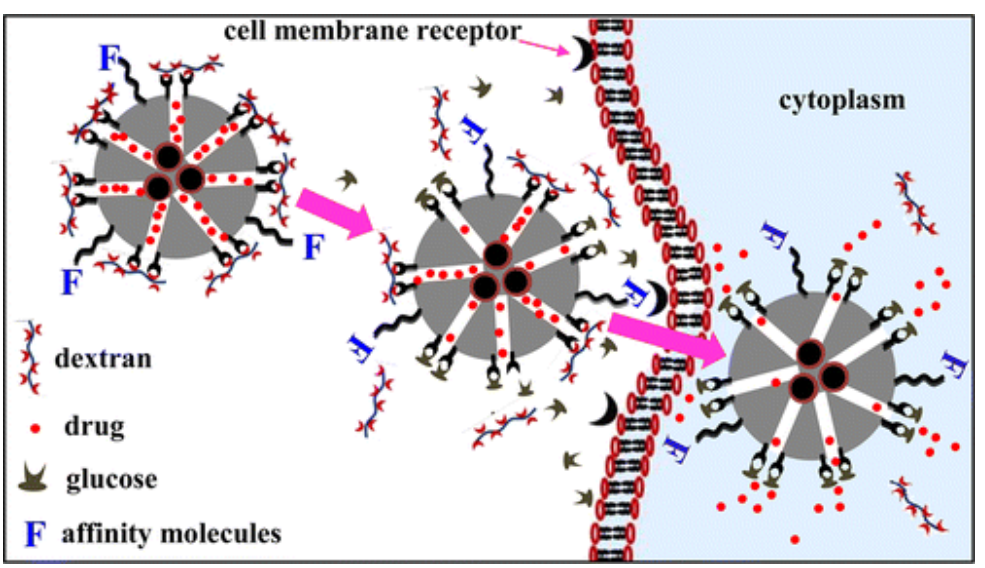


Figure 6. Dextran-Gated Multifunctional Mesoporous Silica Nanocarrier (Reprinted with permission from [31] Copyright © 2014, American Chemical Society).

In addition, a magnetic nanoparticle inside a mesopore can be used for magnetic manipulation and imaging-based tracking of nanocarrier. Compared to earlier approaches where glucose-responsive gates are prepared by protein or enzyme, here a gate is prepared by low cost and stable dextran molecule. Dextran-based gating has two additional advantages. It provides polyethylene glycol like functionalization on particle surface that minimizes nonspecific binding interaction with bio environment and specifically target the cells having glucose transporter. Folate functionalization of this nanocarrier targets cancer cells having folate receptors and offers glucose-responsive cellular delivery of cancer drug. This developed strategy can be used to treat diabetes/cancer with more efficient therapy

## 4.6. Dextran Based Nanoparticles

Nanoparticles (NPs) formulated using self-assembly of block copolymers has attracted significant attention as nano-scaled drug delivery system. The synthesis of NPs by self assembly process of linear amphiphilic block copolymer (Dex-*b*-PLA) using poly (*D*, *L*-lactide) and dextran. This nanoparticle (Dex-*b*-PLA) can self-assemble into core–shell structured NPs with size less than 40 nm. The size of NPs was controlled by varying the molecular weight of dextran and PLA. These NPs demonstrated efficient doxorubicin encapsulation, controlled drug release in *in-vitro* release study, hemocompatibility and enhanced blood circulation half-life in *in-vivo* studies. These NPs provide promising tools for developing a controlled drug delivery system for nanomedicine applications [32].

The non-covalent functionalization of graphene oxide (GO) with chitosan (CS) and dextran (Dex) was successfully developed via layer-by-layer self-assembly technique. The CS/Dex functionalized GO nanocomposites (GO-CS/Dex) exhibited a diameter of about 300 nm and a thickness of 60 nm. Anticancer drug doxorubicin hydrochloride (DOX) was loaded into the nanocomposites via p–p stacking and electrostatic attraction. DOX-loaded nanocomposites exhibited noticeable pH-sensitive DOX release behaviors with release acceleration in an acidic environment. The functionalization with CS and Dex not only strongly improved the dispersibility of both GO and DOX loaded GO nanosheets in physiological conditions, but also decreased the non-specific protein adsorption of GO nanosheets, which was beneficial for the biomedical applications. Additionally, it was observed that the GO-CS/Dex nanocomposites has able to uptake by MCF-7 cells and DOX loaded GO-CS/Dex nanocomposites had a strong cytotoxicity to the cancer cells. Overall, GO-CS/Dex could confirm to be a suitable candidate for anticancer drug delivery [33].

## 4.7. Modified Biopolymers in Disease Diagnosis

Magnetic MPs with higher magnetic moments and biocompatible surface coating that assure better colloidal stability, nontoxicity, biodegradability and labelling efficiency are highly desired. Biocompatible coating not only produces more hydrophilic nanostructures, but also develops diverse surface functional groups to inhibit aggregation, binding drug molecules and improve stability [34]. Surface modifications render good hydrophilicity and

stability to MNPs, but they may cause cytotoxicity when used beyond the threshold level [35].

Modified chitosan was prepared by using bovine serum albumin (BSA), chitosan (CS) and carboxy methyl cellulose (CMC). These biopolymers have many merits as drug carriers and easy chemical modification as they consist of a number of amino acids and carboxylic groups, which easily modify the surface of MNPs. Nontoxicity, hydrophilicity and cancer-specific capability of these biopolymers coated NFs can be used as a new biocompatible MR contrast agent for specific imaging of MCF-7 cells. Then the fabricated $NiFe_2O_4$ were immobilized with a layer of three different biopolymers and evaluated these coated particles as potential T2 contrast agents for MR imaging. The results demonstrated that the coated NFs showed excellent biocompatibility, higher T2 relaxivity (223 to 369 ± 3 $mM^{-1}$ $s^{-1}$) and specific capability of BSA, CS and CMC toward cancer cells. They concluded that BSA@NFs, CS@NFs and CMC@NFs can be used as new biocompatible nano MR imaging probes for targeting MCF-7 cancer cells without any further vectorization [36].

## 5. HYALURONIC ACID

Hyaluronic acid (HA) is a component of extracellular matrix (ECM) of all higher animals. This anionic linear polysaccharide is comprised of P-I A-linked D-glucuronic acid (P-I, 3) N-acetyl-D-glucosamine disaccharide units with a range of naturally occurring molecular sizes from 1-10,000 kDa (Figure 7). HA has unique physicochemical properties and distinctive biological functions [37]. HA is an attractive building block for new biocompatible and biodegradable polymers with applications in drug delivery, tissue engineering and visco supplementation. Chemical modification allows the physicochemical properties and *in-vivo* residence time of HA without affecting its biocompatibility and biodegradability [38].

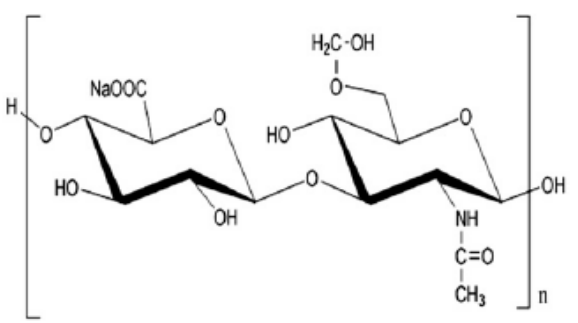


Figure 7. Chemical structure of HA.

### 5.1. Modified Hyaluronic Acid

Photochemically triggered cytosolic delivery system was developed for the delivery of anticancer drugs by combining tumor targetable (CD44 receptor mediated), pH responsive hyaluronic acid nanoparticles with light-induced endosomal escape. The DOX@PHANs is

composed of a photosensitizer PS and a pH-responsive moiety conjugated with acetylated hyaluronic acid copolymer allows controlled cytosolic drug release [39]. After cellular uptake via receptor-mediated endocytosis due to hyaluronic acid interaction with the CD44 receptor and DOX@PHANs disruption by DIP protonation in acidic endolysosomes, low-intensity laser irradiation stimulated the free PS to produce reactive singlet oxygen, which released DOX into the cytosol of cancer cells (Figure 8). *In-vitro* cell and *in- vivo* animal studies demonstrated that the treatment of DOX@PHANs with laser irradiation has powerful therapeutic efficacy regardless of low laser dose. The study result concludes that the photochemical triggered cytosolic drug delivery of therapeutic agents for light-induced cancer therapy has many advantages compared to other forms of cancer therapy.

## 5.2. Functionalized HA Derivatives /Modifications in Hyaluronic Acid

Carboxyl group has a great impact also in the recognition sites for HA receptors and hyaluronidase, therefore the chemical modification of this moiety would change its biological behaviors in the body. Functionalized HA derivatives can be used as drug delivery systems in various forms (hydrogels, gels, nanoparticles) due to its physicochemical and biological properties.

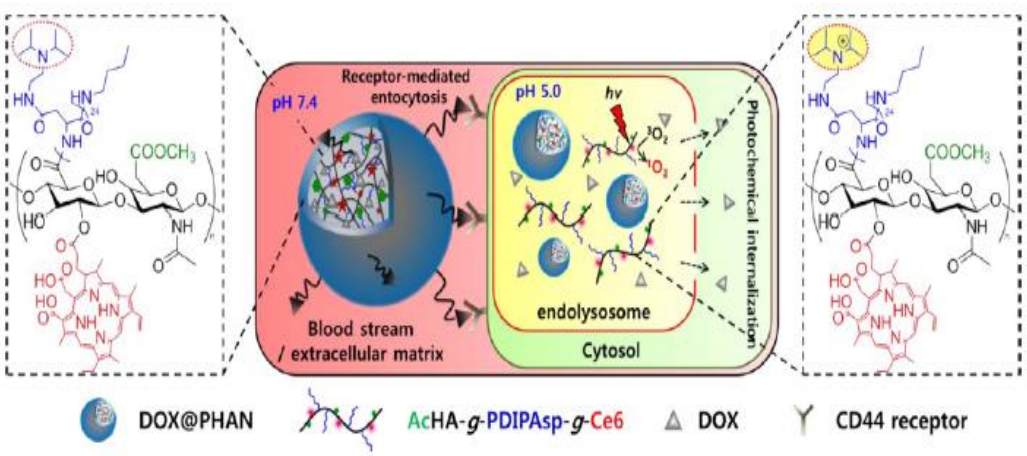


Figure 8. First, DOX@PHANs are administered systemically through intravenous injection. In the tumor site, DOX@PHANs are received into cells via CD44 receptor-mediated endocytosis and accumulate in endolysosomes. DOX is then released from DOX@PHANs due to the protonation of diisopropylethylamine (DIP) groups, which causes a hydrophobic-to-hydrophilic transition in the core. Upon laser irradiation, Ce6 generates singlet oxygen that induces the disruption of endolysosomal membranes and cytosolic release of DOX (Reprinted from [39] Copyright © 2014, American Chemical Society).

HA based gels were formulated by using the acrylic acid copolymerization technique. The model drug Pilocarpine, an ophthalmic therapeutic agent was loaded efficiently by embedding into the gel network. *In- vitro* drug loading and release tests established that the presence of interconnected circular pores within the matrix is the key factor that governs the ability of the gels to load and release pilocarpine hydrochloride. These properties correlated

with its biocompatibility and confirm its suitability as drug delivery carriers in ocular cell therapy [40].

Hyaluronyl reduced graphene oxide (rGO) nanosheets used as a tumor targeting delivery system for anticancer agents. Hyaluronyl modified rGO nanosheets were prepared by synthesizing cholesteryl hyaluronic acid (CHA) and using it to coat rGO nanosheets, yielding CHA-rGO. Compared with rGO, CHA-rGO nanosheets showed increased colloidal stability under physiological conditions and improved *in- vivo* safety, with a survival rate of 100% after intravenous administration in mice. The doxorubicin (Dox) loading capacity of CHA-rGO was 4-fold greater than that of rGO. Uptake of Dox by CD44-overexpressing KB cells was higher for CHA-rGO than for rGO, and was decreased in the presence of hyaluronic acid through competition for CD44 receptor binding. After intravenous administration in tumor-bearing mice, CHA-rGO/Dox showed higher tumor accumulation than rGO/Dox. The *in-vivo* antitumor efficacy of Dox delivered by CHA-rGO was significantly increased compared with free Dox or rGO/Dox. In CHA-rGO/Dox-treated mice, tumor weights were reduced. They concluded that CHA-rGO nanosheets possess greater stability, safety, drug loading capacity and CD44-mediated delivery of Dox than rGO nanosheets to produce the enhanced anticancer effects [41].

## 5.3. Functional Modifications in Hyaluronic Acid

HACE (hyaluronic acid–ceramide), as an amphiphilic HA oligomer, has been used in tumor targeted delivery of anticancer drugs and *in- vivo* cancer imaging using near-infrared fluorescence (NIRF) and MR techniques. An amphiphilic hyaluronic acid derivative (hyaluronic acid–ceramide; HACE) - coated nanohybrid liposomes were prepared for targeted delivery of anticancer drug and MR imaging of cancer [42]. Amphiphilic HACE was embedded into the lipid bilayer of the liposomal formulation and hybrid nanoliposomes were formed. This nanohybrid liposome can exhibit the advantages of both components; the tumor targetability of HACE and the *in- vivo* stability of the liposome. Specifically, the hydrophobic residue (CE) may be anchored in the hydrophobic lipid bilayer and the hydrophilic chain (HA) attached to the outer surface of the liposome. It is known that HA can bind to the CD44 receptor overexpressed in many types of cancer cells; thus it can be used as a tumor-targeting moiety. Both modulation of physicochemical properties (i.e., b200-nm particle size) of nanocarriers and HA–CD44 receptor interaction can provide passive, mainly due to enhanced permeability and retention (EPR) effects, and active tumor targetability in cancer therapy.

Reversibly-cross-linked polymeric DOX-loaded nanoparticles have been developed through the conjugation of lysine, HA (35 kDa) with lipoic acid, a natural antioxidant produced by the human body. The lipoic ring is prone to ring-opening polymerization, forming a linear polydisulfide in the presence of a catalytic amount of dithiothreitol under aqueous conditions, rapid drug release occurs in the presence of 10 mM GSH. This study results concluded that the prepared multifunctional nanoparticles possess complete biocompatibility, biodegradability, the ability to uncross-link and become destabilized under cytoplasmic reductive conditions, resulting in an enhanced antitumor effect in CD44+ drug-resistant human breast MCF-7 tumor xenografts in nude mice [43].

Gagomers (glycosaminoglycan clusters of particles; GAGs) are lipid-based non-liposome forming nanostructures that self-assemble into nanoparticle like clusters, which are then

covalently coated with HA by carbodiimide activation of carboxyl groups. HA is the main component of the GAGs surface; their inner structure can contain large quantities of nucleic acids and small (hydrophilic or hydrophobic) molecules. The HA coating naturally targets GAGs to cells expressing specific receptors and gives these particles stealth properties without triggering an immune response. PTX-loaded GAGs with 500-1200 kDa HA were prepared, their structure and physicochemical properties were characterized. The cytotoxicity of PTX-GAGs were evaluated *in vitro* in the mouse colorectal carcinoma cell line CT-26, expressing CD44; it was demonstrated to be the same as that of free PTX. After *in vivo* administration in CT-26 colon adenocarcinoma bearing mice, pharmacokinetics, biodistribution and therapeutic properties of PTX-GAGs were evaluated. The results showed a good safety profile, marked tumor accumulation and antitumor potency superior than that of the FDA-approved PTX formulations (Taxol® and Abraxane®) [44].

Protein cage based pH-responsive delivery system for controlled release of apoferritin was developed based on apoferritin as delivery vehicles to encapsulate the anticancer drug daunomycin (DN) and alleviate the side effect. The hydrophobic drug daunomycin DN was encapsulated into the interior of apoferritin by the hydrophobic channels of the cage with swelling at slight acidic pH and electrostatic adsorption. The negatively charged poly-L-aspartic acid (PLAA) was further introduced into the apoferritin to absorb the positively charged DN. The mixture of PLAA and DN easily flew into the apoferritin cage and was stable in the physiological fluids. PLAA protected the leakage of DN and encapsulated a sufficient amount of drug molecules in the cage. Further, specifically target the tumor cells, the surface of apoferritin was modified with hyaluronic acid (HA) which can easily bind to the HA-receptor CD44. Human embryonic lung MRC-5 cells and lung cancer A549 cells were used to observe the specific binding of HA and morphological changes *in vitro* and examine the antitumor activity. This unique protein based drug delivery platform using the apoferritin cage shows great potential in the therapeutic administration of the anticancer agents [45].

### 5.4. Smart Nanocarrier Based on PEGylated Hyaluronic Acid for Cancer Therapy

Tumor targetability and site-specific drug release of therapeutic nanoparticles are the key factors for effective cancer therapy. Poly (ethylene glycol) (PEG) - conjugated hyaluronic acid nanoparticles (P-HA-NPs) as a carrier for anticancer drugs including doxorubicin and camptothecin (CPT). P-HA-NPs were internalized into cancer cells (SCC7 and MDAMB-231) via receptor-mediated endocytosis, but were rarely taken up by normal fibroblasts (NIH-3T3). During *in- vitro* drug release tests, P-HA-NPs rapidly release drugs when incubated with cancer cells, extracts of tumor tissues, or the enzyme Hyal-1, which is abundant in the intracellular compartments of cancer cells. CPT-loaded P-HA-NPs (CPT-P-HA-NPs) showed dose-dependent cytotoxicity to cancer cells (MDA-MB-231, SCC7, and HCT 116) and significantly lower cytotoxicity against normal fibroblasts (NIH-3T3) than free CPT. Unexpectedly, high concentrations of CPT-P-HANPs demonstrated greater cytotoxicity to cancer cells than free CPT. An *in-vivo* biodistribution study indicated that P-HA-NPs selectively accumulated into tumor sites after systemic administration into tumor-bearing

mice, primarily due to prolonged circulation in the blood and binding to a receptor (CD44) that was overexpressed in the cancer cells. In addition, when CPT-P-HA-NPs were systemically administrated into tumor bearing mice, we saw no significant increases in tumor size for at least 35 days, implying high antitumor activity. Overall, P-HA-NPs showed promising potential carrier for hydrophobic anticancer drug for cancer therapy [46].

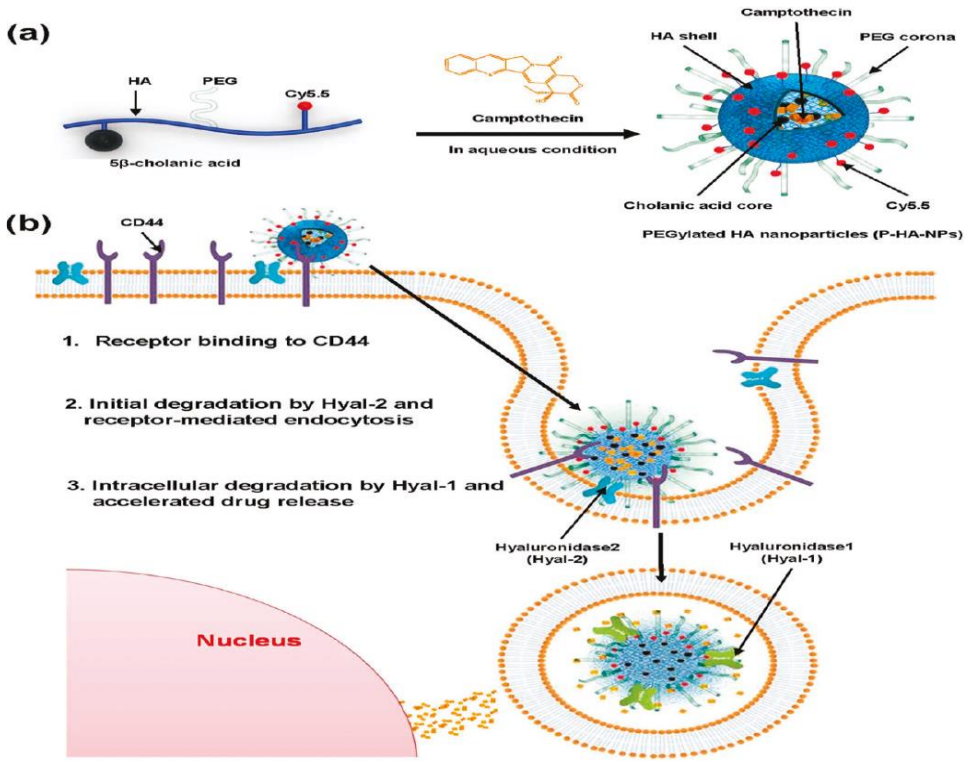


Figure 9. Schematic illustrations of (a) the formation of drug-loaded P-HA-NPs and (b) hypothetical cellular uptake pathways and subcellular drug release behaviors (Reprinted from [46] Copyright © 2011, American Chemical Society).

A novel nanohybrid of hyaluronic acid (HA) decorated graphene oxide (GO) based targeting and pH-responsive drug delivery system for controlling the release of anticancer drug doxorubicin (DOX) for cancer therapy. In this method, DOX was first loaded onto GO nanocarriers via π−π stacking and hydrogen-bonding interactions, and then it was decorated with HA to produce HA−GO−DOX nanohybrids via H-bonding interactions. In this strategy, HA served as both a targeting moiety and a hydrophilic group, making them as prepared nanohybrids targeting, stable and disperse. A high loading efficiency (42.9%) of DOX on nanohybrids was also obtained and cumulative DOX release from HA− GO−DOX was faster in pH 5.3 phosphate buffered saline solution than that in pH 7.4, providing the basis for pH-response DOX release in the slightly acidic environment of tumor cells, while the much slower DOX release from HA−GO−DOX than DOX showed the sustained drug release capability of the nanohybrids. Fluorescent images of cellular uptake and cell viability analysis studies illustrated that these HA−GO−DOX nanohybrids significantly enhanced DOX accumulation in HA-targeted HepG2 cancer cells compared to that of the HA-nontargeted

RBMEC cells and subsequently induced selective cytotoxicity to HepG2 cells. *In vivo* antitumor efficiency of HA−GO−DOX nanohybrids showed obviously enhanced tumor inhibition rate for H22 hepatic cancer cell-bearing mice compared with free DOX and the GO−DOX formulation. Hence the results revealed that the HA−GO−DOX nanohybrids have potential clinical applications for anticancer drug delivery [47].

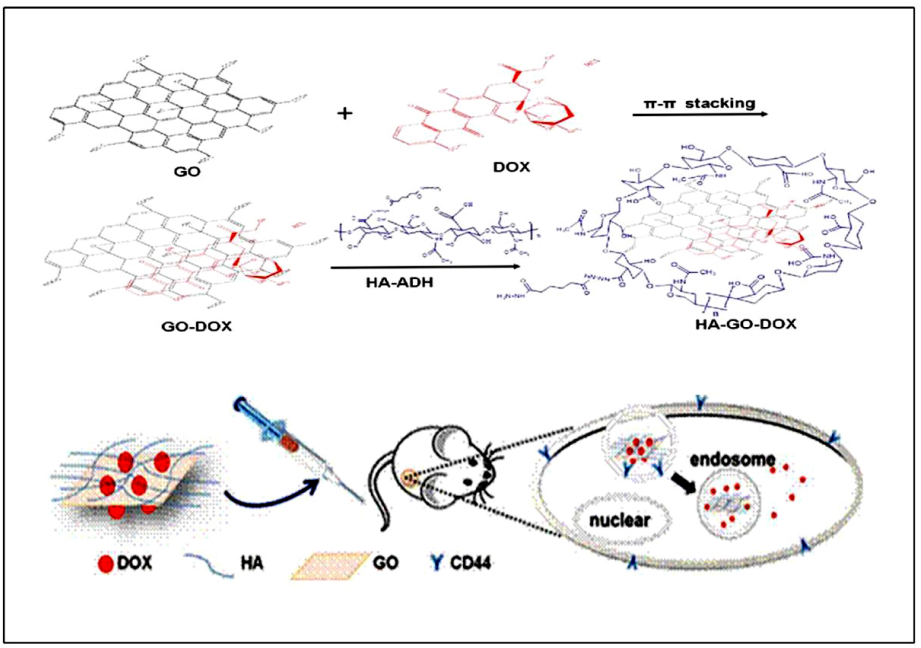


Figure 10. Schematic Illustration of the Preparation of HA−GO−DOX Nanohybrid and delivery of drug molecules to cancer cells (Reprinted with permission from [47] Copyright © 2014, American Chemical Society).

## 6. HEPARIN

Heparin, a negatively charged polysaccharide that used as an anticoagulant, is often applied for the preparation of self-assembled nanoparticles. For heparin functionalized polymeric nanoparticles, heparin has been used as coating material and also as a building block of the nanoparticle. Chemical structure of heparin was shown in Figure 11. As heparin protein interactions and antitumor effects continue to be of interest, heparin based/modified polymeric nanoparticles have been widely studied as therapeutic delivery vehicles in the field of tissue engineering and cancer therapy. Heparin plays an important role in many biological processes, via its interaction with various proteins, hydrogels and nanoparticles comprising heparin exhibit attractive properties such as anticoagulant activity, growth factor binding, as well as anti-angiogenic and apoptotic effects, making them as great candidates for emerging drug delivery applications.

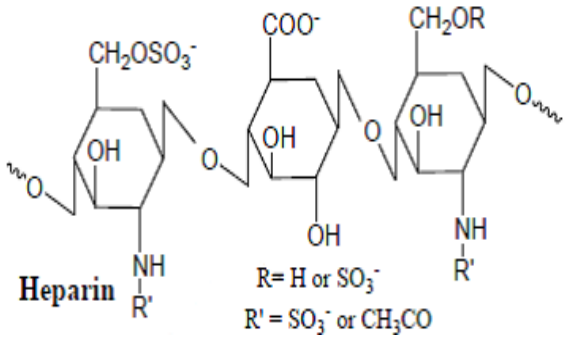


Figure 11. Chemical structure of heparin.

## 6.1. Modified Heparin

Immobilised chitosan/heparin system was developed for the delivery of sorafenib (SRF) for gastric cancers by the SRF NP was nanosized with spherical shape and exists as amorphous form. The SRF NP exhibited a sustained release of drug at pH 7.4 and enhanced drug release at pH 5.5. Flow cytometer analysis showed that cellular uptake of NP increased two-fold after 4h of incubation compared to 1h incubation. The SRF NP showed a superior anticancer effect compared to that of free SRF in BGC-823 cancer cells. SRF NP induced a remarkable apoptosis of cancer cells consistent with the cytotoxicity assay. Approximately, ~50% of cell fractions were observed in early apoptosis phase with ~15% of cells in the late apoptosis stage. Importantly, SRF NP showed a superior anticancer effect in xenograft tumor model making it a promising delivery vehicle in the treatment of gastric cancers [48].

## 6.2. Heparin Based Binary Drug Delivery Systems

Dendronized heparin-doxorubicin (heparine-DOX) conjugates used as pH-sensitive drug delivery vehicle by combination of the features of dendrimer and heparin. Dendronized heparin and its nanoparticles with drug demonstrated no significant toxicity to healthy organs of both tumor bearing and healthy mice, which was confirmed by histological analysis compared with free drug DOX. In this study, we described the preparation and characterization of dendronized heparin DOX conjugate as pH-stimuli and nanoscale drug delivery system for breast tumor therapy. Its antitumor efficacy and biosafety were assessed well. The heparin was dendronized with low generation dendron via click reaction; DOX was conjugated to the surface of dendron through a pH-sensitive hydrazone bond, resulting in compact nanoparticle via the self- assembly [49].

## 6.3. Modified Heparin in Combination Therapy

Use of single chemotherapy agents has shown some limitations in anti-tumor treatment, such as development of drug resistance, severe adverse reactions and limited regime for

therapeutic use. A combination of two or more therapeutic drugs is a feasible strategy to overcome these limitations. Co-delivery of doxorubicin and curcumin by core–shell nanoparticles (NPs) were performed by using core shell nanoparticle contains hydrophobic PLLA core loaded with curcumin (Cur) and hydrophilic heparin shell adsorbing doxorubicin (DOX). Studies on cellular uptake of DOX-Cur-NPs demonstrated that both drugs were effectively taken up by 4T1 tumor cells. Furthermore, DOX-Cur-NPs suppressed 4T1 tumor cells growth more efficiently than individual either DOX or Cur alone at the same concentrations, as measured by flow cytometry (FCM). The result reveals that intravenous injection of DOX-Cur-NPs efficiently inhibited growth of subcutaneous 4T1 breast carcinoma *in-vivo* and prolonged survival of the treated 4T1 breast carcinoma mice. Moreover, the pathological damage to the cardiac tissue in mice treated with DOX-Cur-NPs were significantly less severe than that of mice treated with free DOX. Thus, the study result concludes that DOX-Cur-NPs may have promising applications in breast carcinoma therapy [50].

## 6.4. Heparin Conjugated Nanoparticles for Drug Delivery

Heparin/$CaCO_3$/CaP hybrid nanoparticles were prepared by via co-precipitation method in aqueous solutions under very mild conditions, which does not involve any organic solvent and surfactant. The size of the hybrid nanoparticles can be controlled by adjusting the ion concentrations. The hybrid nanoparticles with heparin enriched surface layers exhibit a negative surface charge, which ensure the better colloidal stability in aqueous media. The antitumor drug DOX could be easily loaded in the heparin/$CaCO_3$/CaP nanoparticles and *in-vitro* release shows that the hybrid nanoparticles could effectively sustain the drug release. The *in-vitro* cytotoxicity evaluation indicates that the DOX loaded nanoparticles exhibit a strong cell inhibition effect. All these results suggest that the heparin/$CaCO_3$/CaP hybrid nanoparticles can be a potential anticancer drug delivery platform for tumor treatment [51].

The new polymeric micelle system for protein delivery by conjugation of heparin to block copolymer that consists of Tetronic and poly (e-caprolactone) (PCL). Amphiphilic multiblock Tetronic–PCL copolymer was synthesized by a ring-opening polymerization of e-caprolactone with Tetronic by using stannous octoate as a catalyst, and Tetronic–PCL–heparin conjugate was prepared by coupling heparin with Tetronic– PCL copolymer by using the EDC/NHS as coupling agents. The diameter of Tetronic–PCL micelle in number averaged scale was observed to be around 25 nm and its size after heparin coupling was increased to 224 nm due to the heparin chain on the hydrophilic shell of the micelle. Tetronic as poloxamer derivative is a surfactant which is thermosensitive and nonionic tetra-functional block copolymer with four PEO–PPO blocks. PCL as a well-known biodegradable polymer in the biomedical field has better biocompatibility and the biodegradability of PCL blocks can help the sustained release of the heparin and the heparin binding proteins. Especially, the introduction of heparin moiety to the Tetronic–PCL backbone can provide the potential for specific affinity with various heparin binding proteins during micelle formation. Therefore, Tetronic–PCL–heparin micelle could be attractive as an injectable PM for the delivery of many heparin binding proteins, including hydrophobic drugs [52].

Heparin has been used to coat nanoparticle surfaces and also as a building block of the nanoparticle for heparin functionalized polymeric nanoparticles. As heparin protein

interactions and antitumor effects continue to be of interest, heparin based/modified polymeric nanoparticles have been widely studied as therapeutic delivery vehicles in the field of tissue engineering and cancer therapy.

## CONCLUSION

This chapter summarizes the potential applications of the modified polysaccharide based biopolymers for biomedical and pharmaceutical applications especially in drug delivery, and disease diagnosis. Modified biopolymers have great utility in developing stimuli responsive drug delivery system, controlled and sustained release mechanism depends on the respective functional modification in biopolymers.

## ACKNOWLEDGMENTS

The authors wish to acknowledge the DST sponsored National Facility for Drug Development (VI-D&P/349/10-11/TDT/1), Nanomission program of the Department of Science and Technology (DST), Ministry of Science and Technology of India (DST/SR/NM/NS-19/2009) and Technical Education Quality Improvement Programme (TEQIP-PHASE II) for their support in this work.

## REFERENCES

[1] Ubaidulla, U., Khar, R.K., Ahmad, F.J. and Tripathi, P. (2009). Optimization of chitosan succinate and chitosan phthalate microspheres for oral delivery of insulin using response surface methodology. *Pharmaceutical Development and Technology* 14: 96-105.

[2] Grabovac, V. and Bernkop-Schnurch, A. (2007). Development and in vitro evaluation of surface modified poly (lactideco-glycolide) nanoparticles with chitosan-4-thiobutylamidine. *Drug Development and Industrial Pharmacy* 33: 767-774.

[3] Bigucci, F., Luppi, B. and Cerchiara, T. (2008). Chitosan/pectin polyelectrolyte complexes: selection of suitable preparative conditions for colon-specific delivery of vancomycin. *European Journal of Pharmaceutical Sciences* 35: 435-441.

[4] Weng, L., Romanov, A., Rooney, J. and Chen, W. (2008). Non-cytotoxic, in situ gelable hydrogels composed of N-carboxyethyl chitosan and oxidized dextran. *Biomaterials* 29: 3905-13.

[5] Kraulan, A.H., Guggi, D. and Bernkop-Schnurch. A. (2006). Thiolated chitosan microparticles: A vehicle for nasal peptide drug delivery. *International Journal of Pharmaceutics* 307: 270-277.

[6] Perioli, L., Ambrogi, V., Venezia, L., Pagano, C., Ricci, M. and Rossi, C. (2008). Chitosan and a modified chitosan as agents to improve performances of mucoadhesive vaginal gels. *Colloids and Surfaces B: Biointerfaces* 66: 141-145.

[7] Ercelen, S., Zhang, X., Duportail, G., Grandfils, C., Desbrieres, J. and Karaeva, S. (2006). Physicochemical properties of low molecular weight alkylated chitosans: A newclass of potential nonviral vectors for gene delivery. *Colloids and Surfaces B: Biointerfaces* 51: 140-148.

[8] Gover Antoniraj, M., Senthil Kumar, C., Linda Jeeva Kumari, H., Subramanian, N. and Ruckmani K. (2017). Atrial natriuretic peptide-conjugated chitosan-hydrazone-mPEG copolymer nanoparticles as pH-responsive carriers for intracellular delivery of prednisone. *Carbohydrate polymers* 157:1677-168.

[9] Gover Antoniraj, M., Senthil Kumar, C. and Ruckmani, K. (2015). Synthesis and characterization of poly (N-isopropylacrylamide)-g-carboxymethyl chitosan copolymer-based doxorubicin-loaded polymeric nanoparticles for thermoresponsive drug release. *Colloid and Polym Science doi:* 10.1007/s00396-015-3804-4.

[10] Chawan, M., Viravaidya-Pasuwat, K. and Nuttaporn, P. (2012). Preparation of Folate-Conjugated Pluronic F127/Chitosan Core-Shell Nanoparticles encapsulating Doxorubicin for Breast Cancer Treatment. *Journal of Nanomaterials* 2: 1-11.

[11] Lai, W.F. and Shum, H.C. (2015). Hypromellose-*graft*-chitosan and Its Polyelectrolyte Complex as Novel Systems for Sustained Drug Delivery. *ACS Applied Material & Interfaces* 7 (19): 10501–10510.

[12] Qi X., Qin, J., Fan, Y., Qin, X., Jiang, Y. and Wu, Z. (2016). Carboxymethyl Chitosan-Modified Polyamidoamine Dendrimer Enables Progressive Drug Targeting of Tumors via pH-Sensitive Charge Inversion. *Journal of Biomedical Nanotechnology*, 12: 667–67.

[13] Mahanta, A.K., Mittal, V., Singh, N., Dash, D., Malik, S. Mohan, K. *et al.*, (2015). Polyurethane-Grafted chitosan as New Biomaterials for controlled drug delivery. *Macromolecules*, 48 (8): 2654–2666.

[14] Goycoolea, F.M., Lollo, G., Remuñán-López, C., Quaglia, F. and Alonso. M.J. (2009). Chitosan-alginate Blended Nanoparticles as Carriers for the Transmucosal delivery of Macromolecules. *Biomacromolecules* 10 (7): 1736–1743.

[15] Sultzbaugh, K.J. and Speaker, T.J.J. (1996). A method to attach lecthins to the surface of spermine alginate microcapsules based on avidin biotin interaction. *Microencapsulation* 13: 363–375.

[16] Gonçalves, V.S.S., Gurikov, P., Poejo, J., Matias, A.A., Heinrich, S. and Duarte, C.M.M. *et al.*, (2016). Alginate-based hybrid aerogel microparticles for mucosal drug delivery. *European Journal of Pharmaceutics and Biopharmaceutics* 107: 160-170.

[17] Du, C., Zhao, J., Fei, J., Gao, L., Cui, W. and Yang, Y. *et al.*, (2013). Alginate-Based Microcapsules with a Molecule Recognition Linker and Photosensitizer for the Combined Cancer Treatment. *Chem Asian J* 8:736-742.

[18] Izawa, H., Kawakami, K., Sumita, M., Tateyama, Y., and Hillab, J.P. *et al.*, (2013). B-Cyclodextrin-crosslinked alginate gel for patient-controlled drug delivery systems: regulation of host–guest interactions with mechanical stimuli. *Journal of Materials Chemistry B* 1: 2155.

[19] Lim, M.P.A., Lee, W.L., Widjaja, E. and Loo, S.C.J. 2013. One-step fabrication of core–shell structured alginate–PLGA/PLLA microparticles as a novel drug delivery system for water soluble drugs. *The Royal Society of Chemistry Biomaterial science* 1: 486.

[20] Joshi, A., Solanki, S., Chaudhari, R., Bahadur, D., Aslam, M. and Srivastava, R. (2011). Multifunctional alginate microspheres for biosensing, drug delivery and magnetic resonance imaging. *Acta Biomaterialia* 7: 3955–3963.

[21] Shi, J., Zhang, Z., Qi, W. and Cao, S. (2012). Hydrophobically modified biomineralized polysaccharide alginate membrane for sustained smart drug delivery. *International Journal of Biological Macromolecules* 50: 747– 753.

[22] Matai, I. and Gopinath, P. (2016). Chemically Crosslinked Hybrid Nanogels of Alginate and PAMAM Dendrimers as Efficient Anticancer Drug Delivery Vehicles. *ACS Biomaterials Science & Engineering* 2: 213–223.

[23] Hsu, F.Y., Yu, D.S. and Huang, C.C. (2013). Development of pH-sensitive pectinate/alginate microspheres for colon drug delivery. *Journal of Material Science: Materials in Medicine* 24: 317–323.

[24] Sun, X., Shi, J., Zhang, Z. and Cao, S. (2011). Biomineralized hydrophobically modified alginate membrane for sustained drug delivery. *Journal of controlled release* 152: e 79-81.

[25] Moebus, K., Siepmann, J. and Bodmeier, R. (2009). Alginate–poloxamer microparticles for controlled drug delivery to mucosal tissue. *European Journal of Pharmaceutics and Biopharmaceutics* 72:42–53.

[26] Lewis, Sharon L. 2010. *Medical Surgical Nursing (8th ed.)*. ISBN 978-0323079150.

[27] Jaleh, V. (2012). Dextran conjugates in drug delivery. *Expert Opinion on Drug Delivery* 9(5): 509-523.

[28] Liu, S., Jones, L. and Gu, F.X. (2012). Development of Mucoadhesive Drug Delivery System Using Phenylboronic Acid Functionalized Poly(D,L-lactide)-*b*-Dextran Nanoparticles. *Macromol. Biosci* 12: 1622–1626.

[29] Bachelder, E.M., Beaudette, T.T., Broaders, K.E., Dashe, J. and Frechet, J.M.J. (2008). Acetal-derivatized dextran: an acid-responsive biodegradable material for therapeutic applications. *Journal of American Chemical Society* 130: 10494-5.

[30] Li, L., Bai, Z. and Levkin. P.A. (2013). Boronateedextran: An acid-responsive biodegradable polymer for drug delivery. *Biomaterials* 34: 8504-8510.

[31] Sinha, A., Chakraborty, A. and Jana. N.R. (2014). Dextran-Gated, Multifunctional Mesoporous Nanoparticle for Glucose-Responsive and Targeted Drug Delivery. *ACS Applied Material. Interfaces* 6: 22183-22191.

[32] Mohit, S.V., Liu, S., Chen, Y.Y., Meerasa, A. and Gu, F.X. (2012). Size-Tunable Nanoparticles Composed of Dextran-*b*-poly (*D*, *L*lactide) for Drug Delivery Applications. *Nano Res* 5(1): 49–61

[33] Xie, M., Lei, H., Zhang, Y., Xu, Y., Shen, S. and Ge, Y. et al., (2016). Non-covalent modification of graphene oxide nanocomposites with chitosan/dextran and its application in drug delivery. *RSC Advances* 6: 9328.

[34] Tong, S., Hou, S., Zheng, Z., Zhou, J. and Bao, G. (2010). Coating Optimization of Superparamagnetic Iron Oxide Nanoparticles for High T(2) relaxivity. *Nano Letters* 10 (11): 4607-461.

[35] Chu, X., Yu, J. and Hou, Y.L. (2015). Surface modification of magnetic nanoparticles in biomedicine. *Chinese Physics B.* 24 (1): 014704.

[36] Bano, S., Zafar, T., Akhtar, S., Buzdar, S.A., Waraich, M.M. and Afzal, M. (2016). Biopolymers coated superparamagnetic Nickle ferrites: Enhanced biocompatibility and

MR imaging probe for breast cancer. *Journal of Magnetism and Magnetic Materials* 417: 284-290.

[37] Laurent, T.C., Laurent, U.B.G. and Fraser, J.R.E. (1995). Functions of hyaluronan. *Annals of Rheumatic Diseases* 54: 429-432.

[38] Vercruysse, K.P. and Prestwich, G.D. (1998). Hyaluronate derivatives in drug delivery, *Critical. Reviews. Therapeutic. Carrier System* 15: 513-555.

[39] Lee, C.S. and Na, K. (2014). Photochemically Triggered Cytosolic Drug Delivery Using pH Responsive Hyaluronic Acid Nanoparticles for Light-Induced Cancer Therapy. *American Chemical Society Biomacromolecules* 15:4228-4238.

[40] Vasi, A.M., Popa, M.I., Butnaru, M., Dodi, G. and Verestiuc, L. (2014). Chemical functionalization of hyaluronic acid for drug delivery applications. *Materials Science and Engineering C* 38: 177–185.

[41] He, M., Zhao, Z., Yin, L., Tang, C. and Yin, C. (2009). Hyaluronic acid coated poly(butyl cyanoacrylate) nanoparticles as anticancer drug carriers. *International Journal of Pharmaceutics* 373(1–2): 165–173.

[42] Park, J.W., Jeon, O.C., Kim, S.K., Al-Hilal, T.A., Jin, J. and Moon, H.T. (2010). High antiangiogenic and low anticoagulant efficacy of orally active low molecular weight heparin derivatives. *Journal of Controlled Release* 148: 317-26.

[43] Zhong, Y., Zhang, J., Cheng, R., Deng, C., Meng, F. and Xie, F. (2015). Reversibly crosslinked hyaluronic acid nanoparticles for active targeting and intelligent delivery of doxorubicin to drug resistant CD44+ human breast tumor xenografts. *Journal of Controlled Release* 205: 144-154.

[44] Rivkin, I., Cohen, K., Koffler, J., Melikhov, D., Peer, D. and Margalit, R. (2010). Paclitaxel-clusters coated with hyaluronan as selective tumor-targeted nanovectors. *Biomaterials* 31:7106-7114.

[45] Luo, Y., Wang, X., Du, D. and Lin, Y. (2015). Hyaluronic acid-conjugated apoferritin nanocages for lung cancer targeted drug delivery. *Biomater Sci.* 3(10): 1386-94.

[46] Choi, K.Y., Yoon, H.Y., Kim, J.O., Bae, S.M., Park, R.W. and Kang, Y.M. *et al.*, (2011). Smart Nanocarrier Based on Pegylated Hyaluronic Acid for Cancer Therapy. *ACS Nano* 5(11): 8591–8599.

[47] Song, E., Han, W., Li, C., Cheng, D., Li, L. and Liu, L. *et al.*, (2014). Hyaluronic Acid-Decorated Graphene Oxide Nanohybrids as Nanocarriers for Targeted and pH-Responsive Anticancer Drug Delivery. *ACS Appl. Mater. Interfaces* 6: 11882−11890.

[48] Yang, Y.C., Cai, J., Yin, J. Zhang, J., Wang, K.L. and Zhang, Z.T. 2016). Heparin-Functionalized Pluronic Nanoparticles to Enhance the Antitumor Efficacy of Sorafenib in Gastric Cancers. *Carbohydrate Polymers* 136: 782–790.

[49] She, W.C., Li, N., Luo, K., Guo, C.H., Wang, G. and Geng, Y.Y. (2013). Dendronized heparin-doxorubicin conjugate based nanoparticle as pH-responsive drug delivery system for cancer therapy. *Biomaterials* 34: 2252-64.

[50] Guo, Q., Li, X., Yang, Y., Wei, J., Zhao, Q. and Luo, F. *et al.*, (2104). Enhanced 4T1 Breast Carcinoma Anticancer Activity by Co-Delivery of Doxorubicin and Curcumin with Core–Shell Drug-Carrier Based on Heparin Modified Poly (L-lactide) Grafted Polyethylenimine Cationic Nanoparticles. *Journal of Biomedical Nanotechnology* 10: 227–237.

[51] Liang, Y. and Kiick, K.L. (2014). Heparin-functionalized polymeric biomaterials in tissue engineering and drug delivery applications. *Acta Biomaterialia* 10(4): 1588–1600.

[52] Lee, J.S., Go, D.H., Bae, J.W., Jung, I.K., Lee, J.W. and Park, K.D. (2007). Synthesis and characterization of heparin conjugated Tetronic–PCL copolymer for protein drug delivery. *Current Applied Physics* 7S1: 49–52.

In: Advances in Polymers for Biomedical Applications ISBN: 978-1-53613-612-8
Editors: Deepak Pathania and Bhuvanesh Gupta 

*Chapter 6*

# VALIDATION OF NANO BIS-DEMETHOXY CURCUMIN ANALOG (NBDMCA) AS ADJUVANTS FOR MULTIDRUG RESISTANT INFECTIONS

***Charanya Sankar, Thiyagarajan Devasena**** ***and Arul Prakash Francis***
Centre for Nanoscience and Technology, Anna University, Chennai, India

## ABSTRACT

Multidrug resistance (MDR) is a phenomenon by which the targeted organisms resist antimicrobials that are aimed at eradicating the organism. The present study was aimed at evaluating the antibacterial activity of nano bis-demethoxy curcumin analog (NBDMCA). NBDMCA was prepared by solvent-assisted process and characterized using HRTEM, DLS, FTIR and NMR. The morphology and size of NBDMCA which was determined by HRTEM and DLS was found to be around 90 nm. Antibacterial activity of NBDMCA was determined by using Agar disc diffusion method and compared with various groups of antibiotics. Further, Bacteria-NBDMCA interaction was visualized using optical microscope. Also Resazurin assay was carried out to determine the Minimal Inhibitory concentration of the drug. Investigation of antimicrobial activity of the derivative demonstrated the ability to inhibit Gram-positive and Gram negative microorganisms with zone of inhibition ranging from 10 mm to 20 mm. In addition to this, the mobility of the BDMCA treated bacteria was found to be reduced when compared to the untreated bacteria. Applications of BDMCA based on these findings may lead to valuable discoveries in various fields such as medical devices and antimicrobial systems.

**Keywords**: multidrug resistance, antimicrobial, characterizations

* Corresponding Author Email: tdevasenabio@gmail.com.

# 1. INTRODUCTION

Since ancient times, plants have been used as source of medicines for the treatment of various diseases [1] and are inspiring researchers in the search of novel drugs. Plants have yielded clinical drugs, either as natural product molecules, or as synthetic modifications, particularly for chemotherapeutic treatment of cancer [2, 3]. The plant and its derivatives of chemical compounds especially flavonoids, alkaloids, saponins, polyphenols, terpenoids and tannins natural product have been widely studied for their potency as drugs [4-6].

The modern pharmaceutical industry was born from botanical medicine. In recent years, botanical therapeutics currently available as dietary supplements, drugs, or botanical drugs have been in high demand due to their less side effects [7]. A primary advantage of botanicals is their complex composition consisting of collections of related compounds having multiple activities that interact for a greater total activity.

## 1.1. Multidrug Resistance

Multiresistance (MDR) is a condition caused by disease causing microorganisms that shows resistance against distinct antimicrobials that are targeted at eradicating the organism. Also the terms extensively-drug resistant (XDR) and pandrug-resistant (PDR) have been introduced to recognize different degrees of MDR [8, 9]. To limit the development of antimicrobial resistance [10], it has been suggested to:

- Use the appropriate antimicrobial for an infection; e.g., no antibiotics for viral infections
- Identify the causative organism whenever possible
- Select an antimicrobial which targets the specific organism, rather than relying on a broad- spectrum antimicrobial
- Complete an appropriate duration of antimicrobial treatment (not too short and not too long)
- Use the correct dose for eradication; sub-therapeutic dosing is associated with resistance, as demonstrated in food animals.

Pathogenic bacteria are the major root of morbidity and mortality in humans. Even with the increased production of antibacterial by pharmaceutical companies, resistance to these drugs has increased [11]. The effectiveness of current drugs was limiting by the emergence of multi-drug resistant (MDR) bacteria, significantly causing treatment failure. This resistance may be due to the over-expression of MDR efflux pumps [12, 13]. Therefore, with increase in MDR, the need to develop new and innovative antimicrobial agents is also increased. Accordingly, the development of new antibacterial agents that could overcome the resistance problem has become the subject of an ongoing research.

## 1.2. Phytochemicals

The plants have been investigated as potential sources of new agents, this is because of the presence of bioactive compounds with therapeutic potential. Phytochemicals are naturally occurring substances found in plants. The term is generally used to refer to those chemicals that may have biological significance, for example carotenoids or flavonoids, but are not established as essential nutrients [14]. Diseases such as cancer, stroke or metabolic syndrome may be cured with by treating with different phytochemicals derived from dietary components. This in turn created considerable public and scientific interest in the use of phytochemicals [15].

Phytochemicals have been considered as possible drugs for millennia even without specific knowledge of their cellular actions or mechanisms. Interestingly, Salicin, active molecule with anti-inflammatory and pain-relieving potential, was originally extracted from the bark of the white willow tree. Previously, their leaves were prescribed by Hippogrates to abate fever and later it was synthetically produced as drug aspirin. Moreover, specific phytochemicals like dietary fibres with limited health claims were approved by the US Food and Drug Administration [16].

## 1.3. Turmeric

The dried ground rhizome of the perennial herb Curcuma longa Linn, have been used in Asian Medicine Since the Second Millennium B.C. Turmeric plants with the native of southwest India, requires temperatures between 20 and 30 °C in addition to a considerable amount of annual rainfall. Curcuma spp. contain turmerin, essential oils and curcuminoids. The utility of turmeric is being referred in Ayurveda, the ancient Hindu scripture. In addition to its aromatic, stimulant and colouring properties, Turmeric along with slaked lime mixture has been used topically for treating wounds, inflammation and tumours [17].

### *1.3.1. Curcuminoids*

Curcuminoids are polyphenols derived from turmeric (Curcuma longa). Curcumin is the principal component of curcuminoids and is now accepted for most of the therapeutic effects viz antiseptic, analgesic, anti-inflammatory, antioxidant and antimalarial. Curcumin was first isolated from turmeric in 1815 and it is about 2–5% of turmeric. Commercial curcumin contains approximately 77% diferuloylmethane, 18% demethoxycurcumin, and 5% bisdemethoxycurcumin. The structure of curcumin is shown in the Figure 1.

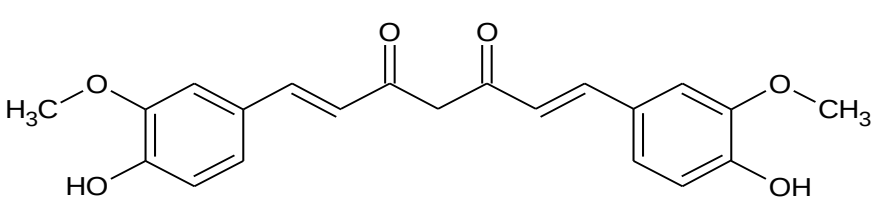


Figure 1. Structure of Curcumin.

Extensive research in the last decade revealed the potential of curcumin against numerous inflammatory diseases, including pancreatitis, arthritis, inflammatory bowel disease (IBD), colitis, gastrititis, allergy and fever [18, 19]. Previous studies on the anti-inflammatory activity of curcumin revealed that the anti-inflammatory response is mainly due to the down-regulation of the activity of cyclooxygenase-2 (COX-2), lipoxygenase, and inducible nitric oxide synthase (iNOS) enzymes. Moreover, down regulation of these enzymes inhibit the production of the inflammatory cytokines tumor necrosis factor-alpha (TNF-α), interleukin (IL) -1, -2, -6, -8, and -12, monocyte chemoattractant protein (MCP), and migration inhibitory protein [20-22]. NF-κB, a ubiquitous eukaryotic transcription factor that regulates the inflammation, cellular proliferation, transformation, and tumorigenesis. Previous reports showed that the nuclear factor kappa B (NF-κB) activation suppressed by curcumin was characterized by the down regulation of COX-2 and iNOS expression. However, the suppression of NF-κB activation and proinflammatory gene expression by curcumin was carried out by blocking phosphorylation of inhibitory factor I-kappa B kinase (IκB) [23,24]. Moreover, the down regulation of cyclooxygenase and lipoxygenase pathways up on curcumin treatment was reported to inhibit arachidonic acid metabolism and inflammation in mouse skin epidermis [25]. Curcumin inhibits inflammatory response through various mechanisms i) by activating transcription factors such as activating protein-1 (AP-1) and NF-κB, ii) by the down-regulation of intercellular signaling proteins, such as protein kinase C, may be another way in which curcumin inhibits cytokine production [26]. Curcuminoids inhibits wnt signaling by inhibiting WIF-1 promoter demethylation and inhibits DNA methyltransferase 1 (DNMT1), inducing apoptosis in non-small cell lung cancer (NSCLC) cells [27]. Curcuminoids also induces apoptosis in other in vitro cancer models through increases in reactive oxygen species (ROS) and increases in the expression of p53, p21, p16, and retinoblastoma (Rb) protein. This compound activates Sirt1 and AMPK signalling [28-30]. In addition, curcuminoids inhibits PDGF signaling in smooth muscle cells, preventing cell migration and proliferation [31]. Curcuminoids may also display potential benefit in the treatment of type 2 diabetes, as it acts as a non-competitive inhibitor of pancreatic α-amylase. Antioxidant property of curcumin was evaluated in chemically induced circulatory, hepatic, pulmonary and renal stress. The result of these studies confirmed the antioxidant property of curcumin, characterized by the fall in lipid peroxidation level followed by the elevation of antioxidant enzymes [32-35].

### *1.3.2. Bisdemethoxy Curcumin Analog*

Bisdemethoxy curcumin analog (BDMCA) chemically called bis-1,7-(2-hydroxyphenyl)-hepta-1,6-diene-3,5-dione (Figure 2) is the structural analog of curcumin. BDMCA exhibit anticancer and antioxidant activities similar to curcumin. In fact, curcumin and BDMCA were reported to be equipotent in preventing colon cancer, lung cancer and toxicity. Moreover, curcumin and BDMCA possess no side effects even after long term administration in laboratory animals [36]. Devasena et al., (2006) reported that the BDMCA treatment decreases the symptoms of DMH-induced colon cancer and normalizes the oxidative stress in the circulation by raising detoxifying and antioxidant enzymes resulting from the treatment of BDMCA. The study also showed that the effects were comparable with that of diferuloyl methane, the primary polyphenol in turmeric. The findings suggest that the methoxy group had no role in the anticarcinogenic/antioxidant properties, however, the phenolic group or the β-diketone moiety in the central 7-carbon chain may be responsible [37, 38].

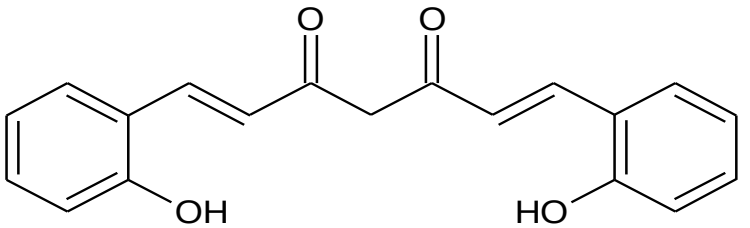


Figure 2. Structure of BDMCA.

In spite of these advantages, curcumin and BDMCA suffer from certain disadvantages. (i) Poor absorption from the gut, (ii) pharmacologically insignificant accumulation in tissue, (iii) poor solubility in physiological pH and (iv) poor bioavailability. Previous studies on rats and human suggested that, even at a dose of 2 g/kg body weight, curcumin is poorly absorbed, with a serum concentration of 1.35 ± 0.23 µg/ml and 0.006 ± 0.005 µg/ml respectively [39, 40]. Therefore, it is essential to enhance the dispersibility and solubility of curcuminoids in order to achieve a complete therapeutic effect at low dose. Moreover, intravenous route of BDMCA delivery needs a non-polar solvent, leads to rapid precipitation in blood vessels. This was supported by the previous studies on intravenous delivery of hydrophobic drugs. This can be circumvented by enhancing the dispersity and stability and also by decreasing the size of the drug by nanotization. Nano-drugs with small size and increased surface area might enhance the dissolution rate and saturation solubility of drug, which reduces the drug dose, cost and side effects [41]. An approach for enhancing the dissolution and dispersion of the particles is to increase the surface volume ratio. The best way to increase the surface area is to scale down the particle to nano size. Previously, Bhawana has converted bulk curcumin into curcumin nanoparticles and confirmed the enhancement of antimicrobial activity at nanoscale [42].

The present study was aimed at evaluating the antibacterial activity of nano bis-demethoxy curcumin analog (NBDMCA) as well as the interaction and aggregation of NBDMCA on bacteria.

## 2. EXPERIMENTAL SECTION

### 2.1. Materials

Acetyl acetone, salicyl aldehyde, boric acid, acetic acid and Resazurin orange were purchased from SRL Labs, Mumbai, India. Dimethyl sulfoxide (DMSO) and diethanolamine, were procured from S. D. Fine Chemicals, Mumbai, India. Nutrient agar was obtained from Hi Media Laboratories, Mumbai, India. Petri dish, Falcon tubes, glass slides, test tubes and coverslips were from Tarsons, Mumbai, India. All other chemicals employed were of analytical or equivalent grade. Candida albicans (NCIM 3628), Candia Parapsilosis (ATCC 7330) and Cryptococcus neoformans (NCIM 3541) were employed for the anti-fungal studies. Milli-Q water was used throughout.

## 2.2. Measurements

NMR spectra were run using a Bruker AV 500 MHz spectrometer (Bruker, Germany) using DMSO D6 as solvent. IR spectra were recorded on FT-IR instrument (Perkin Elmer, USA). UV-Visible spectra were recorded on Jasco spectrophotometer (JascoV-650 Series, USA). Morphology of NBDMCA was examined using High resolution transmission electron microscope (HRTEM) (TECHNAI T20 instrument). Microplate reader used was from Multiskan MS Lab system, Helsinki, Finland.

## 2.3. Methods

### *2.3.1. Preparation of NBDMCA*

Initially, BDMCA was prepared by simple chemical method followed by nanotization using solvent assisted co-precipitation results in NBDMCA as reported by previously Francis et al., 2014 [43]. Briefly, to the mixture acetyl acetone and boric acid, dimethyl formamide (DMF) was added and heated for 15 min. Then salicylaldehyde was added and heated for 5 min. A few drops of glacial acetic acid and diethanolamine mixture was added and heated for 5 to 6 h. The mixture was kept for overnight and then DMF was added and warmed to form a flow paste. This paste was added slowly into the 10% acetic acid and stirred for 2 to 3 h. After stirring, the mixture was sonicated for 15 min. Then the mixture was filtered in a Whatman No 1 filter paper using a vacuum pump and dried on a watch glass at room temperature for 1-2 hours. BDMCA was purified using column chromatography [44] and then converted to NBDMCA by anti-solvent precipitation method using dimethyl sulfoxide (DMSO). Briefly about 50 mg of BDMCA was dissolved in 10 ml of the DMSO and added into 40 ml of water in drop wise under constant stirring at 800 rpm. The resulting mixture was homogenized at 2000 rpm for 30 min and followed by centrifugation at 10000 rpm for 20 min. The pellet was washed thrice with water and then dried at room temperature, and referred here as NBDMCA. The percentage yield of NBDMCA was determined from the absorbance of the supernatant at 418 nm and was found to be 85-90%.

### *2.3.2. Characterization of NBDMCA*

#### 2.3.2.1. Particle Size and Zeta Potential Measurement

Particle size and zeta potential was determined using dynamic light scattering (DLS) analysis (Malvern Zetasizer). Nanoparticles were first suspended in 100 ml of distilled water and subjected to sonication for 30 seconds and vortex mixing for 10 seconds before analysis. The size of the particle was measured based on the scattering of laser light by the particle. The angular intensity of the scattered light was then measured by a series of photosensitive detectors. The map of scattering intensity versus angle is the primary source of information used to calculate the particle size.

#### 2.3.2.2. Microscopic Imaging

TEM is a microscopy technique whereby a beam of electrons is transmitted through an ultrathin specimen, interacting with the specimen as it passes through it. An image is formed

from the electrons transmitted through the specimen, magnified and focused by an objective lens and appears on an imaging screen.

High resolution transmission electron (HRTEM) analysis of NBDMCA was carried out in TECHNAI T20 instrument operated at 200kV. For HR- TEM analysis few grams of powder dispersed in vial containing water. The mixture is sonicated for 10min to obtain complete suspension. Then, a drop of the suspension was applied on copper grid of 300 mesh coated with carbon. The grid was allowed to dry in air before analysis.

#### 2.3.2.3. Spectral Studies

Fourier Transform-Infrared Spectroscopy (FTIR) is an analytical technique used to identify the organic materials. When a material is irradiated with infrared radiation, absorbed IR radiation usually excites molecules into a higher vibrational state. The wavelengths that are absorbed by the sample are characteristic of its molecular structure. This unique absorbance or transmittance bands of molecular components and structures was helpful in the identification. The FTIR spectra are usually presented as plot of transmittance versus wave number (in $cm^{-1}$). Wave number is the reciprocal of the wavelength. The intensity can be plotted as the percentage of light transmittance or absorbance at each wave number. Absorption bands in the range of 4000 - 1500 wavenumbers are typically due to functional groups (e.g., -OH, C=O, N-H, CH3, etc.). The region from 1500 - 400 wavenumbers is referred to as the fingerprint region. Absorption bands in this region are generally due to intramolecular phenomena and are highly specific to each material. The specificity of these bands allows computerized data searches within reference libraries to identify a material.

Fourier Transform Infrared spectrum was recorded using PERKIN ELMER Spectrum1 FT-IR spectrometer in the region of 400-4000cm-1. The procedure involves dispersing a sample in potassium bromide (200-400mg) and compressing into discs by applying a pressure of 5 tons for 5min in a hydraulic press to prepare the pellet. The pellet was placed in the light path and the spectrum was obtained.

Carbon-13 (13C) NMR spectrum of NBDMCA was recorded in DMSO-d6 using Bruker AVANCE III 500 MHz (AV 500) multi nuclei solution NMR.

## 2.4. Antimicrobial Screening

Bacterial strains were obtained from Armats Biotek, Chennai and The Med Lab, Salem for carrying out *in-vitro* Antimicrobial activity. A disk diffusion assay reported in the literature by Bauer *et al. was carried out [45]*. Further confirmation tests include Resazurin assay to check the viability of cells and also microscopic visualization of drug-microorganism interactions.

### *2.4.1. Agar Disc Diffusion Method*

This method [45] is suitable for organism that grows rapidly over night at 35-37°C. Kirby–Bauer antibiotic testing (KB testing or disc diffusion antibiotic sensitivity testing) is a test which uses antibiotic-impregnated filter papers to test whether bacteria are affected by antibiotics. The antibiotic (specific concentration) impregnated disc absorbs moisture from

the agar and antibiotic diffuses in to the agar medium. The rate of extraction of the antibiotic from the disc is greater than the rate of diffusion.

In this test, disc containing antibiotics are placed on an agar plate where bacteria have been placed, and the plate is left to incubate. If an antibiotic stops the bacteria from growing or kills the bacteria, there will be an area around the wafer where the bacteria have not grown enough to be visible. This is called a zone of inhibition. As the distance from the disc increases, there is a logarithmic reduction in the antibiotic concentration. Zone of inhibition of bacterial growth around each disc is measured and the susceptibility is determined.

The size of this zone depends on how effective the antibiotic is at stopping the growth of the bacterium. A stronger antibiotic will create a larger zone, because a lower concentration of the antibiotic is enough to stop growth.

#### 2.4.1.1. Medium

3.8g of Nutrient Agar is added to 100 ml distilled water and autoclaved at 121°C for 15 minutes at 15 lbs and poured in sterile Petri plates up to a uniform thickness of approximately 4mm and the agar is allowed to set at ambient temperature and used.

#### 2.4.1.2. Inoculum

The microorganisms were inoculated in Nutrient agar medium and incubated at 37° C for 3-4 hours and this was used as inoculum.

#### 2.4.1.3. Method

The antibacterial activity of NBDMCA against bacterial isolates was evaluated by using agar disc diffusion method. A sterile cotton swab was inserted into the bacterial suspension and then rotated and compressed against the wall of the test tube so as to express the excess fluid. The surface of Nutrient Agar plate was inoculated with the swab. To ensure that the growth is uniform and confluent (or semi confluent) the swab is passed three times over the entire surface, by repeating the procedure. The prepared disc that contains NBDMCA was also placed on the bacteria inoculated Nutrient Agar plate. The plates were incubated overnight at 37°C for 18-24 hours. Antimicrobial activity was evaluated by measuring zone of inhibition by using Hi Media zone scale.

### *2.4.2. Resazurin Based Antibacterial Activity*

Resazurin is an oxidation–reduction indicator used for the evaluation of cell growth, particularly in various cytotoxicity assays. Resazurin (7-Hydroxy-3*H*-phenoxazin-3-one 10-oxide) is a blue dye, itself weakly fluorescent until it is irreversibly reduced to the pink coloured and highly red fluorescent resorufin. It is used as an oxidation-reduction indicator in cell viability assays for bacteria and mammalian cells, and for measuring aerobic respiration and exchange with the hyporheic zone in streams. Usually it is available commercially as the sodium salt. Usually, in the presence of NADPH dehydrogenase or NADH dehydrogenase as the enzyme, NADPH or NADH is the reductant that converts resazurin to resorufin. Resorufin is further reduced to hydroresorufin (uncoloured and nonfluorescent). Hence the resazurin/diaphorase/NADPH system can be used to detect NADH, NADPH, or diaphorase level, and any biochemical or enzyme activity that is involved in a biochemical reaction generating NADH or NADPH. This method allows the detection of microbial growth in

extremely small volumes of solution in microtitre plates without the use of a spectrophotometer.

### 2.4.2.1. Minimal Inhibitory Concentration

In microbiology, *minimum inhibitory concentration* (MIC) is the lowest concentration of an antimicrobial that will inhibit the visible growth of a microorganism after overnight incubation (Figure 3).

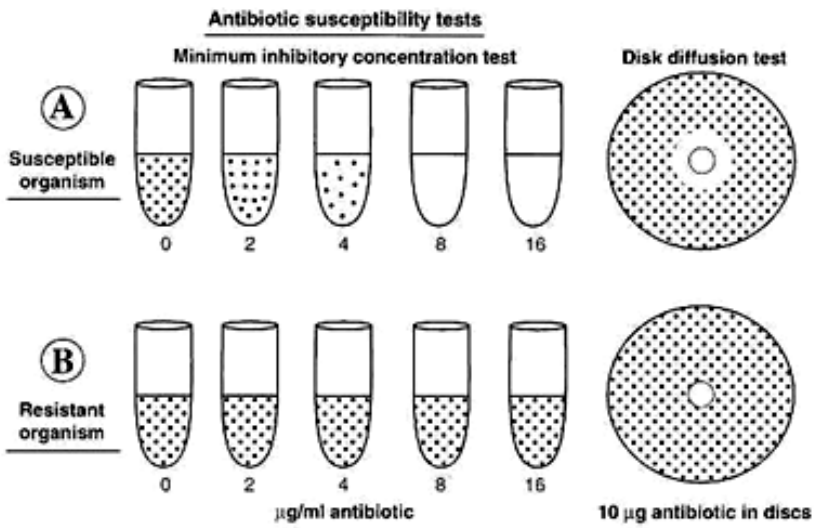


Figure 3. Assessment of Minimum Inhibitory Concentration.

Minimum inhibitory concentrations are important in diagnostic laboratories to confirm resistance of microorganisms to an antimicrobial agent and also to monitor the activity of new antimicrobial agents. A MIC is generally regarded as the most basic laboratory measurement of the activity of an antimicrobial agent against an organism.

### 2.4.2.2. Inoculum Preparation

Using aseptic techniques, a single colony was transferred into a 100 mL bottle of nutrient broth and placed in incubator overnight at 35 °C. After 12–18 h of incubation, using aseptic preparation and the aid of a centrifuge, a clean sample of bacteria was prepared. The broth was spun down using a centrifuge set at 4000 rpm for 5 min with appropriate aseptic precautions. The supernatant was discarded into an appropriately labelled contaminated waste beaker. The pellet was resuspended using 20 mL of sterile normal saline and centrifuged again at 4000 rpm for 5 min. This step was repeated until the supernatant was clear. The pellet was then suspended in 20 mL of sterile normal saline and used for the assay.

### 2.4.2.3. Preparation of Resazurin Solution

The resazurin solution was prepared by dissolving a 270 mg tablet in 40 mL of sterile distilled water. A vortex mixer was used to ensure that it was a well-dissolved and homogenous solution.

**2.4.2.4. Method**

Plates were prepared under aseptic conditions. A sterile 96 well plate was labelled. A volume of 100 µL of test material in 10% (v/v) DMSO or sterile water (usually a stock concentration of 1 mg/mL for purified compounds and 10 mg/mL for crude extracts) was pipetted into the first row of the plate. To all other wells 50 µL of nutrient broth or normal saline was added. Serial dilutions were performed using a multichannel pipette. Tips were discarded after use such that each well had 50 µL of the test material in serially descending concentrations. To each well 10 µL of resazurin indicator solution was added. Finally, 10 µL of bacterial suspension was added to each well. Each plate had a set of controls: a column with a broad-spectrum antibiotic as positive control, a column with all solutions with the exception of the test compound, and a column with all solutions with the exception of the bacterial solution adding 10 µL of nutrient broth instead [46].

## 2.5. Visualization of Bacteria NBDMCA Interaction

It becomes necessary to know the interaction of nanoparticles (NPs) with bacterial cell membranes that would help in providing direction in the design of bactericidal agents and sensor systems. Therefore, to determine this interaction between bacteria and nanoparticles, preliminary studies were done using optical microscopy.

***2.5.1. Medium***

3.8g of Nutrient Broth is added to 100 ml distilled water and autoclaved at 121°C for 15 minutes at 15 lbs and 10 ml of the Nutrient broth was poured in sterile test tubes.

***2.5.2. Inoculum***

The microorganisms were inoculated in Nutrient agar broth and incubated at 37°C for 3-4 hours and this was used as inoculums.

***2.5.3. Method***

500 µL of 1mg/ml concentration BDMCA was aliquoted into 500 µL of bacterial suspension (30 µL, $OD_{600\ nm}$ = 0.33). Sterilized Glass slides were taken and a loopful of bacterial suspension with BDMCA was applied and the slides were covered with a cover slip. After incubating for three hours, the slides were viewed under optical microscope using 20X, 50X, 100X. The mobility of the bacteria without drug was compared with the mobility of bacteria with drug using optical microscope.

# 3. RESULTS AND DISCUSSION

## 3.1. Characterisation of BDMCA

The particle size, polydispersity index and zeta potential data of NBDMCA are given in the Table as well as Figure 4 and 5. The results revealed that the particles produced were of nano size and exhibits low polydispersity index, which specifies relatively narrow particle

size distribution for all preparations. The mean diameter, polydispersity index (PI) and zeta potential of NBDMCA was found to be 90 nm, 0.112 and -24.17 respectively. The particle size data indicated that NBDMCA was in nano size and had low poly dispersity which indicates relatively narrow particle size distribution [47]. The low PI of NBDMCA may be due to surface charges, which prevent the flocculation of particles and enhance dispersion. Moreover, narrow particle size distribution circumvents the Ostwald ripening, i.e., the crystallization of various sized nanoparticles into larger particles. According to a previous report, a colloidal suspension with PI lower than 0.200 is considered to be stable [48, 49]. This report coincides with our present PI value of 0.112. In addition, Zeta potential is a measure of the electrostatic interaction between individual particles, indicating stability of a suspension with uniform dispersion (which indicates the degree of repulsion between adjacent, similarly charged particles in dispersion) [50]. The NBDMCA obtained using DMSO solvent system has shown good stability with zeta potential of -24.17 mV. The DMSO is miscible with water while the BDMCA is insoluble. This difference in the water solubility might precipitate the BDMCA leading to the formation of nanoparticles.

**Table 1. Particle Size, Polydispersity Index and Zeta Potential of NBDMCA**

| Solvent | Particle Size (nm) | Polydispersity Index | Zetapotential (mV) |
|---|---|---|---|
| DMSO | 90 | 0.112 | -24.17 |

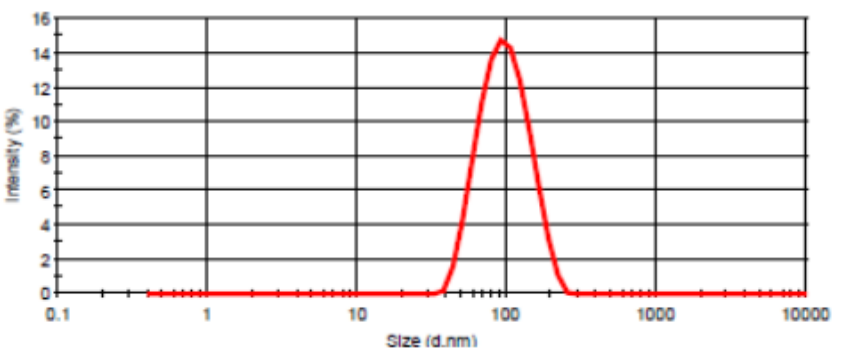


Figure 4. Particle size distribution of NBDMCA.

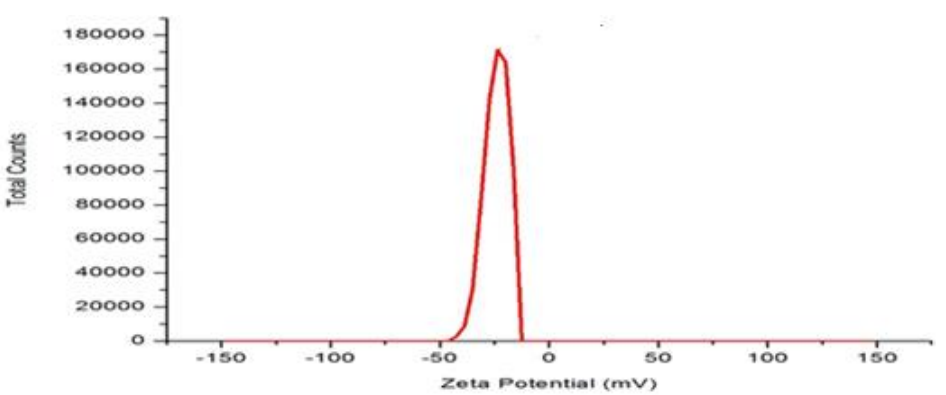


Figure 5. Zeta Potential of NBDMCA.

The FTIR of bulk BDMCA and NBDMCA were performed to validate the structural similarities between them. Figure 6 displays the FTIR of bulk BDMCA and NBDMCA. The prominent stretching observed in the spectra are summarized in the Table 2. The FTIR spectra of both bulk BDMCA and NBDMCA exhibit peaks corresponding to benzene ring, alkene, ketone and hydroxyl functional groups. O-H stretching frequency at 3250 - 3650 $cm^{-1}$, C=C aromatic stretching frequency at 1314-1654 $cm^{-1}$, C=O stretching frequency at 1654 $cm^{-1}$ being assigned to the C=O stretching frequency and C-H vibration stretches at 2926 $cm^{-1}$ were also observed. The most characteristics C=C Stretch occurs at 1654-1437 $cm^{-1}$. Band characteristics of aromatic mono substitution were explained by the vibration at 749 $cm^{-1}$. On the whole, the FTIR spectral characteristics reveal the presence of i) conjugated carbon chain with unsaturated double bond, ii) aromatic ring (Benzene), iii) ortho hydroxy group in the benzene ring.

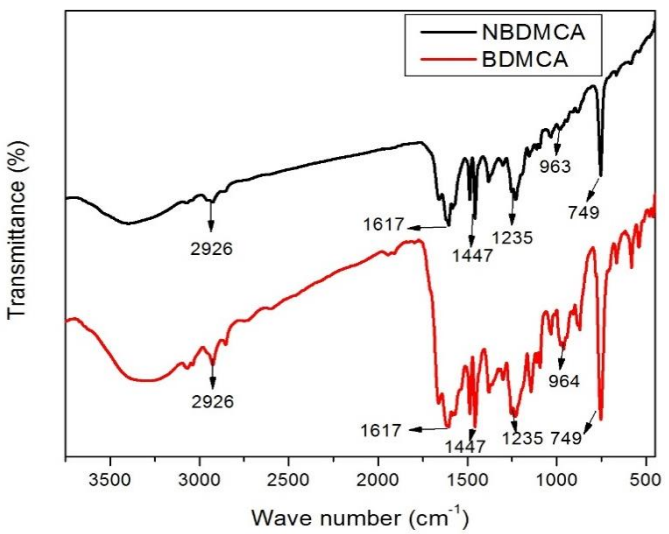


Figure 6. FTIR spectra of BDMCA and NBDMCA.

**Table 2. FTIR Interpretation of BDMCA and NBDMCA**

| Wave number ($cm^{-1}$) | Assignment | Expected Bonds in NBDMCA | Interpretation |
|---|---|---|---|
| 3600-3300 | phenolic OH stretch | O-H at ortho position | O-H stretching |
| 2926 | Methylene C-H asym./sym. stretch | Methylene C-H in the conjugated chain | C-H stretching |
| 1654 -1314 | Alkenyl C=C Conjugated ketone | Ketone in the linear chain | C=O olefinic stretching frequency bands |
| 1447 | Aromatic ring stretches | Aryl C=C bond | C=C stretching indicates the presence of the benzene ring |
| 1028 – 954 | Aromatic C-H out-of-plane bend | Skeletal C-C vibrations | C-C stretching of conjugated chain |
| 749 | Substitution at ortho position | Phenolic (C-O-H) stretch | Presence of ortho hydroxyl group |

The similarities in the FTIR spectral peaks between the bulk and NBDMCA confirms that the integrity of the functional groups is maintained and that, no structural changes occurred during the synthesis of nano BDMCA. The structure and the functional moieties play a crucial role in establishing the therapeutic activities. Our previous reports on bulk BDMCA suggest that the anticancer and antioxidant activities are due to its terminal phenolic groups and the unsaturated central seven carbon chain, clearly revealing the role of functional groups in the therapeutic activities [37, 47]. These reports together with the present findings suggest that the nano BDMCA can be used as a therapeutic tool for cancer and other diseases associated with oxidative stress and antioxidant imbalance. Moreover, the scaled down size and the enhanced surface area of NBDMCA could make it a better drug than its bulk counterpart.

NMR spectra of NBDMCA is shown in the Figure 7. The $^{13}C$ NMR spectra data scanned at 100 MHz using DMSO as solvent were δ 15.5, 101.73, 116.28, 119.59, 121.47, 123.49, 128.55, 131.73, 135.78, 156.93, 183.59. The signals at δ 116.28, 119.59, 128.55, 131.73, 135.78, 156.93 were corresponds to the carbon (-CH, C) in the benzene ring and the signal at δ 123.49 represent the ethylene group. Moreover, the signal at δ 183.59 and 101.73 indicates the carbonyl carbon and methylene linkage respectively. The spectral data on the whole reveal that the structure of NBDMCA was similar to bulk BDMCA. Thus, our synthesis protocol reported here increased the dispersibility and bioavailability without influencing the structural integrity of BDMCA.

The surface morphology like size and shape of NBDMCA was determined using HRTEM. HRTEM images describe the shape and size of NBDMCA respectively as shown in the Figure 8 NBDMCA particles were found to be spherical and within a size range of 70 - 100 nm. Moreover, the images indicate the uniform distribution of NBDMCA.

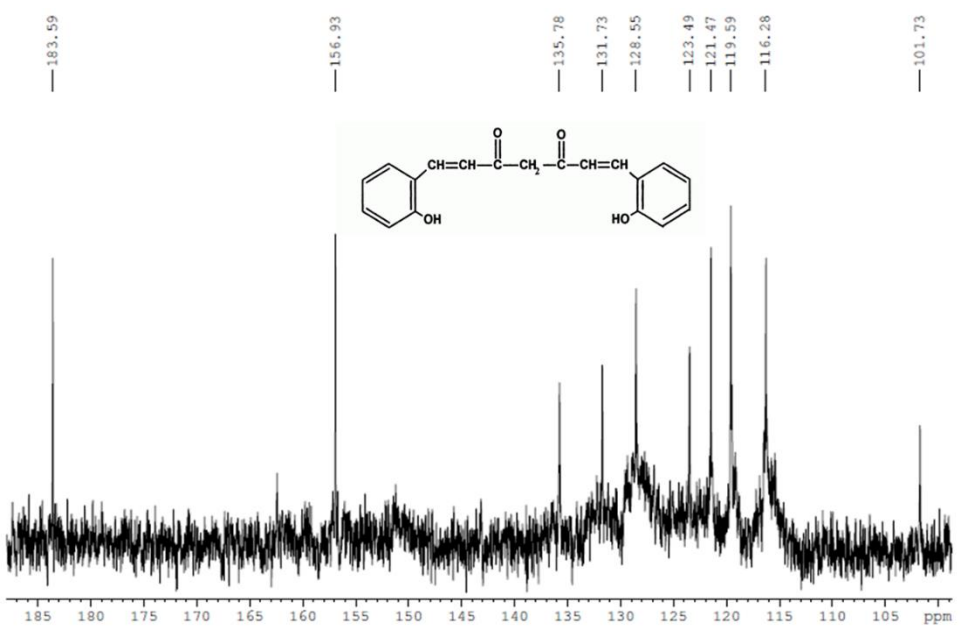


Figure 7. 13C NMR spectrum of NBDMCA.

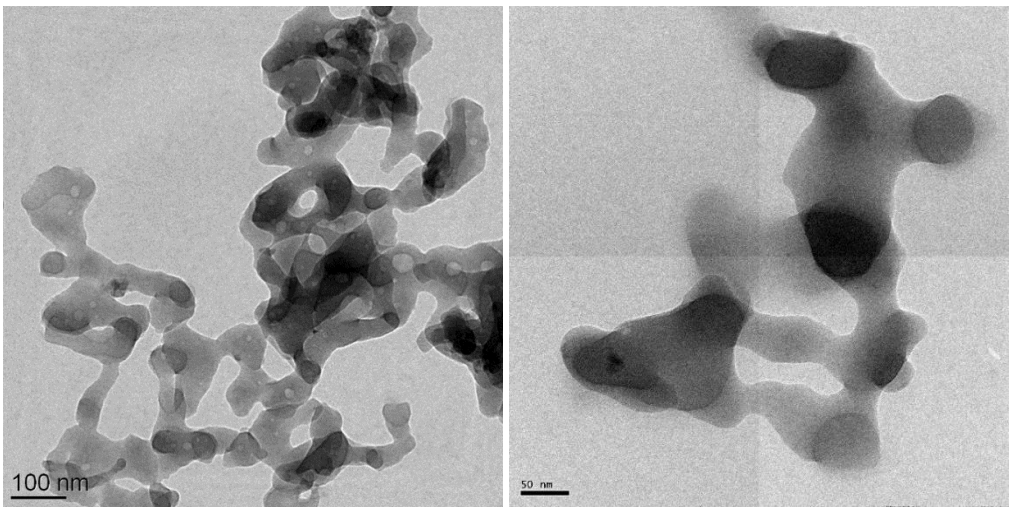


Figure 8. TEM micrograph of NBDMCA.

Previous reports suggest that the size of the nanoparticles should be less than 100 nm in order to prevent their rapid leakage into blood capillaries and also escape capture by macrophages accumulate in the recticulo endothelial system (liver and spleen) [51]. We have obtained NBDMCA with average size of 90 nm, which is very well all in the cut-off range, thus correlates with the previous report. Over all the size analysis of NBDMCA using HRTEM and DLS indicates that the particle synthesized by the present protocol very well fall under nanoscale. Therefore, NBDMCA may possess unique characteristic features like high surface to volume ratio, and monodispersion, which would render them an ideal therapeutic and pharmacological properties [42]. In addition, we could justify that the protocol is described here is valid and optimal to synthesize NBDMCA.

## 3.2. Anti-Bacterial Activity

Different gram positive (Enterococci, Staphylococcus) & gram negative (E.Coli, Pseudomonas, Proteus, Klebsiella) bacterial strains were obtained from urine samples of patients. Gram staining was done for identification (Figure 9).

Antibacterial activity results revealed that NBDMCA acted as excellent antibacterial agents against bacteria. NBDMCA exhibited bacterial growth inhibition against gram positive S. aureus (Table 3 and Figure 10) gram negative bacteria E. coli (Table 4 and Figure 11), in the form of zone-of-inhibition studies, where diffusion of nanoparticles on nutrient agar plates inhibits growth. The zone of inhibition was measured to be prominent to confirm the antibacterial activity when compared with the positive control. Through this, it can be demonstrated that the antibacterial activity of the drug increases with increase in surface-to-volume ratio due to the decrease in size of nanoparticles. The results show that NBDMCA were found to be more effective against all the microbes tested.

| | |
|---|---|
| 1. E.coli | 2. Enterococci |
| 3. Pseudomonas sp. | 4. Klebsiella sp. |
| 5. Proteus sp. | 6. Staphylococcus sp. |
| 7. Klebsiella sp. | 8. Staphylococcus sp. |

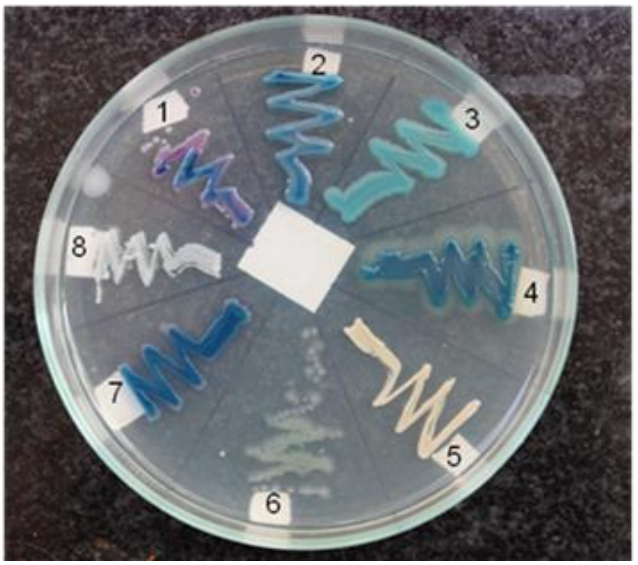


Figure 9. UTI plate with bacterial colonies.

**Table 3. Zone of Inhibition in NBDMCA treated *Staphylococcus aureus***

| S.No | NBDMCA (concentration in µg) | Zone of Inhibition (mm) |
|---|---|---|
| **1.** | 5 | 8 |
| **2.** | 10 | 12 |
| **3.** | 15 | 14 |
| **4.** | 20 | 16 |
| **5.** | 25 | 16 |

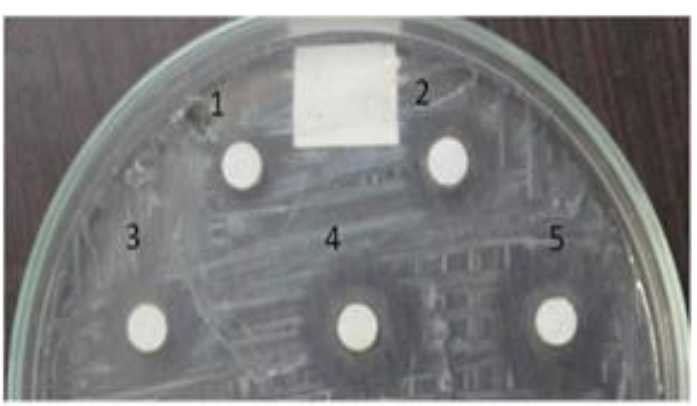


Figure 10. Zone of Inhibition in NBDMCA treated *Staphylococcus aureus.*

**Table 4. Zone of Inhibition in NBDMCA treated *Escherichia coli***

| S. No | NBDMCA (concentration in µg) | Zone of Inhibition (mm) |
|---|---|---|
| **1.** | 5 | 12 |
| **2.** | 10 | 17 |
| **3.** | 15 | 19 |
| **4.** | 20 | 22 |
| **5.** | 25 | 24 |

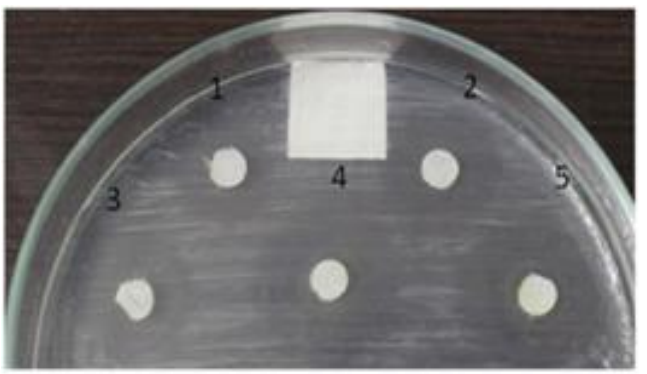


Figure 11. Zone of Inhibition in NBDMCA treated *Escherichia coli.*

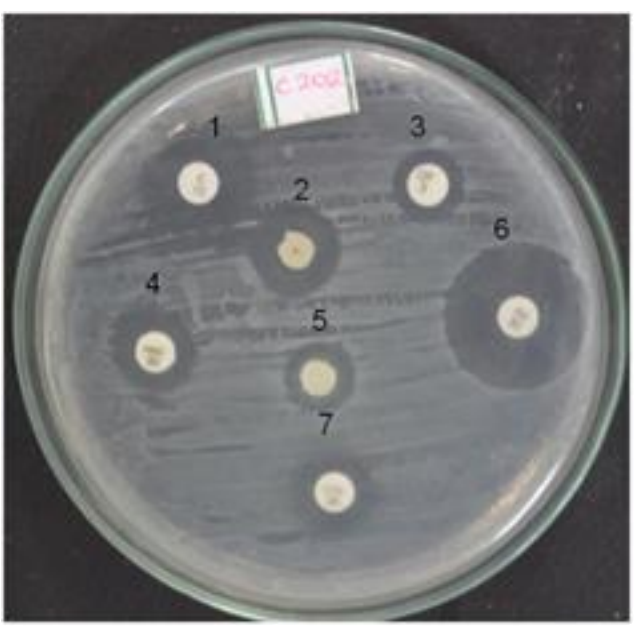


Figure 12. Comparison of antibacterial activity of NBDMCA with different positive controls like Erythromycin (Macrolides) (1), 20 µg of NBDMCA (15 mm) (2), Ofloxacin (Fluoroquinolones) (3), Amoxycillin clavulanic acid (Penicillin/ β lactamase inhibitor) (4), 10 µg of NBDMCA (10 mm) (5), Amikacin (Aminoglycosides) (6), Cefotaxime (Cephalosporins) (7) on S. aureus.

In addition, the antibacterial potential of 10 and 20 µg of NBDMCA were compared with various group of antibiotics such as Erythromycin (Macrolides), Ofloxacin (Fluoroquinolones), Amoxycillin clavulanic acid (Penicillin/β lactamase inhibitor), Amikacin (Aminoglycosides) and Cefotaxime (Cephalosporins). The results are shown in Figure 12. It was identified that NBDMCA has antibacterial activity that increases linearly with increase in concentration (µg/ml). As compared with standard antibiotics, the results revealed that bacterial strains were more sensitive towards in NBDMCA. Moreover, the antibacterial potential of NBDMCA at the concentration of 20 µg/ml was found to be comparable with all the standard antibiotics except Amikacin.

## 3.3. Resazurin Assay

The effectiveness of resazurin assay has been demonstrated with various concentrations of NBDMCA and the positive controls that include a variety of antibiotics. The plates were prepared and placed in an incubator set at 37 °C for 18–24 h. The colour change was then assessed visually. Any colour changes from purple to pink or colourless were recorded as positive. Choosing the correct assay to assess the antimicrobial potential of NBDMCA is important for generating high-quality data with the greatest accuracy, speed and efficiency, enabling the addition of potential new antimicrobial compounds.

Figure 13 indicates the antibacterial efficacy of NBDMCA at the concentration of 15 µg/ml was significantly high when compared to most of the standard antibiotics and comparable with aminoglycosides. This result is matching with the zone of inhibition of NBDMCA compared with antibiotics by disc diffusion method.

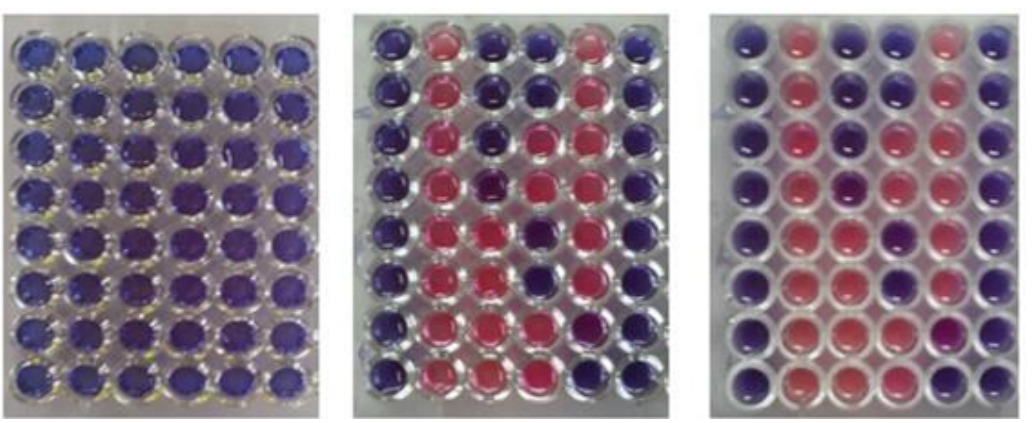

(a) (b) (c)

Figure 13. Resazurin assay: a) plates at the $0^{th}$ minute; b) plates after 4 hours in Resazurin assay [pink colour indicates growth and blue means inhibition of growth: the test organism]; c) plates aft 10 hours in Resazurin assay.

**Table 5. Representation of NBDMCA and Antibiotics in 96 well (Resazurin assay)**

| Col 1 | Col 2 | Col 3 | Col 4 | Col 5 | Col 6 |
|---|---|---|---|---|---|
| **Blank** | Control | 25 µg | Gentamycin | Cephalexin | Blank |
| **Blank** | Control | 20 µg | Amikacin | Cephadroxil | Blank |
| **Blank** | Control | 15 µg | Ciprofloxacin | Cefaclor | Blank |
| **Blank** | Control | 10 µg | Methicillin | Cefixime | Blank |
| **Blank** | Control | 5 µg | Doxycillin | Cefuroxime | Blank |
| **Blank** | Control | 2.5 µg | Amoxycillin/Clav | Ceftizidime | Blank |
| **Blank** | Control | 1 µg | Amoxycillin | Ceft/ Clav | Blank |
| **Blank** | Control | 0.5 µg | Ofloxocin | Ceft/ Tazo | Blank |

## 3.4. Visualization of Bacteria NBDMCA Interaction

Positive control that contains bacterial suspension without drug was observed with rapid mobility when compared with the bacterial suspension with drug. And also aggregation of bacteria surrounding NBDMCA drug molecules could be visualized (Figure 14). The decrease in mobility may be due to the bacteria- NBDMCA interaction (Data not Shown).

Overall NBDMCA was found to be more effective against *S. aureus* and *E. coli.* This could be believed that NBDMCA get attached to the cell wall of the bacterial cell and resulting the destruction of peptidoglycan layer, then penetrating inside the cell, and disrupting the structure of cell organelles ended with cell lysis.

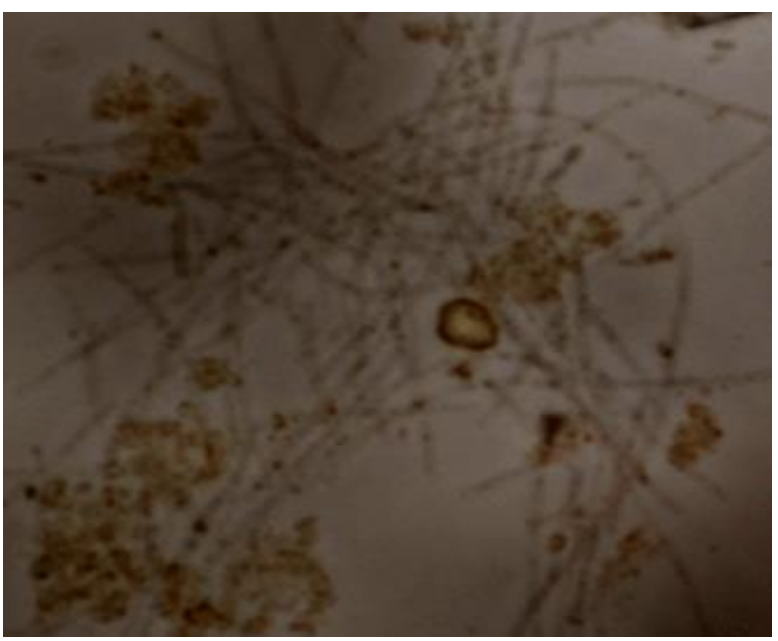

Figure 14. Interaction between bacteria and NBDMCA.

## CONCLUSION

Because of the various side effects caused by existing synthetic drugs, drug development of plant based compounds could be useful in meeting the demand for newer drugs with minimal side effects. Nano bis-demethoxy curcumin analog (NBDMCA) the synthetic compound possess anti-oxidant and anti-carcinogenic properties. Hence, this study focus on the determination of antibacterial property of NBDMCA. This is important to know about the capability of NBDMCA to use against Multidrug resistant infections. The zone of inhibition obtained from Agar disc diffusion assay shows the presence of antibacterial activity of the drug. Also from the Resazurin assay, Minimal Inhibitory Concentration of the drug has been determined and it was found to be 10 µg/ml. Bactericidal activity of NBDMCA which was determined optical microscope may be due to BDMCA- Bacteria interaction which is confirmed by the bacterial aggregates. In addition, antibacterial activity of NBDMCA is confirmed using Disc diffusion method. Therefore, NBDMCA can be used as an adjuvant for Multidrug resistant infections. Applications of NBDMCA based on these findings may lead to valuable discoveries in various fields such as medical devices and antimicrobial systems.

## REFERENCES

[1] Rakotoarivelo N. H., Rakotoarivony F., Ramarosandratana A. V., Jeannoda V. H., Kuhlman A. R., Randrianasolo A. and Bussmann R. W. 2015. Medicinal plants used to treat the most frequent diseases encountered in Ambalabe rural community, Eastern Madagascar. *J Ethnobiol Ethnomed.* 11:68. doi: 10.1186/s13002-015-0050-2.

[2] Cragg G. M. and Newman D. J. 2013. Natural products: a continuing source of novel drug leads. *Biochimica et Biophysica Acta (BBA)-General Subjects* 1830:3670-95.

[3] Hartwell J. L. *Plants used against cancer: a survey*. Lawrence, MA. Quarterman Publications, 1982, pp. 438-39.

[4] Mutai P., Heydenreich M., Thoithi G., Mugumbate G., Chibale K. and Yenesew A. 2013. 3-Hydroxyisoflavanones from the stem bark of Dalbergia melanoxylon: Isolation, antimycobacterial evaluation and molecular docking studies. *Phytochem. Lett.* 6:671-5.

[5] Gundidza M. and Gaza N. 1993. Antimicrobial activity of Dalbergia melanoxylon extracts. *J Ethnopharmacol.* 40:127-30.

[6] Donnelly D. M., O'Reilly J. and Whalley W. B. 1975. Neoflavanoids of Dalbergia melanoxylon. *Phytochemistry* 14:2287-90.

[7] Wachtel-Galor S. and Iris F. F. Benzie An Introduction to Its History, Usage, Regulation, Current Trends, and Research Needs. In: Benzie IFF, Wachtel-Galor S, editors. *Herbal Medicine: Biomolecular and Clinical Aspects*. 2nd edition. Boca Raton (FL): CRC Press/Taylor & Francis; 2011.

[8] Manchanda V., Sanchaita S. and Singh N. 2010. Multidrug resistant acinetobacter. *J Glob Infect Dis.* 2:291-304.

[9] Viehman J. A., Nguyen M. H. and Doi Y. 2014. Treatment options for carbapenem-resistant and extensively drug-resistant Acinetobacterbaumannii infections. *Drugs* 74:1315-33.

[10] Lee C. R., Cho I. H., Jeong B. C. and Lee S. H. 2013. Strategies to Minimize Antibiotic Resistance. *Int J Environ Res Public Health.* 10:4274-305.

[11] Fair R. J. and Tor Y. 2014. Antibiotics and Bacterial Resistance in the 21st Century. *Perspect Medicin Chem.* 6:25-64.

[12] Hancock R. E. 2005. Mechanisms of action of newer antibiotics for Gram-positive pathogens. *The Lancet infectious diseases* 5:209-18.

[13] Li X. Z. and Nikaido H. 2004. Efflux-mediated drug resistance in bacteria. *Drugs* 64:159-204.

[14] Pandey K. B. and Rizvi S. I. 2009. Plant polyphenols as dietary antioxidants in human health and disease. *Oxi Med Cell Longev.* 2:270-8.

[15] Srinivasan M., Sudheer A. R. and Menon V. P. 2007. Ferulic Acid: Therapeutic Potential Through Its Antioxidant Property. *J Clin Biochem Nutr.* 40:92-100.

[16] Tyagi S., Singh G., Sharma A. and Aggarwal G. 2010. Phytochemicals as candidate therapeutics: An overview. *Int J Pharma Sci Review Res.* 3:53-5.

[17] Ricky A. Sharma, William P. Steward, Andreas J. Gescher. Pharmacokinetics and pharmacodynamics of curcumin. In: Aggarwal, Bharat B., Young-Joon Surh, and Shishir Shishodia, eds. *The molecular targets and therapeutic uses of curcumin in health and disease.* Vol. 595. Springer Science & Business Media, 2007, pp.453-470.

[18] Holt P. R., Katz S. and Kirshoff R. 2005. Curcumin therapy in inflammatory bowel disease: a pilot study. *Digestive diseases and sciences* 50:2191-3.

[19] Tourkina E., Gooz P., Oates J. C., Ludwicka-Bradley A., Silver R. M. and Hoffman S. 2004. Curcumin-induced apoptosis in scleroderma lung fibroblasts: role of protein kinase Cε. *Am J Respirat Cell Mol Biol* 31:28-35.

[20] Gulcubuk A., Altunatmaz K., Sonmez K., Haktanir-Yatkin D., Uzun H., Gurel A. and Aydin S. 2006. Effects of Curcumin on Tumour Necrosis Factor-α and Interleukin-6 in the Late Phase of Experimental Acute Pancreatitis. *Transboundary and Emerging Diseases* 53:49-54.

[21] ABE Y., Hashimoto S. and HORIE T. 1999. Curcumin inhibition of inflammatory cytokine production by human peripheral blood monocytes and alveolar macrophages. *Pharmacol Res* 39:41-7.

[22] Goel A., Kunnumakkara A. B. and Aggarwal B. B. 2008. Curcumin as "Curecumin": from kitchen to clinic. *Biochemical pharmacology* 75:787-809.

[23] Jobin C., Bradham C. A., Russo M. P., Juma B., Narula A. S., Brenner D. A. and Sartor R. B. 1999. Curcumin blocks cytokine-mediated NF-κB activation and proinflammatory gene expression by inhibiting inhibitory factor I-κB kinase activity. *The Journal of Immunology* 163:3474-83.

[24] Surh Y. J., Chun K. S., Cha H. H., Han S. S., Keum Y. S., Park K. K. and Lee S. S. 2001. Molecular mechanisms underlying chemopreventive activities of anti-inflammatory phytochemicals: down-regulation of COX-2 and iNOS through suppression of NF-κB activation. *Mutation Research/Fundamental and Molecular Mechanisms of Mutagenesis* 480:243-68.

[25] Huang M. T., Lysz T., Ferraro T., Abidi T. F., Laskin J. D. and Conney A. H. 1991. Inhibitory effects of curcumin on in vitro lipoxygenase and cyclooxygenase activities in mouse epidermis. *Cancer research* 51:813-9.

[26] Liu J. Y., Lin S. J. and Lin J. K. 1993. Inhibitory effects of curcumin on protein kinase C activity induced by 12-O-tetradecanoyl-phorbol-13-acetate in NIH 3T3 cells. *Carcinogenesis* 14:857-61.

[27] Liu Y. L., Yang H. P., Gong L., Tang C. L. and Wang H. J. 2011. Hypomethylation effects of curcumin, demethoxycurcumin and bisdemethoxycurcumin on WIF-1 promoter in non-small cell lung cancer cell lines. *Molecular medicine reports* 4:675-9.

[28] Ravindran J., Prasad S. and Aggarwal B. B. 2009. Curcumin and Cancer Cells: How Many Ways Can Curry Kill Tumor Cells Selectively? *The AAPS Journal* 11:495-510.

[29] Tuorkey M. J. 2014. Curcumin a potent cancer preventive agent: Mechanisms of cancer cell killing. *Interventional Medicine & Applied Science* 6:139-46.

[30] Abdal Dayem A., Choi H. Y., Yang G. M., Kim K., Saha S. K. and Cho S. G. 2016. The Anti-Cancer Effect of Polyphenols against Breast Cancer and Cancer Stem Cells: Molecular Mechanisms. *Nutrients* 8:581.

[31] Hua Y., Dolence J., Ramanan S., Ren J. and Nair S. 2013. Bisdemethoxycurcumin inhibits PDGF-induced vascular smooth muscle cell motility and proliferation. *Molecular nutrition & food research* 57:10.1002/mnfr.201200852.

[32] Trujillo J., Chirino Y. I., Molina-Jijón E., Andérica-Romero A. C., Tapia E. and Pedraza-Chaverrí J. 2013. Renoprotective effect of the antioxidant curcumin: Recent findings. *Redox biology* 1:448-56.

[33] Otuechere C. A., Abarikwu S. O., Olateju V. I., Animashaun A. L. and Kale O. E. 2014. Protective Effect of Curcumin against the Liver Toxicity Caused by Propanil in Rats. *International Scholarly Research Notices* 2014:853697.

[34] Wu J., Pan X., Fu H., Zheng Y., Dai Y., Yin Y., Chen Q., Hao Q., Bao D. and Hou D. 2017. Effect of curcumin on glycerol-induced acute kidney injury in rats. *Scientific Reports* 7.

[35] Aggarwal B. B. and Harikumar K. B. 2009. Potential Therapeutic Effects of Curcumin, the Anti-inflammatory Agent, Against Neurodegenerative, Cardiovascular, Pulmonary, Metabolic, Autoimmune and Neoplastic Diseases. *The international journal of biochemistry & cell biology* 41:40-59.

[36] Anto R. J., Kuttan G., Babu K. D., Rajasekharan K. and Kuttan R. 1996. Anti-tumour and free radical scavenging activity of synthetic curcuminoids. *International journal of pharmaceutics* 131:1-7.

[37] Devasena T., Rajasekaran K. and Menon V.P. 2002. Bis-1, 7-(2-hydroxyphenyl)-hepta-1, 6-diene-3, 5-dione (a curcumin analog) ameliorates DMH-induced hepatic oxidative stress during colon carcinogenesis. *Pharmacological research* 46:39-45.

[38] Devasena T., Menon V. P. and Rajasekharan K. N. 2006. Prevention of 1, 2-dimethylhydrazine-induced circulatory oxidative stress by bis-1, 7-(2-hydroxyphenyl)-hepta-1, 6-diene-3, 5-dione during colon carcinogenesis. *Pharmacological Reports* 58:229.

[39] Ravindranath V. and Chandrasekhara N. 1981. Metabolism of curcumn-studies with [3H] curcumin. *Toxicology* 22:337-44.

[40] Pan M. H., Huang T. M. and Lin J. K. 1999. Biotransformation of curcumin through reduction and glucuronidation in mice. *Drug metabolism and disposition* 27:486-94.

[41] Liversidge G. G. and Cundy K. C. 1995. Particle size reduction for improvement of oral bioavailability of hydrophobic drugs: I. Absolute oral bioavailability of nanocrystalline danazol in beagle dogs. *International journal of pharmaceutics* 125:91-7.

[42] Bhawana, Basniwal R. K., Buttar H. S., Jain V. and Jain N. 2011. Curcumin nanoparticles: preparation, characterization, and antimicrobial study. *J Agric Food Chem* 59:2056-61.

[43] Francis A. P., Murthy P. B. and Devasena T. 2014. Bis-demethoxy curcumin analog nanoparticles: synthesis, characterization, and anticancer activity in vitro. *Journal of nanoscience and nanotechnology* 14:4865-73.

[44] Babu K. D. and Rajasekharan K. 1994. Simplified condition for synthesis of curcumin I and other curcuminoids. *Organic preparations and procedures international* 26:674-7.

[45] Bauer A. W. Kirby W. M. Sherris J. C. Turck M. 1966. Antibiotic susceptibility testing by a standardized single disk method. *Am J Clin Pathol.* 45:493–496.

[46] Sarker S. D., Nahar L. and Kumarasamy Y. 2007. Microtitre plate-based antibacterial assay incorporating resazurin as an indicator of cell growth, and its application in the in vitro antibacterial screening of phytochemicals. *Methods* (San Diego, Calif) 42:321-4.

[47] Francis A. P., Ramaprabhu S. and Devasena T. 2016. Towards Intravenous Drug Delivery: Augmenting the Stability and Dispersity of Bis-Demethoxy Curcumin Analog by Bottom-Up Strategy. *Journal of Nanoscience and Nanotechnology* 16:1186-9.

[48] dos Santos K. C., da Silva M. F. G., Pereira-Filho E. R., Fernandes J. B., Polikarpov I. and Forim M. R. 2012. Polymeric nanoparticles loaded with the 3, 5, 3′-triiodothyroacetic acid (Triac), a thyroid hormone: factorial design, characterization, and release kinetics. *Nanotechnology, science and applications* 5:37.

[49] Wu L., Zhang J. and Watanabe W. 2011. Physical and chemical stability of drug nanoparticles. *Advanced drug delivery reviews* 63:456-69.

[50] Honary S. and Zahir F. 2013. Effect of zeta potential on the properties of nano-drug delivery systems-a review. *Tropical Journal of Pharmaceutical Research* 12:265-73.

[51] Yuan F., Dellian M., Fukumura D., Leunig M., Berk D. A., Torchilin V. P. and Jain R. K. 1995. Vascular permeability in a human tumor xenograft: molecular size dependence and cutoff size. *Cancer research* 55:3752-6.

In: Advances in Polymers for Biomedical Applications ISBN: 978-1-53613-612-8
Editors: Deepak Pathania and Bhuvanesh Gupta 

*Chapter 7*

# PLASMA FUNCTIONALISATION OF POLYCAPROLACTONE SURFACE FOR BIOMEDICAL APPLICATIONS

***Jincy Joy, Surabhi Singh, Sadiya Anjum and Bhuvanesh Gupta****

Bioengineering Laboratory, Department of Textile Technology,
Indian Institute of Technology Delhi, New Delhi, India

## ABSTRACT

Polycaprolactone (PCL) has been extensively used for biomedical applications because of its strength and its slow rate of biodegradation. However, its inert nature has stimulated the surface functionalization of PCL, without the compromise of its bulk properties which can be carried out by plasma functionalization. Thus, this chapter highlights the plasma modification of PCL surface so that immobilization of biomolecules transforms the inert PCL surface to a bioreceptive surface finding vivid applications in tissue engineering. Emphasis has been made on generating specific chemical functionalities on PCL surface by the modulation of the nature of the gas. This consequently changes the surface properties; wettability, nanotopography and nanoroughness which play a vital role in cell adhesion and proliferation. Moreover, the reactive functionalities and the altered surface properties facilitate the covalent attachment of biopolymers and bioreactive substrates rendering durability and ligands for cell receptors to adhere to the PCL surface. The chapter details the application of the plasma modified surface for bioimmobilization and tissue engineering applications. Greater cell adhesion and proliferation was observed with the plasma modified PCL surface enhancing its biocompatibility. Therefore, plasma modification of PCL could elevate its applicability in the biomedical field.

* Corresponding address: bhuvanesh.universe@gmail.com.

## 1. INTRODUCTION

For the past few decades, surface modification has gained much attention for enhancing the biocompatibility of the surface of a polymeric material to promote immobilization of biomolecules such as collagen, gelatin, chitosan etc., onto their surfaces for tissue engineering applications, an interdisciplinary area that combines knowledge from cellular biology and materials engineering to bring about construction of artificial tissues or organs such as skin, heart valves, bones etc., [1-3].

Several researchers have stated the fact that bioimmobilization of hydrophilic and protein containing moieties improve the cell adhesion and proliferation onto the surfaces of polymeric scaffolds [4-6]. Among different materials, poly ε-caprolactone (PCL) (Figure 1) has been considered an ideal scaffolding material owing to its inherent biodegradability, biocompatibility and slow resorbability [7].

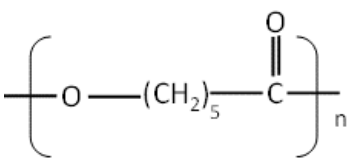


Figure 1. Structure of polycaprolactone (PCL).

PCL based devices have been commercialized for clinical applications as tissue repair patches (i.e., Ethicon Inc., Edinburgh, U.K.) [8]. After implantation, PCL gets broken down by the body in harmless end products (ideally $CO_2$ and $H_2O$) that can be secreted by the body, making a second surgery no longer necessary [9,10] and its structural and mechanical properties are sufficient for their field of application. Unfortunately, the hydrophobic character of PCL, and of most polyesters in general, limits the penetration of aqueous cell suspensions in the scaffold's core [11]. In addition, the top layer of cells settled on the scaffold limits the diffusion of nutrients by consuming most of it, thus reducing the amount available for pioneer cells which further inhibits their migration and differentiation into the scaffold structure [12].

To address this problem with PCL based scaffolds, various surface modification techniques have been employed to create and/or enhance functional changes on the surfaces to accelerate cell-material interactions for tissue engineering applications [13, 14]. Plasma functionalization is one of the most suitable and versatile techniques due to the ability of different plasma entities to react with the polymeric material and transfer energy by elastic and inelastic collision. Outcome of inelastic collision is degradation of the polymer and free radical formation along with surface functionalization [15-17]. To generate functional groups, such as hydroxyl, carboxyl, and amino groups on the polymer surface, gases; mostly carbon dioxide ($CO_2$), oxygen ($O_2$) are utilized in plasma modification process as shown in Figure 2.

The chemical surface treatment of scaffolds is often carried out but is complicated, as the pore size limits the infiltration efficiency of (wet)-chemical treatments and often degrades the structural stability of the delicate biomaterials [18]. Whereas, gas based plasma is chemical free technique and promising to penetrate more easily into the scaffold structure. At the same time, it only alters the surface without affecting the bulk, restoring the mechanical and

structural integrity of the modified biomaterial [18, 19]. PCL scaffolds were designed and exposed to $CO_2$ plasma [18].

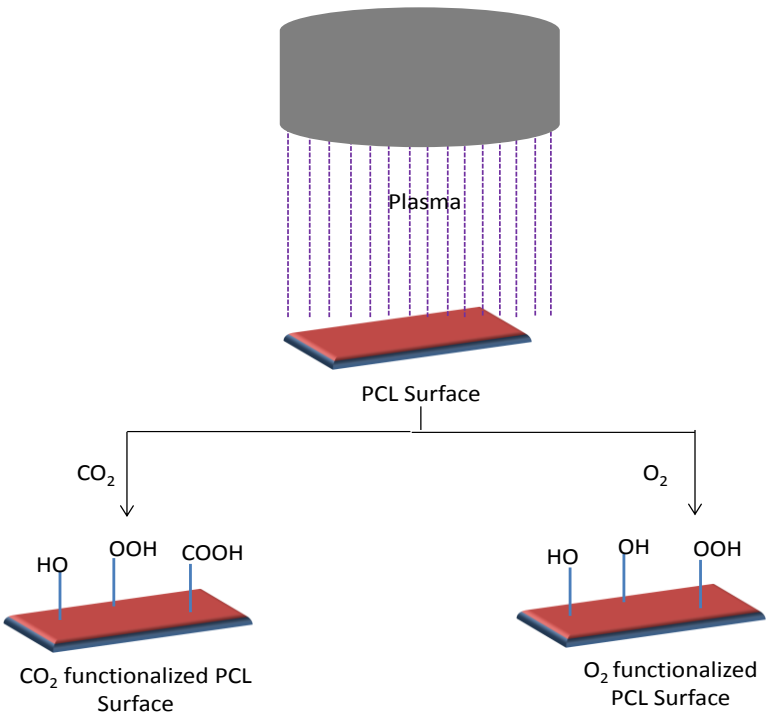


Figure 2. Plasma functionalization of PCL surface using $CO_2$ and $O_2$ gases.

Almost unaltered mechanical properties and morphological characteristics along with sufficient functionalization prove the advantage of plasma mediated surface modification. By proper choice of gas, it is possible to manipulate these functional groups and change their nature, which alters their surface wettability and surface energy, which both have a drastic impact on protein and cell adhesion [15, 17]. Prabhakaran et al., seeded neurolemmocytes (or Schwann) cells onto the PCL nanofibrous scaffolds and found an increase in proliferation rate at all times, with a maximum of 17% compared to the untreated material after 10 days[20]. It was claimed that the treatment is as effective as a collagen coating, making it a cost-effective alternative for nerve cell regeneration applications. Martins et al., came to the same conclusion after treating their PCL nano-textile scaffolds both with Ar and $O_2$ plasma [21]. Min et al., tested the $O_2$ plasma treated PCL nanotextile with primary astrocytes and noted an increase in adherence and viability in the first 24 hours [22]. In a study, cross-linked PEO-like domains interspaced with native PCL ones were deposited only on top of the scaffold, were effective in promoting Saos-2 cells colonization and increasing penetration of up to 3 mm below the periphery of the scaffold [23]. Plasma treatment had shown pronounced effect on the surface wettability of a polymeric surface [24]. Differences in contact angle upon exposure to $CO_2$ and $O_2$ gases are depicted in Figure 3.

Similar studies were conducted where plasma modification using Ar gas, Ar + $O_2$, Ar + $O_2$ + $N_2$ gas mixtures and dry air plasma was performed on electrospun

PCL/Chitosan/PCL hybrid scaffolds which increased biocompatibility performance of L929 fibroblast cells. It was observed that the samples treated with Ar + $O_2$ + $N_2$ gas mixtures for 1 min and air dried for 9 min have better hydrophilicity; 78.9° ± 1.0 and 75.6° ± 0.1, respectively compared to the untreated samples (126.5°) [25]. A research conducted indicated that the contact angle of PCL electrospun scaffolds lies between 120° and 140°, indicating a hydrophobic surface, which is not favoured by most cells. After treatment with either air, Ar, $NH_3$ or $O_2$ plasmas, all research groups were able to reduce the contact angle [26, 27]. Our work on $O_2$ and $CO_2$ plasma treated PCL scaffolds has demonstrated that $O_2$ plasma exposure reduced the contact angle to a greater extent as compared to $CO_2$ which can be ascribed to higher hydrophilicity of functional moieties; peroxides and hydroxyl; generated on the surface after $O_2$ treatment resulting in enhanced interaction with water [18, 24]. The micrographs showing the change in contact angle after plasma treatment on PCL cast films and electrospun mats with $CO_2$ and $O_2$ gas has been presented in Figure 3. A clear change in the increase of hydrophilicity of the surface was observed after plasma treatment in lieu of the introduced reactive groups with the gases; that interact with water.

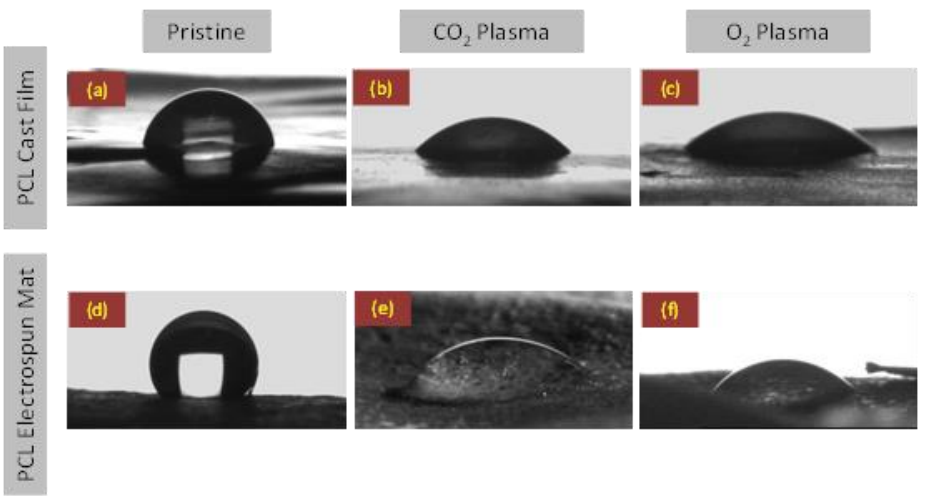


Figure 3. Effect of Plasma treatment on surface wettability. Contact angle measurement on PCL cast film; (a) pristine, (b) $CO_2$ plasma treated, (c) $O_2$ plasma treated. Contact angle measurement on electrospun PCL mats (d) pristine, (e) *$CO_2$ plasma treated; (f) $O_2$* plasma treated. Reaction condition: RF Incident power: 60W, exposure time; 60s.

The contact angle of 81 ± 10 for pristine PCL film dropped to 49 ± 5 after $CO_2$ plasma treatment and 43 ± 5 for $O_2$ plasma treatment. The same pattern was emulated for PCL electrospun mats wherein the contact angle for pristine; 117 ± 6 dropped to 54 ± 4 and 49 ± 7 after $CO_2$ and $O_2$ treatment respectively. This fact was coherent to the comparative contact angle values on PCL films after $CO_2$ and $O_2$ treatment at increasing exposure times represented in Figure 4.

Thereby, the nature of the gas used for plasma treatment and the consequent groups generated on the surface can have a profound change in the surface chemistry of the polymer.

Other similar reports on PCL scaffolds involved treatment with plasma created with $O_2$, $NH_3$ or $SO_2$ gas at identical conditions and their influence on the adhesion and proliferation of human umbilical vein endothelial cells (HUVEC) on scaffolds. MTT assay showed that

treatment with $O_2$ and $NH_3$ plasma stimulated endothelial cell proliferation on PCL surfaces by 60% as measured at 24 h, showing significant improvement in endothelialization of this biomaterial [28].

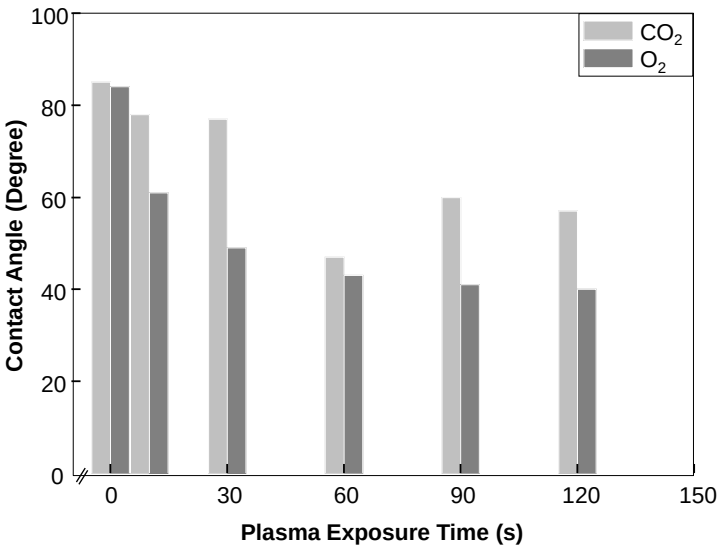


Figure 4. Variation of contact angle with the plasma exposure time on PCL cast films using $CO_2$ and $O_2$ gases.

Changes in surface wettability are accompanied by nanotopographical changes that occur on the surface after plasma exposure. During exposure, chain fragments evolved from photon absorption get ablated and lead to surface etching. Also, these ablated chain fragments and polymer fragments from utilized gas gets redeposited on to the surface and form a hill-valley surface topography, which is a typical outcome of plasma exposure. The changes in topography of the substrate lead to an increase in surface roughness, thus providing more favourable environment for cell adhesion. It was noticed that PCL film treated for 5 min with DBD plasma showed good degree of total surface energy, mouse osteoblast cell proliferation and surface roughness [29].

Examination of roughness can be carried out using atomic force microscopy as shown in Figure 5. Surface roughness values of PCL scaffold after plasma treatment range were in nanodimension; lesser than 70nm which acts as topographical cue for cell adhesion [18].

It was observed that the plasma treatment transforms morphology and topography of PCL significantly with exposure time from relatively smooth surface to rough surface with prominent hill-valley feature. It was also affirmed that increasing exposure time leads to broader hills and valleys on the surface as depicted in Figure 5. Lee et al., also used an atmospheric pressure DBD operating in air to modify PCL films. The cell attachment and proliferation of human prostate epithelial cells (HPECs) was found to be ten times better on plasma-treated PCL films compared to untreated film [30]. In another study, Saos-2 osteoblasts exhibit enhanced cell growth on $N_2/H_2O$ plasma treated PCL scaffolds with respect to untreated ones. Moreover, those treated in 50/50 $H_2O/N_2$ feeds showed the highest level of cell growth [31].

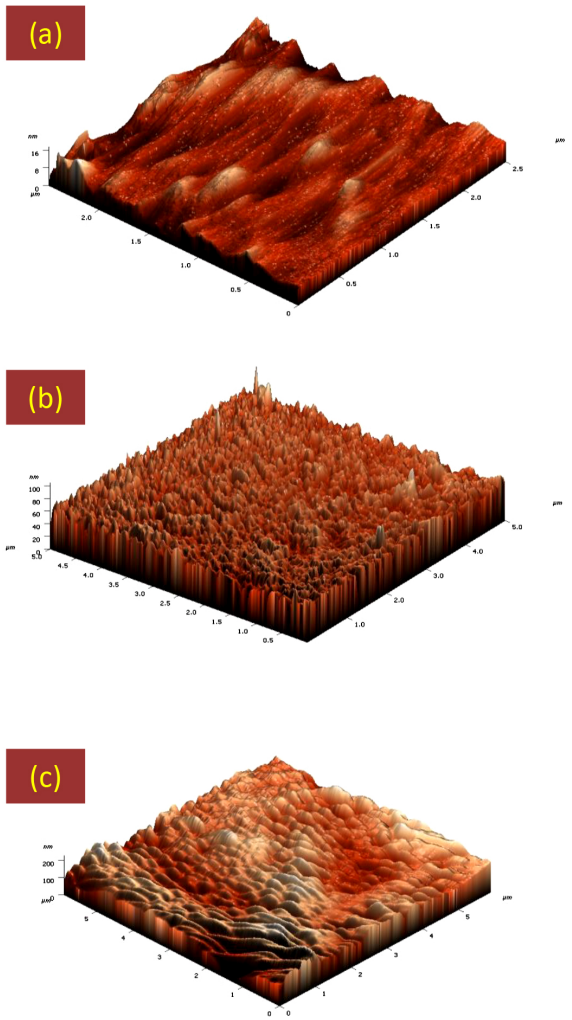


Figure 5. Topographical studies using AFM on PCL cast films with increasing exposure time; (a) 0s (pristine film) (b) 60s (c) 90s.

This review highlights the strategies to develop hydrophilic functional PCL scaffolds for anchoring desired biomolecules to induce cell receptive surface for effective tissue regeneration without much alteration in the bulk properties of the PCL polymeric material.

## 2. Applications of PCL Based Scaffolds

### 2.1. Tissue Engineering

Tissue engineering deals with the precise designing of the scaffold for guiding cells to grow and proliferate into a three-dimensional tissue structure with proper diffusion of oxygen, nutrients and metabolic waste. For successful organ regeneration, scaffolds must meet the basic requirements of biocompatibility and mechanical compatibility with the virgin tissue. Similarly, biodegradability, matching of degradation rate with neo-tissue generation rate and

a nontoxic degraded component along with high porosity and interconnected pores are necessary for a scaffold to achieve sufficient cell-to-cell and cell-to-matrix communication for better tissue generation [32, 33].

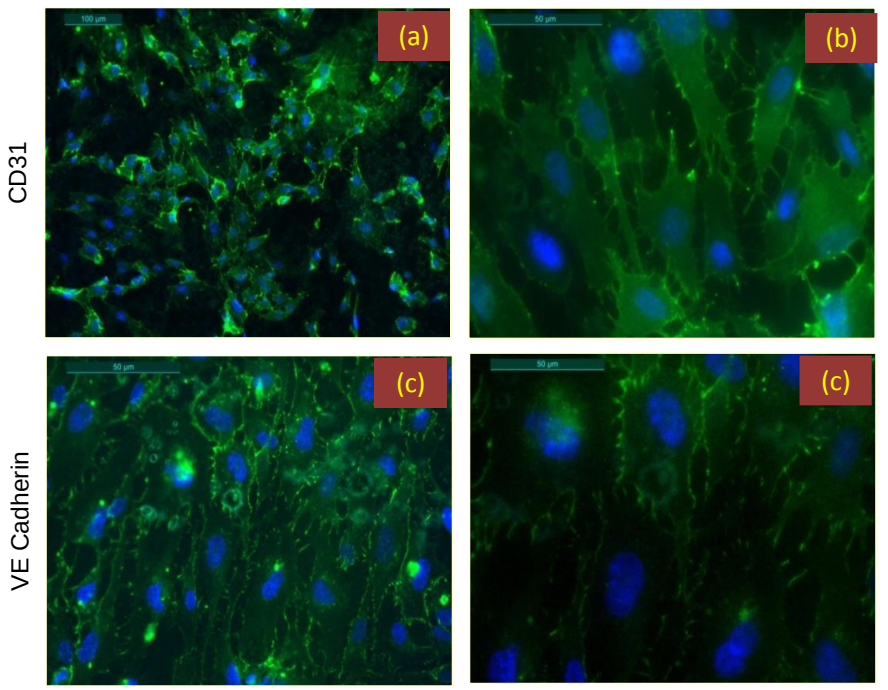


Figure 6. Immunofluoroscent staining of seeded progenitor derived endothelial cells on gelatin immobilized PCL scaffold for cell markers CD31 (a-b) and VE cadherin (c-d). Scale 50 µm.

Combination of biopolymers with PCL has also been utilized to obtain scaffolds with desired biological and mechanical properties. Nanofibrous structure of collagen with PCL has been developed by electrospinning and has been found to be a good candidate for vascular prosthesis [34]. It exhibited good tensile behaviour, compliance, suture retention and burst properties, and has a favourable response to endothelial and smooth muscle cell seeding. In a similar manner, a tissue engineered blood vessel scaffold was designed using combination of gelatin and porous PCL to achieve excellent growth of progenitor-derived endothelial cells as shown in Figure 6 [7]. Here, cell coverage and proliferation on the scaffold surface can be co-related to the cell-to-cell interactions estimated by CD-31 marker. The immunofluorescence images clearly show the cell extensions and their interactions with each other, forming colonies. The VE cadherin is characteristic of functionality of endothelial cells. A positive expression of VE cadherin shows the retained functionality of endothelial cells after seeding and culture. Thereby, the surface cytocompatibility offered by gelatin immobilization on plasma functionalized surface did not alter the identity or the biological characteristic of the cells. While immobilized gelatin facilitated cell adhesion, the interconnected porosity helped in cell migration and cell infiltration which led to the confluency of functional endothelial cells on PCL scaffold.

Along with the use of PCL in combination with other biopolymers, single PCL based nanofibrous scaffolds that mimic the original extracellular matrix to achieve better cell

attachment, proliferation and growth, have been a focus of enormous research [34]. Augustine et al., fabricated novel electrospun PCL nanofibrous tissue engineering scaffolds with the incorporation of pro-angiogenic europium hydroxide nanorods (EHNs), to promote effective vascularization. Biological examination indicated enhanced cell growth and density of endothelial cells grown on the scaffolds incorporated with EHNs (PCL-EHNs) along with good hemo-compatibility towards the blood cells. The PCL-EHNs demonstrated augmented growth of blood vessels in an in vivo angiogenesis chick embryo model [35]. Likewise, it was observed that the incorporation of ZnO nanoparticles in PCL scaffolds enhanced cell adhesion, migration and proliferation both in vitro and in vivo [36].

## 2.2. Bioimmobilization

Immobilization of certain cell recognition motives on the surface of a substrate is not the only means to enhance the biocompatibility of the substrate; the adsorption of either unspecific or specific proteins also plays a major role [37].

Gelatin immobilized PCL scaffolds were characterized and observance of slow release of gelatin from the scaffold surface; unlike a burst behaviour indicated fair adherence of gelatin onto the surface as depicted in Figure 7. Washing of immobilized gelatin led to removal of excess unattached gelatin; not clogging the pores vital for cell migration as observed with our work which proved beneficial for cell adhesion and migration [18].

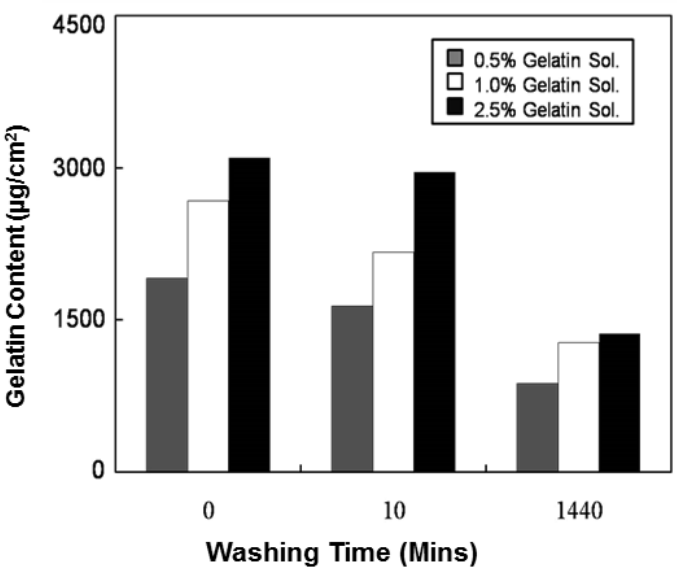


Figure 7. Release of gelatin with respect to washing time from the gelatin immobilized plasma functionalized PCL scaffold. Variation of the concentration of gelatin immobilized are: 0.5%, 1% and 2.5%.

In a study, the hydrophilicity and cytocompatibility of the surface of the electrospun PCL fibrous scaffolds was improved by treatment with 1,6- hexamethylenediamine (HMD) and using the induced amino groups as precursors for subsequent immobilization with three

different biomolecules, e.g., collagen, chitosan, and Gly-Arg-Gly-Asp-Ser (GRGDS) peptide. Cytocompatibility of the biomolecule-immobilized scaffolds was then assessed in vitro with keratinocytes (HEK001), fibroblasts (L929), and osteoblasts (MC3T3-E1) for cell viability, cell adhesion, and cell proliferation. Both the neat and the modified PCL fibrous scaffolds released no substances in the levels that were harmful to these cells. Among the various biomolecule immobilized PCL fibrous scaffolds, the ones that had been immobilized with type I collagen showed the greatest ability to support both the attachment and the proliferation of all of the investigated cell types, followed by those that had been immobilized with GRGDS peptide [38].

Santiago et al., performed immobilization of three different peptides [i.e., RGD, Tyr-Ile-Gly-Ser-Argand Cys-Arg-Ala-Arg-Lys-Gln-Ala-Ala-Ser-Ile-Lys-Val-Ala-Val-Ser-Ala-Asp-Arg] on the surface of solvent-cast PCL disks for adipose derived stem cell applications [39].

## CONCLUSION

Plasma modification of PCL using various gases for developing bioreceptive surface to enhance their biological properties for tissue engineering applications is a simplistic and clean approach with preservation of bulk properties of the polymeric scaffold. Several findings have suggested that topographical changes in terms of surface roughness of the polymeric materials after plasma treatment augments cell adhesion and proliferation on the scaffold surface. These scaffolds with improved hydrophilicity and biocompatibility can serve as potential candidates for tissue reconstruction.

## REFERENCES

[1] Zhu, Y., Gao, C., Liu, X., Shen, J., *J. Biomed. Mater. Res.* A 2004, 69, 436-443.
[2] Cheng, Z., Teoh, S. H., *Biomaterials* 2004, 25, 1991-2001.
[3] Zhu, Y., Gao, C., Shen, J., *Biomaterials* 2002, 23, 4889-4895.
[4] Zhu, Y., Gao, C., He, T., Shen, J., *Biomaterials* 2004, 25, 423–430.
[5] Ding, Z., Chen, J., Gao, S., Chang, J., Zhang, J., Kang, E. T., *Biomaterials* 2004, 25, 1059–1067.
[6] Liao, J. D., Lin, S. P., Wu, Y. T., *Biomacromolecules* 2005, 6, 392–399.
[7] Patra, S., Remy, M., Ray, A. R., Brouillaud, B., Amedee, J., Gupta, B., Bordenave, L., *J. Biomater. Tissue Eng.* 2013, 3, 289-299.
[8] Woodruff, M. A., Hutmacher, D. W., *Prog. Polym. Sci.* 2010, 35, 1217−1256.
[9] Desmet, T., Morent, R., Geyter, N. D., Leys, C., Schacht, E., Dubruel, P., *Biomacromolecules* 2009, 10, 2351-2378.
[10] Ulery, B. D., Nair, L. S., Laurencin, C. T., *J. Polym. Sci. Part B. Polym. Phys.* 2011, 49, 832-864.
[11] Bacakova, L., Filova, E., Parizek, M., Ruml, T., Svorcik, V., *Biotechnol. Adv.* 2011, 29, 739−767.

[12] Martin, I., Padera, R. F., Vunjak-Novakovic, G., Freed, L. E., *J. Orthop. Res.* 1998, 16, 181−189.
[13] Am, S., Kim, J. K., Ryu, S. H., *Appl. Surf. Sci.* 2006, 252, 5714-5722.
[14] Sasmazel, H. T., Manolache, S., Gumusderelioglu, M., *J. Biomater. Sci.* 2009, 20, 1137-1162.
[15] Recek, N., Vesel, A., *Materiali in Tehnologije* 2014, 48, 893-897.
[16] Jaganjac, M., Vesel, A., Milkovic, L., Recek, N., Kolar, M., Zarkovic, N., Latiff, A., Kleinschek, K. S., Mozetic, M., *J. Biomed. Mater. Res.* A 2014, 102, 2305–2314.
[17] Recek, N., Jaganjac, M., Kolar, M., Milkovic, L., Mozetic, M., Stana-Kleinschek, K., Vesel, A., *Molecules* 2013, 18, 12441-12463.
[18] Patra, S., Anjum, S., Ray, A. R., Gupta, B., *Polym. Bull.* 2016, 73, 1875-1890.
[19] Jacobs, T., Morent, R., De Geyter, N., Dubruel, P., Leys, C., *Plasma Chem. Plasma Process* 2012, 32, 1039-1073.
[20] Prabhakaran, M. P., Venugopal, J., Chan, C. K., Ramakrishna, S., *Nanotechnology* 2008, 19, 455102.
[21] Martins, A., Pinho, E. D., Faria, S., Pashkuleva, I., Marques, A. P., Reis, R. L., Neves, N. M., *Small* 2009, 5, 1195-1206.
[22] Min, S. K., Jung, S. M., Kim, S. H., Kim, C. R., Shin, H. S., *J. Biomed. Mater. Res. B. Appl. Biomater.* 2013, 101, 1267-1274.
[23] Sardella, E., Salama, R. A., Waly, G. H., Nour Habib, A., Favia, P., Gristina, R., *ACS Appl. Mater. Interfaces* 2017, 9, 4966−4975.
[24] Gupta, B., Krishnanand, K., Deopura, B. L., Atthoff, B., *J. Appl. Polym. Sci.* 2012, 127, 1744-1750.
[25] Surucua, S., Masurb, K., Sasmazela, H. T., Von Woedtkeb, T., Weltmann, K. D., *Appl. Surf. Sci.* 2016, 385, 400-409.
[26] Yan, D., Jones, J., Yuan, X., Xu, X., Sheng, J., Lee, J. M., Ma, G., Yu, Q., *J. Biomed. Mater. Res.* A 2013, 101, 963-972.
[27] Jeon, H. J., Lee, H., Kim, G. H., *Plasma Process. Polym.* 2014, 11, 142-148.
[28] Recek, N., Resnik, M., Motaln, H., Lah-Turnšek, T., Augustine, R., Kalarikkal, N., Thomas, S., Mozetic, M., *Int. J. Polym. Sci.* 2016, Volume 2016, 9 pages.
[29] Yildirim, E. D., Ayan, H., Vasilets, V. N., Fridman, A., Guceri, S., Sun, W., *Plasma Process Polym.* 2008, 5, 58-66.
[30] Lee, H. U., Jeong, Y. S., Koh, K. N., Jeong, S. Y., Kim, H., Bae, J. S., Cho. C. R., *Curr. Appl. Phys.* 2009, 9, 219-223.
[31] Sardella, E., Fisher, E. R., Shearer, J. C., Trulli, M. G., Gristina, R., Favia, P., *Plasma. Process Polym.* 2015, 12, 786–798.
[32] Soucacos, P. N., Johnson, E. O., Babis, G., *Injury* 2008, 39, 636−642.
[33] Dhandayuthapani, B., Yoshida, Y., Maekawa, T., Sakthi Kumar, D., *Int. J. Polym. Sci.* 2011, 2011, 1−19.
[34] Leonard, S. S., Harris, G. K., Shi, X., *Free Radic. Biol. Med.* 2004, 37, 1921-1942.
[35] Augustine, R., Nethi, S. K., Kalarikkal, N., Thomas, S., Patra, C., *J. Mater. Chem. B*, 2016, 00, 1-3.
[36] Augustine, R., Dominic, E. A., Reju, I., Kaimal, B., Kalarikkal, N., Thomas, S., *RSC Adv.* 2014, 4, 24777-24785.

[37] Krishnanand, K., Deopura, B. L., Mishra, A., Gupta, B., *J. Biomater. Tissue Eng.* 2013, 1-7.

[38] Mattanavee, W., Suwantong, O., Puthong, S., Bunaprasert, T., Hoven, V. P., Supaphol, P., *ACS Appl. Mater. Interfaces* 2009, 1, 1076-1085.

[39] Santiago, L. Y., Nowak, R. W., Rubin, J. P., Marra, K. G., *Biomaterials* 2006, 27, 2962–2969.

In: Advances in Polymers for Biomedical Applications ISBN: 978-1-53613-612-8
Editors: Deepak Pathania and Bhuvanesh Gupta 

*Chapter 8*

# ADVANCES IN DIRECTIONAL DELIVERY OF DNA AND SIRNA

***Adesh K. Saini*, Yash Raj Rastogi and Reena V. Saini***
Faculty of Applied Sciences and Biotechnology, Shoolini University,
Solan, Himachal Pradesh, India

## ABSTRACT

Medical research has been greatly benefited with the discovery of biomedical application of natural or synthetic polymers as biomaterial which could help in medical treatment. In this chapter, we are going to discuss the use of biomaterials for the directional delivery of molecules that could either modulate the gene expression or directly benefit a tissue or cell. Materials like poly(lactide-co-glycolide), polyacetals, collagen, polysaccharides, chitin, polyanhydrides and other polymers are discussed with respect to their applications for delivering DNA or siRNA.

**Keywords:** siRNA, DNA delivery, photochemical internalization, chitosan

## INTRODUCTION

### Advances in Directional Delivery of DNA and siRNA

One of the major leaps in molecular biology and biotechnology came on 14th September, 1990 when Dr. W. French Anderson and Michael Blaese at National Institutes of Health, Clinical center performed the first successful gene therapy on a four year old girl with adenosine deaminase (ADA) deficiency [1]. Since then a lot of progress has been made in the realms of gene therapy but still there remains a long way to go.

* Corresponding author: Faculty of Applied Sciences and Biotechnology, Shoolini University, Solan, Himachal Pradesh, India, Email: sainiade@gmail.com.

A basic requirement for gene therapy or any other biotechnological investigation or application is the successfully transfection of a cell with the desired gene or nucleotide sequence [2-4]. This can be achieved either through transduction (using modified viral vectors) or non-viral physical or chemical methods. Earlier the viral gene transfer techniques were popular but they posed some serious clinical problems such as toxicity, induced immune or inflammatory responses in the cell or caused insertional mutagenesis. Moreover, due to the large size of the viral vectors they could not be used for systemic delivery as they could not cross many barriers in the body such as the blood-brain barrier.

It was then that the non-viral vectors for gene transfer were developed such as liposomes, polyplexes, dendrimers, etc. The major advantages of using them are that they are comparatively easy to develop or assemble, cause less cytotoxicity, their size can be reduced to nanoscale for effective transfection [5, 6] and they did not pose any danger like the the viral vectors of recovering their ability to cause disease. Liposomes have been most extensively used as non-viral gene transfer vectors because of their cationic nature, bioreducibility, cost efficiency, ease of production and low cytotoxicity caused by them. But the major disadvantage of using these liposomes is that they have poor transfection efficiency and are somewhat unstable molecules [7, 8].

This led to the development of polyplexes for efficient gene transfer. Polyplexes are the complexes formed by the gene and the carrier polymer. Some popular polymers that have been used for polyplex formation are polyethylene glycol (PEG), chitin, polyethylenemine(PEI), poly(lactide co-glycolide)(PLGA), etc. A good polyplex must have the following characteristics:-

I. It must be biodegradable so that it does not accumulate inside the cell causing problems like toxicity.
II. It must efficiently cause transfection releasing the gene into the cell before being destroyed by lysosomes.
III. It may be cationic in nature so that it can easily attach to the anionic DNA or siRNA. Moreover, cationic molecules are preferentially phagocytosed by cells from the blood stream due to accumulation of opsonins on them.
IV. They must have a low to moderate zeta potential (ς) [9] so that they may easily disintegrate releasing the gene inside the cell.

In recent times significant and ingenious research has been done to develop such polymers that besides meeting the above mentioned requirements can also perform directional or targeted delivery of the therapeutic molecule inside the body. When we precisely target the desired cells or tissues in the body without influencing the other cells or tissues then it is called targeted or directional method of delivery. It increases the efficiency of the delivered therapeutic molecule and prevents any adverse effects on other cells or tissues due to the molecule.

## DNA DIRECTIONAL DELIVERY THROUGH POLYMERS

Although cationic lipids and polymers were a popular method for negatively charged DNA transfer, still the poor shielding of the positively charged part of the vector posed

problems *in-vivo* [10]. New techniques for gene transfer using non-viral polymeric vectors that can solve this problem have been developed that have the potential for efficient directional delivery of the molecule in-vivo. Some of the most advance and major techniques have been discussed below:-

## Asymmetric Polyplex-Nanocapsules Loaded with Photosensitizer for Light Assisted Gene Transfer [11]

Endo-lysosomal sequestration of the gene is a major obstacle in the efficient gene transfection. Endosome vesicles are formed as a result of the endocytosis of the polyplex by the cell. The DNA must break away from the endosomal membrane for its release into the cytosol before reaching the lysosome. This problem can be overcome by a novel technique called photochemical internalization (PCI) [12]. In this technique, certain photosentisizers (PS) are used that upon activation by light can cause the release of DNA from the endosomal vesicle. This technology can also be used for the release of other macromolecules in the cell. In this technique of gene transfer, asymmetric polyplex based on the triblock co-polymers of poly(ethylene glycol)-b-polycaprolactone-b-poly(ethylene imine)(PEG-PCL-PEI) are used. According to the theory of polymer self assembly, the amphiphilic block polymers can self-assemble to form polymerosome in aqueous environment (that are analogous to liposomes) with hydrophobic membranes [13-14]. Like liposomes, polymerosomes also contain an aqueous interior where the DNA or siRNA can be stored. The aforementioned triblock co-polymer of PEG-PCL-PEI is similar to a polymerosome that can be used to store the DNA as well as the photosensitizer (PS) through hydrophopic interactions with the polyplex nanocapsules. In this method, the activation of photosensitizer by light generates reactive oxygen species (ROS) at sub-lethal levels that then cause the rupture of the endosomal vesicle.

If the light radiated on the photosensitizer can be tuned or controlled externally using lasers then we can precisely regulate the DNA delivery intracellularly as well as when systemic delivery is done making the targeted delivery of gene possible. The other advantages of this method are that the polyplex complex formed is stable enough for prolonged blood circulation without being eradicated and it is biodegradable in nature. It is an ingenious method in the sense that it employs both physical and chemical methods of gene transfer.

## Chitosan Nanoparticle Based Delivery of Fused NKG2D-IL-21 Gene Suppresses Growth of Colon Cancer in Mice

Interlukin-21(IL-21) is a cytokine that can antagonize the growth of tumors in-vivo by activating lymphocytes-6 [15-21]. NKG2D is a proteinaceous lectin like activating receptor that can identify tumor cells in the body of mice as well as humans by two different pathways respectively [22, 23]. Hence, theoretically NKG2D-IL-21 fusion protein can specifically suppress tumors. The NKG2D moiety can identify the tumor cells whereas the IL-21 segement shall activate the T-cells to suppress the tumor growth. In this method the genes encoding for NKG2D and IL-21 were joined together and inserted into pcDNA 3.1 (minus)

plasmid. The delivery of this plasmid was done by enclosing them in chitosan nanoparticles [24]. Chitosan nanoparticles are biodegradable and non-toxic in nature. This method has been successfully tested in mice to suppress colon cancer by injecting the chitosan polyplexes intravenously. This method has great potential in curing tumors and cancers in humans also. Unlike previous method, in this method there is nothing inherently special about the polymer for target specific gene delivery, rather it is the gene itself in the polyplex that make it target specific. A similar to treat tumors in humans is of chitosan nanoparticles coated NKG2D-IL-12 fused genes.

## PAMAM/DNA Dendriplex Coated with Hyaluronic Acid for Efficient Targeted Gene Delivery to Tumor Cells [25]

Dendrimers are highly branched spherical molecules the surface of which is functionalized to get desired properties for efficient gene transfer. The complex of dendrimers with DNA or RNA leads to the formation of structures known as dendriplexes. In this technique positively charged polyamidoamine (PAMAM) dendrimers are used for gene transfer because of their low polydispersity index and balanced molecular weight [26]. The most important feature of this dendriplex is its coating with hyaluronic acid (a polysaccharide formed of D-glucoronic acid and N-acetyl-D-glucosamine) that is responsible for its tumor cells specific delivery of gene. Hyaluronic acid is biodegradable in nature, conceals the exposed surface charge of the dendriplex and does not cause any toxicity.

It has been found that CD44, a receptor for hyaluronic acid, is overexpressed on the surface of tumor cells compared to that on the surface of normal cells [27]. This technique makes use of this finding because of which the tumor cells have a considerably greater uptake of these hyaluronic acid coated dendriplexes than normal cells in the body. Once endocytosed, these dendriplexes easily release the DNA in the cell via proton sponge mechanism [28, 29] preventing the problem of endosomal sequestration of the DNA. The same technique of using hyaluronic acid for tumor specific DNA delivery can be used with liposomes or conventional polymers like polyethylemine [30-37] but they may not confer the additional benefits of PAMAM dendriplexes. This technique of gene transfer can be employed to cure tumors of lung, breast, stomach, etc. and can even cure melanoma [38].

## Phenylboronic Acid-Sugar Grafted Polymer Construct as a Dual Stimuli-Responsive Gene Carrier for Targeted Anti-Angiogenic Tumor Therapy [39]

This is a highly efficient method of targeted gene delivery that depends upon the cell characteristics and chemistry for its functioning. In this method phenylboronic acid (PBA) CH5B(OH)2 is bound to the cis-diol moieties of the common sugar [40]. This complex is then bound to the commonly used cationic carrier polyethylemine (PEI) for gene delivery. The polyplex nanocomplex remains stable in the blood stream due it's alkaline pH so it can be administerd intravenously [41]. This technique induces dual stimuli-response in the cell for gene delivery [42, 43]. Firstly, the bond between phenylboronic acid and sugar via cis-diol moieties is strong at the basic pH outside the cell but weakens at acidic pH as that exists in

endosomes thus causing the release of the DNA from the polymeric construct inside the cell. Secondly, the ATP inside the cell also has cis-diol moiety in its ribose ring and the PBA preferentially bind to ATP by breaking its bond with common sugar leading to greater thermodynamic stability [44, 45]. The breaking of the PBA-common sugar bond also leads to the release of DNA in the cell. The easy disintegration of this architecture prevents its accumulation inside the cell and any toxicity thereby as a repercussion. The PBA is responsible for the tumor cell specific delivery of the gene [46]. The sialylated glycoproteins that are generally over-expressed on the surface of the tumor cells have an affinity for PBA causing this architecture to be endocytosed by the tumor cells [47-50]. This method holds promise in anti-angiogenic tumor therapy [51-53]. A major drawback of this technique is that it cannot be used for systemic administration as the PBA could bind to any cis-diol moiety of various biological membranes. This problem can be overcome by further modifying the above given structure by adding a pH dependent removable PEG coating that shall get removed in acidic environment inside the cell but remain stable in blood stream [54].

**Table 1. DNA polyplexes and their importance**

| S. No. | DNA Polyplex | Details | Significance |
|---|---|---|---|
| 1. | Single walled carbon nanotubes(SWCNTs) conjugated with PEG, PEI and 5TR1 aptamer [55] | Delivers Bcl class of protein's gene for cell apoptosis, the aptamer 5TR1 recognises the tumor cells through MUC1 glycoprotein on cancer cells | In the treatment of breast cancer |
| 2. | SWCNTs conjugated with PEI and AS1411 aptamer [56] | Targets tumor cells through AS1411 aptamer moiety having affinity for nucleoin receptors over expressed on cancer cells | In the treatment of gastric cancers |
| 3. | PEI electrostaticaly conjugated with sgc-8c aptamer [57] | The aptamer recognizes the protein tyrosine kinase 7 on the cancer cells for targeted delivery | In the treatment of leukemia |
| 4. | DMPGTVLP peptide conjugated to PEI via disulfide bond[58] | Performs target specific gene delivery using aptamers or antibodies recognized cancer cell receptors | In the killing of breast adenocarcinoma cells |
| 5. | FQHPSF peptide conjugated with chitosan linked with PEI [59] | Combines interlukin-12 for target specific gene delivery | In the treatment of liver cancer |

Polyplexes can be an important milestone in DNA delivery because of the many advantages that they possess. They are easy to assemble, are small in size, cost efficient, do not cause toxicity or provoke immune response like viral vectors. They can be modified for target specific drug delivery and so can be used for convenient systemic delivery. We can

now also cure neurological disorders using gene therapy which was once difficult using viral vectors because of their large size making them unable to cross the blood brain barrier [60].

## siRNA Directional Delivery through Polymers

Small interfering RNA (siRNA) has a significant role in gene therapy (RNA interference) and in general research to understand the physiology of the cell. Till now, non-viral vectors used for DNA delivery were also used for the siRNA delivery but none of them could transfer the siRNA efficiently because of its inherently different properties from that of DNA [9]. The supercoiled plasmid DNA can easily form polyplexes with cationic polymers but this is not so with siRNA. The rigid and large 19-20 bp long siRNA molecule non-uniformly interacts with the cationic polymers forming loose complexes leading to inefficient delivery of siRNA [61, 62]. Recent advancements have led to the development of such nano-polymeric constructs that besides efficiently transfecting siRNA into the cell can also perform its target specific delivery making them useful for complex systemic administrations. Some examples have been discussed below:-

### Arginine Engrafted Biodegradable Polymer for the Systemic Delivery of siRNA for Gene Therapy Purposes

This is a bioreducible polymer of poly(disulfide amine) (ABP) used for efficient systemic delivery of siRNA to otherwise inaccessible tumor cells in the body [63]. The polymer is cystaminebisacrylamide-diaminohexane [poly(CBA-DAH)] whose primary amine groups are all attached to arginine residues. Arginine has good siRNA binding properties. In this case, the disulfide bonds remain stable in the oxidative extracellular environment but they decay in the reducing intracellular environment and thus, ensuring the release of siRNA in the cytosol of target cells. The positively charged arginine residues ensure that the polyplex penetrates into the cell.

The target specific delivery of siRNA results from the larger size of the polymeric nanoparticles (around 300 nm). The tumor microvessels have a larger pore size compared to the microvessels of the normal cells with tight junctions. This leads to the accessibility and accumulation of ABP into these tumors. This enhanced permeability and accumulation of the polyplex into the tumor cells is called EPR effect or enhanced permeability and retention effect. But the method fails to target tumors in kidneys and liver due to lack of EPR effect there [64, 65]

This is a very efficient, non-toxic and cost efficient method of systemic siRNA delivery in remote parts of body having tumors. The target specificity of the polyplex towards certain types of tumors can be increased by easily modifying it [66], making it prone to certain receptors on the tumor cell surface. This technology is used for plasmid DNA delivery also.

## Methods for Hepatocyte Specific Delivery of siRNA

Asialoglycoprotein (ASGP) receptors are present on the surface of liver cells and certain cancerous cells. The receptor binds to galactosyl residues in glycoproteins (N-Acetyl galactosamine) and endocytoses them [67]. The ASGP receptors are responsible for the clearing of the serum glycoproteins. The following two polymeric complexes make use of these ASGP receptors for hepatocyte specific delivery of siRNA.

(a) Biodegradable polypeptide based polymer conjugates [68]
This technique makes use of poly(amide) based polymers synthesized using a facile N-carboxy anhydride polymerization method given by Leuchs [69, 70]. The polymer is conjugated with N-acetylgalactosamine targeting ligands for a hepatocyte specific uptake. The mechanism for siRNA release in the cell takes place by the acidic pH dependent cationic group disintegration.

(b) Glycosylated RAFT polymers with PEG linkers [71]
This method makes use of Reversible Addition-fragmentation chain transfer (RAFT) polymerization technique to synthesize polymers (such as repeating unit of dimmers composed of 2-hydroxymethyl methacrylamide and 2-aminoethyl methacrylamide) that are glycosylated so as to be endocytosed by the same mechanism of clathrin mediated endocytosis by ASGP receptors present on hepatocyte. This technique aims to cure viral liver infections such as hepatitis A, B, C and E and liver related cancers.

## Targeted siRNA Delivery to Prevent Nitric Oxide Mediated Cell Death after Spinal Cord Injury

A spinal cord injury is ensued by a cascade of cellular and biochemical events that amplify the initial injury [72, 73]. The production of nitric oxide, superoxides and peroxynitrites by the damaged cells further damage the cellular proteins, DNA and membrane phospholipids leading to the complete death of the neurons in the spinal cord. The reactive oxygen and nitrogen species are produced by an inducible enzyme nitric oxide synthase (iNOS). The pro inflammatory M1 macrophages provoke the release of this enzyme [74-82]. This technology aims to obstruct the iNOS expression in M1 macrophages to attenuate the secondary injures occurring post primary spinal cord injuries using siRNA carried in chitosan nanoparticles [83].

Chitosan nanoparticles have high transfection efficiency, do not cause any cytotoxicity and studies have shown that chitosan nanoparticles attenuate lipid peroxidation thus helping in reducing post initial spinal cord injury damages [84]. The chitosan nanoparticles ensure the release of siRNA into the M1 macrophages by proton sponge effect preventing endosomal sequestration of siRNA [83].

The chitosan nanoparticles are conjugated with specific antibodies such as INFγ (interferon γ) so that they are phagocytosed by the Fc receptors present on the M1 macrophages. Fc receptors antibody receprtors present on the membranes of various immune cells like macrophages, neutrophils and B-lymphocytes, etc. This ensures a targeted delivery of siRNA to M1 macrophages. The method has been successfully tested *in-vivo* mice and in

future can help prevent chronic spinal cord injuries in humans thus improving the quality of life of patients with spinal cord injuries. Moreover, we may further apply such related technologies to prevent old age related degradation and ageing.

## Targeted siPLK1 Delivery Using Polymerosomes to Treat Lung Cancer

This method aimed to suppress the expression of polo like kinase 1 to cure orthotopic human lung cancer by delivering its specific siRNA (siPLK1) into the tumor cells[85]. It used cNGQGEQCc peptide with reversibly cross linked chimaeric polymerosomes cNGQ/RCCPs for target specific efficient delivery of siPLK1. The outer surface of the peptide is PEGylated. The cNGQ/RCCPs are co self assembled from poly(trimethylene carbonate-co-dithiolane-trimethylene carbonate)-b-polyethylenemine (PEG-P(TMC-DTC).PEI) asymmetric triblock copolymer [86].

It is a bioreducible complex rendering high transfection efficiency. The disulfide cross linking bonds keep the complex stable in the blood stream but disintegrate in the acidic environment of the cytosol thus easily releasing the siRNA [87].

**Table 2. Some more examples of siRNA polyplexes and their importance**

| S. No | siRNA polyplex | Details | Significance |
|---|---|---|---|
| 1. | Folic acid functionalized PEG- PEI superparamagnetic iron oxide nanoparticles for PD-L1 siRNA delivery [89] | Blocks PD-1/PD-L1 interaction on gastric cancer cells to provoke immune response, PD-l is overexpressed on gastric cancer cells | To treat gastric cancers |
| 2. | Folate PEG-siRNA lipopolyplexes [90] | Specifically targets the folate receptor expressing tumors | In the treatment of leukemia |
| 3. | Luminescent/magnetic PLGA based nanocomposites [91] | Its endocytosis is done via folate receptors, delivers the VEGF-shRNA | In the imaging and treatment of cancer by suppressing the expression of vascular endothelial growth factor (VEGF) |
| 4. | Fentanyl initiated polymers prepared by atom transfer radical polymerization(ATRP) [92] | Targets Mu opioid receptors | To treat neuronal disorders |
| 5. | Glycosylated polyaspartamide copolymers [93] | Targets the hepatocyte via ASGP receptors through glycosylated segment | To treat liver cancer |

The α3β1 integrins are over expressed on these lung cancer cells. The cNGQ peptide are picked up by these α3β1 integrin receptors causing the polymerosome's target specific

endocytosis by the tumor cells [88]. The technique has been succesfuly tested *in-vivo* on mice injected with the orthotopic lung cancer cells.

The majority of recent advances in polymeric delivery of DNA and siRNA make use of the natural physiological and biochemical aspects of the cell (such as cell surface receptors) for target specific efficient delivery. The methods for siRNA delivery can as well be applied to plasmid DNA delivery but vice-versa is not feasible in every case.

The targeted specific bioreducible polplexes are a remarkable example of man's ingenuity and unfailing spirit to find ways to survive against natural odds. They have wide therapeutic implications in not only curing cancers but also have potential to cure malfunctions like obesity, diabities, accidental injuries, neuropsychological disorders, ageing and old age related issues.

## REFERENCES

[1] Fabio Candotti et al. Gene therapy for adenosine deaminase–deficient severe combined immune deficiency: clinical comparison of retroviral vectors and treatment plans. *Blood*. 2012 Nov 1, 120(18).

[2] Guinn, BA; Mulherkar, R. International progress in cancer gene therapy, *Cancer Gene Ther*., *15* (2008) 765–775.

[3] Sridharan, K; Gogtay, NJ. Therapeutic nucleic acids: current clinical status, *Br. J. Clin. Pharmacol*., 82, (2016), 659–672.

[4] Saffari, M; Moghimi, HR; Dass, CR. Barriers to liposomal gene delivery: from application site to the target, Iran, *J. Pharm. Res*., 15, (2016), 3–17.

[5] Raisin, S; Belamie, E; Morille, M. Non-viral gene activated matrices for mesenchymal stem cells based tissue engineering of bone and cartilage, *Biomaterials*, 104, (2016), 223–237.

[6] Parlea, L; Puri, A; Kasprzak, W; Bindewald, E; Zakrevsky, P; Satterwhite, E; Joseph, K; Afonin, KA; Shapiro, BA. Cellular delivery of RNA nanoparticles, *ACS Comb. Sci*., 18, (2016), 527–547.

[7] Muller, LK; Landfester, K. Natural liposomes and synthetic polymeric structures for biomedical applications, *Biochem. Biophys. Res. Commun*., 468, (2015), 411–418.

[8] Kim, HJ; Kim, A; Miyata, K; Kataoka, K. Recent progress in development of siRNA delivery vehicles for cancer therapy, *Adv. Drug Deliv. Rev*., 104, (2016), 61–77.

[9] Badwaik, Vivek. D. Structure property relationship for *in vitro* siRNA delivery performance of 2-hydroxypropyl-β-cyclodextrin: PEG-PPG-PEG polyrotaxane vectors. *Biomaterials*, April. 84, 86-98.

[10] Xumein, Lu. Asymmetric polyplex nanocapsules loaded with photosentisizer for light assisted gene transfer. *Journal of photochemistry and photobiology, B:biology*. 2017 August.

[11] Berg, K; et al. Photochemical internalization (PCI): a technology for drug delivery *Methods Mol Biol*., 2010.

[12] Brinkhuis, RP; Rutjes, F; van Hest, JCM. Polymeric vesicles in biomedical applications, *Polym. Chem*., 2, (2011), 1449–1462.

[13] Liao, J; Wang, C; Wang, Y; Luo, F; Qian, Z. Recent advances in formation, properties, and applications of Polymersomes, Curr. *Pharm. Des*., *18*, (2012), 3432–3441.

[14] Rhim, T; Lee, KY. Exosome and Polymersome for potential Theranostic applications, *Macromol. Res*., 24, (2016), 577–586.

[15] Tan, Lunmei. Chitosan nanoparticle-based delivery of fused NKG2D–IL-21 gene suppresses colon cancer growth in mice. *Int J Nanomedicine*., 2017, 12, 3095–3107.

[16] Sim, GC; Radvanyi, L. The IL-2 cytokine family in cancer immunotherapy. *Cytokine Growth Factor Rev*., 2014, 25(4), 377–390. [PubMed].

[17] Floros, T; Tarhini, AA. Anticancer cytokines: biology and clinical effects of interferon-α, Interleukin (IL)-2, IL-15, IL-21, and IL-12. *Semin Oncol*., 2015, 42(4), 539–548. [PMC free article] [PubMed].

[18] Tian, Y; Zajac, AJ. IL-21 and T cell differentiation: consider the context. *Trends Immunol*., 2016, 37(8), 557–568. [PMC free article] [PubMed].

[19] Al-Chami, E; Tormo, A; Khodayarian, F; Rafei, M. Therapeutic utility of the newly discovered properties of interleukin-21. *Cytokine*., 2016, 82(6), 33–37. [PubMed].

[20] Tangye, SG. Advances in IL-21 biology – enhancing our understanding of human disease. *Curr Opin Immunol*., 2015, 34(3), 107–115. [PubMed].

[21] Leonard, WJ; Wan, CK. IL-21 signaling in immunity. *F1000Res*., 2016, 5 pii: F1000 Faculty Rev-224.[PMC free article] [PubMed].

[22] Chávez-Blanco; A; Chacón-Salinas; R; Dominguez-Gomez; G, et al. Viral inhibitors of NKG2D ligands for tumor surveillance. *Expert Opin Ther Targets*., 2016, 20(11), 1375–1387. [PubMed].

[23] Lanier, LL. NKG2D receptor and its ligands in host defense. *Cancer Immunol Res*., 2015, 3(6), 575–582. [PMC free article] [PubMed].

[24] Cerqueira, BB; Lasham, A; Shelling, AN; Al-Kassas, R. Nanoparticle therapeutics: technologies and methods for overcoming cancer. *Eur J Pharm Biopharm*., 2015, 97(Pt A), 140–151. [PubMed].

[25] Urbiola, K; Sanmartin, C; Fernandez, LB; Ilarduya, CT, de. Efficient Targeted gene delivery by a novel PAMAM/DNA dendriplex coated with hyaluronic acid. *Nanomedicine (Lond)*, 2014, Dec, 9(18), 2787-801.

[26] Mintzer, MA; Grinstaff, MW. Biomedical applications of dendrimers: a tutorial. *Chem. Soc. Rev*., 40(1), 173–190 (2011).

[27] Haensler, J; Szoka, FC. Polyamidoamine cascade polymers mediate efficient transfection of cells in culture. *Bioconjug. Chem*., 4(5), 372–379 (1993).

[28] Kukowska-Latallo, JF; Bielinska, AU; Johnson, J; Spindler, R; Tomalia, DA; Baker, JR. Efficient transfer of genetic material into mammalian cells using Starburst polyamidoamine dendrimers. *Proc. Natl Acad. Sci. USA*, 93(10), 4897–4902 (1996).

[29] Underhill, C. CD44, the hyaluronan receptor. *J. Cell. Sci*., 103, 293–298 (1992).

[30] Ito, T; Iida-Tanaka, N; Niidome, T; et al. Hyaluronic acid and its derivative as a multi-functional gene expression enhancer: protection from non-specific interactions, adhesion to targeted cells, and transcriptional activation. *J. Control. Release*, 112(3), 382–388 (2006).

[31] Hornof, M; De, La; Fuente, M; Hallikainen, M; Tammi, RH; Urtti, A. Low molecular weight hyaluronan shielding of DNA/PEI polyplexes facilitates CD44 receptor mediated uptake in human corneal epithelial cells. *J. Gene Med*., 10(1), 70–80 (2008).

[32] Wang, Y; Xu, Z; Zhang, R; Li, W; Yang, L; Hu, Q. A facile approach to construct hyaluronic acid shielding polyplexes with improved stability and reduced cytotoxicity. *Colloids Surf. B Biointerfaces*, 84(1), 259–266 (2011).

[33] Jiang, G; Park, K; Kim, J; Kim, KS; Hahn, SK. Target specific intracellular delivery of siRNA/PEI–HA complex by receptor mediated endocytosis. *Mol. Pharm*., 6(3), 727–737 (2009).

[34] Han, SE; Kang, H; Shim, GY; et al. Cationic derivatives of biocompatible hyaluronic acids for delivery of siRNA and antisense oligonucleotides. *J. Drug Target*., 17(2), 123–132 (2009).

[35] Yao, J; Fan, Y; Du, R; et al. Amphoteric hyaluronic acid derivative for targeting gene delivery. *Biomaterials*, 31(35), 9357–9365, (2010).

[36] Needham, CJ; Williams, AK; Chew, SA; Kasper, FK; Mikos, AG. Engineering a polymeric gene delivery vector based on poly (ethylenimine) and hyaluronic acid. *Biomacromolecules*, 13(5), 1429–1437 (2012).

[37] Surace, C; Arpicco, S; Dufay-Wojcicki, A; et al. Lipoplexes targeting the CD44 hyaluronic acid receptor for efficient transfection of breast cancer cells. *Mol. Pharm*., 6(4), 1062–1073 (2009).

[38] Han, M; Lv, Q; Tang, XJ; et al. Overcoming drug resistance of MCF-7/ADR cells by altering intracellular distribution of doxorubicin via MVP knockdown with a novel siRNA polyamidoamine-hyaluronic acid complex. *J. Control. Release*, 163(2), 136–144 (2012).

[39] Kim, J; Lee, YM; Kim, H; Park, D; Kim, J; Kim, WJ. Phenylboronic acid-sugar grafted polymer architecture as a dual stimuli-responsive gene carrier for targeted anti-angiogenic tumor therapy. *Biomaterials*., 2016 Jan, 75, 102-111.

[40] Springsteen, G; Wang, B. A detailed examination of boronic acid-diol complexation, *Tetrahedron*, 58, (2002) 5291-5300.

[41] Yan, J; Springsteen, G; Deeter, S; Wang, B. The relationship among pKa, pH, and binding constants in the interactions between boronic acids and diols - it is not as simple as it appears, *Tetrahedron*, 60, (2004), 11205-11209.

[42] Chen, L; Zhao, X; Lin, Y; Su, Z; Wang, Q. Dual stimuli-responsive supramolecular hydrogel of bionanoparticles and hyaluronan, *Polym. Chem*., 5, (2014), 6754e6760.

[43] Liu, H; Li, Y; Sun, K; Fan, J; Zhang, P; Meng, J; et al., Dual-responsive surfaces modified with phenylboronic acid-containing polymer brush to reversibly capture and release cancer cells, *J. Am. Chem. Soc*., 135, (2013), 7603-7609.

[44] Cambre, JN; Sumerlin, BS. Biomedical applications of boronic acid polymers, *Polymer*, 52, (2011) 4631-4643.

[45] Nishiyabu, R; Kubo, Y; James, TD; Fossey, JS. Boronic acid building blocks: tools for sensing and separation, *Chem. Commun*., 47, (2011), 1106-1123.

[46] Gao, H; Shi, W; Freund, LB. Mechanics of receptor-mediated endocytosis, *Proc. Natl. Acad. Sci. U. S. A.*, 102, (2005), 9469-9474.

[47] Goldstein, JL; Brown, MS; Anderson, RG; Russell, DW; Schneider, WJ. Receptor-mediated endocytosis: concepts emerging from the LDL receptor system, *Annu. Rev. Cell Biol*., 1, (1985) 1-39.

[48] Deshayes, S; Cabral, H; Ishii, T; Miura, Y; Kobayashi, S; Yamashita, T; et al., Phenylboronic acid-installed polymeric micelles for targeting sialylated epitopes in solid tumors, *J. Am. Chem. Soc*., 135, (2013), 15501-15507.

[49] Djanashvili, K; Frullano, L; Peters, JA. Molecular recognition of sialic acid end groups by phenylboronates, *Chem. Eur. J*., 11, (2005), 4010-4018.

[50] Matsumoto, A; Cabral, H; Sato, N; Kataoka, K; Miyahara, Y. Assessment of tumor metastasis by the direct determination of cell-membrane sialic acid expression, *Angew. Chem. Int. Ed*., 49, (2010), 5494-5497.

[51] Kendall, RL; Thomas, KA. Inhibition of vascular endothelial cell growth factor activity by an endogenously encoded soluble receptor, *Proc. Natl. Acad. Sci. U. S. A.*, 90, (1993), 10705-10709.

[52] Kim, WJ; Yockman, JW; Jeong, JH; Christensen, LV; Lee, M; Kim, YH, et al., Anti-angiogenic inhibition of tumor growth by systemic delivery of PEI-g-PEG-RGD/pCMV-sFlt-1 complexes in tumor-bearing mice, *J. Control. Release*, 114, (2006), 381-388.

[53] Millauer, B; Shawver, LK; Plate, KH; Risaui, W; Ullrich, A. Glioblastoma growth inhibited *in vivo* by a dominant-negative Flk-1 mutant, *Nature*, 367, (1994), 576-579.

[54] Fan, B; Kang, L; Chen, L; Sun, P; Jin, M; Wang, Q; Bae, YH; Huang, W; Gao, Z. Systemic siRNA Delivery with a Dual pH-Responsive and Tumor-targeted Nanovector for Inhibiting Tumor Growth and Spontaneous Metastasis in Orthotopic Murine Model of Breast Carcinoma. *Theranostics*., 2017 Jan 1, 7(2), 357-376

[55] Taghavi, S; HashemNia, A; Mosaffa, F; Askarian, S; Abnous, K, Ramezani, M. Preparation and evaluation of polyethylenimine-functionalized carbon nanotubes tagged with 5TR1 aptamer for targeted delivery of Bcl-xL shRNA into breast cancer cells. *Colloids Surf B Biointerfaces*., 2016 Apr 1, 140, 28-39.

[56] Taghavi, S; Nia, AH; Abnous, K; Ramezani, M. Polyethylenimine-functionalized carbon nanotubes tagged with AS1411 aptamer for combination gene and drug delivery into human gastric cancer cells. *Int J Pharm.*, 2017 Jan, 10, 516 (1-2), 301-312.

[57] Shahidi-Hamedani, N; Shier, WT; Moghadam, Ariaee F; Abnous, K; Ramezani, M. Targeted gene delivery with noncovalent electrostatic conjugates of sgc-8c aptamer and polyethylenimine. *J Gene Med*., 2013 Jun-Jul, 15(6-7), 261-9.

[58] Mokhtarzadeh, A; Parhiz, H; Hashemi, M; Ayatollahi, S; Abnous, K; Ramezani, M. Targeted Gene Delivery to MCF-7 Cells Using Peptide-Conjugated Polyethylenimine. *AAPS Pharm Sci Tech*., 2015 Oct, 16(5), 1025-32.

[59] Zhao, QQ[1]; Hu, YL; Zhou, Y; Li, N; Han, M; Tang, GP; Qiu, F; Tabata, Y; Gao, JQ. Gene-carried hepatoma targeting complex induced high gene transfection efficiency with low toxicity and significant antitumor activity. *Int J Nanomedicine*., 2012, 7, 3191-202.

[60] Lu, Y[1]; Jiang, C[2,3]. Brain-Targeted Polymers for Gene Delivery in the Treatment of Brain Diseases. *Top Curr Chem (Cham)*., 2017 Apr, 375(2), 48.

[61] Gary, DJ; Puri, N; Won, YY. Polymer-based siRNA delivery: perspectives on the fundamental and phenomenological distinctions from polymer-based DNA delivery. *J Control Release*, 2007, 121(1-2), 64-73.

[62] Spagnou, S; Miller, AD; Keller, M. Lipidic carriers of siRNA: differences in the formulation, cellular uptake, and delivery with plasmid DNA. *Biochemistry*, 2004, 43(42), 13348-56.

[63] Beloor, J[1]; Choi, CS; Nam, HY; Park, M; Kim, SH; Jackson, A; Lee, KY; Kim, SW; Kumar, P; Lee, SK. Arginine-engrafted biodegradable polymer for the systemic delivery of therapeutic siRNA. *Biomaterials*., 2012 Feb, 33(5), 1640-50

[64] Matsumura, Y; Maeda, H. A new concept for macromolecular therapeutics in cancer chemotherapy: mechanism of tumoritropic accumulation of proteins and the antitumor agent smancs. *Cancer Res*, 1986, 46(12 Part 1), 6387-92.

[65] Bundgaard, M. Transport pathways in capillaries-in search of pores. *Annu Rev Physiol*, 1980, 42(1), 325-36.

[66] Nam, HY; Kim, J; Kim, S; Yockman, JW; Kim, SW; Bull, DA. Cell penetrating peptide conjugated bioreducible polymer for siRNA delivery. *Biomaterials*, 2011, 32(22), 5213-22

[67] Shim, G; Lee, S; Choi, H; Lee, J; Kim, CW; Byun, Y; Oh, YK. Nanomedicines for Receptor-Mediated Tumor Targeting. *Recent Patents on Nanomedicine*, 2011, 1 (2), 138-148.

[68] Barrett, SE[1]; Guidry, EN[2]. Liver-Targeted SiRNA Delivery Using Biodegradable Poly(amide) Polymer Conjugates. *Methods Mol Biol*., 2016, 1364, 11-25.

[69] Leuchs, H. Ueber die Glycin-carbonsäure, *Ber. Dtsch. Chem. Ges*., 39 (1), (1906), 857–861.

[70] Leuchs, H; Geiger, W. Über die Anhydride von α-Amino-N-carbonsäuren und die von α-Aminosäuren, *Ber. Dtsch. Chem. Ges*., 41 (2), (1908), 1721–1726.

[71] Williams, EGL; Hutt, OE; Hinton, TM; Larnaudie, SC; Le, T; MacDonald; JM; Gunatillake, P; Thang, SH; Duggan, PJ. Glycosylated Reversible Addition-Fragmentation Chain Transfer Polymers with Varying Polyethylene Glycol Linkers Produce Different Short Interfering RNA Uptake, Gene Silencing, and Toxicity Profiles. *Biomacromolecules*., 2017 Nov 9.

[72] Gao, W, LiJ. Targeted siRNA delivery reduces nitric oxide mediated cell death after spinal cord injury. *J Nanobiotechnology*., 2017 May 8, 15(1), 38.

[73] Borgens, RB; Liu-Snyder, P. Understanding secondary injury. *Quar Rev Biol*., 2012, 87, 89–127. doi: 10.1086/665457. [PubMed] [Cross Ref].

[74] Kong, Q; Lin, CL. Oxidative damage to RNA: mechanisms, consequences, and diseases. *Cell Mol Life Sci*., 2010, 67, 1817–1829. doi: 10.1007/s00018-010-0277-y. [PMC free article] [PubMed] [Cross Ref].

[75] Hall, ED. Antioxidant therapies for acute spinal cord injury. *Neurotherapeutics*., 2011, 8, 152–167. doi: 10.1007/s13311-011-0026-4. [PMC free article] [PubMed] [Cross Ref].

[76] Kong, X; Gao, J. Macrophage polarization: a key event in the secondary phase of acute spinal cord injury. *J Cell Mol Med*., 2016, 8(2), 941–954. [PMC free article] [PubMed].

[77] David, S. Mechanisms underlying macrophage polarization in spinal cord injury—detrimental and beneficial influences on recovery. *FASEB J*., 2015, 29, 210–214.

[78] Kigerl, KA; Gensel, JC; Ankeny, DP; Alexander; JK; Donnelly; DJ; Popovich, PG. Identification of two distinct macrophage subsets with divergent effects causing either neurotoxicity or regeneration in the injured mouse spinal cord. *J Neurosci*., 2009, 29, 13435–13444. doi: 10.1523/JNEUROSCI.3257-09.2009. [PMC free article][PubMed] [Cross Ref].

[79] Liu; D; Ling; X; Wen; J; Liu; J. The role of reactive nitrogen species in secondary spinal cord injury: formation of nitric oxide, peroxynitrite, and nitrated protein. *J Neurochem*., 2000, 75, 2144–2154. doi: 10.1046/j.1471-4159.2000.0752144.x. [PubMed] [Cross Ref].

[80] Liu, D; Bao, F; Prough, DS; Dewitt, DS. Peroxynitrite generated at the level produced by spinal cord injury induces peroxidation of membrane phospholipids in normal rat cord: reduction by a metalloporphyrin. *J Neurotrauma*., 2005, 22, 1123–1133. doi: 10.1089/neu.2005.22.1123. [PubMed] [Cross Ref].

[81] Scott, GS; Szabó, C; Hooper, DC. Poly(ADP-ribose) polymerase activity contributes to peroxynitrite-induced spinal cord neuronal cell death *in vitro*. *J Neurotrauma*., 2004, 21, 1255–1263. doi: 10.1089/neu.2004.21. 1255. [PubMed] [Cross Ref].

[82] Xiong, Y; Rabchevsky, AG; Hall, ED. Role of peroxynitrite in secondary oxidative damage after spinal cord injury. *J Neurochem*., 2007, 100, 639–649. doi: 10.1111/j.1471-4159.2006.04312.x. [PubMed] [Cross Ref].

[83] Isaksson, J; Farooque, M; Olsson, Y. Improved functional outcome after spinal cord injury in iNOS-deficient mice. *Spinal Cord*., 2005, 43, 167–170. doi: 10.1038/sj.sc.3101672. [PubMed] [Cross Ref].

[84] Maggio, DM; Chatzipanteli, K; Masters, N; Patel, SP; Dietrich, WD; Pearse, DD. Acute molecular perturbation of inducible nitric oxide synthase with an antisense approach enhances neuronal preservation and functional recovery after contusive spinal cord injury. *J Neurotrauma*., 2012, 29, 2244–2249. doi: 10.1089/neu.2012.2371. [PMC free article] [PubMed] [Cross Ref].

[85] Zou, Y; Zheng, M; Yang, W; Meng, F; Miyata, K; Kim, HJ; Kataoka, K; Zhong, Z. Virus-Mimicking Chimaeric Polymersomes Boost Targeted Cancer siRNA Therapy *In Vivo*. *Adv Mater*., 2017 Nov, 29(42).

[86] Zou, Y; Fang, Y; Meng, H; Meng, F; Deng, C; Zhang, J; Zhong, Z. *J. Controlled Release* 2016, *244*, 326.

[87] a) Yang, W; Zou, Y; Meng, F; Zhang, J; Cheng, R; Deng, C; Zhong, Z. *Adv. Mater*. 2016, *28*, 8234, b) Liao, C; Chen, Y; Yao, Y; Zhang, S; Gu, Z; Yu, X; *Chem. Mater*. 2016, *28*, 7757, c) Talelli, M; Barz, M; Rijcken, CJ; Kiessling, F; Hennink, WE; Lammers, T. *Nano Today* 2015, *10*, 93, d) Li, YL; Zhu, L; Liu, Z; Cheng, R; Meng, F; Cui, JH; Ji, SJ; Zhong, Z. *Angew. Chem., Int. Ed.*, 2009, *48*, 9914.

[88] Lau, D; Guo, L; Liu, R; Marik, J; Lam, K. *Lung Cancer* 2006, *52*, 291.

[89] Luo, X; Peng, X; Hou, J; Wu, S; Shen, J; Wang, L. Folic acid-functionalized polyethylenimine superparamagnetic iron oxide nanoparticles as theranostic agents for magnetic resonance imaging and PD-L1 siRNA delivery for gastric cancer. *Int J Nanomedicine*., 2017 Jul 26, 12, 5331-5343.

[90] Lee, DJ; Kessel, E; Lehto, T; Liu, X; Yoshinaga, N; Padari, K; Chen, YC; Kempter, S[7]; Uchida, S[3,4]; Rädler, JO[2,7]; Pooga, M[5]; Sheu, MT[6]; Kataoka, K[3,8]; Wagner, E[1,2]. Systemic Delivery of Folate-PEG siRNA Lipopolyplexes with Enhanced Intracellular Stability for *In Vivo* Gene Silencing in Leukemia. *Bioconjug Chem*., 2017 Sep 20, 28(9), 2393-2409.

[91] Shen, X; Li, T; Chen, Z; Geng, Y; Xie, X; Li, S; Yang, H; Wu, C; Liu, Y. Luminescent/magnetic PLGA-based hybrid nanocomposites: a smart nanocarrier system fortargeted codelivery and dual-modality imaging in cancer theranostics. *Int J Nanomedicine*., 2017 Jun 6, 12, 4299-4322.

[92] Cohen-Karni, D; Kovaliov, M; Li, S; Jaffee, S; Tomycz, ND; Averick, S. Fentanyl Initiated Polymers Prepared by ATRP for Targeted Delivery. *Bioconjug Chem*., 2017 Apr 19, 28(4), 1251-1259.

[93] Cavallaro, G; Farra, R; Craparo, EF; Sardo, C; Porsio, B; Giammona, G; Perrone, F; Grassi; M; Pozzato, G; Grassi, G; Dapas, B. Galactosylated polyaspartamide copolymers for siRNA targeted delivery to hepatocellular carcinoma cells. *Int J Pharm*., 2017 Jun 20, 525(2), 397-406.

In: Advances in Polymers for Biomedical Applications ISBN: 978-1-53613-612-8
Editors: Deepak Pathania and Bhuvanesh Gupta 

*Chapter 9*

# CHITOSAN CONTAINING BIOMATERIALS FOR TISSUE ENGINEERING APPLICATIONS

***Mihaela Baican[1] and Cornelia Vasile[2,*]***
[1]Pharmaceutical Physics Department,
"Grigore T. Popa" Medicine and Pharmacy University,
Iaşi, Romania
[2]Physical Chemistry of Polymers Department,
"P. Poni" Institute of Macromolecular Chemistry,
Iaşi, Romania

## ABSTRACT

Chitosan, an aminopolysaccharide with strong positive electrical charge, is of great interest as a biomaterial for tissue engineering. Chitosan-based biomaterials show a wide variety of physico-chemical characteristics as: they are non-toxic, biocompatible, bioabsorbable, biodegradable, arise from renewable resources, offering also antimicrobial, haemostatic, analgesic and stimuli responsiveness activities. This chapter reviews the applications of the chitosan containing biomaterials, as hydrogel, powder, porous scaffold, sponge, film, fiber, and nanoparticles in tissue engineering. Tissue engineering, a multidisciplinary research, is devoted to the reconstructing or regenerating damaged biological tissue in clinical/pathological situations, such as lesions, infections, traumas, and sequelae. Chitosan – containing systems exhibit affinity for biomolecules, are promising biomaterials to develop biological substitutes capable to restore, maintain, or to improve the organs and tissues function. Such biomaterials in combination with cells or bioactive molecules (such as cytokines and growth factors) can promote cell proliferation, differentiation, and migration.

**Keywords**: chitosan, wound healing, bone tissue engineering

* Corresponding Author Email: cvasile@icmpp.ro.

## ABBREVIATIONS

ACF-HS powder of alginate, chitin/chitosan and fucoidan
ACL cells cells from the human ligaments
A-dECM adipose-derived extracellular matrix
Ag-NP silver nanoparticles
ALP alkaline phosphatase
Az-CS-LA chitosan containing both azide, and lactose groups
BCP biphasic calcium phosphate
bFGF fibroblast growth factor
BMP-2 bone morphogenetic protein
CA chitosan-alginate
CaP calcium phosphate
CNT carbon nanotubes
CS chitosan
CX diacetate of clorhexidine
EGF epidermal growth factor
FDA Food and Drug Administration
Gel/CS gelatine-chitosan
HA hyaluronic acid
HANa sodium hyaluronate HA
HaCaT human keratinocyte
HAp hydroxyapatite
LBL layer-by-layer deposition method
MRSA meticycline
OCP osteocalcium phosphate
PEC polyelectrolyte complex
PEGDA diacrylate polyethylene glycol
PEO polyethylene oxide
PET polyethylene terephthalate
PHB poly(3-hydroxybutyrate)
PLGA Poly-(DL-lactide-co-glycolide)
PMMA poly(methacrylate)
PMN polymorphonuclear leukocytes
PNIPAM poly(N-isopropyl acrylamide)
PVA polyvinyl alcohol
QCS quaternary chitosan
ROS oxygen reactive species
Saos-2 cells Sarcoma osteogenic cells
$scCO_2$ supercritical carbon dioxide
SCS sulphadiazine-chitosan conjugate
sHA sintered hydroxyapatite
TCP tricalcium phosphate
VEGF vascular growth factor

## 1. INTRODUCTION

The term of tissue engineering describes a multidisciplinary domain including biology, medicine, and engineering. Its purpose is to improve the quality of the human life by restoring, maintaining or improving the function of the tissues or of the organs (van Winterswijk and Nout, 2007). This purpose could be attained by *in vitro* growth of the tissues, starting from donor cells. The success of the tissue engineering is related to the importance of imitation of the composition and the structure of the original tissue.

The domain of the tissue engineering deals with the study of the technical aspects of the regenerative medicine, in particular with restoring the function of the damaged tissues, by using a scaffold matrix obtained from a biomaterial (e.g.: any implantable scaffold, used for assuring the environment necessary for developing the natural tissue and for restarting its function) (Williams, 2006). In bone tissue engineering, there have been often used as biomaterials, the autografts and the allografts. However, these ones present a series of limitations due to the induction of a possible infection at the place of the implant, to the rejection by the organism in the case of the allografts transplant and to the small quantity of the grafting material (Lieder, 2013; Fleming et al., 2000; Wheeler and Enneking, 2005). Frequently, there are used inorganic, natural and/or synthetic biomaterials and their composites, bioactive materials that could be modified from the chemically point of view in order to obtain the characteristics necessary for being used in a certain type of application and to be resorbable and bioactive (Rezwan et al., 2006; Hench, 2002). Chitosan is an important component in these materials.

## 2. CHITOSAN ACTIVITIES AND PROPERTIES USEFUL FOR APPLICATIONS IN TISSUE ENGINEERING

Chitosan is a natural polymer, characterized by the presence of primary amines groups along its backbone. Such a structure allows this polysaccharide to present not only very good physico-chemical properties, but also particular interactions with the proteins, the cells, and the living organisms. Chitosan, obtained by chitin deacetylation, presents important properties of hydrophilicity, nontoxicity, biocompatibility, and biodegradability. In the meantime, this polycationic (after protonation in acid conditions) polysaccharide is characterized by an improved solubility in respect with that of chitin, this allowing its easy processing, in very mild conditions, in a wide variety of forms. Soft gels and thin films, as well as sponges and nanofibers are easily prepared, with a good control of the composition and of the morphology. The porous structures, membranes or particles are obtained by lyophilisation of the chitosan solution or of the gels, the medium pores size being varied by controlling the freezing temperature and the lyophilisation rate (Vereştiuc, 2006).

Chitosan (CS), as well as the alginates, the collagen and the hyaluronic acid are characterized by biological and chemical properties, similar to those corresponding to the natural tissues. In the same time, it was proved that the chitosan degrades *in vivo*, by hydrolysis mediated especially by the lysozyme (Nordtveil et al., 1994).

Some of the chitosan properties offer unique opportunities for its applications in the biomedical field. The presence of the protonable amino groups from the *D*-glucosamine

residues is responsible for a series of these properties. For example, chitosan mucoadhesiveness could be explained by the presence of the negatively charged residues from the mucin, the glycoprotein that composes the mucus. In acidic medium, the amino groups of the chitosan are positively charged, thus interacting with the mucin.

The *haemostatic activity* of the chitosan could be, also, related to the presence of the positive charges from the chitosan backbone. The membranes of the red cells negatively charged interact with the positively charged groups of the chitosan. Due to its positive charges, the chitosan could interact also with the negative parts of the cellular membranes, thus explaining the improved permeability properties of this polysaccharide.

As it concerns the *antimicrobial activity* of the chitosan, two mechanisms have been proposed to explain it. The first mechanism refers to the fact that the positive charges of the chitosan could interact with the negative charges of the groups found at the surface of the cell membranes, consequently affecting their permeability. This fact could inhibit the penetration of the essential substances in cells and/or the exit of the solvents out from the cell. The second mechanism implies the binding of chitosan to the DNA (by the protonated amino groups), thus inhibiting the synthesis of the microbial RNA. In fact, the antimicrobial properties of the chitosan could be a result between the combination of these two mechanisms (Sudarshan et al., 1992; Chung and Chen, 2008).

It is known that some chitosan derivatives with quaternary ammonium groups present antimicrobial properties (Jayakamur et al., 2012). Electrospun photo-crosslinked tissues that contain quaternary chitosan (QCS) proved to be efficient in the growth inhibition of gram-positive and gram-negative bacteria (Ignatova et al., 2007). In meantime, tissues obtained from nanofibrilar photo-crosslinked QCS/polyvinyl alcohol (PVA) present good antibacterial activities against gram-negative and gram-positive bacteria (Ignatova et al., 2006). These characteristics prove the high potential of CS-based materials for being applied in obtaining wound dressings.

Factors related both on the chitosan molecule and/or its environment could influence the antimicrobial properties of the systems based on chitosan, such as: molecular weight, deacetylation degree, ionic strength, and pH of the dissolution medium. In the same time, the physical shape of the chitosan-based materials (e.g., in form of films, hydrogels, coating layers, in solution, or being mixed with other materials etc.) could induce different antimicrobial properties (Tianhong et al., 2011). In Table 1 are presented the main effects of several systems based on chitosan against various microorganisms, evidenced by *in vitro* experiments.

Polycationic nature of chitosan explains also its *analgesic effects*. The amino groups of the *D*-glucosamine residues can protonate in the presence of the ions that are released in the inflammed zone, thus leading to an analgesic effect (Okamoto et al., 2002). Chen et al. evaluated the nanofibrous membranes produced from chitosan/collagen composites, known for their beneficial effects on the wounds healing. It was proved that these membranes accelerate the wound healing, inducing the cellular migration and proliferation. The studies realized on animals proved that these membranes are more efficient than commercial chitosan sponges (Chen et al., 2008).

Biomaterials used to produce dressings should *be bio-compostable and to promote the increase of the derma and epidermis layers.*

**Table 1. Antimicrobial effects of the chitosan based systems**

| Studied system | Tested microorganisms | Main results | Ref. |
|---|---|---|---|
| Chitosan powder | *E. coli, Pseudomonas aeruginosa, Enterococcus faecalis* and *Staphylococcus saprophyticus* | Effective antimicrobial effect | (Andres et al., 2007) |
| Chitosan solution | *Staphylococcus aureus* | - Chitosan led to multiple modifications in the expression of the bacteria genes<br>- Binding chitosan to the teichoic acid determined bacteria death | (Raafat et al., 2008) |
| Chitosan and chitosan oligomer | Gram-positive and Gram-negative bacteria | Chitosan generally presented bactericide effects, stronger for Gram-positive bacteria than for Gram-negative ones | (No, 2002) |
| Chitosan *N*-carboxybutil | Gram-positive, Gram-negative bacteria and *Candidaspp*. | - Active, especially, against *Candida* Gram-positive bacteria<br>- Without bactericide activity for streptococcus and enterococcus | (Muzzarelli et al., 1990) |
| Solutions of chitosan chloride, chitosan carboxymethyl, chitosan oligosaccaharide and *N*-acetyl-*D*-glucosamine | *Candida albicans, Candida krusei* and *Candida glabrata* | Antifungal activity decreases with the decrease in the molecular weight and with the increased masking of the amino protonated groups by the functional groups | (Seyfarth et al., 2007) |
| Derivatives of chitosan tiazolidinone | *E. coli, Shigella dysenteriae, P. aeruginosa* and *Bacillus subtilis* | Better antimicrobial activity when compared with Schiff bases of chitosan | (Kulkarni et al., 2005) |
| Chitosan hydrolysate | *Bacillus cereus, E. coli, S. aureus, P. aeruginosa, Salmonella enterica* and *Saccharomyces cerevisiae* | Strong activity at 100 ppm against the pathogens | (Tsai et al., 2004) |
| Chitosan film charged with thyme oil | *E. coli, Klebsiella pneumoniae, P. aeruginosa* and *S. aureus* | Antimicrobial activity for all the tested microorganisms | (Altiok et al., 2010) |
| Chitosan hydrochloride, chitosan 5-methyl-pyrolidinone | *S. aureus, Staphylococcus epidermidis, P. aeruginosa, C. albicans* and *Aspergillus niger* | Antimicrobial activity against bacteria and *C. albicans* | (Rossi et al., 2007) |
| Chitosan incorporated with polyphosphate and silver | *S. aureus* and *P. aeruginosa* | Complete destruction of *P. aeruginosa* and of > 99,99% for *S. aureus* | (Ong et al., 2008) |
| Chitosan functionalized with arginine | *Pseudomonas fluorescens* and *E. coli* | At concentrations of 5000 mg/l, 6%- and 30%-chitosan substituted with arginine, there have been destroyed 2.7 logs and 4.5 logs from *P. fluorescens* and, respectively, 4.8 logs and 4.6 logs from *E. Coli*, in 4 h | (Tang et al., 2010) |
| Chitosan hydrogel | *P. aeruginosa, E. coli, S. aureus* and *Fusarium solani* | Excellent antimicrobial/antifungal activities | (Li et al., 2010) |

As it concerns with the chitosan *biodegradability*, it has to mention that this polycation is not only a polymer which contains amino groups, but also a polysaccharide that contains glycosidic bonds which could be broken. Chitosan is degraded *in vivo* by some proteases and, principally, by lysosome. Degradation rate of chitosan is firstly related to its deacetylation degree, but also to the distribution of the *N*-acetyl *D*-glucosamine residues and to the chitosan molecular weight (Aiba, 1992; Tomihata and Ikada, 1997; Zhang and Neau, 2001).

Due to all these mentioned properties, it is not surprising that this polymer is tested for a lot of biomedical and pharmaceutical applications, especially for sutures, dental and bone implants, as well as for artificial skin (Rinaudo, 2006). The applied *in vitro* and *in vivo* tests proved the good biocompatibility of chitosan, this material being approved by Food and Drug Administration (FDA) for being used in wound healing (Wedmore, 2006).

The chitosan *compatibility* with the physiological environment depends on the preparation method (the residual proteins could lead to allergenic reactions). Chitosan proved to be more cytocompatible *in vitro*, when compared with chitin. It is known that higher the number of positive charges, higher the interaction between cells and chitosan, this fact leading to an improved biocompatibility. Some chemical modifications of the chitosan could, however, induce toxicity (Dash, 2011).

Chitosan-based structures are characterized by good properties for the development of hepatocyte cultures, regeneration of articular cartilage and, if it is combined with inorganic materials, even for bone reconstruction (Wang et al., 2005; Di Martino et al., 2005).

Monomeric unit *N*-acetyl-*D* glucosamine from chitosan is found also in hyaluronic acid, an extracellular macromolecule with important role in wound healing. That is why it is expected that this natural polymer be adequate for use in applications related to the quick skin regeneration and to accelerate wound healing.

It is also important to mention that the incorporation into chitosan of a fibroblastic growth factor (bFGF) accelerates the healing (Khor and Lim, 2003). Incorporation of the antimicrobial agents such as garlic oil, potassium sorbate and nisin into chitosan structure is another strategy used for wound healing; this combination proved to be efficient in controlling *Pseudomonas Aeruginosa* and *Staphyloccocus Aureus* from cellular cultures (Pranoto et al., 2005). The plant extracts are also considered as being natural antimicrobials, being characterized by a high capacity to heal the wounds. That is why, elaboration of systems based on chitosan, in which plant extracts is incorporated has been also developed (Qin et al., 2013).

The polyelectrolyte complex (PEC) formed by chitosan and alginates has also a wound healing potential, this one being used in tissue engineering (Rinaudo, 2006). PEC-chitosan-alginate system is water insoluble, biodegradable, but it is characterized by an increased stability at variable pH and has a much higher efficiency for controlled release, when compared with chitosan or alginate. The wound treated with such a system heals after 14 days after the surgical intervention; the epidermis presents a keratinized surface, with a normal thickness (Li and Zhang, 2005).

An interesting application refers to a system of chitosan glycerophosphate mixed with calcium phosphate and citric acid that forms an injectable system which hardens itself and that can be used as a filling material, or for bone repair (Rinaudo, 2006).

## 3. CHITOSAN-BASED PRODUCTS USED IN TISSUE ENGINEERING

Because chitosan is characterized by excellent basic properties for applications as bioactive coatings and scaffolds in tissue engineering, this natural polymer was used in various medical domains. As it was already mentioned, in order to be used in different systems, chitosan must be processed in various forms, such as: soft gels, thin films, nanofibers, sponges (Di Martino et al., 2005), and also it can be combined with other biomaterials. *Chitosan membranes* have been prepared by film casting method. Their bioactivity and its surface properties strongly depend on those of the starting material (Chatelet, 2001). A higher degree of deacetylation is associated with an increased wettability, a higher crystallinity degree, improved tensile strength and elasticity modulus, higher adsorption of negatively charged proteins and decreased surface roughness (Tomihata and Ikada, 1997; Amaral, 2007). The appropriate selection of the substrate for the casting solution procedure determines the final crystallinity degree. The crystal structure is strongly influenced by the substrate surface structure (Uygun, 2010). The materials based on chitosan with a deacetylation degree of approximately 50% are soluble in aqueous solutions. In order to improve their stability, the crosslinking is necessary (Sannan, 1976).

Before being used in experiments that imply cell cultures and animal models, the chitosan membranes need sterilization. It was found that the most used sterilization methods could induce chemical modifications in polymer structure, finally affecting its biological performance (Lim, 1998; Rao and Sharma, 1995; Lim, 1999). Thus, autoclaving and sterilization by heating lead to the molecular weight decrease and negatively affect the solubility in aqueous media (Rao and Sharma, 1995; Lim, 1999). Sterilization with gamma radiations and with ethylene oxide is associated with chain scission, thus leading to the decrease in mechanical properties and to the increase in degradation susceptibility (Azuma et al., 2014; França et al., 2013; Mayol et al., 2014).

### 3.1. 3D Chitosan-Based Scaffolds

The implantable scaffolds have to fulfil a series of properties such as: the compatibility with the host environment, adequate mechanical properties, as well as the ability of wound healing or of tissue replacement (Dutta et al., 2011). In the same time, the scaffold has not to induce acute or chronic responses, it has to be biodegradable (case in which the healed tissue is replaced by the biomaterial), to present surface properties which allow cell attachment, their differentiation and proliferation, and it is necessary that this one could be processed in a wide variety of forms (Zhu et al., 2005). Due to all its properties above discussed, the chitosan proved to be a very useful material for preparing such systems. Throughout the time, several methods have been developed to obtain 3D scaffolds from chitosan hydrogels and sponges.

#### *3.1.1. Chitosan Hydrogels*

Hydrogels are networks of polymer chains that are sometimes found as colloidal gels in which water is the dispersion medium. The high water content of the hydrogels confers them a good compatibility with most living tissues. Moreover, they are soft and flexible; therefore

the deterioration of the surrounding tissue is reduced during and after their implantation. The mechanical properties of the hydrogels are similar to those corresponding to the soft tissues in the body, this fact making the hydrogels to assure both the functional and morphological characteristics of the tissue which should be repaired.

Three types of chitosan hydrogels that present reversible or irreversible gelation have been developed. Chitosan hydrogels could be formed by physical association, bounding through metallic ions or by complexation, and by irreversible chemical crosslinking (Dash et al., 2011).

### 3.1.1.1. Chitosan Hydrogels Formed by Physical Association

The hydrogels are formed by reversible interactions of non-covalent nature, as electrostatic, hydrophobic, hydrogen bonds that manifest between the polymeric chains (Berger et al., 2004; Boucard et al., 2005) (Scheme 1). These interactions depend on a series of parameters, such as: pH, concentration and temperature. These hydrogels are not very stable, and suffer reversible gelation. Wettability of these hydrogels could be adjusted by modifying the nature and the quantity of each component, thus increasing or decreasing the number of interactions.

Chitosan has gel-forming capability, by itself, without any additive. The process is based on neutralization of the amino groups of chitosan and on inhibiting the repulsion between its chains.

Gels containing chitosan could be obtained also by its mixing with other non-ionic water soluble polymers, (i.e., polyvinyl alcohol PVA) (Berger et al., 2004; Cascone et al., 1999). Thermosensitive chitosan hydrogels could be obtained by mixing chitosan with polyol salts (i.e., disodic salt of glycerol phosphate). Chitosan structures could be modified in order to form hydrogels by physical association; in this way, the grafted copolymer chitosan-*g*-polyethylene glycol is capable of self-organization in function of temperature, stable hydrogels being formed (Dash et al., 2011).

The preparation of the physical chitosan hydrogels do not need using of catalysts or other toxic reactive agents, a first demand in biomedical applications. The use of gelation without the need of toxic additives, in simulated conditions with the human body, led to the development of injectable solutions which suffer a sol/gel transition after there are injected in the organism, offering a unique opportunity to allow the gel to take the form of the deteriorated tissue, used as matrix, the scaffold perfectly adjusting to the respective defect. However, the resistance of this type of hydrogels is limited, being possible its uncontrolled dissolution (Peppas, 1986).

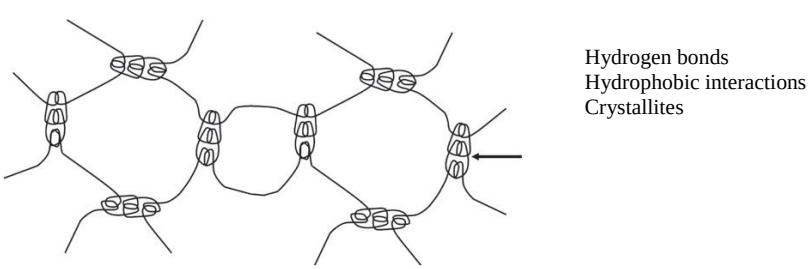


Scheme 1. Schematically representation of chitosan hydrogel resulted by physical association, without additives.

### 3.1.1.2. Chitosan Coordination Complexes

Between chitosan and some metallic ions (Pt (II), Pd (II) and Mo (VI)) (Dambies et al., 2001), covalent coordinative bonds could be established, leading to the formation of another hydrogel type, with less applications in the biomedical domain (Croisier, and Jerome, 2013).

### 3.1.1.3. Polyelectrolyte Complexes (PEC)

Polyelectrolyte complexes (PECs) are obtained by electrostatic interactions between the amino groups in C2 position from the glucopyranose units of CS and the anionic groups (e.g., the carboxyl groups) of the polyanions of natural origin (e.g., hyaluronic acid, pectin, alginates, xanthan gum, carboxy methyl cellulose, chondroitin sulphate, dextran sulphate etc.), or synthetic one (e.g., polyacrylic acid, polyphosphoric acid, poly(L-lactide) (Ong et al., 2008). Polyelectrolyte complexation takes place in mild reaction conditions. PEC exhibit a higher swelling sensitivity towards pH changes, compared to covalently crosslinked chitosan hydrogels, which extends their potential application. Certain complexed polymers, such as glycosaminoglycans, can exhibit interesting intrinsic properties. Since PECs are formed by non-permanent networks, dissolution can occur. Chitosan/PVA complexes represent an interesting alternative for preparing biocompatible drug delivery systems if pH-controlled release is not required. Grafted chitosan hydrogels are more complex to prepare and do not always improve biocompatibility compared to covalently crosslinked hydrogels, but can enhance certain intrinsic properties of chitosan such as bacteriostatic and wound-healing activity (Berger et al., 2004).

Swelling in different fluids of the polyelectrolyte hydrogels is very dependent on the pH environment, especially when this one is compared with that corresponding to the hydrogels obtained by covalent crosslinking; that is why these ones could be used for drug release, are pH responsive, in different conditions and in a wide application area (Vasile et al., 2013). PECs protect the sodium hyaluronate (HANa) against the enzymatic hydrolysis, but only for pH values different from the optimum one for the enzymatic activity. CS/HANa based PEC, under sponge or film form, allows the culture of different specific cells, such as the ketocytes, which produce the skin matrix, accelerating the wound healing, without inflammatory and toxic reactions (Denuziere et al., 1998). CS/HANa PEC are adequate materials for treating the wounds and the burns, because these ones allow a humid treatment, thus preventing the wound injury during the treatment; the properties of the two components assure wound healing, and also present antimicrobial activity (Vasile et al., 2013).

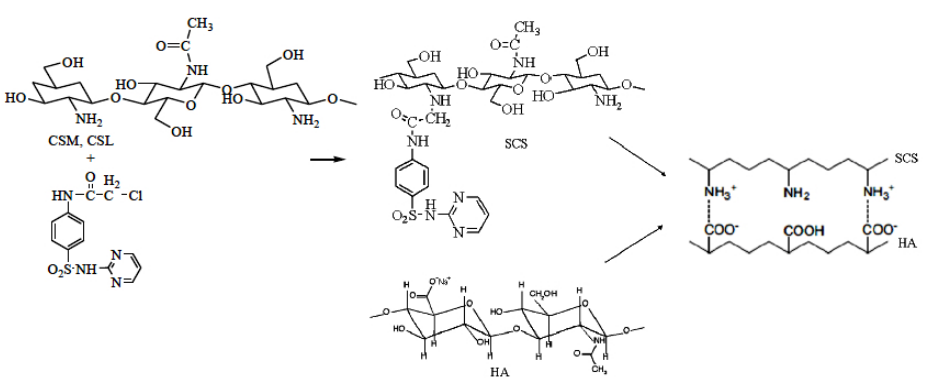


Scheme 2. Formation of the polyelectrolytic complex (PEC) using sulphadiazine-chitosan conjugate (SCS) and sodium hyaluronate (HANa) (reprinted from Profire et al., 2013; Dumitriu et al., 2015).

Incorporation in the PECs of modified chitosan with sulphadiazine led to the obtainment of a new form of PEC (Scheme 2), which improved the bacteriostatic effect of chitosan against the bacteria *Escherichia coli*, *Listeria monocytogenes* and *Salmonella thyphymurium*, and also allowed the control of the properties and of the antimicrobial activity in the treatment of the wounds and the burns (Profire et al., 2013; Dumitriu et al., 2015). The PEC hydrogels of CS/sodium hyaluronate (HANa) type present a porous heterogeneous morphology, with strong interconnected pores (Figure 1).

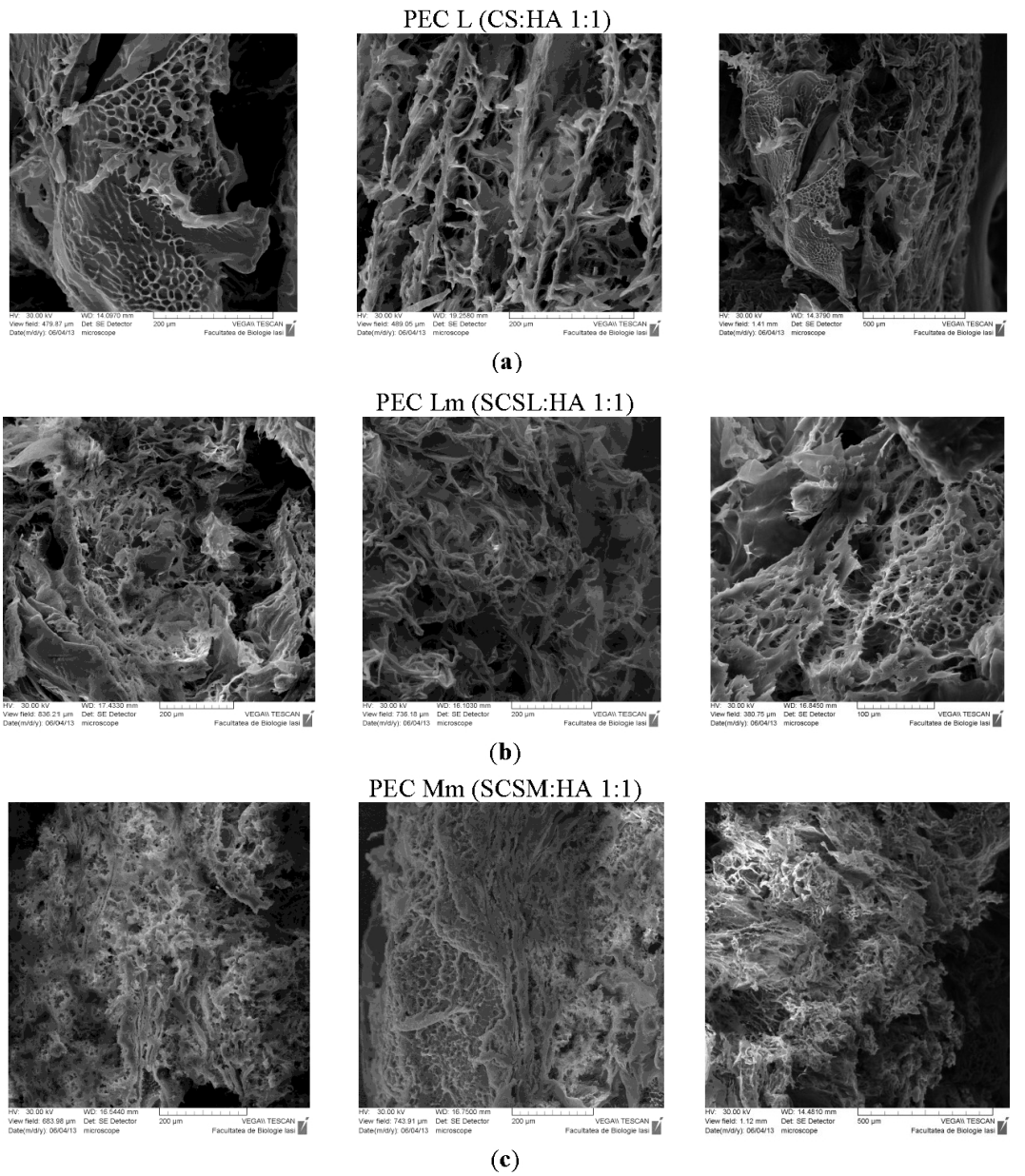


Figure 1. SEM images of the PEC: (a) PEC L (low molecular weight chitosan – HA); (b) PEC Lm (low molecular weight chitosan modified with sulfadiazine - HA); (c) PEC Mm (medium molecular weight chitosan modified with sulfadiazine - HA) (reprinted from Dumitriu et al., 2015).

PEC of CS and hyaluronic acid (HA) have been obtained under nanofibers form by electrospinning and proved as being good biomaterials in tissue engineering (Ma et al., 2012).

Freeze-drying method was used by Rossi et al. (Rossi S. et al., 2007) to obtain mixtures of hydrochlorinated CS, chitosan modified with 5-methyl-pyrolidinone and hyaluronic acid (HA). In the obtained blends, an antimicrobial drug was incorporated, i.e., the diacetate of chlorhexidine (CX). The obtained dressings based on these systems presented good mechanical properties that are necessary for the systems applied on the skin. Adding of HA to both chitosan types leads to the decrease in the hydration properties of the dressings and to the modulation of drug release. Dressings containing modified chitosan have superior elastic properties and inhibit the radical activity. The antimicrobial activity is evident even in the absence of the CX drug.

#### 3.1.1.4. Chemically Crosslinked Chitosan Hydrogels

Obtainment of such hydrogels takes place by covalent bonds formation between the polymer chains, in the presence of a crosslinking agent. These hydrogels are more stable when compared with physical ones, and the gelation is irreversible (Croisier, and Jerome, 2011). In this case, it is necessary to chemically modify the primary structure of the chitosan, fact which could alter its initial properties, particularly if the amino groups are implied in the reaction. In the same time, this reaction could be a source of contamination with the residual reactants or by the catalyst traces.

For obtaining irreversible chitosan hydrogels, crosslinkers based on dialdehyde are used, such as glyoxal and glutaraldehyde that quickly react with the amino groups of the D-glucosamine units from chitosan and also with the chitosan hydroxyl groups. Tripolyphosphate, ethylene glycol, diglycidyl ether and diisocianate could be also crosslinkers for obtaining chitosan hydrogels (Leung, 2001). All these crosslinkers could induce the toxicity of the obtained hydrogels, this fact being a major disadvantage when such hydrogels are used for biomedical applications.

#### 3.1.1.5. Applications of the Chitosan Hydrogels

Boucard et al. (2007), prepared bi-layer physical hydrogels from chitosan and water, used for treating the burn wounds. The experiments have been realized on pigs, biopsies being taken after 9, 17, 22, 100 and 293 days. It was evidenced a good tolerability of chitosan by tissues, this polymer inducing a good regeneration of these ones. In the 22-nd day, it was observed the synthesis of collagen of I and IV type under the granulation tissue, as well as the formation of a junction dermis-epidermis. After 100 days, the new formed tissue was similar to the native skin, especially in respect with its aesthetic aspect and its high flexibility.

Using chitosan hydrogel as dressing (Boucard et al., 2007) evidenced its ability to induce the cellular adhesion and proliferation. The positive charges of chitosan allow electrostatic interactions with the glicosaminoglycans, which attract growth factors that improve the growth and the proliferation of the cells (Lee et al., 2009).

Studies on the cellular viability evidenced that the chitosan hydrogel and its degradation products do not present cytotoxicity. Evaluation of chitosan applicability in treatment of burns induced to Wistar rats was realized on deep wounds, at the dermis level. Macroscopic analysis evidenced that the wounds in animals treated with chitosan are significantly smaller when compared with those induced in the control, untreated group. The histological analysis proved the lack of an inflammatory reaction in the lesions of the skin treated with chitosan

and the absence of the pathological abnormalities in the organs obtained by necropsy, a proof of the local and systemic histocompatibility of the biomaterial (Boucard et al., 2007).

UV irradiation of an aqueous photo-crosslinkable chitosan solution leads to the obtainment of a flexible and insoluble hydrogel (Ishihara et al., 2001; Ishihara et al., 2002). To evaluate its effect on the quickly wound healing, deep incisions in the rat skin were performed, on which this chitosan solution was added and subsequent it was UV irradiated, for 90 seconds. Using of chitosan hydrogel led to the significant contraction of the wound, accelerating its healing. Histological examination evidenced an increased rate of wound contraction in the first two days after the application.

In order to create a humid medium for quickly heal the wounds, it was developed a hydrogel system, composed from powder of alginate, chitin/chitosan and fucoidan (ACF-HS; 60:20:2 w/w) (Murakami et al., 2010). This dressing is characterized by good properties, such as easily application and in removing from the wound surface. After 7 days of application, the obtainment of a granulation tissue with an extended surface was observed.

Yang et al. (2010) developed hydrogels based on water soluble PVA, chitosan and glycerol. The extract from these hydrogels proved to not present toxicity for the mouse fibroblasts L929, and the wounds treated with this system healed after the 11-th day of application, after this period the mature epidermis being already formed.

### *3.1.2. Chitosan Sponges*

Sponge or foam porous scaffolds have been used in tissue engineering. Sponge is a very light soft substance with many little holes in it.

Chitosan sponge solid structures are able to absorb a great fluid quantity (higher than 20 times their dry mass), due to the characteristic micro-roughness. These materials generally offer a better interaction with the cells, remaining soft and flexible.

Chitosan sponges are often used as materials for wound healing, because they catch the exudate arising from the wounds, thus helping the surrounding environment to regenerate (Jayakumar et al., 2011; Mori et al., 2016). In the meantime, these materials could be successfully applied in bone tissue engineering, as well as filling materials. Sponges produced from pure chitosan, or from mixtures of chitosan with tricalcium phosphate and collagen (Seol et al., 2004; Costa-Pinto et al., 2011; Lee et al., 2000; Arpornmaeklong et al., 2008) have been prepared by lyophilisation and used as scaffolds for bone regeneration. Composite sponges made from chitosan-ZnO presented a good wettability, and were characterized by antibacterial and haemostatic properties, confirming their potential use in applications related to wound healing. Chitosan crosslinked sponges, charged with norfloxacine, also presented adequate properties for being used as dressing (Denkbas et al., 2004). For obtaining chitosan scaffolds with adequate roughness, supercritical carbon dioxide ($scCO_2$) was used, the obtained materials proving to be adequate for cell growth (Rinki et al., 2009).

Han et al. (2014) prepared gelatine-chitosan (Gel/CS) sponge scaffold, with different ratios between the two polymers. Biocompatibility and *in vivo* studies indicated that the obtained sponge presented adequate properties for cell adhesion, and proliferation, proving to be a potential system for applications related to skin tissue engineering.

## 3.2. 2D Chitosan Scaffolds, Used for Wound Healing

Materials used for wound healing have to satisfy a series of specific conditions in order to be efficient. The dressings have to be non-toxic and non-allergenic, to allow gas change, to maintain the environment moisture, to protect the wound against the microbes and to absorb the exudates from the wound (Jayakumar et al., 2011). As it was already mentioned, chitosan sponges satisfy pretty well all these conditions. When skin tissues are implied, 2D scaffolds as films, or porous membranes are also useful.

### *3.2.1. Chitosan Films*

Surface properties of the dressings in contact with the damaged tissue are extremely important in what is concerning an efficient healing. In order to obtain adequate properties of the different medical devices, nanostructured thick films and multilayer coatings have been used. To obtain chitosan films with improved properties in respect with their thickness, composition, morphology and roughness (Pavinatto et al., 2010), Langmuir-Blodgett technique, and the layer-by-layer deposition method (LBL) can be used. LBL films entirely composed of polysaccharides (i.e., chitosan and hyaluronic acid (Salomaki and Kankare, 2009), or chitosan and alginate (Wittmer et al., 2008)) present important abilities in wound healing.

Chitosan films can be easily prepared from chitosan salt solutions. For example, HemCon is prepared from chitosan acetate and it is used as haemostatic dressing (Jayakumar et al., 2011). Properties of these films could be improved by a series of physico-chemical methods, such as:

- treatment in a nitrogen or argon plasma (Silva et al., 2008) which, being applied to chitosan membranes, induces surface roughness, improving cell adhesion and proliferation
- irradiation with ozone or UV radiations, which determines chitosan depolymerisation (Matienzo and Winnacker, 2002)
- incorporation of silicon particles or of polyethylene glycol (Clasen et al., 2006) in chitosan films, leading to roughness modification (pore size is between 0.5 and 100 μm)

When, in different applications good mechanical properties are required, mixing and chemical modification of chitosan proved to be efficient. Chitosan films prepared in the presence of dialdehyde starch presented improved mechanical properties and a better wettability (Tang et al., 2003). Improved wettability was also proved for films of chitosan/diacrylate polyethylene glycol mixtures (PEGDA) (Zhang et al., 2008). Films of chitosan/polyvinyl alcohol/alginate (which maintain the environment moisture, accelerating wound healing) (Pei et al., 2008), and non-adherent chitosan/β-glucan films (Kofuji et al., 2010; Xu et al., 2007) have been obtained.

Chemical modification of chitosan films could be used for obtaining surface properties adequate for subsequent applications. For example, when a stearoil group was attached to such films, they became more hydrophobic, thus favouring protein adsorption. When chitosan films reacted with succinic anhydride or phthalic anhydride, more hydrophilic surfaces have

been obtained, which promoted lysozyme adsorption (Tangpasuthadol et al., 2003). A thermosensitive film obtained by combining the chitosan thiolate with poly(*N*-isopropyl acrylamide) and ciprofloxacin was easily removed from the wound surface (Radhakumary et al., 2011).

Incorporation of inorganic particles in chitosan films allows the obtainment of combined effects, due to both materials, this fact leading to a high performance in wound healing. Silver nanoparticles are characterized by antimicrobial activity, property used especially in dressings applied for wound healing (Rai et al., 2009). These silver particles can be added to chitosan films, thus avoiding microorganisms proliferation (Lu et al., 2008; Mi et al., 2003; Thomas et al., 2009; Vimala et al., 2010). Besides silver nanoparticles, those of zinc oxide ZnO proved to be non-toxic and presented antibacterial properties (Cohen, 2000; Díez-Pascual and Díez-Vicente, 2015). Films prepared from chitosan, Ag and ZnO nanoparticles are characterized by a high antibacterial activity, being extremely promising in the domain of wound healing (Li et al., 2010).

### *3.2.2. Porous Membranes from Chitosan Nanofibers*

Chitosan nanofibers have been frequently used both for preparation of dressings, as well as in tissue engineering (Jayakumar et al., 2010). Chitosan/polyethylene oxide nanofibers, prepared by electrospinning, are characterized by cellular biocompatibility (Jayakumar et al., 2010, Bhattarai et al., 2005), keeping their morphology and their viability after human cell adhesion. Adding polyethylene oxide (PEO) of high molecular weight at chitosan solutions allows formation of fibers having dimensions between less than 100 nanometers and some tens of micrometers (Zhang et al., 2008), while adding of polyvinylpirolydone induces the decrease of the chitosan based fibers diameter (Ignatova et al., 2007). That is why these blends offer great possibilities for being used in tissue engineering (Jayakumar et al., 2010). Blending polyvinyl alcohol with chitosan induces the obtainment of fibers with high biocompatibility, used in a wide variety of biomedical applications (Huang et al., 2007; Duan et al., 2006; Li and Hsieh, 2006). Besides biocompatibility, chitosan/polyethylene terephthalate (PET) nanofibers are characterized by improved antibacterial properties, when compared with PET fibers, or with chitin/PET ones (Zhang et al., 2008).

Adding another polymer in order to obtain a much simple electrospinning process represents a way to improve the properties of the obtained fibers, as follows: mechanical properties, biocompatibility and antibacterial behaviour (Jayakumar et al., 2010). Chitosan based nanofibers, obtained by this procedure are recognized as being an adequate biomaterial for being used in wound healing, affirmation also sustained by their application in commercial products, such as Chitoflex.

### *3.2.3. Chitosan Membranes Used for Coating of the Titanium Surfaces*

Titanium is a metal that is generally regarded as one of the most biocompatible metals, available for clinical applications (Brunette et al., 2001). Together with its alloys, titanium is used as implants in dentistry, orthopedics and the cardiovascular system. The advantages of titanium and its alloys used for biomedical devices include (Elias et al., 2008): high corrosion resistance, biocompatibility, high ratio between tensile strength and density, lack of toxicity. However, there are some other properties which have to be improved, such as: the stabilization of the implant, the osteointegration at the bone-implant interface, and the prevention of bone stress shielding (Goodacre et al., 1999). Successful integration and

stabilization of the implant critically depends on the surface characteristics, i.e.: surface chemistry, roughness, topography, and wettability (Esposito et al., 2004). One of the methods used to improve the titanium surface characteristics is to cover it with a layer of chitosan (Lieder, 2013).

Coating of the titanium and of its alloys with chitosan membranes can be realized by several methods such as: solvent casting, silanization, electrophoretic deposition and layer-by-layer self-assembling (Bumgardner et al., 2003, 2007; Thierry et al., 2003; Martin et al., 2007, 2008; Boccaccini et al., 2010; Mehdipour et al., 2012; Cai et al., 2005, 2008).

Titanium coated with chitosan, by silanization, proved to improve the osteoblast attachment when compared with non-coated titanium; it remained stable during 8 weeks after implantation and positively affected the implant integration at the bone-biomaterial interface (Bumgardner et al., 2003 and 2007). In a similar way, chitosan membranes deposed using layer-by-layer technique, were significantly more appropriate for cell attachment and osteogenic differentiation stimulation, compared with non-coated titanium films (Cai et al., 2005; and 2007). With all these advantages, there are a lot of other problems to be solved for titanium implants coated with chitosan, in order to be clinically used on a large scale. Evaluation of the bioactivity of the chitosan membrane is realized before coating the titanium surface, using *in vitro* methods that allow the obtainment of adequate surface and biological properties. Coating of titanium is realized only after it was proved that the general properties of the chitosan membranes satisfy the conditions necessary for the implants used in tissue engineering.

Bioactivity of each chitosan membrane is essentially affected by the surface properties and by the deacetylation degree that alter the cell behavior (Hsu et al., 2004). A higher deacetylation degree generally induces an increase in cell attachment and proliferation, while a smaller deacetylation degree induces the healing, without forming a healing tissue (Mi et al., 2001; Chatelet, 2001). Cationic charge seems to mediate the osteoblast attachment rather than the fibroblast one, behavior that could be very useful for preventing the formation of fibrous tissue capsule around the implants (Fakhry et al., 2004).

Chitosan membranes used as biological substrates have been studied for a wide variety of cell types, including the osteoblast and pre-osteoblast cells, as well as non-osteoblast cellular lines and primary cells. Generally, the osteoblast cell attachment and proliferation is favored by a high deacetylation degree of the chitosan membranes (Bumgardner et al., 2003). Mesenchymal stem cell attachment and proliferation seems to be a more complex process, highly dependent on the membrane thickness and needing a deacetylation degree of at least 96% (Uygun et al., 2010; Amaral et al., 2005). Non-osteoblast cellular lines and the primary mouse hepatocytes adhered at chitosan membranes, but no differentiation was observed in what is concerning the type of the adhered cell (Uygun et al., 2010; Abarrategi et al., 2009).

Main advantages/disadvantages of the chitosan based systems could be summarized as follows (Croisier and Jérôme, 2013):

- *Hydrogels (3D)*, used for tissue replacement/controlled release:
  - **a)** *if physically associated (reversible)*, they have the *advantages* of being soft, flexible, non-toxic; as *disadvantages*: they are unstable, could produce uncontrolled dissolution; low mechanical resistance; difficulty in controlling pore sizes;

**b)** *if chemically crosslinked (irreversible)*, they have the *advantages* of being soft, flexible, with an easy control of the pore sizes; as *disadvantages*: they could be toxic; crosslinking could affect the intrinsic chitosan properties

- *Sponges (3D)*, used in tissue engineering (as filling material), or as dressings and skin substitutes, have the *disadvantage* of possible agglutination if they have a high porosity, or they present the *disadvantage* of low porosity if they are soft
- *Thin films (2D)*, used as coatings for a wide variety of scaffolds, dressings, skin substitutes, have the *disadvantage* of a laborious obtainment procedure, even if they are obtained by Langmuir-Blodgett method, or by layer-by-layer technique
- *Porous membranes (2D)*, used as coatings for a wide variety of scaffolds, dressings, skin substitutes, have high porosity, but electrospinning for chitosan is not easy to obtain.

## 4. Chitosan Applications in Tissue Regeneration

### 4.1. Wound Healing

Skin is the more extended organ of the human organism, which functions as a barrier against harmful environments. A wound could appear as a consequence of a physical, chemical, mechanical, and/or thermal injury. Natural healing process of the skin is complex and continuously. Wound healing is a dynamic and a complex process of regeneration, which consists in a series of interdependent stages, which overlap, in which a variety of cellular components act together to re-establish the integrity of the damaged tissue and to replace the lost tissue (Boateng et al., 2008; Ahmed and Ikram, 2016). Process of wound healing was described as consisting in five stages, that imply complex cellular and biochemical processes, such as: haemostasis, inflammation, migration, proliferation and remodelling (Hani and Satya, 2013; Beanes et al., 2003; Dai et al., 2011).

Generally, the treatment against skin injury is represented by the traditional autografts and allografts. Tissue engineering, however, became an alternative method for skin excessive loss. Nowadays, a series of new materials have been used in the domain of skin regeneration, such as a wide variety of polymers, including natural or synthetic materials, or combinations between these ones, immobilized nanoparticles at the surfaces of polymeric materials etc. (Wen et al., 2015).

#### *4.1.1. Chitosan Based Systems Used for Wound Healing*

There are three main types of dressings, such as: biological, synthetical and biological-synthetic (Azuma et al., 2015). The most used ones are the biological dressings. However, these ones present some disadvantages, between which one can mention: high antigenicity, low adhesiveness, contamination risk. Synthetic dressings are characterized by a longer lifetime, induce a minimum inflammatory reaction and do not present high risk for pathogen transmission. Combined biologic-synthetic dressings are prepared from two layers consisting from a polymer and a biological material (Bruin et al. 1990; Matsuda et al., 1990; Suzuki et al., 1990). Whatever their type, the materials used as dressings have to satisfy, as it was already mentioned, a series of requirements, such as: to maintain the moisture of the

surrounding environment at the interface with the wound, to allow the gas change, to action as a barrier against the microorganisms and to allow the removal of the excess exudates. In the same time, the dressing has to be non-toxic, non-allergenic, non-adherent and it has to be easily removed from the wound surface, without inducing its further trauma. Moreover, the dressing has to be prepared from biomaterials already existent that need minimum processing, to be characterized by antimicrobial properties and to induce the most rapidly healing of the wounds (Jayakumar et al., 2011).

Chitosan proved to be an attractive candidate for treating major burns. This one can form – directly at the wound surface – a biocompatible and compact film, by immersing the damaged tissue in an aqueous chitosan acetate solution. The resulting film is permeable to oxygen and presents a high capacity of water absorption, both characteristics being useful properties in wound healing. Chitosan is also slow degraded by the lysozyme, present in the wound regions; therefore this system is not necessary to be so frequently removed from the wound surface.

Chitin and chitosan based materials used in wound healing have to satisfy some requirements (Shigemasa and Minami, 1996) such as: to accelerate the healing process, to be useful in less hygienic conditions, to decrease the frequency of the applied treatment, to assure comfortable protection and without pain at the wound surface, to simplify the treatment procedure, to avoid antibiotics use. In what is concerning this last aspect, of the therapy with drugs, a series of problems that could appear have been evidenced, such as: bacteria resistance at drug action, possible allergies, death of the useful bacteria in the digestive tract etc. That is why, it is desirable to use non-toxic biodegradable materials capable to activate the response reaction of the host organism in order to prevent infections and to accelerate wound healing. Wounds treated with chitosan do not follow classical healing process, but it induces only the regeneration of the elements of the normal tissue, with no visible traces.

Recent research made possible to prepare chitosan based materials under the form of nanofibers, which are more flexible and which can be used for developing new bio-products used as dressings (Naseri et al., 2014a, b).

Abdelgawad et al. (2014) described a green method to produce the antibacterial nano-textiles loaded with silver nanoparticles (Ag-NP, with the diameter of 25 nm), wrapped in chitosan after reducing with glucose. Obtained materials presented improved properties and synergistic antibacterial effects, by combining the effect of chitosan with that of Ag-NP.

Chitosan/hyaluronic acid films, very transparent, were tested *in vivo* on animals, and it was observed that these ones are very efficient in accelerating wound healing, reducing the tissue re-deterioration when the dressing was removed from the wound surface (Xu et al., 2007). Membranes prepared from chitosan combined with alginate (Dong et al., 2010) proved a high stability at pH variations and a high efficiency as membranes for controlled release when compared with chitosan or alginate, separately. These membranes could be used for healing of the wound with a high quantity of exudate, in order to prevent the bacteria infections. β-glucan and chitosan films presented therapeutic effects comparable or superior to those induced by Beschitin W, a commercial dressing prepared from chitosan (Kofuji et al., 2010). Moreover, the complex β-glucan-chitosan does no dissolve during the application period, does not adhere at the wound surface, being easily removed.

Mi et al. (1999) prepared porous microspheres from chitosan and its derivatives, for antigen controlled release. Mucoadhesiveness of chitosan and of its cationic derivatives is

known to improve drug adsorption, especially at a neutral pH. *N*-trimethyl chitosan chloride interacts with the negatively charged cellular membranes, thus inhibiting growth of microorganisms (Hamman and Kotzé, 2002). Heterogeneous chemical modification of chitosan films could be used to obtain improved surface properties. For example, when a stearoil group is attached at the surface of a chitosan film, this one becomes more hydrophobic, inducing protein adsorption. When chitosan films react with the succinic anhydride or with the phthalic anhydride, more hydrophilic surfaces are obtained, which facilitate lysozyme adsorption (Tangpasuthadol et al., 2003).

In Table 2 are presented a series of systems containing chitosan, used for wound healing, together with the corresponding effects, induced by these ones.

**Table 2. Chitosan based products used for wound healing**

| System type | Results/Properties/Observations | Reference |
|---|---|---|
| chitosan powder | - improved re-epithelialization<br>- decrease of the number of inflammatory cells | (Okamoto et al., 1995) |
| chitosan N-carboxybutyl system | - improved vascularization and no inflammatory cells were present in the vicinity of the tissue<br>- formation of organized cutaneous tissue<br>- decrease in the number of anomalous healings | (Biagini et al., 1991) |
| asymmetric chitosan membrane | - controlled water lose by evaporation<br>- excellent oxygen permeability<br>- drainage ability of the fluids from the wound surface<br>- inhibition of the exogenous microorganisms invasion<br>- increase of the epithelialization rate<br>- improved ability for wound healing | (Mi et al., 2001) |
| carboxymethyl hexanoyl chitosan | - antimicrobial activity<br>- increased biocompatibility for fibroblasts | (Huang et al., 2012) |
| gels from chitosan, crosslinked under the action of UV radiation | - resistance against *E. Coli*<br>- efficiency in inhibiting the infection | (Fujita et al., 2004) |
| chitosan gel (1% w/v) | - periodontal regeneration | (Boynuegri et al., 2009) |
| nanofibers of chitosan/carboxyethyl blends (CECS) and polyvinyl alcohol (PVA), prepared by electrospinning | - improvement of the adhesion and proliferation of L929 cells | (Zhou et al., 2008) |
| hydrogels of chitosan immobilized at the surface of composites prepared from gel of poly(N-isopropyl acrylamide)/polypropylene, using glutaraldehyde as crosslinking component | - antibacterial activity against *E. coli* and *Staphylococcus aureus*<br>- the product is easily removed from the wound surface, without affecting the new regenerated tissue | (Chen et al., 2005a, 2005b) |
| chitosan hydrogel | - promoting of the cellular adhesion and proliferation<br>- the hydrogel and its degradation products are not cytotoxic<br>- enables to restore skin architecture | (Ribeiro et al., 2009) |
| Scaffolds from blends of chitosan and synthetic/natural polymers | | |
| films of chitosan/polyethylene diacrylate glycol blends | - good biocompatibility<br>- non-cytotoxicity for growing of L929 fibroblasts | (Zhang et al., 2008) |
| chitosan water soluble/heparin | - improved capacity of wound healing, due to the attraction or to the binding of the growth factor | (Kweon et al., 2003) |

| System type | Results/Properties/Observations | Reference |
|---|---|---|
| films of chitosan/Ag/ZnO blends | -excellent antimicrobial properties against Bacillus subtilis, E. coli, S. aureus, Penicillium, Aspergillus, Rhizopus | (Li et al., 2010) |
| biocompatible chitosan carboxyethyl (CECS)/polyvinyl alcohol (PVA) | - non-toxicity<br>- improvement of the cellular attachment and proliferation | (Zhou Y. et al., 2008 |
| nanofibrous membranes of water soluble chitosan N-carboxyethyl/PVA/silk | - good biocompatibility | (Zhou Y. et al., 2013) |
| membranes of chitosan and alginate | - non-toxicity<br>- increased potential for wound healing | (Wang et al., 2002) |
| Scaffolds from chitosan based composites | | |
| chitosan/sericine composite nanofibres | - good antibacterial activity against Gram-positive and Gram-negative bacteria<br>- promoting of cellular proliferation<br>- good biocompatibility<br>- non-toxicity | (Zhao et al., 2014) |
| chitosan hydrogels/PVA/bentonite nanocomposite, PVA/Ag nanoparticles | - significant antimicrobial activity against *E. coli*<br>- good transmission rate for the water vapour<br>- adequate capacity of water absorption, due to the filling effect of Ag nanoparticles | (Gonzalez et al., 2011) |
| membranes of chitosan incorporated with sulphadiazine silver | - controlled release of the sulphadiazine silver<br>- controlled evaporation of the water vapours<br>- adequate ability for wetting<br>- cytocompatibility<br>- prolonged antibacterial activity | (Fwu et al., 2003) |
| sulphadiazine silver incorporated in membranes of chitosan - alginate composite | - improvement in the kinetic release at a concentration of approximate 50%<br>- very good mechanical properties | (Meng et al., 2010) |
| tannic acid/chitosan/pullulan nano-composites | -antibacterial activity against *E. Coli* and Gram-negative bacteria<br>- good water absorption<br>- favouring of fibroblast attachment<br>- growth of an inter-layer which favours the wound healing in depth | (Xu et al., 2015) |
| thiolate chitosan/ poly(*N*-isopropyl acrylamide)/ciprofloxacin | - thermo-sensitive film, which can be easily removed from the wound surface, when temperature decreases | (Radhakumary et al., 2011) |
| coverage biocomposite prepared from chitosan, silver and hydroxyapatite on a titanium substrate | - antibacterial activity<br>- uniform and porous surface, appropriate for cellular adhesion<br>- decrease in the infection risk | (Yajing et al., 2015) |
| silver nanoparticles incorporated in a composite dressing based on chitosan hydrogel | - increased wetting rate<br>- controlled biodegradability<br>- excellent coagulation properties of the blood<br>- antibacterial potential against *S. aureus* and *E. Coli*<br>- non-toxicity | (Wu., 2011) |
| composite membranes of chitosan and gelatine, filled with $Fe_3O_4$ nanoparticles | - improved properties for inhibiting *S. aureus* and *E. Coli*<br>- good mechanical properties<br>- antibacterial activity | (Ning et al., 2016) |
| nanocomposite hydrogels of polyvinyl alcohol/chitosan/ montmorillonite | - improved mechanical properties<br>- biocompatibility<br>- antimicrobial activity<br>- good wetting capacity | (Noori et al., 2015) |

**Table 2. (Continued)**

| System type | Results/Properties/Observations | Reference |
|---|---|---|
| Chitosan-based sponges | | |
| biodegradable sponge, prepared from chitosan and sodium alginate, filled with curcumin | - improved capacity for wound healing | (Mei et al., 2009) |
| sponge type composite of curcumin/chitosan/gelatine, with different content of chitosan | - improved water absorption<br>- antimicrobial activity<br>- collagen formation was increased, thus inducing an improvement in wound healing | (Van et al., 2013) |
| sponge type dressings based on chitosan glutamate (high molecular weight) and sericine | - realized for treatment of chronic ulcerations of the skin<br>- effect of protection of human fibroblasts against the oxidative stress<br>- improvement of fibroblast proliferation | (Mori et al., 2016) |
| chitosan scaffolds, which porosity was induced using supercritical $CO_2$ | - fiber structure, useful for applications in wound healing | (Kumari et al., 2009) |
| crosslinked chitosan scaffolds, loaded with antibiotic | - increased tolerance and safety<br>- antibacterial protection against the most common wound pathogens | (Denkbaş et al., 2004; Panoraia et al., 2016) |
| Scaffolds of chitosan/plant extract systems | | |
| films based on castor oil reinforced with different quantities of chitosan modified with ZnO nanoparticles | - antimicrobial activity against Gram-positive and Gram-negative bacteria, in the presence or in the absence of UV light<br>- good thermal stability<br>- cytocompatibility<br>- improved capacity of wound healing | (Diez-Pascual and Diez-Vicente, 2015) |
| films of chitosan hydrogels in which gentamicin sulphate and extracts from leaves of Salix alba and Juglena regia were encapsulated | - antibacterial and antifungal activity | (Mohammad, Fehmeeda, Sakeel, 2015; Mohammad, and Fehmeeda, 2014) |
| chitosan and aloe vera based membrane | - improved antimicrobial properties<br>- improvement in cell adhesion and proliferation | (Silva et al., 2013) |
| Scaffolds based on chitosan charged with drugs | | |
| thiolate chitosan with poly(*N*-isopropyl acrylamide) charged with ciprofloxacin | - cytocompatibility<br>- modulating capacity for ciprofloxacin release, thus protecting the wound for a high period of time<br>- antimicrobial properties against *E. coli* | (Radhakumary et al., 2011) |
| textiles from chitosan ethylene diamine tetra acetic acid/PVS (ratio 30/70) nanofibers, charged with lysozyme | - improvement in wound healing rate | (Charernsriwilaiwat et al., 2012) |
| films of crosslinked hydrogel, prepared from PVA and chitosan and charged with minocycline | - improvement in wound healing rate | (Sung et al., 2010) |
| chitosan gel (1% w/w) incorporated with 15% metronidazole | - significant improvement after 24 weeks of treatment in chronic periodontitis | (Akincibay et al., 2007) |

### *4.1.2. Chitosan-Based Adhesives for Tissues*

Adhesives for tissues gained, in the last years, popularity in different clinical applications, which include: wound healing, drug delivery, implant of medical devices, tissue engineering and applications related to bones and teeth (Mehdizadeh et al., 2013; Wheat and Wolf, 2009; Spotnitz and Burks, 2008). Adhesives and sealing agents are extremely important in situations where other techniques such as suturing are impracticable. An ideal adhesive should present strong and rapid adherence, decreased immunogenicity, good biocompatibility and biodegradability. During the time, a series of adhesives have been developed, which include: natural derived tissues (glue from fibrin and gelatine-resorcine-formaldehide-glutaraldehyde) (Valbonesi, 2006; Spotnitz and Prabhu, 2005; Elvin et al., 2010), synthetic tissues (sealing agents based on cyanoacrylates and polyethylene glycol (Mehdizadeh and Yang, 2013; Spotnitz and Burks, 2008), as well as adhesives inspired from nature (adhesive proteins from mussels and adhesives inspired from gecko) (Ryan et al., 2004). All these adhesives present both advantages, as disadvantages. For example, the adhesives that contain bovine thrombin could induce allergenic reactions, or could transmit some diseases from animal to human (Radosevich et al., 1997). Although the cyanoacrylates are characterized by a high polymerization rate and a strong adherence, it is possible that the corresponding adhesives to be not enough flexible, especially for the applications related to soft tissues (Leggat et al., 2004). Moreover, Smith and co-workers observed that ethyl-2-cyanoacrylate induces inflammation, embolization, bleeding and necrosis of the vascular walls in cats (Smith et al., 1985).

Detailed research tried to develop adhesives for tissues, evaluating, in the same time, their efficiency. Thus, Ono et al. (2000) prepared an adhesive for soft tissues, based on photo-crosslinked chitosan, in which they introduced both azide groups, and lactose (Az-CS-LA). Lactose induced the obtainment of a more water soluble chitosan at a neutral pH. UV irradiation of Az-CS-LA led to the obtainment of an insoluble hydrogel, after 60 s of exposure, hydrogel that proved to be more efficient than the fibrin based adhesive. Nor the Az-CS-LA, or the obtained hydrogel from this one did not present cytotoxicity for human skin fibroblasts, endothelial cells and the cells from soft muscles. Moreover, all the studied mice survived for at least one month after the implant of 200 µl of photo crosslinked chitosan gel and after administration of up to 1 mL of 30 mg/mL Az-CS-LA solution.

Renbutsu et al. (2005) synthesized chitosan based systems, irradiated with UV light, using less toxic agents, which have been implanted in subcutaneous tissues of the animals and were histologically followed during 7 days after the implantation. After this period of time, it was observed that the implant is covered with a fibrous granular tissue, without inflammatory aspects.

Nie et al. (2013) realized a new polysaccharide/polypeptide hydrogel, in order to be applied as haemostatic adhesive material. Chitosan modified with thiol was rapidly crosslinked *in situ*, using an efficient crosslinker (polypeptide). The obtained hydrogel proved to be characterized by an intensity of the adhesion force four times higher than that corresponding to a commercial adhesive based on fibrin. In the meantime, this adhesive is biocompatible, is not toxic for L929 cells and presents very good haemostatic properties.

Lih et al. (2012) reported the rapid *in situ* formation of the hydrogels chitosan-poly(ethylene-glycol)-tyramine, using peroxidase extracted from radish and hydrogen peroxide. A polyethylene glycol modified with tyramine was grafted on a chitosan chain, in order to improve its solubility and its crosslinking in a tridimensional network. The obtained

hydrogels were characterized by an adhesiveness of 3 to 20 times higher than that corresponding to Greenplast – a commercial adhesive based on fibrin. In the same time, the haemostatic properties and the effect of wound healing were significantly improved; after two weeks after the implantation, the wound was entirely healed, with a new formed dermis.

### *4.1.3. Effects of the Chitosan Based Products, Evidenced by In Vitro and Preclinic Studies*

Depending on its molecular weight, some chitosan-based biomaterials could show a negative effect on the human keratinocyte (HaCaT) viability and proliferation. In the same time, chitosan with an average molecular weight of 120 kDa or 5 kDa stimulated the release of inflammatory cytokines by the CaHaT cells, depending on the incubation time and on the concentration. Both types of chitosan induced the cellular death (Wiegand et al., 2010). Studies realized by Jin et al. (2007) comparing the effects of chitosan and heparin in treating the dorsal burns in rats evidenced that the highest healing rate is obtained when chitosan with a higher molecular weight is used.

In the case of chitosan with a high deacetylation degree (89%), the proliferation of fibroblasts was strongly stimulated, while chitosan with a low deacetylation degree was characterized by a decreased activity (Howling et al., 2001).

**Table 3. Wound healing effects induced by chitosan, evidenced by *in vitro* studies using various mammalian cells**

| Sample | Mammalian cells | Main results | Reference |
|---|---|---|---|
| chitosan | Keratinocytes | - induction of cellular death, depending on molecular weight<br>- stimulation of inflammatory cytokines release | (Wiegand et al., 2010) |
| chitosan | fibroblasts and keratinocytes | - stimulation of fibroblast proliferation<br>- inhibition of keratinocyte mitogenesis | (Howling et al., 2001 |
| chitosan based porous systems for skin regeneration | Keratinocytes | -cytocompatibility; stimulation of cell proliferation; induction of ADN deterioration; release of TNF-α and IL-8 | (Lim et al., 2010) |
| chitosan | Osteoblasts | -significant improvement of osteoblast differentiation | (Klokkevold et al., 1996) |
| chitosan | ACL | - chitosan stimulated the ACL cells to secrete more fibronectin, TGF-β1 and collagen III<br>- after coverage of chitosan surface with fibronectin, the ACL cells adhesion was improved | (Shao et al., 2010) |
| chitosan based membranes | PMN | -chitosan did not activate PMN | (Santos et al., 2007) |
| chitosan | polymorphonuclear neutrophils | -chitosan accelerated osteopontin production from polymorphonuclear leukocytes | (Ueno et al., 2001) |
| chitosan | Macrophage | - stimulating effect both for NO macrophage production, and for chemotaxis | (Peluso et al. 1994) |

Burkatovskaya et al. (2006) compared the antimicrobial activity of HemCom™ dressing based on chitosan acetate, with that of a dressing based on alginate sponge containing sulphadiazine and silver, using rats infected with *P. aeruginosa* and *P. mirabilis*. Chitosan acetate proved to be more efficient in reducing the colonies of bacteria.

Chitosan also stimulated ACL cells (cells from the human ligaments) to secrete more fibronectin, TGF-β1 and collagen III; in the same time, small quantities of fibronectin were adsorbed on chitosan surface (Shao et al., 2009).

Santos et al. (2007) investigated the effect of the chitosan based membranes on activating the polymorphonuclear leukocytes (PMN). The obtained results evidenced that PMN, in the presence of chitosan, secrete similar quantities of lysozyme, when compared with the control group, and the tested materials do not stimulate the production of oxygen reactive species (ROS).

Table 3 presents some aspects related to the wound healing effects induced by chitosan based systems.

#### *4.1.4. Effects of the Chitosan Based Products Evidenced by Clinical Studies*

For the patients who suffered plastic surgical interventions, Biagini et al. (1991) used soft dressings of lyophilized *N*-carboxybutyl chitosan. Comparing with the control group, without dressings, the chitosan *N*-carboxybutyl based dressings induced the formation of a regularly organized cutaneous tissue that reduced the risk of anomalous healing. At the dermis level, the inflammatory cells were not observed, while at the epidermis level, a Malpighian layer was developed.

The wounds produced after skin sampling for obtaining grafts were treated with chitosan based dressings (Stone et al., 2000). These ones proved to be easy to apply and to maintain at the wound surface, being also easy to remove from the wound, without causing pain. The small nervous fibers from the dermis were more numerous and presented major differences when compared with the skin treated with conventional dressings.

Azad et al. (2004) prepared membranes from chitosan obtained from shrimps, with a deacetylation degree of 75%, and an average molecular weight of $1.5 \cdot 10^6$ Da. The efficiency of these dressings was compared with that of Bactigras, a formulation based on chlorhexidine acetate. The chitosan based system induced an efficient adherence at the wound surface, haemostasis, healing and re-epithelialization. Pruritus and pain sensitivity were smaller and, under the chitosan membrane, the cells stimulate skin regeneration and aid to recover tissue architecture.

A chitosan/dextran gel was tested on patients with chronic rhinosinusitis for the healing effect on wounds produced by endoscopic sinus surgery (Valentine et al., 2010). The used gels induced a rapid haemostasis, after only two minutes after the application, comparatively with 10 minutes in the case of the control group. Even if the adhesion between the chitosan based gel and the wound surface manifested in less points, no major difference was observed between the studied gel and the control system for crust formation, mucosa edema, or formation of a granulation tissue.

### *4.1.5. Chitosan Based Dressings as Devices for Drug Release for Improving the Antimicrobial Effect and the Wound Healing Rate*

Chitosan and its derivatives were studied in order to obtain systems to treat the wounds and the bursts, not only due to their antimicrobial effects and their capacity of wound healing, but also because they present adequate properties for being used as vehicles for drug controlled release. Reported studies include the use of chitosan based systems for releasing antimicrobial drugs (Rossi et al., 2007; Noel et al., 2008; Vimala et al., 2010; Tunney et al., 2008; Aoyagi et al., 2007), growth factors (Park et al., 2009; Obara et al., 2005; Mizuno et al., 2002) and other type of drugs (Dai et al., 2009; Jayakumar et al., 2007).

#### 4.1.5.1. Chitosan Used For Antimicrobial Drug Carriers

There have been developed a lot of studies concerning chitosan ability to act as a vehicle for antimicrobial drug release, because some portions from the wound contain no vascularized zones, which inhibit the release of systemic antibiotics towards the infected tissue. While the administration of a drug dose for the entire organism should lead to systemic toxicity, the systems that allow the local drug release could assure high concentrations of active substance only for the implied zones.

A preliminary study to evaluate the abilities of chitosan films loaded with daptmicyn and vancomycin in reducing and preventing the infections in bone fractures was reported by Smith et al. (2010). The film was applied on the devices for musculoskeletal fixation, or on the implant surfaces. Chitosan based films with a deacetylation degree of 61%, 71%, and 80%, prepared using as solvent lactic or acetic acid were analysed from the point of view of the antibiotic absorption properties, elution, adhesion strength and degradation. It was observed that, after 1 minute of rehydration, chitosan films maintained the mechanical integrity necessary to fix the bone fracture. The percentage degradation of the film increased with increasing the deacetylation degree (from 61% to 80%), but the film degradation rate decreased in the presence of the antibiotics. A deacetylation degree of 80% was optimum for absorbing and eluting the antibiotics, these ones being active against *S. aureus*.

In Table 4 are presented some chitosan based systems used as antimicrobial drug release.

A porous chitosan-silver composite, with possible applications as wound dressings with antibacterial properties, was developed by Vimala et al. (2010) using a three steps process, consisting in: preparation of the silver ions-PEG matrix, adding of chitosan and removal of PEG from the matrix. Both PEG and chitosan were essential in reducing the metallic ions and for a good stability of the formed nanoparticles. The chitosan-silver nanoparticles based composite presented improved mechanical properties and superior microbial inhibition. Excellent antimicrobial properties against *E. coli* and *Bacillus* have also been found by other researchers *(*Thomas et al., 2009).

In a preliminary study, Greene et al. investigated if a coating layer of chitosan, loaded or not with antibiotic (gentamicin) could reduce or prevent the beginning of an infection (Greene et al., 2008). They demonstrated that gentamicin from the chitosan coating maintained at a detectable level during 72-96 h, the obtained system being characterized by biocompatibility with the fibroblasts and with the stem cells and presenting bacteriostatic properties for *S. aureus.*

**Table 4. Chitosan based systems used as carriers for antimicrobial drugs**

| Chitosan based carrier | Loaded antimicrobial | Main results/observations | Reference |
|---|---|---|---|
| Chitosan film | Amikacin, daptomicyn | - The system does not need further removal from the wound place, due to its biodegradability<br>- Effective local release of the antimicrobial drugs<br>- The eluents inhibited the growth of *S. aureus*<br>- Possible alternative methods for treating the musculoskeletal infections | (Noel et al., 2008) |
| Matrix from porous chitosan | Amikacin, vancomycin | - Inhibition of *S. aureus* and *P. Aeruginosa* growth<br>- Potential applicability in debridement and lavage therapy | (Noel et al., 2010) |
| Dressings based on chitosan hydrochloride, chitosan 5-methylpirolydinone and their blends with hyaluronic acid | Chlorhexidine diacetate | - All the systems presented adequate properties for the active substance release<br>- Modulation in drug release for the systems that contain hyaluronic acid<br>- Applications in the therapy of skin ulcer | (Rossi et al., 2007) |
| Film of chitosan-polyurethane, used for treating severe burns | Minocycline | -Very good effect in accelerating the wound healing for the systems based on chitosan with a deacetylation degree of 83% | (Aoyagi et al., 2007) |

Mi et al. obtained a bilayer of chitosan membrane, which consisted in a superior dense layer and an inferior layer with a sponge like structure, used for the silver sulphadiazine release in controlling the infections at the wound place *(*Mi et al., 2001). Such bilayer dressing presented very good oxygen permeability, thus controlling the evaporation rate and increasing the water absorption capacity. Sulphadiazine release from the bilayer dressing based on chitosan was higher in the first day, after this period presenting a slower release profile, with a sustained increase in the silver concentration. In vitro studies realized on *P. aeruginosa* and *S. Aureus* cultures evidenced antimicrobial activity for a week. In vivo antibacterial tests followed using Wistar rats confirmed that these dressings are effective for inhibition, for a long period of time, of *P. aeruginosa* and *S. aureus* growth at the infected wound place.

#### 4.1.5.2. Chitosan Systems as Carriers of Growth Factors

Chitosan and its derivatives were often used to release growth factors at the wound place, in order to accelerate the healing process. Growth factors were known as a problem in what it concerns the sustained biodisponibility at the wound place. A series of formulations have been developed to slow their release and thus to prolong their period of activity. While the antibacterial agents prevent or treat the infections, leading to an accelerated healing process, the growth factors are not active from the physiological point of view in this process. These factors are implied in cellular division, migration, differentiation, protein expression and enzyme production, affecting the inflammatory, proliferation and migration phases implied in

the healing process. Between the growth factors that are implied in the healing process, one can mention: EGF, PDGF, bFGF, TGF-β1, IGF-1, and the human growth hormone.

Mizuno et al. (2002) studied the stability of the fibroblast growth factor (bFGF) loaded into a chitosan film, used as carrier for the sustained release of bFGF. Pristine chitosan films, or loaded with bFGF, were applied on the wounds on the rats backs, diagnosed with diabetes. After 20 days of application, the wounds became smaller for the group where chitosan-bFGF was used. This fact is explained by the acceleration of the wound healing due to the combined effects of chitosan and bFGF. A similar study was realized on chitosan scaffolds loaded with bFGF contained in gelatine microparticles (Park et al., 2009), proving that both chitosan and chitosan-bFGF accelerate the wound healing.

A formulation based on chitosan gel containing EGF was tested for healing the wounds produced by second degree burns (Alemdaroglu et al., 2006). *In vitro* studies evidenced that the release rate of epidermal growth factor (EGF) from the obtained formulations was of 97.3% after 24 hours of application. During this study, chitosan/EGF formulations were repeatedly applied on the regions affected by burns, for a period of 14 days (an application every day). The obtained results after the immune-histochemical investigations evidenced significant increases in the cellular proliferation for the group which was treated with gel containing EGF. In the same time, in this group, an increased epithelialization rate was observed, when compared with the group treated with gel without EGF.

#### 4.1.5.3. Chitosan Systems Used as Carriers of Other Drugs

A biodegradable sponge, composed of chitosan and sodium alginate, was obtained by Dai et al. for curcumin release, in order to improve the wound healing effects **(**Dai et al., 2009). Curcumin release from such systems could be controlled by the crosslinking degree. The prolonged release for an extended period, up to 20 days, was obtained. *In vivo* tests, realized on rats, proved that these systems have improved therapeutic effects when compared with the classical cotton dressing.

### *4.1.6. Other Systems Obtained from Chitosan and Hyaluronic Acid*

Hyaluronic acid (HA), a component of the extracellular matrix (ECM), has a high lubrication, water sorption and retention capacity, thus influencing some cellular processes, such as: the cellular attachment, migration and proliferation. These characteristics are essential for obtaining dressings of superior quality.

***Composite films.*** Xu et al. (2007) prepared composite films from chitosan (CS) and HA, by solvent casting, on glass or poly(methacrylate) (PMMA) substrates. The HA content varied between 0.1, 0.25, and 0.5 wt %. The increase in the HA content led to an increase in water absorption (Figure 2), and to the decrease of the permeability to water vapours, of the bovine albumin adsorption and of the fibroblast adhesion, all of these characteristics being adequate for the dressings used in wound healing.

*In vivo* tests proved that these composite films accelerate the wound healing process and decrease the further injury after removing the dressing. Due to the small HA quantity, these composite films are relatively inexpensive and present good properties for different applications.

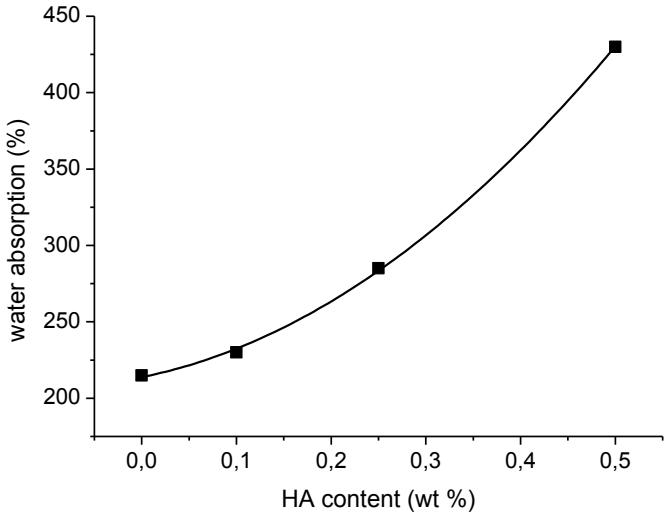


Figure 2. Effect of HA on water absorption of CS/HA films (adapted from Xu et al., 2007).

CS/HA and silver nanoparticles (AgNPs) sponges (5–20 nm), with antimicrobial properties against *Escherichia coli*, *Staphylococcus aureus* bacteria, resistant to meticycline (MRSA), *Pseudomonas aeruginosa* and *Klebsiella pneumonia*, are used for the treatment of the wounds produced by the diabetic ulcer at feet level, that are infected by bacteria resistant at drugs. The CS/HA/AGNPs flexible and porous sponges were prepared by mixing the components, followed by lyophilisation (Anisha et al., 2013). Sponges containing higher AgNP concentrations (0.005% - 0.02%) present antimicrobial activity for the infections caused by *Staphylococcus aureus*, resistant at meticycline (MRSA), a type of bacterium resistant at most of the antibiotics. Depending on AgNPs concentration, the nanocomposites could be cytotoxic for human fibroblasts, at high concentrations.

Endothelial vascular growth factor (VEGF) is the most important growth factor which stimulates the multiple phases of angiogenesis of wound healing and, thus their recovery. A small content of endogenous growth factors and a reduced angiogenesis are the necessary conditions which contribute at wound healing for diabetic patients. Sponges of CS/HA composites with fibrin nanoparticles (150–180 nm), loaded with VEGF, induce the angiogenesis process for healing the wounds at diabetic patients, VEGF release taking place especially during the first three days of application (Annapoorna et al., 2015).

An injectable hydrogel formed from HA modified with aldehyde 1-amino-3,3-dietoxy-propane and chitosan, which improves wound healing by initiating the keratinocyte migration, cell proliferation, granulation and angiogenesis, was prepared by Chang et al. (2015). The facility in injecting, as well as the stability of this hydrogel, were demonstrated by rheological tests. The hydrogel accelerates wound healing, it increases the cellular proliferation and initiates the keratinocyte migration. In the same time, the histologically exam proved the progress in tissue granulation and in capilar formation.

## 4.2. Bone Tissue Engineering

In contrast to other tissues, the bone has the remarkable ability of regeneration when it is broken. In many cases, the bone fractures could be immobilized to allow the spontaneous healing during the time. However, when the bone defects are severe enough, or of critical dimension, they cannot be regenerated by normal physiological processes and need intervention under the form of bone grafts. It is often the case of the segmental defects and of the traumatic fractures (Jayachandran and Se-Kwon, 2010). For being used in bone tissue engineering, the implanted biomaterial has to be characterized by the following properties: biocompatibility, osteoconductivity, increased porosity and biomechanical compatibility (Pizzoferrato et al., 2002). To achieve these conditions, the autografts and the allografts are often used for bone grafts. In the technique that implies the use of an autograft, a portion of bone will be taken from another part of the organism, which will fill the lack portion from another bone zone in the respective organism. Besides the advantages related to the optimum osteoinductivity and osteoconductivity, as well as to the osteogenic properties, the autograft technique also presents some disadvantages, such as: possible complications that often accompany the wound healing process, the need of the additional surgical interventions, and supplementary pain induced to the patient (Wagh, 2004). In the technique using an allograft, bones are taken from the corpses. In this case, problems related to immunogenic reactions and to the transmission risk of some diseases (i.e., SIDA, hepatitis) could appear. Often, supplementary materials (i.e., needles, plates, fillers for bones) are necessary for graft immobilization.

Use of synthetic grafts for tissue engineering offers promising alternatives for autografts and allografts. A synthetic graft, known as a scaffold, should action as a filler at the defect place and promotes bone regeneration. Such a scaffold should satisfy a minimum of requirements, such as: to be osteoconductive for facilitating bone formation at its surface and to present a high porosity in order to allow the transport of nutrients and residues, the neovascularization/angiogenesis and the bone incarnation. Furthermore, a scaffold should be characterized by adequate mechanical hardness to allow the bone growth at the implant place and to maintain the structural integrity during *in vivo* tissue remodelling, as well as by an adequate degradation during the regeneration of the deteriorated bone. The scaffolds are often combined with cells and/or with growth factors, in order to improve the osteoinductivity and the tissue engineering (Levengood and Zhang, 2014).

In order to obtain scaffolds, different classes of materials have been used, including ceramics and polymers (synthetic and natural). The investigated natural polymers for this type of applications include: polysaccharides (i.e., alginate and chitosan), proteins (i.e., collagen, gelatine and silk fibroin) and glycosaminoglicans (i.e., chondroitin sulphate and hyaluronic acid) (Ueno et al., 2001). A series of polysaccharides were used for the treatment of the diseases related to the bone system (i.e., osteoporosis (Iwata et al. 2005), arthritis, (Porporatto et al., 2009) etc.).

Among the investigated polymers, chitosan proved to be a very important material to be used in bone tissue engineering, due to its capability to support mineral rich matrix deposition by osteoblasts, and local anti-inflammatory action along with its other biological properties (Pandey et al., 2017). In contrast to the natural polymers derived from proteins taken from mammalians, the chitosan produces minimum response when interacting with a biological system, as well as fibrous encapsulation (Hu, 2004; Teng et al., 2009; Xianmiao et al., 2009).

Contrary to many synthetic polymers, chitosan has a hydrophilic surface, which promotes the cellular adhesion and proliferation, the degradation products being nontoxic. Chitosan is often preferred as material for bone scaffolds, because it allows the attachment and the proliferation of the osteoblast cells responsible for bone formation, as well as *in vitro* formation of mineralized bone matrix (Chen et al., 2002). Moreover, modified chitosan scaffolds present *in vivo* osteoconductivity, near the bone defects surgically created (Zhang et al., 2008). It is also important that this natural polymer is a material easy to be processed in various forms, being thus possible to produce a high diversity of tri-dimensional scaffolds, with different pore structures. Chitosan can be combined with a series of other materials, including ceramics and polymers, thus obtaining composites with improved mechanical and biological properties.

### *4.2.1. Chitosan Scaffolds in Bone Tissue Engineering*

Scaffolds prepared by pure chitosan are not, generally, appropriate for bone tissue engineering, due to their low mechanical strength. In a study of Jana et al. (2012) it was reported the obtainment of scaffolds from pure chitosan, by phase separation, chitosan concentration varying between 4 wt% and 12 wt%. For the highest chitosan concentration, the obtained systems presented a compression modulus of 17.99 ± 0.11 MPa. All the obtained systems had a pore size of 30 – 220 μm, but the porosity decreased and the thickness of the pore walls increased with increasing the chitosan concentration (Figure 3). As a consequence the mechanical strength was higher, the swelling decreased and the structural integrity in aqueous media was better. This behavior was explained by the increase in the walls thickness and by a higher crystallinity of chitosan for higher concentrations, this fact having an important role in improving the mechanical properties of the respective scaffolds. Proliferation of the MG-63 cells after 7 days of culture was significantly improved by the scaffolds with a chitosan concentration of 12 wt% in respect to those whose concentration was of only 4 wt%. It can be concluded that the systems with better mechanical properties are the most efficient in promoting the osteogenic cell proliferation.

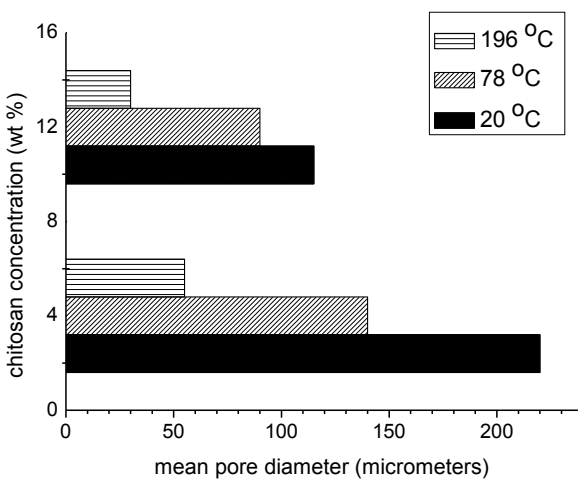


Figure 3. Variation of pore diameter depending on chitosan concentration in scaffolds (adapted from Levengood and Zhang, 2014).

### *4.2.2. Scaffolds for Bone Tissue Based on Chitosan Hydrogels*

Thermally induced gelation was found in different systems based on chitosan hydrogels, such as: chitosan-glycerophosphate (Ahmadi and de Bruijn, 2008; Niranjan et al., 2013), chitosan-polyethylene glycol (Jo et al., 2012; Bhattarai et al., 2005) and grafted copolymers chitosan-g-poly(N-isopropylacrylamide). A chitosan-collagen hydrogel was used as a carrier for the culture and the release of mesenchymal stem cells, or of the mononuclear cells from the bone marrow (Wise et al., 2014).

Poly(N-isopropyl acrylamide) (PNIPAM) is a well-known thermo-sensitive polymer, with a critical temperature in solution (LCST) of 33°C, for higher temperatures the polymer suffering a solution-gel transition. One of the limitations in using PNIPAM in bone tissue engineering is related to its insignificant biodegradability and biocompatibility. To overcome these disadvantages, PNIPAM was grafted with natural polymers. One example is a hyaluronic acid-*g*-chitosan-*g*-PNIPAM copolymer, which is more biocompatible and more biodegradable, due to the presence of hyaluronic acid and of chitosan (Liao et al., 2011). In this hydrogel, mesenchymal stem cells derived from the bone marrow have been incorporated, this system being used for *in vitro* studies dealing with the proliferation, the differentiation and the osteogenic activity of the cells. *In vitro* cultures realized inside this hydrogel evidenced improved proliferation and osteogenic activity, when compared with the cells cultivated in polystyrene. In the same time, the system cells-hydrogel was more flexible after the osteogenic differentiation.

A hydrogel based on photocrosllinked chitosan was obtained by combining the chitosan with polylactide and with methacrylic anhydride, system that was gelled under UV irradiation (Kim et al., 2014). Hydrogel composition in terms of the density of lactide side chains grafted onto the chitosan chain, as well as the crosslinking density controlled by the irradiation time, allowed the control of the mechanical properties and of the degradation rate, as well as of the kinetics for the active substance release. Higher the chitosan/lactide ratio and more prolonged the irradiation time, the degradation rate decreased, and the effect of the crosslinking time was more important in respect with the protein release. Thus, a higher crosslinking time reduced the release of the albumin from bovine serum and extended the total time of release. Chitosan-lactide hydrogels proved to be useful in controlling the release of BMP-2 cells, which promote the *in vitro* osteogenic differentiation of the pre-osteoblastic cells from the mice bone marrow.

Injectable hydrogels based on chitosan, which suffer *in situ* gelation, represent a significant promise for bone tissue engineering, because they constitute an adequate medium for cells and/or growth factors encapsulation, their application at the defect site being realized in a minimum-invasive way. It is also important that these hydrogels could be combined with porous scaffolds; in such systems, biological factors could be incorporated.

### *4.2.3. Chitosan/CNT Composites*

Carbon nanotubes (CNT) present a cylindrical nanostructure, the length/diameter ratio being up to 28,000,000:1. These nanotubes are characterized by very good mechanical properties, high chemical and structural stability, as well as remarkable electrical, thermal, optical, and bioactive properties (Ajayan and Zhou, 2001; Samal and Bal, 2008). All these properties make from CNTs promising candidates as reinforcing fillers and as biomaterials used in contact with bones (i.e., prosthesis for arthroplasty, screws for fixing the fractures, scaffolds for bone regeneration). The carbon nanotubes also present a good compatibility with

bone tissues, allowing bone restoration and being easily integrated in the bone tissue (Usui et al., 2008). Carbon nanotubes could be used to improve the mechanical properties of the chitosan based composites.

CNTs are similar to an inert matrix, in which cells can easily proliferate. Zanello et al. (2006) suggested that carbon nanotubes could be used as an alternative material for treating the bone pathologies, with potential for normal bone reconstruction. Osteoblast cells were grown on CNT neutral from the electric point of view, which induced the production of mineralized bone. The impurities from CNT (such as: metallic catalysts and amorphous carbon particles) are however toxic for the cells and could induce oxygen reactive intracellular species (ROS). The incorporation of chitosan with amino functional groups induces the cytotoxicity decrease. When CNTs are grafted with chitosan, cell proliferation and cells attachment are improved. A possible explanation is that the cellular membranes are negatively charged, the cells being more easily attached and they better grow on the positively charged surfaces (Zhang et al., 2009).

### *4.2.4. Chitosan Blends and Composite Scaffolds*

While chitosan is characterized by several properties which make this polymer to be an important biomaterial used in bone tissue engineering, some of its properties are not suitable for this type of applications. For example, the mechanical strength and the compression modulus for most forms of pure chitosan are two orders of magnitude smaller than those corresponding to the normal bone. In the meantime, chitosan is unstable from the structural point of view in aqueous media. This polymer can not maintain a pre-established form when it is hydrated, property needed when it is implanted at the bone defect, when it should act as a filler to facilitate the processes of bone regeneration. Consequently, chitosan is often blended with other synthetic or natural polymers, in order to improve its mechanical properties and its structural integrity when hydrated. In the next sections, the main types of chitosan based systems, used in bone tissue engineering are briefly presented.

#### 4.2.4.1. Physical Blends

A simple method to form scaffolds is to blend two or more polymers before preparing the respective scaffold. In order to prepare such systems, chitosan was combined with polyesters, obtaining a continuous polymeric network (Correlo et al., 2009; Costa-Pinto et al., 2009; Oliveira et al., 2008).

Mendonca et al. (2013) prepared 3D scaffolds using poly(3-hydroxybutyrate) (PHB) and chitosan blends that proved to favourable interact with the mammalian cells (in particular, with osteoblasts). These systems are not cytotoxic, and present a compressive modulus of (13.07 ± 0.014) MPa, value close to that of the cancellous bone. By their morphological, chemical, and physical properties, PHB/chitosan blends have potential applications in bone-tissue engineering, with drug-delivery capabilities.

#### 4.2.4.2. Polyelectrolyte Complexes

The polyelectrolyte complex (PEC) presents improved properties when compared with the systems obtained from pure chitosan and they are relatively easy processed. The polyelectrolyte complexes based on chitosan, used in bone tissue engineering, include the chitosan complexed with alginate, gelatine and chondroitin sulphate (Park et al., 2013, Li et

al., 2005; Miranda et al., 2011). Particularly, the chitosan-alginate scaffolds (CA) are obtained by the formation of a complex between the amino groups of chitosan and the carboxyl groups of alginate. PEC scaffolds are, generally, more resistant than those processed from individual materials. It is interesting the obtainment of improved mechanical hardness, even if an increase of the PEC scaffolds porosity is achieved, due to a more open chain structure. The structural stability in aqueous media of the PEC scaffolds is superior in respect with those prepared from pure chitosan (Li et al., 2005).

Another example of PEC is represented by the formation, via hydrogen and electrostatic interactions between the anionic carboxyl groups from gelatine and the cationic chitosan. Gelatine, generated by collagen hydrolysis, retains the RGD sequences of collagen, leading to the promotion of the cellular adhesion and to the improvement of cells spreading by integrin binding (Mao et al., 2003). Chitosan and gelatine complexation decreases the scaffold crystallinity, obtaining a more amorphous structure, less subjected to degradation (Miranda et al., 2011). Consequently, a certain control could be realized on the degradation of such scaffolds, by controlling the ratio between chitosan and gelatine. Such a control on the degradation rate is very important in bone tissue engineering, where it is necessary that the degradation of the system do not be produced before the initiation of bone regeneration and also the obstruct of the regeneration do not take place.

#### 4.2.4.3. Scaffolds Based on Chitosan-Calcium Phosphate Composites

Pure chitosan is appropriate for the osteogenic cells attachment and proliferation, but it can not induce bone formation and bond formation between the scaffold and the bone. Contrary, calcium phosphate (CaP) is bioactive, this fact meaning that it can be bound to the bone and, sometimes, it presents osteoinductivity properties. This material is similar with the mineral phase of the bone. The most relevant biological forms for scaffolds used in bone tissue engineering include: hydroxyapatite (HAp), tricalcium phosphate (TCP), biphasic calcium phosphate (BCP), osteocalcium phosphate (OCP), and dicalcium phosphate, forms which are different in Ca/P ratio, crystalline structure and dissolution rate (Barrere et al., 2006). While the macroporous monolithic calcium scaffolds are often too breakable, the scaffolds based on chitosan-calcium phosphate composites accomplish the requirements needed in applications related to uncharged bone grafts. The calcium phosphate increases the osteoblast reaction and directs the phenotype of the mesenchymal stem cells, thus improving the biological answer at the contact with the chitosan scaffolds (LeGeros, 2008; Muller et al., 2007).

Biphasic calcium phosphate (BCP) is composed by insoluble hydroxyapatite and very soluble tricalcium phosphate. When they are exposed to a medium of cell cultures, chitosan scaffolds that contain BCP particles are rapidly wrapped in a mineral layer, such as the partial dissolution of the BCP microparticles induces the re-precipitation of the calcium ions and of the phosphate ions found at the scaffold surface. Comparing with the scaffolds prepared from pure chitosan, the BCP-chitosan scaffolds promoted the osteogenic activity of MC3T3-E1 cells in terms of the cellular attachment, morphology, and mineralization and marker expression of osteogenesis proteins.

Hydroxyapatite-chitosan-alginate (HAp-CA) scaffolds, *in situ* created by co-precipitation and lyophilisation (Jin et al., 2012), have been placed in defects of critical dimensions (4 mm) realized in mice, for 4 and 8 weeks and were compared with the effects induced by CA control scaffolds. After 4 weeks, the defects containing HAp-CA scaffolds presented

mineralization of low density, while for the defects filled with CA, the formation of apparent bone was not observed. After 8 weeks, the defects filled with HAp-CA contained mineralized bone, osteoblasts, and osteoclasts, while in the defects filled with CA it was evidenced only a mineralization of low density.

*4.2.4.3.1. Chitosan/Hydroxyapatite Composites (CS/HAp)*

CS/HAp composites seem to be promising for mimicking both of the organic portion, as well as of the inorganic one from the natural bone. Hydroxyapatite ($Ca_{10}(PO_4)_6(OH)_2$) is one of the most stable forms of the calcium phosphate, representing the major component in bones (60 - 65%) (Kim and Mendis, 2006). HAp is used in orthopaedic, dental and maxillofacial applications. HAp was also used as important compound in the systems applied for obtaining artificial bones, being gradually replaced by the host bone, after implantation. However, the mechanical properties of HAp are weak. For their improvement, HAp is combined with various polymers (Nath et al., 2009). When chitosan is combined with HAp, it is possible to obtain a system that mimics the function of the natural bone, the osteoblast growth on the surface of such scaffolds being significantly improved (Di Martino et al., 2005; Xianmiao et al., 2009; Thein-Han and Misra, 2009; Madhumathi et al.,2009; Li et al. 2005). All the obtained results proved that the system CS/HAp does not present toxicity for the attachment of cells and for the increase of osteoblast proliferation (Di Martino et al., 2005; Xianmiao et al., 2009; Manjubala et al., 2006). Scaffolds prepared from these composites have a pore size between 100 and 200 μm, allowing a spatial arrangement of the cells (10–30 μm), so they can migrate inside the composite (Aronow et al., 1990). It was observed that, when osteoblasts were cultivated in a CS/phosphorylated HAp medium, the cell morphology changed after 30 minutes of culture and they became triangular after 24 hours, polygonal after 48 hours and, finally, they aggregated up to become indistinguishably after 5 days (Li et al., 2008). Besides HAp, other calcium phosphates assure the adhesion and the proliferation of some types of cells when they are combined with CS (i.e., MC3T3-E1 mice osteoblasts and L929 cells) (Xu and Simon, 2005). The activity of the alkaline phosphatase (ALP) is considered as an important marker in osteoblast differentiation, in a relatively initial stage in bone formation. Scaffolds based on CS/HAp composites present a high ALP when compared with the CS based scaffolds, the highest value of the ALP being obtained for the system with a HAp content of 30-40 wt%; cellular proliferation decreases, however, with increasing HAp concentration (Teng et al., 2009; Li et al., 2005; Zhang et al., 2003).

*4.2.4.3.2. Chitosan/Calcium Phosphate Composites*

Scaffolds based on chitosan-calcium phosphate composites are obtained by physical blending of the microparticles of calcium phosphate with chitosan, before producing the respective scaffolds. (Zhang and Neau, 2001; Zhao et al., 2006), or by incorporating nano-hydroxyapatite (nanoHAp) in chitosan based materials (Sionkowska, and Kaczmarek, 2017). NanoHAp particles, when compared with HAp particles of micro dimensions, are more similar with biological apatite from bones, and they have an increased surface area to volume ratio. In the case of the nano material, the interaction between the particles and the polymeric matrix is improved. HAp nanoparticles can be incorporated in chitosan scaffolds in different ways; these ones can be physically incorporated into the chitosan solutions, or they can co-precipitate with chitosan (Peng et al., 2012; Zhang et al., 2010). Because HAp is insoluble in neutral and basic solutions and because chitosan precipitation takes place in solutions with pH

> 6, the conditions for precipitation of both materials are almost the same. In situ co-precipitation forms a mineral phase associated with a polymeric phase during the bone physiological mineralization, leading to a stronger interfacial bonding between the mineral and the polymer. Physical blending is a rapid and simple process, but in situ co-precipitation is more advantageous, due to a homogeneous distribution of HAp in the polymer matrix, the resulted particles being more intimate integrated in this one (Kong et al., 2005). Chitosan and nanoHAp co-precipitation presents a good miscibility for different ratios between nanoHAp and chitosan, the dimension of nanoHAp being controlled by changing the ratio between chitosan, calcium and phosphate ions from the solution (Rusu et al., 2005).

Incorporation of microparticles of hydroxyapatite (microHAp) in scaffolds based on chitosan-gelatine also improved the scaffold-cells interactions and the potential of osteogenic differentiation (Zhao et al., 2006). In this case, because HAp is characterized by a low solubility, the mechanism that controls the scaffold-cells interactions is different from that implied in the case of using BCP microparticles. However, HAp adsorbs proteins such as fibronectin and vitronectin from serum, which could play an important role in improving the mesenchymal stem cells (MSC) binding and proliferation (Wang et al., 2013). Commercial nanoHAp powder was combined with chitosan in order to obtain scaffolds by phase separation (Thein-Han and Misra, 2009). It was observed an improved proliferation of MC3T3-E1 pre-osteoblasts on the scaffolds based on nanoHAp – chitosan composites, when compared with those produced only from chitosan. Cells attached at the surface of the composite scaffolds have more rough surfaces, due to the significant accumulation of particles rich in calcium on the cellular membrane. This behaviour could be attributed to a significant higher mineralization on the composite scaffold. The obtainment of chitosan-nanoHAp composites could be realized also if HAp component is formed *in situ* in chitosan solution. The co-precipitation is a biomimetic process, because the mineral phase is formed in association with the polymeric phase, leading to stronger interfacial bonding, similar with bone physiological mineralization. This method is more advantageous than the physical blending with nanoHAp, because it can generate a more homogeneous distribution of nanoHAp in the polymeric matrix.

Inclusion of nanoHAp in a polymer matrix seems to improve the scaffolds based on chitosan by three ways: the osteogen cells reaction is improved in terms of attachment, proliferation and cellular differentiation, the compression modulus of the scaffold increases, while the scaffold swelling decreases. Improvement in osteogenic cells reaction could be related to the changes in roughness/topography of the scaffold, improved binding of proteins on nanoHAp leading to a better adherence and/or formation of biological apatite being facilitated by nanoHAp which acts like nucleation agents.

*4.2.4.3.3. Coating of the Chitosan Scaffolds with Calcium Phosphate*

Calcium phosphate could be combined with chitosan by the direct formation of a coating layer or of a biological apatite layer at the chitosan scaffold surface. Coating with calcium phosphate improves the binding ability of the respective scaffolds to the bone, as well as their osteoinductivity (LeGeros, 2008; Li et al., 2010; Manjubala et al., 2006).

By scaffolds soaking in SBF, *in vivo* some aspects of the natural biomineralization are mimicked, because the components of the anionic solution, pH and temperature are similar to those corresponding to the sanguine plasma (Suarez-Gonzalez et al., 2012). In this case, the biomineral is nucleated on the surfaces, from the aqueous solution, thus this process is

enough versatile and can be applied to the scaffolds prepared from different materials and having different forms. Formation of apatite from SBF is accelerated on scaffolds based on chitosan-chondroitin sulphate and chitosan-alginate, in comparison with the pure chitosan scaffolds (Park et al., 2013). It is possible that the negative charges associated with chondroitin sulphate and alginate to promote $Ca^{2+}$ electrostatically accumulation on the scaffold surface, inducing the nucleation and the growth of the apatite layer (Zhu et al., 2004). Double diffusion method implies the calcium and phosphate ions diffusion, ions previous segregated inside the scaffold which allows the precipitation of an apatite layer on the pore walls of this one.

*4.2.4.3.4. Multicomponent Chitosan-Based Scaffolds*

Besides adding micro- and nanoparticles of calcium phosphate in chitosan-based scaffolds, the incorporation or immobilization of a second or third functional component improves even more the properties of the scaffolds used in bone tissue engineering.

Such a study refers to the enzymatically assisted co-precipitation of the amorphous calcium phosphate and of ciprofloxacin from a chitosan solution (Nardecchia et al., 2012), finally obtaining porous scaffolds. Ciprofloxacin precipitation determined the obtainment of crystals similar to needles, with granular aggregates of amorphous calcium on their surfaces. Amorphous calcium phosphate is more soluble than hydroxyapatite and, as a consequence, its dissolution in the presence of calcium and phosphate ions induces the biomineralization and the possible osteoinductivity of the scaffolds. Ciprofloxacin is extremely useful in controlling the possible post-surgical infections resulted after scaffolds implantation.

Recently, adipose-derived extracellular matrix (A-dECM) was studied by Wang et al. (2017) for potential applications in bone tissue engineering. They produced chitosan/gelatine/A-dECM scaffolds (C/G/A-dECM) via freeze-drying and crosslinking. *In vitro* tested A-dECM scaffolds promoted the attachment and proliferation of BMCS, better osteogenic differentiation being observed for C/G/A-dECM scaffolds when compared with the C/G scaffolds, used as control.

Isikli et al. (2012) prepared 3D porous chitosan-gelatine scaffolds for bone tissue engineering, with either non-sintered (nsHA) or sintered (sHA) hydroxyapatite. When nsHA and sHA were added, the obtained scaffolds exhibited similarity with human spongy bone. The highest Saos-2 (Sarcoma osteogenic) cells affinity was observed with CS-Gel/sHA composites in comparison with other scaffolds. This study proved that the composites prepared from chitosan, gelatine and hydroxyapatite were suitable as cell carriers, specifically those which were incorporated with sHA.

Porous scaffolds of chitosan and poly (vinyl alcohol) containing various concentrations of methyl cellulose (25%, 50%, and 75%) were characterized by improved tensile strength, swelling ratio, degradation rate and porosity when compared to CS/PVA scaffolds, being thus considered a promising biomaterial for application in tissue engineering (Kanimozhi et al., 2016).

Osteoinductivity (the ability of the scaffolds to attract and induce the differentiation of the mesenchymal cells in osteoblasts bone generating) could be obtained for the chitosan based scaffolds even by calcium phosphate incorporation, which dissolves and re-precipitates, thus obtaining an apatite layer, with the further incorporation and release of growth factors such as BMP-2 (bone morphogenetic protein). While the growth factors are often combined with chitosan scaffolds by physical encapsulation and release controlled by diffusion, the

quantity of growth factors needed for obtaining a biological reaction is often at a supra-physiological level. Often a sudden release of these factors was found. An alternative for the adequate release of the growth factors is to mimic the non-covalent interactions between the growth factor and the extracellular matrix. Heparin, an anionic glycosaminoglycan, plays an important role in modulating the activity of the growth factors, such as the bone morphogenetic proteins (Hudalla and Murphy, 2011). Therefore it can improve the chitosan based scaffolds. For example, heparin was covalently conjugated with chitosan-alginate PEC, used for controlled release (Ho et al., 2009). When PECs were exposed to bFGF-2 fibroblastic factors, the heparin presence and its interaction with bFGF-2 determined the location of the growth factor activity, thus significantly decreasing its release.

Heparin was covalently or non-covalently immobilized (by electrostatic interactions) on porous chitosan based scaffolds used in bone tissue engineering. It was observed that these scaffolds functionalized with heparin have a significant improved effect in what is concerning the differentiation of the MC3T3-E1 pre-osteoblast cells, in terms of an improved activity of alkaline phosphatase and of osteocalcin expression, when compared with using scaffolds based on chitosan without heparin (Gumusderelioglu and Aday, 2011).

Non-covalent immobilization of heparin on microsphere scaffolds based on chitosan-poly(lactide-co-glycolide) (PLGA), via electrostatic interactions, allowed the further BMP-2 immobilization in a manner that mimics the non-covalent interactions of ECM growth factor (Jiang et al., 2010). Presence of heparin and of BMP determined a more rapid bone formation, when compared with the experimental control group. Functionalization of scaffolds based on chitosan with heparin and heparin sulphate glycosaminoglycans could be also very useful for *in vivo* immobilization of endogenous growth factors (Hudalla et al., 2011), in view of bone tissue regeneration.

Poly-(DL-lactide-co-glycolide) (PLGA) microparticles containing 10% w/w simvastatin were embedded in porous chitosan based scaffolds showing controlled drug release at the targeting site, thus enhancing cell proliferation and mineralisation and promoting bone regeneration (Gentile et al., 2016).

Chitosan based systems could be also used for applications in the cartilage, nerves and blood vessel repair. Chitosan hydrogel prepared by cross linking with 5 wt% genipin proved to be effective in disc and cartilage engineering (Yan et al., 2010). Silk fibroin and chitosan scaffolds with an interconnected porous structure, characterized by adequate antimicrobial, degradation and mechanical properties can facilitate the growth and the attachment of feline fibroblast cells; that is why these scaffolds might be a desirable hybrid material for cartilage engineering (Bhardwaj and Kundu, 2011).

## CONCLUSION

Chitosan-based biomaterials represent a family of polymers with distinct structural features, including provenance, degree of deacetylation, acetyl distribution pattern, average molecular weight, and activities. Chitosan-based products are promising materials in the production of scaffolds for tissue engineering because of their antimicrobial, haemostatic and stimuli responsiveness activities. These systems also present special features, such as: non-toxicity, biocompatibility, biodegradability, bioavailability and possibility to be processed in

different forms. Chitosan based materials are also good carriers for drugs and genes. They are able to deliver particles or scaffolds that rapidly break down into microparticles that can be readily phagocytosed.

However, the absence of clinical studies in humans, the inadequate experimental designs, and the lack of information concerning chitosan's characteristics limit the reproducibility and relevance of studies and the clinical applicability of chitosan. Therefore many studies are necessary to promote the wide application of chitosan based materials in tissue engineering.

## REFERENCES

Abarrategi A., García-Cantalejo J., Moreno-Vicente C., Civantos A., Ramos V, Casado J. V., Pérez-Rial S, Martńez-Corriá R. and López-Lacomba J. L. 2009. "Gene Expression Profile On Chitosan/Rhbmp-2 Films: A Novel Osteoinductive Coating For Implantable Materials." *Acta Biomaterialia* 5 (7): 2633-2646.

Abdelgawad A. M., Hudson S. M. and Rojas O. J. 2014. "Antimicrobial Wound Dressing Nanofiber Mats From Multicomponent (Chitosan/Silver-Nps/Polyvinyl Alcohol) Systems." *Carbohydrate Polymers* 100: 166-178.

Ahmadi R. and de Bruijn J. D. 2008. "Biocompatibility And Gelation Of Chitosan–Glycerol Phosphate Hydrogels." *Journal Of Biomedical Materials Research Part A* 86A (3): 824-832.

Aiba S., (1992). Studies on chitosan: 4. Lysozymic hydrolysis of partially N-acetylated chitosans. *International Journal of Biological Macromolecules*, 14(4), pp.225-228.

Ajayan P. and Zhou O. 2001. "Applications of carbon nanotubes." *Carbon Nanotubes*80: 391–425.

Akincibay H., Senel S. and Ay Z. Y. 2007. "Application Of Chitosan Gel In The Treatment Of Chronic Periodontitis." *Journal Of Biomedical Materials Research Part B: Applied Biomaterials* 80B (2): 290-296.

Alemdaroglu C., Degim Z., Celebi N. Zor F., Öztürk S., and Erdoğan D. 2006. "An Investigation On Burn Wound Healing In Rats With Chitosan Gel Formulation Containing Epidermal Growth Factor." *Burns* 32 (3): 319-327.

Altiok D., Altiok E. and Tihminlioglu F. 2010. "Physical, Antibacterial And Antioxidant Properties Of Chitosan Films Incorporated With Thyme Oil For Potential Wound Healing Applications." *Journal Of Materials Science: Materials In Medicine* 21 (7): 2227-2236.

Amaral I. F., Cordeiro A. L., Sampaio P. andBarbosa M. A. 2007. "Attachment, Spreading And Short-Term Proliferation Of Human Osteoblastic Cells Cultured On Chitosan Films With Different Degrees Of Acetylation." *Journal Of Biomaterials Science, Polymer Edition* 18 (4): 469-485.

Amaral I. F., Lamghari M., Sousa S. R., Sampaio P. andBarbosa M. A. 2005. "Rat Bone Marrow Stromal Cell Osteogenic Differentiation And Fibronectin Adsorption On Chitosan Membranes: The Effect Of The Degree Of Acetylation." *Journal Of Biomedical Materials Research Part A* 75A (2): 387-397.

Amidi M., Mastrobattista E., Jiskoot W. and Hennink W. E. 2010. "Chitosan-Based Delivery Systems For Protein Therapeutics And Antigens." *Advanced Drug Delivery Reviews* 62 (1): 59-82.

Andres Y., Giraud L., Gerente C. and Le Cloirec P. 2007. "Antibacterial Effects Of Chitosan Powder: Mechanisms Of Action." *Environmental Technology* 28 (12): 1357-1363.

Anisha B. S., BiswasR., Chennazhi K. P. and Jayakumar R.2013. "Chitosan–Hyaluronic Acid/Nano Silver Composite Sponges For Drug Resistant Bacteria Infected Diabetic Wounds." *International Journal Of Biological Macromolecules* 62: 310-320.

Annapoorna M., Anisha B. S., Chennazhi K. P. and Jayakumar R. 2015. "Chitosan–Hyaluronic Acid/VEGF Loaded Fibrin Nanoparticles Composite Sponges For Enhancing Angiogenesis In Wounds." *Colloids And Surfaces B: Biointerfaces* 127: 105-113.

Anselme K., Bigerelle M., Noel B., Dufresne E., Judas D., Iost A., Iost A., and Hardouin P. 2000. "Qualitative And Quantitative Study Of Human Osteoblast Adhesion On Materials With Various Surface Roughnesses." *Journal of Biomedical Materials Research* 49 (2): 155-166.

Anselme K., Linez P., Bigerelle M., Le Maguer D., Le Maguer A., Hardouin P., Hildebrand H. F., Iost A., and Leroy J. M. 2000. "The Relative Influence Of The Topography And Chemistry Of Tial6v4 Surfaces On Osteoblastic Cell Behaviour." *Biomaterials* 21 (15): 1567-1577.

Aoyagi S., Onishi H. and Machida Y. 2007. "Novel Chitosan Wound Dressing Loaded With Minocycline For The Treatment Of Severe Burn Wounds." *International Journal Of Pharmaceutics* 330 (1-2): 138-145.

Aranaz I., Mengibar M., Harris R., Panos I., Miralles B., Acosta N., Galed G. and Heras A. 2009. "Functional Characterization of Chitin And Chitosan." *Current Chemical Biology* 3 (2): 203-230.

Aronow M. A., Gerstenfeld L. C., Owen T. A, Tassinari M. S., Stein G. S. and Lian J. B. 1990. "Factors That Promote Progressive Development Of The Osteoblast Phenotype In Cultured Fetal Rat Calvaria Cells." *Journal of Cellular Physiology* 143 (2): 213-221.

Arpornmaeklong P., Pripatnanont P. and Suwatwirote N. 2008. "Properties Of Chitosan–Collagen Sponges And Osteogenic Differentiation Of Rat-Bone-Marrow Stromal Cells." *International Journal of Oral And Maxillofacial Surgery* 37 (4): 357-366.

Azad A. K., Sermsintham N., Chandrkrachang S. and Stevens W. F. 2004. "Chitosan Membrane As A Wound-Healing Dressing: Characterization And Clinical Application." *Journal of Biomedical Materials Research* 69B (2): 216-222.

Azuma K., Ifuku S., Osaki T., Okamoto Y. and Minami S. 2014. "Preparation And Biomedical Applications Of Chitin And Chitosan Nanofibers." *Journal of Biomedical Nanotechnology* 10 (10): 2891-2920.

Azuma K., Izumi R., Osaki T., Ifuku S., Morimoto M., Saimoto H., Minami S. and Okamoto Y. 2015. "Chitin, Chitosan, And Its Derivatives For Wound Healing: Old And New Materials." *Journal of Functional Biomaterials* 6 (1): 104-142.

Barrere F., van Blitterswijk C. A., de Groot K. 2006. "Bone regeneration: molecular and cellular interactions with calcium phosphate ceramics."*International Journal of Nanomedicine* 1(3): 317–332.

Beanes S. R., Dang C., Soo C. and Ting K. 2003. "Skin Repair And Scar Formation: The Central Role Of TGF-[Beta]." *Expert Reviews In Molecular Medicine* 5 (08).

Berger J., Reist M., Mayer J. M., Felt O. and Gurny R. 2004. "Structure And Interactions In Chitosan Hydrogels Formed By Complexation Or Aggregation For Biomedical Applications." *European Journal of Pharmaceutics And Biopharmaceutics* 57 (1): 35-52.

Berger J., Reist M., Mayer J. M., Felt O., Peppas N. A. and Gurny R. 2004. "Structure And Interactions In Covalently And Ionically Crosslinked Chitosan Hydrogels For Biomedical Applications." *European Journal of Pharmaceutics And Biopharmaceutics* 57 (1): 19-34.

Bhardwaj N. and Kundu S. C. 2011. "Silk Fibroin Protein And Chitosan Polyelectrolyte Complex Porous Scaffolds For Tissue Engineering Applications." *Carbohydrate Polymers* 85 (2): 325-333.

Bhattarai N., Edmondson D., Veiseh O., Matsen F. A. and Zhang M. 2005."Electrospun chitosan-based nanofibers and their cellular compatibility." *Biomaterials* 26(31): 6176–6184.

Bhattarai N., Gunn J. and Zhang M. 2010. "Chitosan-Based Hydrogels For Controlled, Localized Drug Delivery." *Advanced Drug Delivery Reviews* 62 (1): 83-99.

Bhattarai N., Matsen F. A. and Zhang M. 2005. "PEG-Grafted Chitosan As An Injectable Thermoreversible Hydrogel." *Macromolecular Bioscience* 5 (2): 107-111.

Biagini G., Bertani A., Muzzarelli R., Damadei A., Di Benedetto G., Belligolli A., Riccotti G., Zucchini C. and Rizzoli C. 1991. "Wound Management With N-Carboxybutyl Chitosan." *Biomaterials* 12 (3): 281-286.

Boateng J. S., Matthews K. H., Stevens H. N. E. and Eccleston G. M. 2008. "Wound Healing Dressings And Drug Delivery Systems: A Review." *Journal of Pharmaceutical Sciences* 97 (8): 2892-2923.

Boccaccini A. R., Keim S., Ma R., Li Y. and Zhitomirsky I. J. 2010. "Electrophoretic Deposition *of* Biomaterials." *Journal of The Royal Society Interface* 7 (Suppl_5): S581-S613.

Boucard N., Viton C. and Domard A. 2005. "New Aspects Of The Formation Of Physical Hydrogels Of Chitosan In A Hydroalcoholic Medium." *Biomacromolecules* 6 (6): 3227-3237.

Boucard N., Viton C., Agay D., Mari E., Roger T., Chancerelle Y. and Domard A. 2007. "The Use Of Physical Hydrogels Of Chitosan For Skin Regeneration Following Third-Degree Burns." *Biomaterials* 28 (24): 3478-3488.

Boyan B. D., Hummert T. W., Dean D. D. and Schwartz Z. 1996. "Role Of Material Surfaces In Regulating Bone And Cartilage Cell Response." *Biomaterials* 17 (2): 137-146.

Boynuegri D., Azcan G., Senel S., Uc D., Uraz A., Ogus E., Cakilci B. and Karaduman B. 2009. "Clinical And Radiographic Evaluations Of Chitosan Gel In Periodontal Intraosseous Defects: A Pilot Study." *Journal of Biomedical Materials Research Part B: Applied Biomaterials* 90B (1): 461-466.

Bruin P., Jonkman M. F., Meijer H. J. and Pennings A. J. 1990. "A New Porous Polyetherurethane Wound Covering." *Journal of Biomedical Materials Research* 24 (2): 217-226.

Brunette, D. M., Tengvall, P., Textor, M., Thomsen, P. 2001, *Titanium in Medicine. Material Science, Surface Science, Engineering, Biological Responses and Medical Applications*. Berlin: Springer-Verlag.

Bumgardner J. D., Chesnutt B. M., Yuan Y., Yang Y, Appleford M., Oh S., McLaughlin R., Elder S. H., and Ong J. L. 2007. "The Integration Of Chitosan-Coated Titanium In Bone: An In Vivo Study In Rabbits." *Implant Dentistry* 16 (1): 66-79.

Bumgardner J. D., Wiser R., Elder S. H., Jouett R., Yang Y., and Ong J. L. 2003. "Contact Angle, Protein Adsorption And Osteoblast Precursor Cell Attachment To Chitosan

Coatings Bonded To Titanium." *Journal of Biomaterials Science, Polymer Edition* 14 (12): 1401-1409.

Bumgardner J. D., Wiser R., Gerard P. D., Bergin P., Chestnutt B., Marin M., Ramsey V., Elder S. H. and Gilbert J. A. 2003. "Chitosan: Potential Use As A Bioactive Coating For Orthopaedic And Craniofacial/Dental Implants." *Journal of Biomaterials Science, Polymer Edition* 14 (5): 423-438.

Burkatovskaya M., Tegos G. P., Swietlik E. Demidova T. N., Castano A. P., and Hamblin M. R. 2006. "Use Of Chitosan Bandage To Prevent Fatal Infections Developing From Highly Contaminated Wounds In Mice." *Biomaterials* 27 (22): 4157-4164.

Cai K., Hu Y., Jandt K. D. and Wang Y. 2007. "Surface Modification Of Titanium Thin Film With Chitosan Via Electrostatic Self-Assembly Technique And Its Influence On Osteoblast Growth Behavior." *Journal of Materials Science: Materials In Medicine* 19 (2): 499-506.

Cai K., Rechtenbach A., Hao J., Bossert J. and Jandt K. D. 2005. "Polysaccharide-Protein Surface Modification Of Titanium Via A Layer-By-Layer Technique: Characterization And Cell Behaviour Aspects." *Biomaterials* 26 (30): 5960-5971.

Cascone M. G., Maltinti S., Barbani N. and Laus M 1999. "Journal Search Results - Cite This For Me." *Journal of Materials Science: Materials In Medicine* 10 (7): 431-435.

Chang Q., Gao H., Bu S., Zhong W., Lu F. and Xing M. 2015. "An Injectable Aldehyded 1-Amino-3,3-Diethoxy-Propane Hyaluronic Acid–Chitosan Hydrogel As A Carrier Of Adipose Derived Stem Cells To Enhance Angiogenesis And Promote Skin Regeneration." *Journal of Materials Chemistry B* 3 (22): 4503-4513.

Charernsriwilaiwat N., Opanasopit P., Rojanarata T. and Ngawhirunpat T. 2012. "Lysozyme-loaded, electrospun chitosan-based nanofiber mats for wound healing." *International Journal of Pharmacy* 427(2): 379–384.

Chatelet C., Damour O., Domard A. 2001. "Influence Of The Degree Of Acetylation On Some Biological Properties Of Chitosan Films." *Biomaterials* 22 (3): 261-268.

Chen F., Wang Z. C. and Lin C. J. 2002. "Preparation And Characterization Of Nano-Sized Hydroxyapatite Particles And Hydroxyapatite/Chitosan Nano-Composite For Use In Biomedical Materials." *Materials Letters* 57 (4): 858-861.

Chen K. S., Ku Y. A., Lee C. H., Lin H. R., Lin F. H. and Chen T. M. 2005a. "Immobilization Of Chitosan Gel With Cross-Linking Reagent On Pnipaam Gel/PP Nonwoven Composites Surface." *Materials Science And Engineering: C* 25 (4): 472-478.

Chen S. P., Wu G. Z., Zeng H. Y. 2005b. "Preparation Of High Antimicrobial Activity Thiourea Chitosan–Ag+ Complex." *Carbohydrate Polymers* 60 (1): 33-38.

Chen Z., Mo X, He C. and Wang H. 2008. "Intermolecular Interactions In Electrospun Collagen–Chitosan Complex Nanofibers." *Carbohydrate Polymers* 72 (3): 410-418.

Chung Y. C. and Chen C. Y., 2008. "Antibacterial Characteristics And Activity Of Acid-Soluble Chitosan." *Bioresource Technology* 99 (8): 2806-2814.

Clasen C., Wilhelms T. and Kulicke W. M. 2006. "Formation And Characterization Of Chitosan Membranes." *Biomacromolecules* 7 (11): 3210-3222.

Cohen M. L. 2000. "The Theory *of* Real Materials." *Annual Review of Materials Science*30 (1): 1-26.

Correlo V. M., Boesel L. F., Pinho E., Costa-Pinto A. R., Alves da Silva M. L., Bhattacharya M., Mano J. F., Neves N. M. and Reis R. L. 2009. "Melt-Based Compression-Molded Scaffolds From Chitosan-Polyester Blends And Composites: Morphology And

Mechanical Properties." *Journal of Biomedical Materials Research Part A* 91A (2): 489-504.

Costa-Pinto A. R., Correlo V. M., Sol P. C., Bhattacharya M., Charbord P., Delorme B., Reis R. L., and Neves N. M. 2009. "Osteogenic Differentiation Of Human Bone Marrow Mesenchymal Stem Cells Seeded On Melt Based Chitosan Scaffolds For Bone Tissue Engineering Applications." *Biomacromolecules* 10 (8): 2067-2073.

Costa-Pinto A. R., Reis R. L. and Neves N. M. 2011. "Scaffolds Based Bone Tissue Engineering: The Role Of Chitosan." *Tissue Engineering Part B: Reviews* 17 (5): 331-347.

Croisier F. and Jérôme C., 2013. "Chitosan-based biomaterials for tissue engineering." *European Polymer Journal* 49: 780-792,

Dai M., Zheng X., Xu X. Kong X. Y., Li X. Y., Guo G., Luo F., Zhao X., Wei Y. Q. and Qian Z. 2009. "Chitosan-Alginate Sponge: Preparation And Application In Curcumin Delivery For Dermal Wound Healing In Rat." *Journal of Biomedicine And Biotechnology* 2009: 1-8.

Dai T., Tanaka M., Huang Y. Y. and Hamblin M. R. 2011. "Chitosan Preparations For Wounds And Burns: Antimicrobial And Wound-Healing Effects." *Expert Review of Anti-Infective Therapy* 9 (7): 857-879.

Dambies L., Thierry V., Domard A., and Guibal E. 2001. "Preparation Of Chitosan Gel Beads By Ionotropic Molybdate Gelation." *Biomacromolecules* 2 (4): 1198-1205.

Dash, M., Chiellini F., Ottenbrite R. M., and Chiellini E. 2011. "Chitosan—A Versatile Semi-Synthetic Polymer In Biomedical Applications." *Progress In Polymer Science* 36 (8): 981-1014.

Denkbas E. B., Ozturk E., Ozdemir N., Kececi K., Agalar C. 2004. "Norfloxacin-Loaded Chitosan Sponges As Wound Dressing Material." *Journal of Biomaterials Applications* 18 (4): 291-303.

Denuziere A., Ferrier D., Damour O. and Domard A. 1998. "Chitosan–Chondroitin Sulfate And Chitosan–Hyaluronate Polyelectrolyte Complexes: Biological Properties." *Biomaterials* 19 (14): 1275-1285.

Di Martino A., Sittinger M. and Risbud M. V. 2005. "Chitosan: A Versatile Biopolymer For Orthopaedic Tissue-Engineering." *Biomaterials* 26 (30): 5983-5990.

Díez-Pascual A. M., and Díez-Vicente A. L. 2015. "Wound Healing Bionanocomposites Based On Castor Oil Polymeric Films Reinforced With Chitosan-Modified ZnO Nanoparticles." *Biomacromolecules* 16 (9): 2631-2644.

Dong Y., Liu H. Z., Xu L., Li G., Ma Z. N., Han F., Yao H. M., Sun Y. H. and Li S. M. 2010. "A Novel CHS/ALG Bi-Layer Composite Membrane With Sustained Antimicrobial Efficacy Used As Wound Dressing." *Chinese Chemical Letters* 21 (8): 1011-1014.

Duan B., Yuan X., Zhu Y., Zhang Y., Li X., Zhang Y. and Yao K. 2006. "A Nanofibrous Composite Membrane Of PLGA–Chitosan/PVA Prepared By Electrospinning." *European Polymer Journal* 42 (9): 2013-2022.

Dumitriu R. P., Profire L., Nita L. E., Dragostin O. M., Ghetu N., Pieptu D. and Vasile C. 2015. "Sulfadiazine—Chitosan Conjugates And Their Polyelectrolyte Complexes With Hyaluronate Destined To The Management Of Burn Wounds." *Materials* 8 (1): 317-338.

Dutta P., Rinki K. and Dutta J., 2011. Chitosan: a promising biomaterial for tissue engineering scaffolds. Chitosan for biomaterials II. In: R. Jayakumar, M. Prabaharan, R.

A. A. Muzzarelli, eds., *Advances in polymer science,* Heidelberg: Springer Berlin, p. 45-79

Elias C. N., Lima J. H. C., Valiev R. and Meyers M. A. 2008. "Biomedical Applications Of Titanium And Its Alloys." *JOM* 60 (3): 46-49.

Elvin C. M., Vuocolo T., Brownlee A. G., Sando L., Huson M. G., Liyou N. E., Stockwell R., Lyons R. E., Kim M., Edwards G. A. *et al.*, 2010. "A Highly Elastic Tissue Sealant Based On Photopolymerised Gelatine." *Biomaterials* 31 (32): 8323-8331.

Esposito M., Coulthard P., Thomsen P. and Worthington H. V. 2004. "Antibiotics To Prevent Complications Following Dental Implant Treatment." *Australian Dental Journal* 49 (4): 205-205.

Fakhry A., Schneider G. B., Zaharias R. and Senel S. 2004. "Chitosan Supports The Initial Attachment And Spreading Of Osteoblasts Preferentially Over Fibroblasts." *Biomaterials* 25 (11): 2075-2079.

Faucheux N., Schweiss R., Lützow K., Werner C. and Groth T. 2004. "Self-Assembled Monolayers With Different Terminating Groups As Model Substrates For Cell Adhesion Studies." *Biomaterials* 25 (14): 2721-2730.

Fleming J. E., Cornell C. N. and Muschler G. F. 2000. "Bone cells and matrices in orthopedic tissue engineering." *Orthopedic Clinics of North America* 31 (3): 357-374.

França R., Mbeh D. A., Samani T. D., Le Tien C., Mateescu M. A., Yahia L. and Sacher E. 2013. "The Effect Of Ethylene Oxide Sterilization On The Surface Chemistry Andin Vitrocytotoxicity Of Several Kinds Of Chitosan." *Journal Of Biomedical Materials Research Part B: Applied Biomaterials* 101 (8): 1444-1455.

Fujita M., Kinoshita M., Ishihara M., Kanatani Y., Morimoto Y., Simizu M., Ishizuka T., Saito Y., Yura H., Matsui T., Takase B., Hattori H., Kikuchi M. and Maehara T. 2004. "Inhibition Of Vascular Prosthetic Graft Infection Using A Photocrosslinkable Chitosan Hydrogel." *Journal of Surgical Research* 121 (1): 135-140.

Fwu L. M., Yu B. W., Shin S. S., Chao A. C., Juin Y. L. and Chia C. S. 2003. "Asymmetric Chitosan Membranes Prepared By Dry/Wet Phase Separation: A New Type Of Wound Dressing For Controlled Antibacterial Release." *Journal of Membrane Science* 212 (1-2): 237-254.

García A. J., Vega M. D. and Boettiger D. 1999. "Modulation Of Cell Proliferation And Differentiation Through Substrate-Dependent Changes In Fibronectin Conformation." *Molecular Biology of The Cell* 10 (3): 785-798.

Gentile P., Nandagiri V. K., Daly J., Chiono V., Mattu C., Tonda-Turo C., and Ramtoola Z 2016. "Localised Controlled Release Of Simvastatin From Porous Chitosan–Gelatine Scaffolds Engrafted With Simvastatin Loaded PLGA-Microparticles For Bone Tissue Engineering Application." *Materials Science and Engineering: C* 59: 249-257.

Golub E. E. and Boesze-Battaglia K. 2007. "The Role Of Alkaline Phosphatase In Mineralization." *Current Opinion In Orthopaedics* 18 (5): 444-448.

Gonzalez J. S., Maiolo A. S., Ponce A. G. and Alvarez V. A. Composites based on poly(vinyl alcohol) hydrogels for wound dressing. *XVIII The Argentine Congress of Bioengineering and Clinical Engineering Conference VII*, SABI, pp. 1–4, 2011

Goodacre C. J., Kan J. Y. and Rungcharassaeng K. 1999. "Clinical Complications Of Osseointegrated Implants." *The Journal of Prosthetic Dentistry* 81 (5): 537-552.

Greene A. H., Bumgardner J. D., Yang Y. Moseley J. and Haggard W. O. 2008. "Chitosan-Coated Stainless Steel Screws For Fixation In Contaminated Fractures." *Clinical Orthopaedics and Related Research* 466 (7): 1699-1704.

Gümüşderelioğlu, M., and Aday S. 2011. "Heparin-Functionalized Chitosan Scaffolds For Bone Tissue Engineering." *Carbohydrate Research* 346 (5): 606-613.

Hamamoto N., Hamamoto Y., Nakajima T. and Ozawa H. 1995. "Histological, Histocytochemical And Ultrastructural Study On The Effects Of Surface Charge On Bone Formation In The Rabbit Mandible." *Archives of Oral Biology* 40 (2): 97-106.

Hamman J. H. and Kotzé A. F. 2002. Paracellular absorption enhancement across intestinal pithelia by N-rimethyl chitosan chloride. In: Muzzarelli, R. A. A., Muzzarelli, C. (Eds.), *Chitosan in Pharmacy and Chemistry. ATEC,* Grottammare, Italy,

Han F., Dong Y., Su Z., Yin R., Song A. and Li S. 2014. "Preparation, Characteristics And Assessment *of* A Novel Gelatine–Chitosan Sponge Scaffold As Skin Tissue Engineering Material." *International Journal of Pharmaceutics* 476 (1-2): 124-133.

Hench, L. L. and Polak J. M. 2002. "Third-Generation Biomedical Materials." *Science* 295 (5557): 1014-1017. doi:10.1126/science.1067404.

Ho Y. C., Mi F. L., Sung H. W. and Kuo P. L. 2009. "Heparin-Functionalized Chitosan–Alginate Scaffolds For Controlled Release *of* Growth Factor." *International Journal of Pharmaceutics* 376 (1-2): 69-75.

Howling G. I., Dettmar P. W., Goddard P. A., Hampson F., Dornish M. and Wood E. J. 2001. "The Effect Of Chitin And Chitosan On The Proliferation Of Human Skin Fibroblasts And Keratinocytes In Vitro." *Biomaterials* 22 (22): 2959-2966.

Hsu S., Whu S. W., Tsai C. L., Wu Y. H., Chen H. W. and Hsieh K. H. 2004. "Chitosan As Scaffold Materials: Effects Of Molecular Weight And Degree Of Deacetylation." *Journal of Polymer Research* 11 (2): 141-147.

Hsu Y. Y., Gresser J. D., Trantolo D. J., Lyons C. M., Gangadharam P. R. and Wise D. L 1997. "Effect Of Polymer Foam Morphology And Density On Kinetics Ofin Vitro Controlled Release *of* Isoniazid From Compressed Foam Matrices." *Journal of Biomedical Materials Research* 35 (1): 107-116.

Hu Q., Li B., Wang M. and Shen J. 2004. "Preparation And Characterization Of Biodegradable Chitosan/Hydroxyapatite Nanocomposite Rods Via In Situ Hybridization: A Potential Material As Internal Fixation *of* Bone Fracture." *Biomaterials* 25 (5): 779-785.

Huang L. Y., Liu T. Y., Liu K. H., Liu Y. Y., Chao C. S., Tung W. L. and Yang M. C. 2012. "Electrospinning *of* Amphipathic Chitosan Nanofibers For Surgical Implants Application." *Journal Of Nanoscience And Nanotechnology* 12 (6): 5066-5070.

Huang X. J., Ge D. and Xu Z. K. 2007. "Preparation And Characterization Of Stable Chitosan Nanofibrous Membrane For Lipase Immobilization." *European Polymer Journal* 43 (9): 3710-3718.

Huang Z. H., Dong Y. S., Chu C. L. and Lin P. H. 2008. "Electrochemistry Assisted Reacting Deposition *of* Hydroxyapatite In Porous Chitosan Scaffolds." *Materials Letters* 62 (19): 3376-3378.

Hudalla G. A. and Murphy W. L. 2011. "Biomaterials That Regulate Growth Factor Activity Via Bioinspired Interactions." *Advanced Functional Materials* 21 (10): 1754-1768.

Hudalla G. A., Kouris N. A., Koepsel J. T., Ogle B. M. and Murphy W. L. 2011. "Harnessing Endogenous Growth Factor Activity Modulates Stem Cell Behavior." *Integrative Biology* 3 (8): 832.-842

Ignatova M., Manolova N. and Rashkov I., 2007. "Novel Antibacterial Fibers *of* Quaternized Chitosan And Poly(Vinyl Pyrrolidone) Prepared By Electrospinning." *European Polymer Journal* 43 (4): 1112-1122.

Ignatova M., Starbova K., Markova N., Manolova N. and Rashkov I. 2006. "Electrospun Nano-Fibre Mats With Antibacterial Properties From Quaternised Chitosan And Poly(Vinyl Alcohol)." *Carbohydrate Research* 341 (12): 2098-2107.

Ishihara M., Nakanishi K., Ono K., Sato M., Kikuchi M., Saito Y., Yura H., Matsui T., Hattori H., Uenoyama M. and Kurita A. 2002. "Photocrosslinkable Chitosan As A Dressing For Wound Occlusion And Accelerator In Healing Process." *Biomaterials* 23 (3): 833-840.

Ishihara M., Ono K., Sato M., Nakanishi K., Saito Y., Yura H., Matsui T., Hattori H., Fujita M., Kikuchi M. and Kurita A. 2001. "Acceleration *of* Wound Contraction And Healing With A Photocrosslinkable Chitosan Hydrogel." *Wound Repair and Regeneration* 9 (6): 513-521.

Isikli C., Hasirci V. and Hasirci N. 2011. "Development Of Porous Chitosan-Gelatine/Hydroxyapatite Composite Scaffolds For Hard Tissue-Engineering Applications." *Journal of Tissue Engineering And Regenerative Medicine* 6 (2): 135-143.

Ito Y., Kajihara M. and Imanishi Y. 1991. "Materials For Enhancing Cell Adhesion By Immobilization *of* Cell-Adhesive Peptide." *Journal of Biomedical Materials Research* 25 (11): 1325-1337.

Iwata H., Yana S., Nasu M. and Yosue T. 2005. "Effects *of* Chitosan Oligosaccharides On The Femur Trabecular Structure In Ovariectomized Rats." *Oral Radiology* 21 (1): 19-22.

Jana S., Florczyk S. J., Leung M. and Zhang M. Q. 2012. "High-Strength Pristine Porous Chitosan Scaffolds For Tissue Engineering." *Journal of Materials Chemistry* 22 (13): 6291-6299.

Jayakumar R., Prabaharan M., Nair S. V. and Tamura H. 2010. "Novel Chitin And Chitosan Nanofibers In Biomedical Applications." *Biotechnology Advances* 28 (1): 142-150.

Jayakumar R., Prabaharan M., Sudheesh Kumar P. T., Nair S. V. and Tamura H.,2011. Biomaterials based on chitin and chitosan in wound dressing applications. *Biotechnol. Adv.* 29: 322-337.

Jayakumar, R., Reis R. L. and Mano J. F. 2007. "Synthesis And Characterization *of* Ph-Sensitive Thiol-Containing Chitosan Beads For Controlled Drug Delivery Applications." *Drug Delivery* 14 (1): 9-17.

Jiang T., Nukavarapu S. P., Deng M., Jabbarzadeh E., Kofron M. D., Doty S. B., Abdel-Fattah W. I. and Laurencin C. T. 2010. "Chitosan–Poly(Lactide-Co-Glycolide) Microsphere-Based Scaffolds For Bone Tissue Engineering: In Vitro Degradation And In Vivo Bone Regeneration Studies." *Acta Biomaterialia* 6 (9): 3457-3470.

Jin H. H., Kim D. H., Kim T. W., Shin K. K., Jung J. S., Park H. C. and Yoon S. Y. 2012. "In vivo evaluation of porous hydroxyapatite/chitosan-alginate composite scaffolds for bone tissue engineering." *International Journal of Biological Macromolecules.*51(5): 1079–1085.

Jin Y., Ling P. X., He Y. L. and Zhang T. M. 2007. "Effects Of Chitosan And Heparin On Early Extension Of Burns." *Burns* 33 (8): 1027-1031.

Jo S., Kim S., Cho T. H., Shin E., Hwang S. J. and Noh I. J. 2012. "Effects Of Recombinant Human Bone Morphogenic Protein-2 And Human Bone Marrow-Derived Stromal Cells Onin Vivobone Regeneration *of* Chitosan-Poly(Ethylene Oxide) Hydrogel." *Journal of Biomedical Materials Research Part A* 101A (3): 892-901.

Kanimozhi K., Basha S. K. and Kumari V. S. 2016. "Processing And Characterization Of Chitosan/PVA And Methylcellulose Porous Scaffolds For Tissue Engineering." *Materials Science and Engineering: C* 61: 484-491.

Keselowsky B. G., Collard D. M. and García A. J. 2003. "Surface Chemistry Modulates Fibronectin Conformation And Directs Integrin Binding And Specificity To Control Cell Adhesion." *Journal of Biomedical Materials Research Part A* 66A (2): 247-259.

Khor E. and Lim L. Y., 2003. "Implantable Applications *of* Chitin And Chitosan." *Biomaterials* 24 (13): 2339-2349.

Kieswetter K., Schwartz Z., Hummert T. W., Cochran D. L., Simpson J., Dean D. D. and Boyan B. D. 1996. "Surface Roughness Modulates The Local Production Of Growth Factors And Cytokines By Osteoblast-Like MG-63 Cells." *Journal of Biomedical Materials Research* 32 (1): 55-63.

Kim I. S, Park J. W., Kwon I. C., Baik B. S. and Cho B. C. 2002. "Role Of BMP, Big-H3, And Chitosan In Early Bony Consolidation In Distraction Osteogenesis In A Dog Model." *Plastic And Reconstructive Surgery* 109 (6): 1966-1977.

Kim S., Kang Y., Mercado-Pagan A. E., Maloney W. J. and Yang Y. 2014. "In Vitroevaluation Of Photo-Crosslinkable Chitosan-Lactide Hydrogels For Bone Tissue Engineering." *Journal of Biomedical Materials Research Part B: Applied Biomaterials* 102 (7): 1393-1406.

Kim S. K. and Mendis E. 2006. "Bioactive Compounds From Marine Processing Byproducts – A Review." *Food Research International* 39 (4): 383-393.

Klokkevold P. R., Vandemark L., Kenney E. B. and Bernard G. W. 1996. "Osteogenesis Enhanced By Chitosan (Poly-N-Acetyl Glucosaminoglycan) In Vitro." *Journal of Periodontology*67 (11): 1170-1175.

Kofuji K., Huang Y., Tsubaki K., Kokido F. Nishikawa K., Isobe T. and Murata Y. 2010. "Preparation And Evaluation Of A Novel Wound Dressing Sheet Comprised *of* B-Glucan–Chitosan Complex." *Reactive And Functional Polymers* 70 (10): 784-789.

Kong L., Gao Y., Cao W., Gong Y., Zhao N. and Zhang X. 2005. "Preparation And Characterization Of Nano-Hydroxyapatite/Chitosan Composite Scaffolds." *Journal Of Biomedical Materials Research Part A* 75A (2): 275-282.

Krukowski M., Shively R. A., Osdoby P. and Eppley B. L. 1990. "Stimulation Of Craniofacial And Intramedullary Bone Formation By Negatively Charged Beads." *Journal of Oral And Maxillofacial Surgery* 48 (5): 468-475.

Kulkarni A. R., Kulkarni V. H., Keshavayya J., Hukkeri V. I. and Sung H. W. 2005. "Anti-Microbial Activity And Film Characterization Of Thiazolidinone Derivatives Of Chitosan." *Macromolecular Bioscience* 5 (6): 490-493.

Kumari R., Shipra T., Dutta P. K., Dutta J., Hunt A. J., Macquarriec D. J. and Clark J. H. 2009. "Direct Chitosan Scaffold Formation Via Chitin Whiskers By A Supercritical Carbon Dioxide Method: A Green Approach." *Journal of Materials Chemistry* 19 (45): 8651.

Kweon D. K., Song S. B. and Park Y. Y. 2003. "Preparation Of Water-Soluble Chitosan/Heparin Complex And Its Application As Wound Healing Accelerator." *Biomaterials* 24 (9): 1595-1601.

Lee D. W., Lim H., Chong H. N. and Shim W. S. 2009. "Advances In Chitosan Material And Its Hybrid Derivatives: A Review." *The Open Biomaterials Journal* 1: 10-20.

Lee J. H., Khang G., Lee J. W. and Lee H. B. 1998. "Interaction Of Different Types Of Cells On Polymer Surfaces With Wettability Gradient." *Journal of Colloid And Interface Science* 205 (2): 323-330.

Lee Y. M., Park Y. J., Lee S. J., Ku Y., Han S. B., Choi S. M. and Chung C. P. 2000. "Tissue Engineered Bone Formation Using Chitosan/Tricalcium Phosphate Sponges." *Journal of Periodontology* 71 (3): 410-417.

LeGeros R. Z. 2008."Calcium Phosphate-Based Osteoinductive Materials." *Chemical Reviews* 108 (11): 4742-4753.

Leggat P. A., Kedjarune U. and Smith D. R. 2004. "Toxicity Of Cyanoacrylate Adhesives And Their Occupational Impacts For Dental Staff." *Industrial Health* 42 (2): 207-211.

Leung H. W. 2001. "Ecotoxicology Of Glutaraldehyde: Review Of Environmental Fate And Effects Studies." *Ecotoxicology and Environmental Safety* 49 (1): 26-39.

Levengood S. L. and Zhang M. 2014. "Chitosan-Based Scaffolds For Bone Tissue Engineering." *Journal of Materials Chemistry B* 2 (21): 3161-3184.

Li L., Li B., Zhao M., Ding S. and Zhou C. 2011. "Single-Step Mineralization Of Woodpile Chitosan Scaffolds With Improved Cell Compatibility." *Journal Of Biomedical Materials Research Part B: Applied Biomaterials* 98B (2): 230-237.

Li L. H., Deng J C., Deng H. R., Liu Z. L. and Li X. L. 2010. "Preparation, Characterization And Antimicrobial Activities Of Chitosan/Ag/Zno Blend Films." *Chemical Engineering Journal* 160 (1): 378-382.

Li P., Poon Y. F. Li W., Zhu H. Y., Yeap S. H., Cao Y., Qi X. et al. 2010. "A Polycationic Antimicrobial And Biocompatible Hydrogel With Microbe Membrane Suctioning Ability." *Nature Materials* 10 (2): 149-156.

Li Q., Wu M., Tang L. 2008. "Bioactivity of a novel nano-composite of hydroxyapatite and chitosan-phosphorylated chitosan polyolectrolyte complex." *Journal of Bioactive and Compatible Polymers* 23(6): 520.

Li Z. and Zhang M. 2005. "Chitosan-Alginate As Scaffolding Material For Cartilage Tissue Engineering." *Journal of Biomedical Materials Research Part A* 75A (2): 485-493.

Li Z., Ramay H. R., Hauch K. D., Xiao D. and Zhang M. 2005. "Chitosan–Alginate Hybrid Scaffolds For Bone Tissue Engineering." *Biomaterials* 26 (18): 3919-3928.

Li Z., Yubao L., Aiping Y., Xuelin P., Xuejiang W., Xiang Z. 2005. Preparation and in vitro investigation of chitosan/nano-hydroxyapatite composite used as bone substitute materials. *J. Mater. Sci. Mater. Med.*16: 213–219.

Lian J. B. and Stein G. S. 1992. "Concepts Of Osteoblast Growth And Differentiation: Basis For Modulation Of Bone Cell Development And Tissue Formation." *Critical Reviews In Oral Biology & Medicine* 3 (3): 269-305.

Liao H. T., Chen C. T. and Chen J. P. 2011. "Osteogenic Differentiation And Ectopic Bone Formation Of Canine Bone Marrow-Derived Mesenchymal Stem Cells In Injectable Thermo-Responsive Polymer Hydrogel." *Tissue Engineering Part C: Methods* 17 (11): 1139-1149.

Lieder R. 2013. "*Chitosan and Chitosan Derivatives in Tissue Engineering and Stem Cell Biology*." PhD diss., School of Science and Engineering at the Reykjavik University, Reykjavik, Iceland; http://skemman.is/stream/get/1946/17342/39457/1/lieder_ramona.pdf.

Lih E., Lee J. S., Park K. M. and Park K. D. 2012. "Rapidly Curable Chitosan–PEG Hydrogels As Tissue Adhesives For Hemostasis And Wound Healing." *Acta Biomaterialia* 8 (9): 3261-3269.

Lim C. K., Yaacob N. S., Ismail Z. and Halim A. S. 2010. "In Vitro Biocompatibility Of Chitosan Porous Skin Regenerating Templates (Psrts) Using Primary Human Skin Keratinocytes." *Toxicology In Vitro* 24 (3): 721-727.

Lim L. Y., Khor E. and Koo O. J. 1998. "Irradiation Of Chitosan." *Journal Of Biomedical Materials Research* 43 (3): 282-290.

Lim L. Y., Khor E. and Ling C. E. 1999. "Effects *of* Dry Heat And Saturated Steam On The Physical Properties *of* Chitosan." *Journal of Biomedical Materials Research* 48 (2): 111-116.

Liu H., Peng H., Wu Y., Zhang C., Cai Y., Xu G., Li Q., Chen X., Ji J., Zhang Y. and OuYang H. W. 2013. "The Promotion Of Bone Regeneration By Nanofibrous Hydroxyapatite/Chitosan Scaffolds By Effects On Integrin-BMP/Smad Signaling Pathway In Bmscs." *Biomaterials* 34 (18): 4404-4417.

Liuyun J., Yubao L. and Chengdong X. 2009. "A Novel Composite Membrane Of Chitosan-Carboxymethyl Cellulose Polyelectrolyte Complex Membrane Filled With Nano-Hydroxyapatite I. Preparation And Properties." *Journal of Materials Science: Materials In Medicine* 20 (8): 1645-1652.

Lu S., Gao W. and Gu H. Y. 2008. "Construction, Application And Biosafety Of Silver Nanocrystalline Chitosan Wound Dressing." *Burns* 34 (5): 623-628.

MaG., Liu Y., Fang D., Chen J., Peng C., Fei X. and Nie J. 2012. "Hyaluronic Acid/Chitosan Polyelectrolyte Complexes Nanofibers Prepared By Electrospinning." *Materials Letters* 74: 78-80.

Madhumathi K., Shalumon K., Rani V., Tamura H., Furuike T., Selvamurugan N., Nair S. and Jayakumar R. Wet chemical synthesis of chitosan hydrogel-hydroxyapatite composite membranes for tissue engineering applications.2009. *Int. J. Biol. Macromol.* 45: 12–15.

Manjubala I., Scheler S., Bossert J. and Jandt K. D. 2006. "Mineralisation Of Chitosan Scaffolds With Nano-Apatite Formation By Double Diffusion Technique." *Acta Biomaterialia* 2 (1): 75-84.

Mao J. S., Zhao L. G., Yin Y. J. and Yao K. D. 2003. "Structure And Properties Of Bilayer Chitosan–Gelatine Scaffolds." *Biomaterials* 24 (6): 1067-1074.

Martin H. J., Schulz K. H., Bumgardner J. D. and Schneider J. A. 2008."Enhanced Bonding Of Chitosan To Implant Quality Titanium Via Four Treatment Combinations." *Thin Solid Films* 516 (18): 6277-6286.

Martin H. J., Schulz K. H., Bumgardner J. D. and Walters K. B. 2007. "XPS Study On The Use Of 3-Aminopropyltriethoxysilane To Bond Chitosan To A Titanium Surface." *Langmuir* 23 (12): 6645-6651.

Matienzo L. J. and Winnacker S. K. 2002. "Dry Processes For Surface Modification Of A Biopolymer: Chitosan." *Macromolecular Materials And Engineering* 287 (12): 871-880.

Matsuda K., Suzuki S., Isshiki N., Yoshioka K., Wada R., Okada T. and Ikeda Y. 1990. "Influence Of Glycosaminoglycans On The Collagen Sponge Component Of A Bilayer Artificial Skin." *Biomaterials* 11 (5): 351-355.

Mayol L., De Stefano D., Campani V., De Falco F., Ferrari E., Cencetti C., Matricardi P., Maiuri L., Carnuccio R., and Gallo A. 2014. "Design And Characterization *of* A Chitosan Physical Gel Promoting Wound Healing In Mice." *Journal of Materials Science: Materials In Medicine* 25 (6): 1483-1493.

Mehdipour M. and Afshar A. 2012. "A Study Of The Electrophoretic Deposition Of Bioactive Glass–Chitosan Composite Coating." *Ceramics International* 38 (1): 471-476.

Mehdizadeh M. and Yang J. 2012. "Design Strategies And Applications Of Tissue Bioadhesives." *Macromolecular Bioscience* 13 (3): 271-288.

Mei D., XiuLing Z., Xu X., Xiang Y. K., Xing Y. L., Gang G., Feng L., Xia Z., Yu Q. W. and Zhiyong Q. 2009. "Chitosan-Alginate Sponge: Preparation And Application In Curcumin Delivery For Dermal Wound Healing In Rat." *Journal of Biomedicine And Biotechnology* 2009: 1-8.

Mendonca R. H., de Oliveira Meiga T., da Costa M. F. and da Silva Moreira Thire. 2012. "Production Of 3D Scaffolds Applied To Tissue Engineering Using Chitosan Swelling As A Porogenic Agent." *Journal of Applied Polymer Science* 129 (2): 614-625.

Meng X., Tian F., Yang J., He C. N., Xing N. and Li F. 2010. "Chitosan And Alginate Polyelectrolyte Complex Membranes And Their Properties For Wound Dressing Application." *Journal of Materials Science: Materials In Medicine* 21 (5): 1751-1759.

Mi F. L., Shyu S. S., Chen C. T. and Schoung J. Y. 1999. "Porous Chitosan Microsphere For Controlling The Antigen Release Of Newcastle Disease Vaccine: Preparation Of Antigen-Adsorbed Microsphere And In Vitro Release." *Biomaterials* 20 (17): 1603-1612.

Mi F. L., Shyu S. S., Wu Y. B., Lee S. T., Shyong J. Y. and Huang R. N. 2001. "Fabrication And Characterization Of A Sponge-Like Asymmetric Chitosan Membrane As A Wound Dressing." *Biomaterials* 22 (2): 165-173.

Mi F. L., Wu Y. B., Shyu S. S., Schoung J. Y., Huang Y. B., Tsai Y. H. and Hao J. Y. 2001. "Control Of Wound Infections Using A Bilayer Chitosan Wound Dressing With Sustainable Antibiotic Delivery." *Journal of Biomedical Materials Research* 59 (3): 438-449.

Mi F. L, Wu Y. B, Shyu S. S, Chao A. C, Lai J. Y and Su C. C. 2003. "Asymmetric Chitosan Membranes Prepared By Dry/Wet Phase Separation: A New Type Of Wound Dressing For Controlled Antibacterial Release." *Journal of Membrane Science* 212 (1-2): 237-254.

Miranda S. C., Silva G. A., Hell R. C., Martins M. D., Alves J. B. and Goes A. M. 2011. "Three-Dimensional Culture Of Rat Bmmscs In A Porous Chitosan-Gelatine Scaffold: A Promising Association For Bone Tissue Engineering In Oral Reconstruction." *Archives of Oral Biology* 56 (1): 1-15.

Mizuno K., Yamamura K., Yano K., Osada T., Saeki S., Takimoto N., Sakurai T. and Nimura Y. 2002. "Effect Of Chitosan Film Containing Basic Fibroblast Growth Factor On Wound Healing In Genetically Diabetic Mice." *Journal of Biomedical Materials Research* 64A (1): 177-181.

Mohammad A. Q. and Fehmeeda K. 2014. "In Vitro Study Of Temperature And Ph-Responsive Gentamycin Sulphate-Loaded Chitosan-Based Hydrogel Films For Wound Dressing Applications." *Polymer-Plastics Technology and Engineering* 54 (6): 573-580.

Mohammad A. Q., Fehmeeda K. and Shakeel A. 2015. "An overview on wounds. Their issues and natural remedies for wound healing." *Biochemistry and Physiology* 4(3): 1-9.

Mori M., Rossi S., Ferrari F., Bonferoni M. C., Sandri G., Chlapanidas T., Torre M. L. and Caramella C. 2016. "Sponge-Like Dressings Based On The Association Of Chitosan And Sericin For The Treatment Of Chronic Skin Ulcers. I. Design Of Experiments–Assisted Development." *Journal of Pharmaceutical Sciences* 105 (3): 1180-1187.

Muller P., Bulnheim U., Diener A., Luthen F., Teller M., Klinkenberg E. D., Neumann H. G., Nebe B., Liebold A., Steinhoff G. and Rychly J. 2007. "Calcium Phosphate Surfaces Promote Osteogenic Differentiation Of Mesenchymal Stem Cells." *Journal of Cellular and Molecular Medicine* 12 (1): 281-291.

Murakami K., Aoki H., Nakamura S., Nakamura S., Takikawa M., Hanzawa M., Kishimoto S., Hattori H., Tanaka Y., Kiyosawa T., Sato Y. and Ishihara M. 2010. "Hydrogel Blends *of* Chitin/Chitosan, Fucoidan And Alginate As Healing-Impaired Wound Dressings." *Biomaterials* 31 (1): 83-90.

Muzzarelli R., Tarsi R., Fillipini O., Giovanetti E., Biagini G. and Varaldo P. E. 1990. "Antimicrobial Properties Of N-Carboxybutyl Chitosan." *Antimicrobial Agents and Chemotherapy* 34 (10): 2019-2023.

Muzzarelli R. A., Mattioli-Belmonte M., Tietz C., Biagini R., Ferioli G., Brunelli M. A., Fini M., Giardino R., Ilari P. and Biagini G. 1994. "Stimulatory Effect On Bone Formation Exerted By A Modified Chitosan." *Biomaterials* 15 (13): 1075-1081.

Nardecchia S., Gutierrez M. C., Dentini M., Barbetta A., Ferrer M. L. and del Monte F. 2012. "In Situ Precipitation Of Amorphous Calcium Phosphate And Ciprofloxacin Crystals During The Formation Of Chitosan Hydrogels And Its Application For Drug Delivery Purposes." *Langmuir* 28 (45): 15937-15946.

Naseri N., Algan C., Jacobs V., John M., Oksman K. and Mathew A. P. 2014a. "Electrospun Chitosan-Based Nanocomposite Mats Reinforced With Chitin Nanocrystals For Wound Dressing." *Carbohydrate Polymers* 109: 7-15.

Naseri N., Mathew A. P., Girandon L., Fröhlich M. and Oksman K. 2014b. "Porous Electrospun Nanocomposite Mats Based On Chitosan–Cellulose Nanocrystals For Wound Dressing: Effect Of Surface Characteristics Of Nanocrystals." *Cellulose* 22 (1): 521-534.

Nath S., Dey A., Mukhopadhyay A. K. and Basu B. 2009. "Nanoindentation Response Of Novel Hydroxyapatite–Mullite Composites." *Materials Science and Engineering: A* 513-514: 197-201.

Nie W., Yuan X., Zhao J., Zhou Y. and Bao H.2013. "Rapidly In Situ Forming Chitosan/E-Polylysine Hydrogels For Adhesive Sealants And Hemostatic Materials." *Carbohydrate Polymers* 96 (1): 342-348.

Ning C., Chao L., Chao H., Xiaogang L., Liang S., Yanan X. anad Faquan Y. 2016. "Tailoring Mechanical And Antibacterial Properties Of Chitosan/Gelatine Nanofiber Membranes With $Fe_3O_4$ Nanoparticles For Potential Wound Dressing Application." *Applied Surface Science* 369: 492-500.

Niranjan R., Koushik C., Saravanan S., Moorthi A., Vairamani M. and Selvamurugan N. 2013. "A Novel Injectable Temperature-Sensitive Zinc Doped Chitosan/B-Glycerophosphate Hydrogel For Bone Tissue Engineering." *International Journal of Biological Macromolecules* 54: 24-29.

Nishimura S., Kai H., Shinada K., Yoshida T., Tokura S., Kurita K., Nakashima H., Yamamoto N. and Uryu T. 1998. "Regioselective Syntheses Of Sulfated Polysaccharides: Specific Anti-HIV-1 Activity Of Novel Chitin Sulfates." *Carbohydrate Research* 306 (3): 427-433.

No H. 2002. "Antibacterial Activity Of Chitosans And Chitosan Oligomers With Different Molecular Weights." *International Journal of Food Microbiology* 74 (1-2): 65-72.

Noel S. P., Courtney H., Bumgardner J. D. and Haggard W. O. 2008. "Chitosan Films: A Potential Local Drug Delivery System For Antibiotics." *Clinical Orthopaedics and Related Research* 466 (6): 1377-1382.

Noel S. P., Courtney H. S., Bumgardner J. D. and Haggard W. O. 2010. "Chitosan Sponges To Locally Deliver Amikacin And Vancomycin: A Pilot In Vitro Evaluation." *Clinical Orthopaedics And Related Research*® 468 (8): 2074-2080.

Noori S., Kokabi M. and Hassan Z. M. 2015. "Nanoclay enhanced the mechanical properties of poly(vinyl alcohol)/chitosan/montmorrilonite nanocomposite hydrogel as wound dressing." *Procedia Materials Science* 11: 152–156.

Nordtveil R. J., Varum K. M. and Smirdsrod O. 1994. "Degradation Of Fully Water-Soluble, Partially N-Acetylated Chitosans With Lysozyme." *Carbohydrate Polymers* 23 (4): 253-260.

Obara K., Ishihara M., Fujita M., Kanatani Y., Hattori H., Matsui T. and Takase B. 2005. "Acceleration Of Wound Healing In Healing-Impaired Db/Db Mice With A Photocrosslinkable Chitosan Hydrogel Containing Fibroblast Growth Factor-2." *Wound Repair and Regeneration* 13 (4): 390-397.

Okamoto Y., Kawakami K., Miyatake K., Morimoto M., Shigemasa Y. and Minami S. 2002. "Analgesic effects of chitin and chitosan." *Carbohydrate Polymers* 49: 249-252.

Okamoto Y., Shibazaki K, Minami S., Matsuhashi A., Tanioka S. and Shigemasa Y. 1995. "Evaluation Of Chitin And Chitosan On Open Wound Healing In Dogs." *Journal of Veterinary Medical Science* 57 (5): 851-854.

Oliveira J. T., Correlo V. M., Sol P. C., Costa-Pinto A. R., Malafaya P. B., Salgado A. J., Bhattacharya M., Charbord P., Neves N. M. and Reis R. L. 2008. "Assessment Of The Suitability Of Chitosan/Polybutylene Succinate Scaffolds Seeded With Mouse Mesenchymal Progenitor Cells For A Cartilage Tissue Engineering Approach." *Tissue Engineering Part A* 14 (10): 1651-1661.

Ong S. Y., Wu J., Moochhala S. M., Tan M. H. and Lu J. 2008. "Development Of A Chitosan-Based Wound Dressing With Improved Hemostatic And Antimicrobial Properties." *Biomaterials* 29 (32): 4323-4332.

Ono K., Saito Y., Yura H., Ishikawa K., Kurita A., Akaike T. and Ishihara M. 2000. "Photocrosslinkable Chitosan As A Biological Adhesive." *Journal of Biomedical Materials Research* 49 (2): 289-295.

Pandey A. R., Singh U. S., Momin M. and Bhavsar C. 2017. "Chitosan: Application In Tissue Engineering And Skin Grafting." *Journal of Polymer Research* 24 (8): 125. doi:10.1007/s10965-017-1286-4.

Pangburn S. H., Trescony P. V. and Heller J. 1982. "Lysozyme Degradation Of Partially Deacetylated Chitin, Its Films And Hydrogels." *Biomaterials* 3 (2): 105-108.

Panoraia I. S., Asimina P. Z., Maria K. M., Ioannis D. K. and Dimitrios N. B. 2016. "Porous Dressings Of Modified Chitosan With Poly(2-Hydroxyethyl Acrylate) For Topical Wound Delivery Of Levofloxacin." *Carbohydrate Polymers* 143: 90-99.

Park C. J., Clark S. G., Lichtensteiger C. A., Jamison R. D. and Wagoner Johnson A. J. 2009. "Accelerated Wound Closure Of Pressure Ulcers In Aged Mice By Chitosan Scaffolds With And Without Bfgf." *Acta Biomaterialia* 5 (6): 1926-1936.

Park H., Choi B., Nguyen J., Fan J., Shafi S., Klokkevold P. and Lee M. 2013. "Anionic Carbohydrate-Containing Chitosan Scaffolds For Bone Regeneration." *Carbohydrate Polymers* 97 (2): 587-596.

Pavinatto F. J., Caseli L. and Oliveira Jr O. N. 2010. "Chitosan In Nanostructured Thin Films." *Biomacromolecules* 11 (8): 1897-1908.

Pei H. N., Chen X. G., Li Y. and Zhou H. Y. 2008. "Characterization And Ornidazole Releasein Vitro *of* A Novel Composite Film Prepared With Chitosan/Poly(Vinyl Alcohol)/Alginate." *Journal of Biomedical Materials Research Part A* 85A (2): 566-572.

Peluso G., Petillo O., Ranieri M., Santin M., Ambrosic L., Calabro D., Avallone B. And Balsamo G. 1994. "Chitosan-Mediated Stimulation Of Macrophage Function." *Biomaterials* 15 (15): 1215-1220.

Peng H., Yin Z., Liu H., Chen X., Feng B., Yuan H., Su B., Ouyang H. and Zhang Y. 2012. "Electrospun Biomimetic Scaffold Of Hydroxyapatite/Chitosan Supports Enhanced Osteogenic Differentiation Of Mmscs." *Nanotechnology* 23 (48): 485102.

Peppas N. A. 1986. *Hydrogels in medicine and pharmacy*. Boca Raton: CRC Press.

Pizzoferrato A., Cenni E., Ciapetti G., Granchi D., Savarino L. and Stea S. 2002. "Inflammatory response to metals and ceramics" In *Integrated Biomaterials Science,* edited by Rolando Barbucci, 735-791. New York: Kluwer Academic/Plenum Publishers.

Porporatto C., Canali M. M., Bianco I. D. and Correa S. G. 2009. "The Biocompatible Polysaccharide Chitosan Enhances The Oral Tolerance To Type II Collagen." *Clinical & Experimental Immunology* 155 (1): 79-87.

Pranoto Y., Rakshit S. K. and Salokhe V. M. 2005. "Enhancing Antimicrobial Activity *of* Chitosan Films By Incorporating Garlic Oil, Potassium Sorbate And Nisin." *LWT - Food Science and Technology* 38 (8): 859-865.

Profire L., Pieptu D., Dumitriu R. P., Dragostin O. and Vasile C. 2013. "Sulfadiazine modified CS/HA PEC destined to wound dressing." *Revista Medico Chirurgicala Societatea de Medici si Naturalisti Iasi* 117(2): 525-531.

Qin Y, Guo XW, Li L, Wang H. W. and Kim W. 2013. "The Antioxidant Property Of Chitosan Green Tea Polyphenols Complex Induces Transglutaminase Activation In Wound Healing." *Journal of Medicinal Food* 16 (6): 487-498.

Raafat D., von Bargen K., Haas A. and Sahl H. G. 2008. "Insights Into The Mode Of Action Of Chitosan As An Antibacterial Compound." *Applied And Environmental Microbiology* 74 (12): 3764-3773.

Radhakumary C., Antonty M. and Sreenivasan K. 2011. "Drug Loaded Thermoresponsive And Cytocompatible Chitosan Based Hydrogel As A Potential Wound Dressing." *Carbohydrate Polymers* 83 (2): 705-713.

Radosevich M., Goubran H. I. and Burnouf T. 1997. "Fibrin Sealant: Scientific Rationale, Production Methods, Properties, And Current Clinical Use." *Vox Sanguinis* 72 (3): 133-143.

Rai M., Yadav A. and Gade A. 2009. "Silver Nanoparticles As A New Generation of Antimicrobials." *Biotechnology Advances* 27 (1): 76-83.

Rao S. B. and Sharma C. P. 1995. "Sterilization Of Chitosan: Implications." *Journal of Biomaterials Applications* 10 (2): 136-143.

Renbutsu E., Hirose M., Omura Y., Nakatsubo F., Okamura Y., Okamoto Y., Saimoto H., Shigemasa Y. and Minami S. 2005. "Preparation And Biocompatibility Of Novel UV-Curable Chitosan Derivatives." *Biomacromolecules* 6 (5): 2385-2388.

Rezwan K., Chen Q. Z., Blaker J. J. and Boccaccini A. R. 2006. "Biodegradable And Bioactive Porous Polymer/Inorganic Composite Scaffolds For Bone Tissue Engineering." *Biomaterials* 27 (18): 3413-3431.

Ribeiro M. P., Espiga A., Silva D., Baptista P., Henriques J., Ferreira C., Silva J. C., Borges J. P., Pires E., Chaves P. and Correia I. 2009. "Development Of A New Chitosan Hydrogel For Wound Dressing." *Wound Repair and Regeneration* 17 (6): 817-824.

Rinaudo M. 2006. "Chitin And Chitosan: Properties And Applications." *Progress In Polymer Science* 31 (7): 603-632.

Rinki K., Tripathi S., Dutta P. K., Dutta J., Hunt A. J., Macquarrie D. J. and Clark J. H. 2009. "Direct Chitosan Scaffold Formation Via Chitin Whiskers By A Supercritical Carbon Dioxide Method: A Green Approach." *Journal of Materials Chemistry* 19 (45): 8651-8655.

Rossi S., Marciello M., Sandri G., Ferrari F., Bonferoni M. C., Papetti A., Caramella C., Dacarro C. and Grisoli P. 2007. "Wound Dressings Based On Chitosans And Hyaluronic Acid For The Release of Chlorhexidine Diacetate In Skin Ulcer Therapy." *Pharmaceutical Development and Technology* 12 (4): 415-422.

Rupp F., Scheideler L., Olshanska N., de Wild M., Wieland M. and Geis-Gerstorfer J. 2006. "Enhancing surface free energy and hydrophilicity through chemical modification and microstructured titanium implant surfaces." *Journal of Biomedical Materials Research A* 76(2):323-34.

Rusu V. M., Ng C. H., Wilke M., Tiersch B., Fratzl P. and Peter M. G. 2005. "Size-Controlled Hydroxyapatite Nanoparticles As Self-Organized Organic/Inorganic Composite Materials." *Biomaterials* 26 (26): 5414-5426.

Ryan B. M., Stockbrugger R. W. and Ryan J. M. 2004. "A Pathophysiologic, Gastroenterologic, And Radiologic Approach To The Management of Gastric Varices." *Gastroenterology* 126 (4): 1175-1189.

Salomaki M. and Kankare J. 2009. "Influence Of Synthetic Polyelectrolytes On The Growth And Properties Of Hyaluronan−Chitosan Multilayers." *Biomacromolecules* 10 (2): 294-301.

Samal S. and Bal S. 2008. "Carbon Nanotube Reinforced Ceramic Matrix Composites- A Review." *Journal Of Minerals And Materials Characterization and Engineering* 07 (04): 355-370.

Santos T. C., Marques A. P., Silva S. S., Oliveira J. M., Mano J. F., Castro A. G. and Reis R. L. 2007. "In Vitro Evaluation Of The Behaviour Of Human Polymorphonuclear Neutrophils In Direct Contact With Chitosan-Based Membranes." *Journal of Biotechnology* 132 (2): 218-226.

Senel S. and McClure S. J. 2004. "Potential Applications Of Chitosan In Veterinary Medicine." *Advanced Drug Delivery Reviews* 56 (10): 1467-1480.

Seol Y. J., Lee J. Y., Park Y. J., Lee Y. M., Young K., Rhyu I. C., Lee S. J., Han S. B. and Chung C. P. 2004. "Chitosan Sponges As Tissue Engineering Scaffolds For Bone Formation." *Biotechnology Letters* 26 (13): 1037-1041.

Seyfarth F., Schliemann S., Elsner P. and Hipler U. 2007. "Antifungal Effect Of High- And Low-Molecular-Weight Chitosan Hydrochloride, Carboxymethyl Chitosan, Chitosan

Oligosaccharide And N-Acetyl-D-Glucosamine Against Candida Albicans, Candida Krusei And Candida Glabrata." *International Journal of Pharmaceutics*. 353(1-2): 139-148.

Shakeel A. and Saiqa I. Shakeel Ahmed, and Saiqa Ikram. 2016. "Chitosan Based Scaffolds And Their Applications In Wound Healing." *Achievements In The Life Sciences* 10 (1): 27-37.

Shao H. J., Chen C. S., Lee Y. T., Wang J. H. and Young T. H. 2009. "The Phenotypic Responses Of Human Anterior Cruciate Ligament Cells Cultured On Poly(E-Caprolactone) And Chitosan." *Journal of Biomedical Materials Research Part A* 93(4): 1297–1305.

Shelton R. M., Rasmussen A. C. and Davies J. E. 1988. "Protein Adsorption At The Interface Between Charged Polymer Substrata And Migrating Osteoblasts." *Biomaterials* 9 (1): 24-29.

Shigemasa Y. and Minami S. 1996. "Applications Of Chitin And Chitosan For Biomaterials." *Biotechnology and Genetic Engineering Reviews* 13 (1): 383-420.

Siebers M. C., ter Brugge P. J., Walboomers X. F. and Jansen J. A. 2005. "Integrins As Linker Proteins Between Osteoblasts And Bone Replacing Materials. A Critical Review." *Biomaterials* 26 (2): 137-146.

Silva S. S., Luna S. M., Gomes M. E., Benesch J., Pashkuleva I., Mano J. F. and Reis R. L. 2008. "Plasma Surface Modification Of Chitosan Membranes: Characterization And Preliminary Cell Response Studies." *Macromolecular Bioscience* 8 (6): 568-576.

Silva S. S., Popa E. G., Gomes M. E., Cerqueira M., Marques A. P., Caridade S. G., Teixeira P., Sousa C., Mano J. F. and Reis R. L. 2013. "An Investigation Of The Potential Application Of Chitosan/Aloe-Based Membranes For Regenerative Medicine." *Acta Biomaterialia* 9 (6): 6790-6797.

Sionkowska A. and Kaczmarek B. 2017. "Preparation And Characterization Of Composites Based On The Blends Of Collagen, Chitosan And Hyaluronic Acid With Nano-Hydroxyapatite." *International Journal of Biological Macromolecules* 102: 658-666.

Smith J. K., Bumgardner J. D., Courtney H. S., Smeltzer M. S. and Haggard W. O. 2010. "Antibiotic-Loaded Chitosan Film For Infection Prevention: A Preliminary In Vitro Characterization." *Journal of Biomedical Materials Research Part B: Applied Biomaterials* 94(1): 203–211.

Smith T. W., DeGirolami U. and Crowell R. M. 1985. "Neuropathological Changes Related To The Transorbital Application Of Ethyl 2-Cyanoacrylate Adhesive To The Basal Cerebral Arteries Of Cats." *Journal Of Neurosurgery* 62 (1): 108-114.

Spotnitz W. D. and Burks S. 2008. "Hemostats, Sealants, And Adhesives: Components Of The Surgical Toolbox." *Transfusion* 48 (7): 1502-1516.

Spotnitz W. D. and Prabhu R. 2005. "Fibrin Sealant Tissue Adhesive - Review And Update." *Journal of Long-Term Effects of Medical Implants* 15 (3): 245-270.

Stone C. A., Wright H., Devaraj V. S., Clarke T. and Powell R. 2000. "Healing At Skin Graft Donor Sites Dressed With Chitosan." *British Journal of Plastic Surgery* 53 (7): 601-606.

Suarez-Gonzalez D., Lee J. S., Lan Levengood S. K., Vanderby R. Jr. and Murphy W. L. 2012. "Mineral Coatings Modulate B-TCP Stability And Enable Growth Factor Binding And Release." *Acta Biomaterialia* 8 (3): 1117-1124.

Sudarshan N. R., Hoover D. G. and Knorr D. 1992. "Antibacterial Action Of Chitosan." *Food Biotechnology* 6 (3): 257-272.

Sung J. H., Hwang M. R., Kim J. O., Lee J. H., Kim Y. I., Kim J. H., Chang S. W., Jin S. G., Kim J. A., Lyoo W. S. 2010. "Gel Characterisation And In Vivo Evaluation Of Minocycline-Loaded Wound Dressing With Enhanced Wound Healing Using Polyvinyl Alcohol And Chitosan." *International Journal of Pharmaceutics* 392 (1-2): 232-240.

Suzuki S., Matsuda K., Isshiki N., Tamada Y. and Ikada Y. 1990. "Experimental Study Of A Newly Developed Bilayer Artificial Skin." *Biomaterials* 11 (5): 356-360.

Szmukler-Moncler S., Salama H., Reingewirtz Y. and Dubruille J. H. 1998. "Timing Of Loading And Effect Of Micromotion On Bone-Dental Implant Interface: Review Of Experimental Literature." *Journal of Biomedical Materials Research* 43 (2): 192-203.

Tang H., Zhang P., Kieft T. L., Ryan S. J., Baker S. M., Wiesmann W. P. and Rogelj S. 2010. "Antibacterial Action Of A Novel Functionalized Chitosan-Arginine Against Gram-Negative Bacteria." *Acta Biomaterialia* 6 (7): 2562-2571.

Tang R., Du Y. and Fan L. 2003. "Dialdehyde Starch-Crosslinked Chitosan Films And Their Antimicrobial Effects." *Journal of Polymer Science Part B: Polymer Physics* 41 (9): 993-997.

Tangpasuthadol V., Pongchaisirikul N. and Hoven V. P. 2003. "Surface Modification Of Chitosan Films." *Carbohydrate Research* 338 (9): 937-942.

Teng S., Lee E., Yoon B., Shin D., Kim H. and Oh J. 2009. "Chitosan/Nanohydroxyapatite Composite Membranes Via Dynamic Filtration For Guided Bone Regeneration." *Journal of Biomedical Materials Research Part A* 88A (3): 569-580.

Thein-Han W. and Misra R. 2009. "Biomimetic Chitosan–Nanohydroxyapatite Composite Scaffolds For Bone Tissue Engineering." *Acta Biomaterialia* 5 (4): 1182-1197.

Thierry B., Winnik F. M., Merhi Y., Silver J. and Tabrizian M. 2003. "Bioactive Coatings Of Endovascular Stents Based On Polyelectrolyte Multilayers." *Biomacromolecules* 4 (6): 1564-1571.

Thomas V., Yallapu M. M., Sreedhar B. and Bajpai S. K. 2009. "Fabrication, Characterization Of Chitosan/Nanosilver Film And Its Potential Antibacterial Application." *Journal of Biomaterials Science, Polymer Edition* 20 (14): 2129-2144.

Tomihata K. and Ikada Y. 1997. "In Vitro And In Vivo Degradation Of Films Of Chitin And Its Deacetylated Derivatives." *Biomaterials* 18 (7): 567-575.

Tsai G. J., Zhang S. L. and Shieh P. L. 2004. "Antimicrobial Activity Of A Low-Molecular-Weight Chitosan Obtained From Cellulase Digestion Of Chitosan." *Journal of Food Protection* 67 (2): 396-398.

Tunney M. M., Brady A. J., Buchanan F., Newe C. and Dunne N. J. 2008. "Incorporation Of Chitosan In Acrylic Bone Cement: Effect On Antibiotic Release, Bacterial Biofilm Formation And Mechanical Properties." *Journal of Materials Science: Materials In Medicine* 19 (4): 1609-1615.

Ueno H., Mori T. and Fujinaga T. 2001. "Topical Formulations And Wound Healing Applications of Chitosan." *Advanced Drug Delivery Reviews* 52 (2): 105-115.

Ueno H., Murakami M., Okumura M., Kadosawa T., Uede T and Fujinaga T. 2001. "Chitosan Accelerates The Production *of* Osteopontin From Polymorphonuclear Leukocytes." *Biomaterials* 22 (12): 1667-1673.

Uygun B. E., Bou-Akl T., Albanna M. and Matthew H. W. 2010. "Membrane Thickness Is An Important Variable In Membrane Scaffolds: Influence Of Chitosan Membrane Structure On The Behavior of Cells." *Acta Biomaterialia* 6 (6): 2126-2131.

Valbonesi M. 2006. "Fibrin Glues Of Human Origin." *Best Practice & Research Clinical Haematology* 19 (1): 191-203.

Valentine R., Athanasiadis T., Moratti S., Hanton L., Robinson S. and Wormald P. J. 2010. "The Efficacy Of A Novel Chitosan Gel On Hemostasis And Wound Healing After Endoscopic Sinus Surgery." *American Journal of Rhinology & Allergy* 24 (1): 70-75.

Van Winterswijk P. J. and Nout E. 2007. "Tissue engineering and wound healing: an overview of the past, present, and future." *Wounds* 19(10): 277-284.

Vasile C., Pieptu D., Dumitriu R. P., Pânzariu A. and Profire L. 2013. "Chitosan/hyaluronic acid polyelectrolyte complex hydrogels in the management of burn wounds." *Revista Medico Chirurgicala a Societatii de Medici si Naturalisti Iasi* 117(2): 565-571.

Venkatesan J. and Kim S. K. 2010. "Chitosan Composites For Bone Tissue Engineering—An Overview." *Marine Drugs* 8 (8): 2252-2266.

Venugopal J., Prabhakaran M. P., Zhang Y., Low S., Choon A. T. and Ramakrishna S. 2010. "Biomimetic Hydroxyapatite-Containing Composite Nanofibrous Substrates For Bone Tissue Engineering." *Philosophical Transactions of The Royal Society A: Mathematical, Physical And Engineering Sciences* 368 (1917): 2065-2081.

Vereştiuc L. 2006. "Chitosanul. Caracteristici şi domenii de aplicabilitate" In *Polimeri degradabili şi biocompatibili*, edited by Cornelia Vasile, Aurica P. Chiriac, and Loredana Elena Niţă, 264-284. Iasi: Editura Tehnopress.

Vermes C., Chandrasekaran R., Jacobs J. J., Galante J. O., Roebuck K. A. and Glant T. T. 2001. "The Effects Of Particulate Wear Debris, Cytokines, And Growth Factors On The Functions Of MG-63 Osteoblasts." *The Journal of Bone And Joint Surgery-American Volume* 83 (2): 201-211.

Vimala K., Mohan Y. M., Sivudu K. S., Varaprasad K., Ravindra S., Reddy N. N., Padma Y., Sreedar B and MohanaRaju K. 2010. "Fabrication Of Porous Chitosan Films Impregnated With Silver Nanoparticles: A Facile Approach For Superior Antibacterial Application." *Colloids And Surfaces B: Biointerfaces* 76 (1): 248-258.

Wagh A. 2004. *Chemically Bonded Phosphate Ceramics: Twenty-First Century Materials with Diverse Applications*; New York: Elsevier Science.

Wagoner Johnson A. J. and Herschler B. A. 2011. "A Review Of The Mechanical Behavior Of Cap And Cap/Polymer Composites For Applications In Bone Replacement And Repair." *Acta Biomaterialia* 7 (1): 16-30.

Wang A., Ao Q., Cao W., Zhao C., Gong Y., Zhao N. and Zhang X. 2005. "Fiber-Based Chitosan Tubular Scaffolds For Soft Tissue Engineering: Fabrication And In Vitro Evaluation." *Tsinghua Science And Technology* 10 (4): 449-453.

Wang J., Zhang H., Zhu X., Fan H., Fan Y. and Zhang X. 2013. "Dynamic Competitive Adsorption Of Bone-Related Proteins On Calcium Phosphate Ceramic Particles With Different Phase Composition And Microstructure." *Journal Of Biomedical Materials Research Part B: Applied Biomaterials* 101B (6): 1069-1077.

Wang L. S., Khor E., Wee A. and Lim L. Y. 2002. "Chitosan-Alginate PEC Membrane As A Wound Dressing: Assessment Of Incisional Wound Healing." *Journal of Biomedical Materials Research* 63 (5): 610-618.

Wang X., Ma J., Wang Y. and He B. 2002. "Bone Repair In Radii And Tibias Of Rabbits With Phosphorylated Chitosan Reinforced Calcium Phosphate Cements." *Biomaterials* 23 (21): 4167-4176.

Wang X., T. Yu, Chen G., Zou J., Li J. and Yan J. 2017. "Preparation And Characterization Of A Chitosan/Gelatine/Extracellular Matrix Scaffold And Its Application In Tissue Engineering." *Tissue Engineering Part C: Methods* 23 (3): 169-179.

Wang X., Tan Y., Zhang B., Gu Z. and Li X. J. 2009. "Synthesis and Evaluation of Collagen-Chitosan-Hydroxyapatite Nanocomposites For Bone Grafting." *Journal of Biomedical Materials Research Part A* 89A (4): 1079-1087.

Webb K., Hlady V. and Tresco P. A. 2000. "Relationships Among Cell Attachment, Spreading, Cytoskeletal Organization, And Migration Rate For Anchorage-Dependent Cells On Model Surfaces." *Journal of Biomedical Materials Research* 49 (3): 362-368.

Wedmore I., McManus J. G., Pusateri A. E. and Holcomb J. B. 2006. "A Special Report On The Chitosan-Based Hemostatic Dressing: Experience In Current Combat Operations." *The Journal of Trauma: Injury, Infection, And Critical Care* 60 (3): 655-658.

Wen Z., Jiaojiao L., Kaixiang J.,Wenlong L., Xuefeng Q. and Chenrui L. 2016. "Fabrication of Functional PLGA-Based Electrospun Scaffolds And Their Applications In Biomedical Engineering." *Materials Science And Engineering: C* 59: 1181-1194.

Wheat J. C. and Wolf J. S. 2009. "Advances In Bioadhesives, Tissue Sealants, And Hemostatic Agents." *Urologic Clinics of North America* 36 (2): 265-275.

Wheeler D. L. and Enneking W. F. 2005. "Allograft Bone Decreases In Strength In Vivo Over Time." *Clinical Orthopaedics And Related Research* &NA; (435): 36-42.

Wiegand C., Winter D. and Hipler U. C. 2010. "Molecular-Weight-Dependent Toxic Effects Of Chitosans On The Human Keratinocyte Cell Line Hacat." *Skin Pharmacology and Physiology* 23 (3): 164-170.

Williams D. F. 2006. "To Engineer Is To Create: The Link Between Engineering and Regeneration." *Trends In Biotechnology* 24 (1): 4-8.

Wise J. K., Alford A. I., Goldstein S. A. and Stegemann J. P. 2014. "Comparison of Uncultured Marrow Mononuclear Cells And Culture-Expanded Mesenchymal Stem Cells In 3D Collagen-Chitosan Microbeads For Orthopedic Tissue Engineering." *Tissue Engineering Part A* 20 (1-2): 210-224.

Wittmer C. R., Phelps J. A., Lepus C. M., Saltzman W. M., Harding M. J. and Van T. P. R. 2008. "Multilayer Nanofilms As Substrates For Hepatocellular Applications." *Biomaterials* 29 (30): 4082-4090.

Xianmiao C., Yubao L., Yi Z., Li Z., Jidong L. and Huanan W. 2009. "Properties And In Vitro Biological Evaluation Of Nano-Hydroxyapatite/Chitosan Membranes For Bone Guided Regeneration." *Materials Science and Engineering: C* 29 (1): 29-35.

Xu F., Weng B., Gilkerson R., Materon L. A. and Lozano K. 2015. "Development Of Tannic Acid/Chitosan/Pullulan Composite Nanofibers From Aqueous Solution For Potential Applications As Wound Dressing." *Carbohydrate Polymers* 115: 16-24.

Xu H. and Simon C. 2005. "Fast Setting Calcium Phosphate–Chitosan Scaffold: Mechanical Properties And Biocompatibility." *Biomaterials* 26 (12): 1337-1348.

Xu H., Ma L., Shi H., Gao C. And Han C. 2007. "Chitosan–Hyaluronic Acid Hybrid Film As A Novel Wound Dressing:In Vitro Andin Vivo Studies." *Polymers For Advanced Technologies* 18 (11): 869-875.

Yajing Y., Xuejiao Z., Caixia L., Yong H., Qiongqiong D. and Xiaofeng P. 2015. "Preparation And Characterization Of Chitosan-Silver/Hydroxyapatite Composite Coatings Ontio2 Nanotube For Biomedical Applications." *Applied Surface Science* 332: 62-69.

Yan L. P., Wang Y. J., Ren L., Wu G., Caridade S. G., Fan J. B. and Mano J. F. 2010. "Genipin-Cross-Linked Collagen/Chitosan Biomimetic Scaffolds For Articular Cartilage Tissue Engineering Applications." *Journal of Biomedical Materials Research Part A* 95A (2): 465-475.

Yang X., Yang K., Wu S., Chen X., Yu F., Li J., Ma M. and Zhu Z. 2010. "Cytotoxicity And Wound Healing Properties Of PVA/Ws-Chitosan/Glycerol Hydrogels Made By Irradiation Followed By Freeze–Thawing." *Radiation Physics And Chemistry* 79 (5): 606-611.

Yao J., Cs-Szabó G., Jacobs J. J., Kuettner K. E. and Glant T. T. 1997. "Suppression Of Osteoblast Function By Titanium Particles* **." *The Journal of Bone And Joint Surgery-American Volume* 79 (1): 107-112.

Zanello L. P., Zhao B., Hu H. and Haddon R. C. 2006. "Bone Cell Proliferation On Carbon Nanotubes." *Nano Letters* 6 (3): 562-567.

Zhang H. and Neau S. H. 2001. "In Vitro Degradation Of Chitosan By A Commercial Enzyme Preparation: Effect of Molecular Weight And Degree of Deacetylation." *Biomaterials* 22 (12): 1653-1658.

Zhang R. and Ma P. X. 1999. "Poly(A-Hydroxyl Acids))/Hydroxyapatite Porous Composites for Bone-Tissue Engineering. I. Preparation and Morphology." *Journal of Biomedical Materials Research* 44(4): 446-455.

Zhang X., Meng L. and Lu Q. 2009. "Cell Behaviors On Polysaccharide-Wrapped Single-Wall Carbon Nanotubes: A Quantitative Study Of The Surface Properties Of Biomimetic Nanofibrous Scaffolds." *ACS Nano* 3 (10): 3200-3206.

Zhang X., Yang D. and Nie J. 2008. "Chitosan/Polyethylene Glycol Diacrylate Films As Potential Wound Dressing Material." *International Journal of Biological Macromolecules* 43 (5): 456-462.

Zhang Y. and Zhang M. 2001. "Synthesis And Characterization Of Macroporous Chitosan/Calcium Phosphate Composite Scaffolds For Tissue Engineering." *Journal of Biomedical Materials Research* 55 (3): 304-312.

Zhang Y., Reddy V. J., Wong S. Y., Li X., Su B., Ramakrishna S and Lim C. T. 2010. "Enhanced Biomineralization In Osteoblasts On A Novel Electrospun Biocomposite Nanofibrous Substrate Of Hydroxyapatite/Collagen/Chitosan." *Tissue Engineering Part A* 16 (6): 1949-1960.

Zhang Y., Venugopal J. R., El-Turki A., Ramakrishna S., Su B. and Lim C. T. 2008. "Electrospun biomimetic nanocomposite nanofibers of hydroxyapatite/chitosan for bone tissue engineering." *Biomaterials* 29: 4314–4322,

Zhang Y. Z., Su B., Ramakrishna S. and Lim C. T. 2008. "Chitosan Nanofibers From An Easily Electrospinnable UHMWPEO-Doped Chitosan Solution System." *Biomacromolecules* 9 (1): 136-141.

Zhang Z., Yang D. and Nie J. 2008. "Chitosan/Polyethylene Glycol Diacrylate Films As Potential Wound Dressing Material." *International Journal Of Biological Macromolecules* 43 (5): 456-462.

Zhang, Yong, Ming Ni, Miqin Zhang, and Buddy Ratner. 2003. "Calcium Phosphate—Chitosan Composite Scaffolds For Bone Tissue Engineering." *Tissue Engineering* 9 (2): 337-345.

Zhao F., Grayson W. L, Ma T., Bunnell B. and Lu W. W. 2006. "Effects Of Hydroxyapatite In 3-D Chitosan–Gelatine Polymer Network On Human Mesenchymal Stem Cell Construct Development." *Biomaterials* 27 (9): 1859-1867.

Zhao Rui., Li X., Sun B., Zhang Y., Zhang D., Tang Z., Chen X. and Wang C. 2014. "Electrospun Chitosan/Sericin Composite Nanofibers With Antibacterial Property As Potential Wound Dressings." *International Journal of Biological Macromolecules* 68: 92-97.

Zhou Y., Yang D., Chen X., Xu Q., Lu F. and Nie J. 2008. "Electrospun Water-Soluble Carboxyethyl Chitosan/Poly(Vinyl Alcohol) Nanofibrous Membrane As Potential Wound Dressing For Skin Regeneration." *Biomacromolecules* 9 (1): 349-354.

Zhou Y., Yang H., Liu X., Mao J., Gu S. and Xu W. 2013. "Electrospinning Of Carboxyethyl Chitosan/Poly(Vinyl Alcohol)/Silk Fibroin Nanoparticles For Wound Dressings." *International Journal of Biological Macromolecules* 53: 88-92.

Zhu P., Masuda Y. and Koumoto K. 2004. "The Effect Of Surface Charge On Hydroxyapatite Nucleation." *Biomaterials* 25 (17): 3915-3921.

Zhu X., Chian K. S., Chan-Park M. B. E. and Lee S. T. 2005. "Effect Of Argon-Plasma Treatment On Proliferation Of Human-Skin-Derived Fibroblast On Chitosan Membranein Vitro." *Journal of Biomedical Materials Research Part A* 73A (3): 264-274.

In: Advances in Polymers for Biomedical Applications ISBN: 978-1-53613-612-8
Editors: Deepak Pathania and Bhuvanesh Gupta 

*Chapter 10*

# DRESSING MATERIALS USING HERBAL DRUGS FOR BETTER WOUND MANAGEMENT

***Arpan Biswas[1], Manoranjan Sahu[2] and Pralay Maiti[1,*]***
[1]School of Materials Science and Technology,
Indian Institute of Technology, Banaras Hindu University, Varanasi, India
[2]Department of Shalya Tantra, Institute of Medical Science,
Banaras Hindu University, Varanasi, India

## ABSTRACT

In this chapter, better wound management using different herbal drugs loaded wound dressing materials has been discussed. The wound healing is a complex phenomenon and it passes through mainly three overlapping phases, where cell to cell and cell to matrix interactions take place. Due to complexity of the wounds, different types of dressing materials are required for faster healing. The traditional herbal medicines have a long history of wound management but often their low bioavailability decreases their efficacy. The encapsulation of herbal drug in polymer matrix increases their efficiency for wound healing. Amongst modern dressing materials, hydrogels, polymeric films and scaffolds have the capability to load very high concentration of drug and also have the ability to release them in a controlled and sustained manner which is essential for optimal therapeutic concentration. Further, they have the capability to absorb the exudate, pass the oxygen and also help the cells to be attached and proliferate. *In-vivo* and clinical studies show better healing efficiency of the herbal drug loaded dressing materials as compared to pure drug or pure dressing materials.

**Keywords:** wounds, herbal medicines, dressing materials

*Corresponding Author Email: pmaiti.mst@itbhu.ac.in.

## 1. INTRODUCTION

Skin, being the largest organ of human being, serves numerous functions of protecting our internal organs and tissues from external and potentially dangerous environments[1]. The partial or complete injury to the dermis or sub-dermis tissues leads to the wound generation which requires to be healed quickly and especially important for burn victims or diabetic patients[2–4]. As per World Health Organization (WHO) report, more than 300 thousands deaths are attributed to fire related burn injuries [5] along with millions suffer from chronic skin ulcers triggered by pressure, venous stasis or diabetes mellitus[6]. Healing of wounds usually proceeds through three overlapping phages[7–10] which consist of a series of interactions between extracellular matrix (ECM), cells and cytokines and may last for years[11,12]. The wound closure by epithelialization is one of the major steps and epidermal barrier is formed which protects the underlying growing tissues[13]. Different approaches are introduced by several researchers to improve the healing process[14,15] to overcome the limitations like non-selectivity, low bioavailability through oral route. Antibiotic loaded wound dressing material is one of them to treat infected wounds[16]. "Darmal patch technology" is widely accepted for delivering the biologically active molecules through skin without using needles [17]. Recently, polymeric templates whose shape changing capabilities [18,19] are also being used in wound dressing applications[20].

Polymeric dressing materials attracted huge attention as drug carriers because of their ability to enhance drug stability, drug solubility by improving transport properties of the biologically active molecules [21, 22]. An international study conducted by Price et al. on pain during the change of wound dressing [22]reveals that it is the worst part of wound management as it increases the swelling, discharge, pain and it also delay the healing by damaging the healthy granulation and epithelial tissues. Considering these acute problems, a good dressing material has to be developed which is cost effective, easily applicable in any position and maintain the therapeutic concentration of the drug on the wound site in a sustained manner. Mandal et al. has developed a wound dressing material by incorporating synthetic antibiotic to improve wound healing [23]. The synthetic drugs which are being used in wound healing are summarized in Table 1. The side effects of the synthetic bioactive molecules used in cosmetics, medicine and food industry become a big concern with growing human awareness and also the multidrug resistance phenomena increase the complications along with the expenditure. These problems drive the medical community to find alternative medicines like herbal products, plant extracts etc. [24]. Different parts of the plants contain various biologically active chemical compounds which exhibit antimicrobial activity [25, 26] and have the ability to treat antimicrobial infections [27, 28]. The different phytochemicals synthesized from the plants are phenolics, terpenoids and alkaloids which have various mechanism of actions against pathogens including disruption of cell membrane, complex formation with the cell wall, substrate deprivation and enzyme inhibition [29].

Generally, the adequate moist environment accelerate the healing through increasing epithelialization of superficial wound as compared to dry bandaged wound and, hence, different types of occlusive dressing materials have been developed to maintain the moisture over the wound [30, 31]. Hydrogels and soft physiological tissues have very identical

physicochemical properties viz. water content, mechanical properties, low interfacial tension to body fluids/water, air permeability, etc. [32]. Further, hydrogels have the capability to release the water soluble drugs in a sustained manner following the appropriate diffusion mechanism [33]. Further, the electrospun scaffolds have drawn the attention in the field of wound healing because of their morphological advancement. The porous structure of the scaffold with high surface area can mimic the extracellular matrix (ECM) [34, 35] and can facilitate/control water evaporation, oxygen permeability, fluid drainage etc. It has the potential to inhibit the ultrafine exogenous microorganism due to their ultra-fine pores [13]. Electrospun scaffolds prepared from biodegradable and biocompatible polymers like poly(ε-caprolactone), poly(lactic acid), poly(vinyl alcohol), poly(lactic acid-co-glycolic acid), chitosan and gelatin provide substrate for cell growth which helps to reconstruct the damaged tissue and thereby promote new tissue restoration [36, 37]. The most challenging part of topical delivery systems is to maintain the therapeutic concentration of the drug in the wound site and it depends on the ability of the drug to be released from the formulation and its permeation through skin barrier. The controlled release of drug reduces the cumulative amount of release at initial stage and ultimately increases the bioavailability of drug for longer period of time which cause faster wound healing [38].

**Table 1. The list of common synthetic drugs which are used for wound healing**

| Drug name | Drug class |
|---|---|
| Silver sulfa diazine | Sulfa antibiotics |
| Santyl Collagen | specific enzyme |
| Urea | Keratolytics |
| Thermazene | Sulfa antibiotics |
| Hibiclens | Antiseptic |
| Sarna | Local Anaesthetic |
| Silver nitrate | Antiseptic |
| Atrapro | Skin Barrier Emollie |

## 2. CLASSIFICATION OF WOUNDS

Wounds are broadly classified as acute and chronic on the basis of physiology of wound healing[39]. Wounds which heal in a estimated time frame through the physiological wound healing process are called acute wounds[40] while chronic wounds are defined as a loss of

integrity of the skin and one or more deeper structures with the lack of healing within a reasonable time frame. Delayed healing in chronic wound is due to an etiological difference and pathological difference from the acute wound. US National Research Council classified wounds according to the extent of contamination present, for understanding the risk factors and better management of wounds [41]. Wounds are further divided into four categories depending on the presence of contamination viz. dirty, contaminated, clean-contaminated and clean wounds. The presence of pus, purulent inflammation and intraperitoneal abscess formation is the sign of a dirty wound. The major breakage in aseptic technique is the characteristics of infected wounds while acute inflammation should present or no break of aseptic technique takes place in clean wounds.

## 3. PHASES OF WOUND HEALING

Wound healing is a physiological mechanism of the body's tissues in response to injury. Proper healing of the wound is essential for the restoration of disrupted anatomical continuity and functional status of the skin. Healing of a wound is a complicated process initiated in response to an injury which helps to restore the function and integrity of the damaged tissues through continuous cell-cell and/or cell-matrix interactions. Healing process proceeds through three overlapping process viz. inflammation (0-3 days), cellular proliferation (3-12 days) and remodeling (3-6 months)[42–44].

### 3.1. The Inflammatory Phase

This phase starts immediately after the creation of wound and usually lasts for 48 to 72 hrs.[45]. The inflammation phase shows some classical signs like redness, swelling, heat and pain. Inflammation is a complex chain of reaction which ultimately leads to healing. Growth factors and cytokine signals are responsible for cell and tissue movements, inflammatory responses to trauma or injury[46]. Immediately after the disruption of skin barrier, keratinocytes release Interlukin-I (IL-1) which alert the surrounding tissues and attract the neutrophiles towards the wound site. This phase introduces the homeostatic mechanism to stop blood loss from the wound site. This phase is recognized by vasoconstriction and platelet aggregation to induce blood clotting and subsequently vasodilation and phagocytosis to produce inflammation at the wound site[47].

### 3.2. Proliferative Phase

The proliferative phase begins from the 3$^{rd}$ day and remains up to 12 days. This phase includes three stages namely, granulation stage; where fibroblasts activity is associated with PDGF (platelet derived growth factor) and the synthesis of ECM by collagen and ground substances such as glycosaminoglycan and proteoglycan, contraction stage; where wound

edges pull together to reduce defect followed by epithelialization stage; where migration of epithelial cells occurs from the adjacent wound area for external shielding of the wound. The epithelialization starts immediately after injury and is activated by the Epidermal Growth Factor (EGF), TGF-$\alpha$ and Fibroblast Growth Factor (FGF). Normally, re-epithelialization takes around 48 hours for properly incised wounds[40].

### 3.3. Remodeling Phase

The last phase of wound healing is the remodeling phase which persists from day 21 to 1 year after injury. The apoptosis of the cells helps to stop the formation of granulation tissue[48]. The characteristics of remodeling phase is identified by the presence of collagen, replacing collagen type III with type I, realignment of collagen along the lines of tension and reduction of vascularity and wound contraction[49]. The oxygen supply, adequate nutrition and cofactors[40] are the essential important factors for collagen synthesis. Scar remodeling continues for 6-12 months post injury and tensile strength of wound tend to increase over the time.

## 4. WOUND MANAGEMENT

A trauma wound is a severe break or injury in the soft tissue of the skin. The term 'trauma' refers to wound in Greek and major trauma can lead to very serious morbidity, injury and systematic inflammatory response syndrome (SIRS) etc. which may need emergency care unless it may lead to death.[50] Careful examination of wounds in details pay attention to its appearance, smell, colour, necrotic tissue type, surrounding skin condition, the type and amount of exudates etc. and plays a crucial role in planning a suitable management for a particular wound. Wound healing society has made a standard protocol to handle the chronic wounds by designing wound bed preparation. Wound bed preparation is a systematic approach for the assessment and management of wounds consisting of four steps namely TIME; **T**issue assessment and debridement of nonviable tissues, **I**nflammation and infection control, **M**oisture balance, and Promote epithelialization of **E**dges[51]. Tissue debridement is the process by which devitalized structures such as necrotic tissue, foreign tissue and wound coatings are removed from the wound area[52]. Control of infection and inflammation are two important factors for wound healing. Wounds with more than $10^5$ CFU bacterial loads are difficult to heal. Bright red colour, friable granulation tissue, exudates, increasing pain are the signs of an infected wound[53]. Moisture balance is also an important factor for proper healing of a wound. Wound dryness inhibits the epithelialization while excessive moisture leads to breakdown and maceration of tissues.[54] Shah et al. has modified TIME principles into $TIMEO_2$ for chronic wound management. Availability of excess oxygen enhances the healing rate[55].

**Table 2. Different wound dressings are used for different types of wounds**

| | Wound type | Dressing type |
|---|---|---|
|  | Clean, medium-to-high exudate (epithelializing) | • Paraffin gauze.<br>• Knitted viscose primary dressing. |
|  | Clean, dry, low exudate (epithelializing) | • Absorbent perforated plastic film-faced dressing.<br>• Vapour-permeable adhesive film dressing. |
|  | Clean, exudating (granulating) | • Hydrocolloids<br>• Foams<br>• Alginates |
|  | Slough-covered | • Hydrocolloids<br>• Hydrogels |
|  | Dry, necrotic | • Hydrocolloids<br>• Hydrogels |

### 4.1. Advancement in Wound Dressing

Wound dressing are used to keep away all the possible reasons which can delay the wound healing rate[56]. Usually, wound dressing contains two parts; primary dressing which makes direct contact with the wound and secondary dressing which covers the primary dressing. Two types of wound dressing materials are available in the market, traditional one which contains cotton wool, gauzes, bandages etc. and modern dressing like hydrocolloids, alginates, hydrogels, semipermeable adhesive film, foams, biological dressings etc. Wound care is an age old practice and there is an evidence of clay tablets which are used for making plaster and bandaging the wounds in ancient time[55]. Wound management was targeted to dry the wound to fasten the healing in old age[53]. Different wound dressing materials such as honey, linen, vegetable fibers and animal fats were used to stop bleeding and absorb exudates[57]. The concept of moist wound healing was introduced in 1960 and occlusive wound dressings were produced in 1980 which maintain the moisture as well as biochemical reactions during the healing process[58]. Modern wound dressing are developed to provide the wound function and they are classified as passive, interactive and bioactive dressings[59]. Passive products are non-occlusive, such as gauze, used simply cover the wound to restore its function underneath and wet gauze is not a good barrier for infection as it is a non-occlusive wound dressing[60]. Interactive dressings are semi-occlusive or occlusive in nature, available

in the form of films, foam, hydrogel and hydrocolloids. Moist dressing and supply of adequate nutrition promotes pressure ulcer healing[61]. Biocompatible and biodegradable dressing materials such as chitosan, collagen, alginates etc. fall under this group[59]. Drug eluting biodegradable scaffolds are the latest addition in this category and are considered as very effective in wound healing management[62]. Scaffolds with porous structure allow better cell attachment, proliferation, absorb exudates and protect from microbial attacks. Further, the sustained and controlled local delivery of the drug increases the bioavailability to the wound site which fastens the healing rate. There is no single wound dressing material which can be applied in all situations because of different types/stages of wounds. Therefore, proper selection of wound dressing is very crucial part for better healing[63]. Different wound dressing materials are required for different types of wounds and at different stages of wound healing. The suitable wound dressing materials for variety of wounds are presented in Table 2[64].

## 5. HERBAL DRUGS WITH WOUND HEALING ACTIVITIES

In India, a large number of medicinal plants were used for the treatment of skin diseases like cuts, wounds and burns in traditional medicinal systems particularly ayurvedic, siddha and unani. Recently, researchers are looking for alternatives to modern medicines like antibiotics, corticosteroids etc. for wound healing to avoid the side effects of those medicines. It is found in a study that wounds and dermatological conditions is one of the common problems of people in rural areas of developing countries for which they need medical attention. As most common people cannot take care of injuries, burns and leg ulcers in their initial stages which become severe in later stage and seeks greater medical care[65]. Better understanding is necessary for pathogenesis of chronic wounds. Otherwise, it fails to heal. Two indifferent aspects, pathogenesis and failure to heal strengthened the use of herbal drugs for the healing of wounds. Herbal medicine does not get sufficient attention although it has minimal side effect and low cost. Further, it does not fall into WHO's priority area. The ethanobotanical information on plants which are extensively used for wound healing as a traditional medicine in India is presented in Table 3[66]. *Aloe vera*[67, 68], *Azadirachta indica*[69], *Carica papaya*[70],*Celosia argentea*[71], *Centella asiatica*[72], *Cinnamomum zeylanicum*[73], *Curcuma longa*[74,] *Nelumbo nucifera*[75], *Ocimum sanctum*[76], *Phyllanthus emblica*[77], *Plumbago zeylanica*[78], *Pterocarpus santalinus*[79], *Terminalia arjuna*[80], *Terminalia chebula*[81], are very well known in Ayurveda, Siddha and Unani systems of medicines for their wound healing activities. There are some active compounds, isolated fromthe plants, have the ability to accelerate the healing of wounds like tannins isolated from *Terminalia arjuna*[82],oleanolic acid from *Anredra diffusa*,[83] polysaccharides from *Opuntiaficus-indica*[84],gentiopicroside, sweroside and swertiamarine from Gentianalutea, shikonin derivatives from *Onosma argentatum*[85],curcumin from *Curcuma longa*[86],proanthocyanidins and reseveratrol from grapes[87],acylatediridoid glycosides from *Scrophularia nodosa*[88], glycoprotein fraction from Aloe-vera[89] etc.

## 5.1. Herbal Drug Loaded Wound Dressings

Ayurvedic drug loaded creams are prepared through water/oil emulsification process by incorporating cow ghee, flax seed oil, *Phyllanthus emblica* fruits, *shorea robusta* resin and Yashada bhasma by varying their compositions. The regular application of herbal dressing materials on excision and incision wound model accelerates the healing. The combination of flex seed oil, *shorea robusta* resin and Yashada bhasma is very effective in wound contraction, improvement of tensile strength and augmentation in hydroxylproline or collagen content [90]. The fruit juice, fruit and peel extract of *Punica granatum*,popularly known as pomegranate, have very good anti-oxidant property along with antibacterial, anticonvulsant, anti-inflammatory, antifungal, immune modulatory, cardioprotective, antimutagenic, antispasmodic and antidiabetic activities [91, 92]. 2% (w/w) pomegranate peel ethanolic extract based hydrogel formulation shows very good wound healing activity on a non-healing chronic ulcer [93]. Herbal drug, chamomile extract incorporated starch-zeolite nanocomposites hydrogel is very effective in wound healing and is also biocompatible in nature [94]. The presence of zeolite nanoparticles controls the release kinetics of the drug. Drug loaded nanocomposite hydrogel shows better efficacy in wound area contraction than that of drug loaded pure starch hydrogel applied in animal model (Figure 1a). The histopathological finding shows complete epithelialization and hair follicles in 21 days with drug incorporated composite hydrogel group. The clinical studies of some refractory ulcers at different position with drug loaded hydrogels reveal the changing of wound surface colour and contraction of wound area which indicates controlled release of the drug along with absorption ability of exudates using nanocomposite hydrogel helps in accelerating the wound healing (Figure 1b). Simvastatin-chitosen microparticles incorporated poly(vinyl alcohol) hydrogel has the ability to sustain the release of the herbal drug (simvastatin) and release the drug up to 92% in 7 days. *In-vivo* study with wistar rats reveals better efficacy of the low dose simvastatin-chitosen microparticles loaded PVA hydrogel in wound healing as compared to conventional simvastatin ointment (1%) [95]. 6% honey loaded chitosan-1% lactic acid hydrogel exhibits higher zone of inhibition against *Staphylococcus aureus* and *E. coli* and also shows significant water vapor transmission and water absorption properties which makes it a very good dressing material [96]. The bark of *Ficusracemosa*, which contains several phytoconstitutes like alkaloids, flavonoids and tannins, is widely used in chronic wound and piles [97]. It has the ability to enhance the wound healing activities because of their antioxidant and anti-microbial properties [98]. The herbal drug incorporated dermal patches of natural polymer Protanal LF10/60 are prepared by incorporating the alkaloids, flavonoids and tannins separately through solvent evaporation technique. *In-vivo* wound healing studies show better wound healing efficacy with the tannins and flavonoids incorporated dermal patches as compared to alkanoid incorporated patch in 15 days (Figure 2). *In-vitro* drug release study indicates greater release of drug on wound site from the patch causing faster healing [98]. The curcumin encapsulated chitosan-poly(vinyl alcohol)-silver nanocomposite film shows better anti-bacterial and anti-fungal activity against pure curcumin and pure film. Further, the release of drug becomes sustained and increases the mechanical strength of the film in presence of nanosilver[99].

**Table 3. List of Indian medicinal plants with their wound healing activity and different wound healing models reported**

| Plant name | Extract used | Model studied |
|---|---|---|
| *Acalypha indica* | Whole plant ethanolic extract | Excision and incision |
| *Aegle marmelos* | Methanolic extract of plant | Excision and incision |
| *Allmanda cathartica* | Aqueous extract | Excision and incision |
| *Anogeissus latifolia* | Ethanolic extract of bark | Excision and incision |
| *Aristolochia bracteolata* | Ethanol extract | Excision, incision and dead space |
| *Areca catechu* | Betel nut extract and its two consitutents arecholine and polyphenols | Excision, Incision and dead space |
| *Argemone mexicana* | Ethanolic extract | Excision, incision and dead space wounds |
| *Azadirachta indica* | Pure neem oil and neem ointment | Incised and gap wounds in bovine calves |
| *Bryophyllum pinnatum* | Leaf, alcoholic and water extracts | Excision, incision and dead space |
| *Butea monosperma* | Alcoholic bark extract | Excision |
| *Calotropis procera* | Latex | Excision |
| *Canthium parviflorum* | Aqueous and ethanolic extract | Excision |
| *Cassia fistula* | Alcoholic leaf extract | Excision |
| *Celosia argentea* | Alcoholic extract | Rat burn wound |
| *Centella asiatica* | Ethanolic extract | Incision, excision, and dead space |
| *Cinnamomum zeylanicum* | Ethanol extract of bark | Excision, incision and dead space |
| *Coronopus didynamous* | Ethanol and aqueous extracts of whole plant | Incision |
| *Cyperus rotundus* | Extract of tuber | Excision, incision and dead space |
| *Datura alba* | Alcoholic leaf extract | Burn rat wound |
| *Desmodium triquetrum* | Ethanolic leaf extract | Excision, incision and dead space |
| *Elephantopus scaber* | Aqueous ethanol extracts isolated compound deoxyelephantopin | Excision, incision and dead space |
| *Eucalyptus globulus* | Ethanolic extract of leaf | Excision, incision and dead space |
| *Euphorbia neriifolia* | Aqueous extract of latex | Excision |
| *Flaveria trinerva* | Methanol extract | Excision and incision |
| *Gentiana lutea* | Alcohol and petroleum ether extract of rhizomes | Excision, incision and dead space models |
| *Glycyrrhiza glabra* | Ethanolic extract of root | Excision |
| *Gmelina arborea* | Alcoholic extract of leaf | Excision, incision and dead space |
| *Heliotropium indicum* | Whole plant ethanolic extract | Excision and incision |
| *Hemigraphis colorata* | Crude leaf paste | Excision |
| *Hippophae rhamnoides* | Aqueous extract of leaf | Excision |
| *Hypericum hookerianum* | Methanolic extracts of leaf | Incision and excision |
| *Hypericum mysorense* | Methanol extract of leaf | Excision and incision |
| *Hypericum patulatum Thumb* | Methanolic extract of leaf | Excision and incision |
| *Hyptis suaveolens* | Ethanolic extract of leaf | Excision, incision and dead space |
| *Indigofera enneaphylla* | Alcoholic extract of aerial parts | Excision and incision |
| *Ixora coccinea* | Alcoholic extract of flowers | Dead space |
| *Lantana camara* | Leaf juice and hydroalcoholic extract | Excision |
| *Laura noblis* | Aqueous extracts | Excision and incision |
| *Lawsonia alba* | Difference extracts of leaf | Excision and incision |
| *Leucas hirta* | Aqueous and methanolic leaf extracts | Excision, incision and dead space |
| *Leucas lavandulaefolia* | Methanol extract | Excision and incision |
| *Moringa oleifera* | Ethyl acetate extract of dried leaf | Excision, incision and dead space |
| *Nelumbo nucifera* | Methanol extract of rhizomes | Excision, incision and dead space |
| *Ocimum sanctum* | Ethanolic extract of leaves | Excision, incision and dead space |
| *Oxalis corniculata* | Alcohol and petroleum ether extracts of whole plant | Excision, incision and dead space |
| *Pentas lanceolata* | Ethanolic extract of flowers | Excision |
| *Phyllanthus emblica* | Plant extract | Excision |
| *Plagiochasma appendiculatum* | Alcohol and ethanolic extract | Excision and incision |

The electrospun fiber has the ability to deliver drug in a faster way to the wound site [100]. The thymol encapsulated PLA-PCL nanohybrid nanofiber shows highest percentage of drug release (~72%) *in-vitro* as compared to pure PCL/PLA nanofiber. The comparative in-vivo wound healing study with commercial wound dressing Comfeel Plus and thymol loaded nanohybridnanofiber reveals better efficacy of the nanohybrid in wound contraction [101].

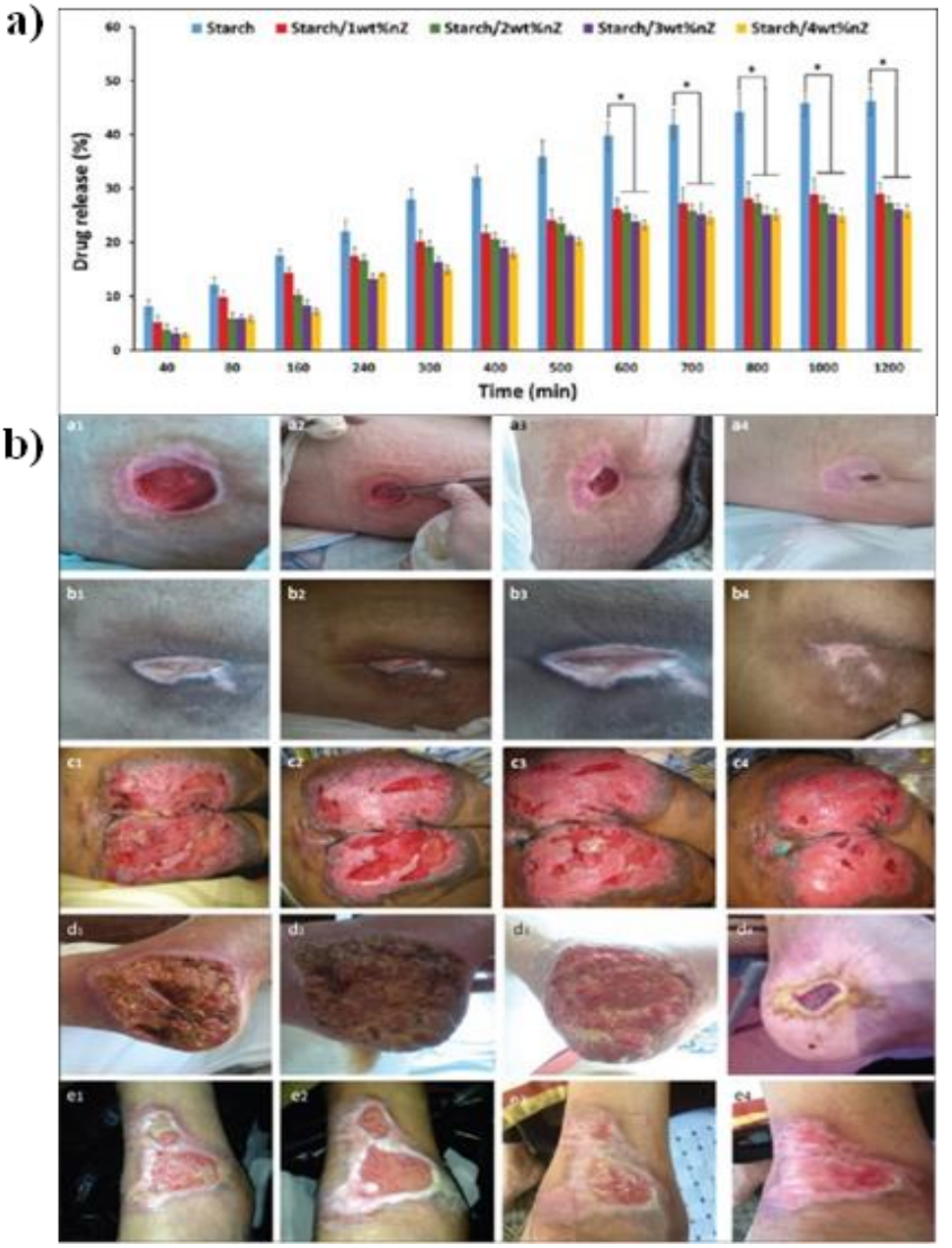


Figure 1. a) The release profile of chamomile from starch-nanozeolitenanocomposites hydrogel. The percentage release decreases with increasing zeolite content.(*$P$< 0.05); b) The representative images of refractory ulcers of five patients which were treated with herbal drug loaded hydrogels (a-e). The wound colour and size changes with treatment time. a1-e1 represent 1$^{st}$day, a2, d2: day 20, b2, c2, e2: day 5, a3, d3: day 40, b3, c3, e3: day 10, a4: day 61, b4: day16, c4: day 25, d4:day 52, e1: day 15(down).

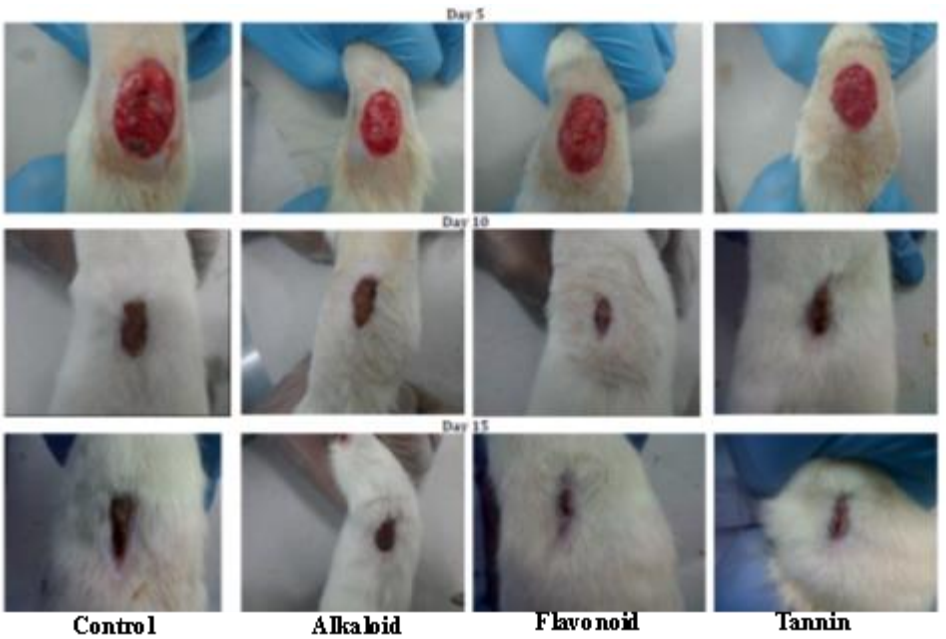


Figure 2. In-vivo study showing the healing pattern of the wounds in presence of alkaloid, flavonoid and tannin loaded dressing materials. The tannin loaded dressing materials heal the wound more effectively than other dressing materials.

Methanolic crude extract of *Centellaasiatica (L.)* is well known for its wound healing activity. Crude extract loaded gelatin fiber [102]controls the release of the drug at higher crosslink density. Curcumin is well known for its anti-oxidant and anti-inflammatory action but poor bioavailability and stability restricts its applications [103]. Effectiveness of curcumin increases when it is impregnated into poly(ε-caprolactone)/gum tragacanth (PCL/GT) nanofiber[104]. The developed material is 99.9% anti-bacterial against MRSA (methicillin-resistant staphylococcus aureus) and 85.1% against ESBL (Extended-spectrum beta-lactamases). Further, *in-vivo* study on diabetic wound model shows markedly fast wound closure with well-defined granulation tissue dominated by fibroblast proliferation, collagen deposition, complete early re-epithelialization and formation of sweat glands and hair follicles. Charernsriwilaiwat et al. prepared chitosan-ethylene diamine tetra acetic acid/poly(vinyl alcohol) (CS-EDTA/PVA) based nanofiber by incorporating various concentrations of *Garciniamangostana* extract for improving the wound healing. In-vitro release study shows 80% release of drug within 1 hr. The nanofiber is cytocompatible in nature against fibroblast cells and shows cytotoxicity against both gram-positive and gram-negative pathogens. Interestingly, the MIC (Minimum inhibition concentration) and MBC (Minimum bacterial concentration) values drop almost 10 times as the concentration of drug in the scaffold improved by ~3 times. Moreover, a faster wound healing in rat model of skin wound is observed with 3% drug loaded electrospun scaffold [105]. The fatty acid containing emu oil encapsulated polyurethane nanofiber has been reported for wound dressing purpose. 10% emu oil loaded scaffold shows antibacterial activity against both type of bacterial strains [106]. The shikonin incorporated poly(ε-caprolactone)/ poly(trimethylene carbonate) composite fiber is prepared by varying poly(ε-caprolactone)/poly(trimethylene carbonate)

ratio and drug loading. The fiber diameter decreases with increasing concentration of poly(trimethylene carbonate). In-vitro release shows initial burst release of shikonin followed by a plateau after 11 hrs. In-vitro drug release can also be tuned using poly(ε-caprolactone)/ poly(trimethylene carbonate) ratio and drug loading concentration. Moreover, the antibacterial and free radical scavenging activity of drug has proven the developed material as good wound dressing material [107]. Dia et al. prepared nanofiber of poly(vinylpyrrolidone) (PVP) encapsulating herbal drug emodin, an extract of *polygonumcaspidate*. In-vitro study shows more desired release kinetics of the drug from the scaffold as compared to pure drug which facilitate the wound healing as revealed form wound contraction and histopathological examinations [108]. *Tecomellaundulate,* is widely known for its medicinal applications, especially for its wound healing ability. Chloroform methanol mixture (4:1) crude bark extract of *Tecomella undulate* loaded PCL/PVP nanofiber inhibits the growth of *Pseudomonas aeruginosa, Staphylococcus aureus, Escherichia coli* very effectively. Microscopic investigation shows no morphological changes due to the encapsulation of the drug in nanofiber. With good drug stability and high drug loading efficacy, the nanofiber can be an effective wound dressing material [109]. The thymoquinone is an active constituent of *Nigella sativa*, known for its anti-bacterial property and wound healing ability. The nanofiber preparation with PLA/cellulose acetate blend by incorporating the thymoquinone control the release kinetic of the drug more effectively than PLA nanofiber as observed through *in-vitro* release study. The drug release profile shows a sustained release of drug with initial burst release. The scaffold shows effective antibacterial property against both types of gram bacteria. Further, the developed material is biocompatible in nature and assists cell proliferation and attachment. The preliminary in-vivo wound healing study shows that scaffold promotes the angiogenesis, re-epithelialization and control the granulation tissue construction [110]. Semelil, a herbal drug used for the treatment of chronic ulcers especially in diabetic foot ulcer, embedded in chitosan-polyethylene oxide electrospun nanofiber keeps the physical property of the chitosan-poly(ethylene oxide) intact. In-vitro release study shows initial burst release up to 1 hour and the mat with lower concentration of drug shows higher cumulative release [111]. In spite of having good mechanical and thermal properties, the hydrophobic nature of the synthetic polyesters inhibits cell proliferation which is the major concern of wound healing. The nanofiber of PCL is prepared by incorporating the aloe-vera which significantly increases the proliferation of fibroblast cells as compared to pure PCL nanofiber. However, degradation of the mat increases in presence of aloe-vera[112]. The electrospun nanomembranes of PCL by incorporating different herbal drugs viz. Tecomella undulate, Asparagus recemosus, Glycyrrhiza glabra and Linum usitatissimum are prepared to improve the wound treatment [113]. An ideal wound dressing material should control the evaporation of moisture from the wound site in such a manner that it may prevent neither excessive dehydration nor it build exudate. The herbal drug loaded dressing materials shows good moisture vapor transmission rate (2900-3100/day), as shown in Figure 3a. Further, the nanomembranes release almost 50% of different incorporated herbal drugs within 24 hours (Figure 3b). In-vivo wound healing study shows faster wound contraction in groups where wounds are dressed with herbal drug loaded nanomembranes as compared to group dressed with commercial wound dressing materials (Figure 3c).

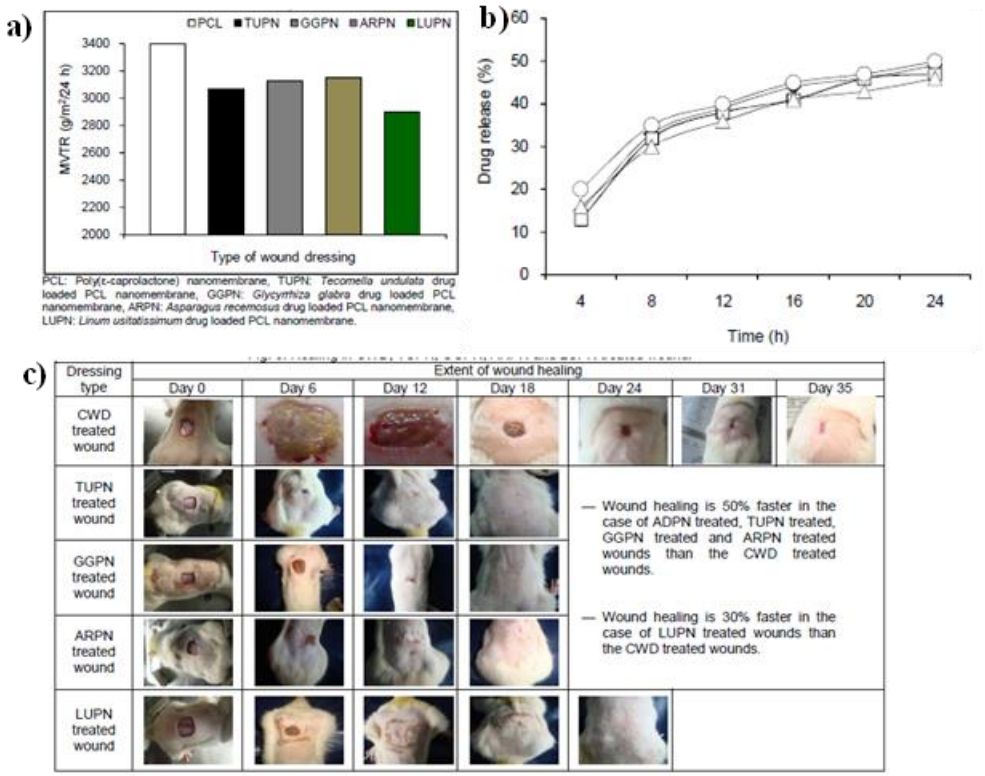


Figure 3. a) The moisture vapor transmission rate of different developed drug loaded electrospun scaffold; b) *In-vitro* drug release profile of different herbal drug loaded electrospun scaffold showing ~ 50% drug released within 24 hours; c) Photographic images of comparative *in-vivo* study using different wounds dressing nanomembranes. The wound closure is faster in all the herbal drug loaded groups as compared to commercial wound dressing material.

Thomas et al. prepared glycosaminoglycan-chitosan-gelatin scaffold, through lyophilization technique, by incorporating hemigraphis colorata silver nanoparticles (herbal nanoparticle). The cytotoxicity measurement and in-vitro scratch wound healing reveals that the material is biocompatible in nature and can be effective as wound healing patch [114]. Incorporation of the curcumin into chitosan nanoparticles and the development of nanohybrid scaffold with collagen improve the stability of the curcumin. Water uptake of the material and sustain release of drug in-vitro condition are reported. In-vivo wound healing studies reveal significant wound closure ($p < 0.001$) with this material as compared to control and placebo groups. Further, histopathological findings show complete epithelialization with thick granulation tissue in nanohybrid scaffold group while incomplete collagen deposition and inflammation is noticed in placebo and control group, respectively [115]. Different types of sponges are prepared by varying chitosan and gelatin ratio and the folding endurances increase with increasing gelatin concentration [116]. Water uptake of the matrix increases with increasing chitosan concentration while the percentage release increases with the increase of gelatin ratio. The porous structure of the prepared sponge is visualized through scanning electron microscope (Figure 4a). The antibacterial property measurement against P. aeruginosa shows greater zone of inhibition for curcumin loaded sponges as compared to sponges without drugs (Figure 4b). Further, the drug loaded sponge with higher chitosen

concentration (SP3) shows greater zone of inhibition as compared to other drug loaded sponges and the cytotoxicity measurement indicate the biocompatible nature of the materials. In-vivo wound healing study with rat model shows better healing of the wounds which are covered with curcumin loaded sponges as compared to control and pure sponge groups after 15 days (Figure 4c).

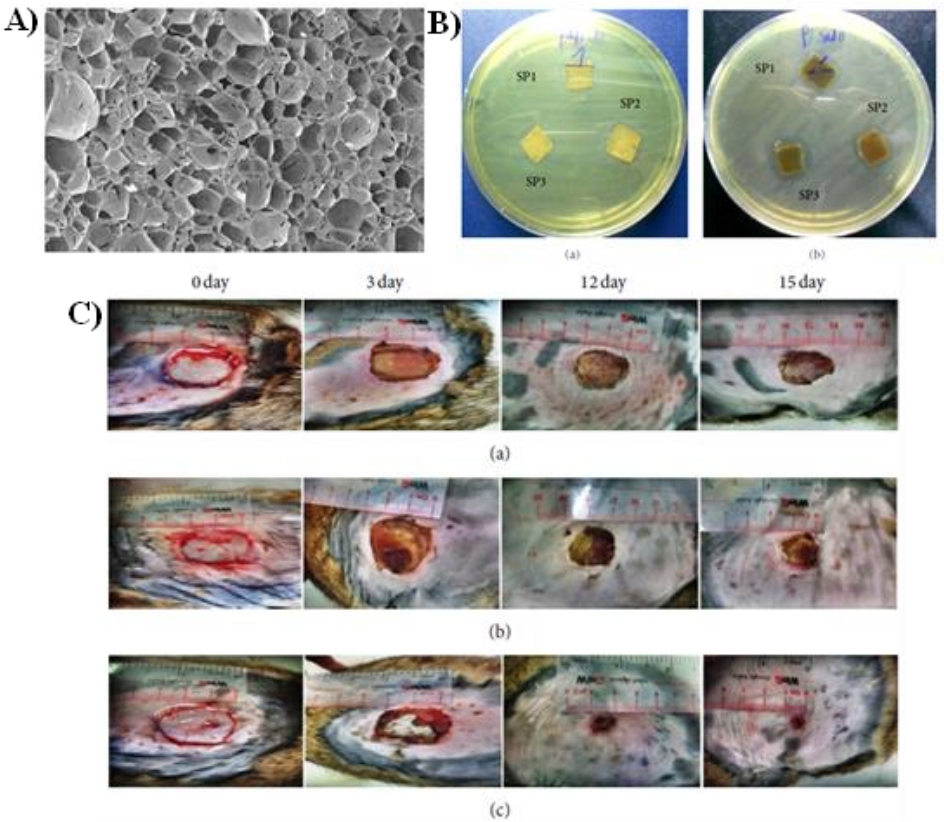


Figure 4. A) The cross-sectional morphology of chitosen/gelatine sponge as observed through scanning electron microscope (SEM); B) The antibacterial activity against Pseudomonas aeruginosa (a) with pure chitosen/gelatin sponges and (b) with curcumin loaded sponges; C) Representative photographic images of in-vivo wound healing when the wounds were covered with (a) control (b) pure sponge and (c) curcumin loaded sponge.The significant wound contraction is observed with curcumin loaded sponge group as compared to other groups in in-vivo study after 15 days.

## CONCLUSION

The wound healing is a complex phenomenon and passes through some overlapping phases and needs special attention for improved healing. The wound dressing material plays an important role to improve the healing pattern. The cream and hydrogel helps to keep the moist condition of the wound while the scaffolds have the ability to absorb the wound exudates, permit oxygenation of the wound and also helps in cell proliferation. The biocompatible and biodegradable polymers are the natural choice as wound dressing materials

because of their inert and green nature. Further, they have the capability to deliver different wound healing drugs in the wound site in a sustained and controlled manner which helps in accelerating the wound healing, keeping the drug concentration within the therapeutic window. The herbal drugs have several advantages in wound healing over modern synthetic drugs in terms of cost effectiveness and less side effect while they also have some limitations like low bioavailability. The incorporation of these herbal drugs in different types of wound dressing materials improves their bioavailability and sustained release over the wound site. The herbal drug incorporated dressing materials shows better cell attachment, cell proliferation and anti-microbial properties and improve the overall quality of wound management.

## REFERENCES

[1] E. Chong, T. Phan, I. Lim, Y. Zhang, B. Bay, S. Ramakrishna, C. Lim, Evaluation of electrospun PCL/gelatin nanofibrous scaffold for wound healing and layered dermal reconstitution, *Acta Biomater.* 3 (2007) 321–330. doi:10.1016/ j.actbio.2007.01.002.

[2] M. Kempf, Y. Miyamura, P. Y. Liu, A. C. H. Chen, H. Nakamura, H. Shimizu, Y. Tabata, R.M. Kimble, J.R. McMillan, A denatured collagen microfiber scaffold seeded with human fibroblasts and keratinocytes for skin grafting, *Biomaterials.* 32 (2011) 4782–4792. doi:10.1016/j.biomaterials.2011.03.023.

[3] M.R. Greives, F. Samra, S.C. Pavlides, K. M. Blechman, S. M. Naylor, C.D. Woodrell, C. Cadacio, J.P. Levine, T.A. Bancroft, M. Michalak, S.M. Warren, L.I. Gold, Exogenous calreticulin improves diabetic wound healing, *Wound Repair Regen.* 20 (2012) 715–730. doi:10.1111/j.1524-475X.2012.00822.x.

[4] J.K. Plichta, K.A. Radek, Sugar-Coating Wound Repair, *J. Burn Care Res.* 33 (2012) 299–310. doi:10.1097/BCR.0b013e318240540a.

[5] J.F. Burke, I. V Yannas, W.C. Quinby, C.C. Bondoc, W.K. Jung, W.K. Jung, Successful use of a physiologically acceptable artificial skin in the treatment of extensive burn injury., *Ann. Surg.* 194 (1981) 413–28. http://www.ncbi.nlm.nih. gov/pubmed/6792993 (accessed December 5, 2017).

[6] I. Jones, L. Currie, R. Martin, A guide to biological skin substitutes, *Br. J. Plast. Surg.* 55 (2002) 185–193. doi:10.1054/bjps.2002.3800.

[7] A.J. Singer, R.A.F. Clark, Cutaneous Wound Healing, *N. Engl. J. Med.* 341 (1999) 738–746. doi:10.1056/NEJM199909023411006.

[8] G. Broughton, J.E. Janis, C.E. Attinger, The Basic Science of Wound Healing, *Plast. Reconstr. Surg.* 117 (2006) 12S–34S. doi:10.1097/01.prs.0000225430. 42531.c2.

[9] L. Braiman-Wiksman, I. Solomonik, R. Spira, T. Tennenbaum, Novel Insights into Wound Healing Sequence of Events, *Toxicol. Pathol.* 35 (2007) 767–779. doi:10. 1080/01926230701584189.

[10] M.B. Dreifke, A.A. Jayasuriya, A.C. Jayasuriya, Current wound healing procedures and potential care., *Mater. Sci. Eng. C. Mater. Biol. Appl.* 48 (2015) 651–62. doi:10.1016/j.msec.2014.12.068.

[11] S. Guo, L.A. DiPietro, Factors Affecting Wound Healing, *J. Dent. Res.* 89 (2010) 219–229. doi:10.1177/0022034509359125.

[12] J.M. Reinke, H. Sorg, Wound Repair and Regeneration, *Eur. Surg. Res.* 49 (2012) 35–43. doi:10.1159/000339613.

[13] A. Schneider, X.Y. Wang, D.L. Kaplan, J.A. Garlick, C. Egles, Biofunctionalized electrospun silk mats as a topical bioactive dressing for accelerated wound healing, *Acta Biomater.* 5 (2009) 2570–2578. doi:10.1016/j.actbio.2008.12.013.

[14] T. Mustoe, Understanding chronic wounds: a unifying hypothesis on their pathogenesis and implications for therapy., *Am. J. Surg.* 187 (2004) 65S–70S. doi:10.1016/S0002-9610(03)00306-4.

[15] Winter, E. D., Epidermal regeneration studied in the domestic pig, *Epidermal Wound Heal.* 85 (1972). http://ci.nii.ac.jp/naid/20001383656/ (accessed December 5, 2017).

[16] F. L. Mi, S. S. Shyu, Y. B. Wu, S. T. Lee, J. Y. Shyong, R. N. Huang, Fabrication and characterization of a sponge-like asymmetric chitosan membrane as a wound dressing, *Biomaterials.* 22 (2001) 165–173. doi:10.1016/S0142-9612(00)00167-8.

[17] M. Segal, *Patches, Pumps, & amp; Timed Release; New Ways to Deliver Drugs.*, FDA Consum. U.S. Gov. Print. Off. (1991). https://www.google.co.in/search?q=Segal%2C+Marian.+%22Patches%2C+Pumps%2C+%26+Timed+Release%3B+New+Ways+to+Deliver+Drugs.%22+FDA+Consumer.+U.S.+Government+Printing+Office.+1991.&oq=Segal%2C+Marian.+%22Patches%2C+Pumps%2C+%26+Timed+Release%3B+New+Ways+to+D (accessed December 5, 2017).

[18] S. Srivastava, A. Biswas, S. Senapati, B. Ray, D. Rana, V.K. Aswal, P. Maiti, Novel shape memory behaviour in IPDI based polyurethanes: Influence of nanoparticle, *Polymer (Guildf).* 110 (2017) 95–104. doi:10.1016/J.Polymer.2016.12.080.

[19] A. Biswas, V.K. Aswal, P.U. Sastry, D. Rana, P. Maiti, Reversible Bidirectional Shape Memory Effect in Polyurethanes through Molecular Flipping, *Macromolecules.* 49 (2016). doi:10.1021/acs.macromol.6b00536.

[20] H. Meng, G. Li, A review of stimuli-responsive shape memory polymer composites, *Polymer (Guildf).* 54 (2013) 2199–2221. doi:10.1016/J.Polymer.2013.02.023.

[21] K. Kazunori, K. Glenn S., Y. Masayuki, O. Teruo, S. Yasuhisa, Block copolymer micelles as vehicles for drug delivery, *J. Control. Release.* 24 (1993) 119–132. doi:10.1016/0168-3659(93)90172-2.

[22] R.D. Price, V. Das-Gupta, I.M. Leigh, H.A. Navsaria, A Comparison of Tissue-Engineered Hyaluronic Acid Dermal Matrices in a Human Wound Model, *Tissue Eng.* 12 (2006) 2985–2995. doi:10.1089/ten.2006.12.2985.

[23] D. Chouhan, B. Chakraborty, S.K. Nandi, B.B. Mandal, Role of non-mulberry silk fibroin in deposition and regulation of extracellular matrix towards accelerated wound healing, *Acta Biomater.* 48 (2017) 157–174. doi:10.1016/J.ACTBIO.2016.10.019.

[24] R. Sridhar, R. Lakshminarayanan, K. Madhaiyan, V. Amutha Barathi, K.H.C. Lim, S. Ramakrishna, Electrosprayed nanoparticles and electrospun nanofibers based on natural materials: applications in tissue regeneration, drug delivery and pharmaceuticals, *Chem. Soc. Rev.* 44 (2015) 790–814. doi:10.1039/C4CS00226A.

[25] K.A. Hammer, C.F. Carson, T. V. Riley, Antimicrobial activity of essential oils and other plant extracts, *J. Appl. Microbiol.* 86 (1999) 985–990. https://s3.amazonaws.com/academia.edu.documents/45498629/Antimicrobial_activity_of_essential_oils20160509-28013-1gru8rh.pdf?AWSAccessKeyId=AKIAIWOWYYGZ2Y53UL3A&Expires=1512544771&Signature=yCAHjER2CMcvXcVAjwDyww58anA%3D&response-content-disposition=inline%3B filename%3DAntimicrobial_activity_of_essential_oils.pdf (accessed December 6, 2017).

[26] M.P. American Chemical Society., A.I. Hopia, H.J. Vuorela, J.P. Rauha, K. Pihlaja, T.S. Kujala, M. Heinonen, *Journal of agricultural and food chemistry.*, American Chemical Society, 1953. http://agris.fao.org/agris-search/search.do?recordID=US201302952411 (accessed December 6, 2017).

[27] M. Friedman, Antibiotic-Resistant Bacteria: Prevalence in Food and Inactivation by Food-Compatible Compounds and Plant Extracts, *J. Agric. Food Chem.* 63 (2015) 3805–3822. doi:10.1021/acs.jafc.5b00778.

[28] H.J. Dorman, S.G. Deans, Antimicrobial agents from plants: antibacterial activity of plant volatile oils., *J. Appl. Microbiol.* 88 (2000) 308–16. http://www.ncbi.nlm.nih.gov/pubmed/10736000 (accessed December 6, 2017).

[29] M.M. Cowan, Plant products as antimicrobial agents., *Clin. Microbiol. Rev.* 12 (1999) 564–82. http://www.ncbi.nlm.nih.gov/pubmed/10515903 (accessed December 6, 2017).

[30] G.D. Winter, Formation of the Scab and the Rate of Epithelization of Superficial Wounds in the Skin of the Young Domestic Pig, *Nature.* 193 (1962) 293–294. doi:10.1038/193293a0.

[31] C.D. Hinman, H. Maibach, Effect of Air Exposure and Occlusion on Experimental Human Skin Wounds, *Nature.* 200 (1963) 377–378. doi:10.1038/200377a0.

[32] M.D. Blanco, O. García, R.M. Trigo, J.M. Teijón, I. Katime, 5-Fluorouracil release from copolymeric hydrogels of itaconic acid monoester. I. Acrylamide-co-monomethyl itaconate., *Biomaterials.* 17 (1996) 1061–7. http://www.ncbi.nlm.nih.gov/pubmed/8718965 (accessed December 6, 2017).

[33] H. Shivakumar, C. Satish, K. Satish, Hydrogels as controlled drug delivery systems: Synthesis, crosslinking, water and drug transport mechanism, *Indian J. Pharm. Sci.* 68 (2006) 133. doi:10.4103/0250-474X.25706.

[34] S. Heydarkhan-Hagvall, K. Schenke-Layland, A.P. Dhanasopon, F. Rofail, H. Smith, B.M. Wu, R. Shemin, R.E. Beygui, W.R. MacLellan, Three-dimensional electrospun ECM-based hybrid scaffolds for cardiovascular tissue engineering, *Biomaterials.* 29 (2008) 2907–2914. doi:10.1016/J.BIOMATERIALS.2008.03.034.

[35] D. Han, P. I. Gouma, Electrospun bioscaffolds that mimic the topology of extracellular matrix, Nanomedicine Nanotechnology, *Biol. Med.* 2 (2006) 37–41. doi:10.1016/J.Nano.2006.01.002.

[36] I.K. Shim, S.Y. Lee, Y.J. Park, M.C. Lee, S.H. Lee, J.Y. Lee, S.J. Lee, Homogeneous chitosan-PLGA composite fibrous scaffolds for tissue regeneration, *J. Biomed. Mater. Res. Part A.* 84A (2008) 247–255. doi:10.1002/jbm.a.31464.

[37] J. J. Lee, H. S. Yu, S. J. Hong, I. Jeong, J. H. Jang, H. W. Kim, Nanofibrous membrane of collagen–polycaprolactone for cell growth and tissue regeneration, *J. Mater. Sci. Mater. Med.* 20 (2009) 1927–1935. doi:10.1007/s10856-009-3743-z.

[38] G. Verreck, I. Chun, J. Rosenblatt, J. Peeters, A. Van Dijck, J. Mensch, M. Noppe, M.E. Brewster, Incorporation of drugs in an amorphous state into electrospun nanofibers composed of a water-insoluble, nonbiodegradable polymer, *J. Control. Release.* 92 (2003) 349–360. doi:10.1016/S0168-3659(03)00342-0.

[39] Schultz G. S., *Molecular Regulation of Wound Healing In Acute, Chronic Wounds*, 2nd. Edition, WB Saunders Publisher, USA, 1999. https://www.google.co.in/search?q=G.S+Schultz.+Molecular+Regulation+of+Wound+Healing+In+Acute,+Chronic+Wounds.+Nursing+Management+WB+Saunders+Publisher,+USA.;+1999;+413-429&spell=1&sa=X&ved=0ahUKEwiGsLj5uvrXAhVHNo8KHcTyAjUQvwUIJSgA&biw=1366&bih=588 (accessed December 8, 2017).

[40] F.C. Brunicardi, S.I. Schwartz, *Schwartz's principles of surgery*, McGraw-Hill, Health Pub. Division, 2005. https://www.google.co.in/search?ei=kL8nWs-RDIrcvgTks73QCw&q=schwartz+principles+of+surgery+8th+edition+pdf&oq=schwartz%27s+principles+of+surgery+8th&gs_l=psy-ab.1.0.0i22i30k1l3.11868.19400.0.23635.4.4.0.0.0.0.331.998.0j1j2j1.4.0....0...1c.1.64.psy-ab..0.4.995...0j0i67k1.0.VKPi8sNwIk0 (accessed December 6, 2017).

[41] S. Kumar, D.J. Leaper, Classification and management of acute wounds, *Surg.* 26 (2008) 43–47. doi:10.1016/j.mpsur.2007.11.003.

[42] L.E. Glynn, *Tissue repair and regeneration*, Elsevier/North-Holland Biomedical Press, 1981.

[43] R.A.F. Clark, Wound Repair, in: *Mol. Cell. Biol.* Wound Repair, Springer US, Boston, MA, 1988: pp. 3–50. doi:10.1007/978-1-4899-0185-9_1.

[44] A. Martin, The use of antioxidants in healing., *Dermatol. Surg.* 22 (1996) 156–60. http://www.ncbi.nlm.nih.gov/pubmed/8608378 (accessed December 6, 2017).

[45] Anon, Wound prevalence and wound management, 2012-2020 | *advanced medical technologies*, 2013. (n.d.). https://blog.mediligence.com/2013/01/29/wound-prevalence-and-wound-management-2012-2020/ (accessed December 6, 2017).

[46] S.J. Leibovich, R. Ross, The role of the macrophage in wound repair. A study with hydrocortisone and antimacrophage serum., *Am. J. Pathol.* 78 (1975) 71–100. http://www.ncbi.nlm.nih.gov/pubmed/1109560 (accessed December 6, 2017).

[47] J. Li, J. Chen, R. Kirsner, Pathophysiology of acute wound healing, *Clin. Dermatol.* 25 (2007) 9–18. doi:10.1016/j.clindermatol.2006.09.007.

[48] D.G. Greenhalgh, The role of apoptosis in wound healing., *Int. J. Biochem. Cell Biol.* 30 (1998) 1019–30. http://www.ncbi.nlm.nih.gov/pubmed/9785465 (accessed December 8, 2017).

[49] N.S. Williams, C.J.K. (Christopher J.K.. Bulstrode, P.R. O'Connell, R.J.M. (Robert J.M. Love, H. Bailey, Bailey & amp; *Love's short practice of surgery.,* CRC Press, 2013.

[50] M.H. Hermans, wounds and ulcers: back to the old nomenclature., *Woundsa Compend. Clin. Res. Pract.* 22 (2010) 289–93. http://www.ncbi.nlm.nih.gov/pubmed/25901519 (accessed December 6, 2017).

[51] K. Carville, Which dressing should I use? It all depends on the "TIMEING."*Aust. Fam. Physician.* 35 (2006) 486–9. http://www.ncbi.nlm.nih.gov/pubmed/16820818 (accessed December 6, 2017).

[52] S. Klein, S. Schreml, J. Dolderer, S. Gehmert, A. Niederbichler, M. Landthaler, L. Prantl, Evidence-based topical management of chronic wounds according to the T.I.M.E. principle, *JDDG J. Der Dtsch. Dermatologischen Gesellschaft.* 11 (2013) 819–829. doi:10.1111/ddg.12138.

[53] A. Sood, M.S. Granick, N.L. Tomaselli, Wound Dressings and Comparative Effectiveness Data, *Adv. Wound Care.* 3 (2014) 511–529. doi:10.1089/wound. 2012.0401.

[54] W. Czaja, A. Krystynowicz, S. Bielecki, R.M. Brown, Microbial cellulose—the natural power to heal wounds, *Biomaterials.* 27 (2006) 145–151. doi:10.1016/ J.Biomaterials.2005.07.035.

[55] J.B. Shah, Correction of Hypoxia, a Critical Element for Wound Bed Preparation Guidelines: TIMEO2 Principle of Wound Bed Preparation, *J. Am. Col. Certif. Wound Spec.* 3 (2011) 26–32. doi:10.1016/j.jcws.2011.09.001.

[56] P. V. Radhika, A. Kumar, Herbal Hydrogel for Wound Healing: A Review, *Int J Pharma Res Heal. Sci.* 5 (2017) 1616–1622. doi:10.21276/ijprhs.2017.02.02.

[57] K. Inngjerdingen, C.S. Nergård, D. Diallo, P.P. Mounkoro, B.S. Paulsen, An ethnopharmacological survey of plants used for wound healing in Dogonland, Mali, West Africa, *J. Ethnopharmacol.* 92 (2004) 233–244. doi:10.1016/J.JEP.2004. 02.021.

[58] S. Sarabahi, Recent advances in topical wound care., *Indian J. Plast. Surg.* 45 (2012) 379–87. doi:10.4103/0970-0358.101321.

[59] S. Dhivya, V.V. Padma, E. Santhini, Wound dressings - a review., *BioMedicine.* 5 (2015) 22. doi:10.7603/s40681-015-0022-9.

[60] A.J. Wodash, Wet-to-Dry Dressings Do Not Provide Moist Wound Healing, *J. Am. Coll. Clin. Wound Spec.* 4 (2012) 63–66. doi:10.1016/J.JCCW.2013.08.001.

[61] B. Dorner, M.E. Posthauer, D. Thomas, The Role of Nutrition in Pressure Ulcer Prevention and Treatment, *Adv. Skin Wound Care.* 22 (2009) 212–221. doi:10.1097/01.ASW.0000350838.11854.0a.

[62] J.J. Elsner, A. Kraitzer, O. Grinberg, M. Zilberman, Highly porous drug-eluting structures, *Biomatter.* 2 (2012) 239–270. doi:10.4161/biom.22838.

[63] Thomas S., ed., Wounds and wound healing in: *Wound management and dressings.*, 1st ed., Pharmaceutical Press, London, 1990. https://www.google.co.in/search?q=Wounds+and+wound+healing+in%3A+Wound+management+and+dressings.+in%3A+Thomas+S.+(Ed.)+1st+edition.+Pharmaceutical+Press%2C+London%3B+1990%3A1–14.&oq=Wounds+and+wound+healing+in%3A+Wound+management+and+dressings.+in (accessed December 6, 2017).

[64] O. Catanzano, *Helping Wound Healing Process through Drug Delivery Sistems*, (2014). http://www.fedoa.unina.it/9976/ (accessed December 6, 2017).

[65] T.J. Ryan, International Foundation for Dermatology-Solving the Problems of Skin Disease in the Developing World, *Trop. Doct.* 22 (1992) 42–43. doi:10.1177/00494755920220S108.

[66] B. Kumar, M. Vijayakumar, R. Govindarajan, P. Pushpangadan, Ethnopharmacological approaches to wound healing—Exploring medicinal plants of India, *J. Ethnopharmacol.* 114 (2007) 103–113. doi:10.1016/J.JEP.2007.08.010.

[67] J.P. Heggers, A. Kucukcelebi, D. Listengarten, J. Stabenau, F. Ko, L.D. Broemeling, M.C. Robson, W.D. Winters, Beneficial Effect of *Aloe* on Wound Healing in an Excisional Wound Model, *J. Altern. Complement. Med.* 2 (1996) 271–277. doi:10.1089/acm.1996.2.271.

[68] R.H. Davis, M.G. Leitner, J.M. Russo, M.E. Byrne, Wound healing. Oral and topical activity of Aloe vera., *J. Am. Podiatr. Med. Assoc.* 79 (1989) 559–62. doi:10.7547/87507315-79-11-559.

[69] WAgle B.R. and Chetri D.K., Evaluation of wound healing properties of neem (Azadirachta indica) in dogs, *Int. J. Herb. Med.* 5 (2017) 5–7.

[70] E. V. Mikhalchik, A. V. Ivanova, M. V. Anurov, S.M. Titkova, L.Y. Penkov, Z.F. Kharaeva, L.G. Korkina, Wound-Healing Effect of Papaya-Based Preparation in Experimental Thermal Trauma, *Bull. Exp. Biol. Med.* 137 (2004) 560–562. doi:10.1023/B:BEBM.0000042711.31775.f7.

[71] K.S. Priya, G. Arumugam, B. Rathinam, A. Wells, M. Babu, Celosia argentea Linn. leaf extract improves wound healing in a rat burn wound model, *Wound Repair Regen.* 12 (2004) 618–625. doi:10.1111/j.1067-1927.2004.12603.x.

[72] B.S. Shetty, S.L. Udupa, A.L. Udupa, S.N. Somayaji, Effect of Centella asiatica L (Umbelliferae) on Normal and Dexamethasone-Suppressed Wound Healing in Wistar Albino Rats, *Int. J. Low. Extrem. Wounds.* 5 (2006) 137–143. doi:10.1177/1534734606291313.

[73] J. V. Kamath, A.C. Rana, A. Roy Chowdhury, Pro-healing effect ofCinnamomum zeylanicum bark, *Phyther. Res.* 17 (2003) 970–972. doi:10.1002/ptr.1293.

[74] K.S. Mehra, I. Mikuni, U. Gupta, K.D. Gode, Curcuma Longa (Linn) Drops in Corneal Wound Healing, *Tokai J. Exp. Clin. Med.* 9 (1984) 27–31. http://ci.nii.ac.jp/naid/110004691073/ (accessed December 7, 2017).

[75] B.P. Mukherjee, P.K., Mukherjee, K., Pal, M., Saha, Wound healing potential of Nelumbo nucifera (Nymphaea) rhizome extract, *Phytomedicine.* 7 (2000) 66. https://www.google.co.in/search?q=Wound+healing+potential+of+Nelumbo+nucifera+

(Nymphaea)+rhizome+extract&spell=1&sa=X&ved=0ahUKEwiJyZrrzPrXAhWJuo8KHSUuCMoQvwUIJSgA&biw=1366&bih=588 (accessed December 8, 2017).

[76] S.L. Udupa, S. Shetty, A.L. Udupa, S.N. Somayaji, Effect of Ocimum sanctum Linn. on normal and dexamethasone suppressed wound healing, *Indian J. Exp. Biol.* 44 (2006) 49–54. http://nopr.niscair.res.in/bitstream/123456789/6337/1/IJEB 44%281%29 49-54.pdf (accessed December 7, 2017).

[77] G. Suguna, L., Sumitra, M., Chandrakasan, Influence of Phyllanthus emblica extract on dermal wound healing in rats., *J. Med. Aromat. Plants.* 32 (2000) 2–3.

[78] D.R. Kodati, S. Burra, K. Goud, Evaluation of wound healing activity of methanolic root extract of Plumbago zeylanica L. in wistar albino rats, *Asian J. Plant Sci. Res.* 1 (2011) 26–34. https://www.researchgate.net/profile/Shashidher_Burra/publication/215868786_Evaluation_of_wound_healing_activity_of_methanolic_root_extract_of_Plumbago_zeylanica_L_in_wistar_albino_rats/links/0e62c44cb060689a55ff02cc.pdf (accessed December 8, 2017).

[79] T.K. Biswas, L.N. Maity, B. Mukherjee, Wound Healing Potential of Pterocarpus Santalinus Linn: A Pharmacological Evaluation, *Int. J. Low. Extrem. Wounds.* 3 (2004) 143–150. doi:10.1177/1534734604268385.

[80] M. Chaudhari, S. Mengi, Evaluation of phytoconstituents of Terminalia arjuna for wound healing activity in rats, *Phyther. Res.* 20 (2006) 799–805. doi:10.1002/ptr.1857.

[81] L. Suguna, S. Singh, P. Sivakumar, P. Sampath, G. Chandrakasan, Influence of Terminalia chebula on dermal wound healing in rats, *Phyther. Res.* 16 (2002) 227–231. doi:10.1002/ptr.827.

[82] M. Chaudhari, S. Mengi, Evaluation of phytoconstituents ofTerminalia arjuna for wound healing activity in rats, *Phyther. Res.* 20 (2006) 799–805. doi:10.1002/ptr.1857.

[83] Gustavo Moura-Letts, León F. Villegas, Ana Marçalo, and Abraham J. Vaisberg, Gerald B. Hammond, *In Vivo Wound-Healing Activity of Oleanolic Acid Derived from the Acid Hydrolysis of Anredera diffusa*, (2006). doi:10.1021/NP0601152.

[84] D. Trombetta, C. Puglia, D. Perri, A. Licata, S. Pergolizzi, E.R. Lauriano, A. De Pasquale, A. Saija, F.P. Bonina, Effect of polysaccharides from Opuntia ficus-indica (L.) cladodes on the healing of dermal wounds in the rat., *Phytomedicine.* 13 (2006) 352–8. doi:10.1016/j.phymed.2005.06.006.

[85] N. Öztürk, S. Korkmaz, Y. Öztürk, K. Başer, Effects of Gentiopicroside, Sweroside and Swertiamarine, Secoiridoids from Gentian (*Gentiana lutea* ssp. s *ymphyandra*), on Cultured Chicken Embryonic Fibroblasts, *Planta Med.* 72 (2006) 289–294. doi:10.1055/s-2005-916198.

[86] G.C. Jagetia, G.K. Rajanikant, Role of curcumin, a naturally occurring phenolic compound of turmeric in accelerating the repair of excision wound, in mice whole-body exposed to various doses of gamma-radiation., *J. Surg. Res.* 120 (2004) 127–38. doi:10.1016/j.jss.2003.12.003.

[87] E. Bråkenhielm, R. Cao, Y. Cao, Suppression of angiogenesis, tumor growth, and wound healing by resveratrol, a natural compound in red wine and grapes., *FASEB J.* 15 (2001) 1798–800. doi:10.1096/FJ.01-0028FJE.

[88] P.C. Stevenson, M.S.J. Simmonds, J. Sampson, P.J. Houghton, P. Grice, Wound healing activity of acylated iridoid glycosides fromScrophularia nodosa, *Phyther. Res.* 16 (2002) 33–35. doi:10.1002/ptr.798.

[89] S. W. Choi, B. W. Son, Y. S. Son, Y. I. Park, S. K. Lee, M. H. Chung, The wound-healing effect of a glycoprotein fraction isolated from aloe vera, *Br. J. Dermatol.* 145 (2001) 535–545. doi:10.1046/j.1365-2133.2001.04410.x.

[90] H.S. Datta, S.K. Mitra, B. Patwardhan, Wound Healing Activity of Topical Application Forms Based on Ayurveda, Evidence-Based Complement. *Altern. Med.* 2011 (2011) 1–10. doi:10.1093/ecam/nep015.

[91] K. Singh, A.S. Jaggi, N. Singh, Exploring the ameliorative potential of *Punica granatum* in dextran sulfate sodium induced ulcerative colitis in mice, *Phyther. Res.* 23 (2009) 1565–1574. doi:10.1002/ptr.2822.

[92] G. Kaur, Z. Jabbar, M. Athar, M.S. Alam, Punica granatum (pomegranate) flower extract possesses potent antioxidant activity and abrogates Fe-NTA induced hepatotoxicity in mice., *Food Chem. Toxicol.* 44 (2006) 984–93. doi:10.1016/j.fct.2005.12.001.

[93] A. Fleck, P. Cabral, F. Vieira, D. Pinheiro, C. Pereira, W. Santos, T. Machado, Punica granatum L. Hydrogel for Wound Care Treatment: From Case Study to Phytomedicine Standardization, *Molecules.* 21 (2016) 1059. doi:10.3390/molecules21081059.

[94] H. Salehi, M. Mehrasa, B. Nasri-Nasrabadi, M. Doostmohammadi, R. Seyedebrahimi, N. Davari, M. Rafienia, M.E. Hosseinabadi, M. Agheb, M. Siavash, Effects of nanozeolite/starch thermoplastic hydrogels on wound healing., *J. Res. Med. Sci.* 22 (2017) 110. doi:10.4103/jrms.JRMS_1037_16.

[95] S. Yasasvini, R. Anusa, B. VedhaHari, P. Prabhu, D. RamyaDevi, Topical hydrogel matrix loaded with Simvastatin microparticles for enhanced wound healing activity, *Mater. Sci. Eng. C.* 72 (2017) 160–167. doi:10.1016/j.msec.2016.11.038.

[96] L. Sasikala, B. Durai, R. Rathinamoorthy, Manuka Honey Loaded Chitosan Hydrogel Films for Wound Dressing Applications, *Int. J. PharmTech Res.* 5 (n.d.) 1774–1785. http://www.sphinxsai.com/2013/OD/PharmOD13/pdfphamOD2013/PT=41(1774-1785)OD13.pdf (accessed December 8, 2017).

[97] K. Rastogi, B. M. N. Delhi,undefined India,undefined 1990, *Compendium of Indian medicinal plants*, Indianmedicine.eldoc.ub.rug.nl. (n.d.). http://indianmedicine.eldoc.ub. rug.nl/root/R/96365/ (accessed December 8, 2017).

[98] V. Ravichandiran, S. Manivannan, *International journal of pharmacy and pharmaceutical sciences.*, *IJPPS*, 2015. https://innovareacademics.in/journals/index.php/ijpps/article/view/3524 (accessed December 8, 2017).

[99] K. Vimala, M.M. Yallapu, K. Varaprasad, N.N. Reddy, S. Ravindra, N.S. Naidu, K.M. Raju, Fabrication of Curcumin Encapsulated Chitosan-PVA Silver Nanocomposite

Films for Improved Antimicrobial Activity, *J. Biomater. Nanobiotechnol.* 2 (2011) 55–64. doi:10.4236/jbnb.2011.21008.

[100] K. Kataria, A. Gupta, G. Rath, R.B. Mathur, S.R. Dhakate, In vivo wound healing performance of drug loaded electrospun composite nanofibers transdermal patch, *Int. J. Pharm.* 469 (2014) 102–110. doi:10.1016/j.ijpharm.2014.04.047.

[101] Z. Karami, I. Rezaeian, P. Zahedi, M. Abdollahi, Preparation and performance evaluations of electrospun poly(ε-caprolactone), poly(lactic acid), and their hybrid (50/50) nanofibrous mats containing thymol as an herbal drug for effective wound healing, *J. Appl. Polym. Sc*i. 129 (2013) 756–766. doi:10.1002/app.38683.

[102] P. Sikareepaisan, A. Suksamrarn, P. Supaphol, Electrospun gelatin fiber mats containing a herbal— *Centella asiatica* —extract and release characteristic of asiaticoside, *Nanotechnology.* 19 (2008) 15102. doi:10.1088/0957-4484/19/01/015102.

[103] Y. Lian, J. C. Zhan, K. H. Zhang, X. M. Mo, Fabrication and characterization of curcumin-loaded silk fibroin/P(LLA-CL) nanofibrous scaffold, *Front. Mater. Sci.* 8 (2014) 354–362. doi:10.1007/s11706-014-0270-8.

[104] M. Ranjbar-Mohammadi, S. Rabbani, S.H. Bahrami, M.T. Joghataei, F. Moayer, Antibacterial performance and in vivo diabetic wound healing of curcumin loaded gum tragacanth/poly(ε-caprolactone) electrospun nanofibers, *Mater. Sci. Eng. C.* 69 (2016) 1183–1191. doi:10.1016/j.msec.2016.08.032.

[105] N. Charernsriwilaiwat, T. Rojanarata, T. Ngawhirunpat, M. Sukma, P. Opanasopit, Electrospun chitosan-based nanofiber mats loaded with Garcinia mangostana extracts, *Int. J. Pharm.* 452 (2013) 333–343. doi:10.1016/j.ijpharm.2013.05.012.

[106] A.R. Unnithan, P.B.T. Pichiah, G. Gnanasekaran, K. Seenivasan, N.A. M. Barakat, Y. S. Cha, C. H. Jung, A. Shanmugam, H.Y. Kim, Emu oil-based electrospun nanofibrous scaffolds for wound skin tissue engineering, *Colloids Surfaces A Physicochem. Eng. Asp*. 415 (2012) 454–460. doi:10.1016/J.COLSURFA.2012.09.029.

[107] J. Han, T. X. Chen, C.J. Branford-White, L. M. Zhu, Electrospun shikonin-loaded PCL/PTMC composite fiber mats with potential biomedical applications, *Int. J. Pharm.* 382 (2009) 215–221. doi:10.1016/j.ijpharm.2009.07.027.

[108] X. Y. Dai, W. Nie, Y. C. Wang, Y. Shen, Y. Li, S. J. Gan, Electrospun emodin polyvinylpyrrolidone blended nanofibrous membrane: a novel medicated biomaterial for drug delivery and accelerated wound healing, *J. Mater. Sci. Mater. Med.* 23 (2012) 2709–2716. doi:10.1007/s10856-012-4728-x.

[109] S. Suganya, T. Senthil Ram, B.S. Lakshmi, V.R. Giridev, Herbal drug incorporated antibacterial nanofibrous mat fabricated by electrospinning: An excellent matrix for wound dressings, *J. Appl. Polym. Sci.* 121 (2011) 2893–2899. doi:10.1002/app.33915.

[110] A. Gasiorowski,N.A. Hurst, R.K. DeLong, The effects of nanoparticles on the structure and function of proteins luciferase and galactosidase, *J. Nanomed. Nanotechnol.* 7 (2016). doi:10.4172/2157-7439.C1.032.

[111] E. Mirzaei, S. Sarkar, S.M. Rezayat, R. Faridi-Majidi, Herbal Extract Loaded Chitosan-Based Nanofibers as a Potential Wound-Dressing, *J. Adv. Med. Sci. Appl. Technol.* 2 (2016) 141. doi:10.18869/nrip.jamsat.2.1.141.

[112] S. Agnes Mary, V.R. Giri Dev, Electrospun herbal nanofibrous wound dressings for skin tissue engineering, *J. Text. Inst.* 106 (2015) 886–895. doi:10.1080/00405000.2014.951247.

[113] K.P. Chellamani, R.S. Vignesh Balaji, D. Veerasubramanian, J. Sudharsan, Wound Healing Ability of Herbal Drug Incorporated PCL (Poly(ε-caprolactone)) Wound Dressing, *J. Acad. Ind. Res.* 2 (2014). http://www.jairjp.com/APRIL 2014/06 CHELLAMANI -01.pdf (accessed February 11, 2018).

[114] L. Thomas, S. Mathew, *Development of Glycosaminoglycan Scaffold Integrated with Herbal Nanoparticle for Wound Healing*, (n.d.). https://ijapsa.com/published-papers/volume-2/issue-6/development-of-glycosaminoglycan-scaffold-integrated-with-herbal-nanoparticle-for-wound-healing.pdf (accessed December 8, 2017).

[115] V.V.S.R. Karri, G. Kuppusamy, S.V. Talluri, S.S. Mannemala, R. Kollipara, A.D. Wadhwani, S. Mulukutla, K.R.S. Raju, R. Malayandi, Curcumin loaded chitosan nanoparticles impregnated into collagen-alginate scaffolds for diabetic wound healing, *Int. J. Biol. Macromol*. 93 (2016) 1519–1529. doi:10.1016/j.ijbiomac.2016.05.038.

[116] V.C. Nguyen, V. B. Nguyen, M. F. Hsieh, Curcumin-Loaded Chitosan/Gelatin Composite Sponge for Wound Healing Application, *Int. J. Polym. Sci*. 2013 (2013) 1–7. doi:10.1155/2013/106570.

In: Advances in Polymers for Biomedical Applications ISBN: 978-1-53613-612-8
Editors: Deepak Pathania and Bhuvanesh Gupta 

*Chapter 11*

# STIMULI-RESPONSIVE HYDROGELS THROUGH GAMMA RADIATION INDUCED GRAFT COPOLYMERIZATION OF HYDROPHILIC MONOMERS ONTO POLYMERIC FILMS: FOR BIOMEDICAL APPLICATIONS

***Teena Sehgal[1] and Sunita Rattan[2]***
[1]HMR Institute of Technology and Management, Hamidpur, Delhi (Affiliated to Guru Gobind Singh Indraprastha University, Dwarka, New Delhi)
[2]Amity Institute of Applied Sciences, Amity University Uttar Pradesh, Noida, India

## ABSTRACT

Many kinds of stimuli-responsive hydrogels that respond to the change in their surroundings such as solvent composition, temperature, pH, and supply of electric field have been developed in the past decades. Gamma radiation induced graft copolymerization of hydrophilic monomers onto polymeric films has been shown particularly useful for the functionalization of surfaces with stimuli-responsive properties. This method involves the formation of active sites (free radicals) onto the polymeric backbone as a result of the exposition to high-energy radiation, in which a proper microenvironment for the reaction among monomer and/or polymer and the active sites takes place, thus leading to propagation which forms side chain grafts. The modification of polymers using high-energy irradiation may be performed by the following methods: direct or simultaneous, pre-irradiation oxidative and pre-irradiation. The most frequent ones correspond to the pre-irradiation oxidative method and the direct one. Radiation-grafting has many advantages over conventional methods considering that it does not require catalyst nor additives to initiate the reaction, and in general, no changes on the mechanical properties with respect to the pristine polymeric matrix are observed. This review focuses on the synthesis of stimuli responsive smart hydrogels by the use of gamma radiation induced grafting. In addition, diverse applications of these materials in the biomedical field are also discussed.

# 1. INTRODUCTION

## 1.1. Hydrogels

Hydrogels by definitions are three-dimensional, cross-linked, hydrophilic, polymeric swollen network structures which swell in water or biological fluids [1-12]. The original polymeric hydrogel network was developed by Wichterle and Lim in Czechoslovakia in 1954 [13] The networks are composed of homopolymers or copolymers, and are insoluble due to the presence of chemical crosslinks (tie-points, junctions), or physical crosslinks, such as entanglements or crystallites [14-19]. The latter provide the network structure and physical integrity as shown in Figure 1.These hydrogels exhibit a thermodynamic compatibility with water which allows them to swell in aqueous media [1, 2, 20-22] and shrinks in its absence [23].

The crosslinks are usually formed by covalent or ionic bonds, although physical crosslinks, such as entanglements, hydrogen bonds, hydrophobic or van der Waals interactions can also provide three-dimensional networks [24, 25]. They swell considerably in an aqueous medium [3, 4] and demonstrate extraordinary capacity (> 20%) for imbibing water into the network structure and retain the volume of the adsorbed aqueous medium in their three-dimensional swollen networks as shown in Figure 2. Such aqueous gel networks are known as hydrogels or aquagels [26]. Their ability to absorb water is due to the presence of hydrophilic groups such as –OH, -COOH, CONH, -$CONH_2$, –$SO_3H$ and other that can be found within the polymer backbone or as lateral chains without undergoing dissolution. This ability to swell, under physiological & biological conditions, makes hydrogels an ideal material for biomedical applications [27]. In general, hydrogels swell to an equilibrium value of 10-98% at physiologic temperature, pH and ionic strength [28]. A dried hydrogel imbibing at least 20 times its own weight of the aqueous media while retaining its original shape could be referred to as superabsorbent. The capacity of hydrogels to absorb in the aqueous media, however, could be enormous and can be as much as 1000 times the weight of the polymer [29, 30]. Figure 2 depicts a hydrogels network upon placement in water [31]. The overall shape of the hydrogels is preserved during the swelling and shrinking process [32].

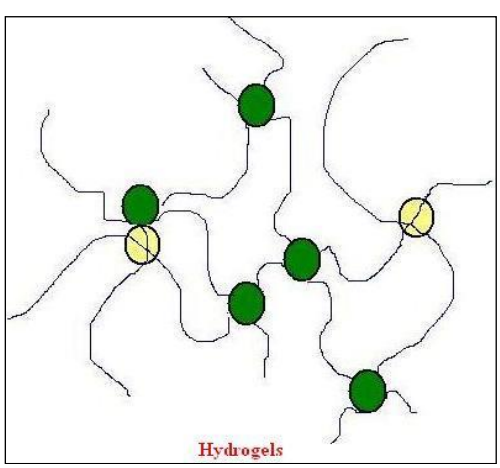


Figure 1. Illustrates the hydrogel network [17].

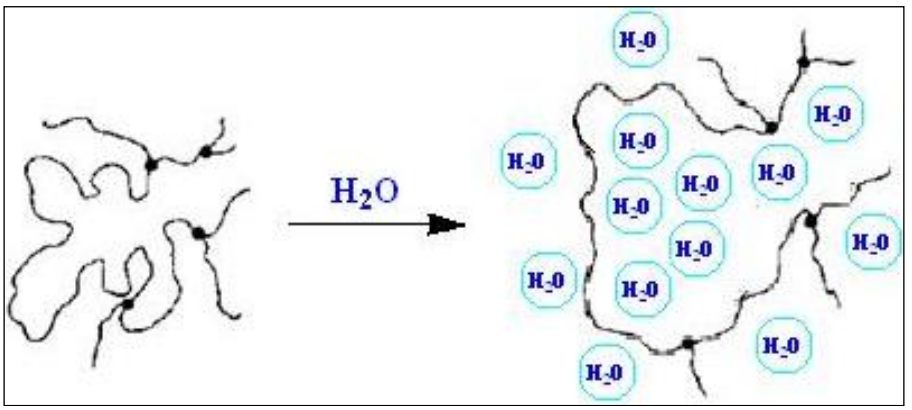


Figure 2. A Schematic representation of a single chain in a hydrogels network upon placement in water.

According to the definition formulated above, hydrogels must be able to hold, in equilibrium, certain amounts of water. This implies that the polymers used in these materials must have at least moderate hydrophilic character. In practice, to achieve high degrees of swelling, it is common to use synthetic polymers that are water-soluble when in non-crosslinked form.

The water holding capacities are the most important characteristic features of a hydrogels. The properties of a specific hydrogels are extremely important in selecting which materials are suitable for a given varied application [33, 34]. However some properties are highly dependent on the environmental conditions.

## 2. CLASSIFICATIONS OF HYDROGELS

Polymeric hydrogels are classified in accordance to their physical and chemical composition, based on the presence of ionic charges on the monomer, based on their physical nature and based on response to the environmental factors (stimuli responsive hydrogels) discussed as below.

### 2.1. Based on Physical and Chemical Composition

The classification of hydrogels depends on their physical structure and chemical composition. Polymeric hydrogels are classified in accordance to their monomeric composition giving some important class of hydrogels which are discussed as below.

#### *2.1.1. Homopolymeric Hydrogels*

Homopolymers are formally referred to as a polymer network derived from a single species of the monomer, which is the basic structural unit comprising of any polymer network [35-37]. Homopolymers could have crosslinked or uncrosslinked skeletal structure depending on the nature of the monomer and polymerization technique.

Homopolymers, which are generally crosslinked, find important applications such as slow drug delivery devices and contact lenses. An important category of crosslinkedhomopolymeric hydrogels of poly(hydroxyalkylmethacrylates) include poly(3-hydroxypropyl methacrylate (PHPMA), poly(glyceryl methacrylate), (PGMA) and poly(2-hydroxyethyl methacrylate) (PHEMA) [38,39]. PHEMA hydrogels is among the most widely studied and used of all synthetic hydrogel materials [40, 41-45].

There are some uncrosslinkedhomopolymers, which have been of interest to a number of researchers [46-47]. Poly(N-vinyl-2-pyrrolidinone) (PNVP), poly(acrylamide) (PAM), poly(ethylene glycol) (PEG) and poly(vinyl alcohol) (PVA) are classed as uncrosslinked water-soluble homopolymers.

### *2.1.2. Copolymeric Hydrogels*

Copolymeric hydrogels networks are comprised of two or more different monomer species with at least one hydrophilic component, arranged in a random, block or alternating configuration along the chain of the polymer network [35-37]. The copolymeric hydrogels network are generally covalently or ionicallycrosslinked structures, which are not water - soluble [48-49].

A wide range of important copolymeric hydrogels with vast combinations of compatible monomers, some of which include poly(NVP-co-HEMA), poly(HEMA-co-MMA) and poly(HEMA-co-AA) have been studied by a number of researchers [50-51]. Copolymers designed to function as hydrogels are confined to the combination of compatible monomers, which will give the hydrogels the desirable properties for their intended potential applications.

### *2.1.3. Interpenetrating Polymer Network (IPN) Hydrogels*

IPN, an important class of hydrogels materials, are defined as two independent crosslinked synthetic and/or natural polymer components contained in a network form as shown in Figures 3 and 4 [52]. A semi-IPN is an IPN where one of the components is a crosslinked polymer while the other component is a non-crosslinked polymer [53-54].

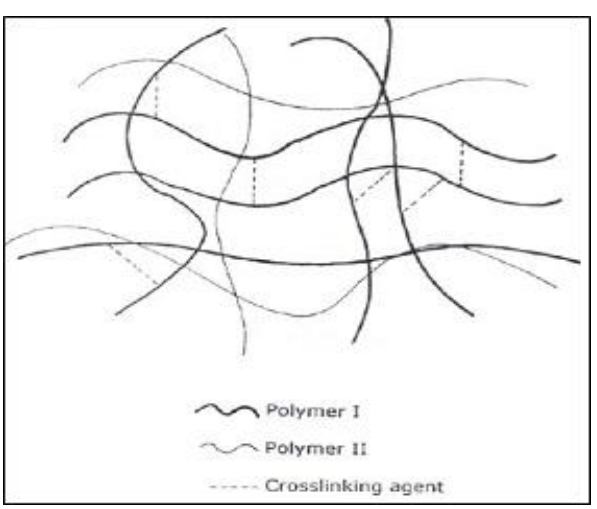


Figure 3. Structure of IPN.

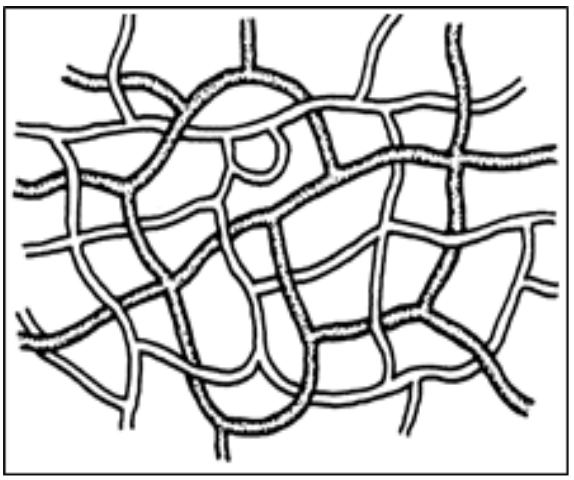

Figure 4. Interpenetrating polymer network.

The two basic synthetic routes to form IPNs are sequential and simultaneous polymerization methods [55]. The formation of an IPN increases the compatibility of the polymer components thus preventing phase separation and allows access to properties that may be hybrids of those of the component macromolecules [56]. Some researchers have described the IPN formation between a pH sensitive hydrogels and temperature sensitive second polymer as an example of such behaviour. The IPN formed will be both, pH and temperature sensitive. Since there is no chemical bonding between the two polymeric components, each component may retain its own property while the proportion of each network can be varied independently thus obtaining the desired combinations of the properties of the two macromolecule components [57].

## 2.2. Based on the Presence of Ionic Charges on the Monomer

The chemical constituent of monomers used in the preparation of hydrogels plays an important role in classifying the hydrogels. The hydrogels are classified as non ionic hydrogels and ionic hydrogels.

### *2.2.1. Non-Ionic Hydrogels*

Non-ionic hydrogels, often referred to as neutral hydrogels, are homopolymeric or copolymeric networks, which do not bear any charged groups in their structure. Neutral hydrogels may be prepared by various polymerization techniques or by conversion of existing polymers. Although generalizations can be made about hydrogels, the wide range of chemical compositions of the monomers used, give them different properties with regards to biocompatibility, physical and chemical properties of the resultant polymer [58].

Neutral hydrogels swell to equilibrium when the osmotic pressure of the solvent is balanced with the sub-chain stretching energy. The collapse and swelling of neutral hydrogels network occur normally as a result of change in the environmental temperature [59]. Some neutral monomers commonly utilized to form hydrogels are shown in Figures 5–8 [58].

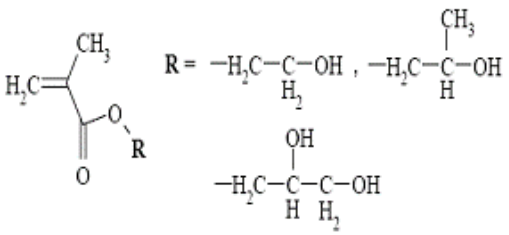

Figure 5. Hydroxyalkyl methacrylates.

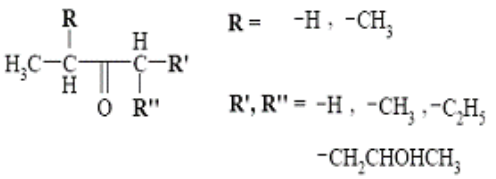

Figure 6. Acrylamide derivatives.

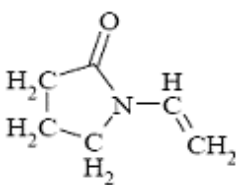

Figure 7. N-vinylprrolidinone.

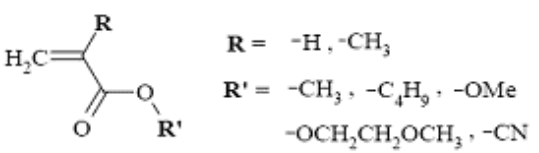

Figure 8. Hydrophobic acrylics.

### *2.2.2. Ionic Hydrogels*

Ionic hydrogels also known as polyelectrolytes are prepared from monomers accompanying ionic charges. The charges could be positive or negative thus classing the hydrogels as cationic or anionic hydrogel respectively and furthermore, a combination of both positive and negative charges gives an ampholytic macromolecule [60, 61]. Inclusion of charged species in the polymer backbone enhances the stimuli responsive properties, which could be controlled, depending on the nature of the pendent group thus widening its scope of bioapplications as hydrogels [58].

#### 2.2.2.1. Anionic Hydrogels

Anionic hydrogels network are usually referred to as either homopolymers of negatively charged acidic or anionic monomers or copolymers of an anionic monomer and a neutral monomer. However, anionic hydrogels could also be prepared through modification of

existing polymeric non-ionic hydrogels such as by the partial hydrolysis of poly(hydroxy alkyl methacrylates) or by the addition of excess polyanions in the case of polyelectrolyte complexes to form anionic hydrogels [58]. Anionic monomers commonly utilized to form anionic hydrogels are shown in Figures 9 [58]. Anionic hydrogels are known to exhibit a marked increase in the swelling ratio with increase in the environmental pH [62].

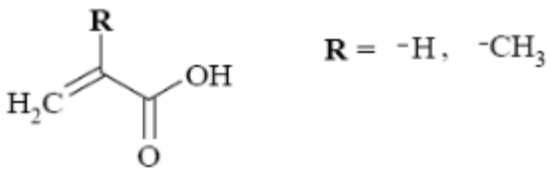


Figure 9. Acrylic acid derivatives.

#### 2.2.2.2. Cationic Hydrogels

Homopolymers of positively charged basic or cationic monomers or copolymers of cationic and neutral monomers are commonly referred to as cationic hydrogels network. Cationic monomers commonly utilized to prepare cationic-based hydrogels network are shown in Figures 10 [60]. Cationic polymeric networks could also be derived through modifications such as partial hydrolysis of the existing non-ionic pre-formed polymer networks. It is also possible to synthesize cationic hydrogels through polyelectrolyte complexation reactions by addition of excess polycations [60].

Cationic pendant groups in polymer network in the contrary behaviour to anionic pendant give rise to hydrogels, which remain collapsed in the basic environment and swollen in the acidic environment due to the electrostatic repulsion between the positively charged groups [63].

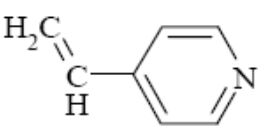


Figure 10. 4-vinylpyridine.

## 3. POLYAMPHOLYTIC HYDROGELS

Polyampholytic hydrogels networks are referred to as macromolecules capable of possessing both positively and negatively charged moieties in the polymer network [64]. The presence of ionic species along the polymer chain has a distinct effect on the solution and solid-state properties of the polyampholytes [65]. The columbic attractions between the oppositely charged sides afford inter and intramolecular ionic interactions that are stronger than Van der Waals forces, yet weaker than covalent bonds as shown in Figure 11 [65].

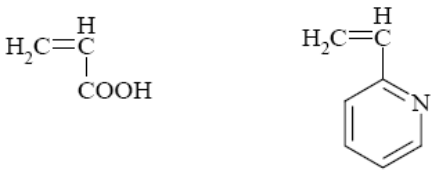


(a) (b)

Figure 11. (a) Acrylic acid(b) 2-vinylpyridine.

## 3.1. Based on Their Physical Nature

The Hydrogels are also classified as amorphous or semi-crystalline materials, bonded structures, supermolecular structures, hydrocolloidal aggregates.

### *3.1.1. Hydrogels Network Structures*

Polymeric hydrogels network structure may have several roles explained by Flory (1953) [65]. In an aqueous medium, the network may dissociate and take the role of the solute as in the case of some water-soluble hydrogels network or swell to equilibrium by imbibing the medium in its structure. As the network expands in an aqueous medium (Figure 2) [66], a force resisting the expansion occurs due to the elongation of the chain into a lesser entropically desirable conformation. The physical and other properties of the hydrogels depend on the structures of the polymeric networks [67]. To maintain the three-dimensional structures, polymer chains of hydrogels are usually crosslinked chemically or physically. In chemically crosslinked hydrogels, polymer chains are connected by covalent bonds and thus it is difficult to change the shape of such networks. Polymer chains of physical gels are connected through non-covalent bonds, such as van der Waals interactions, ionic interactions, hydrogen bonding, or hydrophobic interactions [68]. Physical and ionotropic forms represent secondary valence networks while the covalent form indicates primary valence networks as shown in Figure 12 [69].

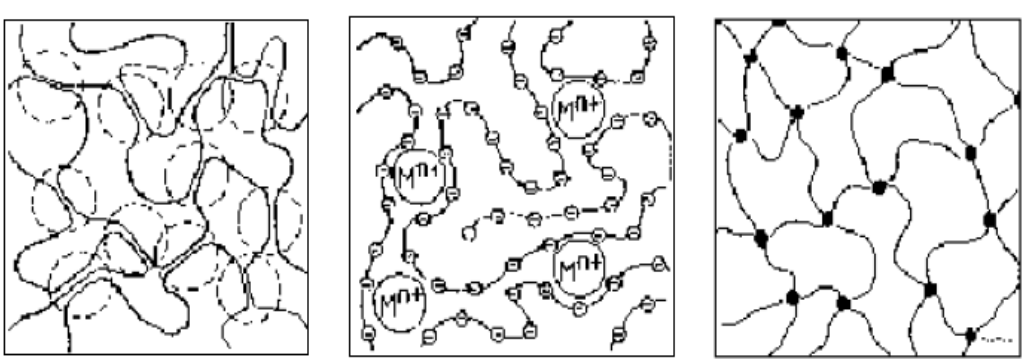


Figure 12. Schematic representation of hydrogels structure.

The extent of crosslinking in the hydrogels network is referred to as crosslinking density. Increased crosslinking density will increase the resistive force to chain elongation consequently reducing the degree of equilibrium swelling in contrast to hydrogels with low crosslinking density [70].

The polymeric hydrogels network can be classified as hydrogen bonded, amorphous, or semi-crystalline based on the structural analysis of the polymer network using a number of physiochemical techniques such as small angle X-ray scattering (SAXS), wide angle X-ray Scattering (WAXS), electron microscopy, differential scanning calorimetry (DSC), along with electron and neutron diffraction [71].

#### *3.1.2. Amorphous Hydrogels Structures*

The term 'amorphous' also known as non-crystalline is usually attributed to optically transparent isotropic polymeric networks that contain randomly arranged macromolecular chains as suggested by Flory [65]. The amorphous hydrogels network often contains localized ordered structures or non-homogeneous structures that are not suggested by the common Flory definition of amorphous polymers. Thus the most acceptable definition of such networks is a collection of Gaussian chains between crosslinks [72].

#### *3.1.3. Semicrystalline Hydrogels Structures*

Semicrystalline hydrogels network are complex mixtures of amorphous and crystalline phases, which contain dense regions of ordered macromolecular chains (crystallites) [73]. The lack of mechanical strength in some conventional crosslinked hydrogels network structures for certain biomedical applications has led the development of anisotropic semicrystalline polymeric networks which are characterized by the presence of strong covalent bonds along the polymer chain [73].

#### *3.1.4. Hydrogen Bonded Hydrogels Structures*

Hydrogen bonding is referred to as an electrostatic interaction between electronegative atoms such as oxygen, nitrogen, fluorine, chlorine and hydrogen atoms that are covalently bound to similar electronegative atoms [74]. The strength of the hydrogen bonding (< 10 Kcal/mol), however, is far weaker than covalent bonding (> 100 Kcal/mol) but still stronger than the van der Walls interactions (~ 1 Kcal/mol) [74].

The formation of multiple hydrogen bonds between two water-soluble macromolecules may result in strong intermolecular structures [25], which are physically crosslinked three-dimensional polymeric networks such as IPNs and semi-IPNs. The driving force behind the formation of the multiple simultaneous hydrogen bonds between the macromolecules is the co-operative interaction between the macromolecules, which is restricted to the chain length of the macromolecule [75].

### 3.2. Based on Response to the Environmental Factors

The past few years have witnessed enormous advances in developing and investigating a unique class of hydrogels. This is called "*intelligent,*" "*smart hydrogels" or stimuli-responsive hydrogels."* Stimuli-responsive hydrogels can exhibit unusual changes in their

swelling behavior, network structure and/or mechanical properties in response to different stimuli such as temperature, pH, light, pressure, ionic strength, solvents, electric field, magnetic field, chemical and biochemical compounds (e.g., glucose and others) [76-83]. These hydrogels can swell or deswell in response to these parameters.

These are functional polymers, which can react, adjust or modulate their physicochemical character, i.e., in most cases their water-solubility and can undergo abrupt volume change in response to small changes in external stimulus environmental parameters. In general, the changes occur to the smart hydrogels in response to any one of the stimuli and disappear upon removal of the stimulus. Consequently, the hydrogels return to their original state in a reversible manner.

Among the various stimulus responsive polymers, the most commonly used ones are temperature- and pH-responsive polymers, since the temperature and pH are relatively easy to change. Polymer–polymer and polymer–solvent interactions show an abrupt readjustment in small ranges of pH or temperature. These two kinds of stimulus responsive polymers will be discussed in detail in the following sections.

### *3.2.1. pH-Sensitive Polymer*

pH-responsive stimuli hydrogels are mainly based on polymers with ionic pendent groups distributed along their backbones such as poly (acrylic acid) (PAA), poly(methacrylic acid) (PMAA) and poly (diethyl-aminoethyl methacrylate) (PDEAEMA)[84].

These pendent ionic groups are responsible for the pH-sensitivity of the hydrogels. At certain pH values, the pendent groups ionize and generate fixed charges on the polymer network that results in developing electrostatic repulsive forces. These repulsive forces are responsible for the pH-dependent swelling/deswelling of the hydrogels as shown in Figure 13 [85-86].

In the case of the hydrogels based on cationic polymers, the pendent groups of the cationic hydrogels are ionized at lower pH and non-ionized at neutral and high pH values. In a contrary situation, the pendent gropus of anionic hydrogels are non-ionized at lower pH and ionized at pHs above the pKa of the polymeric network respectively as shown in Figure 14 [87].

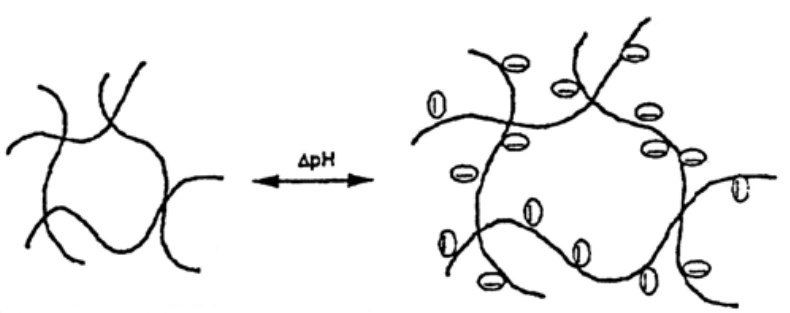


Figure 13. Swelling of an ionic hydrogels network due to ionization of pendent groups at specific pH values.

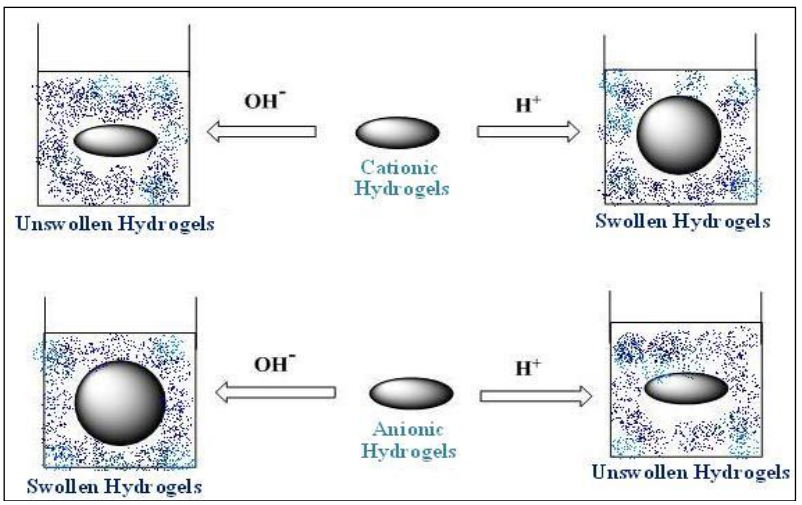


Figure 14. Schematic representation of pH-dependent swelling of a stimuli-responsive hydrogels.

### *3.2.2. Temperature-Sensitive Polymer*

Temperature-sensitive hydrogels, like pH responsive systems, are probably the most commonly studied class of environmentally sensitive polymer systems in biomedical filed [88]. Most polymers increase their water-solubility as the temperature increases. Polymers with Lower critical solution temperature (LCST), however, decrease their water-solubility as the temperature increases. Hydrogels made of LCST polymer shrink as the temperature increases above the LCST. This type of swelling behavior is known as inverse (or negative) temperature-dependence. The inverse temperature-dependent hydrogels are made of polymer chain that either possess moderately hydrophobic groups (if too hydrophobic, the polymer chains would not dissolve in water at all) or contain mixture of hydrophilic and hydrophobic segments.

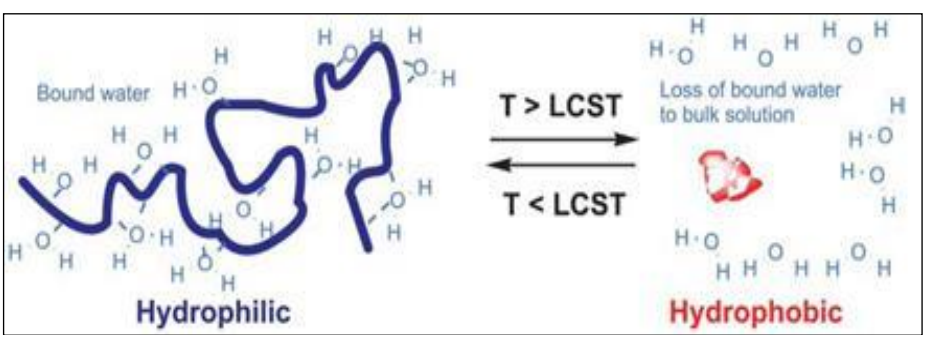


Figure 15. Schematic representation of temperature dependent swelling of a stimuli-responsive hydrogels.

At lower temperature, hydrogen bonding between hydrophilic segments of the polymer chain and water molecules are dominates, leading to enhanced dissolution in water. As the temperature increases, however, hydrophobic interactions among hydrophobic segments become strengthened, while hydrogen bonding becomes weaker. The net result is shrinking of

the hydrogels due to inter-polymer chain association through hydrophobic interactions. In general, as the polymer chain contains more hydrophobic constituents, LCST becomes lower [89]. The LCST can be changed by adjusting the ratio of hydrophilic and hydrophobic segments of the polymer as shown in Figure 15 [90].

Many polymers composed of both hydrophobic and hydrophilic residues are characterized by LCST. Example of these polymers include poly (N-alkylacrylamide), poly (ethylene oxide) - poly(propylene oxide) (PEO-PPO) block copolymers, pyrrolidone containing polymers, and cellulose ethers [91]. These polymers dissolve in aqueous media at about room temperature, and precipitate from solution at certain higher temperatures.

The applications of these two types of stimuli-responsive hydrogels are now attracting the interest of a large number of researchers [92]. Most of the applications are directed towards the stimuli-responsive diffusion studies, controlled drug delivery, cell encapsulation and tissue engineering [93-96]. The main reason for the interest in using smart hydrogels in the controlled drug delivery is that, a good drug delivery system should respond to the physiological requirements, sense the changes and accordingly amend the drug delivery pattern. Stimuli-responsive polymers play an important role in the development of novel smart hydrogels [97].

## 4. APPLICATIONS OF HYDROGELS

Hydrogels are found to meet the requirements for a variety of applications in the present time and many more are being developed for the future. Polymeric hydrogels, owing to their dynamic structural properties have been commonly utilized in numerous biomedical and agricultural applications. One may fashion tailorable "smart" functional materials from stimuli responsive polymers. These find applications in controlled drug delivery, sustained drug delivery systems [98], industrial paints and coatings, sensors and actuators, viscosity modifiers, microfluidic devices, colloid stabilization, surface modification [99] and water remediation [100]. Hydrogels show good compatibility with blood and other body fluids, thus are used as materials for contact lenses, burn wound dressings and membranes surfaces.

Hydrogels have varied applications in fields such as food additives [101], pharmaceuticals [102] as well as biomedicine. From their research, and discovery of the hydrophilic and biocompatible properties of hydrogels, there emerged a new class of hydrogel technologies based on biomaterial application as shown in Figure 16.

### 4.1. Biomedical Applications of Hydrogels

During the past decades, hydrogels have played a very essential role in biomedical applications and used in the wide range of drugs, peptides, and protein delivery applications and the diffusion-controlled systems. Biomedical and biological applications of hydrogels are one of the applications that have been receiving an increasing attention [103]. Recent enhancements in the field of polymer science and technology have led to the development of various stimuli sensitive hydrogels. Fixing (trapping) biological components into hydrophilic polymer matrics such as hydrogels (polymeric materials capable of swelling in water) and

affinity membranes prepared by radiation-induced graft polymerization provides preferable biocompatible materials. Hydrogels membranes prepared by grafting of monomers such as N-vinyl-2-pyrrolidone onto PE, PP, PTEF and FEP were found to have potential for biomedical applications [104]. These properties allow for usage in a number of applications, such as separation membranes, biosensors, artificial muscles, and drug delivery devices.

### *4.1.1. Hydrogels Useful in Drug Delivery*

Hydrogels possess several properties that make them an ideal material for drug delivery. First, hydrogels can be tailored to respond to a number of stimuli [105]. This enables sustained drug delivery corresponding to external stimuli such as pH or temperature. These pH sensitive hydrogels are useful in oral drug delivery as they can protect proteins in the digestive track. Second, Hydrogels can also be synthesized to exhibit bioadhesiveness to facilitate drug targeting, especially through mucus membranes, for non-invasive drug administration [106]. Finally, hydrogels also have a "stealth" characteristic in vivo circulation time of delivery device by evading the host immune response and decreasing phagocytic activity [107-108].

### *4.1.2. Transdermal Delivery*

Drug delivery to the skin has been generally used to treat skin diseases or for disinfection of the skin. In recent years, transdermal route for the delivery of drugs has been investigated. Swollen hydrogels can be delivered for long duration and can be easily removed. These hydrogels can also bypass hepatic first-class metabolism, and are more comfortable for the patient.

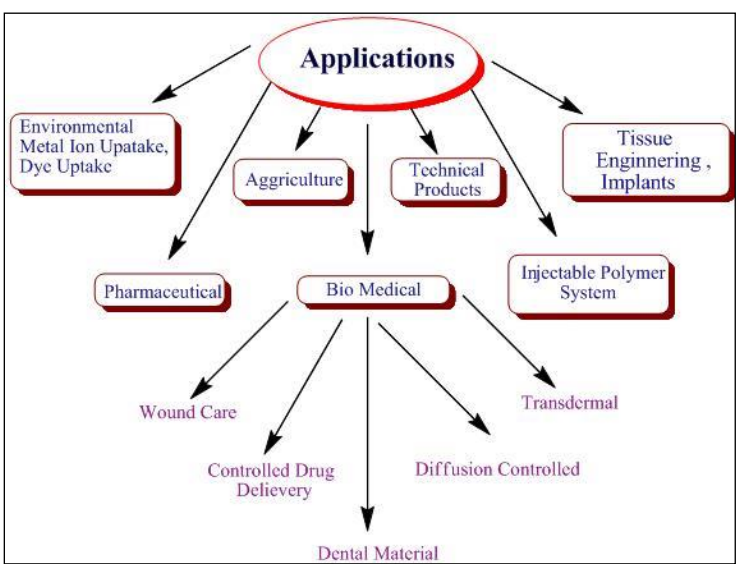


Figure 16. Schematic representation of hydrogels applications.

### *4.1.3. Diffusion-Controlled Delivery Systems*

Diffusion-controlled is the most widely applicable mechanism for describing drug release from hydrogels.

## 4.2. Agricultural Applications

Hydrogels have been commonly utilized in agricultural field mainly as water storage granules [109-110]. The need for improving the physical properties of soil to increase productivity in the agricultural sector was visualized in 1950s [111]. This led to the development of water-soluble polymers such as PVA, PEG and PAM to function as soil conditioners [112] followed by the introduction of water-swellable polymeric hydrogels in the early 1980s [113-114]. Water-swellable hydrogels from crosslinked PAM, crosslinked polyacrylates and copolymers of acrylamide and acrylates for such applications have been reported. Soils with moist hydrogels acting as conditioners, increase water-holding capacity of the potting media by 50 to 100%. The increased water supply enhances the germination process by reducing the relative amount of water loss via evaporation and drainage. Swellable hydrogels delivery systems are also commonly utilized for controlled release of agrochemicals and nutrients of importance in agricultural applications to enhance plant growth with reduced environmental pollution. A number of researchers have reported the versatility of polymeric hydrogels in agricultural applications [115].

## 4.3. Environmental Applications

Removal of heavy metals ($Cu^{2+}$, $Pb^{2+}$, $Ni^{2+}$, $Cd^{2+}$, $Zn^{2+}$, $Mn^{2+}$, $Co^{2+}$, $Hg^{2+}$ and Fe3+) from waste-water of chemical industries including metallurgical and metal finishing has been receiving an increasing attention in the recent years. This is due to the severity of environmental pollution by heavy metals as they impose direct toxic effect on human and animal health. Moreover, selective separation of some metals such as silver and gold from other components is of practical interest, either with the aim to separate these metals from natural resources or to treat industrial effluents and waste-water [116].

## 4.4. Dye Uptake

Dye uptake techniques are widely used to remove certain classes of pollutants from waters, especially those that are not easily biodegradable. Amongst the numerous techniques of dye removal, adsorption is the procedure of choice and gives the best results as it can be used to remove different types of coloring. If the adsorption system is designed correctly it will produce a high-quality treated effluent. Most commercial systems currently use activated carbon as sorbent to remove dyes in wastewater because of its excellent adsorption ability. Many non-conventional low-cost adsorbents, including natural materials, biosorbents, and waste materials from industry and agriculture, have been proposed by several workers.

## 4.5. Other Applications

Hydrogels have been commonly utilized commercially in other important industrial areas such as cosmetics, food industry, photography and instrumentation. A list of some important industrial applications of polymeric hydrogels system is summarized given below [117].

a) Hydrogels are used as thickening agents (e.g., starch and gelatin) in foods.
b) Technical and electronic instruments can be protected from corrosion and short-circuit exposure of, sheathing with highly absorbent hydrogels forming agents.
c) The addition of hydrogel forming agents to incontinence products increases the fluid uptake and ensures the improved retention.
d) Hydrogels are used in photography technology because they are light permeable and can also store light sensitive substances.
e) In electrophoresis and chromatography, the separation and diffusion characteristics of the gel structure are exploited. Hydrogels, thus applied, operate within only a very limited range of swelling.

## 5. CHALLENGES IN THE FIELD OF HYDROGELS

### 5.1. Hydrogels on Polymeric Surfaces

Despites many advantageous properties, the low tensile strength of many hydrogels limits their use in many applications [118-119]. The low tensile strength of many hydrogels lose mechanical properties as they absorb water. One of the major problems in the application of these hydrogels is their relatively poor mechanical strength, attributed to the high degree of hydration of hydrogels.

Unlike, the majority of other polymers which are tested, swollen hydrogels are extremely weak material which can exhibit poor mechanical strength. It is often necessary to improve them in some manner to make the material suitable for the desired applications. The prediction and control of mechanical properties in hydrogels is of great importance in assessing the applicability of hydrogels. It is important to characterize the hydrogels for their mechanical properties.

An usual attempt to overcome this drawback is, grafting hydrophilic groups to strong supports, often hydrophobic polymers, to prepare mechanically strong hydrogels required for many biomedical applications. Graft copolymerization has been utilized to achieve the desired mechanical property of the stronger hydrogels.

Polymeric surface plays a positive role in membrane performances such as biomedical and environmental applications. Surface modification of polymeric membranes provides the mechanical strength and chemical stability.

In polymeric age, it is essential to modify the properties of a polymer according to tailor-made specifications designed for target applications. A large variety of hydrogels were obtained from many suitable monomers. Their properties depend on the chemical nature of the starting compounds and the degree of the resulting polymeric networks. They satisfy the requirements imposed by different applications in food industry, cosmetics, agriculture, medicine, pharmacy, technical and electronic instrumentation, photography etc.

### 5.2. Graft-Copolymerization

The modification of polymers has received much attention recently. Among the methods of modification of polymers, graft co-polymerization is one of the most general, promising

and powerful method of affecting modification in polymers. Copolymerization is most accurately defined as polymerization in which two or more structurally distinct monomers are incorporated into the same polymer chain. It involves a definite chemical reaction between two monomers $M_1$and $M_2$ and is not a simple process of mixing two different monomers to produce polyblends. The terms used to describe various types of copolymers, are explained in the accompanying illustrations as follows: graft polymerization of monomers to the surfaces [120].

Graft Copolymerization is the

a) Alternating copolymers -$M_1$ $M_2$ $M_1$ $M_2$ $M_1$ $M_2$ $M_1$ $M_2$—
b) Random copolymers - $M_1M_1M_1$ $M_2$ $M_1$ $M_2M_2$ $M_2$—
c) Block copolymers -$M_1M_1M_1$ $M_2M_2M_2$ $M_1M_1$ $M_1$—
d) Graft copolymers - $M_1M_1M_1M_1M_1M_1M_1$ $M_1$— $M_2M_2M_2$

In principle, graft co-polymerization is an attractive method to impart a variety of functional groups to a polymer or in which the side chain grafts are covalently attached to form branched copolymer. Graft copolymerization takes place as a result of formation of active cites on the polymer backbone. The active sites may be free radicals or ionic chemical groups, which initiate polymerization reaction. The formation of active cites on the polymer backbone can be carried out by several methods such as plasma treatment [121], ultraviolet (uv) light radiation [122], decomposition of chemical initiator [123] and high energy radiation [124].

Grafting generally requires three reactants: a backbone polymer, the monomer to be grafted and the initiator which can create the active sites. There are two methods of graft copolymerization.

A graft copolymer can be represented as follows:

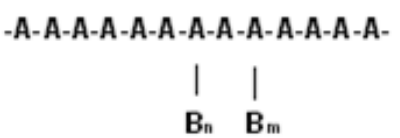


Where, A is the main polymer chain, $B_n$ and $B_m$ are the side chain grafts originated from the monomer B. The extent of polymerization in $B_n$ and $B_m$ grafts is called the degree of grafting (grafting yield) which is gravimetrically determined as the percentage of mass increase. Both the backbone and side chain grafts can be either homopolymer or copolymer.

It can be described as having the general structure shown in Scheme 1, where the main polymer backbone poly(A), commonly referred to as the trunk polymer, has branches of polymer chain poly(B) emanating from different points along its length.

The common nomenclature used to describe this structure, where poly(A) is grafted with poly (B), is poly(A)-graft-poly(B), which can be further abbreviated as poly(A)-g-poly(B). Grafting of synthetic polymer is a convenient method to add new properties to a natural polymer with minimum loss of the initial properties of the substrate.

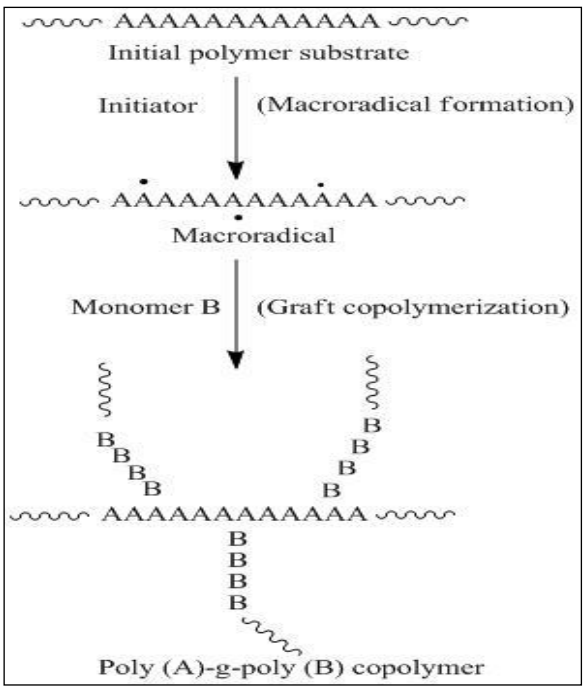


Scheme 1.General Free Radical Mechanism of Graft Copolymerization of Vinyl Monomer B onto Trunk Polymer Poly (A) to form the Graft Copolymer Poly (A)-*G*-Poly (B).

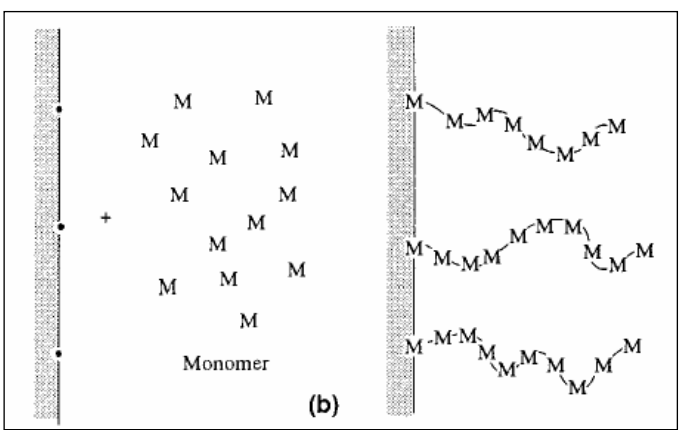


Scheme 2. Grafting of Monomers to the Surface.

Graft copolymers are prepared by first generating free radicals on the polymer backbone and then allowing these radicals to serve as macroinitiators for the vinyl (or acrylic) monomer. The grafting of monomers to the surface shown in Scheme 2 [125].

Mino and Kaizerman firstly reported this approach in 1958 for graft copolymer preparation using a ceric ion redox initiating system [126]. Then, the chemistry and technology of the radical graft copolymerization technique [127-128] was developed especially in the case of cellulose [129] and starch [130]. The properties of the resulting graft copolymers may be controlled widely by the characteristics of the side chains including molecular structures, length, number, and frequency. One of the most important features of

graft polymerization is unwanted formation of homopolymer, homopoly (B) that is not chemically bonded to the substrate poly (A). Homopolymer can result if the initiator used is one that produces free radicals in solution (in the presence of vinyl monomer B initiating homopolymerization) before creating the macroradicals. Once a grafted chain has been initiated and begins to propagate, chain transfer from the growing grafted chain end can occur with some species in the medium to yield free radicals that could initiate the growth of homopoly (B) chains.

Form above discussion, we can say that the graft **copolymer has** gained importance in the development of various commercial hydrogels. Grafting is an excellent technique for preparing copolymeric hydrogels. It is a very simple method to obtain a 'tailor-made' membrane with specific properties by introducing specific monomers.

## 5.3. Advantages of Grafting Method

- The graft copolymerization may introduce some desirable properties into the polymer without a change in the architecture of the polymer backbone and thus gives rise to commercial importance for polymer applications.
- The modified properties of polymers by grafting results in increased intermolecular interactions and possible crosslinking of the macromolecules.
- By these interactions, grafting improves adhesion, tensile strength, abrasion resistance and enhances thermal and photochemical stability, and it improves compatibility.
- Grafting offers a versatile method for incorporating new molecular functionalities into the existing polymer.
- Well controlled process.
- Gives rise to selected polymer combinations with highly specific properties tailor made for particular application.
- Grafting opens the door to the development of various commercial hydrogels membranes with high specificity and permeability.

Considerable work has been done on techniques of graft co-polymerization of different monomers on polymeric backbones.

Two major types of grafting may be considered:

i. Grafting with a single monomer
ii. Grafting with a mixture of two (or more) monomers. The first type usually occurs in a single step, but the second may occur with either the simultaneous or sequential use of the two monomers. Two different monomers are grafted side-by-side to obtain the requisite property. This is the origin of bipolar membranes.

These grafting techniques include chemical, radiation, photochemical, plasma-induced techniques and enzymatic grafting. The use of radiation processing of polymeric materials has been explored for the last 50 years and yet extensive publications describing development efforts and renewed interest in this area continue to appear [131-132]. Particularly, in the last

three decades, the use of radiation-induced graft copolymerization for preparation of various types of membranes has received considerable attention with the aim to develop new materials with modified properties for various applications [133].

## 5.4. Radiation Induced Graft Copolymerization

Radiation induced graft copolymerization can be achieved by ionizing radiation or ultra-violet light [134-136]. It is well known for its merits and potential in modifying the chemical and the physical properties of pre-existing polymeric materials without altering their inherent properties. This is one of the most promising methods because of several advantages:

- A variety of the radiation doses produces different initiation rates, hence different products.
- The effect of temperature, which is relatively unimportant for radiation initiation, can be better assessed, controlled and utilized on propagation rate.
- The lack of any chemical initiator results in the product not contaminated by any side products brought about by the initiators.
- High penetration of energetic radiation onto the polymer matrix, rapid and also uniformly distributed active sites for initiating grafting though out the matrix are some of the major advantages in radiation.
- It is also have the ability to initiate the polymerization in a wide range of temperature including low region in various states of monomers such as bulk, solution and emulsion and even at solid state.
- It offers a unique way to combine two highly incompatible polymers and impart new properties to the obtained graft copolymers [137, 138].

Radiation based technologies (gamma rays or electron beam) are considered to be among the most convenient ways to produce and sterilize polymer gels and membranes.

Radiation induced grafting differs from chemical initiation in many aspects. In a mechanistic way, as in a radiation technique, free radical formation is on the backbone polymer/monomer whereas in a chemical method, a free radical form first on to the initiator and it is transferred to the monomer/polymer backbone. Unlike the chemical initiation method, the radiation-induced process is free contamination, so that the purity of the processed products may be maintained. Chemical initiation is limited by the concentration of the initiator, and it may be difficult to determine an accurate concentration of the initiator, and it may be difficult to determine an accurate concentration of the initiator in pure form. Chemical initiation often brings about problems arising from local heating of the initiator, an effect that is absent in the formation of free-radical sites by radiation, which is only dependent upon the absorption of high-energy radiation. Due to large penetrating power of higher energy radiation, methods using radiation initiation provide the opportunity to carry out grafting at different depths of the base polymer matrix. Moreover, the molecular weight of the products can be better regulated in radiation techniques, and these are also capable of initiation in solid substrates. Also, irradiation methods are simple, and the degree of crosslinking which

strongly determines the extent of swelling of hydrogels, can be easily controlled by varying the irradiation dose [139-141].

Due to these advantages, this technique has found great utilization in *preparing hydrogels* for medical and pharmaceutical applications, where even the slightest contamination is undesirable [142]. Simple procedure control, no initiators, crosslinkers, no waste and relatively low operating costs make an irradiation technique a suitable choice for the synthesis of hydrogels.

There are many other advantages of the radiation-based technologies of polymer-based materials over the conventional techniques. Radiation-based technologies can easily be handled also by small companies and the costs of production, being an important component of the final shelf-price of the product, are considerably lower than for the corresponding conventional procedures, as proven by the already implemented radiation-based technologies, e.g., hydrogel wound dressings. Moreover, some of these products cannot be synthesized by conventional methods [143].

The versatile nature of this technique is attributed to the ability to control the degree of grafting by proper selection of irradiation conditions [144]. For, applications, which requires thin membranes, this technique shows superior advantage where the difficulty of shaping the graft copolymer into thin foil of uniform thickness could be circumvented by the possibility of starting the process with the film already having the physical shape of the membrane [145]. Moreover, high energy radiation offers the ability to control both the graft copolymer composition and properties (such as morphology and structure, as well as the thickness of the grafted layer) through the selection of suitable grafting conditions.

In the present work, gamma radiations have been used to graft copolymerization of monomers with the aim to prepare hydrogels. Gamma radiation involves emission of γ-rays by radioactive isotopes covering a wide range of energies [146].

### *5.4.1. Controlling Factors of Graft Copolymerization*

There are several of the many parameters which affect the degree of grafting in membrane prepared through radiation induced graft copolymerization. This includes parameters directly related to irradiation source and others related to the grafting mixture and its components. The effect of following parameters on the degree of grafting is studied.

- Monomer Concentration
- Reaction Temperature
- Reaction Time
- Irradiation Dose and Dose Rate
- The type of Solvents used

## 6. METHODS OF RADIATION GRAFTING

The most recent research in radiation-induced graft copolymerization proceeds in three different ways:

### 6.1. Simultaneous Radiation Grafting Method (Direct or Mutual)

Simultaneous irradiation is the simplest irradiation technique for preparation of graft copolymers. In this method, a polymer backbone is irradiated in the presence of a monomer available in different forms: vapor, liquid or in bulk solution. Irradiation can be carried out in air, inert atmosphere (e.g., $N_2$) or preferably under vacuum leading to the formation of active free radicals on both polymer backbone and monomer units. The reaction mechanism in this grafting system can be represented as follows:

$$\text{Irradiation :} \quad P \xrightarrow{\gamma\text{-rays}} P^{\cdot} \quad \text{(primary radicals)}$$

$$\text{Initiation :} \quad P^{\cdot} + M \rightarrow PM^{\cdot} \quad \text{(graft chain)}$$

$$\text{Propagation :} \quad PM^{\cdot} + nM \rightarrow PM^{\cdot}_{n+1} \quad \text{(graft growing chains)}$$

$$\text{Termination :} \quad PM^{\cdot}_{n} + PM^{\cdot}_{m} \rightarrow PM_{n+m} \quad \text{(graft copolymer)}$$

Where P is the polymer matrix, M is the monomer units and P· and M· are their primary radicals, respectively. PM· is the initiated graft chain. $PM^{\cdot}_{n}$ and $PM^{\cdot}_{m}$ are the graft growing chains of the copolymer.

In simultaneous irradiation, there is a high possibility for deactivation of the primary radicals of the polymer backbone (P·) by mutual recombination. This deactivation can be represented by equation given below:

$$P^{\cdot} + P^{\cdot} \rightarrow PP \quad \text{(recombination)}$$

The obvious advantage is that the method is relatively free from homopolymer formation, which occurs with the simultaneous technique. Homopolymerization initiated by the reaction of radicals formed from radiolysis of monomer with monomer molecules remaining in the grafting solution can be represented by equation given below:

$$M \xrightarrow{\gamma\text{-rays}} M^{\cdot} \text{ (primary radicals)}$$

$$M^{\cdot} + nM \rightarrow M^{\cdot}_{n}$$

(homopolymer growing chains)

$$M^{\cdot}_{n} + M^{\cdot}_{m} \rightarrow M_{n+m} \quad \text{(homopolymer)}$$

Where $M^{\cdot}_n$ and $M^{\cdot}_m$ are the growing chains of the homopolymer, respectively. The method is thus limited to the system in which the radical yield from the backbone polymer is higher than that from the monomer. Diffusion of monomer into polymer plays an important role in the direct radiation method, as it is by this means that the monomer reaches the active sites within the polymer.

## 6.2. Pre-Irradiation Method

In pre-irradiation technique, the polymer backbone is first irradiated in vacuum or in the presence of an inert gas to form free radicals [147-149]. The irradiated polymer substrate is then treated with the monomer, in liquid or vapor state or as a solution in a suitable solvent.

$$P \rightsquigarrow P^{\cdot} + M \rightarrow PM^{\cdot}$$

## 6.3. Per-Oxidation Grafting Method

In the peroxidation grafting method, the trunk polymer is subjected to high-energy radiation in the presence of air or oxygen to form hydroperoxides or diperoxides, depending on the nature of the polymeric backbone and the irradiation conditions. The stable peroxy products are then treated with the monomer at higher temperature, when the peroxides undergo decomposition to radicals, which then initiate grafting [150-152]. The overall reaction in graft copolymerization of a monomer onto hydrocarbon backbone by pre-irradiation method can be represented by equation given below:

## 6.4. Formation of Hydroperoxides

$$PH + O_2 \xrightarrow{\gamma\text{-rays}} POOH$$

$$\text{Thermal decomposition} \quad POOH \xrightarrow{\Delta} PO^{\cdot} + OH^{\cdot}$$

$$\text{Initiation} \quad PO^{\cdot} + M \rightarrow POM^{\cdot}$$

$$\text{Propagation} \quad POM^{\cdot} + nM \rightarrow POM^{\cdot}_{n+1}$$

Where PH is the polymer backbone, POOH is the hydroperoxide radical, $PO^{\cdot}$ is the primary radical, $POM^{\cdot}$ is the initial chain graft and $POM^{\cdot}_{n+1}$ is the graft growing chain.

This method has been given much attention because the homopolymer formation is little and the grafting can be carried out at any time, away from radiation source. The advantage of this technique is that the intermediate peroxy products can be stored for long periods before performing the grafting step. Thus, this is of particular interest for achieving desired

membrane properties since various commercial polymers available in different forms (films, resins and fibers) can be used as grafting substrates.

## 7. APPLICATIONS

Many radiation grafted membranes were found to meet the requirement for a variety of applications in the present time and many more are being developed the present time and many more are being developed for the future, especially in biomedical in applications.

## 8. FUTURE DIRECTIONS

Stimuli-Responsive hydrogels prepared through gamma radiation induced graft copolymerization method have been created using different approaches in recent decades, but most of the work has been focused on how the different responsive interactions within the membranes can be monitored in biomedical fields. Stimulation of responsive membranes will shift from nonspecific triggers such as temperature and pH to specific, affinity type triggers. A less well developed research area that is ripe for exploration is the synthesis of membranes that respond to biochemical stimuli. Stimuli-responsive hydrogels have strong potential for future applications in tissue engineering, bioseparations, antifouling surfaces, and drugdelivery among others. Reversible changes to surface composition, surface energy, adhesion and wettability of Switchable membrane surface properties will improve the efficiency of many technological processes.

## CONCLUSION

Radiation induced graft copolymerization is a broad and promising method that provides a suitable and an economical technique for preparation of various types of membranes. This is due to their relatively simple preparation procedure and easy control of membrane most important properties such as swelling. This review has examined in detail the significantly important and rapidly developing field of stimuli-responsive hydrogels. We used gamma radiation induced graft copolymerization method to prepare stimuli-responsive hydrogels to use as potential applications in biomedical fields specially in controlled drug delivery system. The responsive properties can be controlled by direct manipulation of the chemistry of membrane materials, structural and morphological factors, and external stimuli. These were generalized into two categories: membrane synthesis from stimuli-responsive materials and membrane modification to incorporate stimuli responsive materials. pH- and ionic strength-responsive membranes are used widely in various applications such as controlled release of chemical and drugs, flow regulation, sensors, self-cleaning surfaces and selective filtration. Finally, this review is meant to provide a better understanding of stimuli-responsive membranes and to encourage further development efforts.

## REFERENCES


[1] N.A. Peppas, A.G. Mikos, F.L. Solute Diffusion in Hydrophilic Network Structures, in *Hydrogels in Medicine and Pharmacy* Vol. 1, (1-25) N.A. Peppas, ed., CRC Press, INC. Boca Raton, Fl., (1986).

[2] B. Bhattacharya, *Prog Polym Sci* (371-401) 25 (2000).

[3] L. Brannon-Peppas, L. Brannon-Peppas, R.S. Harland (Eds.), *Absorbent Polymer Technology*, Elsevier, Amsterdam., (45-66) (1990).

[4] J. Chen, Wu. Zaiqian, Y. Liming, Qu. Zhang, Li. Wang, Lu. Yan, *Journal of Radioanalytical and Nuclear Chemistry.* Vol. 275, No.1 (81–88) (2008).

[5] F.C. Jin, C. Jie, G.Y. Liming, Li. Han, C. Fangqi, *Bull. Mater. Sci.,* Vol. 32, No. 5 (521–526) (2009).

[6] J. Swarbrick, *Encyclopedia of Pharmaceutical Technology*, Informa Healthcare, New York., 3rd edn. (2006).

[7] K. Nguyen, West *J. Biomaterials.*, 23 (4307) (2002).

[8] N. Peppas, P. Bures, *Eur. J. Pharm. Biopharm.*, 50 (27) (2000).

[9] A. Sawhney, C. Pathak, *J. Biomed. Mat. Res.*, 28 (831) (1994).

[10] G. Iwon,J. Helena, *Chemistry & Chemical Technology.*, Vol. 4 No. 4 (2010).

[11] T. Miyata, T. Uragami, K. Nakamae, *Adv. Drug Deliv. Rev*., 54 (79) (2002).

[12] C. Chang, B. Duan, J. Cai, L. Zhang, *Eur. Polym. J.*, 46 (92) (2010).

[13] D. Williams, Pergamon Press, Oxford., (1990).

[14] N.A. Peppas, E.W. Merrill, *J. Polym. Sci. Polym. Chem.* Ed., 14 (441-457) (1976).

[15] N.A. Peppas, E.W. Merrill, *J. Appl. Polym. Sci*., 20 (1457-1465) (1976).

[16] N.A. Peppas, CRC Press, Boca Raton, FL, Vol. 2 (1-48) (1986).

[17] S.R. Stauffer, N.A. Peppas, *Polymer.*, 33 (3932-3936) (1992).

[18] A.S. Hickey, N.A. Peppas, *J. Membr. Sci.*, 107 (229-237) (1995).

[19] N.A. Peppas, N.K. Mongia, *Eur. J. Pharm. Biopharm.*, 43 (51-58) (1997).

[20] P.J. Flory, J. Rehner, *J. Chem. Phys.*, 11 (521-526) (1943).

[21] P.J. Flory, *J. Chem. Phys.*, 18 (108-111) (1950).

[22] P.J. Flory, N.Y. Ithaca, *Cornell University Press*., (1953).

[23] H. Park, K. Park, R. M. Ottenbrite, S. J. Huang, K. Park, *American Chemical Society*, Washington, D.C., 1-10, (1996).

[24] K. Kamath, K. Park, *Adv. Drug Deliv.*, 11 (59-84) (1993).

[25] K. Park, W.S.W. Shalaby, H. Park, *Technomic*, lanscaster., (1993).

[26] K. Park, W. S. W. Shalaby, H. Park., *Technomic Publishing Company*, Inc. Basel., (1-12) (35-66) (1993).

[27] H. Xu. Gao, M.A. Philbert, R. Kopelman, *Angew Chem Int Ed.*, 46 (2224-2227) (2007).

[28] O. Güven, M. Şen, E. Karadağ, D. Saraydın, *Radiation Phys. Chem.*, 56 (381-386) (1999).

[29] W. M. Kulicke, H. Nottelmann, *American Chemical Society*, Washington, D.C., (15-44) (1989).

[30] J. Gross, Elsevier, New York., (3-32) (1990).

[31] J. H, Kuo, G. L. Amidon, P. I. Lee, *Pharm. Res.*,5 (592-597) (1988).
[32] K. Bajpai, S. K. Shukla, S. Bhanu, S. Kankane, *Progress in Polymer Science.*, Volume 33 Issue 11 1088-1118 (2008).
[33] N.A. Peppas, R. Langer, *Science.*, 263 (1715-1720) (1994).
[34] A.S. Hickey, N.A. Peppas, *J. Membr. Sci.*, 107 (229-237) (1995).
[35] R. J. Young, P.A. Lovell, Chapman & Hall, London., (241-306) (1991).
[36] P. C. Hiemenz,Marcel Dekker, Inc, New York., (1-72) (1984).
[37] A. D. Jenkins, K. L. Loening, Pergamon Press, Oxford., Vol 1, pp. 13-54, (1989).
[38] H. R. Allcock, F. W. Lampe, *Contemporary Polymer Chemistry* 2nd Ed, Prentice-Hall, Inc., New Jersey., (420-442) (1990).
[39] A. S. Hoffman, *Adv. Drug Deliv. Rev.*, 54 (3-12) (2002).
[40] H. He, X. Cao, J.L. Lee, *J. Controlled Release.*, 95 (391-402) (2004).
[41] Q. Liu, E. L. Hedberg, Z. Liu, R. Bahulekar, R. K. Meszlenyi, A. G. Mikos, *Biomaterials.*,21, (2163-2169) (2000).
[42] R. Barbieri, M. Quaglia, M. Delfini, E. Brosio, *Polymer.*, 39 (1059-1066) (1998).
[43] Y. C. Lai, *J. Appl. Polym. Sci.*, 66 (1475-1484) (1997).
[44] A. Güner, M. Kara, *Polymer.*, 39 (1569-1572) (1998).
[45] L. Lopérgolo, C. Lugão, A. B. Catalani, L. H. *Polymer.*, 44 (6217-6222) (2003).
[46] A.B. Lugão, S.O. Rogero, S.M. Malmonge, *Radiation Phys. Chem.*, 63 (543-546) (2002).
[47] J.A. Stammen, S. Williams, D.N. Ku, R.E. Guldberg, *Biomaterials.*, 22 (799-806) (2001).
[48] H. Park, K. Park, R.M. Ottenbrite, S.J. Huang, K. Park, *American Chemical Society*, Washington, D.C., (1-10) (1996).
[49] C.S. Brazel, N.A. Peppas, *Polymer.*, 40 (3383-3398) (1999).
[50] M.T. Am Ende, N. A. Peppas, *J. Controlled Release.*, 48 (47-56) (1997).
[51] M.M. Amiji, United States Patent., 5904927 (1999).
[52] C.E. Carraher, *Polymer Chemistry*, Marcel Dekker, Inc., New York., (345-347) (1996).
[53] Z. Maolin, L. Jun, Y. Min, H. Hongfei, *Radiation Phys Chem.*, 58 (397-400) (2000).
[54] L. H. Sperling, *Plenum Press*, New York., (1-10) (1981).
[55] K. B. Visscher, I. Manners, H. R. Allcock, *Macromolecules.*, 23 (4885-4886) (1990).
[56] J. Zhang, N. A. Peppas, *J. Biomater. Sci. Polymer.*, 13 (511-525) (2002).
[57] J. Zhang, N. A. Peppas, *J. Biomater. Sci. Polymer.*, Edn. 13, 511-525, (2002).
[58] B. D. Ratner, A. S. Hoffman, *American Chemical Society*, Washington, D.C., (1 – 29) (1976).
[59] J. Ostroha, M. Pong, A. Lowman, N. Dan, *Biomaterials.*,25 (4345-4353) (2004).
[60] L. T. Ng, A. Arsenin, D. Nguyen, *Proc. Rad Tech Asia'03,* Yokohama, Japan., (669-672) (2003).
[61] K. Sutani, I. Kaetsu, K. Uchida, Y. Matsubara, *Radiation Phys. Chem.*,64 (331-336) (2002).
[62] W.F. Lee, R.J. Chiu, *Mater. Sci. Eng.*, 20 (161-166) (2002).
[63] K.C. Gupta, R.M.N.V. Kumar, *J. Appl. Polym. Sci.*, 76 (672-683) (2000).

[64] J.C. Salamone, W.C. Rice, H.F. Mark, J.J. Kroschwitz, New York, Wiley., *Vol II*, (514-530) (1985).
[65] P.J. Flory, Cornell University Press, New York., (576-589) (1953).
[66] E.J. Mack, T. Okano, S.W. Kim, *Polymers*, CRC Press, Inc. Florida, ed., Vol II (85-93) (1987).
[67] B.D. Ratner, D.F. William, ed., CRS Press, Inc., Florida., Vol 2 (145-175) (1981).
[68] H. Park, K. Park, R.M. Ottenbrite, S.J. Huang., K. Park, eds., *American Chemical Society*, Washington D.C., (1-10) (1996).
[69] W.M. Kulicke, H. Nottelmann, J.E. Glass, ed., *American Chemical Society*, Washington, D.C., (15-44) (1989).
[70] B.D. Ratner, S.K. Aggarwal, ed., Pergamon Press, Oxford., Vol 7(201-247) (1989).
[71] B.Y. Shekunov, P. Taylor, J.G. Grossmann, *J. Crystal Growth.*, 198/199 (1335-1339) (1999).
[72] N.A., Peppas, A.G, Mikos, CRC Press, Inc., Florida., ed., Vol I (1-25) (1986).
[73] S. H. El-Taweel, G.W.H., Höhne, A.A. Mansour, B. Stoll, H. Seliger, *Polymer.*,45 (983-992) (2004).
[74] J.N. Israelachvili, 1stEd, *Academic Press*, London., (97-107) (1985).
[75] B. Bednar, Z. Li, Y. Huang, L.C.P. Chang, H. Morawetz, *Macromolecules.*,18 (1829-1833) (1985).
[76] C.C. Lin, A.T. Metters, *Advanced Drug Delivery Reviews.*, 58 No.12-13 (1379-1408) (2006).
[77] H. Ji, et al., *International Journal of Solids and Structures.*,43(7-8) (1878-1907) (2006).
[78] J. Dolbow, E. Fried, Ji H., *Computer Methods in Applied Mechanics and Engineering*.,194 (42-44)(4447-4480) (2005).
[79] N.A. Peppas, *J. Bioact. Compat. Polym.*, 6 (241-246) (1991).
[80] M. Yang, L.Y. Chu,Li. Y,X.J. Zhao,H. Song, W.M. Chen, *Chem. Eng. Technol.*,29 631 (2006).
[81] L.Y. Chu, Y. Li, J.H. Zhu, W.M. Chen, *Angew. Chem. Int.* Ed., 44 (2124) (2005).
[82] T. Peng, Y.L. Cheng, *J. Appl. Poly. Sci.*, 76 (778) (2000).
[83] J.B. Qu, L.Y. Chu, M. Yang, R. Xie, L. Hu, W.M. Chen, *Adv. Funct. Mater.*,16 (1865) (2006).
[84] A.M. Lowman, N.A. Peppas, *John wiley & Sons Inc*., 397 (1999).
[85] J. Kost, *John Wiley & Sons Inc*., 445 (1999).
[86] F. Rosso. A. Barbarisi, M. Barbarisi, O. Petillo, S. Margarucci, A. Calarco, G. Peluso, *Mater. Sci., Eng.*, 23 (371-376) (2003).
[87] P. Gupta, K. Vermani, S.Garg, *Drug Discov. Today.*, 7569 (2002).
[88] N. Kashyap, N. Kumar, N.M.V. Ravi Kumar, *Crit. Rev. Ther. Drug Carrier Sys.*, 22 116 (2005).
[89] Y. Zhang, W. Zhu, J. Ding, *J. Biomed. Mater. Res.*, 75A (342) (2005).
[90] D.L.H.A. Carolina, P. Sivanand, A. Cameron. *Chem. Soc. Rev.*, 34 (276–285) (2005).
[91] A.S. Carreira, F.A.M.M. Goncalves, P.V. Mendonca, M.H. Gil, J.F.J. Coelho,

*Carbohydr. Polym.,* 80 (618) (2010).
[92] L. Ferreira, M.M. Vidai, M.H. Gil, *Int. J. Pharm., 194* 169 (2000).
[93] K.N. Plunkett, K.L. Berkowski, J.S. Moore. *Biomacromolecules.,* 6 (632–7) (2005).
[94] N. Bhattarai, H.R. Ramay, J. Gunn, F.A. Matsen, M. Zhang, *J Control Release.,* 103 (609–24) (2005).
[95] C.D.L. Alarcon, S. Penndam, C. Alexander *Chem Soc Rev.,* 34 (276–85) (2005).
[96] C.M. Schilli, M. Zhang, E. Rizzardo, S.H. Thang, Y.K. Chong, K. Edwards, *Macromolecules.,* 37 (7861–6) (2004).
[97] X.Z. Zhang, Y.Y. Yang, T.S. Chung, K.X. Ma. *Langmuir.,* 17 (6094–9) (2001).
[98] W. Yuan, G. Jiang, J. Wang, Y. Song, L. Jiang, *Macromolecules.,* 39 (1300) (2006).
[99] S. Dai, P. Ravi, K.C. Tam, *Soft matter*.,5 (2513) (2009).
[100] X. Chen, et al., *Carbohydrate Polymers.,* 28(1) (15-21) (1995).
[101] N.A. Peppas., et al., *European Journal of Pharmaceutics and Biopharmaceutics.*,50(1) (27-46) (2000).
[102] A.S. Hoffman, Reviews, *Advanced Drug Delivery*., 54(1) (3-12) (2002).
[103] R. Clough, *Nucl. Instrum Meth Phys Res.,* B 185 (8–33) (2001).
[104] A. Dessouki, N. Taher, M. El-Arnaouty. *Polym Int.,* 45 (67–76) (1998).
[105] C.C. Lin, A.T. Metters, *Advanced Drug Delivery Reviews.,* 58 (12-13) (1379-1408) (2006).
[106] L. Achar, N.A. Peppas, *Journal of Controlled Release*.,31(3) (271-276) (1994).
[107] F.M. Veronese, C. Mammucari, P. Caliceti, O. Schiavon, S. Lora., *Journal of Bioactive and Compatible Polymers.,* (315-330) (1999).
[108] P. Bawa, V. Pillay, Y.E. Choonara, L.C. du Toit, *Biomed. Mater.,* 4 022001 (2009).
[109] A. Hüttermann, M. Zommorodi, K. Reise, *Soil and Tillage Res.,* 50 (295-304) (1999).
[110] G. Burillo, T. Ogawa, *Radiation Phys. Chem.,*18 (1143-1147) (1981).
[111] R.M. Hedrick, D.T. Mowry, *Soil Sci.,*73 (427-441) (1952).
[112] R.L. Flannery, W.J. Busscher, *Commun. Soil Sci.,* 13 (103-111) (1982).
[113] M.S. Johnson, *J. Sci. Food Agriculture*., 35 (1063-1066) (1984).
[114] U. Shavit, M. Reiss, A. Shaviv, *J. Controlled Release.,* 88 (71-83) (2003).
[115] U. Shavit, M. Reiss, A. Shaviv, *J. Controlled Release.,* 88 (71-83) (2003).
[116] E.A, Hegazy, H. Kamal, N. Maziad, A. Dessouki. *NuclInstrum Meth Phys Res.,* B151 (386–92) (1999).
[117] W.M. Kulicke, H. Nottelmann, *American Chemical Society*, Washington, D.C., (15-44) (1989).
[118] A.B. Lugao, L.D.B. Machado, L.F. Miranda, M.R. Alvarez, J.M.Rosiak, *Radiat. Phys. Chem.,* 52 (16) 319-322 (1998).
[119] H. Gehrke, P.I. Lee. *Specialized Drug Delivery Systems*, Marcel Dekker., (333–392) (1990).
[120] V.D. Athawale, S.C. Rathi, J. Macromol. *Sci. Rev. Macromol.Chem. Phys.,* C 39(445-480) (1999).
[121] Y.J. Choi, M.S. Kang, S.H. Kim, J. Cho, S.H. Moon. *J. Membr. Sci.,* 223 (201–15) (2003).

[122] Z. Xu, J. Wang, L. Shen, D. Men, Y. Xu. *J Membr Sci.*, 196(221–9) (2002).
[123] I. Guilmeau, S. Esnouf, N. Betz, A. Le Moel. *NuclInstrum Meth Phys Res*., B 131 (270–5) (1997).
[124] L.C. Lopérgolo, A.B. Lugão, L.H. Catalani, *Polymer*., 44 (6217-6222) (2003).
[125] U. Yoshikimi, K. Koichi, I. Yoshito, *Advances in Polymer Scien*ce., 147 (1-39) (1998).
[126] D.W Jenkins, S.M. Hudson, *Chem. Rev.*, 101 (3245-3273) (2001).
[127] Ad. A. Berlin., V.N. Kislenko, *Prog. Polym. Sci*., 17 (765-825) (1992).
[128] A. Hebeish., J.T. Guthrie., *Springer*, Berlin., Ch. (2-6) (1981).
[129] V.D. Athawale., S.C. Rathi., J. Macromol. *Sci. Rev. Macromol. Chem. Phys.*, C39 (445-480) (1999).
[130] D. Wavhal, E. Fisher. *J Membr Sci.*, 209 (255–69) (2002).
[131] J.O. Abu, K.G. Duodu, A. Minnaar, *Food. Chem.*, 95 (386-393) (2006).
[132] M.R. Cleland, L.A, Parks, S. Cheng, *NuclInstrum Meth Phys Res.*, B 208 (66–73) (2003).
[133] N. Betz, J. Begue, M. Goncalves, K. Gionnet, G. Deleris, A. Le Moel. *NuclInstrum Meth Phys Res.*, B 208 (434–41) (2003).
[134] P.K. Pandey, A. Srivastava, J. Tripathy, K. Behari. *Carbohydr. Polym.*, 65 (414-420) (2006).
[135] G. Huacai, P. Wang, L. Dengke, *Carbohydr. Polym.*, 66, 372-378 (2006).
[136] A. Vahdat, H. Bahrami, N. Ansari, F. Ziaie, *Radiat.Phys. Chem.*, 76 787-793 (2007).
[137] I. Guilmeau, S. Esnouf, N. Betz, A. Le Moel. *NuclInstrum Meth Phys Res*., B 131 (270–5) (1997).
[138] A. Bhattacharya, *Prog. Polym. Sci.*, 25 (371) (2000).
[139] E. Jabbari, S. Nozari, *Eur. Polym. J.*, 36 (2685) (2000).
[140] J.M. Rosiak, P. Ulanski, *Radiat. Phys. Chem.*, 55 139 (1999).
[141] E.A. Hegazy, H.A. AbdEl-Rehim, H. Kamal, K.A. Kandeel, *NuclInstum methods Phys Res B.*, 185 (p.235-240) (2001).
[142] S.E. Park, Y.C. Nho, Y.H. Lim, H. Kim, J. *Appl. Polym. Sci.*, 91 636 (2004).
[143] E.M. Abdel-Bary, E.M. El-Nesr, *Handbook of engineering polymeric materials*. New York: Marcel Dekker., 501 (1997).
[144] A. Chapiro. *Int. J. Radiat Phys. Chem.*, 9 (55–67) (1977).
[145] B. Gupta, G. Scherer. *Chimia.*, 48 (127–37) (1994).
[146] J.F. Kunzier, John Wiley and Sons. Inc., *Vol 2* 691 (2003).
[147] J. Chen, H. Iwata, Y. Maekawa, M. Yoshida, N. Tsubokawa. *Radiat Phys Chem*., 67 (3-4) (397–401) (2003).
[148] P. Marmey, M.C. Porte, C. Baquey. *Nucl Instrum Methods* B., 208 (429–33) (2003).
[149] T. Yamaki, M. Asano, Y. Maekawa, Y. Morita, T. Suwa, J. Chen, N. Tsubokawa, K. Kobayashi, H. Kubota, M. Yoshida, *Radiat. Phys. Chem*., 67 (403–7) (2003).
[150] B. Aydinli, T. Tincer. *Radiat Phys Chem.*, 60 (237–43) (2001).
[151] T. Sehgal, S. Rattan, J. *Radioanal. Nucl. Chem., 286* 71–80 (2010).
[152] T. Sehgal, S. Rattan, *Indian Journal of Pure and Applied Physics*., 48 (823-829) (2010).

In: Advances in Polymers for Biomedical Applications ISBN: 978-1-53613-612-8
Editors: Deepak Pathania and Bhuvanesh Gupta 

*Chapter 12*

# THERAPEUTIC APPLICATIONS OF POLYMERIC HYDROGELS

***Poonam Negi[1,*], Chetna Verma[2] and Sarita Kumari[3]***
[1]School of Pharmaceutical Sciences,
Shoolini University, Solan, India
[2]School of Chemistry, Shoolini University,
Solan, Himachal Pradesh, India
[3]Department of Zoology, Saifia Science College
(Affiliated to Barkatullah University), Madhya Pradesh, India

## ABSTRACT

Hydrogels are three-dimensional networks that are able to absorb large quantities of water or biological fluids, and hence have the potential to be used as primary candidates, for various drug delivery systems, and carriers or matrices, for cells in tissue engineering. Hydrogels prepared from natural materials *viz*., polysaccharides and polypeptides, along with different types of synthetic hydrogels from the recent reported literature, are presented in this chapter. The most widely employed natural polymers for the preparation of hydrogels are cellulose, chitosan, hyaluronic acid, dextran and alginate, while synthetic polymers are poly(ethylene glycol), poloxamer, Poly(hydroxyethyl methacrylate) (pHEMA), Polyacrylamide (PAAm) and polyvinyl alcohol. All the classifying properties of hydrogels affect their applicability, and types of therapeutic areas, in which they can be utilized.

**Keywords:** polysaccharide, poloxamer, polyacrylamide, controlled release, mucoadhesive and release mechanism

* Corresponding Author Email: poonamgarge@gmail.com.

# 1. HYDROGELS

Hydrogel, a three-dimensional, hydrophilic polymeric matrix, is capable of imbibing large quantities of water, and tends to simulate biological tissues when present in swollen form [1–3]. During initial years, after the discovery of hydrogels in 1960 by Wichterle and Lim, its biomedical potential was affected owing to the toxicity of cross-linking agents, and restricted application in operating within physiological conditions [3]. Nevertheless, increased research in polymer chemistry, and advanced understanding of human-physiology, have allowed scientists to design more innovative, and biocompatible therapies [4]. The presence of special hydrophilic molecules, in the gel's polymeric components, generates the hydrophilic characteristics of hydrogels, and account for their distinct absorption potential. When hydrogels are swollen, they become soft and rubbery, having a low interfacial tension with water and other biological fluids. In addition, the elastomeric consistency of the gel facilitates in reducing mechanical friction between tissues during implantation [5]. Sometimes, hydrogel networks tend to have low mechanical strength, which is a drawback of its swelling potential [6]. This limitation resulted in the development of multi-polymeric networks, which provided both a higher absorption capacity, and improved mechanical strength.

## 1.1. History of Hydrogels

The word "hydrogel," according to Lee, Kwon and Park, dates back to an article published in 1894. Later, the same material was described as not the hydrogel, indeed a colloidal gel, made with inorganic salts [7]. The first cross-linked network material with its typical hydrogel properties, one for all the high water affinity, was a polyhydroxyethylmethacrylate (pHEMA) hydrogel developed much later, in 1960. The hydrogels were developed with the ambitious goal of using them in permanent contact applications with human tissues, and are in fact the first materials developed for uses inside the patients [8, 9]. Since then the number of studies about hydrogels for biomedical applications began to rise, especially from the decade of 70's [10]. The aims, and goals, and the number of materials used for hydrogels evolved, and enlarged constantly over the decades. According to Buwalda et al., 2014, the development of hydrogels over the years could be divided into three main blocks as depicted in Figure 2 [11]. First generation hydrogels (era of sixties) are cross-linked hydrogels with relatively high swelling, and good mechanical strength. While second generation hydrogels (era of seventies) are capable of responding (by swelling or by other events) to specific stimuli such as pH, temperature, biological molecules, etc., the third generation hydrogels comprise of stereo complexed materials (e.g., poly (ethylene glycol)-poly (lactic acid), PEG-PLA cross-linked by cyclodextrin). Now the progress in hydrogel's science is quickly leading to an increasing interest in the development of the so called "smart hydrogels," polymeric matrixes with a wide spectrum of tunable properties and trigger stimuli [12-16]. Present day smart hydrogels with stimuli sensitive properties can be exploited to make modern day medical devices. In 1980, Lim and Sun [17] used calcium alginate to prepare microcapsules for successful application in cell encapsulation whereas, later on, Yannas and co-workers [18] prepared

hydrogels of collagen and shark fish cartilage for artificial burn dressings. Recently, hydrogels especially gained much attention for stereocomplexed material in biomedical field.

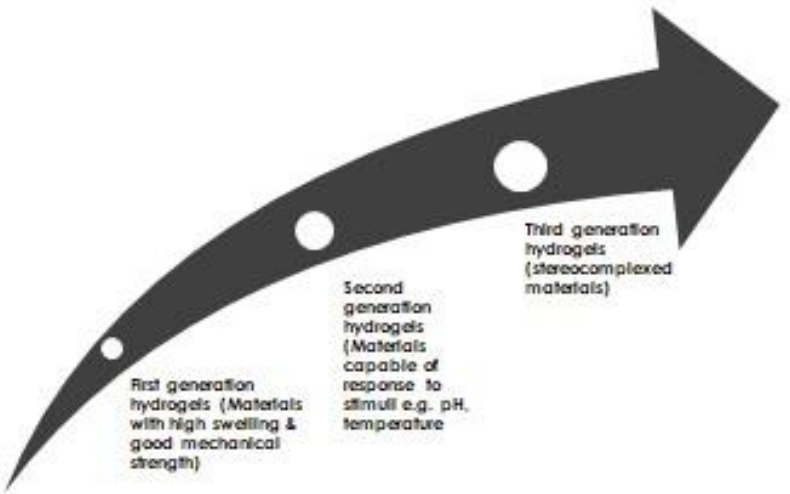


Figure 1. Developmental history of hydrogels.

## 1.2. Classification of Polymeric Hydrogels

Polymeric hydrogels can be classified in many ways. Based on source or origin [19], these can be natural polymeric hydrogels, synthetic polymeric hydrogels, and semi-synthetic polymeric hydrogels. Natural polymers are the polymers that are produced by living organisms. These biopolymers are highly versatile materials that can be modified to meet the needs of the desired biomedical applications. The examples of natural materials employed for hydrogels include collagen, chitin, fibrin, dextran, agarose, pullulan, hyaluronic acid, alginic acid, pectin, carrageenan etc. Synthetic polymers that are exploited for hydrogel construction composed of either biodegradable or non-biodegradable polymer backbone, e.g., polyethylene, polypropylene, polyvinylchloride, polyethylene glycol (PEG), Poly lactic-co glycolic acid (PLGA), Poly (hydroxyethyl methacrylate) (pHEMA), etc. Besides, semi-synthetic polymers derived from naturally occurring polymers by chemical modifications are also employed, *viz*., cellulose diacetate, carboxymethyl cellulose. Depending upon their response to stimuli, polymeric hydrogels can also be classified as smart hydrogels, and conventional hydrogels. While, the polymer network of smart hydrogels is able to respond to external stimuli through abrupt changes in the physical nature of the network, conventional hydrogels is not able to do so [20]. The other classification of polymeric hydrogels depends on, presence or absence of charge as anionic, cationic, neutral, and ampholytic. The crosslinked polymeric chain of anionic hydrogels, contains negative charge, while cationic hydrogels bear positive charge, neutral hydrogels exhibits no charge, and ampholytic hydrogels contain both acidic and basic groups. Further, polymeric hydrogels can also be classified based on structure, as amorphous and semi-crystalline. The polymeric hydrogels, which do not have regular symmetry in their structure, are categorized as amorphous

hydrogels, whereas, hydrogels having both regular and irregular symmetry in their structure, are categorized as amorphous hydrogels. Finally, polymeric hydrogels are also classified as homopolymer, co-polymer, and semi-interpenetrating network, depending on their composition. Polymer network derived from a single species of monomer, is a basic structural unit comprising of any polymer network. Homopolymers may have cross-linked skeletal structure depending on the nature of the monomer, and polymerization technique. On the other hand, co-polymer comprised of two or more different monomer species, with at least one hydrophilic component, arranged in a random, block or alternating configuration along the chain of the polymer network. Semi-interpenetrating (IPN) network, an important class of hydrogels is made of two independent cross-linked synthetic and/or natural polymer components, contained in a network form. In semi-IPN hydrogel, one component is a cross-linked polymer and other component is a non-cross-linked polymer [21-23].

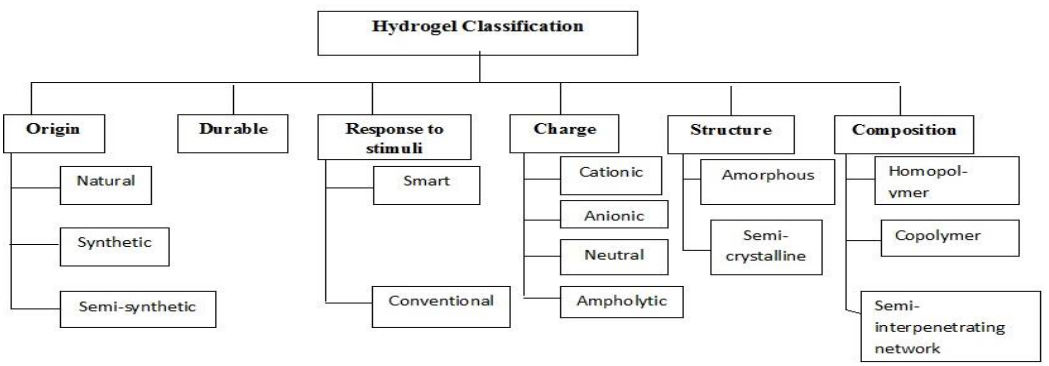


Figure 2. Classification of hydrogels.

## 1.3. Natural Polymer Based Hydrogels

Natural polymers are materials of large molecular weights from natural origins such as plants, micro-organisms and animals. Natural polymers have low toxicity, renewability, flexibility to modification, biodegradability, and low cost. Natural polymer based hydrogels possess high capacity of water absorption, and high gel strength. Modification of natural polymers enhances their drug delivery properties and versatility. Natural polymers based hydrogels are continually being explored in innovative approaches to biomedical applications.

### *1.3.1. Cellulose Based Hydrogels*

Cellulose is a naturally occurring polysaccharide, and is composed of β-D-glucose units linked through 1-4, glycosidic linkages, to form linear chains [24]. It is mainly found in plants and natural fibres, *viz.*, cotton and linen. The most distinct characteristics of cellulose are its biocompatibility and biodegradability, which makes the cellulose an attractive component in biomedical field. Cellulose and its derivative have successfully employed in burn wound regeneration, as well as in cardiac, vascular, neural, cartilage and bone tissue regeneration. Cellulose nanocrystals/poly (acrylamide based temperature/pH sensitive hydrogels are reported for controlled drug delivery for the model drug methylene blue/methylene orange. These hydrogels exhibited excellent pH sensitivity and have maximum swelling at pH 7.4

[25]. Bacterial cellulose currently used as promising hydrogels for the development of functional nano-biocomposites, for biomedical and electroconductive fields [26-27]. The derived materials can display appropriate mechanical properties when being used as membranes. Recently in one research article, composite systems of bacterial cellulose with collagen were, employed in order to promote cell adhesion and viability. Herein, bacterial cellulose membrane surfaces were coated with collagen and alginate on each sides to favour cell adhesion, and protected the transplanted cells from immune rejection, respectively [28, 29]. A promising feature for cellulose is its use as a material for cell encapsulation, and its ability to release dopamine through the composite membrane. The high purity and hydrophilicity of bacterial cellulose also makes it as a favourable material for wound-healing applications with different products already commercialized for dressings, e.g., XCell, Biofill, or Dermafill [30-32].

### *1.3.2. Chitosan Based Hydrogels*

Chitosan is a term referred to deacetylated chitin, containing at least 60% D-glucosamine [33]. Chitosan is mainly obtained from the deacetylation of the natural polymer chitin, and is considered the most abundant natural biopolymer after cellulose [34]. Chitosan hydrogels have the great capability to be formulated in the form of chitosan beads, which are micro/nano-sized, spherical particles, and encapsulate different bioactive molecules *viz.* drugs, proteins or enzymes. Ghanem et al. 2004, developed a method of synthesizing chitosan beads for the purpose of enzyme immobilization. In this method chitosan beads were synthesised by adjoining glucose oxidase enzyme to the biopolymer through carbodiimide conjugation to form enzyme-biopolymer complex. Development of chitosan-based hydrogel cross-linked with glutaraldehyde, loaded with cholesterol and was evaluated in a breast cancer xeno-graft mouse model [35, 36]. This hydrogel remarkably showed a reduction in the progression rate of the tumor, and prevented 69% of tumor recurrence, and metastatic spread [37]. The mucoadhesive property of chitosan hydrogels, has greatly interested the researchers, in expending them as drug delivery systems since the bioavailability of loaded bioactive drugs can be increased [38]. Chitosan beads have the capacity to swell in acidic media, thus, facilitating drug release. An additional advantage of chitosan beads is their relative high hydrophobicity, which facilitates intestinal absorption [39]. The chitosan hydrogels have also provided matrices for radioisotopes, so that it can be exploited for the controlled exposure. Further, these radioisotope drugs encapsulated chitosan matrices have also been reported for the targeted cancer therapy. These chitosan hydrogels can display photo-responsiveness, and a thermos-reversible gelling capacity. Numerous hydrogel systems based on chitosan have also been developed for the treatment of colon [40] and hepatic diseases [41, 42].

### *1.3.3. Hyaluronic Acid Hydrogels*

Hyaluronic acid (HA) is a linear copolymer of 2- acetamido-2-deoxy-D-glucoronic acid. It was discovered by scientists from Columbia University in NewYork in 1934 by isolating it from the vitreous fluid of cow's eyes, and since then has shown a great promise clinically. Strong electrostatic interactions with other components like Pluronic F-27, and collagen, make it an appropriate material to be used for various biomedical applications. Hyaluronic acid is known to promote particular medicinal advantages when used in tissue healing, aids in increase in the cell proliferation and migration, and inflammatory response control [43-45]. Song et al., 2016, developed an injectable hydrogel, consisting of N,O-carboxymethyl

chitosan, and aldehyde hyaluronic acid (AHA), that would assist in alleviating the post-surgical adhesion occurring in the peritoneal cavity which is a severe and unbearable complication to patients. The non-toxic, biodegradable and biocompatible gel, was evaluated in both *in vitro* and *in vivo* test models. The results revealed the hydrogel to reduce the levels of peritoneal adhesion, and thus, could be a promising candidate for anti-adhesion applications. Recently, Jung et al., 2017, also developed an injectable thermosensitive hydrogel made from Hyaluronic acid (HA) and Pluronic F-27 (HP) for the long-term sustained release of Piroxicam (PX). The pharmacokinetic levels were analyzed after injection into the articular cavity and it was determined that the HP not only provided a sustained release of PX, but also showed a high bioavailability in physiological environments [46].

### *1.3.4. Dextran Hydrogels*

Dextran is a polymer of glucose and has a linear 1,6-glycosidic bond, with a certain degree of branching through 1,3-linkage. The dextran polymer was first isolated in 1861, utilizing a bacterial culture of the genus *Leuconostoc*, which produced dextran from sucrose during bacterial growth. Dextran hydrogels, introduced as a bioadhesive in the last few years, was used by Li et al. to synthesize a photocrosslinked tissue adhesive gel [47]. Dextran hydrogels using human serum albumin (Dex-HSA) as both a drug transport medium, as well as a crosslinking agent were prepared as a macroscale delivery medium of insoluble drugs *viz*., Ibuprofen, Paclitaxel, and Dexamethasone [48]. Bae et al. 2015, reported using dextran hydrogel microstructures storage units for the sustained release of PEGylated protein carriers. This microstructured design allowed the proteins to be gradually released, while preserving their therapeutic properties, and increasing their half-life [49]. Liu et al. synthesized dextran injectable hydrogels as a site specific, trackable, chemotherapeutic devices. This hydrogel system was synthesized using sericin, a photoluminescent protein extracted from silk, with hydrazone as the crosslinking agent to construct a sericin/dextran injectable hydrogel. The sericin enabled the mechanism to be monitored in real-time *in vivo*, while successfully disintegrating without leaving traces of photoluminescent material behind. The gel achieved successful entrapment of the drug Doxorubicin, and its controlled release, efficiently suppressing tumor growth [50].

### *1.3.5. Alginate Hydrogels*

Alginate polysaccharide, is a copolymer of linear block containing polyanionic blocks (1,4)D-mannuroic b-(M unit) and a-L-guluronic (block G) acid. Alginate is a naturally occurring anionic polymer obtained from the extract of brown seaweeds, and is produced by two types of bacteria, *Azotobacter* and *Pseudomonas*. Alginate has been successfully used for the embedding and transport of cells and therapeutic agents and consequently, is the most investigated natural polymer for use in the encapsulation of living cells [51]. Alginate has the ability to form polyelectrolyte structures upon interaction with polycations such as chitosan and polylysine [52]. Alginate gels, like many other natural polymer hydrogels, are also frequently employed, as tissue engineering matrices. Alginate hydrogel spheres, range from antimicrobial wound dressings, and as tissue engineering frameworks, to articular cartilage grafts. Moreover, the polymer blend of alginate and silk fibroin (SF), when tested on human umbilical vein endothelial cells proved the viability of the polymer in the area of tissue-engineering, and regeneration [53]. Ivanovska et al. 2016, developed a hydrogel which was

designed in such a manner that it was able to simulate the physical structure, arrangement and biological activity, of the extracellular matrix (ECM) for the purpose of advancing cancer research. The study involved the biofabricated pure alginate and cross-linked alginate-gelatine (ADA-GEL) matrices as models for human colon cancer HCT116. The results showed that the ADA-GEL matrix provided a more accurate visual of the cellular network and its proliferation and in particular the mRNA expression. Evaluation of the ADA-GEL and the pure alginate hydrogels showed that ADA-GEL hydrogel was a more efficient 3D system than pure alginate as it simulated the physiology of the tumor micro-environment [54]. These materials are low in cost, available abundantly, and show good biocompatibility with negligible inflammatory effect, after implanting in *in vivo* conditions [55].

## 1.4. Synthetic Polymer Based Hydrogels

Hydrogels synthesized from synthetic polymers, constitute a group of materials used in various therapeutic applications. Synthetic polymers are hydrophobic, and are chemically and mechanically stronger in nature when compared with natural polymers. The improved mechanical strength provides excellent durability of the biomaterial by reducing the rate of its degradation. Hydrogels synthesized in the past for various therapeutic purposes tend to incorporate synthetic polymers such as polyacrylamide and its derivatives; poly vinyl alcohol (PVA), polyethylene glycol (PEG), and poloxamers.

### *1.4.1. Poly(ethylene glycol) (PEG) and Poly (ethylene oxide) (PEO) Hydrogels*

The compounds poly (oxyethylene) (POE), poly(ethylene oxide) (PEO) and Poly(ethylene glycol) (PEG) are chemically synonymous, referring to an oligomer or polymer of ethylene oxide, that can be differentiated based on the molecular weight. The polymer with a molecular weight of <100,000 are usually called PEGs, contrary to those of higher molecular weights that are categorized as PEOs [56]. PEG is the most popular polymer known for its biocompatibility, non-immunogenicity, and resistance to protein adsorption. PEG hydrogels have been exploited greatly in the field of drug delivery, due to its therapeutic actions in directing cellular functions, such as proliferation and differentiation. In addition, it provides localized release of the drug, within the therapeutic range, while minimizing adverse reactions and preserving the bioactivity of therapeutic agents. PEG is also popularly applied to sol-gel chemistry [57]. This process occurs when hydrogel formulations are injected instead of implanted, and undergo gelation spontaneously at the site of injection. In comparison to implants, PEG injectable hydrogels not only avoid use of potentially toxic and denaturing cross-linking agents, as well as increasing the ease of administration resulting in comfort for the patient. These types of hydrogels are useful because they are conveniently able to swell after being administered into the body under specific conditions often referred to as trigger [58].

### *1.4.2. Poloxamer Hydrogels*

Polymers with hydrophobic character might be cross-linked in aqueous environments utilizing reverse thermal gelation process in sol-gel chemistry to yield a modified polymer with utmost desired characteristics [59]. This type of polymer blending is designed to

combine different polymers with preferred attributes, e.g., thermo-responsiveness and pH sensitivity, and is a much economical and quicker option than developing new polymers, or utilizing new polymerization techniques for each polymer. Poloxamers, also known as pluronics, are groups of tri-block polymers, which generally comprise of two hydrophilic blocks adjoining a hydrophobic block. Poloxamer 188 is a triblock co-polymer consisting of poly (ethylene oxide), poly (propylene oxide), poly (ethylene oxide) (PEO-PPO-PEO), while poloxamer 407 is a triblock copolymer consisting of Poly (ethylene glycol), poly (propylene glycol), and poly (ethylene glycol) (PEG-PPG-PEG). Within the process of hydrophobic gelation, hydrophobic fragments are paired to the hydrophilic fraction of the polymers utilizing the copolymerization process or directly using an amphiphilic copolymer [60]. Amphiphilic block copolymers possess many advantages when applied in drug delivery, including: their stability, biocompatibility, potential to be used in site-specific drug delivery, and in the delivery of poorly soluble drugs due to their amphiphilic nature [61]. Heparin-poloxamer (HP) is thermo-sensitive hydrogel designed to boost spinal cord regeneration of nerve growth factor (NGF). Salbutamol sulfate (SS)-poloxamer bioadhesive hydrogel was developed as a drug delivery mechanism for buccal administration using TR146 human buccal epithelium cells due to its cellular toxicity, and trans epithelial diffusion. The Salbutamol sulphate solution produced extreme cell change, after only 2 h of treatment, which the hydrogels averted based on concentrations of both the poloxamer and xanthan gum. These results suggest that salbutamol sulfate-poloxamer bioadhesive hydrogels are feasible for buccal drug delivery [62]. The HA/poloxamer hydrogels having various conformations were synthesized, and biominerlized for the purpose of simulating the extracellular matrix of bone. Pluronics have been candidate materials for use in bioprinting, which is a novel approach in the field of tissue engineering, providing a more accurate and realistic 3D arrangement of the biomaterials [63-65].

### *1.4.3. Poly(hydroxyethyl methacrylate) pHEMA Hydrogels*

Poly (hydroxyethyl methacrylate), is one of the pioneering synthetic hydrogel polymers, introduced by Wichterle and Lim in 1960. It is being exploited in the various fields mainly in the medical and biological areas, due to its characteristics, like non-toxic and biocompatible nature, and high water absorbing capacity [66]. PHEMA is well known for its contribution to tissue engineering as bone substitutes, scaffolds, synthetic biomaterials and drug delivery applications, therefore, its mechanical and swelling properties are often specific to the desired application. The ability of the pHEMA hydrogel to facilitate the delivery of drugs and bioactive agents is directly proportional to its swelling properties. These swelling properties are dependent on the crosslinking agents which are used in the hydrogel synthesis [67]. The pHEMA hydrogel was successfully synthesized by microwave polymerization, potassium persulphate, and polycaprolactone, as initiator and crosslinking agent respectively, and was quantified using FTIR and NMR techniques. This novel hydrogel proved to be a promising addition to tissue engineering owing to its excellent biocompatibility, and degradation profiles along with its non-toxicity *in vitro* assays [68]. In tissue engineering for cancer research, 3D synthetic biomaterial is an emerging technology for *in vivo* and *in vitro* testing, due to the fact that they were more applicable to the body's physiological conditions [69].

### *1.4.4. Polyacrylamide (PAAm) Hydrogels and Its Derivatives*

Polyacrylamide (PAAm) hydrogels are generally synthesized from monomers of acrylamide. Depending on the type of application, its properties can be altered by either adjusting the conditions of synthesis, by copolymerization with other monomers, or by chemical modification of the synthesized hydrogels. PAAm hydrogels generally have a structured cross-linked network, and are often employed as stimuli-responsive polymers, particularly responsive to temperature and pH [70]. The swelling of pH-responsive hydrogels is controlled by the level of ionization, protonation or deprotonation of various tissues and cellular compartments. The primary characteristic of a pH sensitive system is the presence of ionizable, weak acidic or basic moieties bonded to a hydrophobic backbone. When ionized, the coiled chains begin to lengthen extensively, responding to the electrostatic repulsions of the ionic (anions or cations) charges [71]. PAAm pH responsive characteristics, PAAm and its derivatives possess properties that make them choice candidates for the production of thermo-responsive hydrogels. Thermoresponsive hydrogels are known to be very sensitive which makes them extremely useful, particularly when they are introduced into the body. In such cases when the temperature rises from room to body temperature, gelation is initiated without any other chemical or environmental trigger [72].

### *1.4.5. Polyvinyl Alcohol (PVA) Hydrogels*

Polyvinyl alcohol (PVA), a hydrophilic synthetic polymer possessing biocompatible and biodegradable properties, and has been used widely in various biomedical fields. This polymer has proven to be an excellent choice for tissue engineering applications, and is being evaluated as a feasible replacement of current artificial grafts. PVA hydrogels are considered highly viable biomaterials suitable for mimicking tissue structure, vascular cell culture, and vascular implantation, due to their nontoxicity, and mechanical strength. The mechanical strength they possess results from their crosslinking hydrogen bonds. In the study carried out by Hoffman, PVA hydrogels were successfully obtained for culturing living cells, since these hydrogels have large pores and are capable of degradation. PVA hydrogels are used in contact lens production, cartilage reconstruction and regeneration, artificial organs, drugs systems and wound dressings, providing the humid environment beneficial for wound healing. Wound dressing PVA applications were made with gamma irradiated chitosan (CS)/gelatin (Gel)/polyvinyl alcohol (PVA) Hydrogels. These hydrogels showed pH-sensitivity, swelling ability and water evaporation rate, confirming the potential of the CS-PVA hydrogel to be applied as wound dressing. Hayes et al. initiated a biomechanical analysis of a salt-modified polyvinyl alcohol hydrogel, evaluating its potential for use as an artificial implant for meniscal tissue. Stocco et al. synthesized a partially oxidized polyvinyl alcohol that could be used to construct scaffolds with modifiable mechanical behavior, protein-loading ability and biodegradability [73-76].

## 2. POLYMERIC HYDROGELS AND THERAPEUTICS

Polymers occupy a major portion of materials used for controlled release formulations and in biomedical applications, because this class of materials presents seemingly endless diversity in topology and chemistry. In comparison with other classes of materials, polymeric

materials, including natural, semi-natural, and synthetic polymers, present countless opportunities to modulate the properties of drug delivery systems other than to meet several criteria such as biodegradability, biocompatibility because of their diversity in chemistry, topology, and dimension.

## 2.1. Hydrogels in Drug Delivery

Drug delivery is the process of observing, an active pharmaceutical compound to attain the therapeutic effect in humans. Drug delivery method is an expedient formulation technology, which not only aids in modification of drug release, absorption, and distribution of drugs, but also facilitates the patient ease and safety, along with improved product effectiveness. The common routes of drug delivery include topical, transmucosal and inhalation [7]. The drug molecules like peptide and protein, antibody, vaccine and gene based drugs, cannot be delivered by old conventional methods owing to their disposal by either enzymatic degradation or poor absorption into the systemic circulation. Polymers have played an integral role in the advancement of drug delivery technology by providing controlled release of therapeutic agents in constant doses over long periods, cyclic dosage, tunable release of both hydrophilic and hydrophobic drugs and targeted delivery. From early beginnings using off-the-shelf materials, the field has grown tremendously, motivated part by the innovations of chemical engineers [78]. Modern advances in drug delivery are now predicated upon the rational design of polymers tailored for specific cargo and engineered to exert distinct biological functions. Hydrogels and other polymer-based carriers have been developed to provide safe passage for pharmaceuticals through inhospitable physiological regions [79]. The porosity of hydrogels could be modified by controlling the density of cross linkers used or by changing the swelling efficiency of hydrogels in the environment. This porosity of hydrogels helps in release of drugs. The drug release from hydrogel could be guarded by controlling the diffusion coefficient of drugs through hydrogel matrix [80, 81]. All polymeric materials, provide a non-cytotoxic interface between the device and native living tissue or cell culture medium [82].

### *2.1.1. Polymeric Hydrogels Used for Colon-Targeted Drug Delivery*

Polymers play a very important role in the colon targeted drug delivery system. It protects the drug from degradation or release in the stomach and small intestine. It also ensures abrupt or controlled release of the drug in the proximal colon. In the recent years, the use of naturally occurring polysaccharides is attracting a lot of attention for drug targeting to the colon, since these polymers of monosaccharides are found in abundance, have wide availability, are inexpensive, and are available in a verity of a structures with varied properties. These include naturally occurring polysaccharides obtained from plant (guar gum, inulin), animal (chitosan, chondrotin sulphate), algal (alginates), or microbial (dextran) origin. Chitosan has been evaluated for colon specific drug delivery mainly in the form of a capsule forming material. Pectin is another non-starch linear polysaccharide used for colon targeted drug delivery system [83].

### *2.1.2. Mucoadhesive Polymeric Hydrogels for Buccal, Nasal and Ocular Drug Delivery*

The new generation mucoadhesive polymers for buccal drug delivery with advantages such as increase in the residence time of the polymer, penetration enhancement, site-specific adhesion and enzymatic inhibiton, site-specific mucoadhesive polymers will undoubtedly be uitilized for the buccal delivery of a wide variety of therapeutic compounds. The class of polymers has enormous applicability for the delivery of therapeutic macromolecules [84]. The various mucoadhesive polymers used for the development of buccal delivery systems include cyanoacrylates, polyacrylic acid, sodium carboxymethylcellulose, hyaluronic acid, chitosan and gellan. Like buccal cavity, nasal cavity also provides a potential site for the development of formulations where mucoadhesive polymers can play an important role. The mucoadhesive polymers used for the ocular delivery include thiolatedpoly(acrylic acid), poloxamer, cellulose acetophthalate, methyl cellulose, hydroxy ethyl cellulose, poly(amidoamine) dendrimers, poly(dimethyl siloxane) and poly (vinyl pyrrolidone).

### *2.1.3. Polymeric Hydrogels as Floating Drug Delivery System for Gastric Delivery*

Polymers are generally employed in floating drug delivery systems so as to target the delivery of drug to a specific region in the gastrointestinal tract i.e., stomach. Many sophisticated techniques have been utilized to develop floating devices, generally consisting of a capsule containing a drug reservoir and a floating reservoir filled with gas or containing a carbon dioxide generating blend. A simple method for producing floating systems uses polymeric materials with a density lower than that of the gastric fluid. Natural polymers which have been explored for their promising potential in stomach specific drug delivery include chitosan, pectin, xanthan gum, guar gum, gellan gum, karkaya gum, psyllium, starch, husk, starch,alginatesetc [85].

## 2.2. Hydrogels for Sustained Delivery

Sustained release systems include any drug-delivery systems that achieve slow release of drug over an extended period of time and have been categorized into two main classes, i.e., controlled release and prolonged release systems. The controlled release system maintain constant drug levels in the blood or target tissue, while in prolonged release system drug is provided for absorption over a longer period of time than from a conventional dosages form. Sustained release formulations, provide vital way to decrease the side effect of drug, by preventing the fluctuation of the therapeutic concentration of the drug in the body with better patient compliance, as well as increased efficacy of drug. Copolymerization of konjac glucomannan with acrylic acid, and cross-linked by *N*, *N*-methylene-bis-(acrylamide) prepared by Chen et al., 2005, showed *in vitro* release of 5- aminosalicylic acid from the pH-sensitive hydrogel in pH 7.4 phosphate buffer containing Cellulase E0240. The drug release reached 95.19% after 36 h and the drug release has been said to be controlled by the swelling and degradation of the hydrogels. Kulkarni et al., 2008, reported Ketoprofen-loaded pH sensitive interpenetrating network hydrogel beads of polyacrylamide-*g*-xanthan, and sodium carboxymethyl cellulose, and evaluated the pH sensitivity and drug release characteristics. Protein loaded nanoparticles (150- 280 nm) of hydrogel are reported. *In vitro* release study showed that these nanoparticles could provide sustained drug release for more than 24h.

Pourjavadi et al., 2005, reported that a novel superabsorbent hydrogel of hydrolyzed alginate-*g*-polymethacrylamide could exhibit high swelling capacity at basic pH and reversible pH responsiveness property, and therefore this hydrogel may be considered as an excellent candidate to design sustained drug delivery systems [86-90]. Chitosan-g-poly (acrylamide)/Zn nanocomposite hydrogels prepared by simple method in presence of microwave radiation. These drug delivery systems using ofloxacinhas are studied for controlled drug delivery and antibacterial activity [91]. CMC/p (LA-co-IA) hydrogel was prepared by grafting of itaconic acid and lactic acid onto carboxymethyl cellulose using MBA and potassium persulphate as crosslinker and initiator respectively for controlled delivery of amoxicillin [92]. A gastroretentive controlled release drug delivery system for Ciprofloxacin hydrochloride, having swelling, floating, and adhesive properties, was successfully formulated by effervescent technique for prolonged release of drug [93].

## 2.3. Polymeric Hydrogels for Tissue Engineering

Tissue engineering has three basic components namely, cells/tissues, scaffolds and implantation and/or grafting. Hydrogels can be used as matrices in tissue engineering either directly or after formulation as scaffolds. Hydrogel-based scaffolds are a very important class of due to the ability to tailor their mechanical characteristics to mimic those of natural tissues. Hydrogel scaffolds are used in particular to provide bulk and mechanical structures to a tissue construct, whether cells are suspended within or adhered to the 3D hydrogel framework. The principles of tissue engineering have been used extensively to restore the function of traumatized/malfunctioning tissues or organs. A wide range of natural origin polymers with special focus on proteins and polysaccharides might be potentially useful as carriers systems for active biomolecules or as cell carriers with application in the tissue engineering field targeting several biological tissues [94]. In general, hydrogels based on polymers from natural origins such as collagen are advantageous in tissue engineering applications due to their intrinsic characteristics of biological recognition, including presentation of receptor-binding ligands, and the susceptibility to cell-triggered proteolytic remodeling, and degradation. Collagen-coated tissue culture inserts are used for growing three- dimensional corneal implant, tracheal gland cells etc. Poly (lactic-co-glycolic acid) (PLGA) polymer foams are seeded with preadipocytes for the epithelial cell culture of the breast. Fedorovich et al., 2012, created a bioprinted osteochondrol graft consisting of chondrocytes in an alginate hydrogel and mesenchymal stem cells in an alginate- hydroxyapatite-tricalcium phosphate hydrogel [95]. Porous scaffolding (e.g., filter, swatch of nylon, biodegradable microcarrier) coated with fibrillar collagen mixed with fibro nectin or with Matrigel are used for the culture of the normal mature liver cells (polyploidy liver cells) [96].

## 2.4. Polymeric Hydrogels Used for the Gene Therapy

Gene delivery from hydrogel biomaterials offers the opportunity to improve current gene delivery technologies for a range of applications in gene therapy and regenerative medicine. Gene delivery from hydrogel biomaterials provides a fundamental tool for a variety of clinical

applications including regenerative medicine, gene therapy for inherited disorders and drug delivery. The high water content and mild gelation conditions of hydrogels support their use for gene delivery by preserving activity of vectors and acting to shield vectors from any host immune response. The use of polymers like polylactic acid (PLA), polylactic-co-glycolic acid (PLGA) and polyglycolic acid (PGA), has gained importance due to their biodegradability. The PEG-PLGA-PEG hydrogel was used for the delivery of plasmid-beta gene, which showed the increased wound healing process in diabetic mouse model [97].

## 3. General Mechanism of Drug Release from Polymeric Hydrogel

In general, the drug release from polymeric hydrogel can follow three basic mechanisms, i.e., diffusion, desorption, and swelling. The diffusion can be exterior or interior diffusion [98]. Exterior diffusion takes place when drug molecules diffuse from surface of the hydrogel matrix to bulk of the liquid phase and vice-versa. However, the rate of drug release is controlled by interior diffusion. In the desorption, drug molecules can be adsorbed either chemically or physically on the pore surface [99]. In chemisorptions, the electronic structure (electronic density) of adsorbate molecule is strongly modified. In physical adsorption the adsorbate is weakly adherent by secondary interactions (e.g., van der Waals forces). Moreover, the processes of shape change (e.g., heterogeneous and homogeneous erosion) and processes of surface change (desorption, reconstruction, and reaction) can overlap to above phenomena. The rate of mass transfer can be controlled by physical adsorption if the rate of desorption is finite (or is comparable to the rate of diffusion). The mechanism of hydrogel swelling is one of the most important factors in drug release phenomena. This mechanism of drug release occurs when diffusion of an active agent is faster than hydrogel swelling [100]. In swelling-controlled systems, hydrogels may undergo a swelling-driven phase transition from a glassy state to rubbery state. This transition occurs when the characteristic glass-rubber polymer transition temperature is lower than temperature of fluid, which surrounds the drug delivery matrix. In the glassy state, entrapped molecules remain immobile. In the rubbery state dissolved drug molecules rapidly diffuse to the fluid through the swollen layer of polymer. Released fluid molecules contact the external layer of hydrogel. This forms a moving front that divides hydrogel matrix into a glassy and swollen region. In these systems the rate of molecule release depends on the rate of gel swelling [101-105].

## Conclusion

Biopolymers based hydrogels, are versatile promising tools for various types of biological applications, and have the capability to be employed for drug delivery therapeutics. Besides this, hydrogels demonstarted significant antiviral, anticancer, antibacterial, antimicrobial, and antifungal activity, which could be combined with the drugs for the benefit of synergitic action and avoidance of dose related side-effects. They also possess a high content of functional groups that can be utilized for cross linking with additional functional cross linkers as well as for further bio-conjugation with cell targeting agents. Many

achievements have been gained in development of polymeric hydrogels for release of therapeutic agents which are described in this chapter. Common natural and synthetic hydrogel formulations, are highlighted and their most current and impactful contributions to biomedical science reviewed. These hydrogels are promising in sustained drug delivery, tissue engineering and regenerative medicine. With consistent efforts of our groups and researchers globally, we hope patients can take a benefit from pH- and temperature-responsive hydrogels in the near future. Future research on biopolymer based delivery systems should focus on developing new methods for fabrication and refining or adapting current methods for their application to medical, pharmaceutical field.

## REFERENCES

[1] Ahmed E. M. 2015. Hydrogel: Preparation, characterization, and applications: A review. *J. Adv. Res.* 6:105–121.

[2] Sun Y., Kaplan J., Shieh A., Sun H. L., Croce C. M., Grinstaff M. W., Parquette J. R. 2016. Self-assembly of a 5-fluorouracil-dipeptide hydrogel. *Chem. Commun.* 52:5254–5257.

[3] Kim S. H., Sun Y., Kaplan J. A., Grinstaff M. W., Parquette J. R. 2015. Photo-crosslinking of a self-assembled coumarin-dipeptide hydrogel. *New J. Chem.* 39: 3225–3228.

[4] Verhulsel M., Vignes M., Descroix S., Malaquin L., Vignjevic D. M., Viovy J. L. 2014. A review of microfabrication and hydrogel engineering for micro-organs on chips. *Biomaterials.* 35:1816–1832.

[5] Daniele M. A., Adams A. A., Naciri J., North S. H., Ligler F. S. 2014. Interpenetrating networks based on gelatine methacrylamide and PEG formed using concurrent thiol click chemistries for hydrogel tissue engineering scaffolds. *Biomaterials.* 35:1845–1856.

[6] Yu X., Jiao Y., Chai Q. 2001. Applications of Gold Nanoparticles in Biosensors. *Nanolife.* 6-164.

[7] Yom Tov O., Neufeld L., Seliktar D., Bianco-Peled H. 2014. A novel design of injectable porous hydrogels with in situ pore formation. *Acta Biomater.* 10: 4236-4246.

[8] Abebe D. G., Fujiwara T. 2012. Controlled thermoresponsive hydrogels by stereocomplexed PLA-PEG-PLA prepared via hybrid micelles of premixed copolymers with different PEG lengths. *Biomacromolecules.* 13: 1828-1836.

[9] Chung H. J., Lee Y., Park T. G. 2008. Thermo-sensitive and biodegradable hydrogels based on stereocomplexedPluronic multi-block copolymers for controlled protein delivery. *J Control Release.* 127: 22-30.

[10] Kirakci K., Šícha V., Holub J., Kubát P., Lang K. 2014. Luminescenthydrogel particles prepared by self-assembly of Î²-cyclodextrinpolymer and octahedral molybdenum cluster complexes. *Inorg Chem.* 53: 13012-13018.

[11] Kono H., Teshirogi T. 2015. Cyclodextrin-grafted chitosan hydrogelfor controlled drug delivery. *Int J Biol Macromol.* 72: 299-308.

[12] Wei Yang Seow, Charlotte A. E. Hauser. 2014. Short to ultrashort peptide hydrogels for biomedical uses. *Materials Today.* 17:381-388.

[13] Lee S. C., Kwon I. K., Park K. 2013. Hydrogels for delivery of bioactive agents: a historical perspective. *Adv Drug Deliv Rev.* 65: 17-20.

[14] Kopecek J. 2007. Hydrogel biomaterials: a smart future. *Biomaterials.* 28: 5185-5192.

[15] Wichterle O., Lìm D. 1960. Hydrophilic Gels for Biological Use. *Nature* 185:117-118.

[16] Buwalda S. J., Boere K. W., Dijkstra P. J., Feijen J., Vermonden T. 2014. Hydrogels in a historical perspective: from simple networks to smart materials. *J Control Release.* 190: 254-273.

[17] Harland R. S., Prud'homme R. K. 1992. *Polyelectrolyte Gels: Properties, Preparation, and Applications;* American Chemical Society: Washington, DC, USA.

[18] Yannas I. V., Lee E., Orgill D. P., Skrabut E. M., Murphy G. F. 1989. Synthesis and characterization of a model extracellular matrix that induces partial regeneration of adult mammalian skin. *Proc. Natl. Acad. Sci. USA.* 86, 933–937.

[19] Peppas N. A. 1987. *Hydrogels in Medicine and Pharmacy.* CRC Press 21:184.

[20] Shin Jinsub, Braun Paul V., Lee Wonmok. 2010. Fast response photonic crystal pH sensor based on templatedphotopolymerized hydrogel inverse opal. *Sens Actuat B: Chem.* 150(1):183–90.

[21] Takashi L., Hatsumi T., Makoto M., Takashi I., Takehiko G., Shuji S. 2007. Synthesis of porous poly(N-isopropylacrylamide) gel beads by sedimentation polymerization and their morphology. *J Appl Polym Sci.* 104(2):842.

[22] Yang L., Chu J. S., Fix J. A. 2002. Colon-specific drug delivery: new approaches and in vitro/in vivo evaluation. *Int J Pharm.* 235:1–15.

[23] Maolin Z., Jun L., Min Y., Hongfei H. 2000. The swelling behaviour of radiation prepared semi-interpenetrating polymer networks composed of polyNIPAAm and hydrophilic polymers. *Radiat Phys Chem.* 58:397–400.

[24] A. S. Hoffman. 2002. Hydrogels for biomedical applications, *Adv. Drug Deliv. Rev.* 54, 3-12.

[25] D. Parveen, K. Reet. 2013. Hyaluronic acid: a boon in periodontal therapy, *N. Am. J. Med. Sci.* 5:309–315.

[26] B. V. Nusgens. 2010. Hyaluronic acid and extracellular matrix: a primitive molecule? *Ann Dermatol. Vener.* 137:3–S8.

[27] N. Shah, M. Ul-Islam, W. A. Khattak, J. K. Park. 2013. Overview of bacterialcellulose composites: A multipurposeadvanced material. *Carbohydrate. Polym.* 98:1585–1598.

[28] M. Ul-Islam, S. Khan, M. W. Ullah, J. K. Park. 2015. Bacterial cellulose composites: Synthetic strategies and multiple applications in bio-medical and electroconductive fields. *J. Biotechnol.* 10:1847–1861.

[29] M. Park, S. Shin, J. Cheng, J. Hyun. 2017. Nanocellulose based asymmetric composite membrane for the multiple functions in cell encapsulation. *Carbohydr. Polym.* 158:133–140.

[30] S. Kusuma, Y. Shen, D. Hanjaya-Putra, P. Mali, L. Cheng, S. Gerecht. 2013. Self-organized vascular networks from human pluripotent stem cells in a synthetic matrix. *Proc. Natl. Acad. Sci. USA.* 110:2601–12606.

[31] N. Petersen, P. Gatenholm. 2011. Bacterial cellulose-based materials and medical devices: Current state andperspectives. *Appl. Microbiol. Biotechnol*. 91:1277–1286.

[32] O. Portal, W. A. Clark, D. J. Levinson. 2009. Microbial cellulose wound dressing in the treatment of nonhealinglower extremity ulcers. *Wounds.* 21:1–3.

[33] Joye, I. J.; McClements, D. J. Biopolymer-based nanoparticles and microparticles: Fabrication, characterization, and application. *Curr. Opin. Colloid Int. Sci.* 2014, 19, 417–427.

[34] M. Rani, A. Agarwal, Y. S. Negi. 2010. Review: Chitosan based hydrogel polymeric beads – As drug delivery system. *Bio Resources.* 5:2765–2807.

[35] J. H. Park, G. Saravanakumar, K. Kim, I. C. Kwon. 2010. Targeted delivery of low molecular drugs using chitosan and its derivatives. *Adv. Drug Deliv. Rev*. 63:28–41.

[36] M. K. Chourasia, S. K. Jain. 2004. Polysaccharides for colon targeted drug delivery. *Drug Deliv.* 11:129–148.

[37] Y. Kato, H. Onishi, Y. Machida. 2001. Biological characteristics of lactosaminated N-succinyl-chitosan as a liver-specific drug carrier in mice. *J. Control. Release.* 70, 295–307.

[38] E. Ruel-Gariepy, M. Shive, A. Bichara, M. Berrada, D. Le Garrec, AChenite, J. C. Leroux. 2004. A thermosensitive chitosan-based hydrogel for the local delivery of paclitaxel. *Eur. J. Pharm. Biopharm.* 57:53–63.

[39] K. Obara, M. Ishihara, Y. Ozeki, T. Ishizuka, T. Hayashi, S. Nakamura, Y. Saito, H. Yura, T. Matsui, H. Hattori. 2005. Controlled release of paclitaxel from photocrosslinked chitosan hydrogels and its subsequent effect on subcutaneous tumor growth in mice. *J. Control. Release.* 110:79–89.

[40] M. Park, H. Chang, D. H. Jeong, J. Hyun. 2013. Spatial deformation of nanocellulose hydrogel enhances SERS. *Biochip J.* 7:234–241.

[41] L. Song, L. Li, T. He, N. Wang, S. Yang, X. Yang, Y. Zeng, W. Zhang, L. Yang, Q. Wu, C. Gong. 2016. Peritoneal adhesion prevention with a biodegradable and injectable N,O-carboxymethylchitosanaldehyde hyaluronic acid hydrogel in a rat repeated-injury model, *Sci. Res.*

[42] Y. Jung, W. Park, H. Parka, D. Lee, K. Na. 2017. Thermo-sensitive injectable hydrogel based on the physical mixing of hyaluronic acid and Pluronic F-127 for sustained NSAID delivery, *Carbohyd. Polym.* 156: 403–408.

[43] K. Farrell, J. Joshi, C. R. Kothapalli. 2016. Injectable uncrosslinked biomimetic hydrogels as candidate scaffolds for neural stem cell delivery, *J. Biomed. Mater. Res.*

[44] P. S. Babo, R. L. Reis, M. E. Gomes. 2016. Production and characterization of hyaluronic acid microparticles for the controlled delivery of growth factors using aspray/dehydration method. *J. Biomater. Appl.* 31: 693–707.

[45] A. Sannino, C. Demitri, M. Madaghiele. 2009. Biodegradable cellulose-based hydrogels: design and applications. *Materials.* 2:353–373.

[46] W. K. Czaja, D. J. Young, M. Kawecki, R. M. Brown. 2007. The future prospects of microbial cellulose in biomedical applications, *Biomacromolecules* 8:1–12.

[47] F. Aouada, M. Moura, W. Orts, L. Mattoso. 2010. Polyacrylamide and methylcellulose hydrogel as delivery vehicle for the controlled release of paraquat pesticide, *J. Mater. Sci.* 45: 4977–4985.

[48] P. L. Nasatto, F. Pignon, J. L. M. Silveira, M. E. R. Duarte, M. D. Noseda, M. Rinaudo. 2015. Methylcellulose, a cellulose derivative with original physical propertiesand extended applications, *Polymers.* 7:777–803.

[49] M. Takigami, H. Amada, N. Nagasawa, T. Yagi, T. Kasahara, S. Takigami, M. Tamada. 2007. Preparation and properties of CMC gel, *Trans. Mater. Res. Soc. Jpn.* 32:713–716.

[50] E. Caló, V. Khutoryanskiy. 2015. Biomedical applications of hydrogels: a review of patents and commercial products. *Eur. Polym. J.* 65:252–267.

[51] D. Seliktar. 2005. Extracellular stimulation in tissue engineering, *Ann. NY Acad. Sci.* 1047:386–394.

[52] G. T. Gold, D. M. Varma, P. J. Taub, S. B. Nicoll. 2015. Development of crosslinked methylcellulose hydrogels for soft tissue augmentation using an ammoniumpersulfate-ascorbic acid redox system, *Carbohyd. Polym.* 34:497–507.

[53] M. P. Rowan, L. C. Cancio, E. A. Elster, D. M. Burmeister. 2015. Burn wound healing treatment: a review and advancements, *Crit. Care.*

[54] S. Kusuma, Yu. I. Shen, D. Hanjaya-Putra, P. Mali, L. Cheng, S. Gerecht. 2013. Self-organized vascular networks from human pluripotent stem cells in asynthetic matrix, *Proc. Natl. Acad. Sci.* 110-31.

[55] H. Li, R. Niu, J. Yang, J. Nie, D. Yang. 2011. Photocrosslinkable tissue adhesive based on dextran, *Carbohyd. Polym*. 86:1578–1585.

[56] R. A. Omer, A. Hughes, J. R. Hama, W. Wang, H. Tai. 2015. Hydrogels from dextran and soybean oil by UV photo-polymerization, *J. Appl. Polym. Sci.* 132:6.

[57] Y. Gao, R. E. Kieltyka, W. Jesse, B. Norder, A. V. Korobko, A. Kros. 2014. Thiolated human serum albumin cross-linked dextran hydrogels as a macroscaledelivery system, *Soft Matter* 10:27.

[58] N. Artzi, T. Shazly, C. Crespo, A. B. Ramos, H. K. Chenault, E. R. Edelman. 2009. Characterization of star adhesive sealants based on PEG/dextran hydrogels, *Macromol. Biosci.* 9:754–765.

[59] K. H. Bae, F. Lee, K. Xu, C. T. Keng, S. Y. Tan, Y. J. Tan, Q. Chen, M. Kurisawa. 2015. Microstructured dextran hydrogels for burst-free sustained release of PEGylated protein drugs, *Biomaterials.* 63:146–157.

[60] R. Jin, C. Hiemstra, Z. Zhong, J. Feijen. 2007. Enzyme-mediated fast in situ formation of hydrogels from dextran-tyramine conjugates. *Biomaterials*. 28:2791–2800.

[61] J. Liu, C. Qi, K. Tao, J. Zhang, J. Zhang, L. Xu, X. Jiang, Y. Zhang. 2016. Sericin/dextran injectable hydrogel as an optically trackable drug delivery systemfor malignant melanoma treatment, *ACS Appl. Mater. Interfaces.* 8:6411–6422.

[62] N. Zeng, N. Mignet, G. Dumortier, E. Olivier, J. Seguin, M. Maury, D. Scherman, P. Rat, V. Boudy. 2015. Poloxamerbioadhesive hydrogel for buccal drug delivery: cytotoxicity and trans-epithelial permeability evaluations using TR146 human buccal epithelial cell line, *Int. J. Pharm.* 495:1028–1037.

[63] Y. Li, J. Rodriques, H. Tomás. 2012. Injectable and biodegradable hydrogels: gelation, biodegradation, and biomedical applications, *Chem. Soc. Rev*. 41:2193–2222.

[64] S. N. Pawar, K. J. Edgar. 2012. Alginate derivatization: a review of chemistry, properties and applications, *Biomaterials.* 33:3279.

[65] K. Yong Lee, D. Mooney. 2012. Alginate: properties and biomedical applications, *Prog. Polym. Sci*. 37:106–126.

[66] L. Gasperini, J. F. Mano, R. L. Reis. 2014. Natural polymers for the microencapsulation of cells, *J. R. Soc. Inter.* 11-100.

[67] W. Zhao, X. Jin, Y. Cong, Y. Liu, J. Fu. 2013. Degradable natural polymer hydrogels for articular cartilage tissue engineering. *J. Chem. Technol. Biot.* 88:327–339.

[68] Madzovska-Malagurski, M. Vukasinovic-Sekulic, D. Kostic, S. Levic. 2016. Towards antimicrobial yet bioactive Cu-alginate hydrogels. *Biomed. Mater.* 11-3.

[69] R. Silva, R. Singh, B. Sarker, D. G. Papageorgiou, J. A. Juhasz, J. A. Roether, I. Cicha, J. Kaschta. 2016. Soft-matrices based on silk fibroin and alginate for tissue engineering, *Int. J. Biol. Macromol.*

[70] J. Ivanovska, T. Zehnder, P. Lennert, B. Sarker, A. R. Boccaccini, A. Hartmann, R. Schneider-Stock, R. Detsch. 2016. Biofabrication of 3D alginate based hydrogel for cancer research: comparison of cell spreading, viability and adhesion characteristics of colorectal HCT116 tumor cells. *Tissue Eng.* 22-708–715.

[71] N. Bhattarai, J. Gunn, M. Zhang. 2010. Chitosan-based hydrogels for controlled, localized drug delivery, *Adv. Drug Deliv. Rev*. 62:83–99.

[72] F. Croisier, C. Jérôme 2013. Chitosan-based biomaterials for tissue engineering, *Eur. Polym. J*. 49:780–792.

[73] L. Fan, H. Yang, J. Yang, M. Peng, J. Hu. 2016. Preparation and characterization of chitosan/gelatin/PVA hydrogel for wound dressings, *Carbohydr. Polym.* 146: 427–434.

[74] J. C. Hayes, C. Curley, P. Tierney, J. E. Kennedy. 2016. Biomechanical analysis of a salt-modified polyvinyl alcohol hydrogel for knee meniscus applications, including comparison with human donor samples, *J. Mech. Behav. Biomed*. 56:156–164,

[75] Armum P. V. 2000. Drug delivery market poised for five years of strong growth. *Chemical Market Reporter.* 258:16-23.

[76] Peng C., Zhao Q., Gao C. 2010. Sustained delivery of doxorubicin by porous $CaCO_3$ and chitosan/alginate multilayer-coated $CaCO_3$ microparticles. *Colloids and Surfaces A: Physicochemical and Engineering Aspects*. 353:132-139.

[77] Anirudhan T. S., Nima J., Divya P. L. 2015. Synthesis, characterization and in vitro cytotoxicity analysis of a novel cellulose based drug carrier for the controlled delivery of 5-Fluorouracil, an anticancer drug. *Applied Surface Science.* 355: 64-73.

[78] Zhang Y., Chan H. F., Leong K. W. 2013. Advanced materials and processing for drug delivery: the past and the future. *Adv Drug Deliv Rev.* 65: 104-120.

[79] Angelova N., Hunkeler D. 1999. *Trends Biotechnol.* 17:409.

[80] Pillai O., Panchagnula R. 2001. Polymers in drug delivery. *Curr Opin Chem Biol.* 5: 447.

[81] Elbert D. L., Hubbell J. A. 1996. Surface Treatments of Polymers for Biocompatibility. *Ann Rev Mater Sci.* 26: 365.

[82] P. Vashisth, K. Nikhil, P. Roy, P. A. Pruthi, R. P. Singh, V. Pruthi. 2016. A novel gellan-PVA nanofibrous scaffold for skin tissue regeneration: fabrication and characterization, *Carbohydr. Polym.* 136:851–859.

[83] E. Stocco, S. Barbon, F. Grandi, P. G. Gamba, L. Borgio, C. Del Gaudio, D. Dalzoppo, S. Lora, S. Rajendran, A. Porzionato, V. Macchi, A. Rambaldo, R. De Caro, P. P. Parnigotto, C. Grandi. 2015. Partially oxidized polyvinyl alcohol as a promising material for tissue engineering, *J. Tissue Eng. Regen. Med.*

[84] R. M. Ribeiro, A. P. Duarte, R. Mampuya, J. O. C. Silva. 2012. Hydrogel as a controlled release system, *Charact. Appl.* 95–129.

[85] M. Chen, H. Tsai, C. Liu, S. Peng. 2009. A nanoscale drug entrapment strategy for hydrogel based systems for the delivery of poorly soluble drugs, *Biomaterials.* 3:2102–2111.

[86] M. Rani, A. Agarwal, Y. S. Negi. 2010. Review: chitosan based hydrogel polymeric beads–as drug delivery system. *Bio Resources.* 5:2765–2807.

[87] Allen, V. Loyd., Popovich, G. Nicholas. 2005. Solid oral modified release dosage form & drug delivery system. In: Ansel's pharmaceutical dosage forms & drug delivery system, 8th, Lippincott Williams & Wilkins company, India. 260-274.

[88] Chen L. G, Liu Z. L., Zhuo R. X. 2005. Synthesis and properties of degradable hydrogels of konjacglucomannan grafted acrylic acid for colonspecific drug delivery. *Polymer*. 46: 6274-6281.

[89] Kulkarni R. V. and Sa B. 2008. Evaluation of pHSensitivity and drug release characteristics of (polyacrylamide-grafted-xanthan)-carboxymethyl cellulose-based pH-sensitive interpenetrating network hydrogel beads. *Drug Dev. Ind. Pharm.* 34:1406-1414.

[90] Qian F., Cui F., Ding J., Tang C., Yin C. 2006. Chitosan graft copolymer nanoparticles for oral protein drug delivery: Preparation and characterization. *Biomacromol.* 7: 2722-2727.

[91] Pourjavadi A., Amini-Fazl M. S., Hosseinzadeh H. 2005. Partially hydrolyzed crosslinked alginate graft polymethacrylamide as a novel biopolymer-based superabsorbent hydrogel having pH responsive properties. *Macromol. Res*. 13:45-53.

[92] D. Pathania, D. Guptaa, N. C. Kothiyal, G. sharma, G. E. Eldesoky, Mu. Naushad. 2016. Preparation of a novel chitosan-g-poly(acrylamide)/Zn nanocompositehydrogel and its applications for controlled drug delivery of ofloxacin. *International Journal of Biological Macromolecules.* 84:340–348.

[93] S. Sood, V. K. Gupta, S. Agarwal, K. Dev, D. Pathania. 2017. Controlled release of antibiotic amoxicillin drug using carboxymethylcellulose-cl-poly(lactic acid-co-

itaconic acid) hydrogels. *International Journal of Biological Macromolecules.* 101: 612–620.

[94] Fedorovich N. E., Schuurman W., Wijnberg H. M., Prins H. J., van Weeren P. R., Malda J. 2012. Biofabrication of osteochondral tissue equivalents by printing topologically defined, cell-laden hydrogel scaffolds. *Tissue Eng Part C Methods.* 18(1):33–44.

[95] Mina Ibrahim Tadros. 2010. Controlled-release effervescent floating matrix tablets of ciprofloxacin hydrochloride: Development, optimization and in vitro–in vivo evaluation in healthy human volunteers. *European Journal of Pharmaceutics and Biopharmaceutics*. 74:332–339.

[96] J. H. Park, G. Saravanakumar, K. Kim, I. C. Kwon. 2010. Targeted delivery of low molecular drugs using chitosan and its derivatives, *Adv. Drug Deliv. Rev.* 63:28–41.

[97] M. K. Chourasia, S. K. Jain. 2004. Polysaccharides for colon targeted drug delivery, *Drug Deliv.* 11:129–148.

[98] S. K. Jain, A. Jain. 2008. Target-specific drug release to the colon. *Exp. Opin. Drug Deliv.* 5:483–498.

[99] Z. Ke, H. Guo, X. Zhu, Y. Jin, Y. Huang. 2015. Efficient peroral delivery of insulin via vitamin B12 modified trimethyl chitosan nanoparticles, *J. Pharm. Pharm. Sci.* 18:155–170.

[100] R. Hejazi, M. Amiji. 2003. Chitosan-based gastrointestinal delivery systems. *J. Control. Release.* 89:151–165.

[101] Lee PY, Li Z, Huang L. 2003. Thermosensitive hydrogel as a Tgf- beta 1 gene delivery vehicle enhances diabetic wound healing., *Pharm Res.* 20: 1995-2000.

[102] Y. Kato, H. Onishi, Y. Machida. 2001. Biological characteristics of lactosaminated N-succinyl-chitosan as a liver-specific drug carrier in mice. *J. Control. Release.* 70:295–307.

[103] Z. Yuan, X. Sun, T. Gong, H. Ding, Y. Fu, Z. Zhang. 2007. Randomly 50% N-acetylated low molecular weight chitosan as a novel renal targeting carrier. *J. DrugTarget.* 15:269–278.

[104] E. Ruel-Gariepy, M. Shive, A. Bichara, M. Berrada, D. Le Garrec, A. Chenite, J. C. Leroux. 2004. A thermosensitive chitosan-based hydrogel for the local deliveryof paclitaxel, *Eur. J. Pharm. Biopharm.* 57:53–63.

In: Advances in Polymers for Biomedical Applications ISBN: 978-1-53613-612-8
Editors: Deepak Pathania and Bhuvanesh Gupta 

*Chapter 13*

# BIOINSPIRED MATERIALS FOR DIAGNOSTIC IMAGING APPLICATIONS

***Enza Torino**, Franca De Sarno and Alfonso Maria Ponsiglione***
Department of Chemical, Materials and Industrial Engineering (DICMaPI),
University of Naples "Federico II," Naples, Italy

## ABSTRACT

Nowadays, advancements in imaging technology would give a more detailed and accurate image for better diagnosis and treatment planning. The requirements of probes for bioimaging include high target selectivity, high stability, low cytotoxicity, biocompatibility, and high contrast. To this aim, we need new materials and approaches.

This chapter reports some fundamental results of biomaterials used to design rational architectures for biomedical imaging application.

**Keywords:** biomaterials, MRI, PET, optical imaging, multimodal imaging

## INTRODUCTION

Today, medical diagnostic methodologies have an enormous impact on the diagnosis and in the clinical management of the diseases. In this scenario, the integration of different imaging modalities enables to acquire information on specific biological processes. Among different diagnostic techniques, Magnetic Resonance Imaging (MRI) is a highly flexible, reproducible and non-invasive imaging modality. In contrast to the other medical imaging methods, which expose patients to ionizing radiation, MRI uses strong non-ionizing electromagnetic fields in the radio frequency range, offers an excellent spatial resolution, is operator independent and provides 3D data [1, 2]. Compared to other imaging techniques

* Corresponding author: enza.torino@unina.it.

(i.e., nuclear medicine techniques), it shows low sensitivity and long acquisition time. However, the use of contrast agents (CAs) is often required in MRI scans to improve the enhancement of MRI signals [3]. The majority of these agents are paramagnetic ion complexes, which contain lanthanide elements such as Gadolinium (Gd), or superparamagnetic iron oxide (SPIO) conjugates [4]. These compounds shorten the T1 (or longitudinal) and T2 (or transverse) relaxation time, thereby increasing signal intensity on T1-weighted images or reducing signal intensity on T2-weighted images. Their effectiveness remains limited owing to nephrotoxic effects, lack of tissue specificity, low relaxivity and short circulation half-lives. Moreover, McDonald et al. [5-7] have recently reported results about progressive Gd deposition in the brain after repeated intravenous administration of CAs. As a result, the Food and Drug Administration (FDA) has alarmed the medical community and has recommended healthcare professionals to limit the use of Gd-based CAs unless necessary and to report any possible related side effects. Despite the valuable role of the CAs for MRI, these latest results confirm the need to have a biocompatible system able to boost a clinical relevant Gd-chelate without its chemical modification.

According to these parameters and by exploiting the versatile properties of nano- and bio-materials several nanostructured CAs with enhanced relaxivity have been investigated. This chapter aims to describe and evaluate clinical aspects related to the use of biomaterials such as polymer nanoparticles, block copolymers structures and liposomes for MRI applications. In addition, taking into account that multimodal imaging techniques have a huge impact on the early diagnosis, the design of novel nanocarriers with multimodal imaging characteristics is also of great interest and requires the integration in a single system of complementary imaging functionalities. The main examples of nanovectors that combine MRI with other diagnostic techniques, such as Optical Imaging and Positron Emission Tomography (PET), are set out below with a particular focus on nanoparticle-based multimodal PET/MRI probes [8].

## POLYMER NANOPARTICLES

Nanostructured materials have been shown to have some advantages over conventional CAs. In this field, Polymer Nanoparticles (PNPs) have attracted considerable interest over the last years due to their properties that can be modulated depending on the particular application [9]. Advantages of PNPs as nanovectors include controlled release, the ability to combine therapy and imaging (theranostics) in one nanocarrier, protection of active molecules and its specific targeting, facilitating improvements in the therapeutic index [10].

Several hydrophilic polymers, such as Hyaluronic Acid (HA), Chitosan (CS), Dextran and many others are widely used to manufacture PNPs for biomedical applications. Among them, HA and its derivatives have been investigated for the development of several carrier systems for cancer diagnosis, staging and therapy [11]. HA salts have also been used in combination with CS for drug delivery and diagnostic applications. In this context, Chen and coworkers [12] report a very interesting example of nanotheranostic system in which disease diagnosis and therapy are combined. This nanocarrier has a yolk-shell structure with a radioluminescent yolk based on $Gd_2O_3$:Eu nanospheres, an upconversion luminescent in a silica shell, and a coating constituted by HA/CS combination for pH-triggered drug release.

The deposition of the polymer combination HA/CS is performed in layer-by-layer manner by alternating addition of the particles in HA and CS solutions. The resulting system is also able to act as dual T1/T2 MRI agents. Mitoxantrone (MTX), selected as anticancer model drug, is loaded in the empty area between the core and the shell. The *in vitro* MTX release from the nanocarrier is studied in PBS (pH 7.4) and in acidic conditions (pH 5.0) and, interestingly, a marked difference is noted. The drug release occurs with a faster kinetic in acidic conditions and it may be favorable in cancer therapy, taking into account that in tumors and in endosomes an acidic environment is present. The usefulness of the combination HA/CS is also well documented for different bio-applications [11]. Particularly relevant results have been achieved by Courant et al. [13]. Their goal is to develop a new and straightforward synthesis of high-relaxivity Gd-PNPs for MRI applications, with an optimized production process, Gd-loading, and relaxivity at the same time. They choose to encapsulate a low-risk CA: gadolinium-tetraazacyclododecanetetraacetic acid (also known as Gd-DOTA). Because of its hydrophilic nature, the encapsulation of Gd-DOTA is made in a hydrophilic polymer matrix. For biocompatibility reasons, CS and HA are chosen as polymer matrix. A boosting in relaxation rate is found in Gd-DOTA-loaded PNPs.

Furthermore, recently, Torino et al. [14] have coupled a flow focused nanoprecipitation to an efficient crosslinking reaction based on Divinyl Sulfone (DVS) to entrap the relevant clinical gadolinium-diethylenetriaminepentaacetic acid (also known as Gd-DTPA) in crosslinked Hyaluronic Acid Nanoparticles (cHANPs) able to increase relaxometric properties of CAs without the chemical modification of the chelate. Authors hypothesize that Gd-chelate modifies the solvent affinity of the polymer solution shifting the supersaturation to a low degree and leads to a slow heterogeneous nucleation followed by the growth of produced nuclei into large or aggregated particles. These specific interactions induce flow perturbation, causing an uncontrolled size variation and formation of aggregated morphologies. Subsequently, the macrocyclic molecules are firmly entrapped within the hydrogel matrix, using a crosslinking reaction simultaneously occurring with the nanoprecipitation. Investigations related to the addition of the DVS in the middle channels or into the side channels have also attributed to the hydrogel nanoparticles some peculiar properties responsible for the modulation of the release behavior and swelling properties. *In vitro* MRI results prove that using the flexible platform it is possible to take advantages from the strong interference detected by the presence of Gd-DTPA producing Gd-entrapped NPs with enhanced MRI properties. This observation is crucial to lead potentially to a significant reduction of administration dosage of T1 contrast agents in clinical practice and to gain advantages in the imaging modalities based on nanotechnologies. Indeed, the nanoparticles (NPs) are widely used for the improvement of imaging techniques and all the tunability features reported for this system can potentially reduce limitation linked to a fast clearance from the bloodstream and low detection due to the dependence on the concentration. The proposed approaches aim to overcome some drawbacks of the traditional procedures for the production of NPs such as high polydispersity, expensive and time-consuming purification/recovery steps. Furthermore, results present the effective strategy to dose all species and to control property the entrapment of CAs within the hydrogel nanostructures that influences MRI performances in the signal intensity and, potentially, the tissue specificity. Then, the same authors propose a high versatile microfluidic platform to design, in a one-step process, PEGylated cHANPs entrapping an MRI contrast agent and a dye for multimodal imaging applications [15]. Clinically relevant biomaterials are shaped in the form of spherical

NPs through a microfluidic flow focusing approach. A comparison between post processing and simultaneous PEGylation is reported to evaluate the potentiality of the chemical decoration of the cHANPs in microfluidics. An accurate control of the NPs in terms of size, PEGylation and loading is obtained. Furthermore, *in vitro* cell viability is reported and their ability to boost the magnetic resonance imaging signal up to 6 times is also confirmed. The proposed microfluidic approach reveals its ability to overcome several limitations of the traditional processes and to become an easy-to-use platform for imaging applications [15]. All these results drive to the conclusions that the hydration of the hydrogel structure can be used to control the relaxometric properties of Gd-DTPA. In particular, this concept is explained for the first time by Torino et al. [16] and called Hydrodenticity. The ability to tune the hydrogel structure is proved through a microfluidic flow-focusing approach able to produce cHANPs, analyzed regarding the crosslink density and mesh size, and connected to the characteristic correlation times of the Gd-DTPA. Hydrodenticity explains the boosting (12-times) of the Gd-DTPA relaxivity by tuning hydrogel structural parameters, potentially enabling the reduction of the administration dosage as approved for clinical use [17, 18].

To date, 1H MRI has been widely used in clinical diagnosis, but in recent years, researchers have focused on exploring alternative MRI atoms. Among them, the 19F atom, as the most promising imaging nucleus, owns several unique features such as 100% natural isotopic abundance, low background 19F in the human body, relatively high sensitivity (83% of protons) and a broad range of chemical shifts. Given that the 19F element present in the human body exists in bones and teeth, low doses of fluorinated agents are required for performing 19F MRI [19].

It has been proved that structure of a fluorinated agent is of crucial importance for achieving satisfactory MRI performance. Preferably, a 19F MRI agent shall display a high fluorine content, high signal-to-noise resonance spectrum, short T1 and long T2. To this end, various types of 19F MRI agents have been developed and manufactured in the form of delivery vectors for MRI. For example, Wang et al. [20] prepare 19F moiety loaded nanocomposites with an organic fluorescent core via a facile strategy by encapsulating organic dyes with oleylamine-functionalized polysuccinimide and 1H,1H,2H,2H-perfluorodecyltriethoxysilane (PDTES). The aggregation of organic fluorescent dyes in the core results in significant fluorescence for optical imaging, while the 19F moieties on PDTES allow for simultaneous 19F MRI. Moreover, the nanocomposites exhibit high water dispersibility and excellent biocompatibility. These properties make them promising for both cell imaging and *in vivo* imaging applications.

Among other biomaterials, silica nanostructures have earned a key role in the MRI field. Indeed, in contrast to many other nanomaterials, silica NPs do not acquire any special property from their sub-micrometer size, except for the corresponding increase in surface area. What makes silica NPs fascinating from a nanotechnology point of view is their well-defined and tunable structures (i.e., size, morphology and porosity) and surface chemistry. By introducing new functional groups via well-established siloxane chemistry, it is possible to modify the silica surface to impart new properties to the particles, such as diagnostic and therapeutic capabilities. Moreover, silica NPs are effectively "transparent" in the sense that they do not absorb light in the near-infrared (NIR), visible and ultraviolet regions, or interfere with magnetic fields. In addition, silica NPs are inexpensive, easy to prepare, relatively chemically inert, biocompatible, and water dispersible. A fundamental use of silica particles has been reported by Decuzzi et al. [21]. In their work, they demonstrate the enhanced

efficiency of Gd-based CAs (Gd-CAs) by confining them within the nanoporous structure of intravascularly-injectable Silicon Micro Particles (SiMPs). Effective enhancement is shown for three different Gd-CAs: Magnevist (MAG), a clinically-used $Gd^{3+}$ polyaminocarboxylate complex, and two carbon nanostructure-based lipophilic agents, Gadofullerenes (GFs) and Gadonanotubes (GNTs). The GFs have a single $Gd^{3+}$ ion encapsulated by a spherical fullerene cage of ~0.7 nm in diameter. The external fullerene cage, which prevents the leakage of the $Gd^{3+}$ ions, can be chemically functionalized to provide solubility and biocompatibility. Even after functionalization, the GFs exist as aggregates in solution. The GNTs are nanoscale carbon capsules (derived from full-length single-walled carbon nanotubes) with a length of 20-80 nm and a diameter of about 1.4 nm, which are internally loaded with $Gd^{3+}$ ion clusters. Within the GNTs, the $Gd^{3+}$ ions are present in the form of clusters (<10 $Gd^{3+}$ ions per cluster), and each GNT contains approximately 50 to 100 $Gd^{3+}$ ions. The $Gd^{3+}$ clusters are stable and the $Gd^{3+}$ ions do not leak from the nanocapsules under physiological conditions. Because of the hydrophobic nature of their external carbon sheath, the GNTs exist in the form of bundles. In this work, a homogeneous dispersion of GNTs (debundled GNTs) is prepared using Na0/THF reduction.

As assessed in the introduction, multimodal imaging is becoming the new perspective into the fields of clinical and preclinical imaging, and nanomedicine represents a valid field of application to support its development. Here, it is reported a successful example, developed by the author of this chapter, to combine boosted MRI with Optical Imaging or PET. To the best of our knowledge, this is the only case reported in literature that describes the development of a nanoprobe for multimodal imaging with improved relaxometric properties and without the chemical modification of the chelate. In particular, core-shell polymer NPs are obtained, which can be encapsulated with both Gd-DTPA and a dye for Dual Imaging applications through a complex coacervation that exploits an innovative double crosslinking to improve the stability of the nanostructure overcoming the interference of the Gd-DTPA in the coacervation process [22]. Furthermore, the adjustment of the process parameters, the coacervation and chemical reaction kinetic promote the interpolation of the hydrophobic core with the hydrophilic shell, controlling the water exchange and, consequently, the relaxation rate T1, enhancing the MRI signal at reduced concentration compared to the relevant clinical CAs. Finally, process conditions able to develop a pH-sensitive behavior of the Hybrid Core-Shell (HyCoS) NPs have been identified.

Further investigations are required to highlight the benefits and the drawbacks of this behavior and to consider the system as an effective and safe platform for theranostic nanomedicine. Further developments of this project have been the upgrade of the designed nanosystem to the trimodal applications and *in vivo* tests. In particular, a study of HyCoS NPs with the Fluorodeoxyglucose ($^{18}$F-FDG) is planned for PET-MRI applications [23].

## BLOCK COPOLYMERS

Polymers containing a mixture of repeat units are known as copolymers. They occupy an extensive research area and are well known in size and chemical composition [24]. For this reason, the interest in synthesis and characterization of copolymers is increased enormously in the last years thanks to their ability to generate nanostructures in aqueous solution by

varying their architectures. Therefore, the synthetic nature of copolymers allows the design of interfaces containing various biochemically active functional groups. Among them, Block Copolymers (BCPs) are a specific type of copolymer system such that each monomer is homopolymerized to create chemically distinct domains.

A broad range of functional BCPs with tailored properties and organic or inorganic components are now accessible especially for pharmaceutical or diagnostic applications [25, 26].

An increased number of reports on the synthesis, structures, properties and applications of copolymers have been published in the last years [27]. A vast majority of di- and tri-block copolymers are used for the creation of nanosystems loaded with imaging agents, not only to protect these agents from degradation or inactivation *in vivo* but also to optimize dosage and efficacy. These molecules can be physically encapsulated into polymer assemblies or covalently conjugated onto polymer chains. Moreover, as known, the polymer carriers with surface bioconjugation is the key to prolong the bioavailability of the encapsulated active molecules.

Particularly remarkable are the data reported by Xiao et al. [28] about a new Gd-copolymer (ACL-A2-DOTA-Gd), developed as a potential liver MRI contrast agent. ACL-A2-DOTA-Gd consists of a poly (aspartic acid-co-leucine) unit bound with Gd-DOTA via the linkage of ethylenediamine. *In vitro* experiments show that new complex is biodegradable, biocompatible and its relaxivity is 2.4 times higher than the clinical Gd-DOTA. *In vivo* MRI study and biodistribution in rats confirm that Gd-copolymers are mainly accumulated in the liver with a long time-window.

Hou et al. [29], instead, report a novel approach to synthesize poly(ethylene glycol) (PEG)-based Gd-NPs with small size (7 nm) and high relaxivity. They construct a pentablock copolymer through two sequential atom transfer radical polymerization (ATRP) reactions. The nanostructure consists of a Gd chelates-conjugated block in the center and PEG-terminated segments at both ends. In this way, the interactions of Gd chelates with proteins are shielded by the hydrated PEG segments. *In vitro* and *in vivo* studies demonstrate that the relaxivity is 20 times higher than commercial CA.

Then, Cao and coworkers [30] synthesize a new type of triblock polymeric micelle-based on biocompatible poly(glycerol) (PG) and poly(caprolactone) (PCL) for tumor-targeted MRI *in vivo*. Gd chelates (such as Gd-DOTA) and folic acid (FA) molecules are conjugated to PG block through efficient click chemistry reaction, and the final structure is T-micelle (PCL-PG-PCL-g-DOTA(Gd)+FA) of 250 nm. T-micelles exhibit a higher longitudinal relaxivity (r1) and show significant targeting specificity to tumor cells. The capability of T-micelle as an MRI contrast agent for better visualization of tumor tissue is evaluated *in vivo* in tumor-bearing mice at different time points. The results indicate that FA functionalized T-micelles could provide efficient contrast effect at the tumor region through targeting specificity.

Luo et al. [31] have successfully synthesized an amphiphilic poly(aminoethyl ethylene phosphate)/poly(L-lactide) (PAEEP-PLLA) copolymer by the ring-opening polymerization reaction, which contains hydrophobic PLLA and hydrophilic PAEEP segments with good biocompatibility and biodegradability. Oleylamine-coated $Fe_3O_4$ magnetic nanoparticles (OAM-MNPs) are encapsulated into the PAEEP-PLLA copolymer nanoparticles, while molecules of lactoferrin (Lf) are conjugated for glioma tumor targeting. The results indicate reliable, long-lasting, tumor targeting, and contrast-enhanced MRI ability of Lf-MPAEEP-PLLA-NPs owing to the selective accumulation in brain glioma tissue.

Another interesting strategy for the development of new contrast reagents is the synthesis of amphiphilic Gd- complexes that can form micelles spontaneously. Jeong and colleagues [32] synthesize biocompatible amphiphilic derivatives of DOTA with hydrophobic alkyl chains, whose Gd are incorporated into DOTA of micelles via ethylenediamine. To prepare the micelle-formed MRI contrast agent with Gd, hydrophilic (mPEG) and hydrophobic moieties (hexadecylamine) are conjugated with the Poly-N-hydroxyethylacrylamide (PHEA) backbone, with PEG chains exposed to the external aqueous phase. The final structure (PHEA-mPEG-C16-ED-DOTA-Gd) has an average diameter of 180 nm and can be used for the detection of liver lesion. *In vitro* experiments show that this nanovector give better imaging contrast than commercial CA at low Gd concentration. Therefore, when the solution of PHEA-mPEG-C16-ED-DOTA-Gd is intravenously injected into an animal model, detailly a rabbit, the T1-weighted image of the liver in an animal model shows prolonged intravascular duration time of about 30 min.

With the rapid development of synthetic polymers and nano-techniques, stimuli-responsive block copolymers and corresponding assemblies are created one after another and used for targeted delivery of drugs to tumor sites. These vehicles are able to react to internal environmental changes (temperature, ionic strength, light, pH level, pressure) or to external stimuli (light and electromagnetic field) exhibiting reversible or irreversible changes in chemical structures and physical properties [33]. In particular, the measurement of pH *in vivo* has received considerable attention because, in presence of solid tumors, it provides the potential not only for early detection and diagnosis of tumors but also for monitoring the efficacy of the treatment plan used to combat the disease [34]. The non-invasive measurement of pH is carried out also by MRI. Gao and coworkers [35] are one of the first groups that prepared a stimuli-responsive BCPs by encapsulating iron oxide NPs in a pH-responsive diblock copolymer, consisting of poly(ethylene oxide) (PEO) as the hydrophilic, biocompatible segment and a poly(β-amino ester) (PAE) as the pH-sensitive segment. When the pH is low (<7.0), the transverse relaxivity (r2) of the imaging agent increases due to the release of the iron oxide nanoparticles from the core of the micelles. Subsequently, Okada et al. [36] develop a different approach to prepare a pH-responsive system by attaching Gd-chelates to poly(methacrylic acid) (PMAA). *In vitro* MRI studies indicate that the relaxivity of the CA increases of two times when the environmental pH is acid. Also Zhu et al. [37] design a pH-responsive MRI contrast agent that demonstrates significant changes in terms of relaxivity upon changes in the environmental pH at physiological relevant values. Recently, to enhance the stability of polymeric micelles, Hu et al. [38] report the fabrication of crosslinked micellar structure, which covalently labeled with Gd-DOTA and green-emitting fluorophores within pH-responsive cores, serving as a dual-modality MR/fluorescence imaging agents. The acidic pH-triggered turn-on and the enhancement of signal intensities for both imaging modalities are reported. Compared with non-crosslinked diblock precursor, this system shows better MR and fluorescence imaging performance due to structural stability. Subsequently, the same group develops a novel theranostic poly-prodrug platform with synergistic imaging/chemotherapy capability consisting of hyperbranched cores conjugated with reduction-activatable prodrugs (an anticancer agent), MRI CA (Gd complex) and hydrophilic coronas functionalized with guanidine residues [39]. The hyperbranched cores avoid the potential interactions between anticancer agent and blood components and serve as the embedding matrix for MR contrast agents to weaken MR background signals. Upon

cellular internalization, the synergistic turn-on of therapeutic potency and enhanced diagnostic imaging in response to tumor environment are achieved.

In addition, Mouffouk et al. [40] report the development of a smart CA composed of pH-sensitive micelles containing a hydrophobic Gd-complex with the aim of specifically detecting cancer by MRI. This vector (35–40 nm) consists of pH-sensitive polymeric micelles formed by self-assembly of a diblock copolymer poly(ethyleneglycol-b-trimethylsilyl methacrylate) (PEG-b-PTMSMA), loaded with the hydrophobic complex tetraaquodichloro(4,4'-di-t-butyl-2,2'-bipyridine) Gadolinium(III) chloride (tBuBipyGd) and decorated with a specific monoclonal antibody (mAb) against the human MUC1 protein, which is more expressed in many epithelial cancers and a specific targeting vector in preclinical and clinical trials. This system is able to amplify the MRI signal chemically and at the same time can remain silent during circulation; in fact, the CA remains in the "off state," being activated only upon micelle disruption in an acidic medium represented by tumour microenvironment. Indeed, the extracellular pH of most tumor tissues is weakly acidic (pH 6.5), which is lower than that of normal tissues (pH 7.2) and this discrepancy is usually used as the trigger factor. Finally, the conjugation of a specific biomolecule to smart agents increases their affinity significantly for cancer cells.

Other stimuli-responsive BCPs are extensively studied. Tsai et al. [41], for example, develop a core-shell structure composed by poly(HEMA-co-histidine)-g-PLA and diblock copolymer PEG–PLA with functional moiety. The inner core of poly(HEMA-co-histidine)-g-PLA exhibits pH stimulate to enable intracellular drug delivery, while the outer shell PEG-b-PLA with functional moiety Cy5.5 for biodistribution diagnosis and folate for cancer specific targeting. The nanospheres has an average diameter of 200 nm. From drug release study, a change in pH destroy the inner core to lead a significant drug release from mixed micelles. Cellular uptake of folate–micelles is found to be higher than that of non-folate–micelles. The *in vivo* study reveal that specific targeting of folate–micelles exhibit cancer targeting and efficiency expression on tumor growth, indicating that multifunctional micelles prepared from poly(HEA-co-histidine)-g-PLA and folate–PEG–PLA have great potential in cancer chemotherapy and diagnosis.

Concomitantly, additional and promising technologies in nanomedicine are currently under investigation such as multimodal imaging and nanotheranostics (integration of therapeutic and diagnostic capabilities in a single nanoplatform). Locatelli et al. [42], for example, report a nanocarrier system for dual PET/MRI imaging. In this case, hydrophilic superparamagnetic maghemite NPs are synthesized and coated with a lipophilic organic ligand and entrapped into polymer NPs made of biodegradable poly(D,L-lactide-co-glycolide)-block-poly(ethylene glycol) copolymer (PLGA-b-PEG-COOH). Moreover, the surface of NPs shows active sites (COOH) that allow a modification with 2,2'-(7-(4-((2-aminoethyl) amino)-1-carboxy-4-oxobutyl)-1,4,7-triazonane-1,4-diyl) diacetic acid (NODA) to chelate $^{68}$Ga for PET imaging. Zhang and coworker [43], instead, realize a copolymer-based single-photon emission computed tomography/magnetic resonance (SPECT/MR) dual-modality imaging agent that can be labeled with technetium-99m ($^{99}$mTc) and Gd simultaneously. The copolymer P(VLA-co-VNI-co-V2DTPA) (pVLND2) is synthesized by radical copolymerization reaction and based on asialoglycoprotein receptor (ASGPR) targeting agent for a hepatic tissue.

An example of theranostic polymer platform is developed by Porsch et al. [44]. In this work, they report the use of natural isotope $^{19}$F as an efficient alternative to the conventional

imaging costrast agents, because this nucleus is not intrinsic to the body, thus enabling MRI images with great spatial selectivity against a zero background and synthesize fluorinated NPs loaded with doxorubicin (Dox). The NPs are formed by self-assembly of amphiphilic BCPs with fluorinated elements incorporated in the hydrophilic corona and anticancer drug in the hydrophobic core. Experimental data show that the nanovector has a controllable drug release kinetics, are detectable by $^{19}$F-MRIand toxic for breast cancer cells.

Recently, Koziolova and colleagues [45] evaluate the influence of molecular weight and dispersity of N-(2-hydroxypropyl)methacrylamide (HPMA) copolymer conjugates with Dox on their biodistribution is studied using two complementary imaging methods PET and Fluorescence Imaging (FI). The HPMA copolymers are synthesized by RAFT polymerization and functionalized with a chelator for further radiolabelling with Zirconium-89 ($^{89}$Zr; t1/2 = 78.4 h) prior to *in vivo* and ex vivo studies. PET/Optical Imaging studies indicate that dispersity and molecular weight of the HPMA polymer carriers have a significant influence on the *in vivo* fate of the polymer conjugates and thanks to presence of anticancer drug bound show higher cytotoxicity and cellular uptake *in vitro*.

## LIPOSOMES

Liposomes are structures composed of hydrophobic head groups and hydrophilic tail groups. They can be prepared by adding lipids in organic solution, which is slowly evaporated to produce a thin film. The film is then hydrated with a desired aqueous buffer and sonicated. Liposomes are generally nano-scaled structures and can be further size refined by passage through physical membrane pores of known size (extrusion). Liposomes are typically characterised by their size, shape and lamellarity. They may be composed of a single bilayer (unilamellar), a few bilayers (oligolamellar), or multiple bilayers (multilamellar). Due to their aqueous cavity and "tunable" bilayer, liposomes have traditionally been used as drug delivery vehicles, encapsulating water-soluble drugs within the aqueous cavity in order to improve drug pharmacokinetics [46].

Zou et al. [47], for example, report an amphiphilic MRI-traceable liposome NPs encapsulating Gd-DOTA for *in vivo* inner ear visualization through MRI. They design these multifunctional NPs through the film hydration method that allows the encapsulation of Gd-DOTA inside the hydrophilic core of the NPs. They observe acceptable relaxivity values enabling visible signal characteristics for MRI. *In vivo* studies demonstrate that these systems are efficiently taken up by the inner ear after both transtympanic and intracochlear injection. The latter shows better NPs distribution throughout the inner ear, including the cochlea and vestibule, and induced stronger MRI signals on T1-weighted images.

Bui et al. [48] produce lipid NPs containing phospholipids that express Gd-chelate or DTPA by incorporating DTPA-PE into the lipid core of the NPs and then adding $Gd^{3+}$ to preformed NPs (for binding to $Gd^{3+}$ as Gd-DTPA-PE chelate). They also add 10-mole percentage of lipid conjugated to mPEG-PE to lipid nanoparticles in order to increase the bound water on the lipid nanoparticle surface, thereby increasing the MRI contrast. In this case, the following nanoparticle system shows an higher longitudinal relaxivity (33-fold) than the current FDA approved Gd-chelated CAs. In addition, intravenous administration of these

Gd-LNP at only 3% of the recommended clinical Gd dose produce MRI signal-to-noise ratios of greater than 300 times in all vasculatures.

Kamaly and colleagues [46] synthesize a bimodal imaging liposome for cell labeling and tumour imaging. The lipid molecules are able to bear both fluorophore and CA on the same structure, thereby representing a useful probe for both MRI and fluorescence microscopy utility. Very briefly, they conjugate a rhodamine moiety onto a DOTA-bearing C-18 dialkyl lipid and complex Gd into the molecule to obtain the bimodal lipid Gd DOTA Rhoda DSA 1. The lipid is used to label IGROV-1 human ovarian carcinoma cells and to image xenograft tumours in mice. The new paramagnetic and fluorescent lipid proved to be a valuable probe to obtain anatomical information, through MRI, and liposome biodistribution, through ex vivo fluorescence microscopy.

Kono et al. [49] synthesize multi-functional pegylated liposomes having both highly thermosensitive polymers and newly synthesized Gd-chelate-attached dendron lipid (G3-DL-DOTA-Gd) with a compact conformation. The multifunctional liposomes show temperature-responsive drug release and MR imaging functions. In particular, authors load liposomes with Dox and tested the stability of the nanostructures, showing that liposomes are able to retain Dox below physiological temperature but release it immediately above 40°C. As far as the MRI properties, the developed liposomes exhibit the ability to shorten the longitudinal relaxation time with a relaxivity (5.5 $mM^{-1}s^{-1}$) higher than that of free Gd-DOTA (4.6 $mM^{-1}s^{-1}$).

In addition, Na and co-worker [50] report dual functional liposomes co-encapsulating Dox and Gd as therapeutic and diagnostic carriers. They measure MR relaxivity and cellular uptake showing that the liposomes can entrap 3.6 mM of Dox and 1.9 mM of Gd. Although the low relaxivity (5.5 $mM^{-1}s^{-1}$) compared to that of MRbester® due to limited water diffusion across the liposome membrane, the surface charge induced good cellular uptake, allowing a higher accumulation of Gd into cells than MRbester®. Additionally, Dox is more easily internalized to the nucleus compared to Doxil®.

Li et al. [51], instead, prepare fluorescent and paramagnetic liposomes for early tumor diagnosis by incorporating a RGD-coupled-lipopeptide, synthesized using a cyclic RGD peptide headgroup coupled to palmitic acid anchors via a KGG tripeptide spacer, into lipid bilayers. As far as the paramagnetic liposomes, they adopted the thin film hydration method and hydrated the lipid film with commercial Gd-DTPA as MRI contrast agent. *In vivo* MRI scanning demonstrate that the signal enhancement in tumor after injection of RGD-targeted liposomes is significantly higher than non-targeted liposomes and pure Gd-DTPA. In addition, biodistribution study also shows specific tumor targeting of RGD-targeted paramagnetic liposomes *in vivo*, proving them an effective means for noninvasive diagnosis of early tumor.

Liao et al. [52] design a core-shell NPs system composed of a PLGA core and a paramagnetic liposome shell for simultaneous MRI and targeted therapeutics. They encapsulate Dox within biocompatible and FDA-approved PLGA NPs, and DTPA-Gd is conjugated to the amphiphilic octadecyl-quaternized lysine-modified chitosan (OQLCS). The paramagnetic liposome shell is based on Gd-DTPA-conjugated OQLCS (Gd-DTPA-OQLCS), folate-conjugated OQLCS (FA-OQLCS), and PEGylated OQLCS (PEG-OQLCS). Briefly, the carboxyl groups of DTPA used as a chelating agent are combined with the amino groups of OQLCS. Then Gd is incorporated into the complex. As a result, the NPs show paramagnetic properties with an approximately 3-fold enhancement in the longitudinal

relaxivity (r1 = 14.381 mM−1s−1) compared to the commercial Gd-DTPA complex and exceptional antitumor effects without systemic toxicity.

Another remarkable example as reported by Gianolio et al. [53]. They prepare pH-responsive Gd-DO3Asa-loaded liposomes which maintain the pH responsiveness of the unbound paramagnetic complex, and their relaxivities are markedly affected by the magnetic field strength, exhibiting a steep change in the relaxivity in the pH range 5-7.5. Moreover, they provide a ratiometric method for measurement of the pH based on a comparison of the relaxation effects at different magnetic fields, offering an alternative tool for accessing measurement of the pH without prior knowledge of the concentration of the paramagnetic agent.

Subsequently, Hossann et al. [54] investigate formulations of 6 clinically approved CAs encapsulated into thermosensitive liposomes (TLs):

(1) Gd-DTPA (Magnograf®) from Marotrast GmbH, Jena, Germany;
(2) Gd-BOPTA (Multihance®) from Bracco Imaging Deutschland GmbH (Konstanz, Germany);
(3) Gd-DOTA (Dotarem®) from Guerbet GmbH (Sulzbach/Taunus, Germany);
(4) Gd-BT-DO3A (Gadovist™) from Bayer Vital GmbH (Leverkusen, Germany);
(5) Gd-DTPA-BMA (Omniscan™) from GE Healthcare Buchler GmbH & Co. KG (Braunschweig, Germany);
(6) Gd-HP-DO3A (Prohance®) from Bracco Imaging Deutschland GmbH (Konstanz, Germany).

They observe that Omniscan™ and Prohance® are the most promising candidates to be encapsulated into DPPG2-TSL. In particular, Prohance® allows the highest loading capability (256 mM) due to the lowest osmolality and yields the highest relaxivity. Omniscan™ is the only formulation that could be stored at 4°C for weeks. The other CAs induce phospholipid hydrolysis, which results in unwanted CA leakage, and therefore reduce the shelf life of TSL. Nevertheless, Omniscan™ is associated with Nephrogenic Systemic Fibrosis (NSF) [55].

The Human Serum Albumin (HSA) and Immunglobulin G (IgG) contribute to the increase of MRI signal at 30°C by increasing Pd. A high concentration of encapsulated CA is a prerequisite to achieve a sufficiently high Δr1 during heat triggered CA release combined with a low r1 at 37°C. Hence, the optimal CA is characterized by a non-ionic structure and a low contribution to osmolality.

Cheng et al. [56], instead, encapsulate Gd within a nanometer-sized stabilized porous liposome in order to increase the Gd relaxivity thanks to the porous structure, enabling a fast water exchange rate. A further increase in relaxivity (up to 9.9 $mM^{-1}s^{-1}$) is achieved by attaching large molecular weight dextran to the Gd moiety (Gd-DOTA) prior to encapsulation.

Others authors report further interesting strategies for the development of new liposome-complexes. Kozlowska et al. [57], for example, synthesize liposomes loaded with Gd ions using different membrane-incorporated chelating lipids and functionalized with monoclonal anti-CD138 (syndecan-1) antibody for multiple myeloma and non Hodgkin's lymphoma diagnosis. In this case, the use of the polychelating amphiphilic polymer increases both the Gd content and the longitudinal relaxivity of the Gd-loaded liposomes as compared to Gd-DTPA-BSA equivalents.

Then, Park and coworker [58] develop nanohybrid liposomes coated with amphiphilic hyaluronic acid-ceramide for targeted delivery of anticancer drug and *in vivo* cancer imaging. Dox, an anticancer drug, and Magnevist, a Gd-based CA for MRI, are loaded into this nanohybrid liposomal formulation. They find that *in vitro* release and *in vivo* clearance of Dox as well as cellular uptake from the nanohybrid liposome is enhanced than that from conventional liposome, thanks to the prolonged circulation of the nanohybrid liposome in the blood stream and to the HA–CD44 receptor interactions.

Another example is reported by Smith and Kong [59]. In this case, they evaluate the stability of liposomes with Gd-loaded in presence of serum. The authors assemble crosslinkable liposomes composed of diyne-containing lipids, conjugate the liposome surface to DTPA-chitosan-g-C18 and then crosslink the liposome via UV irradiation. The particles are mixed with Gd to enhance the quality of MRI contrast. They demonstrate that the crosslinking strategy after the adsorption of the polymer fastener allows stabilizing the thermodynamically favorable association between liposome and DTPA-chitosan-g-C18. In the end, they observe that CS-coated crosslinked liposomes are more effective than non-crosslinked liposomes in terms of stability, showing reduced liposome degradation and chitosan desorption.

Concomitant, Gu et al. [60] develop novel Gd-loaded liposomes guided by GBI-10 aptamer for enhanced tumor MRI. They conjugate GBI-10, as targeting ligand, onto the liposome surface and the so obtained system shows an accumulation of Gd at the periphery of C6 glioma cells, where the targeting extracellular matrix protein tenascin-C is overexpressed. This novel design strategy, obtained by simply replacing the aptamers with other kinds of aptamers, can be applied to a variety of target cells with high efficiency and specificity.

Silva et al. [61] synthesize and incorporate complexes of Gd with aliphatic chain ligands of N-alkyl-N-methylglucamine series into liposomes in order to enhance MRI contrast. The presence of two aliphatic chains is conceived to reduce the local rotational motion of the Gd-complexes after incorporation in the liposomal bilayer. They show that the incorporation into liposomes is accompanied by an increase of the vesicle zeta potential and in relaxation effectiveness ($r_1$ up to 15 $mM^{-1}s^{-1}$) compared to commercial Gd-DTPA, presumably because of the slower molecular rotation due to the elevated molecular weight and incorporation in liposomes.

Xiao et al. [62] report liposomes loaded with Sorafenib (SF) and commercial Gd-based CA (Gd-DTPA) for theranostic applications. Thin film hydration method is used to prepare liposomes exhibiting spherical shapes or ellipsoidal shapes, uniform particle size distribution (around 180 nm), negative zeta potential, high encapsulation efficiency and drug loading. As far as the longitudinal relaxivity, they achieve a value of 3.2 $mM^{-1}s^{-1}$, slightly lower than the commercial CA (4.5 $mM^{-1}s^{-1}$) and the MRI test show longer imaging time and higher signal enhancement at the tumor tissue. Furthermore, they demonstrate *in vivo* antitumor efficacy of the developed SF/Gd-liposomes on hepatocellular carcinoma (HCC) in mice. To sum up, the authors show that SF/Gd liposomes could be promising nano-carriers for MRI-guided *in vivo* visualization of the delivery and HCC treatment.

In the end, Tian et al. [63] synthesize Gd-DTPA-loaded mannosylated liposomes (M-Gd-NL) and test their ability to target macrophages in Acute Pancreatitis (AP) and discriminate between mild and severe AP. Lipid film-based method is used to synthesize DSPE-PEG2000-Man liposomes encapsulating DPPE-DTPA-Gd, with size around 100 nm. *In vitro* tests show efficient bind and readily release of Gd-DTPA into macrophages, resulting in enhanced MRI

ability. Indeed, M-Gd-NL show a longitudinal relaxivity 1.8-1.9 higher than Gd-DTPA, as a consequence of the embedding of DPPE-DTPA-Gd into the bilayer of liposomes, which slowed down the tumbling motion of Gd complexes. As far as the safety profile, M-Gd-NL do not show any severe organ toxicity in rats, thus proving to be promising nanocarriers for clinical use and for the early detection of AP.

## REFERENCES

[1] Mansfield, P., Snapshot magnetic resonance imaging (nobel lecture). *Angewandte Chemie-International Edition* 2004, *43* (41), 5456-5464.

[2] Caravan, P., Ellison, J. J., McMurry, T. J., Lauffer, R. B., Gadolinium(III) chelates as MRI contrast agents: Structure, dynamics, and applications. *Chemical Reviews* 1999, *99* (9), 2293-2352.

[3] Sethi, R., Ananta, J. S., Karmonik, C., Zhong, M., Fung, S. H., Liu, X., Li, K., Ferrari, M., Wilson, L. J., Decuzzi, P., Enhanced MRI relaxivity of Gd3+-based contrast agents geometrically confined within porous nanoconstructs. *Contrast Media & Molecular Imaging* 2012, *7* (6), 501-508.

[4] Xue, S. H., Qiao, J. J., Pu, F., Cameron, M., Yang, J. J., Design of a novel class of protein-based magnetic resonance imaging contrast agents for the molecular imaging of cancer biomarkers. *Wiley Interdisciplinary Reviews-Nanomedicine and Nanobiotechnology* 2013, *5* (2), 163-179.

[5] McDonald, R. J., McDonald, J. S., Kallmes, D. F., Jentoft, M. E., Murray, D. L., Thielen, K. R., Williamson, E. E., Eckel, L. J., Intracranial Gadolinium Deposition after Contrast-enhanced MR Imaging. *Radiology* 2015, *275* (3), 772-782.

[6] McDonald, R. J., McDonald, J. S., Kallmes, D. F., Jentoft, M. E., Murray, D. L., Thielen, K. R., Williamson, E. E., Eckel, L. J., Gadolinium Deposition after Contrast-enhanced MR Imaging Response. *Radiology* 2015, *277* (3), 925-925.

[7] McDonald, R. J., McDonald, J. S., Kallmes, D. F., Jentoft, M. E., Murray, D. L., Thielen, K. R., Williamson, E. E., Eckel, L. J., Dose-Dependent Neurotoxicity (Seizures) Due to Deposition of Gadolinium-based Contrast Agents in the Central Nervous System Response. *Radiology* 2015, *277* (3), 926-926.

[8] Biffi, S., Voltan, R., Rampazzo, E., Prodi, L., Zauli, G., Secchiero, P., Applications of nanoparticles in cancer medicine and beyond: optical and multimodal *in vivo* imaging, tissue targeting and drug delivery. *Expert Opinion on Drug Delivery* 2015, *12* (12), 1837-1849.

[9] Patel, T., Zhou, J. B., Piepmeier, J. M., Saltzman, W. M., Polymeric nanoparticles for drug delivery to the central nervous system. *Advanced Drug Delivery Reviews* 2012, *64* (7), 701-705.

[10] Zhong, Y. A., Meng, F. H., Deng, C., Zhong, Z. Y., Ligand-Directed Active Tumor-Targeting Polymeric Nanoparticles for Cancer Chemotherapy. *Biomacromolecules* 2014, *15* (6), 1955-1969.

[11] Tripodo, G., Trapani, A., Torre, M. L., Giammona, G., Trapani, G., Mandracchia, D., Hyaluronic acid and its derivatives in drug delivery and imaging: Recent advances and

challenges. *European Journal of Pharmaceutics and Biopharmaceutics* 2015, *97*, 400-416.

[12] Chen, H. Y., Qi, B., Moore, T., Wang, F. L., Colvin, D. C., Sanjeewa, L. D., Gore, J. C., Hwu, S. J., Mefford, O. T., Alexis, F., Anker, J. N., Multifunctional Yolk-in-Shell Nanoparticles for pH-triggered Drug Release and Imaging. *Small* 2014, *10* (16), 3364-3370.

[13] Courant, T., Roullin, V. G., Cadiou, C., Callewaert, M., Andry, M. C., Portefaix, C., Hoeffel, C., de Goltstein, M. C., Port, M., Laurent, S., Vander Elst, L., Muller, R., Molinari, M., Chuburu, F., Hydrogels Incorporating GdDOTA: Towards Highly Efficient Dual T1/T2 MRI Contrast Agents. *Angewandte Chemie-International Edition* 2012, *51* (36), 9119-9122.

[14] Russo, M., Bevilacqua, P., Netti, P. A., Torino, E., A Microfluidic Platform to design crosslinked Hyaluronic Acid Nanoparticles (cHANPs) for enhanced MRI. *Scientific Reports* 2016, *6*.

[15] Russo, M., Grimaldi, A. M., Bevilacqua, P., Tammaro, O., Netti, P. A., Torino, E., PEGylated crosslinked hyaluronic acid nanoparticles designed through a microfluidic platform for nanomedicine. *Nanomedicine* 2017, *12* (18), 2211-2222.

[16] Russo, M., Ponsiglione, A. M., Forte, E., Netti, P. A., Torino, E., Hydrodenticity to enhance relaxivity of gadolinium-DTPA within crosslinked hyaluronic acid nanoparticles. *Nanomedicine* 2017, *12* (18), 2199-2210.

[17] Russo, M., Bevilacqua, P., Netti, P. A., Torino, E., Commentary on "a microfluidic platform to design crosslinked hyaluronic acid nanoparticles (cHANPs) for enhanced MRI". *Molecular imaging* 2017, *16*.

[18] Ponsiglione, A. M., Russo, M., Netti, P. A., Torino, E., Impact of biopolymer matrices on relaxometric properties of contrast agents. *Interface focus* 2016, *6* (6), 20160061-20160061.

[19] Srinivas, M., Heerschap, A., Ahrens, E. T., Figdor, C. G., de Vries, I. J. M., F-19 MRI for quantitative *in vivo* cell tracking. *Trends in Biotechnology* 2010, *28* (7), 363-370.

[20] Wang, K. W., Peng, H., Thurecht, K. J., Whittaker, A. K., Fluorinated POSS-Star Polymers for F-19 MRI. *Macromolecular Chemistry and Physics* 2016, *217* (20), 2262-2274.

[21] Gizzatov, A., Stigliano, C., Ananta, J. S., Sethi, R., Xu, R., Guven, A., Ramirez, M., Shen, H. F., Sood, A., Ferrari, M., Wilson, L. J., Liu, X. W., Decuzzi, P., Geometrical confinement of Gd(DOTA) molecules within mesoporous silicon nanoconstructs for MR imaging of cancer. *Cancer Letters* 2014, *352* (1), 97-101.

[22] Vecchione, D., Grimaldi, A. M., Forte, E., Bevilacqua, P., Netti, P. A., Torino, E., Hybrid Core-Shell (HyCoS) Nanoparticles produced by Complex Coacervation for Multimodal Applications. *Scientific Reports* 2017, *7*.

[23] Vecchione, D., Aiello, M., Cavaliere, C., Nicolai, E., Netti, P. A., Torino, E., Hybrid core shell nanoparticles entrapping Gd-DTPA and F-18-FDG for simultaneous PET/MRI acquisitions. *Nanomedicine* 2017, *12* (18), 2223-2231.

[24] Tsitsilianis, C., Gotzamanis, G., Iatridi, Z., Design of "smart" segmented polymers by incorporating random copolymers as building blocks. *European Polymer Journal* 2011, *47* (4), 497-510.

[25] van Nostrum, C. F., Covalently cross-linked amphiphilic block copolymer micelles. *Soft Matter* 2011, *7* (7), 3246-3259.

[26] Epps, T. H., O'Reilly, R. K., Block copolymers: controlling nanostructure to generate functional materials - synthesis, characterization, and engineering. *Chemical Science* 2016, *7* (3), 1674-1689.

[27] Feng, H. B., Lu, X. Y., Wang, W. Y., Kang, N. G., Mays, J. W., Block Copolymers: Synthesis, Self-Assembly, and Applications. *Polymers* 2017, *9* (10).

[28] Xiao, Y., Xue, R., You, T. Y., Li, X. J., Pei, F. K., A new biodegradable and biocompatible gadolinium (III) -polymer for liver magnetic resonance imaging contrast agent. *Magnetic Resonance Imaging* 2015, *33* (6), 822-828.

[29] Hou, S. J., Tong, S., Zhou, J., Bao, G., Block copolymer-based gadolinium nanoparticles as MRI contrast agents with high T-1 relaxivity. *Nanomedicine* 2012, *7* (2), 211-218.

[30] Cao, Y., Liu, M., Kuang, Y., Zu, G. Y., Xiong, D. S., Pei, R. J., A poly(epsilon-caprolactone)-poly(glycerol)-poly(epsilon-caprolactone) triblock copolymer for designing a polymeric micelle as a tumor targeted magnetic resonance imaging contrast agent. *Journal of Materials Chemistry B* 2017, *5* (42), 8408-8416.

[31] Luo, B. H., Wang, S. Q., Rao, R., Liu, X. H., Xu, H. B., Wu, Y., Yang, X. L., Liu, W., Conjugation Magnetic PAEEP-PLLA Nanoparticles with Lactoferrin as a Specific Targeting MRI Contrast Agent for Detection of Brain Glioma in Rats. *Nanoscale Research Letters* 2016, *11*.

[32] Jeong, S. Y., Kim, H. J., Kwak, B. K., Lee, H. Y., Seong, H., Shin, B. C., Yuk, S. H., Hwang, S. J., Cho, S. H., Biocompatible Polyhydroxyethylaspartamide-based Micelles with Gadolinium for MRI Contrast Agents. *Nanoscale Research Letters* 2010, *5* (12), 1970-1976.

[33] Ge, Z. S., Liu, S. Y., Functional block copolymer assemblies responsive to tumor and intracellular microenvironments for site-specific drug delivery and enhanced imaging performance. *Chemical Society Reviews* 2013, *42* (17), 7289-7325.

[34] Kato, Y., Ozawa, S., Miyamoto, C., Maehata, Y., Suzuki, A., Maeda, T., Baba, Y., Acidic extracellular microenvironment and cancer. *Cancer Cell International* 2013, *13*.

[35] Gao, G. H., Im, G. H., Kim, M. S., Lee, J. W., Yang, J., Jeon, H., Lee, J. H., Lee, D. S., Magnetite-Nanoparticle-Encapsulated pH-Responsive Polymeric Micelle as an MRI Probe for Detecting Acidic Pathologic Areas. *Small* 2010, *6* (11), 1201-1204.

[36] Okada, S., Mizukami, S., Kikuchi, K., Application of a Stimuli-Responsive Polymer to the Development of Novel MRI Probes. *Chembiochem* 2010, *11* (6), 785-787.

[37] Zhu, L. P., Yang, Y., Farquhar, K., Wang, J. J., Tian, C. X., Ranville, J., Boyes, S. G., Surface Modification of Gd Nanoparticles with pH-Responsive Block Copolymers for Use As Smart MRI Contrast Agents. *Acs Applied Materials & Interfaces* 2016, *8* (7), 5040-5050.

[38] Hu, J. M., Liu, T., Zhang, G. Y., Jin, F., Liu, S. Y., Synergistically Enhance Magnetic Resonance/Fluorescence Imaging Performance of Responsive Polymeric Nanoparticles Under Mildly Acidic Biological Milieu. *Macromolecular Rapid Communications* 2013, *34* (9), 749-758.

[39] Hu, X. L., Liu, G. H., Li, Y., Wang, X. R., Liu, S. Y., Cell-Penetrating Hyperbranched Polyprodrug Amphiphiles for Synergistic Reductive Milieu-Triggered Drug Release and Enhanced Magnetic Resonance Signals. *Journal of the American Chemical Society* 2015, *137* (1), 362-368.

[40] Mouffouk, F., Simao, T., Dornelles, D. F., Lopes, A. D., Sau, P., Martins, J., Abu-Salah, K. M., Alrokayan, S. A., da Costa, A. M. R., dos Santos, N. R., Self-assembled polymeric nanoparticles as new, smart contrast agents for cancer early detection using magnetic resonance imaging. *International Journal of Nanomedicine* 2015, *10*, 63-76.

[41] Tsai, H. C., Chang, W. H., Lo, C. L., Tsai, C. H., Chang, C. H., Ou, T. W., Yen, T. C., Hsiue, G. H., Graft and diblock copolymer multifunctional micelles for cancer chemotherapy and imaging. *Biomaterials* 2010, *31* (8), 2293-2301.

[42] Locatelli, E., Gil, L., Israel, L. L., Passoni, L., Naddaka, M., Pucci, A., Reese, T., Gomez-Vallejo, V., Milani, P., Matteoli, M., Llop, J., Lellouche, J. P., Franchini, M. C., Biocompatible nanocomposite for PET/MRI hybrid imaging. *International Journal of Nanomedicine* 2012, *7*, 6021-6033.

[43] Zhang, P., Guo, Z. D., Zhang, D. L., Liu, C., Chen, G. B., Zhuang, R. Q., Song, M. L., Wu, H., Zhang, X. Z., A Novel Copolymer-Based Functional SPECT/MR Imaging Agent for Asialoglycoprotein Receptor Targeting. *Molecular Imaging* 2016, *15*.

[44] Porsch, C., Zhang, Y. N., Ostlund, A., Damberg, P., Ducani, C., Malmstrom, E., Nystrom, A. M., *In vitro* Evaluation of Non-Protein Adsorbing Breast Cancer Theranostics Based on 19F-Polymer Containing Nanoparticles. *Particle & Particle Systems Characterization* 2013, *30* (4), 381-390.

[45] Koziolova, E., Goel, S., Chytil, P., Janouskova, O., Barnhart, T. E., Cai, W. B., Etrych, T., A tumor-targeted polymer theranostics platform for positron emission tomography and fluorescence imaging. *Nanoscale* 2017, *9* (30), 10906-10918.

[46] Kamaly, N., Miller, A. D., Paramagnetic Liposome Nanoparticles for Cellular and Tumour Imaging. *International Journal of Molecular Sciences* 2010, *11* (4), 1759-1776.

[47] Zou, J., Sood, R., Ranjan, S., Poe, D., Ramadan, U. A., Kinnunen, P. K. J., Pyykko, I., Manufacturing and *in vivo* inner ear visualization of MRI traceable liposome nanoparticles encapsulating gadolinium. *Journal of Nanobiotechnology* 2010, *8*.

[48] Bui, T., Stevenson, J., Hoekman, J., Zhang, S., Maravilla, K., Ho, R. J. Y., Novel Gd Nanoparticles Enhance Vascular Contrast for High-Resolution Magnetic Resonance Imaging. *Plos One* 2010, *5* (9).

[49] Kono, K., Nakashima, S., Kokuryo, D., Aoki, I., Shimomoto, H., Aoshima, S., Maruyama, K., Yuba, E., Kojima, C., Harada, A., Multi-functional liposomes having temperature-triggered release and magnetic resonance imaging for tumor-specific chemotherapy. *Biomaterials* 2011, *32* (5), 1387-1395.

[50] Na, K., Lee, S. A., Jung, S. H., Shin, B. C., Gadolinium-based cancer therapeutic liposomes for chemotherapeutics and diagnostics. *Colloids and Surfaces B: Biointerfaces* 2011, *84* (1), 82-87.

[51] Li, W., Su, B., Meng, S. Y., Ju, L. X., Yan, L. H., Ding, Y. M., Song, Y., Zhou, W., Li, H. Y., Tang, L., Zhao, Y. M., Zhou, C. C., RGD-targeted paramagnetic liposomes for early detection of tumor: *In vitro* and *in vivo* studies. *Eur. J. Radiol.* 2011, *80* (2), 598-606.

[52] Liao, Z. Y., Wang, H. J., Wang, X. D., Zhao, P. Q., Wang, S., Su, W. Y., Chang, J., Multifunctional Nanoparticles Composed of A Poly(DL-lactide-coglycolide) Core and A Paramagnetic Liposome Shell for Simultaneous Magnetic Resonance Imaging and Targeted Therapeutics. *Advanced Functional Materials* 2011, *21* (6), 1179-1186.

[53] Gianolio, E., Porto, S., Napolitano, R., Baroni, S., Giovenzana, G., Aime, S., Relaxometric investigations and MRI evaluation of a liposome-loaded pH-responsive gadolinium (III) complex. *Inorg. Chem.* 2012, *51* (13), 7210-7217.

[54] Hossann, M., Wang, T. T., Syunyaeva, Z., Wiggenhorn, M., Zengerle, A., Issels, R. D., Reiser, M., Lindner, L. H., Peller, M., Non-ionic Gd-based MRI contrast agents are optimal for encapsulation into phosphatidyldiglycerol-based thermosensitive liposomes. *J. Control. Release* 2013, *166* (1), 22-29.

[55] Thomsen, H. S., Morcos, S. K., Almen, T., Bellin, M. F., Bertolotto, M., Bongartz, G., Clement, O., Leander, P., Heinz-Peer, G., Reimer, P., Stacul, F., van der Molen, A., Webb, J. A. W., Nephrogenic systemic fibrosis and gadolinium-based contrast media: updated ESUR Contrast Medium Safety Committee guidelines. *European Radiology* 2013, *23* (2), 307-318.

[56] Cheng, Z., Al Zaki, A., Jones, I. W., Hall, H. K., Aspinwall, C. A., Tsourkas, A., Stabilized porous liposomes with encapsulated Gd-labeled dextran as a highly efficient MRI contrast agent. *Chemical Communications* 2014, *50* (19), 2502-2504.

[57] Kozlowska, D., Biswas, S., Fox, E. K., Wu, B., Bolster, F., Edupuganti, O. P., Torchilin, V., Eustace, S., Botta, M., O'Kennedy, R., Gadolinium-loaded polychelating amphiphilic polymer as an enhanced MRI contrast agent for human multiple myeloma and non Hodgkin's lymphoma (human Burkitt's lymphoma). *RSC Advances* 2014, *4* (35), 18007-18016.

[58] Park, J. H., Cho, H. J., Yoon, H. Y., Yoon, I. S., Ko, S. H., Shim, J. S., Cho, J. H., Kim, K., Kwon, I. C., Kim, D. D., Hyaluronic acid derivative-coated nanohybrid liposomes for cancer imaging and drug delivery. *Journal of Controlled Release* 2014, *174*, 98-108.

[59] Smith, C. E., Shkumatov, A., Withers, S. G., Yang, B. X., Glockner, J. F., Misra, S., Roy, E. J., Wong, C. H., Zimmerman, S. C., Kong, H., A Polymeric Fastener Can Easily Functionalize Liposome Surfaces with Gadolinium for Enhanced Magnetic Resonance Imaging. *Acs Nano* 2013, *7* (11), 9599-9610.

[60] Gu, M. J., Li, K. F., Zhang, L. X., Wang, H., Liu, L. S., Zheng, Z. Z., Han, N. Y., Yang, Z. J., Fan, T. Y., *In vitro* study of novel gadolinium-loaded liposomes guided by GBI-10 aptamer for promising tumor targeting and tumor diagnosis by magnetic resonance imaging. *International Journal of Nanomedicine* 2015, *10*, 5187-5204.

[61] Silva, S. R., Duarte, E. C., Ramos, G. S., Kock, F. V. C., Andrade, F. D., Frezard, F., Colnago, L. A., Demicheli, C., Gadolinium(III) Complexes with N-Alkyl-N-methylglucamine Surfactants Incorporated into Liposomes as Potential MRI Contrast Agents. *Bioinorg. Chem. Appl.* 2015.

[62] Xiao, Y., Liu, Y., Yang, S., Zhang, B., Wang, T., Jiang, D., Zhang, J., Yu, D., Zhang, N., Sorafenib and gadolinium co-loaded liposomes for drug delivery and MRI-guided HCC treatment. *Colloids and Surfaces B: Biointerfaces* 2016, *141*, 83-92.

[63] Tian, B., Liu, R., Chen, S., Chen, L., Liu, F., Jia, G., Dong, Y., Li, J., Chen, H., Lu, J., Mannose-coated gadolinium liposomes for improved magnetic resonance imaging in acute pancreatitis. *International journal of nanomedicine* 2017, *12*, 1127.

In: Advances in Polymers for Biomedical Applications ISBN: 978-1-53613-612-8
Editors: Deepak Pathania and Bhuvanesh Gupta 

*Chapter 14*

# RECENT ADVANCES IN POLYMERIC DRUG DELIVERY CARRIER SYSTEMS

***P. Sharma, P. Negi* and N. Mahindroo****
School of Pharmaceutical Sciences, Shoolini University, Solan, India

## ABSTRACT

There is a tremendous progress in the field of drug delivery in last few decades with introduction of novel delivery systems for improving therapeutic objectives, and minimizing side effects. Polymeric Drug Delivery Carrier Systems (PDDCS) have emerged as systems of choice, for targeted and controlled release formulations. PDDCS improve both pharmacokinetic and pharmacodynamic profiles of biopharmaceuticals by altering plasma half-life, decreasing immunogenicity, improving solubility, and stability of drug. For developing an ideal PDDCS, safety, efficacy, hydrophilicity, absence of immunogenicity, biological inertness, suitable pharmacokinetics, and the presence of functional groups for covalent conjugation of drug, targeting moiety, or formation of copolymer are important. Discussion covering various factors impacting the success of PDDCS is very broad and cannot be covered exhaustively in this chapter, so this review focuses on:

1. General introduction to various types of PDDCS and their various therapeutic advances
2. Types of polymers used and essential properties of an ideal carrier for drug delivery
3. Responsive PDDCS based on physical and chemical stimuli
4. Mechanism of drug release from the PDDCS

**Keywords**: polymeric drug delivery systems (PDDCS), microspheres, nanoparticles, polymeric vesicles, polymer drug conjugates, dendrimers, polymeric gels and hydrogels, capsosomes, micelles and responsive systems

* Corresponding authors. neeraj.mahindroo@yahoo.com, poonamgarge@gmail.com.

## 1. INTRODUCTION

The developments in polymeric drug delivery carrier systems (PDDCS) over the past sixty years, revolutionized the medical therapy and led to the significant therapeutic advantages. The short half-lives, non-specific distribution, increase in hydrophobicity and toxicity of small molecule drugs, are major driving forces for the development of polymeric drug delivery platforms. The successful clinical conversion of the macro/micro drug delivery systems, led to the progress in controlled-release nano-drug delivery carrier systems that are capable of overcoming pharmacological limitations, and have substantial benefits over conventional dosage forms. Further, research in synthetic methodologies, fabrication methods, and mathematical models for studying the mechanisms of controlled drug release have led to development of tunable polymeric nanoparticle drug delivery systems capable of localized and sustained delivery, facilitating improvements in the therapeutic index of drugs. The ability to control the release of therapeutics and the extremely versatile nature of polymeric drug delivery platforms offer numerous advantages. Polymeric drug delivery has flourished since 1960s with pioneering contributions from researchers such as Folkman, Langer, Higuchi, Roseman, Peppas, Heller, Ringsdorf, and Speiser [1-18]. PDDCS are used to entrap or fix the drug in a polymeric matrix for effective, safe and convenient administration. Higher efficacy of drug is achieved by improving water solubility [19-21], controlling release in a site-specific manner [22-23], or preventing undesired degradation in the stomach or during blood circulation [24-25]. PDDCS can also improve drug safety by alleviating systemic side effects [26-27], inhibiting gastric damage due to the drug release in stomach [28], and preventing drug distribution in normal tissues [29-31]. PDDCS have found applications in diverse biomedical fields such as drug delivery systems, tissue engineering, implantation medical devices and artificial organs, prosthesis, ophthalmology, dentistry, bone repair, and many other medical fields. The most important criteria, for the design of PDDCS, are the choice of polymer and the selection of the carrier system. Polymers are the backbone of pharmaceutical drug delivery systems [32] and are an important tool for controlling the drug release rate from the formulation. Further, advances in drug delivery are focused on the rational design of polymers tailored for specific payload to exert distinct biological functions.

## 2. POLYMERS USED IN DRUG DELIVERY CARRIER SYSTEMS

Polymers are used as inert carriers for conjugated drug or bioactive molecules. There are several advantages of using polymers as carriers, for example, they can enhance the pharmacodynamic and pharmacokinetic properties of bioactives by either increasing the plasma half-life, decreasing the immunogenicity, increasing stability, improving solubility, and site-directed drug delivery [33]. Polymers used for drug delivery carrier systems can be classified based on their origin, natural or synthetic. The natural polymers are obtained as such from nature, for example, starch, cellulose, proteins, and nucleic acids while synthetic polymers are artificially synthesized, for example, poly(lactic-co-glycolic acid) (PLGA), poly *N*-vinyl pyrrolidone (PVP), poly acrylic acid (PAC), poly 2-hydroxyethylmethacrylate (PHEMA), polyacrylamide (PAM), poly methacrylicglycol (PMAG) and polyethylene glycol (PEG) [34-48]. For utility of a polymer in the drug delivery carrier systems, it should be

biodegradable, nontoxic, non-immunogenic, non-thrombogenic, non-inflammatory and inexpensive. Besides, it should not activate neutrophils, cause platelet aggregation, and affect reticulo-endothelial system or prolong circulation time. It should have wide applicability for drugs with different chemical origin, such as small molecules, proteins, peptides, or nucleic acids (platform technology) and should have scalable and inexpensive manufacturing process [33]. Most commonly used polymers for the preparation of biodegradable PDDCS are, poly-lactic acid (PLA), poly-D-L-glycolide (PLG), PLGA, poly-cyanoacrylate (PCA), PEG, gelatin, chitosan, and alginate. The biggest advantage of these degradable polymers is the ability of biological systems to break them into biologically acceptable molecules, which are metabolized and removed from the body *via* normal metabolic pathways. Natural polymers have the advantage of high biocompatibility and less immunogenicity [49]. Polymers are able to: 1) prolong drug availability; if fabricated as hydrogels or micro particles; 2) favorably alter bio-distribution, if fabricated into dense NPs; 3) facilitate hydrophobic drug administration, if fabricated as micelles; 4) carry a drug to usually inaccessible site of action, if fabricated as gene medicines; 5) present drugs available in response to stimuli [50].

Selection of the polymer for a particular PDDCS depends upon the carrier related factors, like various design related requirements, and the application. These include size of the desired carrier system, properties of the drug or bioactive molecule (aqueous solubility, stability, etc.) to be encapsulated in the polymer, surface characteristics and functionality, degree of biodegradability, biocompatibility, and drug release profile of the final product [51]. As stated earlier, biodegradable polymers are metabolized, and removed from the body *via* normal metabolic pathways, however, they do produce degradation byproducts that must be tolerated with little or no adverse reactions within the biological environment. These degradation products, both desirable and potentially non-desirable, must be tested thoroughly, since there are a number of factors that will affect the biodegradation of the original materials [52-58].

## 3. POYMERIC DRUG DELIVERY CARRIER SYSTEMS

With the availability of new fabrication technologies and interdisciplinary drug research, the field of PDDCS has evolved from simple polymeric microspheres, nanoparticles, vesicles to more complex systems *viz*., polymer drug conjugates, dendrimers, polymeric gels and hydrogels, capsosomes and micelles. This section discusses the unique carrier properties of these systems, and the progress in the recent research, for various therapeutic applications [33, 52].

### Polymeric Microspheres

Microspheres are tiny spheres consisting of porous/non-porous inner polymeric matrix with an outer, porous and regular to nonporous and irregular, polymeric surface. Diameter of these structures varies from 1-500 μm. Encapsulated drug is dispersed throughout the inner matrix and is released through pores of inner polymeric matrix by diffusion. Recent developments in these PDDCS include, paclitaxel (PTX) PLGA microspheres for tumor and revaprazan for gastric problems etc. [33, 52, 54]. Yang et al. reported microspheres held with

thermo-sensitive hydrogels for vaginal local drug delivery. These systems release drug on coming in contact with body. The microspheres controlled the burst release of drug [59]. Additionally, Liu et al. developed novel microspheres based on oleic acid-conjugated chitosan (OA-CTS) loaded with PTX, and quercetin (QUE), as double drug delivery system for prolonging PTX retention time for pulmonary delivery. The particle size of the microspheres was kept in the range of 250 and 350 nm to retain the drug in the lungs for better efficacy due to small size [60]. Recently, Chen et al. reported a unique drug delivery system based on surface molecular imprinting method using β-cyclodextrin (β-CD)-grafted chitosan (CS) (CS-g-β-CD) microspheres as matrix, and sinomenine hydrochloride (SM) as the template molecule. These systems have a better ability to control release of template drug molecule [61].

## Polymeric Nanoparticles

Oral administration of nucleic acid, and peptide-based drugs, is limited due to extensive metabolism leading to degradation, which can be avoided by using PDDCS. These systems elegantly control drug distribution at cellular, or even at sub-cellular level. Polymeric nanoparticles contains drug in an inner core reservoir surrounded by a polymeric membranous cover (Figure 1), which controls the rate of release of drug. Diameter of these structures varies from 10-200 nm. The nano size of these polymeric particles is responsible for physical and biochemical site-specific delivery [62]. One of the major limitations of the formulation of nanoparticles is the brisk clearance of the encapsulated drug/bioactive molecule from the blood stream. Lately, various types of long circulating nanoparticles have been prepared for delaying the systemic circulation time of nanoparticles for releasing the encapsulated gene/drug at the desired site of action [63]. Ebeid et al. designed polymeric nanoparticles of PTX for enhancing the therapeutic efficacy in endometrial cancer with mutant p53. Not only were PTX-loaded NPs superior to PTX in solution, the combination of PTX-loaded NPs with the antiangiogenic molecular inhibitor, BIBF 1120 (BIBF), promoted synthetic lethality specifically in cells with the loss-of-function (LOF) p53 mutation [64]. Mirzaei et al. reported chitosan nanoparticles (CS NPs) using ionic gelation method for loading *Echis carinatus* (EC) venom as an adjuvant and antigen delivery system. These unique systems were used for hyperimmunization of horse [65].

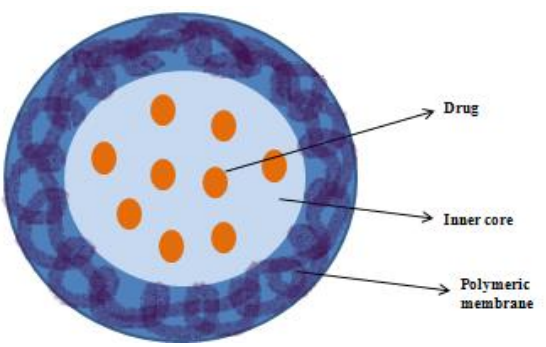


Figure 1. Polymeric nanoparticle representing reservoir system

## Polymeric Vesicles

These are amphiphillic macromolecule architectures, designed as block copolymers, and polymers containing lipophilic low molecular weight terminal groups. The polymeric vesicle is typically composed of lipophilic polymeric core, and lipophobic tail or shell (Figure 2). The drug can be encapsulated either in the interior core or in the shell. They range from micro to nano-sized particles. Polymeric vesicles show immense potential as versatile drug delivery systems due to their tunable membrane formulations, physicochemical properties, controlled release mechanisms, targeting abilities, *in vivo* stability in comparison to conventional lipid vesicles such as liposomes, and capacities to encase a wide range of drugs, and other molecules [66]. Polymeric vesicles are applied as PDDCS for drug targeting to various sites in the biological system, stimuli-responsive release systems, and in various other drug delivery applications [33, 52]. *Li* et al. studied the adsorption of a semi flexible polymer onto a fluid membrane vesicle by using Monte Carlo computer simulations. For small vesicles, polymer adsorption also induces dumbbell-like vesicle shapes with a narrow membrane constriction circled by the polymer. Large-scale deformations of the vesicle include invaginations of the membrane that internalizes the polymer in a membrane bud. These may alter the drug release from the carrier system [67]. Ribeiro et al. isolated and characterized human islet-derived polymeric extra cellular vesicles (h-Islet-EVs), and added them to human induced pluripotent stem cell (iPSC) clusters, during pancreatic differentiation, and showed positive expression of CD63, and CD81 EV markers as measured by ELISA [68]. Vardhan et al. optimized polymeric nanoparticles of polyhydroxybutyrate-co-hydroxyvalerate (PHBV), a biodegradable polymer, utilizing modified emulsification solvent evaporation method for treatment of breast cancer [69].

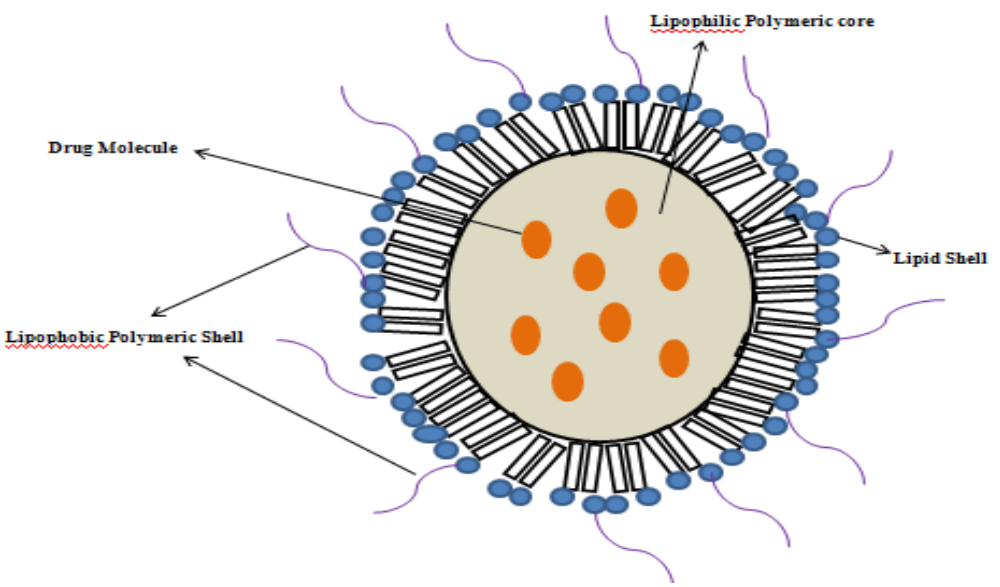


Figure 2. Typical structure of a polymeric vesicle.

## Polymeric Micelles

These are one of the most potent type of PDDCS. They are made of amphipathic linear polymers formed spontaneously by self-assembly in water, and a hydrophobic core in which the drug is encapsulated. The size of the micelles should be within the diameter range of 20-100 nm for ensuring that they do not cross the normal vessel walls, hence decreasing the volume of distribution and reducing the chances of side effects of the drugs [70]. They can carry a wide variety of poorly soluble pharmaceutical agents due to their high *in vitro* and *in vivo* stability. They can effectively accumulate in body areas with compromised vasculature (for example in infarcts, tumors), and act as carrier systems for drug targeting as they can carry specific ligands on their surface (Figure 3). They have applications in both therapeutic and diagnostic areas. Recently, polymeric micelles were evaluated for delivery of poorly soluble, and toxic chemotherapeutic agents for treatment of cancer. The micelles can reach tumors by a passive mechanism (Enhanced Permeation and Retention effect) or an active mechanism through conjugated targeting moieties for enhanced delivery to a specific site [71]. The block-copolymer micelles form spontaneously by self-assembly in water when the concentration of the amphiphilic block copolymer is above the critical micelle concentration (CMC) [72]. Guo et al. reported an acid-active tumor-targeting nano-platform consisting of 2,3-dimethylmaleic anhydride-Trans-activating transcriptional activator-poly (ethylene glycol)-poly(ε-caprolactone) (DA-TAT-PECL) which can inhibit the nonspecific interactions of TAT in the bloodstream. These micelles are capable of circulating under the physiological condition for a long time, promote cell penetration upon accumulation at the tumor site, and then deshield the DA group [73]. Yang et al. studied the impact of PEGylation degree on *in vivo* tumor-targeted accumulation activities of cRGD-installed nanoparticulates revealing the importance of design of active-targeting PEGylated nanomaterials to fulfill the targeting strategies in systemic applications [74]. Kataoka et al. designed block copolymer micelles of poly(ethylene oxide) (PEO) and poly(β-benzyl l-aspartate) (PBLA) and chemically tailored these for enhancing drug loading [75].

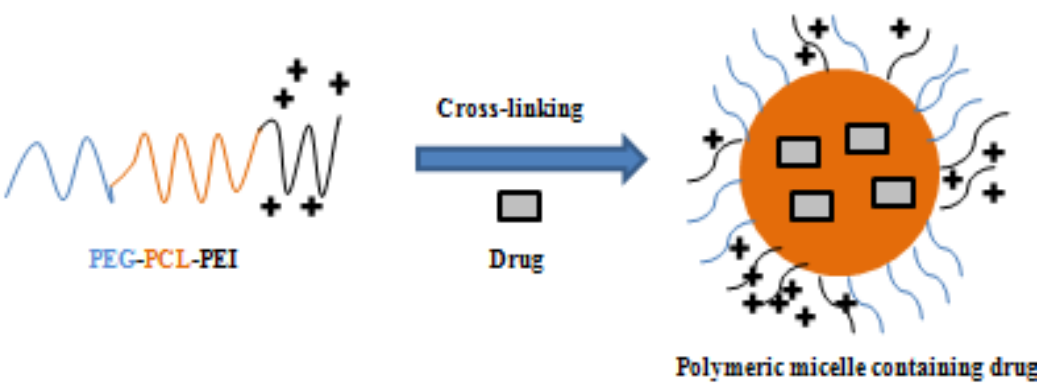


Figure 3. Schematic illustration of the formation of polymeric micelle. Here, PE is Poly (ethylene glycol); PCL is polycaprolactone and PEI is polyethyleneimine.

## Polymer Drug Conjugates

In last few years, there is a considerable increase in interest in design and chemical properties of polymer-drug conjugates. Various polymers, such as PEG, HPMA, poly(glycolic acid) (PGA) and PLGA have been successfully used in clinics. The polymer drug conjugates have polymer attached with drug for targeting specific tissues as shown in Figure 4 and thus reducing the toxicity of drugs. At present, various polymer drug conjugates are under clinical trial for the treatment of disease such as cancer, diabetes, AIDS, and rheumatoid arthritis [76]. Studies to elucidate the mechanism of action of free and polymer bound drugs at the cellular and subcellular levels for polymer anticancer drug conjugates are being pursued [77]. On swelling the cells show increase in the vascular permeability, same is the case of tumors, thus allowing polymer drug conjugates to target cancer cells. Several drug-polymer conjugates have entered clinical development [78]. Some of these compounds, for example, HPMA copolymer-doxorubicin galactosamine (PK2) [79], HPMA copolymer platinate (AP 5346), carboxymethyldextranpolyalcoholboundexatecan (DE-310), poly(L-glutamic acid)-paclitaxel (Xyotac), PEG-SN38 (EZN-2208), linear cyclodextrinbound-camptothecin (IT-101) and poly(L-glutamic acid)camptothecin (CT-2106), have progressed further into the clinical phase [80]. Islam et al. developed a tumor environment-responsive polymeric anticancer prodrug containing pirarubicin (THP) conjugated to *N*-(2-hydroxypropyl) methacrylamide copolymer (PHPMA) [P-THP] through a spacer containing pH-sensitive hydrazone bond. It showed a remarkable therapeutic effect against various tumor models and in a human pilot trials [81]. Bolu et al. prepared nontoxic, biodegradable, and modularly tunable micellar delivery systems using two types of dendron-polymer conjugates [82]. Aina et al. synthesized a new drug delivery system consisting of chondroitin sulfate linked to 5-ASA using a carbodiimide as conjugating agent [83].

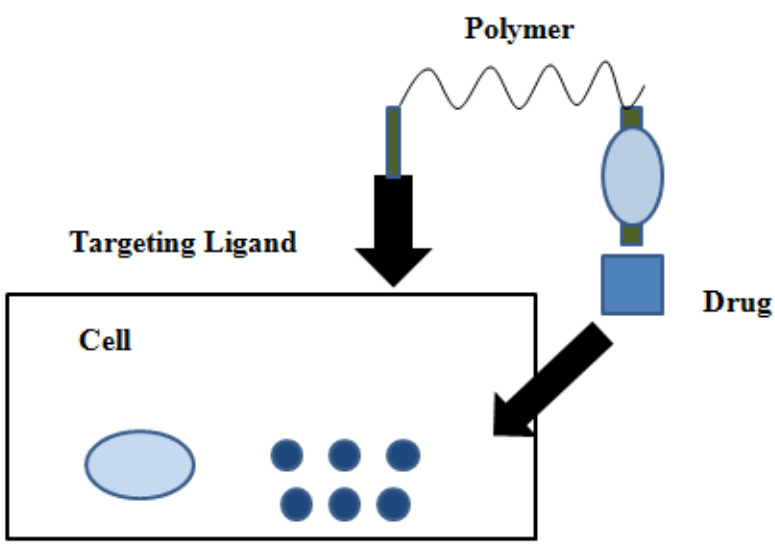


Figure 4. Polymer-drug-targeting ligand conjugation.

## Dendrimers

Dendrimers are nanostructures showing high degree of branching with a core shell. They show low polydispersity with highly precise architectures. Synthesis of these systems, is carried out around a core unit in a generation-by-generation fashion, with a high level of control over size, branching points, and surface functionality. Drug incorporation can be done by passive encapsulation, in which the drug is physically encapsulated in the interior, or by covalently attaching the drug to the dendrimer surface through chemically reactive functional groups to generate a drug-dendrimer conjugate. Dendrimers for drug targeting can be synthesized by adding a targeting moiety on the peripheral surface of the dendritic carrier. Dendrimers help in enhancing bioavailability, and solubility of small molecules, as well as help in multidrug delivery of hydrophobic, and hydrophilic drugs. Recently, Quintana et al. [84] synthesized a generation 5 polyamidoamine dendrimer. The polyamidoamide (PAMAM) dendrimer, was conjugated with folic acid (FA) to obtain a specific focus, and with fluorescein isothiocynate (FITC), which is used as an imaging agent to track the localization of the dendrimer. Finally, it was conjugated to methotrexate, a drug that inhibits FA metabolism. This drug specifically acts during DNA and RNA synthesis; its cytotoxic activity occurs during the S-phase of the cell cycle [52]. Hove et al. constructed particle-in-a-box-in-a-box systems by assembling dendrimer-encapsulated gold nanoparticles (DENs) into dendrimicelles [85]. Kutz et al. formed a self-assembled nanostructure with selective photocatalytic activity from anionic polyoxometalate clusters and cationic dendrimers by electrostatic self-assembly [86]. Siriwardena et al. reported that second generation (G2) peptide dendrimers bearing a fatty acid chain at the dendrimer core efficiently kill Gram-negative bacteria including *Pseudomonas aeruginosa*, and *Acinetobacter baumannii*, two of the most problematic MDR bacteria worldwide [87].

## Polymeric Gels and Hydrogels

Polymeric gels and hydrogels are different hydrophilic structures made of polymers. Polymeric gels have a linear structure while the polymeric hydrogels are networks with three-dimensional covalent cross-linking. Long-chain monomer units linked by covalent bonds, such as, amides, esters, orthoesters, and glycosidic bonds, form the linear polymer gels. Once the linear polymers are formed, other types of interactions (hydrogen bonds or Van der Waals interactions) contribute to achieve the three-dimensional structure. Covalent bonds between chains are responsible for controlling polymeric properties, and making these polymers convenient for use as drug carriers in the form of micro- or nano-particles. These systems can absorb a large quantity of water due to the presence of hydrophilic groups in the structure, which can be utilized in various fields of biotechnology, such as biosensors and drug carriers. Pishko et al. [88] developed a fluorescent biosensor consisting of seminapthofluorescein conjugated with the enzyme organophosphorus hydrolase (SNALF-1) encapsulated in a PEG hydrogel. This enzyme catalyzes the hydrolysis of neurotoxins, thus leading to an increase in the pH. In addition, the fluorescent compound, seminapthofluorescein, which is conjugated to the enzyme, is labile to changes in pH, thereby causing a change in its emission spectrum. Therefore, when the biosensor is incubated in an aqueous medium containing a neurotoxin

such as paraoxon, at first the polymer swells, thus allowing diffusion of the water and toxin inside the polymer. Once the organophosphorus hydrolase enters into contact with toxin, the latter is hydrolyzed, resulting in a change in the pH of the medium, and thus a change in the emission spectrum of the seminapthofluorescein. Another interesting example is the study carried out by Syu et al. [89] for design and synthesis of biosensors for urea concentration measurement. They immobilized urease enzymes in a core of carbon paper on which a polypyrrole matrix was deposited forming an external layer. Urea concentration measurement is based on ammonia concentration, which is the product obtained from the catalysis reaction of urease enzymes [52]. Thambi et al. reviewed the development of biocompatible, biodegradable, and pH- and temperature-responsive injectable hydrogels for sustained release of therapeutic agents [90]. Davoodi et al. developed a polymeric hydrogel system to treat triple negative breast cancer [91].

## Capsosomes

These micron size carrier systems (Figure 5) can be defined as the polymeric structures with a biodegradable outer layer and contain liposomes in the inner compartment of the carrier system. The release of small molecules of drug from these systems takes place by passive diffusion due to permeability of outer membrane. Liposomes in the interior compartment of the capsules may contain the same molecule or different ones. These encapsulated molecules can be either hydrophobic, so will bind to the liposome membrane, or hydrophilic, which will be located in the aqueous core of liposomes. Enzymes such as glucose oxidase [92], peroxidase, chymotrypsin [93], catalase [94] and urease [95], have been encapsulated into capsosomes and these systems have been reported to show catalytic activity [52]. Recently, Yoo et al. prepared polyelectrolyte multilayered liposome alternating adsorption of negatively charged sodium hyaluronate (HA), and positively charged chitosan (CH) on the surface of a cationic core liposome (CL) *via* layer-by-layer (LbL) deposition [96]. Maina et al. reported polymer capsules containing liposomal sub compartments, and checked their ability for the sustained delivery of protein therapeutics [97].

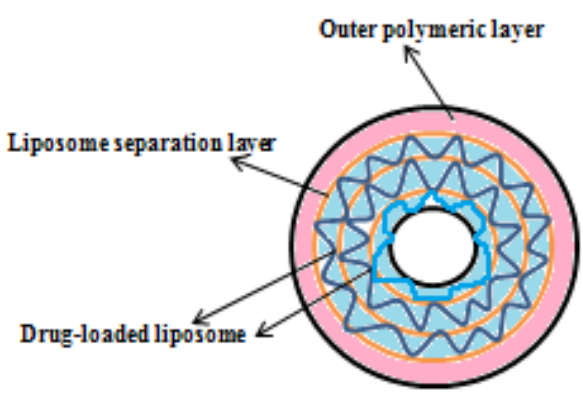


Figure 5. Polymeric capsosome.

## 4. RESPONSIVE POLYMERIC DRUG DELIVERY CARRIER SYSTEMS

Responsive PDDCS(s), or smart PDDCS(s), is a class of carrier system based on the responsive polymer in their design. The superiority of these systems lies in the fact that they undergo dramatic physical or chemical changes, in response to an external stimulus, such as temperature, pH change, and redox potential. These stimuli can be classified as physical or chemical. Physical stimuli (e.g., temperature, ultrasound, light, magnetic, and electrical fields) modulate directly the energy level of the polymer, or the solvent system, and at a critical energy level to induce a polymer response. Chemical stimuli (e.g., pH, redox potential, ionic strength, and chemical agents) induce response by alteration of molecular interactions between polymer, and solvent, or between polymer chains (influencing crosslink or backbone integrity, proclivity for hydrophobic association, or electrostatic repulsion) [98]. Behavioral changes may also induce polymeric changes including transitions in solubility, hydrophilic-hydrophobic balance, and conformation [99]. These changes are manifested in many ways, such as the coil-globule transition of polymer chains [100], swelling/deswelling of covalently crosslinked hydrogels [101], sol-gel transition of physically crosslinked hydrogels [102], and self-assembly of amphiphilic polymers [103]. The most important responsive PDDCS that are widely employed for therapeutic applications are based on temperature, pH and redox potential.

### 4.1. Responsive Systems Based on Temperature

Temperature plays an important role for stimulating PDDCS. Thermo-responsive polymer falling under this category includes Poly(N-isopropylacrylamide) PNIPAAm, which has been studied thoroughly for its potential for reversible or irreversible temperature-dependent phase transition [104]. Lipophobic coils of PNIPAAm were found to be present at a temperature under LCST i.e., lower critical solution temperature (LCST) which is close to 32°C, however above LCST collapsed as lipophilic globules [105]. Volume phase transition is dependent upon lipophilic/lipophobic balance of the polymeric chains [106]. Modulation of these is regulated by continuous establishment and disruption of inter- and intramolecular electrostatic and lipophilic interactions. Under LCST, the water molecules come in contact with local environment of polymeric chains and exist in an orderly manner [107]. Above LCST, lipophilic interactions dominate [105], resulting in collapse of polymeric chain leading the water molecule to the bulk thus causing net entropic increment for polymer/solvent system [108]. In PDDCS the shifting of critical temperature can be achieved by formulating inclusion complex of lipophilic or lipophobic moieties. Polymers with wide lipophlic hydration area show stronger lipophilic interactive forces which collapse at lower temperature [109, 110]. LCST can be increased by increasing the lipophobic content in the polymeric chain. Polymers exhibiting positive temperature-dependent swelling behavior show upper critical solution temperature (UCST). The examples of such materials are poly(acrylic acid) and poly(acrylamide) interpenetrating networks (IPNs) [111].

### 4.2. Responsive Systems Based on pH

Physiological pH differs systematically in the body, predominantly along the GI tract, where degradation of macromolecules takes place by harsh pH and enzymatic conditions of stomach (pH ~ 2). The small intestine is alkaline, with pH ~ 6.2-7.5. Physiological pH also changes in cellular compartments. For example, endosomes typically show pH values of 5.0--6.8 and lysosomes 4.5-5.5 [112-113]. Tumors are reported widely for having acidic conditions (pH ~ 6.5) in the extracellular milieu [114]. Thus, scientists and engineers have dedicated considerable efforts towards rational design of PDDCSs capable of exploiting these pH variations to selectively deliver valuable therapeutics to specific intracellular or extracellular sites of action. By judicious materials selection and careful engineering of molecular architecture, pH-responsive PDDCSs can be developed to give well-controlled pH response and drug release. The polymer system, a mixture of two block copolymers, poly(L-histidine)-b-PEG (polyHis-b-PEG), and poly(L-lactic acid)-b-PEG-b-polyHis-ligand (pLLA-b-PEG-b-polyHis ligand), self-assembled into mixed micelles capable of ligand exposure, micelle destabilization, and endosomal disruption in response to pH [115-116]. Promising work by Hu et al. [117] described the development of pH-responsive core-shell hydrogels, for intracellular delivery of ovalbumin to dendritic cells, a class of cells intimately involved with adaptive immunity. Emulsion polymerization was used to create cross-linked poly (2-diethylamino) ethyl methacrylate (PDEAEMA), core-poly (2-aminoethyl methacrylate) (PAEMA), shell nanoparticles measuring 205 nm in diameter. Authors hypothesized that PDEAEMA would exhibit pH-responsive behavior, whereas PAEMA would remain constitutively ionized throughout the physiological pH range. Interestingly, the cationic PAEMA shell was used to adsorb and protect a model ovalbumin protein rather than the archetypal practice of loading therapeutics into the hydrogel core. Subsequent studies demonstrated the versatility of this approach through intracellular delivery of siRNA and influenza A particles [118].

### 4.3. Responsive Systems Based on Redox Potential

Polymers employed for PDDCS containing labile linkages present an attractive opportunity to develop biodegradable or bioerodible delivery devices. Much of the early work in this field focused on acid labile linkages of polyanhydrides [119,120], poly(lactic/glycolic acid) [121], and more recently poly(β-amino esters) [122,123]. However, intracellular cues are now being investigated as a means to trigger cytoplasmic degradation of polymer carriers incorporating advanced therapeutics such as siRNA, and anticancer drugs. Disulfide linkages are well known to be unstable in a reductive environment as the disulfide bond is readily cleaved in favor of corresponding thiol groups. Polymers with disulfide cross-links have been synthesized as polymersomes [124], nanogels [125], and core-cross-linked polyplexes and degrade when exposed to cysteine or glutathione, reductive amino-acid based molecules present at intracellular concentrations, 50–1000 fold greater than those of the extracellular milieu [126]. Glutathione-degradable nanogels were prepared by inverse emulsion atom transfer radical polymerization (ATRP) [125]. Upon exposure to 10 wt% glutathione, half of the polymer degraded in nearly 6 hours. Exposing polymers to 20 wt% glutathione resulted in

85% degradation within 1 hour. In a more recent investigation, Kataoka and colleagues [126] synthesized and thoroughly characterized a core-cross-linked polyplex composed of iminothiolane-modified PEG-block-poly(L-lysine), or [PEG-b-(PLL-IM)], for intracellular siRNA delivery. The use of a block copolymer affords modular functionality; the polycationic poly(L-lysine) segment serves to bind siRNA and provide endosomal buffering capacity [127] whereas the hydrophilic PEG segment prolongs circulation time, prevents aggregation, and reduces opsonization [128]. Lysine groups of the PEG-b-PLL copolymer were reacted with 2-iminothiolane and subsequently oxidized to form disulfide cross-links. Introducing crosslinks to the micelle core confers stability to the system, as crosslinked polymers maintained micellar structure in physiological salt conditions whereas their noncrosslinked counterparts could not. The resulting polyion complex micelles were approximately 60 nm in diameter, a particle size well within the accepted limits (20–100 nm) for avoiding uptake by the RES and renal exclusion [129].

## 5. General Mechanism of Drug Release from PDDCS

Drug release typically refers to the mechanism that how a drug molecule is transported from a PDDCS to surrounding environment which can be achieved by (a) drug diffusion through water-filled pores or polymer matrix, (b) osmotic pumping, and (c) erosion [130].

Diffusion: Diffusion can take place through water filled pore or polymeric matrix. The former process can be explained by the random movement of drug molecules driven by a chemical potential gradient similar to concentration gradient. In degradable polymeric systems, the rate of drug release rate is approached by the diffusion through a network of pores, with degradation of polymeric matrix. Water absorption is done by polymeric structures immediately; this step is faster than actual drug release. The water in the polymeric structure cause increase in size of the pores, eventually result in drug release through these pores [131]. In latter case i.e., drug diffusion through the polymer matrix; diffusion simply takes place through polymer matrix. In non-degradable drug systems, diffusion is the main driving force for drug release. In these systems the rate of drug release is independent on concentration gradients and remains constant but can be affected by properties of the polymeric membrane (permeability and thickness) [132].

Osmotic pumping: This mechanism of drug release is dependent on convection drive. Osmotic pressure causes influx of water into a non-swelling polymeric system, and thus enhancing the permeability [133].

Erosion: Erosion can take place either from the surface or through the bulk. Surface erosion takes place when the degradation of the polymer starts at the matrix surface, causing size reduction from the outer surface to the inner bulk [134]. It occurs when the degradation rate of polymeric matrix surface is greater than the water penetration rate in the bulk polymer [135]. Bulk erosion takes place when water penetrates in the bulk of the polymeric carrier system causing homogeneous degradation of the entire matrix [136]. Here, water penetration rate is greater than the degradation rate, resulting in hydrolysis of bulk of the matrix. Surface erosion is more predictable than bulk erosion, and protects drugs from the external environment, thus an optimal mechanism for PDDCS.

## CONCLUSION

Research in polymer therapeutics has achieved a great success over the past few decades, in mediating safe and effective delivery of drugs, and various other bioactive agents, for treating variety of medical conditions. The polymeric drug delivery carrier systems *viz*., microspheres, nanoparticles, vesicles, micelles, dendrimers, and polymer drug conjugates highlighted in this chapter show a promising future not only in therapeutics but also in various other biomedical applications. These systems can also be tuned for their responsive release by means of the use of polymers, which release the encapsulated cargos on change of pH, temperature or redox potential. These responsive carrier systems have promising future in endosomal and intracellular delivery, and tumor targeting.

## REFERENCES

[1] Cullins VE. Injectable and implantable contraceptives. *Curr. Opin. Obstet. Gynecol.* 1992; 4:536–543.
[2] Langer R. Implantable controlled release systems. *Pharmacol. Ther*. 1983; 21:35–51.
[3] Zaffaroni A. Systems for controlled drug delivery. *Med Res Rev.* 1981; 1:373–386.
[4] Hoffman AS. The origins and evolution of "controlled" drug delivery systems. *J Controlled Release.* 2008; 132:153–163.
[5] Folkman J, Long DM. The Use of Silicone Rubber as a Carrier for Prolonged Drug Therapy. *J Surg Res.* 1964; 4:139–142.
[6] Langer R, Folkman J. Polymers for the sustained release of proteins and other macromolecules. *Nature.* 1976; 263:797–800.
[7] Higuchi T, Kuramoto R. Study of possible complex formation between macromolecules and certain pharmaceuticals. I. Polyvinylpyrrolidone with sulfathiazole, procaine hydrochloride, sodium salicylate, benzyl penicillin, chloramphenicol, mandelic acid, caffeine, theophylline, and cortisone. *J Am Pharm AssocSci Ed*. 1954; 43:393–397.
[8] Theeuwes F, Hussain A, Higuchi T. Quantitative analytical method for determination of drugs dispersed in polymers using differential scanning calorimetry. *J Pharm Sci.* 1974; 63:427–429.
[9] Roseman TJ, Higuchi WI. Release of medroxyprogesterone acetate from a silicone polymer. *J Pharm Sci.* 1970; 59:353–357.
[10] Roseman TJ. Release of steroids from a silicone polymer. *J Pharm Sci.* 1972; 61:46–50.
[11] Peppas NA, Merrill EW. Development of semicrystallinepoly(vinyl alcohol) hydrogels for biomedical applications. *J Biomed Mater Res.* 1977; 11:423–434.
[12] Langer RS, Peppas NA. Present and future applications of biomaterials in controlled drug delivery systems. *Biomaterials*. 1981; 2:201–214.
[13] Heller J. Controlled release of biologically active compounds from bioerodible polymers. *Biomaterials.* 1980; 1:51–57.
[14] Heller J, Himmelstein KJ. Poly(ortho ester) biodegradable polymer systems. *Methods Enzymol.* 1985; 112:422–436.

[15] Batz HG, Franzmann G, Ringsdorf H. Model reactions for synthesis of pharmacologically active polymers by way of monomeric and polymeric reactive esters. AngewChem, *Int Ed Engl.* 1972; 11:1103–1104.
[16] Przybylski M, Zaharko DS, Chirigos MA, Adamson RH, Schultz RM, Ringsdorf H. DIVEMA-methotrexate: Immune-adjuvant role of polymeric carriers linked to antitumor agents. *Cancer Treat Rep.* 1978; 62:1837–1843.
[17] Khanna SC, Jecklin T, Speiser P. Bead polymerization technique for sustained-release dosage form. *J Pharm Sci.* 1970; 59:614–618.
[18] Birrenbach G, Speiser PP. Polymerized micelles and their use as adjuvants in immunology. *J Pharm Sci.* 1976;65:1763–1766.
[19] Alam MA, Ali R, Al-Jenoobi FI, et al. Solid dispersions: a strategy for poorly aqueous soluble drugs and technology updates. *Expert Opin Drug Deliv.* 2012; 9:1419–40.
[20] Alani AW, Rao DA, Seidel R, et al. The effect of novel surfactants and Solutol HS 15 on paclitaxel aqueous solubility and permeability across a Caco-2 monolayer. *J Pharm Sci.* 2010; 99:3473–85.
[21] Yoshida T, Kurimoto I, Yoshihara K, et al. Aminoalkyl methacrylate copolymers for improving the solubility of tacrolimus I: evaluation of solid dispersion formulations. *Int J Pharm.* 2012; 428:18–24.
[22] Sawada T, Kondo H, Nakashima H, et al. Time-release compression-coated core tablet containing nifedipine for chronopharmacotherapy. *Int J Pharm.* 2004; 280:103–11.
[23] Katsuma M, Watanabe S, Kawai H, et al. Effects of absorption promoters on insulin absorption through colon-targeted delivery. *Int J Pharm.* 2006; 307:156–62.
[24] Tirpude RN, Puranik PK. Rabeprazole sodium delayed-release multiparticulates: effect of enteric coating layers on product performance. *J Adv Pharm Technol Res.* 2011; 2:184–91.
[25] Lai TC, Bae Y, Yoshida T, et al. pH-sensitive multi-PEGylated block copolymer as a bioresponsivepDNA delivery vector. *Pharm Res.* 2010; 27:2260–73.
[26] Maeda A, Shinoda T, Ito T, et al. Evaluatingtamsulosin hydrochloride-released microparticles prepared using single-step matrix coating. *Int J Pharm.* 2011; 408:84–90.
[27] Yoshida T, Nakanishi K, Maeda A, et al. *Pharmaceutical composition containing lipophilic IL-2 production inhibitor.* 2009 WO2009054463.
[28] Babish J, Tripp M, Howell T, Bland JS. *Anti-inflammatory pharmaceutical compositions for reducing inflammation and the treatment or prevention of gastric toxicity*. 2010 US7811610.
[29] Adams ML, Lavasanifar A, Kwon GS. Amphiphilic block copolymers for drug delivery. *J Pharm Sci.* 2003; 92:1343–55.
[30] Maeda H. The link between infection and cancer: tumor vasculature, free radicals, and drug delivery to tumors via the EPR effect. *Cancer Sci.* 2013 In press.
[31] Matsumura Y. Preclinical and clinical studies of NK012, an SN-38-incorporating polymeric micelles, which is designed based on EPR effect. *Adv Drug Deliv Rev.* 2011; 63:184–92.
[32] Raizada A, Bandari A, Kumar B;Polymers in drug delivery : A Review. International *Journal of pharma research and development,* 2010; 2(8):9-20.
[33] Duncan R; The dawning era of polymer therapeutics. *Nature Reviews Drug Discovery,* 2003; 2:347–360.

[34] Laufman H, Rubel T. Synthetic absorable sutures. *SurgGynecol Obstet.* 1977; 145:597–608.

[35] Kulkarni RK, Moore EG, Hegyeli AF, Leonard F. Biodegradable poly(lactic acid) polymers. *J Biomed Mater Res*. 1971;5:169–181.

[36] Pitt CG, Chasalow FI, Hibionada YM, Klimas D.M. and Schindler A. (1983). "Aliphatic polyesters 1. The degradation of poly-caprolactone in vivo", *J. Appl. Polym. Sci.,* 28: 3779–87.

[37] Fahlman, BD. (2007). "Materials Chemistry", *Springer: Mount Pleasant, MI, Vol. 1,* pp 282–283.

[38] O. Kayser, A. Lemke and N. Hernández-Trejo.(2005). "The Impact of Nanobiotechnology on the development of new drug delivery systems". *Current Pharmaceutical Biotechnology*. 6(1):3-5.

[39] Aminabhavi, TM, Balundgi, RH, Cassidy, PE. (1990). "Review on biodegradable plastics". *Polymer Plastics Technology and Engineering.* 29(3): 235-262.

[40] Andreopoulos, A.G. (1994). "Degradable plastics: A smart approach to various applications". *Journal of Elastomers and Plastics.* 24(4): 308-326.

[41] Chandra, R., Rustgi, R. (1998). "Biodegradable polymers". *Progressive Polymer Science*. 23: 1273-1335.

[42] Chau, H., Yu, P. (1999). "Production of biodegradable plastics from chemical wastewater – A novel method to resolve excess activated sludge generates from industrial wastewater Treatment". *Water Science and Technology.* 39(10-11): 273-280.

[43] Chiellini, E., Cinelli, P., Imam, S., Mao, L. (2001). "Composite films based on biorelatedagroindustrial waste and PVA. Preparation and mechanical properties characterization". *Biomacromolecules.* 2: 1029-1037.

[44] Frisoni, G., Baiardo, M., Scandola, M. (2001). "Natural cellulose fibers: Heterogeneous acetylation kinetics and biodegradation behavior". *Biomacromolecules.* 2: 476-482.

[45] Grigat, E., Kock, R., Timmermann, R. (1998). "Thermoplastic and biodegradable polymers of cellulose". *Polymer Degradation and Stability.* 59(1-3): 223-226.

[46] Kolybaba M., Tabil LG, Panigrahi S., Crerar WJ, Powell T., Wang B. (2003). *"Biodegradable Polymers: Past, Present, and Future"*, the American Society of Agricultural Engineers: RRV03-0007.

[47] Huang, JC, Shetty, AS, Wang, M.S. (1990). "Biodegradable plastics: A review". *Advances in Polymer Technology.* 10(1): 23-30.

[48] Jopski, T. (1993). *Biodegradable plastics. Starch.* 83(10): 17-20.

[49] Chandel P, Rajkumari, Kapoor A, Polymers – A Boon To Controlled Drug Delivery System, *International research journal of pharmacy (IRJP)*, 2013; 4(4), 28 – 34.

[50] V Sri Vajra Priya, Hare Krishna Roy, N jyothi, N Lakshmi Prasanthi, "Polymers in Drug Delivery Technology, Types of Polymers and Applications". *Sch. Acad. J. Pharm.,* 2016; 5(7): 305-308.

[51] SatyabrataBhanja, Sudhakar M, Neelima V, Panigrahi BB, Harekrishna Roy. Development and Evaluation of Mucoadhesive Microspheres of Irbesartan. *International Journal of Pharma Research and Health Sciences,* 2013; 1(1): 817.

[52] Gemma Vilar, JuditTulla-Puche and Fernando Albericio, "Polymers and Drug Delivery Systems" *Current Drug Delivery,* 2012, Vol. 9, No. 4.

[53] Harekrishna Roy, Sanjay Kumar Panda, Kirti Ranjan Parida, Asim Kumar Biswal. Formulation and In-vitro Evaluation of Matrix Controlled Lamivudine Tablets. *International Journal of Pharma Research and Health Sciences* 2013; 1(1): 1-7.

[54] Park JH, Kim DS, Mustapha O et. Al Comparison of a revaprazan-loaded solid dispersion, solid SNEDDS and inclusion compound: Physicochemical characterisation and pharmacokinetics. *Colloids Surf B Biointerfaces.* 2017 Dec 12;162:420-426.

[55] V Sri Vajra Priya*, Hare Krishna Roy, N jyothi, N Lakshmi Prasanthi,"Polymers in Drug Delivery Technology, Types of Polymers and Applications" *Sch. Acad. J. Pharm.,* 2016; 5(7): 305-308.

[56] Mahammad Rafi Shaik, MadhuriKorsapati and DinakarPanati (2012). "Polymers in Controlled Drug Delivery Systems", *International Journal of Pharma Sciences, Vol. 2,* No. 4 (2012): 112-116.

[57] Santini Jr, JT, Richards AC, Scheidt R., Cima M.J, and Langer R (2000). "Microchips as Controlled Drug-Delivery Devices", *Angew. Chem. Int. Ed* 39:2396-407.

[58] Kopecek J (2003). "Smart and genetically engineered biomaterials and drug delivery systems", *European Journal of Pharmaceutical Sciences* 20:1-16.

[59] Ting-Ting Yang, Yuan-ZhengCheng, MengQin, Yong-HongWang et al. Thermosensitive Chitosan Hydrogels Containing Polymeric Microspheres for Vaginal Drug Delivery. *BioMed Research International, Volume 2017* (2017), Article ID 3564060.

[60] Liu K, Chen W, Yang T[1], Wen B, Ding D, Keidar M, Tang J, Zhang W. Paclitaxel and quercetin nanoparticles co-loaded in microspheres to prolong retention time for pulmonary drug delivery. *International Journal of Nanomedicine,* 13 November 2017 Volume 2017:12 Pages 8239-8255.

[61] Chen, H., Zhang, W., Yang, N. et al. Chitosan-Based Surface Molecularly Imprinted Polymer Microspheres for Sustained Release of Sinomenine Hydrochloride in Aqueous Media. *Appl. Biochem. Biotechnol.* (2017). https://doi.org/10.1007/s12010-017-2658-2.

[62] Hickey JW, Santos JL, Williford JMet al.Control of polymeric nanoparticle size to improve therapeutic delivery. *J Control Release.* 2015 Dec 10;219:536-547.

[63] Hu J, Sheng Y, Shi J, Yu B, Yu Z, Liao G. Long circulating polymeric nanoparticles for gene/drug delivery. *Curr Drug Metab.* 2017 Dec 7.

[64] Ebeid K, Meng X, Thiel KW, Do AV, Geary SM, Morris AS, Pham EL et al. Syntheticallylethalnanoparticles for treatment of endometrial cancer. *Nat Nanotechnol.* 2017 Dec 4.

[65] Mirzaei F, MohammadpourDounighi N, Avadi MR, Rezayat M. A new approach to Antivenom preparation using chitosan nanoparticles containing *Echiscarinatus* (EC) venom as a novel antigen delivery system. *Iran J Pharm Res.* 2017 Summer;16(3):858-867.

[66] Zhao Y, Li X, Zhao X, Yang Y et al. Asymmetrical Polymer Vesicles for Drug delivery and Other Applications. *Front Pharmacol.* 2017 Jun 20;8:374. doi: 10.3389/fphar.2017.00374. eCollection 2017.

[67] Bing Li, Steven M. Abel. *Shaping membrane vesicle by adsorption of a semi flexible polymer.* Soft matter, 2017, Advance article.

[68] Ribeiro D, Andersson EM, Heath N, Persson-Kry A et al. Human pancreatic islet-derived extracellular vesicles modulate insulin expression in 3D-differentiating iPSC

clusters. *PLoS One.* 2017 Nov 8; 12(11):e0187665. doi: 10.1371/journal.pone. 0187665. eCollection 2017.

[69] Vardhan H, Mittal P, Adena SKR, Upadhyay M et al. Process optimization and in vivo performance of docetaxel loaded PHBV-TPGS therapeutic vesicles: A synergistic approach. *Int J BiolMacromol.* 2017 Oct 27. pii: S0141-8130(17)32121-9. doi: 10.1016/j.ijbiomac.2017.10.172.

[70] Yasuhiro Matsumura. Polymeric Micellar Delivery Systems in Oncology. *Japanese Journal of Clinical Oncology, Volume 38,* Issue 12, 1 December 2008, Pages 793–802.

[71] Boddu, S. H. S.; Jwala, J.; Chowdhury, M. R.; Mitra, A. K. *J. Ocul. Pharmacol. Ther.,* 2010, 26, 459-468.

[72] Kwon, G. S.; Naito, M.; Kataoka, K.; Yokoyama, M.; Sajurai, Y.; Okano, T. *Colloids Surf.* B., 1994, 2, 429-434.

[73] Guo X, Wang L, Duval K, Fan J et al. Dimeric Drug Polymeric Micelles with Acid-Active Tumor Targeting and FRET-Traceable Drug Release. *Adv Mater.* 2017 Dec 6. doi: 10.1002/adma.201705436.

[74] Yang X, Chen Q, Yang J, Wu S, Liu J et al. Tumor-targeted accumulation of ligand-installed polymeric micelles influenced by surface PEGylation crowdedness. *ACS Appl Mater Interfaces.* 2017 Dec 1. doi: 10.1021/acsami.7b16764.

[75] Banerjee SL, Singha NK. A new class of dual responsive self-healable hydrogels based on a core crosslinked ionic block copolymer micelle prepared via RAFT polymerization and Diels-Alder "click" chemistry. *Soft Matter.* 2017 Dec 6;13(47):9024-9035. doi: 10.1039/c7sm01906h.

[76] Jasbir Singh, Sapna Desai, Snehlata Yadav et al. Polymer Drug Conjugates: Recent Advancements in Various Diseases. *J Current Pharmaceutical Design, Volume 22,* Issue 19, 2016.

[77] Tong, R.; Cheng, *J. Polymer reviews,* 2007, 47, 345-381.

[78] Vicent, M. J.; Duncan, R. Trends Biotechnol. 2006, 24, 39-47. (b)Haag, R.; Kratz, F. Angew. Chem. Int. Ed. Engl., 2006, 45, 1198-1215. (c) Duncan, R.; Vicent, M. *J. Adv. Drug Deliv. Rev.,* 2010, 62, 272-282.

[79] Lammers, T. *Adv. Drug Deliv. Rev.* 2010, 62, 203-230.

[80] Hopewel, J. W.; Duncan, R.; Wilding, D.; Chakrabarti, K. Hum. Exp. Toxicol., 2001, 20, 461-470. (b) Julyan, P. J.; Seymour, L. W.; Ferry, D. R.; Daryani, S.; Boivin, C. M.; Doran, J.; David, M.; Anderson, D.; Christodoulou, C.; Young, A. M.; Hesslewood, S.; Kerr, D. J. *J. Control. Release,* 1999, 57, 281-290.

[81] WaliulIslam, JunFang, TomasEtrych, PetrChytil et al. HPMA copolymer conjugate with pirarubicin: In vitro and ex vivo stability and drug release study. *International Journal of Pharmaceutics, Volume 536,* Issue 1, 30 January 2017, Pages 108-115.

[82] Bolu BS, Golba B, Boke N, Sanyal A, Sanyal R. Designing Dendron-Polymer Conjugate Based Targeted Drug Delivery Platforms with a "Mix-and-Match" Modularity. *Bioconjug Chem.* 2017 Dec 6. doi: 10.1021/acs.bioconjchem.7b00595.

[83] AinaL.A.Cesar, Fernanda A.Abrantes, LuanaFarah, Rachel O.Castilho. New mesalamine polymeric conjugate for controlled release: Preparation, characterization and biodistribution study. *European Journal of Pharmaceutical Sciences, Volume 111,* 1 January 2017, Pages 57-64.

[84] Quintana, A.; Raczka, E.; Piehler, L.; Lee, I.; Myc, A.; Mahoros, I.; Patri, A. K.; Thomas, T.; Mulé, J.; Baker, J. R. *Pharm. Res.,* 2002, 19, 1310-1316.

[85] J. B. ten Hove, J. Wang, F. W. B. van Leeuwen and A. H. Velders. Dendrimer-encapsulated nanoparticle-core micelles as a modular strategy for particle-in-a-box-in-a-box nanostructures. *Nanoscale*, 2017, 9, 18619-18623.

[86] Kutz, G. Mariani, R. Schweins, C. Streb and F. Gröhn. Self-assembled polyoxometalate–dendrimer structures for selective photocatalysis. *Nanoscale, 2*017, Advance Article.

[87] Siriwardena TN, Stach M, He R, Gan BH et al. Lipidated Peptide Dendrimers Killing Multidrug Resistant Bacteria. *J Am Chem Soc.* 2017 Dec 5.

[88] Russell, J. R.; Pishko, M. V.; Simonian, A. L.; Wild, J. R. *Anal. Chem.* 1999, 71, 4909-4912.

[89] Syu, M.J,; Chang, Y.S. *BiosensBioelectron.,* 2009, 24, 2671-2677.

[90] ThavasyappanThambi, YiLi, Doo SungLee. Injectable hydrogels for sustained release of therapeutic agents. *Journal of Controlled Release, Volume 267,* 10 December 2017, Pages 57-66.

[91] Davoodi P, Ng WC, Srinivasan MP, Wang CH. Codelivery of anti-cancer agents via double-walled polymeric microparticles/injectable hydrogel: A promising approach for treatment of triple negative breast cancer. *BiotechnolBioeng.* 2017 Dec;114(12):2931-2946.

[92] Srivastava, R.; Brown, J. Q.; Zhu, H.; McShane, M. J. *Macromol. Biosci.*, 2005, 5, 717-27.(b) Z.-l. Zhi, Z. I.; Haynie, D. T. *Chem. Commun.*, 2006, 147-149.

[93] Petrov, A. I.; Volodkin, D. V.; Sukhorukov, G. B. Biotechnol. Prog. 2005, 21, 918-925. (b) Tiourina, O. P.; Antipov, A. A.; Sukhorukov, G. B.; Larionova, N. I.; Lvov, Y.; Mohwald, H. *Macromol. Biosci.*, 2001, 1, 209-214.

[94] Caruso, F.; Trau, D.; Mohwald, H.; Renneberg, R. Langmuir, 2000, 16, 1485-1488. (b)Wang, Y.; Caruso, F. Chem. *Commun.(Camb),* 2004, 7, 1528-1529.

[95] Antipov, A.; Shchukin, D.; Fedutik, Y.; Zanaveskina, I.; Klechkovskaya, V.; Sukhoroukov, G.; Mohwald, H. Macromol. *Rapid Commun.*, 2003, 24, 274-277. (b) Yu, A.; Gentle, I.; Lu, G.; Caruso, F. Chem. Commun. (Camb), 2006, 20, 2150-2152.

[96] Cha YoungYoo, JoonSeobSeong, Soo NamPark. Preparation of novel capsosome with liposomal core by layer-by-Layer self-assembly of sodium hyaluronate and chitosan. *Colloids and Surfaces B: BiointerfacesVolume 144,* 1 August 2016, Pages 99-107.

[97] James W. Maina, Joseph J. Richardson, Rona Chandrawati, Kristian Kempe et al. Capsosomes as Long-Term Delivery Vehicles for Protein Therapeutics. *Langmuir*, 2015, 31 (28), pp 7776–7781.

[98] Gil ES, Hudson SA. Stimuli-reponsive polymers and their bioconjugates. *Prog. Polym. Sci.* 2004; 29(12):1173–222.

[99] Schmaljohann D. Thermo- and pH-responsive polymers in drug delivery. *Adv. Drug Deliv. Rev.* 2006;58(15):1655–70.

[100] Schild HG. Poly (N-isopropylacrylamide): experiment, theory and application. *Prog. Polym. Sci.* 1992; 17(2):163–249.

[101] Khare AR, Peppas NA. Swelling/deswelling of anionic copolymer Gels. *Biomaterials.* 1995; 16(7):559–67.

[102] Malmsten M, Lindman B. Self-assembly in aqueous block copolymer solutions. *Macromolecules.* 1992;25(20):5440–45.

[103] Topp MDC, Jijkstra PJ, Talsma H, Feijen J. Thermosensitive micelle-forming block copolymers of poly(ethylene glycol) and poly(N-isopropylacrylamide) *Macromolecules.* 1997;30(26):8518–20.

[104] Qiu Y, Park K. Environment-sensitive hydrogels for drug delivery. *Adv. Drug Deliv. Rev.* 2001; 53(3):321–39.

[105] Heskins M, Guillet JE. Solution properties of poly(N-isopropylacrylamide) *J. Macromol. Sci. Pure Appl. Chem.* 1968; 2(8):1441–55.

[106] Bae YH, Okano T, Kim SW. Temperature-dependence of swelling of cross-linked poly(N,N'-alkyl substituted acrylamides) in water. *J. Polym. Sci. Part B.* 1990; 28(6):923–36.

[107] Shibayama M, Tanaka T. Volume phase-transition and related phenomena of polymer gels. *Adv. Polym. Sci.* 1993; 109:1–62.

[108] Kopecek J. Smart and genetically engineered biomaterials and drug delivery systems. *Eur. J. Pharm. Sci.* 2003; 20(1):1–16.

[109] Schild HG. Poly (N-isopropylacrylamide): experiment, theory and application. *Prog. Polym. Sci.* 1992; 17(2):163–249.

[110] Inomata H, Goto S, Saito S. Phase-transition of N-substituted acrylamide gels. *Macromolecules.* 1990; 23(22):4887–88.

[111] Katono H, Maruyama A, Sanui K, Ogata N, Okano T, Sakurai Y. Thermoresponsive swelling and drug release switching of interpenetrating polymer networks composed pf poly(acrylamide-co-butyl methacrylate) and poly(acrylic-acid) *J. Control. Release.* 1991; 16(1--2):215–27.

[112] Mukherjee S, Ghosh RN, Maxfield FR. Endocytosis. *Physiol. Rev.* 1997; 77(3):759–803.

[113] Mellman I. Endocytosis and molecular sorting. *Annu. Rev. Cell Dev. Biol.* 1996; 12:575–625.

[114] Vaupel P, Kallinowski F, Okunieff P. Blood-flow, oxygen and nutrient supply, and metabolic microenvironment of human-tumors: A review. *Cancer Res.* 1989; 49(23):6449–65.

[115] Lee ES, Gao Z, Kim D, Park K, Kwan IC, Bae YH. Super pH-sensitive multifunctional polymeric micelle for tumor pHe specific TAT exposure and multidrug resistance. *J. Control. Release.* 2008;129(3):228–36.

[116] Lee ES, Na K, Bae YH. Super pH-sensitive multifunctional polymeric micelle. Nano Lett. 2005;5(2):325–29.

[117] Hu Y, Litwin T, Nagaraja AR, Kwong B, Katz J, et al. Cytosolic delivery of membrane-impermeable molecules in dendritic cells using pH-responsive core-shell nanoparticles. *Nano Lett.* 2007;7(10):3056–64.

[118] Hu Y, Atukorale PU, Lu JJ, Moon JJ, Um SH, et al. Cytosolic delivery mediated via electrostatic surface binding of protein, virus, or siRNA cargos to pH-responsive core-shell gel particles. *Biomacromolecules.* 2009; 10(4):756–65.

[119] Mathiowitz E, Jacob JS, Jong YS, Carino GP, Chickering DE, et al. Biologically erodable microspheres as potential oral drug delivery systems. *Nature.* 1997;386(6623):410–14. This contribution was the first serious effort to use biodegrablemicroparticles for oral delivery of proteins and DNA.

[120] Leong KW, Brott BC, Langer R. Bioerodiblepolyanhydrides as drug-carrier matrices. I: Characterization, degradation, and release characteristics. *J. Biomed. Mater. Res.* 1985; 19(8):941–55.

[121] Cohen S, Yoshioka T, Lucarelli M, Hwang LH, Langer R. Controlled delivery systems for proteins based on poly(lactic/glycolic acid) microspheres. *Pharm. Res.* 1991; 8(6):713–20.

[122] Shenoy D, Little S, Langer R, Amiji M. Poly(ethylene oxide)-modified poly(β-amino ester) nanoparticles as a pH-sensitive system for tumor-targeted delivery of hydrophobic drugs. 1. In vitro evaluations. *Mol. Pharm.* 2005; 2(5):357–66.

[123] Shenoy D, Little S, Langer R, Amiji M. Poly(ethylene oxide)-modified poly(β-amino ester) nanoparticles as a pH-sensitive system for tumor-targeted delivery of hydrophobic drugs: Part 2. In vivo distribution and tumor localization studies. *Pharm. Res.* 2005; 22(12):2107–14.

[124] Cerritelli S, Velluto D, Hubbell JA. PEG-SS-PPS: reduction-sensitive disulfide block copolymer vesicles for intracellular drug delivery. *Biomacromolecules.* 2007; 8(6):1966–72.

[125] Oh JK, Siegart DJ, Lee H, Sherwood G, Peteanu L, et al. Biodegradable nanogels prepared by atom transfer radical polymerization as potential drug delivery carriers: synthesis, biodegradation, in vitro release, and bioconjugation. *J. Am. Chem. Soc.* 2007; 129(18):5939–45.

[126] Matsumoto S, Christie RJ, Nishiyama N, Miyata K, Ishii A, et al. Environment-responsive block copolymer micelles with a disulfide cross-linked core for enhanced siRNA delivery. *Biomacromolecules.* 2009; 10(1):119–27.

[127] Dufresne MH, Elsabahy M, Leroux JC. Characterization of polyion complex micelles designed to address the challenges of oligonucleotide delivery. *Pharm. Res.* 2008; 25(9):2083–93.

[128] Owens DE, Peppas NA. Opsonization, biodistribution, and pharmacokinetics of polymeric nanoparticles. *Int. J. Pharm.* 2006; 307(1):93–102.

[129] Davis ME, Chen Z, Shin DM. Nanoparticle therapeutics: an emerging treatment modality for cancer. *Nat. Rev. Drug Discov.* 2008; 7(9):771–82.

[130] Langer R. New methods of drug delivery. *Science.* 1990; 249:1527–1533.

[131] Webber WL, Lago F, Thanos C, Mathiowitz E. Characterization of soluble, salt-loaded, degradable PLGA films and their release of tetracycline. *J Biomed Mater Res.* 1998; 41:18–29.

[132] Fu Y, Kao WJ. Drug release kinetics and transport mechanisms of non-degradable and degradable polymeric delivery systems. *Expert Opin Drug Delivery.* 2010; 7:429–444.

[133] Keraliya RA, Patel C, Patel P, Keraliya V, Soni TG, Patel RC, Patel MM. Osmotic drug delivery system as a part of modified release dosage form. *ISRN Pharm.* 2012;2012:528079.

[134] Uhrich KE, Cannizzaro SM, Langer RS, Shakesheff KM. Polymeric systems for controlled drug release. *Chem Rev.* 1999; 99:3181–3198.

[135] Marin E, Briceno MI, Caballero-George C. Critical evaluation of biodegradable polymers used in nanodrugs. *Int J Nanomed.* 2013; 8:3071–3090.

[136] Park H, Park K, Shalaby WS. *Biodegradable Hydrogels for Drug Delivery.* CRC Press; Boca Raton, FL: 2011.

In: Advances in Polymers for Biomedical Applications ISBN: 978-1-53613-612-8
Editors: Deepak Pathania and Bhuvanesh Gupta 

*Chapter 15*

# VALUE ADDED WOUND HEALING MATERIAL OF CROSS LINKED PVA-ALGINATE NETWORK

***N. Gobi[1], T. Devasena[2,*] and P. Pathmaja[1]***
[1]Department of Textile Technology,
[2]Centre for Nanosceince and Technology,
Alagappa College of Technology, Anna University, Chennai, Tamil Nadu, India

## ABSTRACT

Conventional textile based wound dressing materials are cost-effective and good absorbents. However, cross linked polymer nanocomposites are best choice due to their ability to provide optimal wound healing conditions like homeostasis, non-adherence, maintenance of a moist wound bed etc. Electrospun polymer web, by virtue of their micro fibrous structures provide suitable environment for wound healing. In this study, we have optimized the preparation of a blend of sodium alginate and polyvinyl alcohol of different proportions. We have mixed the blend with different proportions of citric acid for cross linking. The blend was then made into fibrous web using electrospinning apparatus. Calcium alginate has many advantages over sodium alginate such as web stability and high performance especially with bleeding wounds. Getting commercial calcium alginate is also expensive. Therefore, we first made the web using sodium alginate and then replaced the sodium for calcium by using calcium chloride. Thus, we formed a web of calcium alginate crosslinked with citric acid.

The web samples were then taken for physiochemical characterization using scanning electron microscopy, Fourier infrared spectroscopy; thermogravimetric analyser and moisture vapour transmission analyser. The SEM micrograph revealed the presence of many interconnections and densely crosslinked web. Moreover, the cross linking was good in the web made from blend as compared to the web made with the individual component. The SEM images clearly suggest that the cross linked web has ideal morphology to give better performance in the process of wound healing. The FTIR spectra clearly revealed the interaction between the groups of the polymer constituents

* Corresponding Author Address: Prof.Dr.Devasena T. Centre for Nanoscience and Technology, A.C. Tech Campus, Anna University, Chennai 600025, Tamil Nadu, India. tdevasenabio@gmail.com; tdevasenabio@annauniv.edu.

and the groups involved in cross linking. This confirms the role of citric acid in making a high performance web. The spectral findings are in line with the SEM morphological images. Thermogravimetric plot is an evidence for the stability of the material under study. The cross linked web has better stability than the non-cross linked counterpart. Also, the stability increased with an increase in the concentration of the cross linking agent. Thus we speculate that, the web which was found to be better as per the SEM micrograph and the FTIR spectra was also stable enough, which is a pre-requisite for a high performance wound healing. MVTR results show that the loss of water is reduced in citric acid crosslinked alginate blend. Since cross linking increases the water absorption capacity of the alginate it would provide moist environment to the wound, which helps in rapid healing thereafter. Compared to the crosslinked web, the non-crosslinked ones showed greater water vapour permeability. The cross linked web was found to inhibit the growth of the *Staphylococcus aureus*as evidenced by zone of inhibition in the growth medium.

**Keywords:** alginate, PVA, citric acid, nanoweb, web, wound healing

# 1. INTRODUCTION

## 1.1. Wound-Type and Healing

A wound refers to a break in the epithelial integrity of the tissues in an area of the body leading to a loss of continuity in that area. This disruption can be deeper and involve sub-epithelial tissues including dermis, fascia, and muscle. It is caused by physical trauma where skin is torn, cut or punctured (open wound) or where a blunt force trauma causes a contusion (closed wound). Wound healing is the process of refurbishment of structure and function of the injured or diseased tissues by means of blood clotting, tissue mending, scarring, and bone healing. In this process, the continuity of the damaged tissue is restored by fibrous adhesion, without formation of granulation tissue ending up in a thin scar.

The mode of wound healing depends on the powers of regeneration of the particular tissue. Types and causes of wounds are wide ranging, and health care professionals have several different ways of classifying them. They may be chronic, such as the skin ulcers caused by diabetes mellitus, or acute, such as a gunshot wound or animal bite. Wounds may also be referred to as open, in which the skin has been compromised and underlying tissues are exposed, or closed, in which the skin has not been compromised, but trauma to underlying structures has occurred [1]. Various types of wounds are summarisedin Table 1.

Wound healing process occurs in five different phases: haemostasis, inflammation, migration, proliferation or granulation and maturation or remodelling.

The phases operate in different days from the wound incidence. On the whole, moisture is the vital determinant of wound healing and pain related to the wound. Excess the moisture, greater the chances for periwound to occur by granulation tissue. This results in maceration or tearing of the affected area, thus increasing the size of the wound. Lesser the moisture content, lesser the granulation thus leading to fissures in the wound bend causing pain and decreasing the healing rate. A hydrogel can produce a rapid healing by creating a moist environment that reduces the build-up of necrotic tissue and scar tissues (cell death). The beneficial effects of a moist wound versus a dry wound environment is prevention of tissue

dehydration, cell death, accelerated angiogenesis, increased breakdown of dead tissue and powerful interaction with their target cells. Hence a balanced stage of moisture results in rapid healing of the wound. In a skin trauma, a regime of organized and predictable cascadeof events occur.This cascade continue till the wound is enclosed by a scar tissue for complete healing [1].

***Hemostasis***

Hemostasis is the first stage of wound healing that occurs during day one to three. In this process, the bleeding of the damaged blood vessels is stopped by coagulation and formation of gel. This results in the formation of fibrin network which produces a clot in the wound. The clot dries to form a scab which provides strength and support to the injured tissue. Haemostasis therefore, plays a protective role and contributes to successful wound healing [2].

***Inflammation***

Inflammation lasts from day three and may extend up to one or two weeks depending on the severity of the damage. It involves both cellular and vascular responses which lead to new frame work for blood vessel growth, the process called angiogenesis. The release histamine and serotonin protein-rich exudate into the wound causes vasodilatation and allows phagocytes to enter the wound which engulfs the dead cells (necrotic tissue). Necrotic tissue is hard and liquefied by enzymatic action to produce an yellowish mass described as slough [3].

**Table 1. Types of wounds**

| Wound type | Etiology | Example |
|---|---|---|
| Abrasions | rubbing friction in the skin, caused by rough surfaces. | Rope burns and skinned knees |
| Avulsions | Forcible mechanical pulling of body surface or the structure. | Bites caused by organisms. |
| Contusions (Bruises) | Forceful trauma that damages the internal structure of the body without damaging the skin, especially due to a blow in the chest, abdomen, or head or knee. with a blunt instrument | Wounds caused by blowing due to blunt tools or balls. |
| Crush Wounds | Splitting of skin and tearing or shattering of the underlying layers. | Wound caused by sudden falling of heavy objects. |
| Cuts | Slicing of skin with sharp instruments leaving even edged wounds. | Surgical incision or cut with a blade. |
| Fish-Hook Wound | Aseptic or infected sharp cut in the tissue without severing in the soft tissue. | An injury caused by a fish-hook |
| Lacerations | Ragged-edged tears produced by tremendous force imposed by an internal source or external source. | Wound due to childbirth force and punch. |
| Open Wound | Breaking of skin | Incised or gun shot wounds |
| Penetrating wound | Breaking of skin with the parallel entry of the wound causing agents into the subcutaneous tissue or a deep lying structure or cavity. | Wounds caused by piercing of nails, splinters, spikes etc. |
| Punctures | Deep narrow pores induced by sharp objects | Wounds caused by knives, and broken glass. |

***Migration***

The process of movement of epithelial cells and fibroblasts to the injured area to replace the damaged and lost tissue is called migration. These cells migrate along the margin to the wound, growing rapidly over the wound under the dried scab (clot).This process is also escorted by epithelial thickening. Fibroblasts produce collagen which in turn contribute strength and integrity to the skin [2].

***Proliferation***

Cell proliferation in the wound site lasts for 2 to 3 days. This phase is characterised by granulation and capillary and lymphatic vessels growth in the wound. At the end of proliferation, epithelial thickening will be formed which will be followed by the fibroblast proliferation and collagen synthesis and this process will go for about 14-15 days. Collagen is responsible for making the wound thicker [2].

***Maturation or Remodelling***

Maturation or remodeling starts after 3 weeks of the wound formation and lasts for an year or more. In this process the wound closes completely due to remodeling of collagen from type III to type I, characterized by alignment and cross linking of collagen fibers which make the repaired skin stronger by increasing the tensile strength. The wounded area is remodeled by a decrease in the scar thickness. Apoptosis occur in this phase for the removal of unwanted cells involved in repairing [3]

## 1.2. Wound Dressing

An increasing demand for skin repair and replacements has urged the researchers to fabricate high quality nanomaterials-based wound cover or dressings, tissues, scaffolds, etc. Polymeric membranes have been intensively used for the fabrication of wound healing material owing to its active role in the treatment of burns, prevention of post-surgical adhesions and cosmetic surgery. Polymers like polyurethane, polyethylene, polylactides, polyglycolides, and polyacrylonitrile are good examples for such polymers used for topical medication. Nonetheless, release of acids and poor stability are disadvantages of the polymers. These demerits can be circumvented by the use of biodegradable polymers like gelatin, chitin, chitosan, collagen, alginates, etc. These materials are natural polymers without eco-toxic and hazardous effects [1]. An ideal wound dressing should have the following criteria:

- Non-toxic and non-allergic on continuous use.
- provide defence against infection
- absorb blood and exudates
- Enhance rapid growth of new blood vessels
- Promote migration of cells in epidermis.
- Support leucocyte migration.
- Maintain moist milieu.
- Permit gas exchange between the wound and the un-wounded surrounding

- Should favour the synthesis of connective tissue and alignment of collagen network.
- Detach from the tissue after healing process with further damage to the scar.
- Suitable for chronic wounds also
- Less expensive
- Easy fabrication method with less time consumption
- Biocompatible
- Maintain local pH and temperature.

### *1.2.1. Traditional Wound Dressing*

Textile-based wound dressings such as gauze, lint, and wadding, are used in traditional dressings which helps to absorb exudates, cushion the wound, allow for a dry site, hide the wound from view, and provide a barrier to contamination. In fact, these traditional dressings are good for non-severe wounds where they induce blood clotting and absorb exudate fluids, prevent infection and contamination and dry the wound without further damage. An open wound dries up faster with a scab covering it. It has been reported that the healing with a wet environment is faster than that with a dry environment. These traditional wound dressings can be stored and used for domestic purpose [4].

### *1.2.2. Advanced Wound Dressings*

Advanced wound dressings are used for clinical purposes in hospitals rather than for domestic purposes.

Band dressing, film dressing, foam dressings, hydrogels, alginates and hydrocolloids are some of the advanced wound dressing materials. The main function of such dressings is to provide a moist environment for subsequent natural healing process, without occluding the wound. These dressings are capable of maintaining a constant local temperature and also preventing infection. This type of dressing also reduces pain and removes dead tissue without damaging the wound. Often, while textile materials provide high absorbency, they tend to allow a wound to dry out, and become incorporated in the healing tissue, thereby disturbing the newly epithelializing layer during wound changes. Various types of wound dressings are amorphous hydrogels, hydrogel dressings, hydrocolloid dressings, alginate dressings, composite dressings, and transparent films [4].

**Hydrogels**

Hydrogels are made of excess water in a gel base to form an effective dressing. Among them are amorphous hydrogels, impregnated hydrogels and sheet hydrogel.

Amorphous hydrogels are free flowing gel fabricated as sterile formulation in tubes, packets or bottles using water and polymers with an intention to provide moisture to the dry wound and maintain a moist healing milieu. Such gels are suitable for partial- and full-thickness wounds, necrotic wounds, minor burns and radiation-induced wounds. Impregnated hydrogels are usually the gel material impregnated into a base like gauze, sponge ropes or sponge strips. Sheet hydrogels are fabricated using combinations of gels amalgamated by mesh of fibre. On the whole, hydrogels can be used for healing of ulcerated wounds, skin tears, surgical wounds, burns, and radiation burns [5].

**Hydrocolloid Dressings**

Hydrocolloid dressings are impervious, elastic wafer which is impregnated with gels of pectin or any other polymer which is used as an adhesive to stick the wafer to the skin. On sticking, the polymer absorb the fluid in the wound and swell. Hydrocolloid wound dressings show good durability as they can withstand in the skin for a week thus making the treatment cost-effective. It also promotes painless and faster healing of wounds. The water proof attribute of the dressing prevents infection risk. The dressing adheres only to the intact skin surrounding the edge of the wound which do not interfere with the newly forming tissues. Hydrocolloid dressings are impermeable to water, oxygen, or bacteria and hence they promote fast blood vessel regeneration and granulation. Hydrocolloids serves as antibacterial site by creating an acidic environment by lowering of the pH [6].

**Chitosan Dressings**

Wound healing activity of chitosan dressing is attributed to antimicrobial activity, cell attachment and proliferation all of which are essential for safe wound healing. Composite sponge of curcumin/chitosan/gelatin exhibits water uptake ability, antibacterial activity, and wound closure efficacy [7].

## 1.3. Alginate-The Signature of Seaweed's Cell Wall

Alginate dressings are made of alginic acid sourced from seaweeds and are widely used for highly exudative wounds. Alginate is present in the cell walls of brown algae as the calcium, magnesium and sodium salts of alginic acid. Alginate is a good absorbent and gel forming agents with haemostatic properties. It is water soluble, biocompatible, biodegradable, polyelectrolyte which has been used in biomedical applications related to tissue engineering, drug delivery, and wound dressing. Previous works have reported the wide usage of scaffolds dental impressions and surgical impressions of alginate in the biomedical fields [9]. High hydrophilicity, biocompatibility and low cost are added advantages of alginate. The common alginate dressings are in the form of sheets that are suitable for superficial wounds or in the form of strip, ribbon or rope that are used for filling deep wounds and cavities. At skin graft donor sites alginates are good choice for providing better healing and reduced pain when compared with paraffin gauze dressings. Alginate can be used in conjunction with an absorbent pad in the case of heavily exudating wounds or with a semipermeable film or foam for the healing of lightly exudating wounds.[8]:

Following are the main advantages of alginate dressings which make an ideal wound healing material of interest:

- High absorptivity
- Non-adherence
- Biodegradability
- Presence of non-woven fiber
- Presence of ionic silver which interact with serum to form hydrophilic gel during healing process.

- Antimicrobial property
- Hemostatic property

Wounds that are possibly effectively healed by alginate dressings include:

- draining wounds
- pressure/vascular ulcers
- surgical wounds
- wound dehiscence
- tunnel wounds
- sinus tracts
- skin graft donor sites
- exposed tendons
- infected wounds
- bleeding wounds

In spite of several advantages, the low mechanical strength and high degradation level of alginate often demands the co-polymerisation and chemical modification custom. This can be done respectively by blending with a copolymer and crosslinking by a cross linking agent. This is discussed in the very next topic here.

## 1.4. Electrospinning Creates Nano-Platform for Wound Healing Applications

Electrospinning is the most fascinating technique for the lab-scale and large scale fabrication of 2D nanostructures of biomedical and environmental importance. With the advent of nanotechnology, technologists are more fascinated in electrospinning, an electrostatic fiber fabrication technique that has grabbed more concern and attention in modern years due to its versatility and potential for applications in diverse fields. High surface area to volume ratio, choices of different pore size and the ability to tune and optimize nanofiber composition in order to get desired properties and function are the advantages of the electro spun nanofibers which can be exploited for many applications. Tissue regeneration, biosensors, water treatment and air filters, wound healing material, drug delivery carriers, and enzyme immobilization matrix are some of the applications. Electrospinning is indeed a simple and cost-effective method to produce nanoplatforms for rapid and safe healing of wounds. By this technique ultra-fine nano fibers can be directly spun into a multifunctional mat or web [10]. Throughout the decade, more than 100 polymers have been electrospun for diverse applications. This technique can produce high quality fibres from polymers such as carboxyethyl chitosan/PVA, collagen/chitosan, Silk fibroin and ABA type poly(dioxanone-*co*-l-lactide)-block-poly(ethylene glycol) (PPDO/PLLA-b-PEG) block copolymer for wound dressing applications. An electrosupun wound healing material of PVA/$AgNO_3$ was proved to exhibit high performance wound healing effect after ultraviolet or heat treatment. Duan et al. have spun nano fibers of poly(ε-caprolactone) (PCL) incorporated with silver-loaded zirconium phosphate nanoparticles for wound healing application. Nanofibres of poly(ε-caprolactone), poly-vinyl-pyrrolidone iodine complex and poly-

ethyleneoxide/poly-vinyl-pyrrolidone iodine complex possess antimicrobial and wound healing efficacy. Poly(3-hydroxy butyrate-*co*-3-hydroxyvalerate) (PHBV) electrospun nanofiber were reported show wound healing activity in cultured hair follicular cells [10].

Electrospinning of alginate however is a tricky task,owing to low polymer solubility, polymer solution instability and high viscosity [11]. Yet, continuous fibers are successfully electrospun from PVA solutions of 7, 8 and 9%. Safi et al. (2007) have spun the fibers by using blends of alginate and PVA in different ratio. The higher the proportion of PVA more uniform were the fibers. With these background, literature on electrospun polymers and citric acid in perspectives, we present and discuss here the results of our experiments on the electro spun web of citric acid-crosslinked alginate/PVA blend.

## 1.5. Electrospinning of Alginate Is a Challenging Task

Electrospun alginate web is a good wound healing material. A bit challenging though. Even at low concentration, alginate undergoes gelation making electrospinning very difficult thus affecting the fibre formation. Sodium alginate is a polyelectrolyte with high conductivity and surface tension. The repulsive force among the polyanions are the crucial aspect that challenges the electrospinning of sodium alginate. At neutral pH, alginate solution appears semi-dilute at a concentration of 2% by weight, where intermolecular interactions are dominant. At a concentration greater than 2% by weight, an alginate solution transforms into a physical gel as a result of increased intermolecular interactions and chain entanglements [13]. However if the repulsive force is circumvented by blending with a copolymer, the electrospinning can be successful. The co-polymerisation can result in the formation of matrices that mimics natural extracellular matrix making them ideal for biomedical applications especially wound healing. For example, alginate blended with poly(ethylene oxide) was electro spun into fibers for biomedical applications [14].

The rigidity of the alginate chain is mainly caused by the glucuronate units, which are linked by diaxial linkages and stabilized by hydrogen bonding. This makes the alginate more rigid and has a similarity to the cellulosic chain. Nie et al. (2008) speculated that the rigid and extended worm-like molecular chains of alginate will not form effective chain entanglements in its aqueous solution. This may be the reason that electrospinning of pure alginate from its aqueous solution is difficult to generate nanofibers. Glycerol, a strong polar co-solvent was used in the literature to solve the aforementioned problem.

## 1.6. A Renowned co-Polymer Candidate - The Poly Vinyl Alcohol (PVA)

Polyvinyl alcohol (PVA) is well known for some attributes like non-toxicity, biocompatibility, rapid film forming efficacy, chemical resistance to oil, grease and solvent, high tensile strength, high oxygen and aroma barrier properties,emulsifying and adhesive nature and mechanical resistance all of which enhances its biomedical performance[15]. As result, a blend of polymer-PVA when woven into a membrane or a film can hold value-added clinical properties and hence be used for wound dressing applications. This was found true as per the reports on dextran and chitosan. Previous reports have revealed the enhanced tensile

strength of alginate on co-polymerisation with polyvinyl alcohol (PVA). PVA-polymer blend will moisten the surface of the wound and diminish the accumulation of necrotic tissues and autolysis As a result quick wound healing will be achieved. Sodium alginate and polyvinyl alcohol based hydrogel showed an improved healing rate of artificial wounds in rats. Still, the hydrophilicity and poor water resistant property (i.e, poor stability in water) of PVA necessitates chemical cross linking which could warrant stable structural integrity and high water reistance ability, making the alginate-PVA blend highly suitable for biomedical and environmental applications such as water treatment [16].

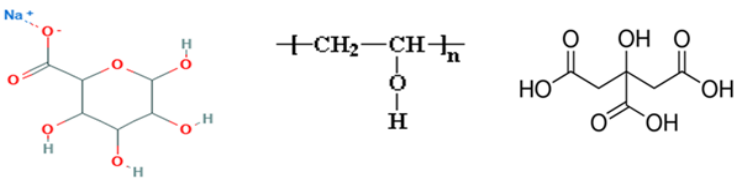


(a) (b) (c)

Figure 1. Structure of the chemicals under discussion a) Alginate b) PVA c) Citric acid.

## 1.7. Citric Acid Is a Promising Choice of Cross Linker for Alginate

Alginate cross linking can be achieved using glutaraldehyde. Nevertheless, the toxic end products and instability due to decomposition in physiological media and generation of undesirable products has overruled the aldehyde cross linkers. Polycarboxylic acids on the other hand can circumvent the aforesaid disadvantages and provide us good quality web or base for wound healing. Therefore, the Poly(carboxylic acids) can be a safe and inexpensive substitute for cross linking in biomedical materials such as wound dressings.

Among polycarboxylic acids, citric acid ($C_6H_8O_7$) is remarkable in that it is non-toxic and occurs naturally in citrus fruits and is also a metabolic product in the Kerb's cycle of all aerobic organisms. It is also inexpensive and reported to possess acidulant and antibacterial property [17]. On the whole, citric acid can be a promising acid for cross linking and wound healing function. Recently, Stone et al. have validated that citric acid can readily crosslink PVA-alginate blend conferring enhanced thermal stability and decreased dissolution in water and simulated body fluid [18].

## 1.8. Calcium Alginate Is Advantageous Over Sodium Alginate

Replacement of sodium ions of sodium alginate with calcium ions can result in calcium alginate. The calcium alginate is expensive than the sodium alginate, however, addition of aqueous calcium chloride to aqueous sodium alginate can result in calcium alginate product at low cost. Calcium alginate is water-insoluble, gelatinous, cream coloured substance. Presence of calcium not only increases the mechanical strength and the stability of the alginate product but also helps in perfect healing of bleeding wounds. This is called as the haemostatic property of calcium. Calcium is a crucial component for platelet aggregation, fibrin formation and blood clotting mechanism. During clotting process of intrinsic pathway, prothrombin is

converted to thrombin in the presence of thromboplastin. Thrombin in turn converts fibrinogen into fibrin which forms a mesh thus clotting the blood. In both of these reactions, calcium is the promoter that drives the reaction towards clotting mechanism.

Calcium alginate is a right option when hydrocolloid type of dressing is not suitable as in the case of excess exudate. Due to high absorptivity, it can be used for dressing of surface wounds, cavities, draining and cleaning applications. Calcium alginate dressings interacts with exudates forming a natural gel that makes the wound environment moist and supple, thus leading to proper healing and proliferation of cells leading to new tissue growth. The gel also act as a natural obstacle toinfectious microbes that may counteract healing by eliciting secondary infections of the wound. Hence, it is reasonable to form web of calcium alginate rather than sodium alginate for wound dressing[19].

## 2. MATERIALS AND METHODS

### 2.1. Chemicals and Equipments

Polyvinyl alcohol ($C_4H_6O_2$) n the copolymer and citric acid, the cross linking agent are obtained from Hi media, Mumbai. Sodium alginate (NaC6H7O6) the gel material, was purchased from Sigma Aldrich. Electrospinning of alginate-PVA blend was done using ESPIN – NANO Electrospinning Apparatus.

### 2.2. Preparation of Alginate-PVA Blend

Sodium alginate and polyvinyl alcohol solutions were prepared by dissolving them in distilled water under mild stirring. Maximum concentration of sodium alginate taken for electrospinning was 2% by weight. The maximum concentration of polyvinyl alcohol taken for electrospinning was 10% by weight. In order to optimize, the solutions of polyvinyl alcohol and sodium alginate were blended in ratios of 100:0, 90:10, and 80:20 with varying concentrations of cross-linking acid. The details of the proportion of the materials and the composition of the blend used for making the web by electrospinning are shown in Table 2.

**Table 2. Composition of the blend used for electrospinning of the fiber web**

| S.No | Sodium alginate (Percentage solution) | PVA (Percentage solution) | Citric acid (Percentage solution) |
|---|---|---|---|
| 1 | 0% | 10% | 0% |
| 2 | 1% | 9% | 0% |
| 3 | 2% | 8% | 0% |
| 4 | 1% | 9% | 6% |
| 5 | 1% | 9% | 9% |
| 6 | 1% | 9% | 12% |
| 7 | 2% | 8% | 6% |
| 8 | 2% | 8% | 9% |
| 9 | 2% | 8% | 12% |

## 2.3. Electrospinning

The blended solutions were taken individually and fed into 5ml syringe fitted with a needle tip. A DC voltage of 18-20kV was applied between the syringe tip and collector covered with aluminium foil. A distance of 20cm was kept between the syringe tip and the collector and flow rate was set as 0.75ml/hr. Droplet emerged from the tip of the needle was split due to repulsive force set at the needle. During this process, the solution evaporated and polymeric fibres deposited on the aluminium foil in the form of nonwoven fibrous mat.

The set-up was left to dry in hot air oven at 80°C for 2hrs. And the webs were subjected to treatment of $CaCl_2$. The webs were then left undisturbed for 2-3hrs at room temperature after which they are washed and cured at 140°C. The resulting fibre web will have its sodium replaced by calcium ions exhibiting high mechanical strength and stability which helps in better wound healing process.

## 2.4. Physiochemical Characterization of the Fibre Web

The morphology of the nanofibers obtained by different compositions wereanalysed using scanning electron microscope (HITACHI S-3400 SEM) at a voltage of 5kV. The diameter of the nanofibers was determined at 5 different points. Fourier transform infrared spectra (FTIR spectra) was obtained using FTIR spectrometer (Jasco FT/IR6600) The spectra were scanned between 500 and 4500 $cm^{-1}$, in order to identify the interaction between the molecular structure of PVA and Alginate and the functional groups involved. It was also used to study the interaction of calcium alginate and PVA blended nanofibre web.

## 2.5. Moisture Vapour Transmission Rate

The moisture vapour permeability of a nanofibrous material can be determined by measuring the Moisture vapour transmission rate (MVTR) across the material. With the diameter of 15mm, the materials were mounted on the mouth of cylindrical beakers containing 5ml of water with negligible water vapour transmittance. The material was fastened using a Teflon tape across the edges to prevent any water vapour loss across the boundary and kept at 37°C and 35% relative humidity in an incubator. The assembly was weighed at regular intervals of time and weight loss versus plot was constructed. From the slope of the plot, MVTR was calculated by the following formula,

$$\text{MVTR} = \frac{\text{slope X 24}}{\text{A}} \text{g/m}^2\text{/day}$$

Where, A is the test area of sample in $m^2$.

### 2.6. Thermogravimetric Analysis

Thermogravimetric analysis (TGA) is one of the members of the family of thermal analysis techniques used to characterize a wide variety of materials. TGA measures the amount and rate (velocity) of change in the mass of a sample as a function of temperature or time in a controlled atmosphere. The measurements are used primarily to determine the thermal and/or oxidative stabilities of materials as well as their compositional properties. The technique can analyse materials that exhibit either mass loss or gain due to decomposition, oxidation or loss of volatiles (such as moisture). It is especially useful for the study of polymeric materials, including thermoplastics, thermo sets, elastomers, composites, films, fibres, coatings and paints. We have determined the thermal stability of the web of different compositions using thermogravimetric analyser (SII TG/DTA 6300).

### 2.7. Antibacterial Activity

Antibacterial activity of the material was studied by disc diffusion method. The protocol is as follows: Nutrient agar solution was prepared by dissolving nutrient agar in distilled water under constant stirring. Nutrient agar and petri plates were autoclaved for further use. After sterilization, nutrient agar was poured into the petri plates and allowed to solidify. After complete solidification, 100µl of organism culture was taken and poured into the petri plates. The culture was spread throughout the plate using L-rod. Then the sample were placed over the agar and left for 24 hrs. After 24 hrs the zone of inhibition was observed and measured and the image was photographed.

## 3. Results and Discussion

### 3.1. The Web Morphology

The scanning electron micrographs of electrospun web of alginate – PVA blend without cross-linking agent are shown in Figure 2. The SEM photographs of nanofibre web spun usinga) 10% PVA(100:0) and and b) 9% PVA + 1% alginate (90:10) are represented. The images clearly show that non-crosslinked PVA and blends of PVA/alginate have uniform fibres and fibre diameter was even and clear. Pure PVA samples showed webs of fibres which are not interconnected. However, addition of alginate resulted in excellent interconnections resulting in dense network of fibre when compared to unblended PVA.

Figure 3 shows the nanofiber web of a) non-crosslinked 8%PVA: 2% alginate blend and b)8% PVA : 2% alginate blend crosslinked with 12% citric acid (CA). The fibres without cross linking shows less interconnection whereas cross linked fibres showed more number interconnected webs with porous look.We therefore, interpret that the presence of citric acid has resulted in intense cross linking of the fibres forming a high quality web which is added advantage for its wound healing applications.

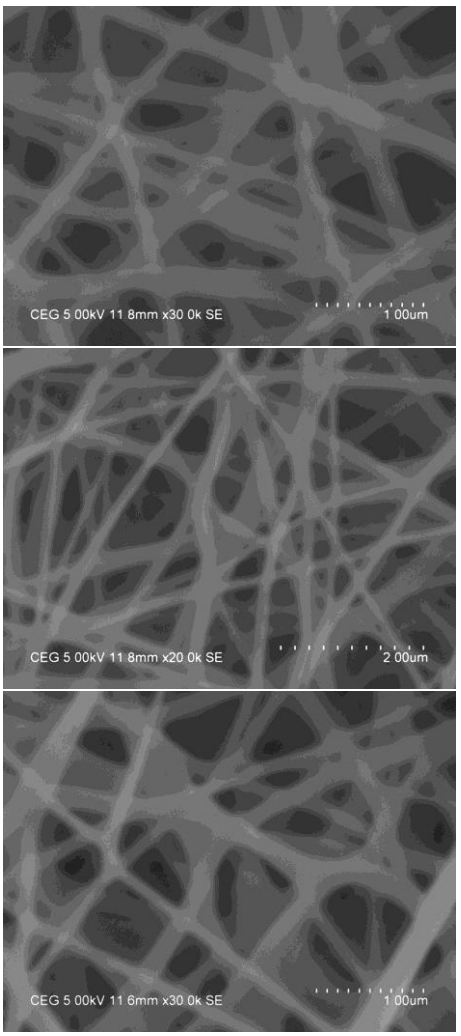


Figure 2. Scanning electron micrographs of nanofibre web of a) 10%PVAand b) 9%PVA + 1% alginate.

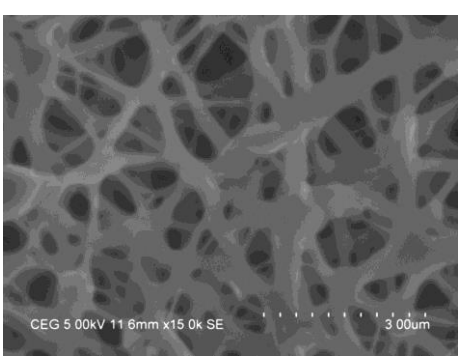


Figure 3. Scanning electron micrographs of nanofibre websobtained from blends of 8%PVA + 2% alginate and b) 8%PVA + 2% alginate + 12%citric acid.

### 3.2. The FTIR Spectral Peaks

FTIR spectrum gives us the peak shift that might be indicative of the interactions between two blended polymers. The interaction may be due to hydrogen bonding or any complex structure formation. The FTIR spectra show spectral features similar to those for individual polymers, but some band may be shifted from their original positions which mark the involvement of the specific group in bonding or interaction. Hydrogen bonding is formed between the proton donor and proton acceptor molecules. The intensity of the hydrogen bonding depends upon the intensity of the hydrogen in proton-donor alkalinity of the proton-acceptor, and distance between the groups.

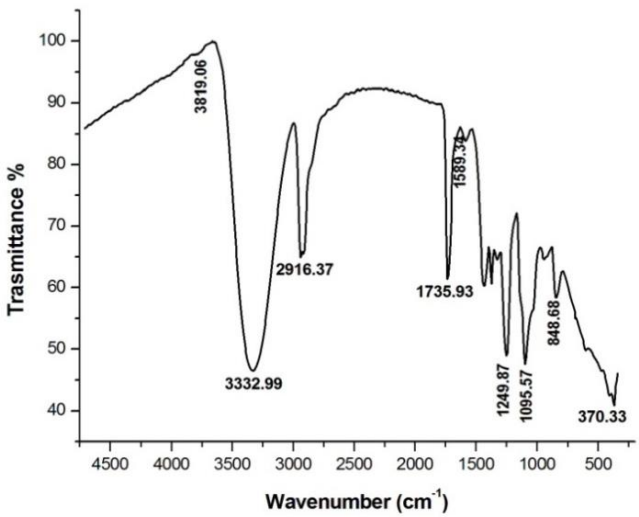


Figure 4a. FTIR spectra of nanofibre web spun from 10%PVA.

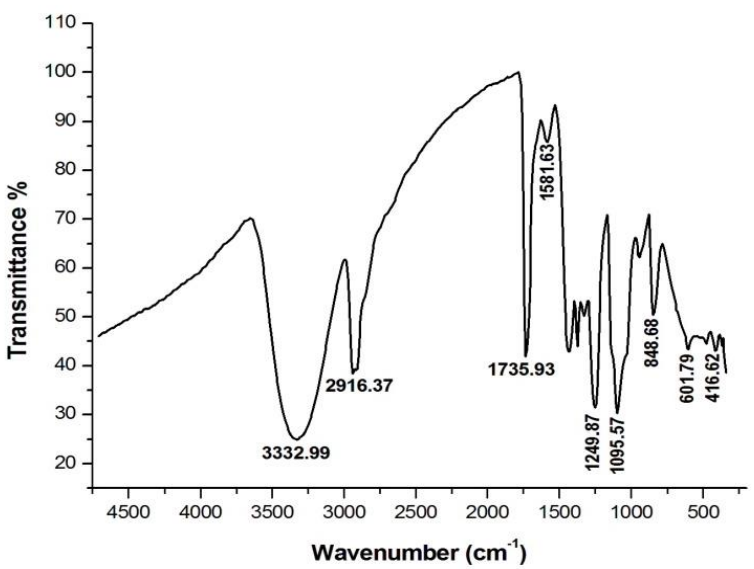


Figure 4b. FTIR spectra of nanofibre web spun from 9%PVA + 1% alginate.

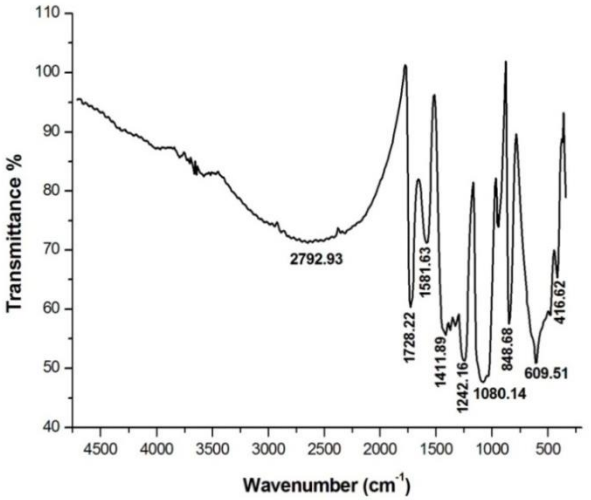


Figure 4c. FTIR spectra of nanofibre web spun from 8%PVA+2% alginate.

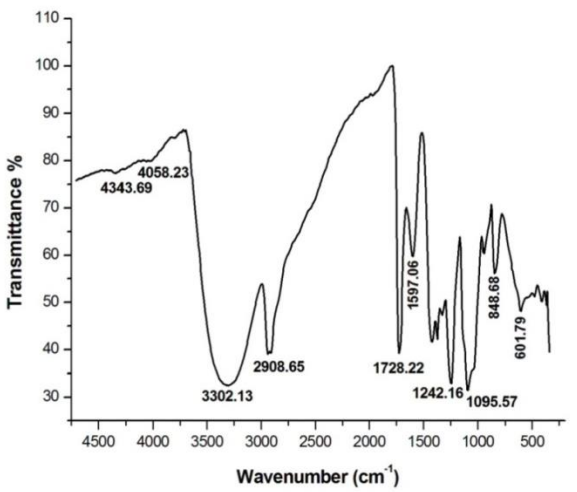


Figure 4d. FTIR spectra of nanofibre web spun from 8%PVA+2% alginate+12%citric acid.

Figure 4a through 4brepresents the FTIR spectra of the web electrospun using blends of PVA and alginate with and without citric acid. The FTIR spectrum of PVA/alginate has its characteristic peaks and cross linked PVA/alginate/citric acid showed similar peaks as PVA/alginate but broadened peak around 3300 cm-1 was observed which maybe due to the hydrogen bonding between the cross linking agent and the polymeric solution with sodium alginate. It was also observed from the spectra that hydroxyl stretching frequency became slightly lowered and broadened with increase of alginate and citric acid content. Our FTIR spectral analysis strongly implies that citric acid plays a major role in altering the morphology of PVA-alginate blend, by posing additional cross linking interactions which might have resulted in interconnected webs. This concept is further supported by the scanning electron micrographs. Therefore, we imply that citric acid-aided cross linking can generate a value added wound healing dressing of PVA-alginate blend with superior stability and haemostatic function.

### 3.3. Thermal Degradation Behaviour of Nanofibrous Web

Thermal degradation behaviour of the nanofibrous web of different composition were analysed by thermogravimetric analysis and differential thermal analysis (TG/DTA). The analysis was done in nitrogen atmosphere. The TGA curves of nanofiber web of different composition in the presence and presence of cross linking agents are drawn in a plot of temperature in x-axis versus weight% in y axis are shown in figure 5a to 5e. Alginate/PVA nanofibers cross-linked with citric acid showed one major weight loss peak at around 350℃. The second broad weight loss peak was observed around 400°C-600°C due to the thermal degradation process. The steepness of the curve indicates the rate of mass loss. IDT (or onset) or Initial decomposition temperature is the point where the study material starts disintegrating and is the measure of thermal stability of that material. Citric acid cross-linking seems to slow the degradation of nanofibers significantly, which indicates a better thermal stability compared to non-cross linked nanofibers and thin film membrane. As high performance application needs increased IDT value, our results clearly shows that, due to the stability of cross linked fibre high performance wound dressing material can be fabricated.

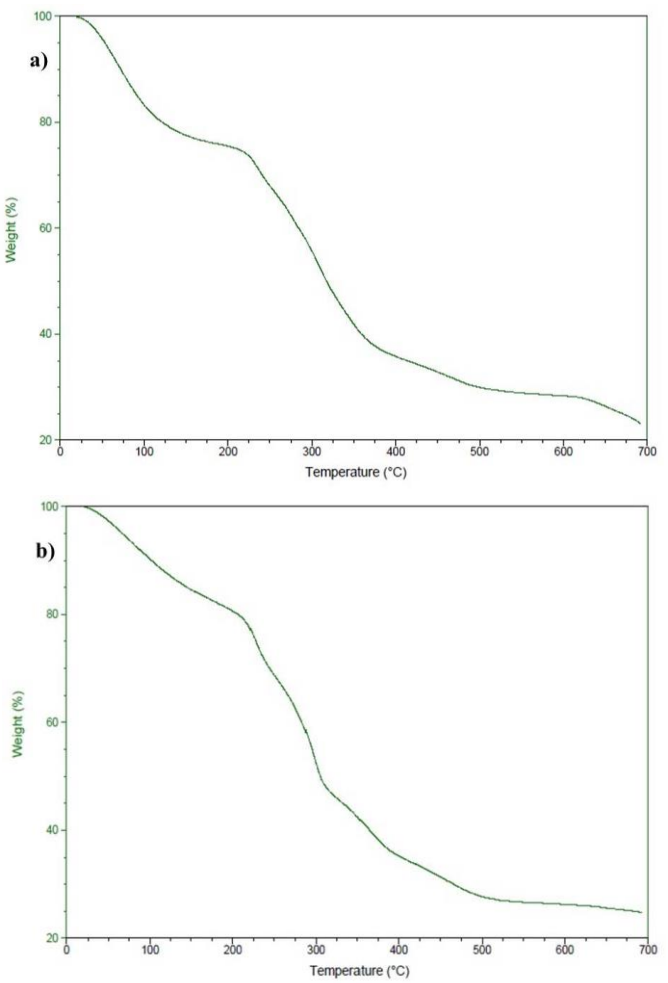


Figure 5. (Continued).

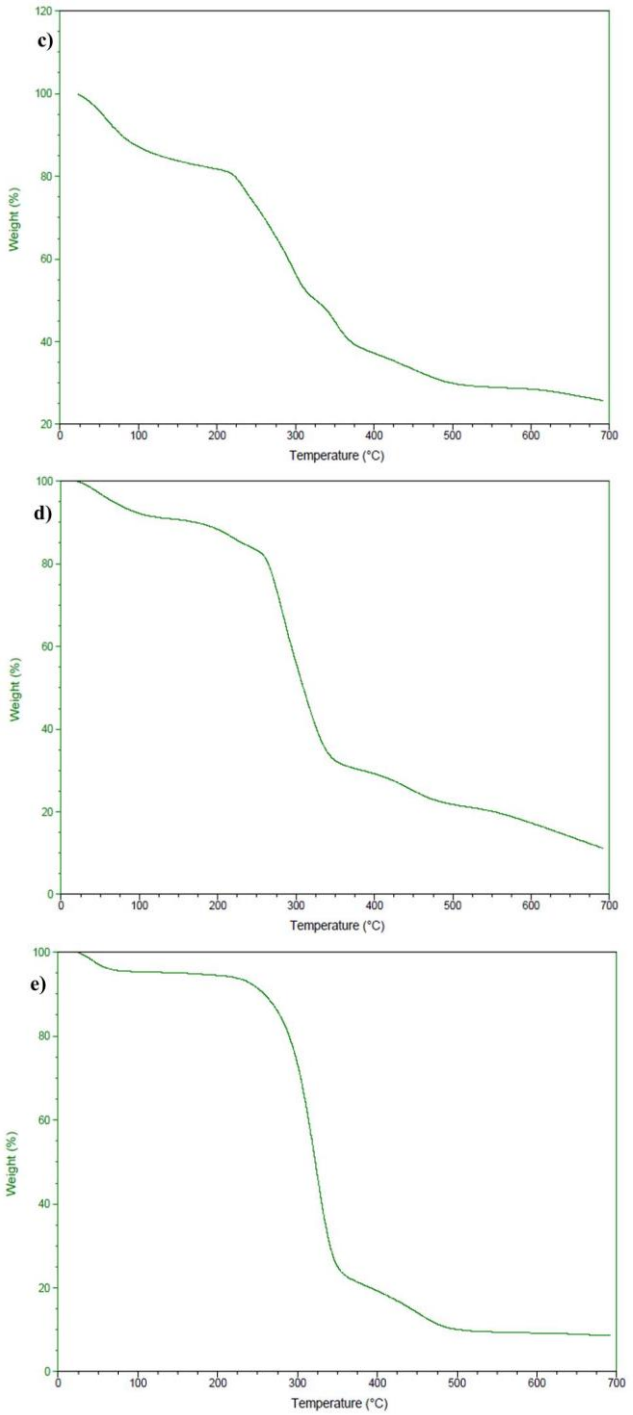


Figure 5. a) TGA curves of a) 3% alginate + 12%citric acid b) 4% alginate + 12%citric acid c) 5%alginate + 12% citric acid d) 8%PVA + 2% alginate + 12% citric acid e) 9% PVA + 1% alginate + 12%citric acid.

### 3.4. Moisture Vapour Transmission Rate

MVTR of the web wound dressing material were calculated as the gradient of the weight loss versus time for every one hour. An ideal wound dressing should control the water vapour loss from wound at an optimal rate. MVTR of the web was characterized under standard conditions set up in the environmental chamber for the samples prepared with and without cross linking agent. The sample was weighed for 24h at a time interval of 1h to calculate MVTR and the dataisrepresented in Table 3 and Figure 6. The water vapour permeability of a wound dressing should prevent excessive dehydration as well as build of exudates. It has been recommended that a rate of 200-300 g/m$^2$/day would provide adequate level of moisture without risking wound dehydration [20]. MVTR results show that the loss of water is reduced in citric acid crosslinked alginate blend. Since cross linking increases the water absorption capacity of the alginateit would provide moist environment to the wound, which helps in rapid healing thereafter. Compared to crosslinked web,non-crosslinkedones showed greater water vapour permeability.

**Table 3. Weight loss versus time of electrospun web and their respective MVTR values**

| Sample tag | Sodium alginate | PVA | Citric acid | Time in minutes | | | | | | | | MVTR |
|---|---|---|---|---|---|---|---|---|---|---|---|---|
| | | | | 0 | 60 | 120 | 180 | 210 | 270 | 320 | 1440 | |
| F1 | 1% | 9% | 6% | 7.201 | 7.181 | 7.141 | 7.081 | 7.011 | 6.986 | 6.926 | 6.526 | 122.8 |
| F2 | 1% | 9% | 9% | 7.85 | 7.77 | 7.745 | 7.72 | 7.683 | 7.658 | 7.638 | 7.2 | 85.35 |
| F3 | 1% | 9% | 12% | 7.731 | 7.689 | 7.67 | 7.655 | 7.635 | 7.615 | 7.565 | 7.207 | 62.74 |
| F4 | 2% | 8% | 6% | 7.178 | 7.15 | 7.137 | 7.07 | 6.749 | 6.689 | 6.619 | 6.272 | 267.9 |
| F5 | 2% | 8% | 9% | 7.49 | 7.445 | 7.425 | 7.41 | 7.4 | 7.35 | 7.15 | 6.94 | 112.9 |
| F6 | 2% | 8% | 12% | 7.665 | 7.628 | 7.61 | 7.599 | 7.588 | 7.576 | 7.559 | 7.116 | 41.27 |

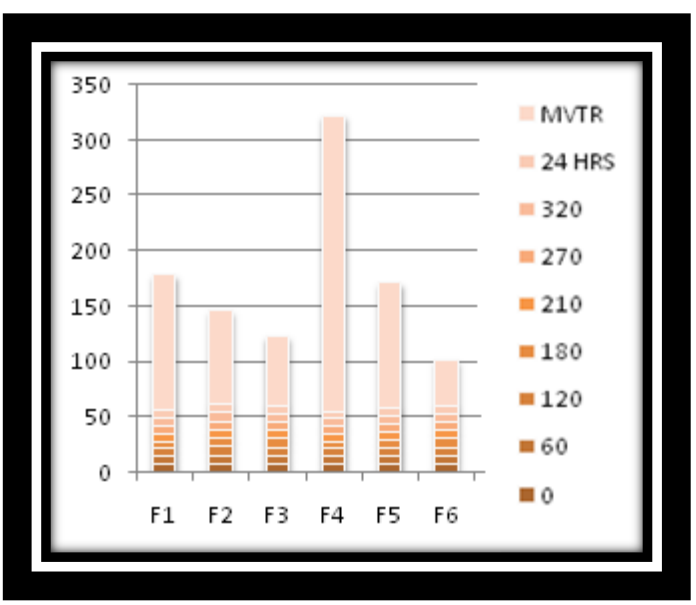


Figure 6. Plot of weight loss vs. time plot for citric acid crosslinked alginate thin film membrane.

Figure 7. Antibacterial activity of cross linked nanofiber web against *Staphylococcus aureus*.

### 3.5. Antibacterial Attribute of the Cross Linked PVA-Alginate Nanoweb

The suspension of Staphylococcus aureus was spread evenly over the face of the sterile agar plate. The nanofibre matrix along with control was placed on the agar plate and incubated. After 24 h of time, zone of inhibition appears around the test product. Figure 7 shows antibacterial activity and the zone of inhibition caused by crosslinked and non-crosslinked nanofiber web. The diameter of the zone of inhibition formed at 5%: 6% alginate:citric acid was 1mm, 5%:9% alginate/citric acid was 2mm, 5%:12% alginate/citric acid was 3mm. It was found that the increase of calcium alginate content shows higher zone of inhibition value and that zone of inhibition was found higher when increasing the cross linking proportions.

## 4. SUMMARY

Initially in this chapter, we have reviewed about the types of wound, wound healing and its phases and types of wound dressings. Traditional wound dressings were discussed with a special focus on alginate based wound dressings. The significance of web matrix in wound dressing was discussed along with the remarkable role of electrospinning and its advantages. Electrospinning of alginate is a challenging task associated with the electrospinning of alginate. The best way of circumventing this challenge is to use a co-polymer. Polyvinyl alcohol was found to be a good co-polymer for making spinnable blends to get a perfect web structure. Efficacy of crosslinking in increasing the performance of web was discussed. Polycarboxylic acids are efficient cross linkers capable of producing many interconnections in the web matrix. Citric acid is one of the best polycarboxylic acid candidates to promote interconnection and cross linking in alginate.

We have prepared a blend of sodium alginate and polyvinyl alcohol of different proportions. We have mixed the blend with different proportions of citric acid for cross

linking. The blend was then made into fibrous web using electrospinning apparatus. Calcium alginate has many advantages over sodium alginate in terms of web stability and high performance especially with bleeding wounds. Getting commercial calcium alginate is also expensive. Therefore, we first made the web and then using calcium chloride solution we replaced the sodium for calcium thus forming a web of calcium alginate crosslinked with citricacid.

The web samples were then taken for physiochemical characterization using scanning electron microscopy, Fourier infrared spectroscopy; thermogravimetric analyser and moisture vapour transmission analyser. The SEM micrograph revealed the presence of many interconnections and dense cross linking in the cross-linked web when compared to the non-cross linked web. Moreover, the cross linking was good in the web made from blend as compared to the web made with the individual component. The SEM images clearly suggest that the cross linked web has ideal morphology to give better performance in the process of wound healing. The FTIR spectra clearly revealed the interaction between the groups of the polymer constituents and the cross linking, thus suggesting the role of citric acid in making a high performance web. The spectral findings are in line with the morphological images derived by SEM. Thermogravimetric plot is an evidence for the stability of the material under study. The cross linked web has better stability than the non-cross linked counterpart. Also, the stability increased with an increase in the concentration of the cross linking agent. Thus we speculate that, the web which was found to be better as per the SEM micrograph and the FTIR spectra was also stable enough which is a pre-requisite for a high performance wound healing. MVTR results show that the loss of water is reduced in citric acid crosslinked alginate blend. Since cross linking increases the water absorption capacity of the alginate it would provide moist environment to the wound, which helps in rapid healing thereafter. Compared to crosslinked web, non-crosslinked ones showed greater water vapour permeability. The cross linked web was found to inhibit the growth of the *staphylococcus aureus* as evidenced by zone of inhibition in the growth medium.

## CONCLUSION

Wound dressings have been electrospun into nanofibers using alginate/PVA and the cross-linking agent, citric acid. Based upon the physiochemical characters such as morphology, fibre alignment, cross linking, interconnections between the fibres and FTIR spectra we conclude that the PVA-calcium alginate blend cross linked with the highest concentration of the citric acid used in our study (that is 12%) has better character which is suitable for an ideal high performance wound healing dressing. Further, from the data of thermogravimetric analysis and moisture vapour transmission rate profile we conclude that the web obtained from the PVA-calcium alginate blend cross linked with the highest concentration of citric acid is the most stable product obtained in our study. It could also be concluded from the antibacterial activity analysed by zone of inhibition that the stable web can prevent bacterial infection of the wound. On the whole, we conclude that the protocol we followed for the fabrication of the web of PVA-calcium alginate blend cross linked with citric acid is optimal. Hence, the product obtained by us can be an ideal high performance wound healing material, owing to its good stability, antibacterial activity and haemostatic efficacy.

The stability is attributed to both the calcium and the cross linking agent while the haemostatic efficacy is attributed to the presence of calcium. Therefore, our material could emerge as a high quality wound dressing material.

## REFERENCES


[1] Boateng J., and Catanzano, O. 2015. "Advanced Therapeutic Dressings for Effective Wound Healing-A Review." *Journal of Pharmaceutical Sciences 104*: 3653–3680.

[2] Gonzalez AC de O., Costa TF., Andrade Z de A., and Medrado ARAP. 2016. "Wound healing - A literature review." *Anais Brasileiros de Dermatologia 91*: 614-20.

[3] Koh, Timothy J., and Luisa, Ann D. 2011. "Inflammation and Wound Healing: The Role of the Macrophage." *Expert reviews in molecular medicine 13*: e23. Accessed September 25, 2017. doi:10.1017/S1462399411001943.

[4] Selvaraj, D., Viswanadha, Vijaya P., and Elango S. 2015. "Wound dressings – a review." *Biomedicine 5*: 24-28.

[5] Bhuvanesh G., Roopali A., and Alam M.S. 2010. "Textile- based smart wound dressings." *Indian Journal of Fibre and Textile Research 35*: 174-187.

[6] Pott, Franciele S., Marineli, Joaquim M., Janislei, Giseli Dorociak S., Karla C., and Janyne Dayane R. 2014. "The Effectiveness of Hydrocolloid Dressings versus Other Dressings in the Healing of Pressure Ulcers in Adults and Older Adults: A Systematic Review and Meta-Analysis." *Revista Latino-Americana de Enfermagem 22*: 511–20.

[7] Shakeel A., and Saiqa I. 2016. "Chitosan Based Scaffolds and Their Applications in Wound Healing." *Achievements in the Life Sciences10:* 27-37.

[8] Aditya S., Mark, Granick S., Nancy, and Tomaselli L. 2014. "Wound Dressings and Comparative Effectiveness Data." *Advanced Wound Care 3*: 511-29.

[9] Zmora S., Glicklis R., and Cohen S. 2002. "Tailoring the pore architecture in 3-D alginate scaffolds by controlling the freezing regime during fabrication." *Biomaterials, 23*: 4087-94.

[10] Mirjalili M. and Zohoori S. 2016. "Review for application of electrospinning and electrospun nanofibers technology in textile industry." *Journal of Nanostructres in Chemistry 6*: 207-13.

[11] Jessica, Schiffman D. and Caroline, Schauer L. 2008. "A review: Electrospinning of biopolymer nanofibers and their applications." *Polymer Review 48*: 317-52.

[12] Safi S., Morshed M., Ravandi S.A.H., and Ghiaci M. 2007. "Study of electrospinning of sodium alginate blended solutions of sodium alginate/poly(vinyl alcohol) and sodium alginate/poly(ethylene oxide)." *Journal of Applied Polymer Science 104*: 3245-55.

[13] Nie H., He A., Zheng J., Xu S., Li J., and Han CC. 2008. "Effects of chain conformation and entanglement on the electrospinning of pure alginate." *Biomacromolecules 9*: 1362-65.

[14] Agnieszka Kyzioł., Justyna M., Ivan M., Enrique G., and Silvia I. 2017. "Preparation and characterization of electrospun alginate nanofibers loaded with ciprofloxacin hydrochloride." *European Polymer Journal Article* In Press.

[15] Seon, Jeong K., Ki, Jung L., In, Young Kim., Young Moo L., and Sun, I. K. 2003. "Swelling kinetics of modified poly(vinyl alcohol) hydrogels." *Journal of Applied Polymer Science 90*: 3310-13.
[16] Nihed, and Ben H. 2016. "Poly(vinyl alcohol): review of its promising applications and insights into biodegradation." *RSC Advances 6*: 39823-32.
[17] Daly CG. 1982. "Anti-bacterial effect of citric acid treatment of periodontally diseased root surfaces in vitro." *Journal of Clinical Periodontology. 9*: 386-92.
[18] Stephanie, Stone A., Pallavi G., Thushara, Athauda J., and Ruya, Ozer R. 2013. "In situ citric acid crosslinking of alginate/polyvinyl alcohol electrospun nanofibers." *Materials Letters 112*: 32-35.
[19] Thomas S. 2000. "Alginate dressings in surgery and wound management--Part 1." *Journal of Wound Care 9*:56-60.
[20] Balakrishnan B., Mahanty M., Umashankar P.R., and Jayakrishnan A. 2005. " Evaluation of an in situ forming hydrogel wound dressing based on oxidized alginate and gelatin." *Biomaterials 26*: 6335-42.

# ABOUT THE EDITORS

**Deepak Pathania** is Professor Cum Head Cum Dean, Central University of Jammu, Jammu and Kashmir, India. He is presently also serving as founder President of Him Science Congress Association, Himachal Pradesh, India, scientific society. Him Science Congress Association is Scientific Society working for inculcating scientific temperament in the youth of state. He had about 19 years of teaching and research experience. He started his teaching career in 2000 from NIT, Jalandhar, Punjab. He joined as Assistant Professor and Head, Department of Applied Sciences, Institute of Engineering and Technology, Phagwara, Punjab in 2005. He also served as Head Chemistry and Dean Faculty of Basic Sciences in Shoolini University, Solan Himachal Pradesh. He also functioned in Punjab University Post Graduates College for three years in Punjab. He was shifted to University at Himachal Pradesh as Headed the Department of Applied Sciences and Humanities. He is members of different professional scientific societies. He had guided 15 Ph.D, 14 M.Phil and 27 M.Sc. research projects for their degree. Presently he is guiding 2 students for their Ph.D degree. He had authorized ten books in different areas of interest from believed publishers. He is editorial members and reviewer of different national and international journals. He had about 120 publications in reputed Journals and 130 publications in conferences to his credit. His area of research includes polymer based composites, nanocomposite ion exchangers, graft copolymerization, fiber reinforced composite, environmental chemistry, photocatalysis etc.

**Dr. Bhuvanesh Gupta** is the Founding President of Asian Polymer Association and Professor of Polymers and Textiles at Indian Institute of Technology, New Delhi, India. Dr. Gupta did his PhD from IIT Delhi and spent a couple of years as post-doc in Paris. Subsequently, Dr. Gupta worked for almost six years in France, Sweden and Switzerland under different capacities. Dr. Gupta initiated research career in the field of polymer functionalisation, biomaterials and tissue engineering. Dr. Gupta has been awarded medals at the University Level and has been granted several Visiting Fellowships in different European countries. Dr. Gupta has about 150 publications in International journals and more than 250 conference presentations in India and abroad along with 24 patents to his credit. Dr. Several PhDs have been along with several graduate students are working on different areas of biomedical technology in the group of Dr. Gupta.

# INDEX

## C



## D

## E



## F



## G



## H

## I



## L



## M



## N



## O

## P

## Q



## R



## S



## T



## U



## V

## W



## X